LEUKEMIA & LYMPHOMA
2023, VOL. 64, NO. S1, S1–S197
https://doi.org/10.1080/10428194.2023.2250219

Taylor & Francis
Taylor & Francis Group

ABSTRACTS

XX International workshop on chronic lymphocytic leukemia

Accepted Abstracts

Abstract ID: 1541946

Title: Endpoint surrogacy in chronic lymphocytic leukemia: a pooled analysis of the German CLL Study Group

Authors: Florian Simon, Rudy Ligtvoet, Sandra Robrecht, Paula Cramer, Nadine Kutsch, Moritz Fürstenau, Valentin Goede, Julia von Tresckow, Petra Langerbeins, Anna Fink, Henriette Huber, Eugen Tausch, Christof Schneider, Clemens Wendtner, Matthias Ritgen, Martin Dreyling, Lothar Müller, Lutz Jacobasch, Werner Heinz, Ursula Vehling-Kaiser, Lilly Sivcheva, Sebastian Böttcher, Peter Dreger, Thomas Illmer, Michael Gregor, Philipp Staber, Stephan Stilgenbauer, Carsten Niemann, Arnon Kater, Kirsten Fischer, Barbara Eichhorst, Michael Hallek and Othman Al-Sawaf

Introduction: Overall survival (OS) is generally considered the most patient-relevant endpoint in oncology trials, however, its implementation can entail several challenges in the context of chronic lymphocytic leukemia (CLL): (1) The competing survival risk due to comorbidities in the mostly elderly CLL patient population; (2) the high efficacy of targeted therapies warrant increasingly long observation periods or extensive patient recruitment, which can be operationally challenging. Hence, surrogate endpoints, such as progression-free survival (PFS), overall response or complete response rate (ORR, CR) or minimal residual disease (MRD), are commonly used in CLL research. However, data supporting a correlation between surrogate endpoints and OS in the treatment for CLL is scarce. Here, we present a large, systematic analysis of over 4,000 patients treated in studies of the German CLL Study Group (GCLLSG) to determine the adequacy of surrogate endpoints in clinical trials for patients with CLL.

Methods: We analysed twelve phase II and phase III trials of the GCLLSG spanning from 1999 to 2022 (Figure 1). Only patients receiving first-line therapy were included in the analysis. To determine correlation, the Kaplan-Meier survival function was estimated for both OS and PFS for each study separately. From these functions, the probability of survival (OS and PFS) was estimated at different time points. These pairs of time points were then correlated across the studies, with each pair of probabilities weighted by the number of patients in each corresponding study using Spearman's correlation coefficients. Additionally, we compared OS according to MRD and iwCLL response status at the end-of-treatment (for fixed-duration regimens) or end-of-induction-treatment (for MRD-guided treatments) (EO[I]T) using Kaplan–Meier functions calculated from the time point of MRD assessment. EO(I)T ranged from month 9 to month 15 after treatment initiation, depending on the study protocol.

Results: The full analysis set comprised 4,237 patients (Panel A). The median observation time was 67 months. Median age was 64 years (range 27–90). 45.1% of patients were older than 65 years. 3,159 patients (74.6%) had received chemo/chemoimmunotherapy (C/CIT), whereas 1,078 (25.4%) were treated with targeted therapies. There were 2,114 progressive disease (PD) events and 1,211 deaths captured within the trial data. The correlation analysis included all trials except for CLL2-BIG, where no OS events were recorded, leading to a total number of 4,204 analysed patients. The Spearman's Rho of estimated survival probabilities for the time points 12/24, 24/36, 36/48 and 60/72 months (PFS/OS) was 0.95, 0.96, 0.94 and 0.92, respectively (Panel B). Focussing on patients with a confirmed OS event ($n = 1,211$), the Spearman's Rho between PFS and OS in months was 0.66 for patients receiving chemo/chemoimmunotherapy and 0.88 for patients receiving targeted treatment (Panel C). ORR and CR rate was 89.8 and 31.5%, respectively. Patients with a CR had a significantly longer PFS (HR 0.38, 95% CI 0.34–0.42, $p < 0.001$) and OS (HR 0.39, 95%CI 0.33–0.46, $p < 0.001$) compared to patients with non-CR. MRD measurements at the EO(I)T were available for 2,521 patients (59.5%), of which 39% were treated with targeted agents. Rates of undetectable (<10^-4), intermediate (≥10^-4 and <10^-2) and high MRD (≥10^-2) were 59.1, 21.7, 19.3%, respectively, across treatment groups. The median OS for undetectable and intermediate MRD was not reached and 60.7 months for high MRD status (Panel D). The estimated 60-month OS was 84.6, 71.3, and 51.1%, respectively. In patients ≤65 years of age, median OS was not reached with undetectable or intermediate MRD and 70.5 months in patients with high MRD status. In patients >65 years, median OS was not reached for undetectable MRD and was 75.2 and 58.8 months, respectively, for patients with intermediate or high MRD. The corresponding hazard ratios for high versus undetectable MRD status at EO(I)T were 3.33 (95% confidence interval 2.57–4.3) in older and 5.89 (4.15–8.35) in younger patients.

Conclusion: In this large analysis of 12 prospective CLL trials, we found a robust correlation between PFS and OS, thereby supporting the use of PFS as a surrogate endpoint in clinical studies. Notably, the MRD status at EO(I)T was associated with OS across all treatment modalities, demonstrating its utility in identifying patients with potentially dismal outcomes and a rationale for MRD-informed treatment strategies.

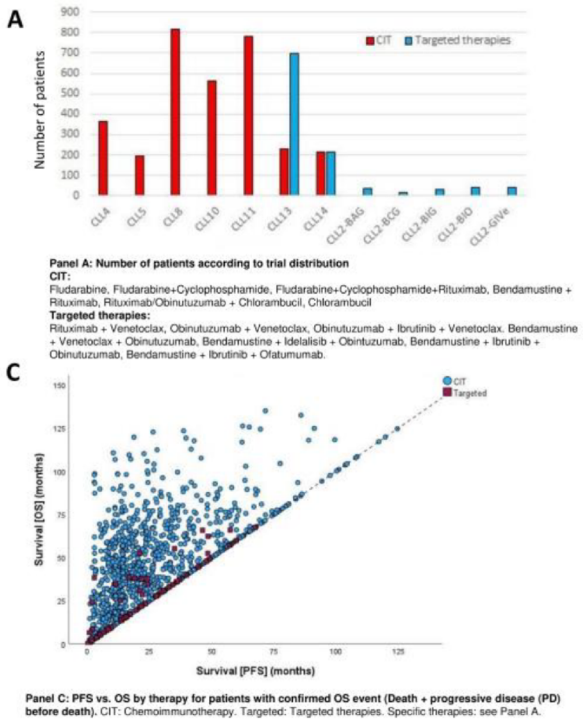

B

Spearman's Rho PFS vs OS	OS				
PFS	24 Months	36 Months	48 Months	60 Months	72 Months
12 Months	0.945	0.947	0.950	0.950	0.950
24 Months		0.963	0.966	0.966	0.966
36 Months			0.936	0.936	0.935
48 Months				0.926	0.926
60 Months					0.922

Panel B: Pairwise Spearman's correlation coefficient (Rho) for PFS vs. OS at different timepoints.

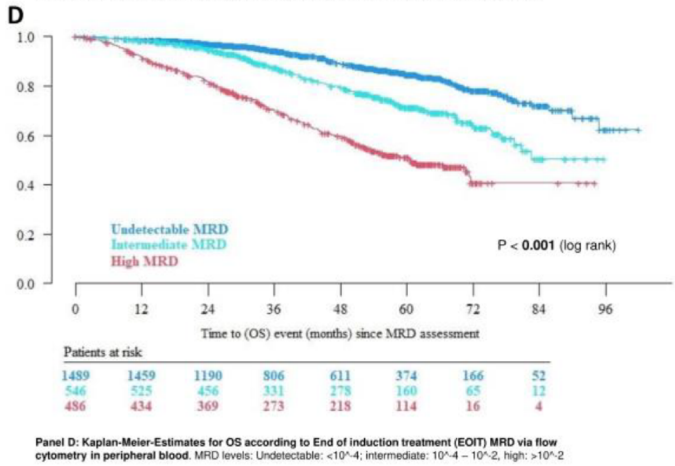

Abstract ID: 1545166

Title: METTL3 contributes to aggressive CLL via post-transcriptional regulation of splicing factor

Authors: Yiming Wu, Meiling Jin, Mike Fernandez, Stacey Fernandes, Alexey Danilov, Jennifer Brown, Steven Rosen, Tanya Siddiqi and Lili Wang

RNA splicing dysregulation is a hallmark of cancers, promoting the onset and progression of disease. In chronic lymphocytic leukemia (CLL), spliceosome mutations leading to aberrant splicing present in ~20% of patients. However, the mechanism for splicing defects in spliceosome unmutated CLL cases remains elusive. Through an integrative transcriptomic and proteomic analysis of primary CLL samples, we discovered proteins involved in RNA splicing are post-transcriptionally upregulated. Coupled with clinical annotation, we found that spliceosome protein abundance is an independent risk factor and associated with poor prognosis. Splice variants found in CLL are highly overlapped with those driven by high spliceosome abundance but not splicing factor mutations, indicating high spliceosome abundance contributes to genetic lesion-independent splicing defects. To identify potential regulators for spliceosome protein expression, we performed a proteome-wide analysis to discover proteins that are highly correlated with splicing factors expression. Our analyses have consistently identified METTL3 as one of the key factors with positive correlation with 77.6% of detected splicing factors. METTL3 is an RNA methyltransferase that modifies N6-methyladenosine (m6A) on mRNA and regulates the translation of m6A-installed transcripts. We found that m6A level on mRNA is increased in CLL cells with differential m6A modification highly enriched for RNA splicing. Moreover, high METTL3 expression in CLL is also associated with poor clinical outcomes. These results suggested that METTL3 may translationally control splicing factors through m6A and plays a role in the progression of CLL. Toward this end, we demonstrated that METTL3 is essential for CLL growth in cell lines in vitro and *in vivo*. Knock out (KO) or pharmaceutical inhibition of METTL3 all decreased CLL cell growth and splicing factor expression. Overexpression of wildtype but not catalytic mutant METTL3 restored the growth and splicing factor expression defects in METTL3 KO cells, indicating that the regulation of splicing factor is m6A-dependent. To dissect the underlying mechanism, we performed an integrated Ribo-seq, RNA-seq, and MeRIP-seq on CLL cell line with or without METTL3. KO of METTL3 decreased overall translation efficiency (TE) with RNA splicing as the most significantly affected pathway. Splicing factors with reduced TE displayed either hypo-m6A at the stop codon region or hyper-m6A at CDS regions upon METTL3 KO, as direct or indirect targets of METTL3. Moreover, we found that m6A at the stop codon and CDS regions regulates splicing factor translation via ribosome recycling and ribosome pausing, respectively. Taken together, our results uncovered a novel regulatory axis for METTL3 that controls splicing factor translation and contributes to CLL progression. Our study highlights a post-transcriptional layer of m6A modification as a major contributor to genetic lesion-independent splicing defects in CLL.

Abstract ID: 1546171

Title: Epcoritamab in patients with relapsed or refractory chronic lymphocytic leukemia: results from the phase 1b/2 EPCORE CLL-1 trial expansion cohort

Table. Best overall response by subgroup

n (%)	Overall n=19[a,b]	Double-exposed n=15[a]	*TP53* mutation/ del(17p) alteration n=12[a]
Overall response rate	11 (58)	8 (53)	8 (67)
Complete response	6 (32)	4 (27)	3 (25)
Partial response	5 (26)	4 (27)	5 (42)
Stable disease	4 (21)	3 (20)	1 (8)
Progressive disease	1 (5)	1 (7)	1 (8)
Not evaluable/no assessment	3 (16)	3 (20)	2 (17)

[a]Based on response-evaluable population, defined as patients who received ≥1 full dose and had ≥1 postbaseline response evaluation, or died within 60 d of first dose.
[b]4 patients were not response evaluable; 1 patient died after step-up dose 1, and 3 patients with ongoing treatment had not received any postbaseline response evaluation at time of data cutoff.

Authors: Arnon Kater, Herbert Eradat, Carsten Niemann, Fritz Offner, Christian Bjørn Poulsen, Thor Høyer, Mar Bellido, Mazyar Shadman, Toshihiko Oki, Alexandra Kuznetsova, Marcia Rios, Rebecca Valentin and Hans Herluf Bentzen

Background: Current treatment options for relapsed/refractory (R/R) chronic lymphocytic leukemia (CLL) primarily include small molecules, such as Bruton tyrosine kinase inhibitors (BTKi) and B-cell lymphoma 2 inhibitors (BCL2i). However, these treatments are not considered curative. As an increasing number of patients are double exposed to BTKi and BCL2i, there is a lack of effective salvage regimens, resulting in poor outcomes. Additionally, these patients would be enriched with poor prognostic factors such as TP53 aberrations and/or unmutated IGHV. Hence, despite recent advances, an unmet need exists for novel, efficacious therapies. In contrast to their use in more aggressive lymphomas, autologous T-cell–based therapies are underdeveloped in CLL, which is due, in part, to the acquired T-cell dysfunction that is a hallmark of this disease. Epcoritamab is a subcutaneous (SC) CD3×CD20 bispecific antibody developed using the DuoBody® platform and has recently been approved by the US FDA for the treatment of adult patients with R/R DLBCL, NOS, including DLBCL arising from indolent lymphoma, and HGBCL after ≥2 lines of systemic therapy. Results from the CLL dose escalation and Richter's syndrome (RS) expansion cohorts of the EPCORE CLL-1 trial showed that single-agent epcoritamab SC had encouraging efficacy and manageable safety in difficult-to-treat, high-risk patients with R/R CLL or RS. Here, we present primary data from the CLL expansion cohort of the EPCORE CLL-1 trial.
Methods: EPCORE CLL-1 (NCT04623541) is a phase 1b/2, multicenter, open-label trial evaluating epcoritamab SC in patients with active R/R CLL in need of treatment per iwCLL 2018 guidelines and ≥2 prior lines of systemic treatment, including treatment with or intolerance to BTKi. Epcoritamab SC is administered in 28 d cycles as follows: cycles 1–3, QW; cycles 4–9, Q2W; cycles 10+, Q4W. Step-up dosing (step-up doses 1 and 2, followed by 48-mg full doses) is used during cycle 1 to mitigate cytokine release syndrome (CRS). The primary endpoint of the expansion cohort is overall response rate (ORR) per iwCLL criteria. All adverse events (AEs), including hematologic toxicities and excluding CRS, immune effector cell–associated neurotoxicity syndrome (ICANS), and clinical tumor lysis syndrome (CTLS), are evaluated per CTCAE v5.0. Hematologic AEs will be updated using iwCLL criteria.
Results: As of 14 April 2023, 23 patients had been enrolled and treated in the CLL expansion cohort (median follow-up, 9.3 mo [range, 0.1–15.9]). Median age was 72 y (range, 55–83) and 74% were men. Patients had a median of 4 (range, 2–10) prior lines of treatment, and median time from initial diagnosis to first epcoritamab dose was 13.0 y (range, 5.5–19.5). TP53 mutation and/or del(17p) chromosomal alterations were present in 61% of patients; 65% had unmutated IGHV. All patients had been previously treated with BTKi, and 83% were double-exposed to BTKi and BCL2i. The most common treatment-emergent AEs (TEAEs) of any grade (G) were CRS (96%), thrombocytopenia (61%), anemia (52%), peripheral edema (43%), fatigue (39%), nausea (39%), diarrhea (35%), injection-site reaction (35%), and neutropenia (35%). CRS events were mostly low grade (78% G1–2, 17% G3) and primarily occurred following the first full dose on cycle 1 day 15; all events resolved in a median of 3 days. ICANS occurred in 3 patients (one G1, two G2); all events resolved. CTLS was reported in 1 patient (G2) and resolved. There were three G5 TEAEs: pneumonia ($n=2$) and metastatic squamous cell carcinoma ($n=1$). Among 19 efficacy-evaluable patients, the ORR was 58%, with 32% achieving complete response (CR). Among double-exposed efficacy-evaluable patients ($n=15$), ORR/CR rate was 53%/27%. Among efficacy-evaluable patients with TP53 mutation and/or del(17p) alteration ($n=12$), ORR/CR rate was 67%/25%. Median time to response was 2.1 mo (range, 1.6–3.3), and median time to CR was 3.2 mo (range, 1.6–10.8).
Conclusions: In patients with R/R CLL, single-agent epcoritamab SC demonstrated a manageable safety profile. CRS events were mostly low grade, and occurrence was predictable and as expected in this disease setting. Preliminary efficacy findings show that epcoritamab SC induces high ORRs and encouraging CR rates in patients with heavily pretreated, high-risk R/R CLL. These findings support continued evaluation of epcoritamab in this setting. Enrollment for EPCORE CLL-1 is ongoing. Updated data with longer follow-up will be presented at the meeting (Table 1).

Abstract ID: 1547411

Title: Minimal residual disease-guided combination of ibrutinib and venetoclax compared to FCR in untreated patients with CLL of intermediate risk: interim results of MRD kinetics in the ERADIC trial from the FILO group

Authors: Anne-Sophie Michallet, Anne Quinquenel, Remi Letestu, Magali Legarff-Tavernier, Fabien Subtil, Thérèse Aurran, Kamel Laribi, Florence Cymbalista, Vincent Levy, Laurence Simon, Damien Roos Weill, Veronique Leblond, Marie-Sarah Dilhuydy, Cecile Tomowiak, Caroline Dartigeas, Romain Guieze, Olivier Tournilhac, Emmanuelle Ferrant, Sophie de Guibert, Pierre Feugier, Fatiha Merabet, Stephane Lepretre, Philippe Carassou, Julie Gay, Benedicte Hivert, Luc Matthieu Fornecker, Jehan Dupuis, Lysiane Molina, Bruno Villemagne, Guillaume Cartron, Bernard Drenou, Beatrice Mahe, Omar Benbrahim, Xavier Cahut, Loic Ysebaert, Florence Nguyen-Khac, Valerie Rouille and Alain Delmer

With the emergence of targeted therapies, defining the best strategy for first-line treatment in chronic lymphocytic leukemia (CLL) patients has become challenging. The aim of the ERADIC phase 2 study was to compare the efficacy of a standard FCR regimen to that of an MRD-guided combination of ibrutinib and venetoclax (IV), in fit patients with CLL of intermediate risk defined by either unmutated IGHV status, 11q deletion or complex karyotype in the absence of TP53 alteration. MRD was assessed in bone marrow (BM) or peripheral blood (PB) by flow cytometry. After a lead-in phase of ibrutinib as a single agent from month (M)1 to M3, the total duration of treatment with the IV combination was based on BM M9 MRD. If it was <0.01% (uMRD) at that time, treatment was continued for 6 additional months (M15) then stopped. If M9 BM-MRD was ≥0.01%, IV treatment was continued for 18 additional months (M27). BM-MRD was reassessed at that time-point in both arms. Additionally, PB-MRD evaluation was performed every 6 months.The primary endpoint will be the percentage of patients with BM uMRD at M27. Here, intermediate safety data and MRD kinetics (M9 to M21) are presented. Between September 2019 and February 2021, 120 patients were randomized 1:1 between the two treatment arms. The median age was 59 [34–72] and 61 [34–74] year-old in the FCR and IV arms, respectively. Patient characteristics were well balanced between the 2 arms in terms of gender (male 72% FCR, 74% IV), PS ECOG 0-1 (59% FCR, 68% IV) and Binet stage (A, B and C 15, 64, 21% for FCR; 8.5, 59 and 32% for IV). An11q deletion was found in 20 and 24% of the cases in the FCR and IV arms, respectively and all patients but one had unmutated IGHV. At the time of data cut-off for this analysis, the median follow-up was 29.7 months [range: 25.3–32.8]. Sixty-three serious adverse events (SAE) have been reported so far, 32 in the FCR arm and 31 in the IV arm. In the FCR arm, the most frequent SAE were infections (Nf12 including 4 COVID-19), febrile neutropenia (Nf5) biological tumour lysis syndrome (Nf3), and secondary malignancies (Nf2, including 1 myelodysplastic syndrome and 1 acute myeloid leukemia). In the IV arm, the most frequently reported SAE were infections (Nf8 including 4 COVID-19), cardiovascular events (Nf7), biological tumour lysis syndrome (Nf5), acute renal failure (Nf2) and secondary malignancies (Nf2, including 1 colorectal cancer and 1 skin basal cell carcinoma). Five grade 5 adverse events were reported, respectively 2 in the FCR arm (1 septic shock and 1 AML) and 3 in the IV arm (2 sudden deaths and one death COVID-19-related). In the FCR arm (intention to treat [ITT] $n=57$), 59.6% of the patients had BM-uMRD at M9. The kinetics of PB-uMRD was 68% at M9, 65% at M15 and 52% at M21. In the IV arm (ITT $n=54$), the rate of BM-uMRD at M9 was much lower at 33%. PB-MRD kinetics showed levels of uMRD of 52, 70, and 67% at M9, M15 and M21, respectively. In terms of response, CR/CRi rates were 56% for the FCR arm and 66% for the IV arm. Three patients progressed in the FCR arm (1 at M9 and 2 at M15) and 2 in the IV arm, at respectively M13 and M39. Among the 13 patients who achieved BM-uMRD at M9 in the IV arm, 10 have indeed stopped according to the protocol and only 1 has progressed at M39. In conclusion, monitoring MRD kinetics in this trial showed a stable level of PB-uMRD in the FCR arm yet a clear increase in the IV arm between M9 and M15. Toxicity remains an important parameter in both treatment arms that will have to be taken into account when determining whether treatment should be continued because of detectable BM-MRD at M9 (IV arm). Upcoming data of the primary enpoint analysis at M27 will be of great interest to try to determine the best strategy.

Abstract ID: 1548000

Title: Autoimmune cytopenias in patients with chronic lymphocytic leukemia treated with targeted drugs: pooled analysis of clinical trials from the German CLL Study Group (GCLLSG)

Authors: Elia Boccellato, Adam Giza, Sandra Robrecht, Paula Cramer, Julia von Tresckow, Othman Al-Sawaf, Moritz Fürstenau, Eugen Tausch, Stephan Stilgenbauer, Kirsten Fischer, Barbara Eichhorst, Candida Vitale, Marta Coscia, Michael Hallek and Petra Langerbeins

Introduction: Chronic lymphocytic leukemia (CLL) can lead to various autoimmune complications in 1–9% of patients. Previous data analyzed their incidence with chemoimmunotherapy and more recently with single agent targeted drugs, i.e. Bruton-tyrosine kinase inhibitors (BTKi) and the anti-BCL2 drug venetoclax. In this context, we wished to investigate autoimmune cytopenias (AIC) in the setting of targeted agents and to identify possible risk factors within a metanalysis.

Methods: A pooled analysis was performed in patients treated with at least one dose of a targeted agent from seven GCLLSG phase 2/3 trials. AIC that occurred after first administration of a targeted agent until 28 days after its last administration were considered. MEDRA terms compatible with AIC (autoimmune hemolytic anemia, AIHA; immune thrombocytopenia, ITP; autoimmune granulocytopenia, AIG; multiple AIC) and cases of anemia/thrombocytopenia/neutropenia with/without related symptoms treated with corticosteroid or immunoglobulin therapy for >2 days in a row in the two weeks preceding the beginning or following the end of the event were included. Patients with at least one AIC vs. no AIC were compared with regard to baseline characteristics. Overall survival (OS) was calculated from 28 days after last administration of targeted agent. Kaplan–Meier methodology and Cox regression with calculation of hazard ratios (HR) and 95% confidence intervals (CI) were used to compare OS between both groups. Logistic regression with calculation of Odds ratios (OR) and 95% CIs was performed to identify risk factors for development of AICs.

Results: With a median observation time of 38.6 months (range 1.1–76.3) a total of 981 patients treated first-line (85.4%) or relapsed/refractory (14.6%) with at least one dose of venetoclax plus CD20 antibody ($n=520$), venetoclax plus BTKi ($n=297$), BTKi ($n=128$), or idelalisib ($n=36$) were included. All patients received therapy with anti-CD20 antibody obinutuzumab ($n=685$), rituximab ($n=231$), or ofatumumab ($n=65$). The median age was 62 years (range, 27–85), 691 (70.4%) were male, and 362 (36.9%) were Binet stage C. A total of 91 AIC events (with incidence of 9.3%) were observed in 58 patients including 42 events in patients treated with venetoclax (8.1%), 45 events in patients treated with venetoclax plus BTKi (15.3%), 3 events in patients treated with BTKi (2.3%) and one event in a patient treated with idelalisib (2.8%). Eighty events (87.9%) occurred during the first 6 months of treatment, and 54 (59.4%) were of CTC grade 3–4, with no grade 5 events. Eighty-one events resolved completely (89%), 2 (2.2%) with sequelae, and 8 (8.8%) were persisting. Nineteen (20.9%) AIC events required dose adjustments, including 11 temporary interruptions, 6 dose reductions (with 4 subsequent interruptions), and 2 permanent discontinuations. When baseline characteristics of the AIC cohort ($n=58$) were compared to the non-AIC cohort ($n=923$), 50 vs. 28.3% were female, 63.8 vs. 35.2% had Binet stage C, 31 vs. 39.8% had B symptoms, 32.8 vs. 24% had creatinine clearance <70 mL/min, 24.6 vs. 11.1% had TP53 aberrations, 69.1 vs. 61.7% were IGHV unmutated, 73.7 vs. 62.6% had β2-microglobulin >3.5 mg/dL, 72.7 vs. 55.4% were in (very) high CLL-IPI risk group, and 27.3 vs. 15% had NOTCH1 mutation. A multivariate analysis identified venetoclax-based treatment (OR 4.913, 95% CI 1.639–14.733, $p=0.004$), Binet stage C (OR 3.459, 95% CI 1.953–6.125, $p<0.001$), female sex (OR 2.428, 95% CI 1.390–4.241, $p=0.002$), and presence of TP53 aberrations (OR 3.163, 95% CI 1.566–6.389, $p=0.001$) as independent adverse prognostic factors for developing an AIC (Table 1). 24-month overall survival from end of treatment was 88.6% for patients with at least one AIC versus 93.9% for patients without any AIC (HR 1.759, 95% CI 0.757–4.087).

Conclusions: Autoimmune cytopenias may occur with an incidence of 9% in patients with CLL treated with targeted drugs. When comparing different treatment modalities, venetoclax plus BTKi had the highest AIC incidence. Adverse risk factors for AIC were venetoclax-based treatment, advanced Binet stage, female sex and TP53 disruptions. Possible mechanisms for AIC therefore may include treatment-induced immunomodulatory and off-target effects, as well as patients' specific factors (Table 1).

Table 1. Multivariable model for prognostic subgroups regarding autoimmune cytopenias.*

Prognostic subgroup	Patients N	AIC N (%)	Odds ratio	95% CI	P value
Ven-based treatment					
No	164	4 (2.4)	*Ref.*		
Yes	814	53 (6.5)	4.913	1.639-14.733	0.004
Binet stage					
Binet A/B	616	20 (3.2)	*Ref.*		
Binet C	362	37 (10.2)	3.459	1.953-6.125	< 0.001
Sex					
Female	289	28 (9.7)	2.428	1.390-4.241	0.002
Male	689	29 (4.2)	*Ref.*		
TP53 status					
None	862	43 (5.0)	*Ref.*		
Mutated and/or deleted	116	14 (12.1)	3.163	1.566-6.389	0.001

*calculated on evaluable patients.

Abstract ID: 1548041

Title: Oncogenic role and target properties of the lysine-specific demethylase KDM1A in chronic lymphocytic leukemia

Authors: Qu Jiang, Johanna Stachelscheid, Johannes Bloehdorn, Alicja Pacholewska, Stephan Stilgenbauer, Michael Hallek, Michal R. Schweiger, Elena Vasyutina and Marco Herling

CLL, the most common leukemia in adults in the Western world, continues to be an incurable disease despite advancements in identifying genomic and molecular changes and improving treatment strategies. Epigenetic modifications play a crucial role in shaping the transcriptional patterns that drive CLL progression and contribute to the development of distinct biological and clinical subgroups. However, characterizations of epigenetic regulators, particularly histone-modifying enzymes, are very rudimentary in CLL. Aberrant expression of the T-cell leukemia/lymphoma 1A (TCL1A) proto-oncogene is a hallmark of CLL and high TCL1A levels are associated with aggressive disease features. As a well-accepted disease model, Eμ-TCL1A transgenic (tg)

mice produce B-cell proliferations that closely resemble human CLL. In the context of the yet-evolving molecular concept of the 14kDa TCL1A protein, it was shown that TCL1A interacts with the DNA methyltransferase 3A (DNMT3A), thereby reducing its enzymatic activity and contributing to epigenetic reprogramming in CLL. Fittingly, induced mono- or bi-allelic losses of Dnmt3a result in murine CLL. Nevertheless, the functional network around TCL1A, particularly with epigenetics, is incomplete and as a causal oncogene in CLL, a better molecular understanding would help in improving disease concepts and treatment rationales in this still incurable neoplasm. Here, we identify the epigenetic modifier, lysine-specific demethylase KDM1A as a novel interaction partner of the TCL1A protein in B cells. This demethylase has been implicated in many cancer entities and its overexpression has been linked to poor prognoses. Currently, KDM1A inhibitors are being investigated for cancer therapy in clinal trials. In this context, we proposed that KDM1A is involved in CLL pathogenesis by altering its epigenetic landscape. We have analyzed the subcellular localization of TCL1A and KDM1A as well as their interacting complex. TCL1A interacted with KDM1A in the nucleus. Interestingly, their protein interaction increased the histone demethylase activity of KDM1A in B cells. TCL1A also affected histone posttranslational modifications (PTMs). Furthermore, we could show that KDM1A is overexpressed in CLL B cells as compared to healthy B cells. By analyzing the gene expression profiling (GEP) data of patients included in the CLL8 trial, we demonstrated that higher KDM1A expression levels and the associated gene signatures correlate with adverse clinical characteristics and unfavorable clinical outcomes, e.g. higher white blood cell (WBC) counts, higher serum thymidine kinase levels, a higher rate of TP53 mutations/deletions, and shorter progression-free survival (PFS). In addition, enrichment of different pathways involved in tumor progression was also associated with KDM1A expression levels. Next, we took advantage of the doxycycline (Dox)-inducible Kdm1a knockdown mouse model and the TCL1A-tg Eμ-TCL1A mice to achieve a whole-organismal Kdm1a knockdown in murine CLL. The genetic Kdm1a depletion in Eμ-TCL1A mice reduced the leukemic burden in peripheral blood, spleen, and bone marrow. This was accompanied by upregulation of p53 and pro-apoptotic pathways identified by RNA-sequencing analysis. The analysis of differentially expressed genes (DEGs) upon Kdm1a knockdown suggested that Kdm1a acts as a transcriptional repressor in murine CLL. This might be due to enrichment of regulatory elements of upregulated genes with H3K4 methylation upon the Kdm1a knockdown, which leads to activation of these genes. Thus, we performed chromatin immunoprecipitation sequencing (ChIP-seq) experiments, which demonstrated an increase in H3K4me3 marks in Kdm1a knockdown leukemic cells. Moreover, KDM1A expression in the components of the microenvironment had an impact on their support for CLL progression. The loss of KDM1A in monocytic cells and stromal cells led to impaired support of CLL cell proliferation and survival *in vitro*. Notably, Kdm1a knockdown in Eμ-TCL1A prolonged the overall survival (OS) of leukemic animals. *In vitro*, KDM1A inhibition by the pharmacologic compounds induced apoptosis and increased H3K4/9 target methylation levels in leukemic B cells. Overall, we established a relevant pathogenic role for KDM1A in CLL, as a pro-oncogenic molecule in CLL cells and in components of their microenvironment. Our data further provide a rationale for therapeutic KDM1A inhibition in CLL.

Abstract ID: 1548495

Title: Mitochondrial dysregulation and metabolite imbalance in Richter's transformation: insights from a mouse model

Authors: Prajish Iyer, Bo Zhang, Tingting Liu, Meiling Jin, Kevyn Hart, Joo Y. Song, Wing Chan, Tanya Siddiqi, Steven Rosen, Alexey Danilov and Lili Wang

Despite significant advancements in genetics and the treatment of CLL, Richter's transformation (RT), a highly aggressive transformation of CLL, poses a clinical challenge. Oxidative stress fuels the pathogenesis of various cancers by disrupting the delicate balance between reactive oxygen species (ROS) production and antioxidant defenses. In CLL, accumulating evidence supports that increased levels of ROS leading to mitochondrial dysfunction may promote CLL progression. In RT, an OXPHOShighBCRlow transcriptional signature was recently reported suggesting mitochondrial dysregulation may be a potential therapeutic target for treating RT. However, the exact role and the molecular mechanisms underlying mitochondrial dysregulation in CLL, and RT are not well explored. MGA (Max gene associated), a functional MYC suppressor, undergoes loss-of-function mutations in approximately 5% of CLL and 36% of RT cases, suggesting a potential driver from CLL to RT. Given MYC is a key regulator for OXPHOS, we hypothesized if MGA deletion could induce mitochondrial dysregulation driving CLL to RT progression. First, we generated a novel murine CLL-RT model by creating a genetic knockout of Mga through the adoptive transfer of genome-edited LSK (Lin-Sca-1+ Kit+) cells derived from CD19Cre/+Cas9fl/+/Mdrfl/+/Sf3b1-K700Efl/+ mice into sub-lethally irradiated recipient mice (control vs. Mga KO, $n=15$ per group; C57BL/6: CD45.1). Three out of fifteen mice with Mga deletion had a clonal expansion of B220+CD5+ CLL-like cells with leukemic cell infiltration in the spleen and bone marrow by the age of 21-month-old; however, no RT signs were observed in these mice. Upon transferring these CLL-like splenic cells into immunocompromised NSG or immunocompetent sub-lethally irradiated CD45.1 mice, these cells had a rapid expansion but with a loss of CD5 at three weeks post-engraftment, with leukemic cells infiltrating various lymphoid tissues. Examination of H&E-stained splenic sections revealed CLL-like cells with a morphology resembling leukemia in the primary engrafted mice, and larger cells resembled aggressive lymphoma (RT) upon secondary engraftment. Furthermore, increased expression of MYC and Ki67, along with the larger size in flow cytometry in RT than CLL, confirmed Mga deletion promotes CLL to RT transition. To assess the impact of Mga/Myc on mitochondrial function, we conducted a series of experiments using murine normal ($n=4$), CLL ($n=2$), and RT ($n=2$) splenic B cells. RT cells displayed elevated oxygen consumption rate and increased utilization of TCA substrates (succinate and glutamine) in Seahorse-based mitostress assays. Second, electron microscopy revealed distinct structural abnormalities in mitochondrial shape and inner membrane in CLL and RT cells, indicating mitochondrial dysregulation. In line with structural and functional mitochondrial changes, RNAseq-based transcriptome profiling demonstrated enrichment of MYC target pathways, OXPHOS, hypoxia, and cell cycle-associated pathways in RT cells compared to CLL and normal B cells. Elevated expression of antioxidant genes (PRDX, TNXRD2) in RT cells confirmed heightened oxidative stress, which was corroborated by flow

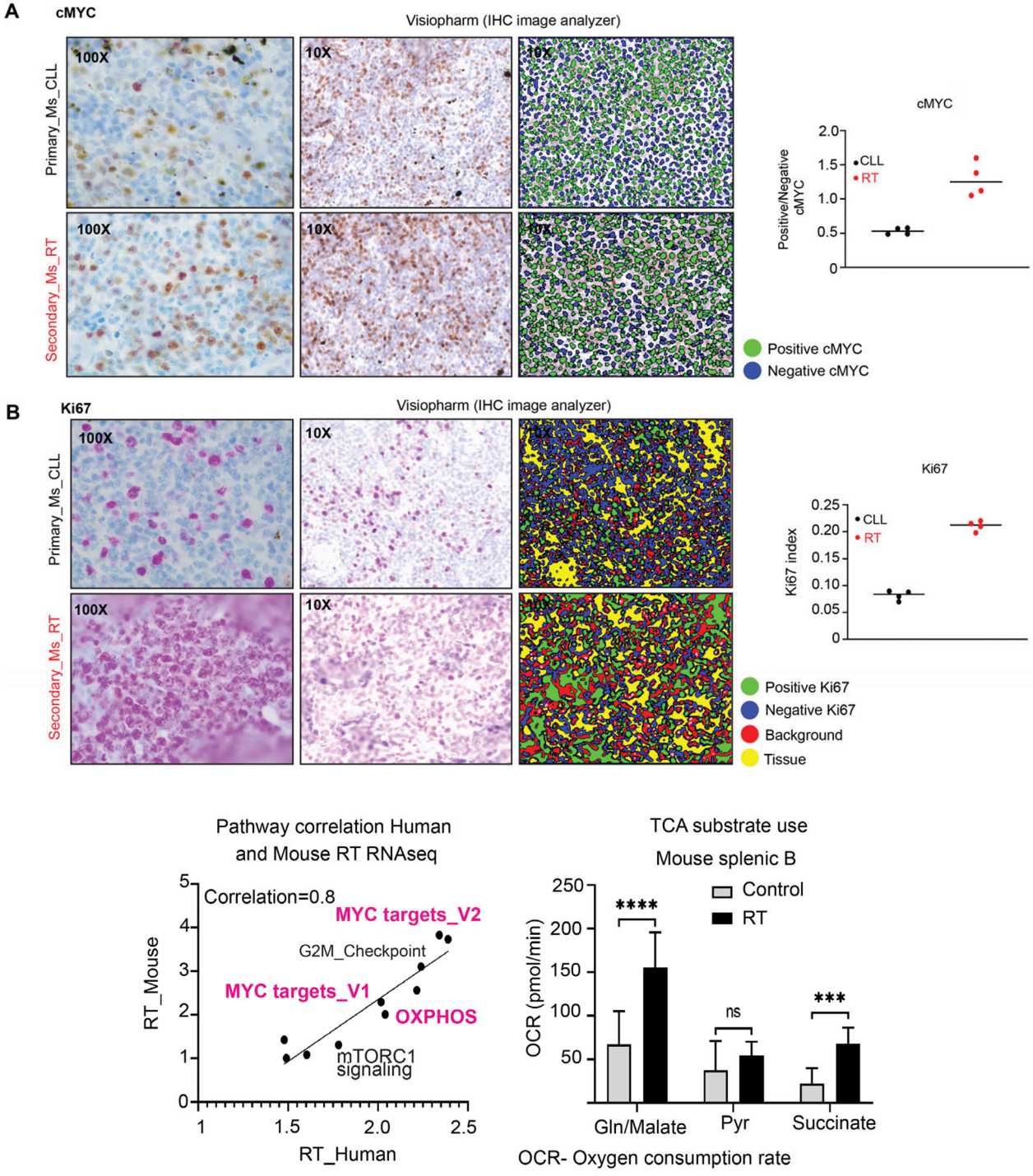

cytometry analysis revealing increased levels of cellular reactive oxygen species (ROS) in RT cells compared to CLL and normal B cells. Immunoblotting confirmed elevated levels of fusion (OPA1), fission (DRP1) proteins, VDAC1 (mitochondrial potential), and MYC targets (NME1 (Nucleoside diphosphate kinase), TFAM (Transcription factor; mitochondrial) in RT cells compared to CLL and normal B samples. Collectively, our findings underscore the significant role of mitochondrial dysregulation in the transition from CLL to RT. To define the metabolites driving mitochondrial dysregulation in RT driven by Mga deletion, we performed unlabeled metabolomics in normal and RT splenic B ($n=3$ each group) followed by LC-MS detection (liquid chromatography-mass spectrometry). Among the 138 identified metabolites, 44/138 were upregulated in RT compared to normal B cells. Notably, glutamine, succinate (TCA), and asparagine exhibited higher levels (fc >1.5, $p<0.05$) than normal B cells. Other elevated metabolites included palmitate, glycerol 3P, and glycine. Pathway analysis revealed enrichment in glycine, serine, glutathione, glycerophospholipid, TCA cycle, and branched-chain metabolism ($p<0.05$). Integrated analysis of RT metabolite and gene expression data unveiled the significance of glycerophospholipid and glutathione pathways ($p<0.001$), suggesting their involvement in energy production and oxidative stress mitigation in RT cells, respectively. Furthermore, we validated increased triglyceride synthesis, NADH production, ATP production, and cellular ROS in CLL cell lines (MEC1) and pre-B ALL cell lines (Nalm6) with MGA deletion. Taken together, our results highlight the importance

of MYC-driven oncometabolites in RT and reveal glycerophospholipid and glutathione pathways as potential therapeutic targets (Figure 1).

Abstract ID: 1549556

Title: Bruton's tyrosine kinase and phospholipase C-gamma 2 mutational profiles in pooled analysis of patients with chronic lymphocytic leukemia treated with ibrutinib

Authors: Inhye Ahn, Adrian Wiestner, Paolo Ghia, John Byrd, Carol Moreno, Susan O'Brien, Daniel Jones, Vincent Girardi, Leo W.-K. Cheung, Melih Acar, Shiquan Wu, James P. Dean, Sima Patel and Jennifer Woyach

Introduction: Although most patients with chronic lymphocytic leukemia (CLL) achieve durable remissions during treatment with ibrutinib, some develop resistance leading to progressive disease (PD). Secondary resistance to BTK inhibitors is associated with acquired mutations in BTK or phospholipase C-γ2 (PLCG2) genes, particularly in relapsed/refractory (R/R) settings. BTK C481 mutation is the most common mutation found in BTK inhibitor-resistant CLL. Novel, non-C481 BTK mutations have been described, including BTK L528W, which has been reported in patients treated with ibrutinib, zanubrutinib, and pirtobrutinib (Maddocks, JAMA Oncol. 2015; Handunnetti, ASH. 2019; Song. Br J Haematol. 2022; Blombery, Blood Adv. 2022; Wang, NEJM. 2022). Of interest, BTK L528W was reported in 54% and 4% of patients treated with zanubrutinib and ibrutinib, respectively (Blombery, Blood Adv. 2022), and is associated with resistance to pirtobrutinib (Blombery, Blood Adv. 2022; Wang, NEJM. 2022), a non-covalent BTK inhibitor with activity in patients with BTK C481 mutations (Mato, Lancet. 2021). Here we evaluate the BTK and PLCG2 somatic mutation status in 419 patients with CLL treated with ibrutinib, including mutations at the BTK L528 locus.

Methods: Blood samples were collected across six clinical trials evaluating ibrutinib in previously untreated (RESONATE-2 [PCYC 1115/1116, NHLBI Phase 2, iLLUMINATE) or R/R CLL (RESONATE, RESONATE-17, NHLBI Phase 2). Samples were obtained at standardized timepoints which varied by study. DNA extracted from peripheral blood mononuclear cells was deeply sequenced using a custom ION Torrent assay covering mutational hotspots and non-hotspots of BTK and PLCG2. Hotspot sites were C481 and T474 in BTK and R665, D993, L845, and S707/708 in PLCG2. The reporting variant allele frequency (VAF) cutoff was set at 0.5% hotspot sites and 2.0% for non-hotspot sites (e.g. BTK L528).

Results: Of 419 patients with available samples (247 previously untreated; 172 R/R), median age was 69 years (range, 39–89), 46% had unmutated IGHV, 39% had deletion 17p and/or TP53 mutation, and 41% had R/R CLL. At the median follow-up of 43.7 months (range 0.2–76.7), 132 patients progressed or died including 69 PD events in R/R CLL (median PFS 56 months, 95% CI 44.4 – 67.3) and 22 PD events in previously untreated CLL (median PFS not reached). The incidence of BTK mutations was over 8-fold higher among patients with R/R CLL (35%) than those with previously untreated CLL (4%). Similarly, PLCG2 mutations were more frequently found in R/R CLL (14%) than previously untreated CLL (6%). The most frequently detected mutations affected BTK C481, which included C481S (16% of all evaluable patients), C481Y (3%), and C481R (2%). BTK T474I and L528W were rare, found in 0.7% (2 previously untreated and 1 R/R CLL) and 0.5% (2 previously untreated CLL), respectively. Sixty-four (15%) patients had mutations exclusively at the BTK C481 locus. Five (1%) patients had co-occurring BTK C481 and non-C481 mutations. Two (<1%) patients had non-C481 mutations only (Figure 1). Two patients with BTK L528W had co-occurring BTK C481 mutations and achieved partial response to ibrutinib before PD (duration of response: 20 and 60 months, respectively); one patient had BTK L528W detectable prior to PD (VAF 4%) but no longer detectable at PD. Mutational hotpots of PLCG2 were more widely dispersed than those observed with BTK mutations. These included well-known PLCG2 mutations affecting Src homology-2 domain (R665W, S707F, L845F in 2% each) and less frequently reported mutations in catalytic (P400L in <1%, V401A in <1%, D993H in 2%) and C2 domains (D1140N, D1140E, M1141K in <1% each).

Conclusion: This is the largest dataset characterizing the incidence and patterns of BTK and PLCG2 mutations in patients with CLL treated with ibrutinib. BTK C481 mutations are the most frequently occurring mutations. PLCG2 mutations occur across the gene at a low incidence per locus (<5%). Non-C481 BTK mutations affecting the L528 locus are rare among patients treated with ibrutinib (<1%), corroborating findings in published literature, and co-occurred with BTK C481 mutations.

Figure. *BTK* mutations in previously untreated and relapsed/refractory CLL patients treated with ibrutinib

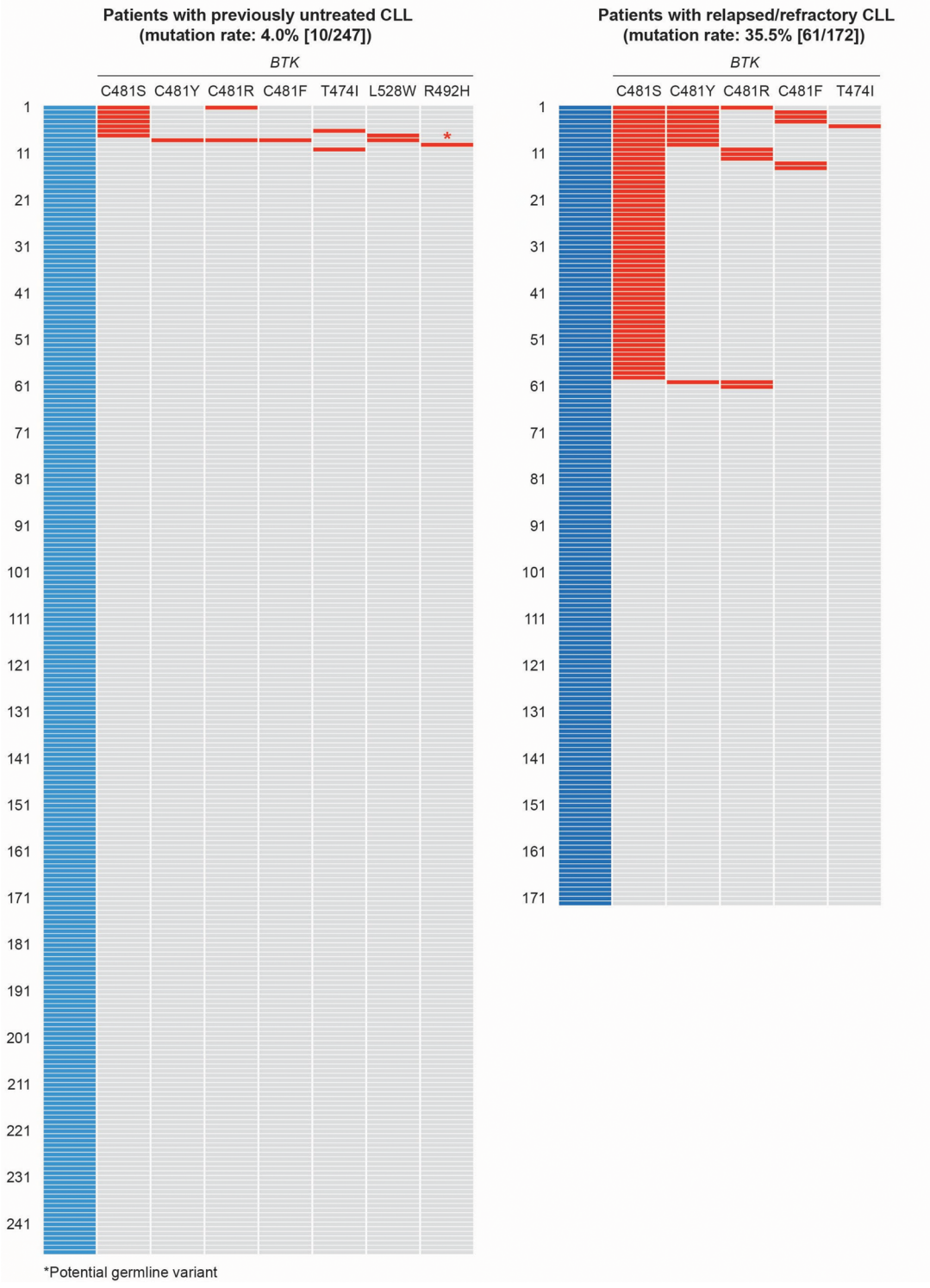

Abstract ID: 1550584

Title: A high proportion of IGHV4-39, subset#8 and #8B in Chinese patients with chronic lymphocytic leukemia: a retrospective analysis of 3154 Ig VH sequences by cwCLL, Chinese workshop on CLL

Authors: Yi Xia, Tonglu Qiu, Shuhua Yi, Chun Qiao, Huayuan Zhu, Yuting Yan, Li Yao, Mingqing Zhu, Hongling Peng, Heng Li, Liang Huang, Min Xiao, Jie Jin, Jianqing Mi, Jiaojiao Zhang, Shaoyuan Wang, Zhengjin Zheng, Bingzong Li, Han Zhang, Wei Xu, Lugui Qiu and Jianyong Li

Introduction: The difference in the usage of IGHV genes and stereotyped BCR between Asian and Western patients with chronic lymphocytic leukemia (CLL) has been a topic of interest. Previous reports on 623 Chinese CLL patients showed that only 19.7% of Chinese patients had stereotyped BCR [1], while the stereotyped fraction of western CLL patients reached 41.2% according to the latest report [2]. It is uncertain whether the proportion of subset users would increase with an increase in sample size. To address this, the study retrospectively collected more than 3000 Ig VH data from different institutions across China.

Methods: A total of 3759 patients diagnosed with CLL from 23 institutes in China were included in this study. All cases met the diagnostic criteria of iwCLL. PCR amplification and sequence analysis were performed in each local institute. Due to lack of records of IGHD, IGHJ and HCDR3 sequences in 612 patients, 3147 patients from 9 institutes were subjected to further analysis. BCR stereotypy was identified using multiple sequence alignment Clustal Omega software according to criteria proposed by Agathangelidis et al. [2,3].

Results: 3154 Ig VH sequences from 3147 Chinese CLL patients were included in this study. Among them, 3105 Ig VH sequences were productive, 49 were unproductive. Following the 98% germline identity cut-off value, 1945 (62.6%) rearrangements were assigned to the mutated subgroup and 1160 (37.4%) were unmutated. The most frequent IGHV genes were IGHV4-34 (365; 11.6%), IGHV3-23 (266; 8.5%), IGHV4-39 (223; 7.1%), IGHV3-7 (208; 6.6%), IGHV1-69 (189; 6.0%), IGHV3-48 (145; 4.6%), IGHV3-30 (139; 4.4%) and IGHV4-59 (121; 3.9%). The most frequent IGHD genes were IGHD3-10 (388; 12.5%), IGHD6-13 (291; 9.4%), IGHD3-22 (243; 7.8%), IGHD6-19 (231; 7.4%), IGHD3-3 (205, 6.6%). The most frequent IGHJ genes were IGHJ4 (1496; 48.2%) and IGHJ6 (702; 22.6%). The data were comparable to our previous reports: Chinese patients showed a higher proportion of mutated IGHV (62.6 vs. 54.1%, $p<0.001$), a more frequent usage of IGHV4-34 (11.8 vs. 8.9%, $p<0.001$), IGHV4-39 (7.2 vs 3.7%, $p<0.001$), IGHV4-59 (3.9 vs. 2.8%, $p=0.002$) and IGHV3-74 (3.7 vs 2.3%, $p<0.001$) and a significantly lower usage of IGHV1-69 (6.1 vs, 12.8%, $p<0.001$), IGHV1-2 (1.9 vs. 4.6%, $p<0.001$) and IGHV3-21 (2.9 vs. 4.7%, $p<0.001$) than western CLL patients (Figure 1A) [3]. We identified 260 sequences (8.4%) belonging to 25 major subsets, lower than the frequency reported by reported by Agathangelidis et al, 2021 (13.5%, $p<0.001$) [2]. The mostly used stereotyped BCR subsets were subset #8 (55, 1.8%), #1

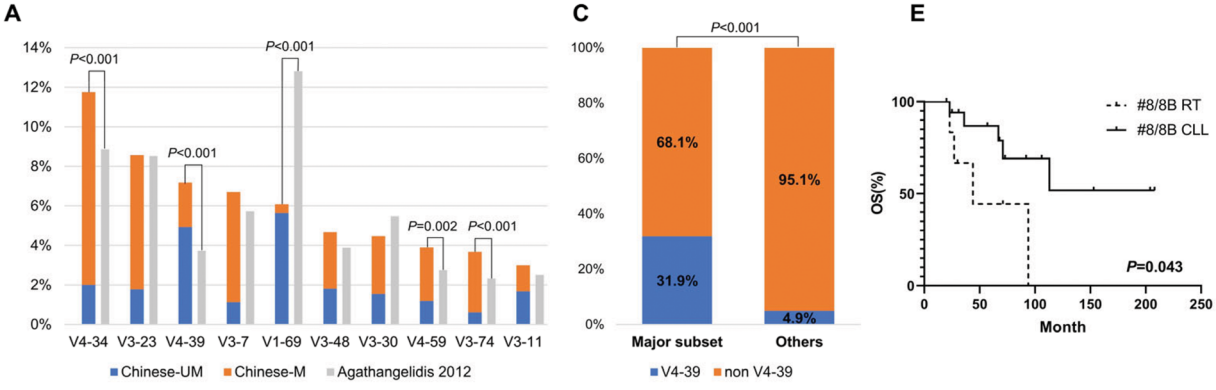

B

Major subset	Chinese (n=3105)	Agathangelidis 2021 (n=30413)
#8	55 (1.77%)	0.5%
#1	45 (1.45%)	2.2%
#4	35 (1.13%)	0.9%
#8B	28 (0.90%)	0.2%
#77	22 (0.71%)	0.4%
#6	13 (0.42%)	0.8%
#3C2	8 (0.26%)	0.2%
#2	7 (0.23%)	2.5%
#99	6 (0.19%)	0.4%
#3C3	4 (0.13%)	0.3%
#12	4 (0.13%)	0.2%
#28A	4 (0.13%)	0.2%
#169	4 (0.13%)	0.2%
#5	4 (0.13%)	0.5%
#14	3 (0.10%)	0.2%
#59	3 (0.10%)	0.3%
#148B	3 (0.10%)	0.5%
#7D3	2 (0.06%)	0.2%
#16	2 (0.06%)	0.3%
#64B	2 (0.06%)	0.3%
#188	2 (0.06%)	0.2%
#7C2	1 (0.03%)	0.2%
#31	1 (0.03%)	0.3%
#73	1 (0.03%)	0.2%
#201	1 (0.03%)	0.2%
#10	0	0.3%
#111	0	0.2%
#202	0	0.2%
#252	0	0.2%

D

Subset	Chinese CLL		Agathangelidis 2021
	Mutational status	No.(%)	No.(%)
#8	UM	55 (1.77%)	151 (0.5%)
#8B	UM	28 (0.90%)	67 (0.22%)
#123	M	4 (0.13%)	45 (0.15%)
#217	UM	4 (0.13%)	25 (0.08%)
#38A	UM	1 (0.03%)	24 (0.08%)
V2.4|J4|10|4	M	1 (0.03%)	2 (0.01%)
V4|J3.4|16|6	UM	1 (0.03%)	5 (0.02%)
V4|J3.4|18|9	UM	1 (0.03%)	2 (0.01%)
V4|J4.5|13|3	UM	1 (0.03%)	11 (0.04%)
V4|J4.5|16|7	M	1 (0.03%)	5 (0.02%)
V4|J6|15|3	UM	1 (0.03%)	2 (0.01%)
V4|J6|19|7	UM	1 (0.03%)	3 (0.01%)
V4-39|J4|12|1	UM	1 (0.03%)	2 (0.01%)
V4-39|J4|20|1	UM	1 (0.03%)	2 (0.01%)
V4-39|J4|21|2	UM	1 (0.03%)	2 (0.01%)
V4-39|J5|22|1	UM	1 (0.03%)	2 (0.01%)

(45, 1.5%), #4 (35, 1.1%), #8B (28, 0.9%), #77 (22, 0.7%) and #6 (13, 0.4%, Figure 1(B)). Compared with CLL patients from western countries, a significantly higher frequency of subset #8 (1.8 vs. 0.5%; $p < 0.001$), #8B (0.9 vs. 0.2%; $p < 0.001$) and #77 (0.7 vs. 0.4%, $p = 0.033$), and a lower frequency of subset #2 (0.2 vs. 2.5%; $p < 0.001$), #1 (1.5 vs. 2.2%; $p = 0.011$), #6 (0.4 vs. 0.8%; $p = 0.017$) were observed. Interestingly, 83 patients were assigned to subset #8 or #8B, which accounted for 31.9% of all major subtype users. In contrast, only 4.9% (140/2845) patients in the non-major-subset cohort used IGHV4-39 ($p < 0.001$, Figure 1(C)). Further analysis compared productive sequences with all IGHV4-39-containing subsets, revealing that among the 223 IGHV4-39 sequences, 103 (46.2%) were assigned to 16 subsets (Figure 1(D)). Patients with unmutated IGHV4-39 gene were more likely to exhibit BCR stereotypy than those with mutated IGHV4-39 gene (61.4 vs. 12.9%, $p < 0.001$). Among the 24 subset #8 or #8B patients with available clinical data, 6 suffered Richter's transformation. With a median follow-up of 67 months, #8 or #8B patients with RT had median survival of 44 months, shorter than that of #8 or #8B patients without RT ($p = 0.043$, Figure 1(E)).

Conclusions: The study provides the most extensive catalogue of BCR features of Chinese CLL. A significant difference was observed between Chinese and western CLL patients in terms of the proportion of IGHV4-39 and subset #8/#8B usage. The results suggest a higher prevalence of these genetic features in Chinese CLL patients. Further analysis on minor subsets is currently underway.

Abstract ID: 1551862

Title: Exploiting the modulation of FOXO1 signalling as a therapeutic target in CLL through combination of ERK and BTK inhibition

Authors: Jodie Hay and Alison Michie

Therapies, such as ibrutinib, that inhibit BTK, a key component of the B cell receptor (BCR) signalling pathway, have revolutionised the clinical treatment of CLL, improving survival rates of poor prognostic patients. However, these treatments are not universally suitable, with the development of resistance mutations presenting a significant problem, with patients ultimately relapsing, therefore new treatment strategies are required. The forkhead box, class O (FOXO) family of transcription factors regulate key cellular processes including cell cycle, apoptosis and proliferation. Evidence largely supports a role for FOXO proteins as tumour suppressors, particularly FOXO1 in B cell malignancies. FOXO1 is negatively regulated, and subsequently inactivated, by a number of signalling pathways including PI3K/AKT/mTOR, which are activated in the CLL tumour microenvironment (TME). We recently demonstrated that inhibiting BCR-mediated mTOR signals promotes the restoration of FOXO activity, enabling the induction of CLL apoptosis. We hypothesise that therapeutically exploiting FOXO1 signalling may reveal new treatments in CLL. Our data shows that treatment of CLL samples with ibrutinib, alone or in combination with a novel ERK-MAPK inhibitor (ERKi), reactivates FOXO1, as indicated by reduced pFOXO1 (Thr24), increased nuclear localisation and increased transcriptional activity. In in vitro pro-proliferative CLL-TME co-culture models, combined inhibition of ERK and BTK significantly reduces CLL proliferation through a G1 cell cycle arrest compared to single treatments, and induced reactive oxygen species. Interestingly, shRNA-mediated knockdown of FOXO1 in CLL cell lines and primary CLL patient samples (inducing ~50% knockdown in expression), resulted in a reduction in CLL cell proliferation. Furthermore, knockdown of FOXO1 sensitised CLL patient samples to ERK and BTK inhibition, with enhanced reduction in metabolically active cells. Our data also suggests that these drugs behave in a CLL selective manner, sparing normal T cells within CLL-PBMC samples, which is therapeutically attractive. Interrogation of the secreted cytokines revealed that FOXO1 knockdown significantly reduced inflammasome components, identifying a novel role for FOXO1 in inflammatory signalling within the TME. Our CLL mouse model, generated by retrovirally transducing murine HSPCs with a catalytically inactive PKCα construct (PKCα-KR), produces a disease resembling a poor prognosis CLL mouse model with elevated BCR signalling. In vitro studies with the mouse CLL-like cells demonstrated that ERKi significantly reduces pFOXO1 (Thr24) *in vitro*. When established in vivo, treatment of the CLL-like disease with ERKi alone or in combination with BTKi significantly reduced tumour burden, across the bone marrow, spleen and blood. In addition to showing a disruption to tumour maintenance in the CLL mouse model, ERK/BTKi combination, but not BTKI alone, blocked disease maintenance in secondary transplant mice. Through *in vitro* CLL/TME modelling, and *in vivo* studies, we have demonstrated that targeting both ERK and BTK signalling simultaneously, to therapeutically activate FOXO1, is an attractive clinical strategy. If trialled in CLL patients, ERKi combined with BTKi may enhance clinical response and may also induce deeper remissions compared to BTKi alone, addressing an unmet clinical need in CLL.

Abstract ID: 1552027

Title: Does the life expectancy of elderly CLL patients receiving upfront targeted agents approach the life expectancy of the general population?

Authors: Stefano Molica, Tait Shanafelt, David Allsup and Diana Giannarelli

Although targeted therapies for patients with CLL have improved clinical outcomes, they are not considered 'curative' treatments. We hypothesized that the change in the CLL treatment paradigm to widespread use of targeted agents (TAs), would improve life expectancy of patients with CLL to approach that of the age- and gender-matched general population (AGMGP). To evaluate this possibility, we compared the 5-year OS of treatment-naive, elderly (>65 years old) or unfit CLL pts enrolled in phase 3 clinical trials of TAs to the 5-year OS of Italian and US AGMGP. The analysis utilized the latest publicly accessible data from the RESONATE2, ILLUMINATE, ALLIANCE, ELEVATE-TN, CLL14, and GLOW trials. We used the method proposed by Liu et al (BMC Med Res Methodol 2021;21(1):111) to reconstruct individual patient data (IPD) from published Kaplan-Meyer survival curves. The expected OS rate for the control population was calculated using 2019 Italian data from the Istituto Nazionale di Statistica (ISTAT) and 2019 US database https://www.ssa.gov/oact/STATS/table4c6.html. These pre-pandemic databases were not subject to biases due to COVID-19-related mortality. The CLL trial analysis group was comprised of 2223 pts with 1293 enrolled in a TA experimental arm

Fig 1

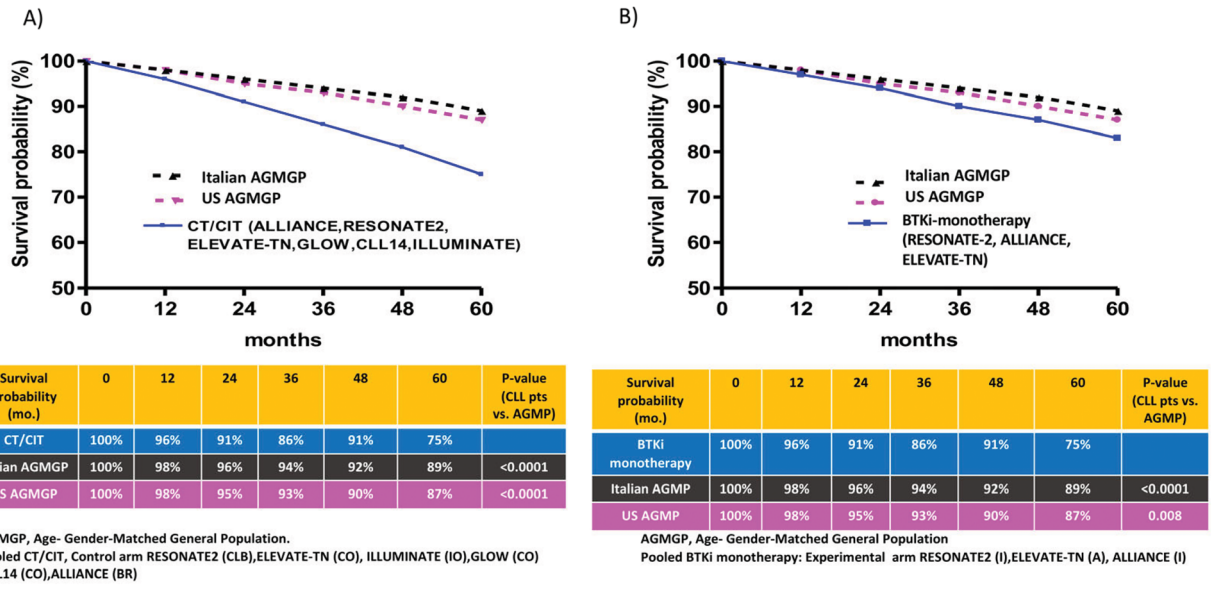

Survival probability (mo.)	0	12	24	36	48	60	P-value (CLL pts vs. AGMP)
CT/CIT	100%	96%	91%	86%	91%	75%	
Italian AGMGP	100%	98%	96%	94%	92%	89%	<0.0001
US AGMGP	100%	98%	95%	93%	90%	87%	<0.0001

AGMGP, Age- Gender-Matched General Population.
Pooled CT/CIT, Control arm RESONATE2 (CLB),ELEVATE-TN (CO), ILLUMINATE (IO),GLOW (CO) ,CLL14 (CO),ALLIANCE (BR)

Survival probability (mo.)	0	12	24	36	48	60	P-value (CLL pts vs. AGMP)
BTKi monotherapy	100%	96%	91%	86%	91%	75%	
Italian AGMP	100%	98%	96%	94%	92%	89%	<0.0001
US AGMP	100%	98%	95%	93%	90%	87%	0.008

AGMGP, Age- Gender-Matched General Population
Pooled BTKi monotherapy: Experimental arm RESONATE2 (I),ELEVATE-TN (A), ALLIANCE (I)

Fig 2

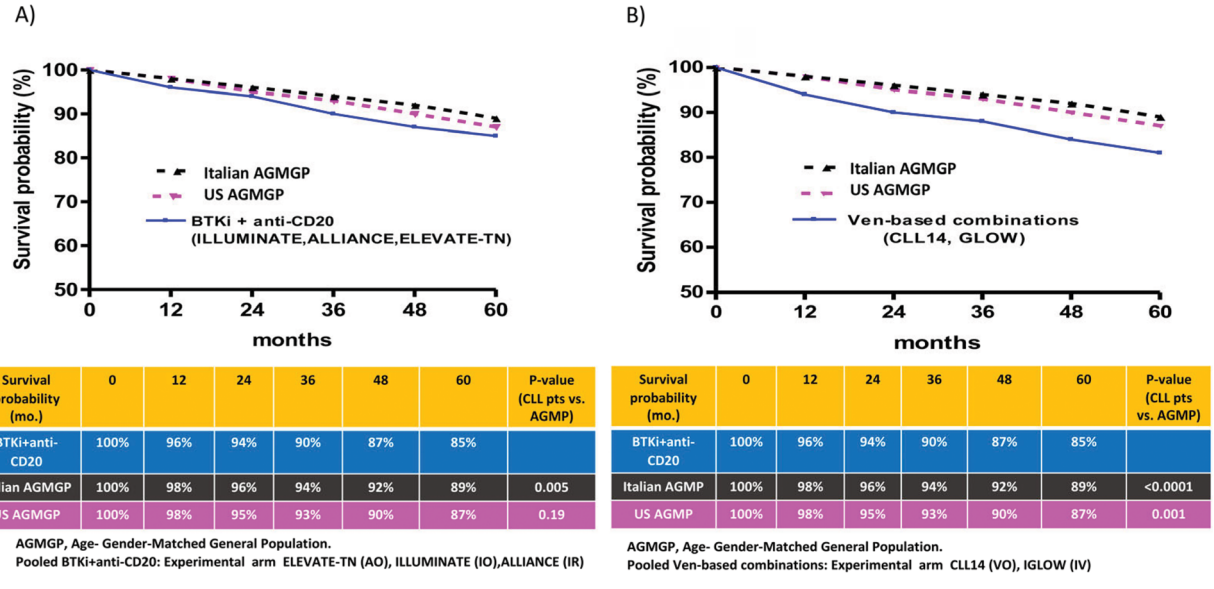

Survival probability (mo.)	0	12	24	36	48	60	P-value (CLL pts vs. AGMP)
BTKi+anti-CD20	100%	96%	94%	90%	87%	85%	
Italian AGMGP	100%	98%	96%	94%	92%	89%	0.005
US AGMGP	100%	98%	95%	93%	90%	87%	0.19

AGMGP, Age- Gender-Matched General Population.
Pooled BTKi+anti-CD20: Experimental arm ELEVATE-TN (AO), ILLUMINATE (IO),ALLIANCE (IR)

Survival probability (mo.)	0	12	24	36	48	60	P-value (CLL pts vs. AGMP)
BTKi+anti-CD20	100%	96%	94%	90%	87%	85%	
Italian AGMP	100%	98%	96%	94%	92%	89%	<0.0001
US AGMP	100%	98%	95%	93%	90%	87%	0.001

AGMGP, Age- Gender-Matched General Population.
Pooled Ven-based combinations: Experimental arm CLL14 (VO), IGLOW (IV)

and 930 in a control chemotherapy (CT) or chemoimmunotherapy (CIT) arm. Among pts treated with TAs, 971 (75%) received continuous therapy with a first-generation Bruton tyrosine kinase inhibitor (BTKi) (ibrutinib [I] monotherapy, 32.7%%; I-obinutuzumab [IO], 11.6%); I-Rituximab [IR], 18.7%; or a second-generation BTKi (acalabrutinib [A] monotherapy, 18.4%; A-obinutuzumab [AO], 18.4%). 322 persons (24.9%) received fixed-duration (FD) therapy with venetoclax (V)-based combinations (V-obinutuzumab: 22.5%; V-Ibrutinib: 10.9%). Patients enrolled in the CT/CIT arms received chlorambucil (C) as a single agent (14.3%), Bendamustine-Rituximab (BR, 19.6%), C-obinutuzumab (CO, 66%). To compare TA data to AGMGP data, pts were merged into 4 treatment groups: (i) BTKi-monotherapy (ALLIANCE, RESONATE2, ELEVATE-TN); (ii) BTKi + anti-CD20 (ALLIANCE, ILLUMINATE, ELEVATE-TN); (iii) FD V-based combinations, (CLL14, and CLL14), (iv) CT or CIT (RESONATE2, ALLIANCE, ELEVATE-TN, ILLUMINATE, CLL14, GLOW). Median age of pts treated with TAs was 70 years (range 47–93). Prevalence of del(17p)/mutated TP53, unmutated IGHV or CIRS score >6 were 9.1% (0–16%); 62.4% (43–66.5%); and 48.6% (11.7–86.1%), respectively. Across six trials, the 5-year OS estimates for CLL patients treated with CT/CIT were less favorable than those of the Italian and US AGMGP ($p < 0.0001$ for both) (Figure 1(A)). BTKi monotherapy mitigated but did not fully reverse the detrimental effect of CLL on OS compared to the Italian ($p < 0.0001$) and US ($p = 0.001$) AGMGP (Figure 1(B)). The ability of BTKi combined

with anti-CD20 to attenuate the OS gap was great, with no statistically significant difference between CLL pts and US AGMGP ($p=0.19$) but a small, statistically significant difference persisting when compared to the Italian AGMGP ($p=0.005$; Figure 2(A)). Finally, FD V-based combinations mitigated but did not fully reverse the detrimental effect of CLL on OS compared to the Italian ($p<0.0001$) and US ($p=0.001$) AGMGP (Figure 2(B)). This analysis is subject to limitations. In this age- and gender-adjusted cross-matched analysis, differences in comorbidity rates between trials and between trials and the AGMGPs may have influenced some of the results. In fact, the proportion of patients with a CIRS score greater than six differed considerably across trials: RESONATE2, 31%; ELEVATE-TN, 11.1% in the A-arm and 16.8% in the AO-arm; ILLUMINATE, 32.7%; CLL14, 86.1%; and GLOW, 69.0%. The AGMGP comorbidity rate was 44.3% (ISTAT 2019 report), making OS comparisons with CLL14 and GLOW trial patients with severe comorbidities less reliable. Additional studies of venetoclax-based therapy in populations with less comorbidity are necessary to fully evaluate the impact of venetoclax-based treatment on OS. Nonetheless, the results of this analysis evaluating the upfront administration of TAs on OS suggest these agents have substantially mitigated but not fully eliminated the shorter OS of CLL patients relative to the AGMGP. Continued development of novel treatment approaches to improve outcome for patients with CLL is needed.

Abstract ID: 1553010

Title: Bruton tyrosine kinase inhibitor ibrutinib induces hypertension by upregulating transcription of CaV1.2 calcium channel

Authors: Juejin Wang, Shumin Yin, Feiran Liu, Ludan Zhang, Xingyu Song, Wei Hou, Xiaoqing Xiong, Jianyong Li and Huayuan Zhu

Background: Ibrutinib, as the first approved Bruton tyrosine kinase inhibitor, is currently a first-line targeted drug for the treatment of chronic lymphocytic leukemia (CLL), but hypertension is a common side effect of ibrutinib therapy. Though previous studies suggest that ibrutinib-induced hypertension is related to the disturbance of intracellular calcium concentration, the underlying mechanisms are uncovered.
Methods and Results: The analysis of clinical CLL patients' data found that ibrutinib treatment for more than 1-month results in ~26.9% of the patients with hypertension. By using animal model, we found that 28 days' oral administration of ibrutinib obviously increases the blood pressure of mice. Moreover, CaV1.2 calcium channel expression and its current density was increased in the vascular smooth muscle cells (VSMCs), and K+-induced vasoconstriction was also enhanced in the mesenteric artery (MA) of ibrutinib-treated mice, suggesting that enhanced vasoconstriction might be mediated by overexpressed CaV1.2 channel. Unexpectedly, Masson and HE staining of MAs didn't show the obvious morphological change of ibrutinib-treated mice in comparison to control mice, indicating there is no structure remodeling in the MAs from the mice feeding with Ibrutinib. At the cell-based level, by using whole-cell patch clamp, we found that application with ibrutinib exhibited hyperpolarized current-voltage curve and increased current size of CaV1.2 channels in vascular smooth muscle cells (VSMCs), which facilitates the channel function. We also found Ibrutinib increases K+-triggered [Ca2+]i elevation in VSMCs by monitoring [Ca2+]i with 4 µmol/L Fluo-4 AM. For investigating the possible mechanisms, we applied RNA-seq, the data identified that the expression of transcription factor C/EBP is specifically upregulated in the MA from ibrutinib-treated mice. ChIP experiments demonstrated that CaV1.2 encoding gene Cacna1c is bound with C/EBP. Furthermore, C/EBP transcriptional expression level was increased under ibrutinib stimulation. Functionally, siRNA-mediated knockdown of C/EBP decreased CaV1.2 current size in VSMCs and K+-induced constriction of MAs.
Conclusions: These results reveal that ibrutinib long-termly increases the expression of CaV1.2 transcription by upregulating C/EBP, thereby enhancing channel functions and increasing vasoconstriction. This study identified a specific molecular mechanism of enhanced vasoconstriction induced by ibrutinib, providing a potential target for the management of hypertension in CLL patients when using ibrutinib.

Abstract ID: 1553031

Title: Constituitive VLA-4 activation is linked to BCR autonomous signaling in circulating CLL cells and promotes pro-survival signals through soluble blood-borne VCAM-1 binding

Authors: Erika Tissino, Riccardo Bomben, Palash Maity, Federico Pozzo, Antonella Nicolò, Annalisa Gaglio, Tamara Bittolo, Francesca Rossi, Moumita Datta, Francesco Zaja, Giovanni D'Arena, Annalisa Chiarenza, Hassan Jumaa, Maria Ilaria del Principe, Roberta Laureana, Jacopo Olivieri, Tanja Hartmann, Valter Gattei and Antonella Zucchetto

CD49d, the alpha chain of the CD49d/CD29 integrin heterodimer very late antigen-4 (VLA-4), expressed in about 40% of chronic lymphocytic leukemia (CLL) cases, has emerged as one of the most relevant biological predictors in CLL, with a negative prognostic impact also in the context of ibrutinib therapies. VLA-4 promotes cell-cell and cell-matrix interactions by binding to its ligands VCAM-1, fibronectin and EMILIN-1 in CLL-involved tissues. The adhesive properties of VLA-4 can be rapidly inside-out activated by signals through the B-cell receptor (BCR), thereby enhancing the integrin's ability to interact with its ligands. In CLL, besides the canonical antigen (Ag)-dependent mechanism, BCR signaling has been demonstrated to occur via an autonomous Ag-independent manner. Our aim is to investigate the effects of autonomous BCR signaling on VLA-4 activation and the consequent ability of circulating CLL cells to interact with VLA-4 ligands in the bloodstream. VLA-4 activation/affinity was determined by flow cytometry (FC) using the conformation-sensitive anti-CD29 mAb HUTS21 in whole blood (WB) as source of VLA-4 ligands, and/or by 'real-time' FC measuring the binding of the VLA-4 ligand LDV-FITC, as reported [1]. ELISA assays were used to quantify soluble(s) VCAM-1 in plasma samples. FC was used to study the

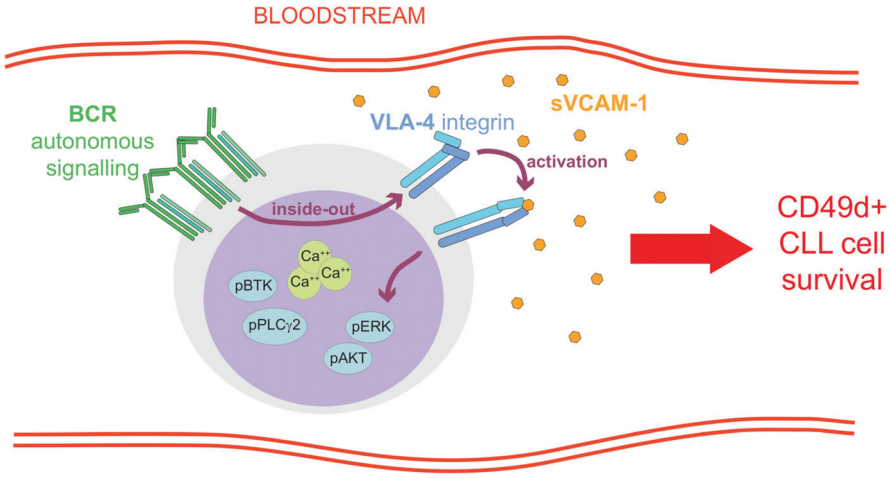

phosphorylation state of integrin and BCR signaling proteins, the sVCAM-1 binding to CLL cells, and Ca++ influx. The 4-idroxy-tamoxifen-inducible murine TKO cells [2], expressing high VLA-4 levels, were used to investigate the interaction between VLA-4 activation and BCR autonomous signaling. From the VLA-4 activation analysis, ($n=1,034$ CD49d+CLL), HUTS-21 positive cells, indicating constitutively activated VLA-4, ranged from 0 and 98.4%, with a median expression of 7.7% (IQR 2.8–18.7). The activated VLA-4 was impaired by depletion of plasma from WB samples ($n=38$), reconstituted by autologous plasma, sVCAM-1 and fibronectin ($n=17$), and impaired by pre-incubation with anti-CD49d HP1/2 blocking mAbs before addition of plasma, sVCAM-1 and fibronectin ($n=8$). Analysis of sVCAM-1 in plasma samples from CD49d+CLL ($n=80$) showed a significant inverse correlation between the amount of sVCAM-1 and the HUTS-21 expression levels ($r=-0.3$; $p=0.005$) suggesting ligand sequestration by activated VLA-4. Concomitant staining of CLL cells with anti-VCAM-1/CD106 mAb and HUTS-21 mAb, confirmed the presence, in all samples analysed, of sVCAM-1 in a subfraction of cells (range 3.3–68.8%) expressing significantly higher HUTS-21 levels compared to sVCAM-1 negative cells (355 vs. 223 MFI, $p<0.0001$). To test whether sVCAM-1 was able to provide pro-survival signals to CD49d+CLL cells, we compared phosphorylation levels of ERK1/2 (pERK1/2) after addition of sVCAM-1 in cells from CD49d+CLL ($n=25$) pre-treated or not with the VLA-4 antagonist Firategrast. Binding of sVCAM-1 significantly increased pERK1/2 levels compared to cells pretreated with Firategrast ($p=0.0074$). We next verified the association between levels of VLA-4 activation and the extent of cell signaling activity within the same CLL cell population. We analysed, in the context of HUTS-21− and HUTS-21+ cells from CD49d+CLL ($n=28$), the phosphorylation levels of ERK1/2 and AKT, both involved in the activation of the integrin pathway, as well as of BTK and PLCγ2, two proteins downstream of the BCR. In all cases, HUTS-21+ cells versus HUTS-21− cells displayed higher pERK1/2 (MFI mean±SD =223±50 vs. 172±43; $p<0.0001$), pAKT (307±93 vs. 261±84; $p=0.0001$), pBTK (1138±391 vs. 813±312; $p<0.0001$) and pPLCγ2 (167±137 vs. 85±57; $p<0.0001$), suggesting the involvement of the BCR pathway in the constitutive VLA-4 activation. This hypothesis was tested using murine TKO cells transfected with different BCRs derived from 4 CLL with high level of constitutively activated VLA-4 (TKO-high) and 4 CLL with low level of constitutively activated VLA-4 (TKO-low). Compared to TKO-low cells, TKO-high cells showed a higher autonomous Ca++ influx ($p=0.03$), and consistently higher VLA-4 affinity ($p=0.01$). Ibrutinib treatment impaired both BCR autonomous signaling and VLA-4 affinity. Notably, anti-IgM stimulation induced high Ca++ influx and high VLA-4 affinity state in both TKO-high and TKO-low, irrespective of ibrutinib treatment. In summary (Figure 1), a constitutively activated form of VLA-4 is detectable in CD49d+CLL cells, probably due to continuous VLA-4 inside-out stimulation by autonomous BCR signalling, which promotes sVCAM-1 binding, providing pro-survival signals to circulating CLL cells. This represents a novel pro-survival mechanism for CD49d+CLL cells that occurs in the bloodstream and exploits two microenvironmental receptors, BCR and VLA-4, both operating independently of tissue-based ligands.

Abstract ID: 1553189

Title: Recurrent genomic alterations in the apoptotic machinery in patients with CLL treated with venetoclax monotherapy following treatment with BCRi

Authors: Jennifer Woyach, Relja Popovic, Emily Rossi, Sanjana Singh, Xifeng Wang, Toshihiko Oki, Tanya S. Rosenberg, Chen Qian, Michael Moran, Michelle Boyer, Jeffrey Jones, Richard Furman, Jason Gotlib, Stephen J. Schuster, Brenda Chyla and Matthew Davids

Introduction: Venetoclax (Ven) monotherapy is efficacious in patients with relapsed/refractory (R/R) chronic lymphocytic leukemia (CLL). Patients previously treated with B-cell receptor pathway inhibitors (BCRi), such as ibrutinib and idelalisib, have lower response rates to Ven; those who are refractory to prior BCRi have a significantly higher risk of relapse than those who are not refractory [1]. Here, we provide updated efficacy and safety of Ven monotherapy in patients with R/R CLL following BCRi therapy with a median follow-up of 68 months. Additional exploratory analyses assessed outcomes in patients with pre-existing BTK mutations and acquired BCL-2 family member mutations after long-term treatment with Ven.

Methods: This Phase 2 multicenter study included patients with CLL previously treated with ibrutinib and/or idelalisib who had relapse or progression after BCRi discontinuation

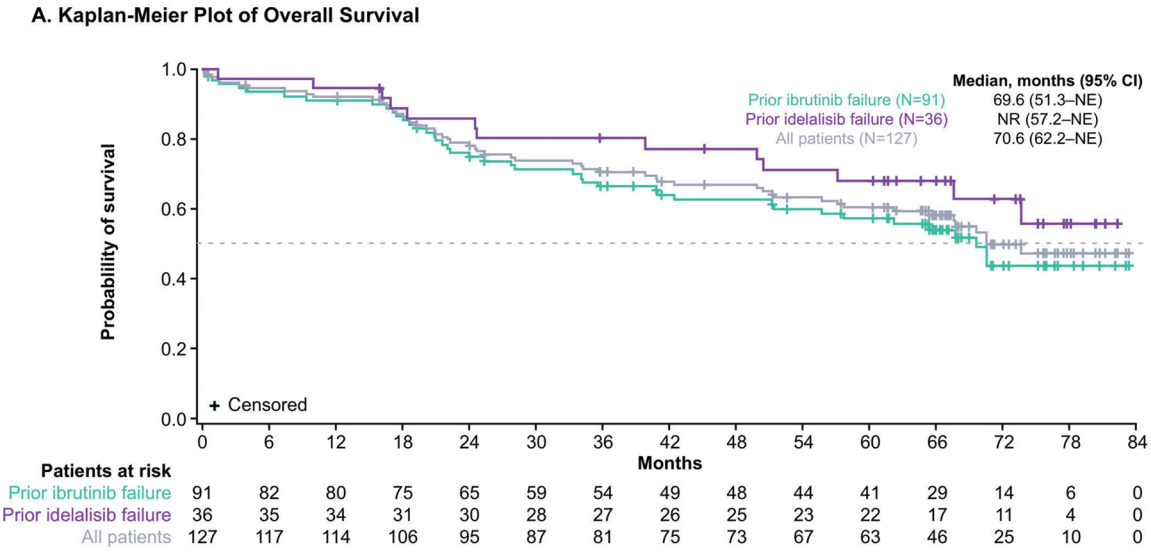

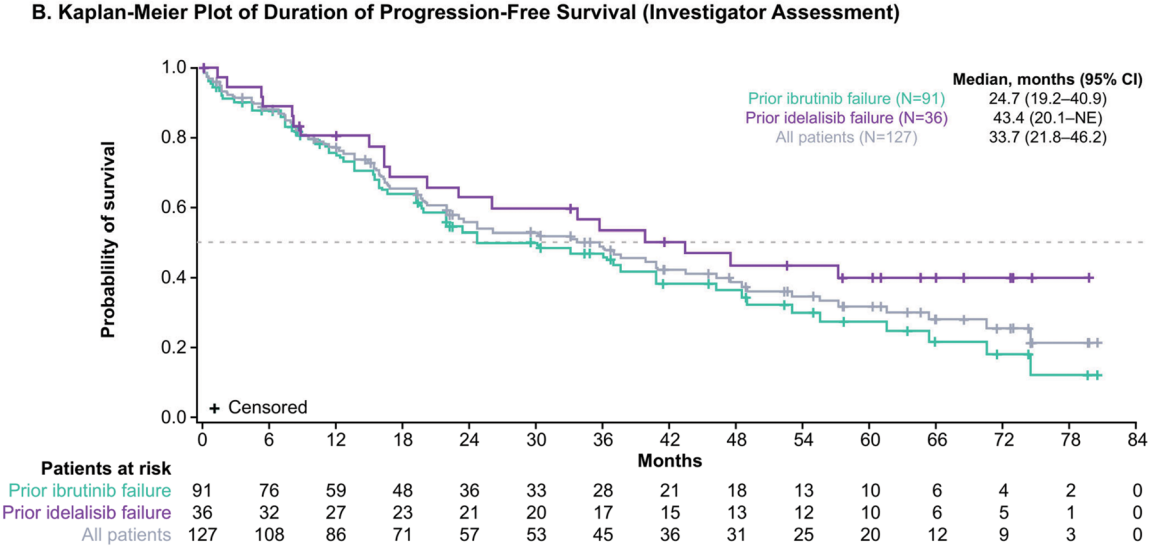

(NCT02141282). The primary objective was overall response rate (ORR); secondary objectives included duration of response (DOR), progression-free survival (PFS), minimal residual disease (MRD, <1 cell in 10 4 assessed by flow cytometry), and overall survival (OS). Study drug was continued, provided no evidence of disease progression or discontinuation criteria were met. Additional *post-hoc* exploratory analyses were conducted on available pre- and post-visit samples, to evaluate pre-existing mutation(s) in BTK (C481) and acquisition of BCL-2 mutations, including variant allele frequency (VAF).

Results: A total of 127 patients with BCRi-R/R CLL were enrolled in the study (patients with ibrutinib as most recent BCRi, $n=91$, and with idelalisib, $n=36$); $n=24$ had received both prior ibrutinib and idelalisib. Twenty-six (38.2%) patients had TP53 mutations and 28 (22.0%) received ≥2 prior BCRi therapies. Patients in the ibrutinib arm received treatment for a median of 20.6 months (range 1.0–60.8) and in idelalisib arm for 9.0 months (0.9–44.9) prior to Ven monotherapy. The median interval between end of BCRi treatment and first dose of Ven was 1.4 months (range 0.0–26.3). Patients received Ven monotherapy for a median of 22.5 months (range 0.1–83.1). Thirty (23.6%) patients discontinued due to progressive disease. The ORR in all patients was 66.1% (84/127; 95% CI 57.2–74.3; 64.8% in patients with ibrutinib failure and 69.4% for patients with idelalisib failure). The complete response (CR/CRi) rate in all patients was 12.6% (16/127; 95% CI 7.4–19.7). Median DOR ($n=84$) was 43.6 months (95% CI 28.6–55.4). Median PFS was 33.7 months (95% CI 21.8–46.2; Figure 1). MRD, evaluable in 77 patients, was negative in 37/127 (29.1%) and positive in 40/127 (31.5%) patients. Median OS was 70.6 months (95% CI 62.2–not estimable). No new safety signals were observed with longer follow-up. During the study, 55 (43.3%) patients died; of those, 10 had fatal TEAEs including acute respiratory failure/respiratory failure ($n=2$), multiple organ dysfunction ($n=2$), Corynebacterium sepsis, pneumonia, septic shock, asphyxia, cytokine release syndrome after CAR-T cell therapy and nonhematologic malignant neoplasm ($n=1$ each). Of 72 patients with mutational data ($n=57$ ibrutinib, $n=15$ idelalisib), 47.0% ($n=34$) had BTK C481 mutation at study entry (VAF range 0.5–99.0%) with 66.7% (22/33) demonstrating a decrease in VAF >20% after initiation of Ven monotherapy. At posttreatment visit, BTK C481 was undetectable in 15.2% (5/33 patients). The ORRs (95% CI) were 79.4% (61.6–90.7) and 86.8% (71.1—95.1) for patients with or without a pre-existing BTK mutation, respectively. Median PFS was similar for patients

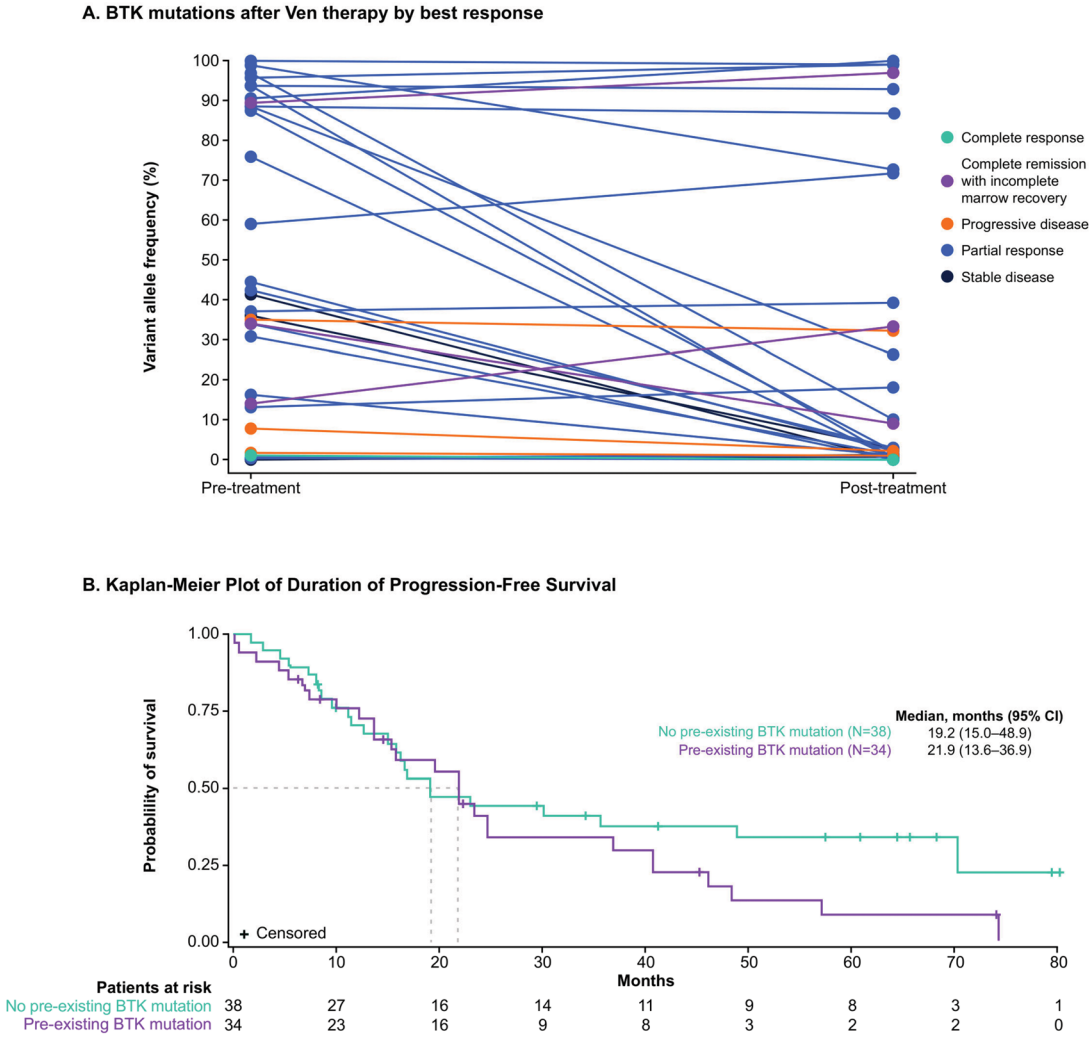

regardless of prior BTK mutations (Figure 2), whereas OS was not reached for patients without pre-existing mutations versus 51.0 months for those with pre-existing mutations. Median time between pre- and post-treatment samples was 17.5 months (range 1.0–52.0). Acquired BCL-2 mutations were identified in 13/68 patients (multiple in 8/13). Most common identified mutations were G101V ($n=8$), D103E/V/Y ($n=3/1/3$), R107-R110dup ($n=5$), A113G ($n=2$), V156D ($n=2$). For these 13 patients, the median time between pre- and post-treatment samples was 32.1 months (range 12.0–48.0) and VAF range was 0.7–34.0%. No mutations in other BCL-2 family members (BAX, BAD or NOXA) were observed.

Conclusions: With extended follow-up, Ven demonstrated durable responses in patients with CLL who progressed on BCRi, irrespective of BTK mutation status. BCL-2 resistance mutations were detected in 19.1% (13/68) of patients, generally at low VAF. These acquired mutations were detectable in patients with prolonged Ven exposure, supporting further exploration of strategies focused on time-limited Ven exposure.

Abstract ID: 1553205

Title: Targeting translation initiation as novel therapeutic in CLL

Authors: Anne Largeot, Jerome Paggetti and Etienne Moussay

CLL cells heavily rely on their surrounding microenvironment for growth and survival. Microenvironmental factors trigger a global increase in translation, affecting specific transcripts such as the MYC oncogene. Notably, heightened translation is considered a vulnerability in cancer cells and is observed across various tumor types. In order to understand if translation inhibition could be relevant in CLL, we used FL3, a synthetic flavagline that binds to prohibitins (PHBs). These proteins exhibit diverse cellular functions depending on their location. At the cell membrane, PHBs are crucial for RAS-induced RAF activation in many cancers, resulting in the phosphorylation of eukaryotic initiation factor 4E (eIF4E) via the MAPK pathway, ultimately leading to increased translation. FL3, by binding to PHBs, impedes RAF activation, subsequently reducing translation. To explore translation initiation as a novel therapeutic target for CLL and investigate FL3's mechanism of action as a translation inhibitor, we conducted experiments using CLL cells from patients, as well as human and murine cell lines. To assess translation rate, our methodology included O-propargyl-puromycin (OPP) and L-homopropargylglycine (HPG) incorporation assays, Proximity Ligation Assay (PLA) to examine the interaction between translation initiation factors eIF4E and eIF4G, pulsed SILAC and polysome

profiling. [U-13C]-glucose and [U-13C]-glutamine tracing were used for metabolomics analysis. We also employed co-immunoprecipitation, PLA, Nano-BRET, and cap-pull down techniques to validate protein interactions. *In vivo* validation was performed through the adoptive transfer of splenocytes from sick Eμ-TCL1 mice. Additionally, we conducted qPCR analyses of six genes involved in translation initiation machinery and PHBs in a cohort of 144 CLL patients to determine correlations between gene expression and clinical parameters. Our findings demonstrated that CLL cells exhibit elevated translation rate, which can be inhibited by FL3. A comprehensive multiomics analysis, including pulsed SILAC, RNA sequencing, and polysome profiling in CLL patient samples and cell lines, revealed reduced translation of the MYC oncogene upon FL3 treatment. Furthermore, translation inhibition was associated with proliferation arrest and a significant metabolic shift at least partially driven by MYC. Intriguingly, unlike other models, we observed that the RAS-RAF-(PHBs)-MAPK pathway in CLL is unaffected by FL3. Instead, we established a direct association between PHBs and the translation initiation complex. Knockdown of PHBs resembled FL3 treatment, confirming their direct involvement in translation initiation. Importantly, translation inhibition effectively controlled CLL development in vivo. Lastly, elevated expression of translation initiation-related genes and PHBs genes correlated with poor survival and unfavorable clinical parameters in CLL patients. In summary, our study demonstrated that inhibiting translation is a promising strategy to control CLL development by blocking the translation of multiple oncogenic pathways, including MYC. Additionally, we unveiled a new and direct role of PHBs in translation initiation, opening up new therapeutic possibilities for CLL patients.

Abstract ID: 1553473

Title: Exposure of progressive immune dysfunction by SARS-CoV-2 mRNA vaccination in patients with chronic lymphocytic leukemia

Authors: Randall Davis, Kai Qin, Kazuhito Honjo, Scott Sherrill-Mix, Weimin Liu, Regina Stoltz, Allisa Oman, Lucinda Hall, Ran Li, Sarah Sterrett, Ellen Frederick, Jeffrey Lancaster, Mayur Narkhede, Amitkumar Mehta, Foluso Ogunsile, Rima Patel, Thomas Ketas, Victor Cruz Portillo, Benjamin Larimer, Anju Bansal, Paul Goepfert and Beatrice Hahn

Background: Patients with chronic lymphocytic leukemia (CLL) have reduced seroconversion rates and lower binding (Ab) and neutralizing antibody (NAb) titers than healthy individuals following SARS-CoV-2 mRNA vaccination. Here, we dissected vaccine-mediated humoral and cellular responses to understand the mechanisms underlying CLL-induced immune dysfunction.

Methods and findings: We performed a prospective observational study in SARS-CoV-2 infection-naïve CLL patients ($n=95$) and healthy controls ($n=30$) who were vaccinated between December 2020 and June 2021. Sixty-one CLL patients and 27 healthy controls received two doses of the Pfizer-BioNTech BNT162b2 vaccine, while 34 CLL patients and 3 healthy controls received two doses of the Moderna mRNA-2173 vaccine. The median time to analysis was 38 days (IQR, 27–83) for CLL patients and 36 days (IQR, 28–57) for healthy controls. Testing plasma samples for SARS-CoV-2 anti-spike and receptor binding domain Abs by enzyme-linked immunosorbent assay (ELISA), we found that all healthy controls seroconverted to both antigens, while CLL patients had lower response rates (68 and 54%) as well as lower median titers (23-fold and 30-fold; both $p<0.001$). Similarly, NAb responses against the then prevalent D614G and Delta SARS-CoV-2 variants were detected in 97 and 93% of controls, respectively, but in only 42% and 38% of CLL patients, who also exhibited >23-fold and >17-fold lower median NAb titers (both $p<0.001$). Interestingly, 26% of CLL patients failed to develop NAbs but had high-titer binding Abs that preferentially reacted with the S2 subunit of the SARS-CoV-2 spike. Since these patients were also seropositive for endemic human coronaviruses (HCoVs), these responses likely reflect cross-reactive HCoV Abs rather than vaccine-induced de novo responses. CLL disease status, advanced Rai stage (III-IV), elevated serum beta-2 microglobulin levels (B2m >2.4 mg/L), prior therapy, anti-CD20 immunotherapy (<12 months), and intravenous immunoglobulin (IVIg) prophylaxis were all predictive of an inability to mount SARS-CoV-2 NAbs (all $p\leq0.03$). T cell response rates determined for a subset of participants were 2.8-fold lower for CLL patients compared to healthy controls (0.05, 95% CI 0.01–0.27, $p<0.001$), with reduced intracellular IFNg staining ($p=0.03$) and effector polyfunctionality ($p<0.001$) observed in CD4+ but not in CD8+ T cells. Surprisingly, in treatment-naïve CLL patients, BNT162b2 vaccination was identified as an independent negative risk factor for NAb generation (5.8, 95% CI 1.6–27, $p=0.006$). CLL patients who received mRNA-2173 had 12-fold higher ($p<0.001$) NAb titers and 1.7-fold higher (6.5, 95% CI 1.3–32, $p=0.02$) response rates than BNT162b2 vaccinees despite similar disease characteristics. The absence of detectable NAbs in CLL patients was associated with reduced naïve CD4+ T cells ($p=0.03$) and increased CD8+ effector memory T cells ($p=0.006$). Limitations of the study were that not all participants were subjected to the same immune analyses and that pre-vaccination samples were not available.

Conclusions: CLL pathogenesis is characterized by a progressive loss of adaptive immune functions, including in most treatment-naïve patients, with pre-existing memory being preserved longer than the capacity to mount responses to new antigens. In addition, higher NAb titers and response rates identify mRNA-2173 as a superior vaccine for CLL patients.

Abstract ID: 1553652

Title: TRAF3 inactivation in chronic lymphocytic leukemia enhances metabolic cellular plasticity through metabolic reprogramming and associates with adverse prognosis

Authors: Claudia Pérez Carretero, Miguel Quijada Álamo, Mariana Tannoury, Léa Dehgane, Alberto Rodríguez Sánchez, David J Sanz, Teresa González, Rocío Benito Sánchez, Elise Chapiro, Florence Nguyen-Khac, Ana E

Rodríguez Vicente, Santos A Susin and Jesús María Hernández Rivas

The TNF receptor-associated factor3 (TRAF3) located in 14q32.32 has been identified as a tumor suppressor gene involved in B-cell survival, immune response, and cellular metabolism. TRAF3 is frequently encompassed within 14q deletion and affected by inactivating mutations in B-cell neoplasms, such as multiple myeloma (20%), diffuse large B-cell lymphomas (15%), and chronic lymphocytic leukemia (CLL) (4%). However, the clinical and biological implications of TRAF3 alterations in CLL are largely unknown. Thus, the aim of this study was to assess the prognostic significance of TRAF3 alterations in a CLL cohort and to elucidate their biological functions in CLL pathogenesis by using CRISPR/Cas9-edited models and CLL primary cells harboring TRAF3 mutations. TRAF3 mutations and deletions were analyzed by next-generation sequencing (NGS) in 350 CLL patients. A total of 14 patients had a TRAF3 loss and 10 of them, additional TRAF3 inactivating mutations, indicating a biallelic inactivation of this gene. Notably, patients with TRAF3 alterations showed and adverse prognosis, being an independent risk factor of time to first treatment (TFT) (median TFT 6 vs. 75 months, $p<0.001$) (HR =0.21, 95% CI =0.05–0.85, $p=0.029$). To explore the implications of TRAF3 in CLL biology, we mimicked the reported mutations in a CRISPR/Cas9-edited CLL cellular model (PGA1 cell line) and performed transcriptomic, metabolomic and functional analyses. RNA-seq studies identified 56 transcripts significantly dysregulated in PGA1-TRAF3mut cells (FDR <0.05). Gene-set enrichment analyses (GSEA) revealed differences in several biological pathways, highlighting a global alteration of the negative regulation of NIK/NF-kB signaling (NES =1.64; FDR =0.03). Specifically, NIK (a direct target of TRAF3-mediated degradation) was overexpressed (p-adj <0.001) in TRAF3mut cells, which resulted in a higher nuclear activity of the non-canonical NF-kB transcription factors p52 ($p=0.01$) and RelB ($p=0.003$). Furthermore, we validated these results in primary CLL cells ($n=22$; 3 TRAF3mut cells). The metabolic studies showed an enrichment of metabolites involved in Warburg effect (pyruvate and lactate), citric acid cycle (TCA-acetyl-CoA, α-ketoglutarate, succinate) and glutamate metabolism (α-ketoglutarate) (FDR <0.001, 0.003, 0.1 resp) in PGA1- TRAF3mut cells. To analyze their metabolic specificities, we evaluated the oxidative phosphorylation (OXPHOS) and glycolytic capacity by assessing the mitochondrial oxygen consumption rate (OCR) extracellular acidification (ECAR), respectively, and cell viability at basal state and in response to metabolic inhibitors. Interestingly, PGA1-TRAF3mut cells exhibited higher basal and maximal respiration levels and a more important spare capacity and generation of ATP-linked to mitochondrial respiration. Glycolysis was also slightly enhanced in the TRAF3mut. Besides, they were more sensitive to 2-deoxy-D-glucose (glycolytic inhibitor), and more resistant to oxamate (lactate-dehydrogenase inhibitor, anaerobic glycolysis marker). These results indicate that, unlike WT, TRAF3mut cells preferentially utilize a mitochondrial glycolytic metabolism. Moreover, upon UK5099 administration (inhibitor of the mitochondrial pyruvate transporter that regulates mitochondrial glycolysis) mutant cells showed higher maximal respiration levels than WT, suggesting a metabolic reprogramming towards an alternative metabolic way fueling mitochondrial metabolism. Therefore, we tested the effect of C968 (glutaminolysis inhibitor), finding that TRAF3mut cells were also more resistant to this drug, what reveals a specific metabolic plasticity (mitochondrial glycolysis/glutaminolysis) in the PGA1-TRAF3mut cells. Interestingly, we identified a dysregulation of gene-sets involved in glutamine metabolism (FDR =0.07) in TRAF3mut, concretely, an upregulation of the glutamine transporter SLC1A4 (p-adj =0.007), what could be favoring glutamine uptake for an enhanced glutaminolysis. Interestingly, by blocking pyruvate import and glutaminolysis simultaneously, we observed a decrease in TRAF3mut CLL cells proliferation ($p=0.03$), with equal levels of the previously dysregulated metabolites to those of the WT, which may indicate that this treatment sensitizes TRAF3mut cells through its relieving effect on metabolic reprogramming. Moreover, primary CLL cells with TRAF3 mutations ($n=22$; 3 TRAF3mut cells) were also sensitive to the combination, in the presence and absence of microenvironment (with and without HS-5 co-culture and IL-2 and CpG stimulation) ($p=0.01$, $p=0.04$ resp.), further demonstrating the potential of the combination of metabolic inhibitors as a new therapeutic approach in TRAF3mut patients. In summary, we demonstrated that TRAF3 mutations had a negative impact on the clinical outcome of CLL patients. In addition, our results indicate a biological role of TRAF3 in NF-kB signaling and CLL cellular metabolism. Specifically, we identified an increased mitochondrial glycolytic activity and distinct metabolic dependencies in CLL cells with TRAF3 inactivation, contributing to an enhanced metabolic plasticity potentially targetable in CLL.

Abstract ID: 1554032

Title: Bendamustine, followed by obinutuzumab, acalabrutinib and venetoclax in patients (Pts) with relapsed/refractory chronic lymphocytic Leukemia (CLL): updated results of the CLL2-BAAG trial of the German CLL Study Group (GCLLSG)

Authors: Paula Cramer, Moritz Fürstenau, Sandra Robrecht, Adam Giza, Anna Fink, Kirsten Fischer, Petra Langerbeins, Othman Al-Sawaf, Eugen Tausch, Christof Schneider, Johannes Schetelig, Peter Dreger, Sebastian Böttcher, Karl-Anton Kreuzer, Anke Schilhabel, Monika Brüggemann, Michael Kneba, Clemens Wendtner, Stephan Stilgenbauer, Barbara Eichhorst and Michael Hallek

Introduction: Several ongoing studies evaluate the triple combination of obinutuzumab (G), acalabrutinib (A) and Venetoclax (Ve). In CLL2-BAAG, the triplet was tested after an optional debulking with two cycles of bendamustine (B) in an all-comer population with relapsed/refractory CLL. The primary endpoint analysis showed an overall response rate (ORR) of 100% and a rate of undetectable measurable residual disease (uMRD, defined as $<10^{-4}$ by flow cytometry) of 76% in peripheral blood (PB) at the end of induction phase, however, the primary endpoint of uMRD was not met (95% CI 61–87%, $p=0.258$) [1] with given sample size. This updated analysis reports longer follow-up data.

Methods: An optional debulking with 2 cycles of B was recommended in pts with lymphocyte counts ≥25,000/µl and/or lymph nodes ≥5cm (70mg/m^2 d1&2 q.28 days). In six induction cycles (28 days), G (1000mg) was administered 3 times in cycle 1 (days 1/2, 8 & 15) and every 4 weeks in cycles 2–6. A (100mg bid) was added in cycle 2 followed by Ve in cycle 3 with a dose ramp-up (to 400mg daily) over 5

weeks. In the MRD guided maintenance phase, consisting of up to eight 84 day-cycles A and Ve remained unchanged while intervals of G were increased to 3 months. MRD was measured centrally with flow from PB. The primary endpoint was the rate of uMRD in PB at the end of induction therapy. Secondary endpoints included iwCLL responses, safety and survival parameters.

Results: Between January 2019 and June 2020, 46 pts were enrolled, 1 pt with a violation of inclusion/exclusion criteria and ≤2 induction cycles was excluded from the analysis. The 45 evaluable pts had relapsed CLL with a median of one prior therapy (range 1–4), 21 pts (47%) had already received a targeted agent, including 8 pts with a BTK-I, 7 pts with Ve-based therapies, and 3 pts with both. Fourteen pts (32%) had a del(17p)/TP53 mutation, 34 (76%) had an unmutated IGHV status and 12 (30%) a complex karyotype. 18/46 pts (40%) received B debulking, 27 (60%) pts immediately started with the induction with G, A and Ve. 44 pts (98%) received 6 induction cycles and 43 pts (96%) received a median of 2 (range 1–8) cycles of maintenance treatment. Nine pts (21%) discontinued maintenance early: 6 due to adverse events, 1 each due to progression, switch to allogeneic stem cell transplantation and physician`s decision. Another 9 pts (21%) completed the full 2 years of maintenance and 25 pts (58%) stopped maintenance due to achievement of a deep remission with uMRD as predefined by protocol. The uMRD in PB rate was 76% at the end of induction, with continued maintenance 42 of 45 pts (93%) achieved uMRD at any time point (best uMRD rate). This rate was similar also among pts with a prior targeted therapy (19 of 21 pts, 90%), including pts with prior venetoclax (9 of 10 pts, 90%). The ORR was 100% at the end of induction, 6 pts (13%) had a CR. Until the end of maintenance this number increased to 19 pts (44%), however, two pts had a clinical progression. With a median observation time of 34 months and all pts off treatment the 36 months-PFS is 88% and 36 months-OS is 97%. Until data cutoff, 1 pt died of a COVID-19 pneumonia. As of 14 February 2023, 50 serious adverse events (SAEs) were reported, including 4 during B debulking, 20 during induction and 10 during maintenance with GAVe, as well as 16 during follow-up. 33 SAEs were of grade 3, 6 grade 4 and one was fatal. Most common were COVID-19 (pneumonia) [8], other pneumonias [5], infusion-related reactions [5] and (febrile) neutropenias [3].

Conclusion: The rate of uMRD increased with the continued maintenance with the GAVe triple combination and 25 pts (58%) stopped maintenance due to achievement of a deep remission with uMRD. Randomized trials will define if the triple combination of a BTK inhibitor, a BCL2 inhibitor and a CD20 antibody is superior to combinations of two of these agents. Until then, the use of this triple combination in routine practice cannot be recommended.

Abstract ID: 1554106

Title: Stopping ibrutinib after 6 years of continuous exposure results in decreased or stable CLL levels for at least a year in most patients, providing further support for the STATIC trial evaluating intermittent BTKi treatment

Authors: Andy Rawstron, Nichola Webster, David Allsup, Sue Bell, Adrian Bloor, David Cairns, Anna Hockaday, Sharon Jackson, Surita Dalal, Ruth de Tute, Natasha Greatorex, Rhiannon Lambkin, Anita Sarma, David Stones, Abraham Varghese, Peter Hillmen and Talha Munir

Background: Bruton Tyrosine Kinase inhibition (BTKi) using treatments such as ibrutinib (IBR) have led to significant improvements in progression-free survival (PFS). BTKi is typically given as continuous therapy, which can lead to the development of treatment resistance or side-effects in some cases. There is some evidence that intermittent treatment may be preferable and this is being investigated in the STATIC trial (ISRCTN51675454) which is a prospective, national, multicentre, open-label, randomised, controlled, 2-arm, parallel-group, non-inferiority, phase III trial to assess whether patients with CLL on long-term treatment with IBR have similar disease control with an intermittent treatment strategy (experimental arm) compared with standard continuous treatment (control arm). In patients who stop IBR due to toxicity the median PFS is approximately 2 years from discontinuation [1] but the impact of stopping treatment in people who are continuing to respond well to IBR is not known. This project assessed the kinetics of disease after treatment cessation in patients who have been treated with IBR for 6 years in the IBR + rituximab (IR) arm of the FLAIR trial (ISRCTN01844152) with the aim of confirming safety parameters and informing patients considering entry into the STATIC trial.

Participants and methods: 172 participants treated in the IR arm of the FLAIR trial had a baseline evaluation before 03 May 2017 (i.e. potential to have 6 years of treatment followed by 1 year of follow-up post-treatment) of which 112 were evaluable at 84 months from baseline. Measurable Residual Disease (MRD) analysis was performed using ERIC-compliant 8-marker flow cytometry with analysis of 0.5–2.2 million total leucocytes at 72 months (72M, end of treatment [EoT]), 78 months (78M) and 84 months (84M) from baseline, respectively.

Results: 112 participants stopped ibrutinib at EoT 72M: • 15/112 (12%) achieved PB uMRD4 (<0.01%) at EoT, of which all evaluable participants maintained uMRD4 in the PB at 6 months (10/15 evaluable) and at 12 months (13/15 evaluable) after EoT. • 41/112 (37%) had 0.01–1% disease at EoT of which 6/41 converted to uMRD4, 20/41 maintained 0.01–1% disease, and 5/41 had disease levels increasing to >1% (2/5

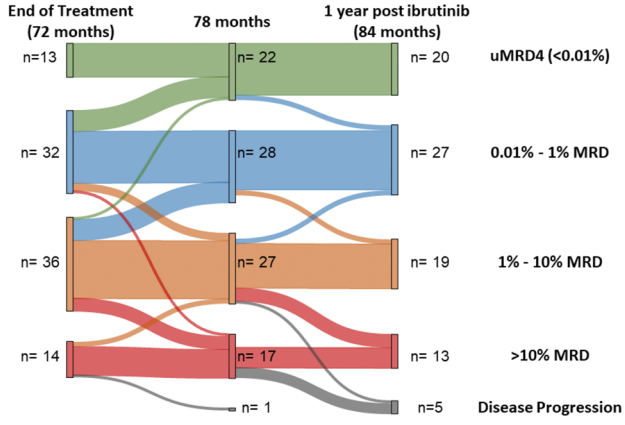

Figure 1: Treatment-naïve patients with CLL on the ibrutinib + rituximab arm of the FLAIR trial. The plot shows the changes in MRD status at end of ibrutinib treatment (72 months from start of ibrutinib exposure) through to 84 months (1 year post treatment) for trial participants with data available at each time point

with >10% disease) at 12 months after EoT (follow-up samples not available in 10/41 cases). • 40/112 (36%) had 1–10% disease at EoT of which 1/40 converted to uMRD4, 7/40 decreased CLL cells to 0.01–1%, 14/40 maintained 1–10% disease and 8/40 developed >10% disease at 12 months after EoT of which 1/8 showed progressive lymphadenopathy (samples not available in 10/40 cases). • 16/112 (14%) participants had >10% disease at EoT, of which 2/12 decreased CLL cells to 1–10%, 4/12 had stable >10% disease, 5 had evidence of disease progression at 12 months after EoT (samples not available in 5/12 cases). Although disease progression was largely restricted to participants with >10% disease at end of treatment, this did not appear to reflect different kinetics because the proportion with stable disease (defined as disease levels at 12 months post EoT remaining within +/−0.5log of EoT disease level) was similar at 41% vs. 38% vs. 38% for those with 0.01–1% vs. 1–10% vs. >10% disease at EoT.

Conclusions: For patients with CLL who have received 6 years of continuous ibrutinib treatment, the levels of residual disease decrease or remain stable for the subsequent 6–12 months after stopping ibrutinib in most cases. Longer follow-up is needed to understand the impact of prolonged ibrutinib exposure on disease kinetics because the initial results are likely to be affected by disease re-distribution from periphery to bone marrow and lymph nodes. However, the stability of disease levels after treatment cessation supports the safety of testing an intermittent treatment strategy to determine whether this could potentially reduce treatment-emergent resistance. This approach is currently being assessed in the STATIC trial that is now open to recruitment for up to 800 patients in the UK. The primary objective is to assess non-inferiority of the intermittent treatment strategy vs. continuous treatment in terms of time to treatment strategy failure, defined as the first documented instance of active disease that does not respond to treatment, or death. The secondary objectives include comparison of overall survival, toxicity and tolerability, cost effectiveness, quality of life, and the rate of resistance mutations and evolution of resistant sub-clones (Figure 1).

Abstract ID: 1554196

Title: SF3B1 mutation and ATM deletion co-drive leukemogenesis via centromeric R-loop dysregulation

Authors: Martina Cusan, Haifeng Shen, Lu Yang, Meiling Jin, Mike Fernandez, Prajish Iyer, Yiming Wu, Catherine Gutierrez, Catherine Wu, Renjang Lin and Lili Wang

The RNA splicing factor SF3B1 is one of the most frequently mutated genes in chronic lymphocytic leukemia (CLL). Co-expression of mutant Sf3b1 and Atm deletion in murine B cells results in CLL development, in which CLL cells exhibit RNA splicing dysregulation, increased DNA damage and recurrent chromosomal amplification, suggest that chromosomal instability (CIN) underlies CLL initiation; however, the linkage among splicing dysregulation, DNA damage and CIN remains elusive. CIN is a well-known hallmark of cancer that originates from inaccurate mitotic process. Faithful chromosome segregation relies on centromeres, a specialized chromosomal domain that serves as docking site for mitotic spindles during mitosis. DNA: RNA hybrids (R-loop) formation at centromeres (centromeric R-loops or cen-R-loops) is essential for CIN regulation. SF3B1 have been previously reported to promote unscheduled R-loop accumulation in myeloid cells while ATM can be activated by transcription-blocking lesions in an R-loop-dependent fashion, remodeling the spliceosome and alternative splicing. We therefore asked whether SF3B1 mutation and ATM deletion may impact CIN via cen-R-loop formation dysregulation. Harnessing murine B cells and human isogenic cell lines with and without SF3B1 mutation (MT), we profiled global R-loop and DNA double strand breaks (DSBs) using dotblot and comet assay, respectively. We found that SF3B1 MT cells have a significantly higher level of R-loop and DSBs. Cen-R-loop is also increased in SF3B1 MT cells by co-staining of phosphorylated replication protein A (p-RPA) (cen-R-loop) and ACA (centromere). Moreover, the disrupted cen-R-loop homeostasis resulted in an impaired centromere-mitotic spindles dynamics, which includes a greater magnitude of chromosome oscillations and altered spindle architecture with wider and more distant mitotic spindle during metaphase, defective centromere-spindles attachment, higher frequency of aberrant mitotic process with misaligned chromosomes in SF3B1 mutant cells. Intriguingly, overexpression of RNaseH1 reduced both the level of global and centromeric R-loops (paired *t*-test *p*-value <0.0001), DNA DSBs (unpaired *t*-test *p*-value <0.0001), and alleviated mitotic stress (unpaired *t*-test *p*-value <0.0001), confirming the causative role of R-loop in CIN. To determine whether SF3B1 mutation-associated RNA splicing dysregulation may directly affect R-loop accumulation, we performed DNA:RNA hybrid immunoprecipitation (DRIP) followed by sequencing (DRIP-seq) to map R-loops in a genome-wide fashion. SF3B1 MT caused minimal changes in overall R-loop distribution and location of R-loops had minimal overlap with SF3B1 MT associated alternative splicing, suggesting that SF3B1 mutation associated R-loops may not directly from RNA splicing per se. We then tested the possibility that SF3B1 MT contributes to cen-R-loop formation through splice variants. Through overlapping conserved SF3B1 MT-associated splice variants across isogenic cell lines and murine model with available R-loop interactome data, we identified that the RNA binding protein SERBP1 as one of the candidate proteins affected by SF3B1 mutation-induced splice variant. Upon overexpression of the canonical, but not the alternative isoform of SERBP1 in SF3B1 MT cells alleviated excessive R-loop, centromeric p-RPA accumulation, and DNA DSBs, implicating direct involvement of SERBP1 in the regulation of R-loop homeostasis. Taken together, we demonstrated that SF3B1 mutation promotes CIN by destabilizing mitotic spindles through aberrant R-loop accumulation at the centromere, via dysregulated splicing in genes such as SERBP1. Our study highlights an unrecognized role of cen-R-loop as a critical link between RNA splicing dysregulation and CIN, providing an opportunity for therapeutic targeting of R-loop in splicing factor mutant leukemias.

Abstract ID: 1554200

Title: Mutations detected in real world clinical sequencing during BTK inhibitor treatment in chronic lymphocytic leukemia (CLL)

Authors: Kiyomi Mashima, Stacey Fernandes, Samantha Shupe, Rayan Fardoun, Aishath Naeem, Matthew Davids and Jennifer Brown

Introduction: Bruton tyrosine kinase inhibitors (BTKi) have significantly improved the treatment of CLL, yet resistance mechanisms emerge.

Methods: We retrospectively analyzed 102 clinical sequencing results performed during BTKi treatment from 85 patients (pts) at Dana-Farber Cancer Institute between 2014 and 2022. The sequencing results come from a comprehensive clinical grade 88-gene NGS panel which has been previously described [1].

Results: Of these 85 patients, 75.3% were male, with a median age at diagnosis of 53 [29–87], and a median age of 60 [39–91] at BTKi start. 68.2% had IGHV unmutated disease, and 29.4 and 30.6% had 17p deletion and 11q deletion, respectively. BTKi was initiated as first line in 31 (36.5%) pts, as second line in 19 (22.3%) pts, and as third line or higher in 35 (41.2%). 73 patients had only one BTKi (ibrutinib (IBR), 64; acalabrutinib (ACA), 9). 12 pts had multiple BTKis, 8 with two drugs with IBR first followed by ACA (Nf3, 37.5%), vecabrutinib (Nf1, 12.5%), and PIR (Nf4, 50.0%); and 4 with three or more drugs. According to disease status at sequencing, we allocated 36 pts with disease progression to PD group, with median observation time from BTKi start of 37.0 months, and 49 pts without disease progression as the NP group, with a median observation period of 26.3 months. Patients in PD group had past history of BTKi treatment more often than those in PD group (PD vs NP, 27.7 vs. 4.1%, $p=0.0019$) with newer generation BTKis (IBR vs. ACA vs. PIR, 68.6, 11.4, 17.1% in PD vs. 81.6, 18.4, 0.0% in NP, respectively). At the time point of NGS, TP53 mutated and/or del(17p) positive pts were significantly enriched in the PD group (PD vs NP, 33.3 vs. 14.2%, $p=0.037$), but del(11q) was not enriched. A higher proportion of complex karyotype was observed in the PD group (PD vs NP, 55.6 vs. 24.5%, $p=0.0035$). A total of 216 different mutations were detected in 57 genes S including 158 variants in the PD group and 121 variants in the NP group. BTK mutations were detected in 15 pts all within the PD group (7 pts during IBR, 2 pts during ACA, 6 pts during PIR) as follows; C481S (c.1442G>C) (10 pts), C481S (c.1441T>A) (6 pts), C481S (c.1442_1443delGCinsCT) (1 pt), C481R (3 pts), C481Y (2pts), C481F (1 pt), L528W (3pts), T474I (3pts) and T474L (2pts). All T474 mutations were detected during PIR (Table 1). L581W was detected in 2 cases on IBR with variant allele frequency (VAF) 2.1 and 62.2%; the high VAF L581W mutation developed during first-line IBR treatment. Mutations in PLCG2 included D993H (1pt), D993Y (1pt), L845F (2pts) and R665W (1pt), and all of them were detected at low VAFs (<10%) in PD pts with BTK mutations. BTK, PLCG2, TP53, SF3B1 and NOTCH2 mutations were significantly enriched in the PD group ($p<0.01$, $p<0.05$, $p<0.01$, $p<0.01$, $p<0.05$, respectively) (Figure 1). The proportion of XPO1 mutations trended higher in the PD group (NP vs PD 2.04 vs 11.1%, $p=0.079$), with significantly higherVAFs (median VAF, NP vs PD 6.0 vs 44.4%, $p=0.021$). The proportion of pts without any mutations was significantly higher in the NP group than the PD group (NP vs PD, 10 vs. 0%, $p=0.048$). No other single CLL driver mutation was enriched in the PD group, but total mutations in MAPK related genes, BRAF, NRAS, KRAS, and MAP2K1, were increased and had higher VAFs compared to the NP group (PD vs NP, number of pts, 19.4 vs 6.1%, $p=0.0596$, median VAF 32.0 vs. 7.5 %, $p=0.041$).

Figure 1. Major mutations observed in CLL pts with or without progression on BTK-is

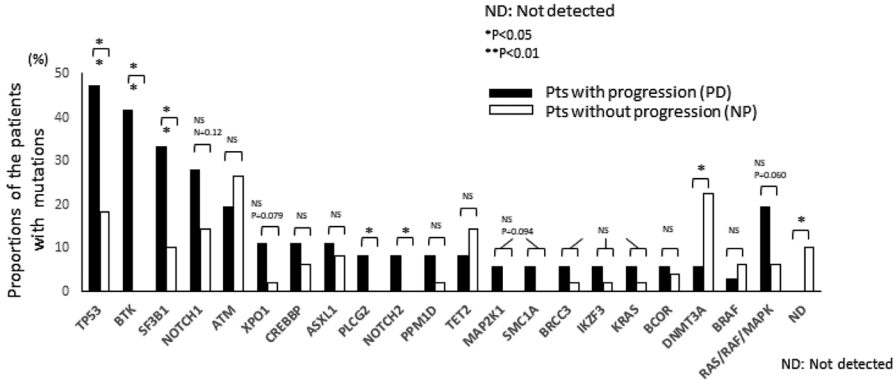

Table 1. BTK mutations and their variant allele frequency detected in patients in PD group according to their treatments

Patient ID	Treatment	*BTK* mutations in the PD group
BTK01	IBR	C481S(c.1442G>C) (29.6%)
BTK02	IBR	C481S(c.1442G>C) (2.1%)
BTK03	IBR	C481S(c.1441T>A) (47.6%), C481S(c.1442G>C) (26.3%)
BTK04	IBR	C481S(c.1441T>A) (60.2%), C481S(c.1442G>C) (1.3%)
BTK05	IBR	C481S(c.1441T>A) (9.9%), C481S(c.1442G>C) (54.6%), C481R (8.4%)
BTK06	IBR	C481S(c.1441T>A) (10.2%), C481R (2.1%), **L528W** (62.2%)
BTK07	IBR	C481S(c.1441T>A) (60.9%), C481S(c.1442G>C) (11.8%), C481Y (4.7%), **L528W** (2.1%)
BTK08	ACA	C481S(c.1442G>C) (46.9%)
BTK09	ACA	C481S(c.1441T>A) (31.2%), C481S(c.1442G>C) (3.0%)
BTK10*	PIR	C481S(c.1442G>C) (5.6%)
BTK11	PIR	C481S(c.1441T>A) (18.0%), C481S(c.1442_1443delGCinsCT) (4.0%), C481F (1.8%), C481Y (3.5%), C481R (16.4%), **L528W** (20.4%)
BTK12	PIR	C481S(c.1442G>C) (2.5%), **T474I** (14.3%)
BTK13	PIR	**T474I** (15.2%)
BTK14	PIR	**T474I** (76.3%)
BTK15	PIR	**T474I** (89.8%), **T474L** (3.2%)

* BTK10 has multiple other mutations including PLCG2 (D993H 7.7% and D993Y 3.1%), SF3B1 (H662L 12.3%) and TP53 (E258D 13.3%).

Conclusions: Our retrospective report summarizes mutations detected during BTKi treatment and shows that BTK L528W can occur during both covalent and non-covalent BTK inhibitor therapy. Four of six patients who progressed on PIR had T474 mutations. In addition, our results may suggest that activating mutations in RAS/RAF/MAPK pathway are related to BTKi resistance.

Abstract ID: 1551554

Title: Association between hypertension and overall survival in chronic lymphocytic leukemia

Authors: Noomi Vainer, Christian Brieghel, Henrik Hjalgrim, Carsten Niemann and Emelie Hamotal Curovic Rotbain

Background: In patients with chronic lymphocytic leukemia (CLL), comorbidities are frequent due to a high median age of 70 years at diagnosis. Comorbidities are often associated with increased mortality. At time of CLL diagnosis, the prevalence of hypertension (HTN) is close to 50%, however, little is known about the impact of HTN on survival and treatment of patients with CLL, which is of particular importance as some CLL treatments may cause or worsen hypertension.

Aim: To assess the impact of HTN on treatment and survival outcomes for patients with CLL from time of CLL diagnosis and following treatment.

Methods: All patients in the National Clinical Quality register, the Danish CLL Register, from 2008-2019 were included. Patients were followed from diagnosis until death or end of follow-up, which was 15 September 2022. HTN was defined as having either ≥2 International Classification of Diseases-10 diagnosis (ICD10) codes registered for hypertension or ≥2 prescriptions for anti-hypertensive drugs (anti-HTN) of first choice drugs or fixed combinations of drugs according to Anatomical Therapeutic Chemical (ATC) codes, one of which was prescribed ≤180 days prior to CLL diagnosis, or ≥2 prescriptions for two different anti-HTN of other ATC groups, both prescribed ≤180 days prior to CLL diagnosis. ICD10 and ATC codes were obtained from the Danish

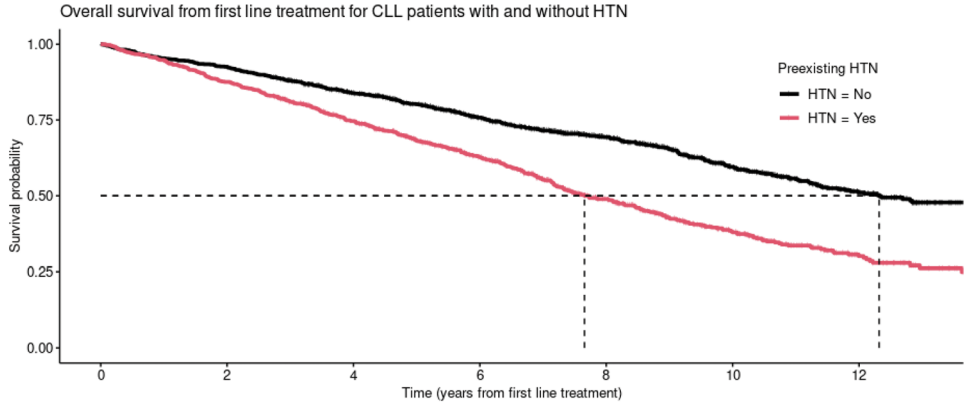

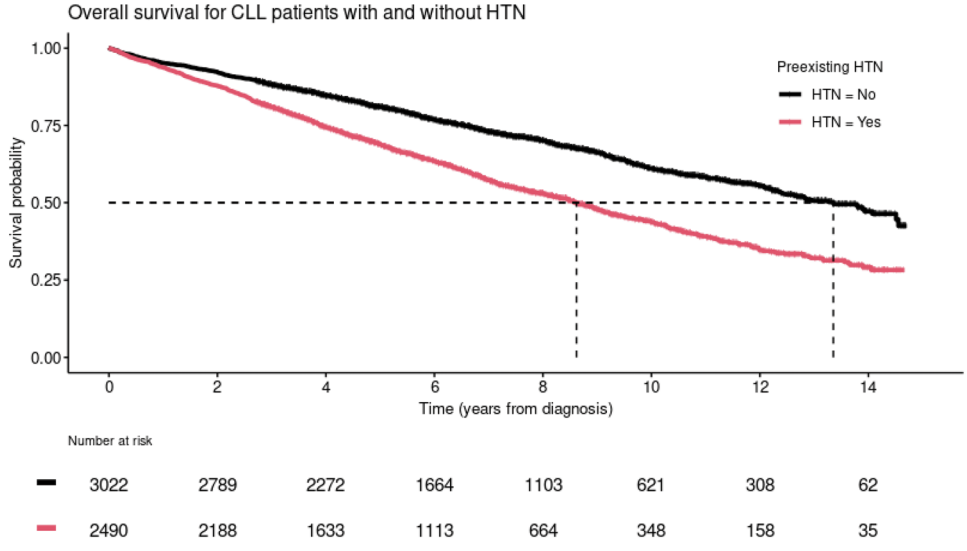

National Patient Register and Epic electronic health record system from January 1994 until CLL diagnosis and the Danish Prescription Register from January 2002 until CLL diagnosis, respectively. Patients were stratified based on presence of HTN at the time of CLL diagnosis or first line treatment for event analysis following first line treatment. Kaplan-Meier estimates and Cox's proportional hazard model adjusted for age at CLL diagnosis (10 years intervals), calendar year of CLL diag-nosis, sex, CLL-IPI category, and comorbidities were performed.

Results: We included 5,512 patients of whom 2,490 had HTN at time of CLL diagnosis (45%); 61% were male and the mean age was 70 years (SD 10.8). The multivariable Cox model showed shorter overall survival (OS) for patients with HTN compared to patients without HTN at CLL diagnosis (hazard ratio (HR): 1.18, 95% confidence interval (CI) [1.08;1.28] (Figure 1). Of the 1.889 patients receiving first line treatment for CLL, 826 had HTN prior to CLL treatment. Patients with both HTN and CLL had a significantly poorer OS following first line treatment compared to CLL patients without HTN (HR: 1.31 [95% CI 1.14;1.51]) in multivariable analysis (Figure 2). Hence, HTN was associated with poorer OS from time of CLL diagnosis and time of treatment independently of comorbidities including cardiac disease.

Conclusion: We demonstrate the clinical association between HTN and survival in CLL, emphasizing the importance of considering optimization of anti-hypertensive treatment in patients with CLL as well as the impact of HTN on treatment choice and outcome in CLL. To further inform management of CLL, these results will be followed up by investigations regarding impact on CLL treatment and cause-specific mortality.

Abstract ID: 1553105

Title: Changes in immune cell numbers and profile during long-term zanubrutinib treatment in treatment-naïve and relapsed/refractory patients with chronic lymphocytic leukemia

Authors: Maria Andersson, Tom Mulder, Kia Heimersson, Sonja Sönnert-Husa, Annika Giertz, Claes Karlsson, Jeanette Lundin, Lotta Hansson, Anders Österborg and Marzia Palma

Introduction: Compromised immune function, in part due to expansion of immunosuppressive immune cells, is one of the hallmarks of chronic lymphocytic leukemia (CLL). Circulating T cells usually have a terminally differentiated and pseudo-exhausted phenotype, with less naive and more effector and effector memory (EM) cells. CD8+ T cells have reduced cytotoxic capabilities and CD4+ T cells are skewed towards a T helper (Th) 2 phenotype. Regulatory T cells (Treg) cells are increased. We have previously shown that long-term treatment with the Bruton's tyrosine kinase inhibitor (BTKi) ibrutinib has a profound impact on immune cells in patients with CLL. We observed a reduction of the absolute number of NK and T cells, which paralleled the decreasing tumor burden. Th1 cell numbers dropped, while Th2 cells remained relatively stable, and CTLA-4 and PD-1 expressing T cells decreased [1]. It has been argued that ibrutinib's effects on T cells are completely 'off-target', i.e. mainly occur through inhibition of kinases other than BTK, interleukin-2-inducible T cell kinase (ITK) in particular. Considering that zanubrutinib (BGB-3111) is a BTKi exerting a more selective relative inhibition of BTK versus other kinases than ibrutinib, we aimed at evaluating whether this drug had a different effect on the immune cells in CLL patients.

Methods: Peripheral blood samples were collected before treatment start and at repeated timepoints, i.e. week (wk) 4, 8, 12, 16, 24 and at 8, 12 and 24 months (mo), from 8 treatment naïve (TN) patients included in the BGB-3111-304 and 8 relapsed/refractory (R/R) patients in the BGB-3111-305 clinical trials. Nine healthy individuals were included as controls. PB mononuclear cells (PBMC) populations were assessed by flow-cytometry including CLL cells, T-cell memory subsets, Th subpopulations, Tregs and NK cells subsets.

Results: At a 24 month follow-up, 6/8 patients in the BGB-304 and in the BGB-305 trial were still on treatment and had achieved partial response. In both groups, CD8+ cell numbers were higher compared to controls at baseline and significantly decreased during treatment, at 12 mo in TN patients and at wk 16 in R/R patients, respectively. At 24 month, normalization of CD8+ cell numbers had occurred in R/R patients but not in TN patients (Figure 1(A,G)). Normalization of CD4+ cell numbers occurred in TN at 8 month and in R/R at wk 12 (Figure 1(B,H)). In both TN and R/R patients, Th1 (CCR6−/CXCR3+) cell numbers were higher at baseline compared to controls while Th2 (CCR6−/CXCR3−) did not significantly differ in TN and were lower compared to controls in R/R patients. (Figure 1(C,D,I,J)). In the TN group, Th1 cells decreased but never reached normal levels (Figure 1(C)), while this occurred in R/R patients (Figure 1(I)). In neither group significant changes were observed for Th2 cells (Figure 1(D,J)). Accordingly, the Th1/Th2 ratio, which was significantly higher in patients at baseline, did not normalize at month 24 in either group. Treg numbers decreased in both groups, in the R/R patients from wk 12 and in TN patients at 12 month and normalized to the levels of the controls, at wk 24 and 8 mo, respectively (Figure 1(E,K)). In both R/R and TN patients, naïve CD4+ and CD8+ T-cells remained unchanged during treatment. Central memory (CM) CD4+ and CD8+ normalized in R/R patients but remained unchanged and were significantly higher compared to controls in TN patients. In both groups, EM CD4+ and CD8+ cells were higher compared to controls and significantly decreased and normalized during treatment. EM CD8+ T effector memory re-expressing CD45RA (TEMRA) were also higher at baseline and decreased and normalized while CD4+ TEMRA remained unchanged in normal levels. The number of cells expressing the immune checkpoints PD-1 and CTLA-4 gradually decreased during the treatment. Finally, NK cells decreased from wk 16 and normalized at wk 12 in R/R patients while remaining stable in TN patients (Figure 1(F,L))

Conclusion: During long-term zanubrutinib therapy, changes in the T and NK cells profiles occur in both TN and R/R patients, similarly to what previously observed in ibrutinib-treated patients. This suggests that the observed changes are related to the reduction of the tumor burden rather than to ITK inhibition.

Fig.1

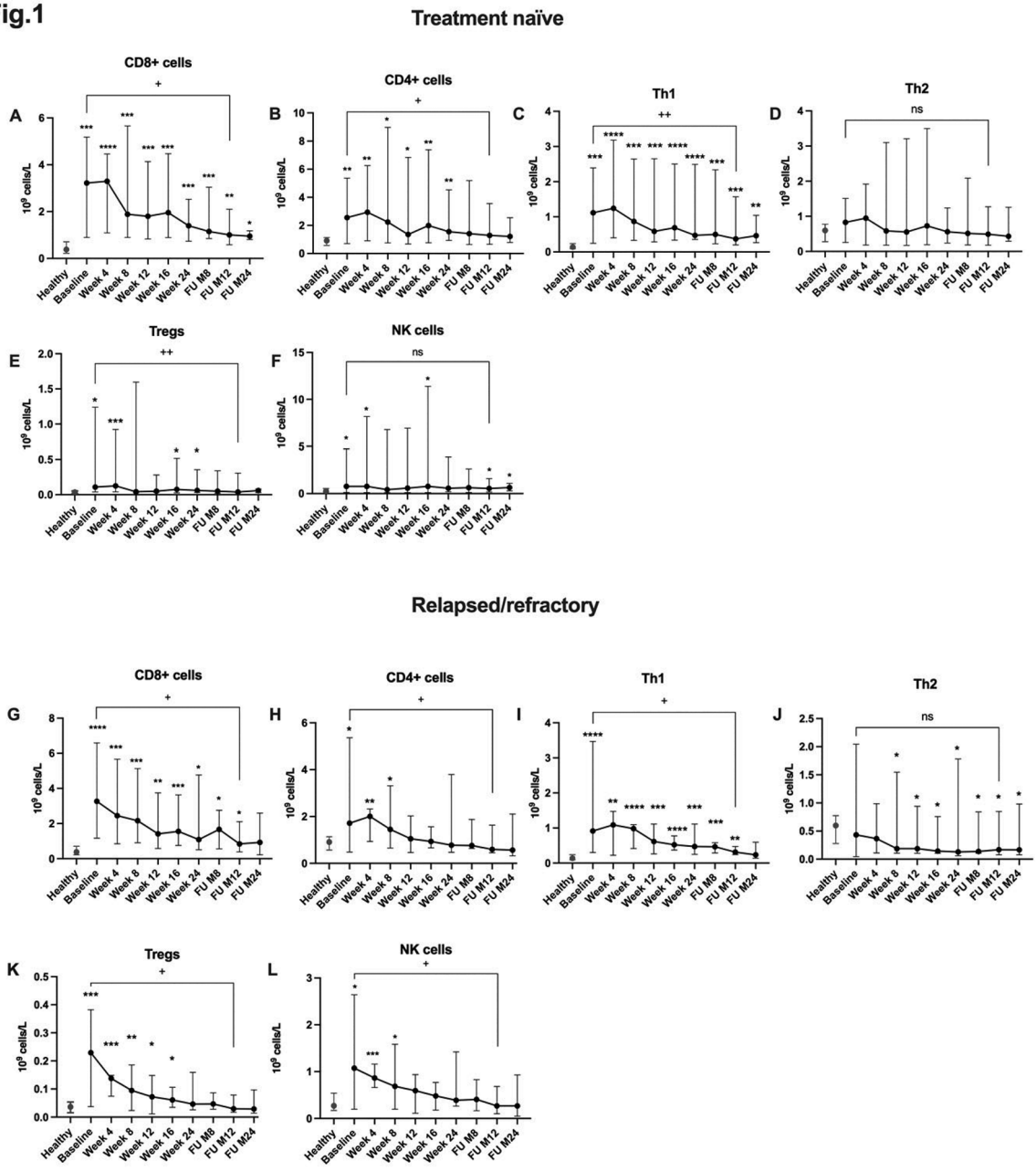

Plus signs indicate a statistically significant difference between baseline and 12 months as analyzed by Wilcoxon signed-rank tests. Stars indicate a statistically significant difference between healthy donors and the respective time point as analyzed by Mann-Whitney U tests. */+ p< 0.05, **/++ p< 0.005, *** p< 0.0005, ns= not significant

Abstract ID: 1550119

Title: Final 7-year follow up and retreatment substudy analysis of MURANO: venetoclax-rituximab-treated patients with relapsed/refractory chronic lymphocytic leukemia

Authors: John Seymour, Arnon Kater, Rosemary Harrup, Thomas Kipps, Barbara Eichhorst, Carolyn Owen, Sarit Assouline, Nicole Lamanna, Tadeusz Robak, Javier de la Serna, Ulrich Jaeger, Guillaume Cartron, Marco Montillo, Clemens Mellink, Brenda Chyla, Maria Thadani-Mulero, Marcus Lefebure, Yanwen Jiang, Rosemary Millen and Michelle Boyer

Introduction: The Phase 3 MURANO trial (NCT02005471) reported superior progression-free survival (PFS) and overall survival (OS) with fixed-duration venetoclax-rituximab (VenR) vs bendamustine (B)R in patients with relapsed or refractory (R/R) chronic lymphocytic leukemia (CLL). At the 5-year update, the median PFS was 53.6 vs 17.0 months (p<0.0001), and 5-year OS rates were 82.1 vs 62.2% (p<0.0001) in patients treated with VenR vs BR, respectively [1]. We report the final analyses of MURANO, with 7 years median follow up:

specifically, updated PFS and OS, with minimal residual disease (MRD) evaluation, in patients treated in the main study, as well as in VenR-retreated patients in the substudy.

Methods: Patients with R/R CLL were randomized to VenR (Ven 400 mg daily for 2 years + monthly R for the first 6 months) or BR (6 months). In the substudy (from 2018 onwards), patients with progressive disease (PD) received VenR (to the same schedule as main study) as either retreatment or as crossover from BR. PFS data are by investigator assessment. Peripheral blood MRD was measured centrally by allele-specific oligonucleotide-PCR and/or flow cytometry, with undetectable (u)MRD defined as <1 CLL cell/10,000 leukocytes.

Results: Baseline characteristics are presented in the Table. At final data cutoff (3 August 2022), VenR-treated patients ($n=194$) had a median PFS (95% confidence interval [CI]) of 54.7 months (52.3, 59.9) vs 17.0 months (15.5, 21.7) for BR-treated patients ($n=195$; hazard ratio [HR] 0.25). Seven-year PFS rates (95% CI) were 23.0% (16.1, 29.9) with VenR, while no patients treated with BR remained progression-free at this time point; 7-year OS rates (95% CI) were 69.6% (62.8, 76.5) with VenR and 51.0% (43.3, 58.7) with BR (HR 0.53). Median time to next treatment with VenR was 63.0 months vs 24.0 months with BR (HR 0.30); 37.1% of VenR-treated patients have not received subsequent anti-CLL treatment. Among VenR-treated patients who had uMRD at end of treatment (EOT) without PD ($n=83/118$; 70.3%), median PFS (95% CI) from EOT was 52.5 months (44.5, 61.5) vs. 18.0 months (8.5, 29.3; $p<0.0001$) in patients who were MRD + at EOT ($n=35$; 29.7%). Fourteen (16.9%) patients had no PD nor confirmed MRD conversion at the 7-year update; in the 63 (75.9%) patients who had MRD conversion, median time to conversion (95% CI) was 19.4 months (8.7, 28.0). Among 63 patients who converted, 39 subsequently had PD or died; median time from conversion to PD (95% CI) was 28.3 months (23.2, 35.0). In the substudy ($n=34$), 25 patients received VenR retreatment (Table), 92.0% of whom had at least one of the following high-risk features: IGHV-unmutated disease, genomic complexity, or del(17p) and/or *TP53* mutations [2]; despite this, 14/25 (56.0%) patients achieved uMRD at EOT in the main study. Best overall response rate (ORR) to retreatment was 72.0% and median PFS (95% CI) was 23.3 months (15.6, 24.3). Median (range) time between the last Ven dose in the main study and Ven ramp-up in the substudy was 2.3 (1.2–3.1) years. Eight (32.0%) patients achieved uMRD at the retreatment end of combination treatment; however, no patients retained their uMRD status at the retreatment EOT. No new safety findings were observed since the 5-year data cut.

Conclusion: In this final long-term analysis of the MURANO trial, PFS and OS benefits for VenR over BR were sustained. Furthermore, achievement of uMRD was associated with prolonged PFS. In VenR-treated patients in the substudy, ORR was high and uMRD was still attainable in this high-risk population. Overall, these data continue to support the use of fixed-duration VenR in R/R CLL, and suggest that retreatment with VenR is a viable option for pretreated patients (Table 1).

Table 1. Baseline characteristics and efficacy of patients in the main study and the substudy.

	Main study		Substudy
	Patients treated with VenR ($n=194$)	Patients treated with BR ($n=195$)	Patients retreated with VenR ($n=25$)
Baseline characteristics			
Mean age, years (SD)	63.9 (10.5)	64.4 (9.6)	65.8 (8.3)
Number of prior cancer therapy, *n* (%)			
1	111 (57.2)	117 (60.0)	0 (0.0)
2	58 (29.9)	43 (22.1)	20 (80.0)
≥3	25 (12.9)	35 (17.9)	5 (20.0)
del(17p) and/or *TP53* mutation (aCGH), *n* (%)			
Mutated	53 (27.3)	55 (28.2)	14 (56.0)
Unmutated	104 (53.6)	98 (50.3)	9 (36.0)
Unknown	37 (19.1)	42 (21.5)	2 (8.0)
Genomic complexity, *n* (%)	$n=48$	$n=46$	$n=20$
3–4	34 (70.8)	29 (63.0)	3 (15.0)
≥5	14 (29.2)	17 (37.0)	8 (40.0)
IGHV, *n* (%)	$n=180$	$n=180$	$n=23$
Mutated	53 (29.4)	51 (28.3)	2 (8.7)
Unmutated	123 (68.3)	123 (68.3)	21 (91.3)
Unknown	4 (2.2)	6 (3.3)	0 (0.0)
Efficacy results			
Median follow-up, months	85.7	85.7	33.4
Best ORR, %	93.3	67.7	72.0
uMRD at EOCT of main study, *n* (%)	121 (62.4)	26 (13.3)	16 (64.0)
uMRD at EOCT of substudy, *n* (%)	N/A	N/A	8 (32.0)
uMRD at EOT of main study, *n* (%)	83 (70.3)*	N/A	14 (56.0)
uMRD at EOT of substudy, *n* (%)	N/A	N/A	0 (0.0)
Median PFS, months (95% CI)	54.7 (52.3, 59.9)	17.0 (15.5, 21.7)	23.3 (15.6, 24.3)
3-Year OS rate, % (95% CI)	88.4 (83.8, 93.0)	78.9 (72.8, 84.9)	53.1 (25.1, 81.0)

*Patients who completed 2 years of Ven without PD ($n=118$)

aCGH: array comparative genomic hybridization; BR: bendamustine-rituximab; CI: confidence interval; del(17p): deletion in chromosome 17p; EOCT: end of combination treatment; EOT: end of treatment; IGHV immunoglobulin heavy chain gene; ORR: overall response rate; OS: overall survival; PD: progressive disease; PFS: progression free survival; SD: standard deviation; *TP53*: tumor protein P53; uMRD: undetectable minimal residual disease; Ven(R): venetoclax-(rituximab)

Abstract ID: 1548587

Title: Genomic evolution and resistance to pirtobrutinib in covalent BTK-inhibitor pre-treated chronic lymphocytic leukemia patients: results from the phase I/II BRUIN Study

Authors: Jennifer Brown, Sai Prasad Desikan, Bastien Nguyen, Helen Won, Shady I. Tantawy, Samuel C. McNeely, Narasimha Marella, Kevin Ebata, Jennifer Woyach, Krish Patel, Constantine S. Tam, Toby A. Eyre, Chan Y. Cheah, Nirav Shah, Paolo Ghia, Wojciech Jurczak, Minna Balbas, Binoj Nair, Paolo Abada, Chunxiao Wang, Denise Wang, Anthony Mato, Varsha Gandhi and William Wierda

Background: Pirtobrutinib, a highly selective, non-covalent (reversible) BTK-inhibitor (BTKi), demonstrated broad efficacy in patients (pts) with chronic lymphocytic leukemia (CLL)/SLL who were resistant to cBTKi. Mechanisms of resistance to pirtobrutinib have not been systematically analyzed to date.

Aim: To explore the genomic evolution of pirtobrutinib resistance in cBTKi pre-treated CLL/SLL pts.

Figure. Number of patients with acquired mutations according to *BTK* status at baseline and prior type of cBTKi. The color gradient indicates the mean VAF at progression.

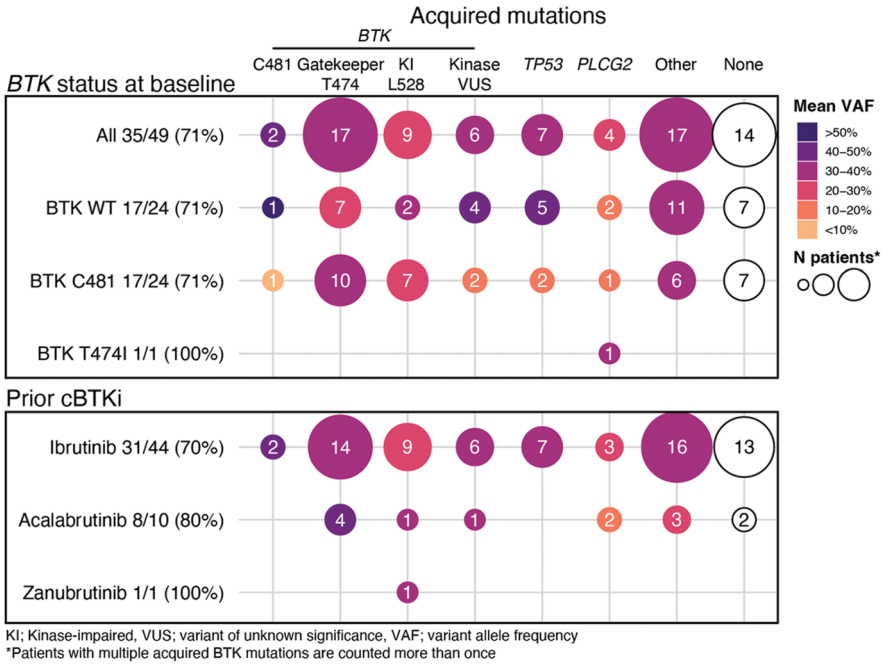

KI; Kinase-impaired, VUS; variant of unknown significance, VAF; variant allele frequency
*Patients with multiple acquired BTK mutations are counted more than once

Methods: cBTKi pre-treated CLL pts treated with pirtobrutinib monotherapy in the phase 1/2 BRUIN trial (NCT03740529) who subsequently developed disease progression (PD) were included in this analysis. Targeted next-generation sequencing (NGS) of all exons of 74 relevant genes was centrally performed on peripheral blood mononuclear cells collected at baseline and at or near PD. Somatic mutations were reported with a limit of detection (LoD) of 5% variant allele frequency (VAF). Manual inspection of *BTK* exons with a LoD of 1% was performed to detect whether *BTK* mutations identified at PD were present at baseline at <5% VAF.
Results: As of 29 July 2022, 49 cBTKi pre-treated CLL pts who progressed on pirtobrutinib had paired NGS data available at baseline and PD. In this group, the median age was 69 y (range, 36–86), median number of prior lines was 4 (range, 1–10), and 41 pts (84%) had discontinued prior cBTKi due to PD. Pts received one or more of the following cBTKi: ibrutinib ($n=44$, 90%), acalabrutinib ($n=10$, 20%), or zanubrutinib ($n=1$, 2%). The ORR to pirtobrutinib (including PR-L) was 80%. The most common alterations at baseline were mutations in *BTK* (51%), *TP53* (49%), *ATM* (27%), *NOTCH1* (20%), *SF3B1* (18%), and *PLCG2* (10%). Among the 25 pts with ≥1 *BTK* mutation detected at baseline, *BTK* mutations included C481S ($n=23$), C481R ($n=4$), C481Y ($n=2$), C481F ($n=1$), T474I ($n=1$). *BTK* C481 VAF decrease or complete clearance was observed at PD in nearly all pts (92%, 22/24, median VAF decrease =100%). NGS of samples at PD showed 71% (35/49) of pts acquired ≥1 mutation, with 55% (27/49) acquiring ≥1 *BTK* mutation. Among these 27 pts, a total of 36 acquired *BTK* mutations were identified; the most common were gatekeeper mutations (T474I/F/L/Y, 17/49, 35%), kinase-impaired (L528W, 9/49, 18%), and variants of unknown significance (VUS) proximal to the ATP-binding pocket (6/49, 12%; including V416L ($n=2$), A428D ($n=2$), D539G/H ($n=1$), Y545N ($n=1$)) (Figure 1). Manual inspection for acquired *BTK* at PD in the corresponding baseline samples revealed that 9 mutations (in 8 pts) pre-existed at baseline at low VAFs (1–4%). These included 6 gatekeeper T474I/L, 2 kinase impaired L528W, and 1 VUS A428D. These pts responded to pirtobrutinib (6/8, 75% ORR) and had received prior ibrutinib ($n=5$) and acalabrutinib ($n=4$). The most commonly acquired non-*BTK* mutations were *TP53* (7/49, 14%) and *PLCG2* (4/49, 8%).
Conclusions: Pts who progressed on pirtobrutinib showed clearance of *BTK* C481 clones and the emergence or outgrowth of non-C481 clones, particularly gatekeeper T474 and kinase-impaired L528W mutations, as well as other VUS. Many acquired *BTK* mutations were shown to pre-exist at baseline at low VAF, reflecting emergence on prior cBTKi. Importantly, these baseline kinase domain *BTK* mutations did not preclude pirtobrutinib efficacy. Approximately half of pts did not acquire *BTK* mutations and 29% did not acquire any mutations in this targeted panel, suggesting alternate resistance mechanisms. Whether similar patterns of resistance would manifest if pirtobrutinib was utilized in earlier lines of therapy or prior to cBTKi treatment remains uncertain.

Abstract ID: 1553491

Title: Identification of novel targets that upregulate CD20 expression in rituximab-resistant cells with the use of genome-wide CRISPR screening

Authors: Lenka Dostalova, Aneta Ledererova, Helena Peschelova, Tomas Loja and Michal Smida

Background: CD20 antigen has been used as a target of monoclonal antibodies (mAb) such as rituximab (RTX) in the therapy of B-cell malignancies for more than two decades. However, CLL B cells tend to express lower levels of CD20 on their surface or downregulate it following the mAb treatment, resulting in mAb resistance and subsequently therapy failure. Therefore, it is crucial to investigate the regulation of CD20 in order to restore sensitivity to anti-CD20 mAb and enhance its efficacy. The aim of this project was to perform genome-wide CRISPR/Cas9 knockout screening to identify genes whose disruption upregulates CD20 surface expression in the resistant cells with low CD20 levels.
Methods: To create a model mimicking the situation in patients who had developed resistance to mAb therapy, we generated

an RTX-resistant CD20-low B-lymphoid cell line by chronic exposure to increasing concentrations of rituximab. These cells were then transduced by the GeCKO (Genome-Scale CRISPR Knock-Out) lentiviral library to obtain a collection of single-gene knockouts. Following a 2.5-week cultivation period allowing the full manifestation of gene knockouts, the top 5% of cells with the highest surface expression of CD20 were sorted out. Using next-generation sequencing and the MAGeCK algorithm, we identified gene knockouts responsible for CD20 upregulation. The most interesting of these genes were subsequently validated using newly designed gRNAs, and the CD20 expression was assessed using flow cytometry and western blot. To determine the response to the anti-CD20 mAb, cells were incubated with rituximab in the presence of human serum for 24 hours and the viability was measured using the CellTiter-Glo assay.

Results: Our CRISPR/Cas9 knockout screening revealed several interesting genes whose disruption led to the increase in CD20 surface expression. As the top hit we identified gene CSK, encoding a negative regulator of Src kinases. CSK is a key kinase in the activation of the B-cell receptor (BCR) pathway – one of the most important pathways in B cells. Another significantly enriched gene involved in BCR signalling was PTEN, a well-known tumour suppressor. Interestingly, among the top ten hits we identified four genes (SSR1, SSR2, SSR3, SSR4) encoding all four subunits of the translocon-associated protein (TRAP) complex, endoplasmic reticular complex involved in protein translocation across ER membrane and other ER processes. The presence of STT3A among the top hits suggests the involvement of another ER complex, oligosaccharyltransferase (OST). OST consists of two subunits encoded by genes STT3A and STT3B and is involved in glycosylation. These results indicate that both BCR signalling and ER play an important role in CD20 regulation. The last gene selected for validation was CD37. It encodes a surface protein, expressed predominantly in B cells, which is involved in immune response, but its function has not been fully described. We indeed observed the upregulation of CD20 upon CD37 disruption. But on the contrary, the loss of CD20 surprisingly led to a decrease in CD37 expression. This suggests the presence of a regulatory loop between these two genes. We generated knockout cell lines for genes CSK, SSR1 and CD37 in our RTX-resistant cells and successfully validated the results from the screening in these cell lines. In each cell line, we observed an increase in both surface and total levels of CD20 compared to wild-type cells. Moreover, in all three cases, cells restored their sensitivity to rituximab. The validation of other selected hits is currently ongoing.

Conclusion: In summary, we have identified several promising genes involved in CD20 regulation and whose disruption may be used to upregulate CD20 expression. The thorough validation and investigation of underlying mechanisms could provide a way for a potential enhancement of anti-CD20 mAb therapy.

Abstract ID: 1552495

Title: Impact of COVID-19 in patients with chronic lymphocytic leukemia treated with venetoclax: a possible role of the association to anti-CD20 antibody? A multicentre SEIFEM study

Authors: Francesco Autore, Andrea Visentin, Marina Deodato, Candida Vitale, Eugenio Galli, Alberto Fresa, Rita Fazzi, Alessandro Sanna, Jacopo Olivieri, Ilaria Scortechini, Maria Ilaria del Principe, Paolo Sportoletti, Luana Schiattone, Nilla Maschio, Davide Facchinelli, Marta Coscia, Alessandra Tedeschi, Livio Trentin, Idanna Innocenti, Anna Candoni, Alessandro Busca, Livio Pagano and Luca Laurenti

Introduction: Severe acute respiratory syndrome coronavirus 2 (SARS-CoV-2), responsible for coronavirus disease 19 (COVID-19), has led to a significant increased morbidity worldwide. The severity of the disease can vary between patients, with history of cancer and administration of antileukemic treatment were associated with worse outcome. A recent meta-analysis showed a high case fatality rate in hospitalized patients with hematological malignancies. Published reports indicated high rates from 27.3 to 35% also in chronic lymphocytic leukemia patients (CLL) patients. The aim of our study was to evaluate the impact of COVID-19 in CLL patients treated with venetoclax.

Methods: The retrospective multicenter study included CLL patients treated since 2017 with venetoclax single agent until progression or toxicity or venetoclax plus anti-CD20 antibody (mainly rituximab as part of VR protocol for 24 months or obinutuzumab as part of VO protocol for 12 months).

Results: We found 114 infections from SARS-CoV-2 in 96 patients out of 287 patients with CLL who received venetoclax during the study period. Basal characteristics of the 96 patients who experienced COVID-19 were compared to those of the 191 patients who did not experience the infection (data are shown in Table 1). Patients of the first group did not show more comorbidities in terms of CIRS, nor renal and pulmonary impairment. Unexpectedly patients without COVID-19 experienced more previous infections in the 12 months before the beginning of the treatment with venetoclax; they also were exposed to a high rate of prophylaxis as immunoglobulin and antiviral drugs. We noted that in the group of COVID-19 a higher rate of patients received venetoclax plus anti-CD20 antibody (64.4% in the group of COVID-19 vs. 38.7% in the group without COVID-19). The rate of vaccination was high in both: 87% in the first and 74.8% in the second with a median of 3 doses each. Analyzing characteristics of the 114 infections we distinguished 64 grade 1–2 COVID-19 and 50 grade 3–4 COVID-19. Patients with grade 1-2 COVID-19 resulted positive for a median time of 10 days (range 5–52), 87% of the patients were vaccinated. Exposure to anti-CD20 antibody associated to venetoclax was present in 61% of the cases. No treatment was administered in 33.3% of the cases, nirmatrelvir/ritonavir was used in 23% of the cases, remdesivir in 18%. Prophylaxis with tixagevimab/cilgavimab was administered in 22.2% of the patients. Patients with grade 3–4 COVID-19 resulted positive for a median time of 18 days (range 5–97), 86% of the patients were vaccinated. Exposure to anti-CD20 antibody associated to venetoclax was present in 66% of the cases. Remdesivir was chosen as treatment in 49% of the cases, nirmatrelvir/ritonavir in 24.4%. Prophylaxis with tixagevimab/cilgavimab was administered in 21.9% of the patients. Venetoclax was withdrawn in 71.5%, and in more than 80% of whom venetoclax was administered together with an anti-CD20 antibody. In most of the cases the discontinuation was only temporary. Sixty-seven % of the patients required hospitalization due to COVID-19, the median time of recovery was 15 days, and 20.7% of them needed intensive care unit admission. Among the 96 patients with COVID-19, 18 patients died, 10 died due to COVID-19, 7 were exposed to anti-CD20 antibody, 3 had a previous grade 1-2 COVID-19, but none experienced a SARS-CoV-2 infection before treatment with venetoclax. All were vaccinated with at least 3 doses except one patient who was not vaccinated but was infected and died in 2020.

Table 1. Patients' characteristics with subdivision in the two subgroups (patients with COVID-19 disease and patients without COVID-19 disease)

		Patients with COVID-19 disease (96 patients)	Patients without COVID-19 disease (191 patients)
CIRS	>6	23.0%	29.8%
Smoking	yes	12.5%	22%
Diabetes	yes	7.3%	14.1%
COPD	yes	14.6%	13.6%
CrCl <70	yes	37.5%	42.4%
Previous lines of treatment	median	2	2
Previous infection	yes	20.8%	38.7%
Previous pneumonia	yes	7.3%	11.5%
Association to anti-CD20	yes	64.6%	38.7%
Immunoglobulin prophylaxis	yes	15.6%	21.5%
Antiviral prophylaxis	yes	28.1%	41.9%

The rate of mortality due to COVID-19 was 10.4% considering patients who were infected by SARS-CoV-2, but 20% among patients with severe grade 3-4 infection.

Conclusions: This is a real-life study on 287 patients affected by CLL treated with venetoclax with the aim to describe COVID-19 in this cohort. The analysis found a significant rate of infections (33.4%), most of grade 1–2, without a high rate of mortality. The increased rate (70%) of venetoclax discontinuation during COVID-19 was a physician choice to decrease the risk of complications since the association of anti-CD20 antibody to venetoclax seems to have a role in the risk of COVID-19.

Abstract ID: 1551859

Title: Inhibition of G protein-coupled receptor kinase 2 (GRK2) as a strategy to modulate leukemic cell homing and activation in CLL

Authors: Chiara Cassarino, Ana Colado, Valeria Sarapura Martinez, Martín Bertini, Claudio Martines, Alice Bonato, Miguel Pavlovksy, Rosario Custidiano, Gregorio Cordini, Fernando R Bezares, Mónica Vermeulen, Romina Gamberale, Mirta Giordano, Dimitar G. Efremov and Mercedes Borge

Proliferation of leukemic cells and resistance to therapy occur within lymphoid tissues, supporting the idea that the retention of leukemic cells within this tumour microenvironment contributes to disease progression and relapse. GRK2 plays a central role in B cell homing to lymphoid organs by inducing Sphingosine-1 phosphate receptor-1 (S1PR1) downregulation, which allows lymphocytes to overcome the S1P-mediated retention in the blood and to enter into lymphoid tissues. Migration towards the high concentration of S1P in the vascular compartment also mediates B cell exit from lymphoid tissues. In mouse models, GRK2-deletion on B cells leads to an increased response to S1P and thus a higher presence of B cells in peripheral blood over bone marrow, lymph nodes and spleen follicles [1]. In addition, GRK2 has been implicated in signalling pathways related to cancer progression [2]. The expression and function of GRK2 in CLL have not been studied yet. Here, we aim to evaluate the role of GRK2 in leukemic cell migration, activation and survival. Primary leukemic B cells were obtained from peripheral blood of untreated CLL patients and normal B cells from healthy volunteers. GRK2 expression was evaluated by western blot and qRT-PCR. Cell activation and drug-induced apoptosis were evaluated by flow cytometry. Chemotaxis towards S1P, CXCL12 or CXCL13 was evaluated in vitro using a Transwell cell migration assay. Murine leukemic B cells were obtained from Eμ-TCL-1 mice (C57BL/6 background). GRK2-deficient murine leukemic cells were generated by CRISPR/Cas9 editing on the mouse cell line TCL1-355 TKO, as previously described [3]. For *in vivo* migration assays, control and GRK2-deficient murine leukemic cells were labeled with CFSE or CTV, mixed in a ratio 1:1 and injected through the tail vein. Twenty hours later, their localization in peripheral blood, bone marrow and spleen was evaluated by flow cytometry. GraphPad Prism software was used for statistical analysis. We found that leukemic cells from CLL patients express similar levels of GRK2 as B cells from healthy volunteers (Figure 1(A–C)). *In vitro* treatment of leukemic cells with the GRK2 inhibitor, CMPD101, did not affect spontaneous or venetoclax-induced apoptosis (not shown). The presence of CMPD101 did not counteract the up-regulation of CD69 expression on CLL cells activated through the BCR (Figure 1(D)). On the other hand, when CLL cells were activated by co-culturing with autologous activated T cells, the presence of CMPD101 decreased the up-regulation of the activation marker CD86 on leukemic B cells, which was accompanied with decreased CD40L expression on T cells and a lower capacity to secrete IL-10 (Figure (E–H)). We then evaluated the effect of GRK2 inhibition on the *in vitro* migratory response of CLL cells towards S1P, CXCL12 and CXCL13. We found that the response of CLL cells to S1P was significantly increased by CMPD101 (Figure 1(I)), while migration towards chemokines was not affected (Figure 1(J)). CMPD101 also increased migration towards S1P of leukemic cells obtained from peripheral blood or lymphoid tissues of Eμ-TCL1 mice (Figure 1(K)). Moreover, using CRISPR/Cas9 technology on the TCL1-355 TKO cell line, we generated GRK2-deficient murine leukemic cells (GRK2KO) (Figure 2(A)) and their control, MOCK-transfected, leukemic cells (MOCK), which allowed us to show that GRK2 deletion increased the *in vitro* response of leukemic cells to S1P (Figure 2(B)). As expected, CMPD101 increased S1P response of MOCK but not on GRK2KO cells (not shown). Migration towards CXCL12 and CXCL13 was similar between GRK2KO and MOCK cells (not shown). Interestingly, GRK2KO cells showed a slightly lower spontaneous proliferation rate when cultured in vitro compared to MOCK cells, which was evident after day 8 of culture (Figure 2(C)), and also proliferated less in response to LPS (Figure 2(D)). Finally, we evaluated the *in vivo* homing capacity of GRK2KO and MOCK cells intravenously injected into mice. At 20 hs post-injection, we found that GRK2KO cells preferentially localized in blood and spleen and were underrepresented in the bone marrow, compared to MOCK cells (Figure 2(E)). Our results suggest that GRK2 inhibition could be explored as a strategy to induce their retention in the blood, increasing their exposure to therapeutic agents and/or to overcome resistance to treatment induced by the protective microenvironment.

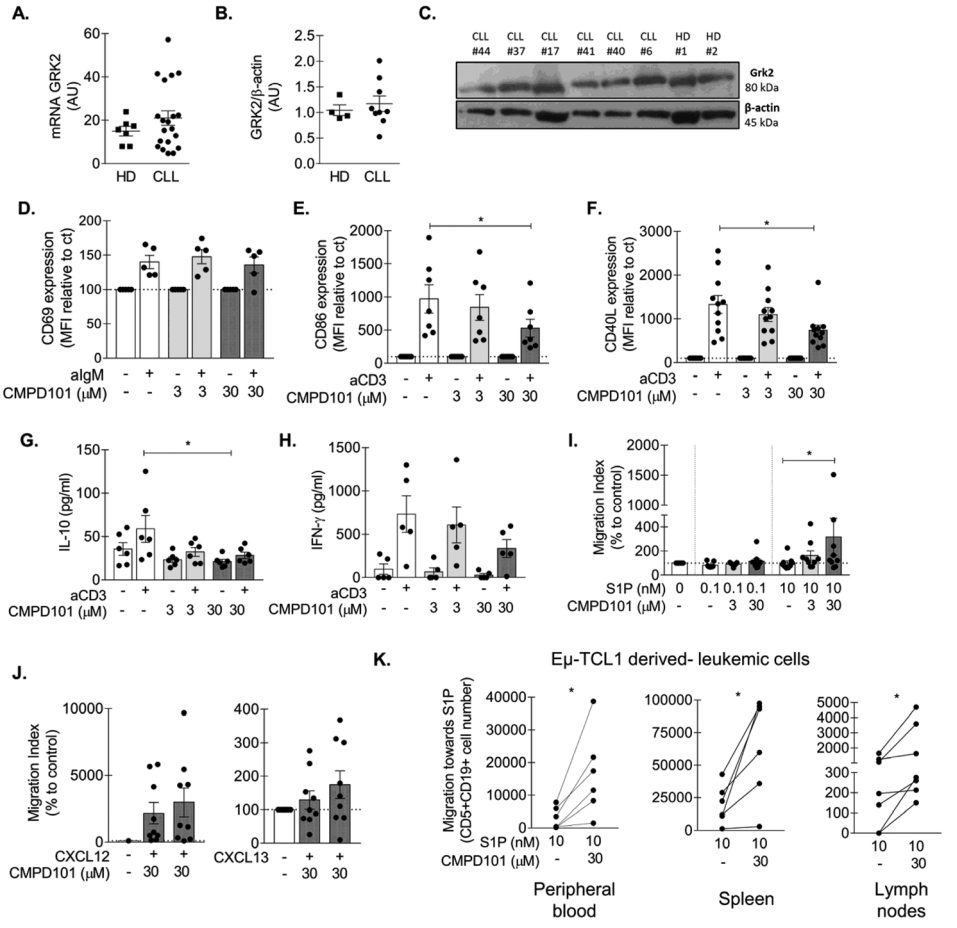

Figure 1. A. GRK2 mRNA levels were measured by qPCR on B cells from healthy donors (HD) and CLL patients purified by immunomagnetic cell separation. AU: arbitrary units. Mean ± SEM, Non statistically significant, Mann-Whitney test. **B.** GRK2 protein expression was measured on HD- and CLL-B cells. β-actin was used as loading control. Mean ± SEM, Mann-Whitney test **C.** Representative image of the western blot. **D-F.** PBMC from CLL patients were pre-incubated with the GRK2 inhibitor, CMPD101, or the drug vehicle (DMSO) for 15 minutes and then plated in wells containing immobilized anti-IgM (25 μg/ml) or anti-CD3 (0.5 μg/ml). CD69 or CD86 (on B cells) **(D-E)** and CD40L (on T cells) **(F)** expression was evaluated by FC. CD69 and CD40L were evaluated after 24h and CD86 after 48h of culture. **G-H.** T cells from CLL patients were purified by immunomagnetic cell separation and activated as detailed before, then IL-10 and IFN-ɣ production was measured in culture supernatants by ELISA. Mean ± SEM, *p<0.05, Friedman test followed by Dunn's post-test. **I-J.** The transwell system was used to evaluate leukemic cell migration towards S1P, CXCL12 (0.5 μg/ml) and CXCL13 (1μg/ml). Cells were pre-treated with CMPD101 or DMSO for 15 minutes before the chemotaxis assay. Migration index: number of cells that had migrated in response to the stimuli/ number of cells that had migrated spontaneously (without stimuli) after 3 h. Mean ± SEM, *p<0.05, Friedman test followed by Dunn's post-test. **K.** Peripheral blood, spleen and lymph nodes were obtained from full leukemic Eμ-TCL1 mice. Cells were pre-treated with CMPD101 or DMSO for 15 minutes and migration in response to S1P was evaluated with the transwell system. For murine cells, migration towards S1P is calculated as the number of CD5+CD19+ cells in the lower chamber with S1P - spontaneous migration (without stimuli), after 3 h. *p<0.05, Wilcoxon matched-pairs signed rank test.

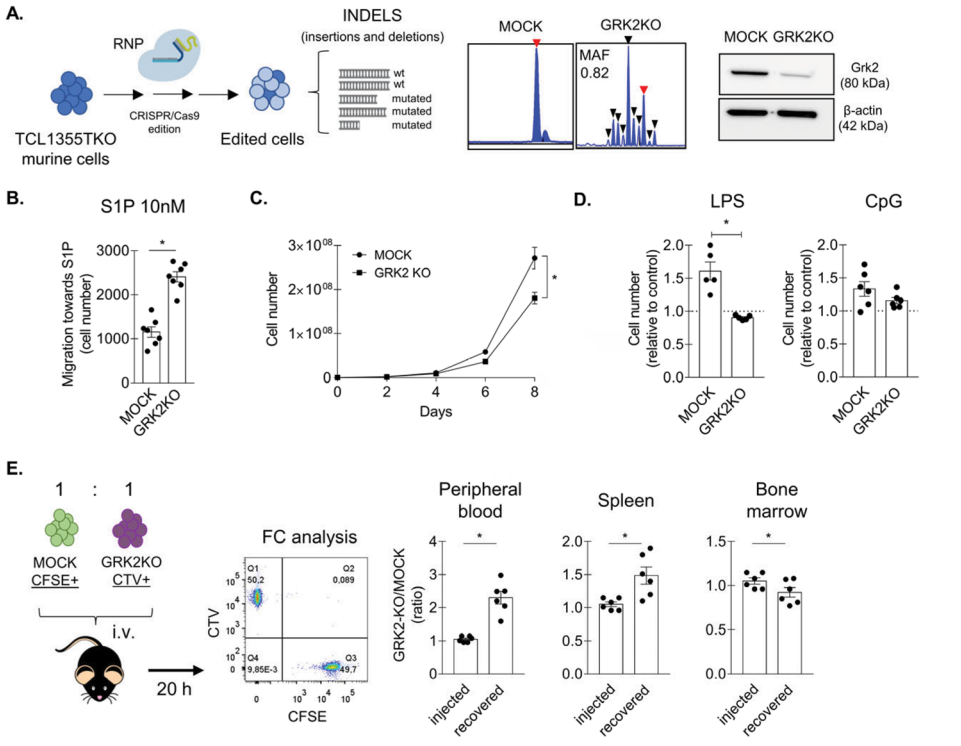

Figure 2. A. TCL1355TKO murine cells were edited using CRISPR/Cas9 technology. TCL1355TKO^{MOCK} cells (MOCK) were electroporated with Cas9 alone and TCL1355TKO^{GRK2KO} cells (GRK2KO) with ribonucleoparticles (RNP) containing recombinant Cas9 enzyme + GRK2 guide RNA. DNA extraction and PCR was performed from the edited population. INDEL analysis of the PCR products was performed by capillary electrophoresis and mutant allele frequency (MAF) was determinate by peak quantification. MAF=mutated alleles/total alleles. Red arrow: peak corresponding to GRK2 wt allele; black arrow: peak corresponding to GRK2 mutated allele. Immunoblotting analysis of GRK2 expression on MOCK and GRK2KO cells **B.** Migration in response to S1P of MOCK and GRK2KO cells was assessed using the transwell system. The number of cells in the lower chamber, after 3 h, is shown. Spontaneous migration (cells in the lower chamber without chemoattractant) was subtracted. Mean ± SEM, *p<0.05, Wilcoxon test. **C.** Spontaneous proliferation of MOCK and GRK2KO cells was evaluated. Absolute number of viable cells at different time point is shown. Each data point represents 3 independent experiments. *p<0.05, Mann Whitney test **D.** Proliferation in response to TLR4 ligand, LPS (5 μg/ml) and TLR9 ligand, CpG (1 μM) was evaluated. Cell number in stimulated condition relative to control condition is shown. Mean ± SEM, *p<0.05, Wilcoxon test **E.** GRK2 KO (CTV+) and MOCK (CFSE+) cells were mixed in a ratio 1:1 and injected intravenously (i.v.) in C57BL/6 mice. After 20 hours, mice were sacrificed and peripheral blood, spleen and bone marrow were obtained and the percentage of each of the injected populations was evaluated by FC. The ratio of GRK2KO cells / MOCK cells in each compartment is shown. Mean ± SEM, *p<0.05, Wilcoxon test.

Abstract ID: 1550959

Title: Integrating multi-omics to reveal the heterogeneous clonal evolutionary characteristics in CLL patients with zanubrutinib resistance

Authors: Huayuan Zhu, Yeqin Sha, Yi Miao, Shuchao Qin, Luomengjia Dai, Tonglu Qiu, Rui Jiang, Wei Wu, Yi Xia, Lei Fan, Wei Xu, Hui Jin and Jianyong Li

Introduction: The drug-resistant mechanisms of the first-generation Bruton's tyrosine kinase (BTK) inhibitor, ibrutinib, has been extensively explored in Chronic Lymphocytic Leukemia (CLL) patients. However, the resistant mechanisms of the second-generation BTK inhibitor such as zanubrutinib remained largely unexplored. We integrated multi-omics to assess the heterogeneous clonal evolutionary characteristics in CLL patients with zanubrutinib resistance.

Methods: We retrospectively identified 8 CLL patients with zanubrutinib resistance. Deep targeted-gene next generation sequencing (NGS) covering BTK (exon 1-19), PLCG2 (exon 1-33) and high sensitivity droplet digital PCR (ddPCR) detecting BTK mutation were assessed in available serial samples. Single-cell RNA sequencing (scRNA-seq) of matching peripheral blood (PB) and lymph node (LN) were performed in 3 zanubrutinib-resistant patients showing progressive lymphadenopathy.

Results: Totally 8 patients were included in our study, the median time from zanubrutinib initiation to progression was 30.5 months, including 2 patients were both histologically confirmed as Richter Transformation (RT) after 13 months' treatment. Five patients presented as LN enlargement at progression received PET-CT imaging scan and further underwent LN biopsy or puncture at the site of maximum Standard Uptake Value (SUVmax), 2 patients were diagnosed as RT, 2 as accelerated CLL (aCLL) and 1 as

CLL progression. Deep targeted-gene NGS showing that BTK Cys481 mutation was detected in 5 of 8 patients (1 patients also harbored BTK Leu528Trp mutation with low frequency) and PLCG2 mutation was detected in one patient without BTK Cys481 mutation. For 3 patients with undetectable BTK mutation by NGS, ddPCR were performed and one patient was identified harboring BTK Cys481Ser mutation (progressed due to lymphadenopathy but NGS performed in bone marrow), suggesting spatial clonal heterogeneity in zanubrutinib-resistant patients. For one patient harboring both BTK Cys481 mutation and BTK Leu528Trp mutation, Cys481Ser (VAF 20.44%) and Cys481Arg (VAF 13.87%), BTK Leu528Trp (5.97%) mutations are in different cells. Crystal structure of BTKCys481Ser-Zanubrutinib suggested the disruption of hydrogen bond compared with BTKWT-Zanubrutinib while BTKLeu528Trp-Zanubrutinib suggested potential steric clashes compared with BTKWT-Zanubrutinib, leading to the decrease of binding free energy between BTK and zanubrutinib. For 3 of 5 patients who showed progressive lymphadenopathy during zanubrutinib resistance, 3 patients displayed different clinical manifestation with one RT, one aCLL and one disease progression. scRNA-seq of matched PB and LN were performed. Highest proportion of proliferating tumor cells was found in RT while lowest proportion of proliferating tumor cells was found in disease progression. Notably, RT patients displayed the most actively upregulated MYC, OXPHOS and G2M pathways and the downregulation of BCR signaling. aCLL showed the median activation of MYC, OXPHOS and G2M pathways and median downregulation level of BCR signaling, indicating its intermediate biological status between RT and disease progression. Moreover, analysis of BCL-2 anti-apoptotic family genes expression showed that tumor cells in RT showed significantly higher expression of MCL-1 while tumor cells in progressive CLL showed relatively higher expression of BCL-2, indicating the shift of BCL-2 family dependence among different disease characteristics.

Conclusion: Integrated multi-omics were performed in our zanubrutinib-resistant CLL patients' cohort. BTK Cys481 and Leu528 were two main BTK resistant mutations in zanubrutinib resistant CLL patients. Due to spatial heterogeneity and clonal evolution among patients, deep targeted-gene NGS and ddPCR should be used comprehensively to evaluate the emergence of resistant clones. Zanubrutinib-resistant RT showed highest upregulation of MYC, OXPHOS and G2M pathways and downregulation of BCR signaling. RT also showed upregulation of MCL-1, indicating underlying mechanism leading to insensitivity to venetoclax treatment following zanubrutinib resistance.

Abstract ID: 1545043

Title: Lisocabtagene maraleucel (liso-cel) in R/R chronic lymphocytic leukemia (CLL)/small lymphocytic lymphoma (SLL): primary analysis of TRANSCEND CLL 004

Authors: Tanya Siddiqi, David G. Maloney, Saad Kenderian, Danielle Brander, Kathleen Dorritie, Jacob Soumerai, Peter A. Riedell, Nirav Shah, Rajneesh Nath, Bita Fakhri, Deborah M. Stephens, Shuo Ma, Tatyana Feldman, Scott R. Solomon, Stephen J. Schuster, Serena K. Perna, Sherilyn A. Tuazon, San-San Ou, Eniko Papp and William Wierda

Introduction: In patients with relapsed or refractory (R/R) CLL/SLL that progressed on Bruton tyrosine kinases inhibitor (BTKi) and failed venetoclax-based regimens, achieving complete response (CR) with current treatment is uncommon. New therapies that achieve deep and durable responses are needed. We report the primary analysis of the phase 1/2, single-arm, multicenter TRANSCEND CLL 004 (NCT03331198) study evaluating liso-cel in patients with R/R CLL/SLL.

Methods: Patients must have received at least 2 prior lines of therapy, including a BTKi. Eligible patients received liso-cel at a target dose of either 50 (dose level [DL] 1) or 100 (DL2) $\times 10^6$ chimeric antigen receptor–positive T cells. The primary endpoint was rate of CR and CR with incomplete marrow recovery (CRi) by independent review committee per 2018 International Workshop on Chronic Lymphocytic Leukemia criteria in the prespecified subset of efficacy-evaluable patients with disease progression on BTKi and venetoclax failure (primary efficacy analysis set [PEAS]) at DL2 (null hypothesis [H0]: ≤5%). Key secondary endpoints were overall response rate (ORR; H0: ≤40%) and rate of undetectable minimal residual disease (uMRD; 10^{-4}) in blood (H_0: ≤5%).

Results: Of 137 leukapheresed patients, 117 received liso-cel (safety set), 96 (DL1 = 9; DL2 = 87) were efficacy evaluable, and 53 (DL1 = 4; DL2 = 49) were in the PEAS. In the safety set, median (range) age was 65 years (49–82), 83% had high-risk features, median (range) lines of prior therapy was 5 (2–12), and all patients had prior BTKi. Median (range) on-study follow-up was 21.1 months (0.4–55.6) for the safety set. In the PEAS at DL2, the primary endpoint of CR/CRi rate was met at 18.4% (95% confidence interval [CI], 8.8–32.0; 1-sided $p = 0.0006$; Table 1). ORR was 42.9% and was not statistically significant (95% CI, 28.8–57.8; 1-sided $p = 0.3931$). The uMRD rate was 63.3% in blood and 59.2% in marrow. Median (95% CI) duration of response was 35.3 months (11.01–not reached [NR]) with a median follow-up of 19.7 months. Median duration of CR/CRi was NR. In the safety set, rate of any-grade cytokine release syndrome (CRS) was 84.6% (grade 3, 8.5%; no grade 4/5) and neurological events (NE) was 45.3% (grade 3, 17.9%; grade 4, 0.9%; no grade 5); 69.2% received tocilizumab and/or corticosteroids for CRS/NEs. Rate of grade ≥3 infections, hypogammaglobulinemia, and prolonged cytopenia was 17.1, 15.4, and 53.8%, respectively. One death related to liso-cel was due to hemophagocytic lymphohistiocytosis. Liso-cel exhibited rapid in vivo expansion and was detected by quantitative polymerase chain reaction in blood up to 36 months after infusion.

Conclusions: Liso-cel demonstrated durable CR/CRi, high uMRD rates, and a manageable safety profile in patients with heavily pretreated, high-risk R/R CLL/SLL and high unmet need.

Table

Efficacy	PEAS at DL2 (n = 49)	Full efficacy set at DL2 (n = 87)
CR/CRi rate[a]	9 (18.4) [8.8–32.0]; ***P* = 0.0006**	16 (18.4) [10.9–28.1]
ORR[a]	21 (42.9) [28.8–57.8]; ***P* = 0.3931**	41 (47.1) [36.3–58.1]
uMRD in blood[a]	31 (63.3) [48.3–76.6]	56 (64.4) [53.4–74.4]
uMRD in marrow[a]	29 (59.2) [44.2–73.0]	51 (58.6) [47.6–69.1]
DOR[b]	35.3 (11.01–NR)	35.3 (19.78–NR)
Duration of CR/CRi[b]	NR (NR–NR)	NR (12.22–NR)
PFS[b]	11.9 (5.72–26.18)	18.0 (9.43–30.13)

[a]n (%) [95% CI]; [b]Median (95% CI), months.
CI, confidence interval; CR, complete response; CRi, complete response with incomplete marrow recovery; DL, dose level; DOR, duration of response; NR, not reached; ORR, overall response rate; PEAS, primary efficacy analysis set; PFS, progression-free survival; uMRD, undetectable minimal residual disease.

Abstract ID: 1538890

Title: m6A-modified circTET2 interacting with HN-RNPC regulates fatty acid oxidation to promote the proliferation of chronic lymphocytic leukemia

Authors: Hui Jin, Zijuan Wu, Huayuan Zhu, Renfu Gui, Jianyong Li, Wei Zhang and Lei Fan

Background: Chronic lymphocytic leukemia (CLL) is a hematological malignancy with high metabolic heterogeneity. The adaptation of CLL cell metabolism is more likely to be dependent upon lipid metabolism, which is one of the most prominent metabolic alterations in cancer because of the abundant lipid deposits when compared with normal B cells. Although accumulating evidence reveals that altered lipid metabolism is associated with the progression and treatment responsiveness of CLL, the extent of its heterogeneity and relationship to molecular heterogeneity have not been systematically studied.N6- methyladenosine (m6A) modification plays an important role in metabolism through regulating circular RNAs (circRNA). However, the underlying mechanism is not yet fully understood in CLL.

Methods: To determine the significance of m6A modification in CLL, we conducted whole-transcriptome sequencing of a cohort of 53 newly diagnosed CLL patients, and 35 m6A regulators were included in the analysis. Next, we constructed a m6A scoring system and found that the m6Sig score displayed a potential prognostic value, and we also explored the differential status of 35 m6A regulators in CLL. To further construct a risk model according to m6A-related circRNAs, we screened circRNAs with a correlation coefficient greater than 0.5. The identification of circTET2 was performed using northern blotting, RNase R treatment, actinomycin D assay, nucleocytoplasmic separation and RNA-FISH. To investigate the potential RBPs involved in this process, catRAPID and RBPBD were then applied, splicing factors RBMX and YTHDC1 was found to bind to the flanking sequences of circTET2, and co-IP assay verified their interaction. We then constructed stable CLL cell lines showing circTET2 overexpression and lentiviral silencing. CCK8 analysis and seahorse assay were performed to detected the cellular viability and oxygen consumption rate (OCR) which represents fatty acid oxidation (FAO) levels of CLL cells. Furthermore, We applied five inhibitors: indisulam (targeting splicing by inducing RBM39 degradation), H3B-8800 (a modulator of the SF3b complex), and the three pre-mRNA splicing inhibitors isoginkgetin, madrasin, and CP028. And the apoptotic rate with the drug combination compared with single-drug treatment was examined by flow cytometric analysis.

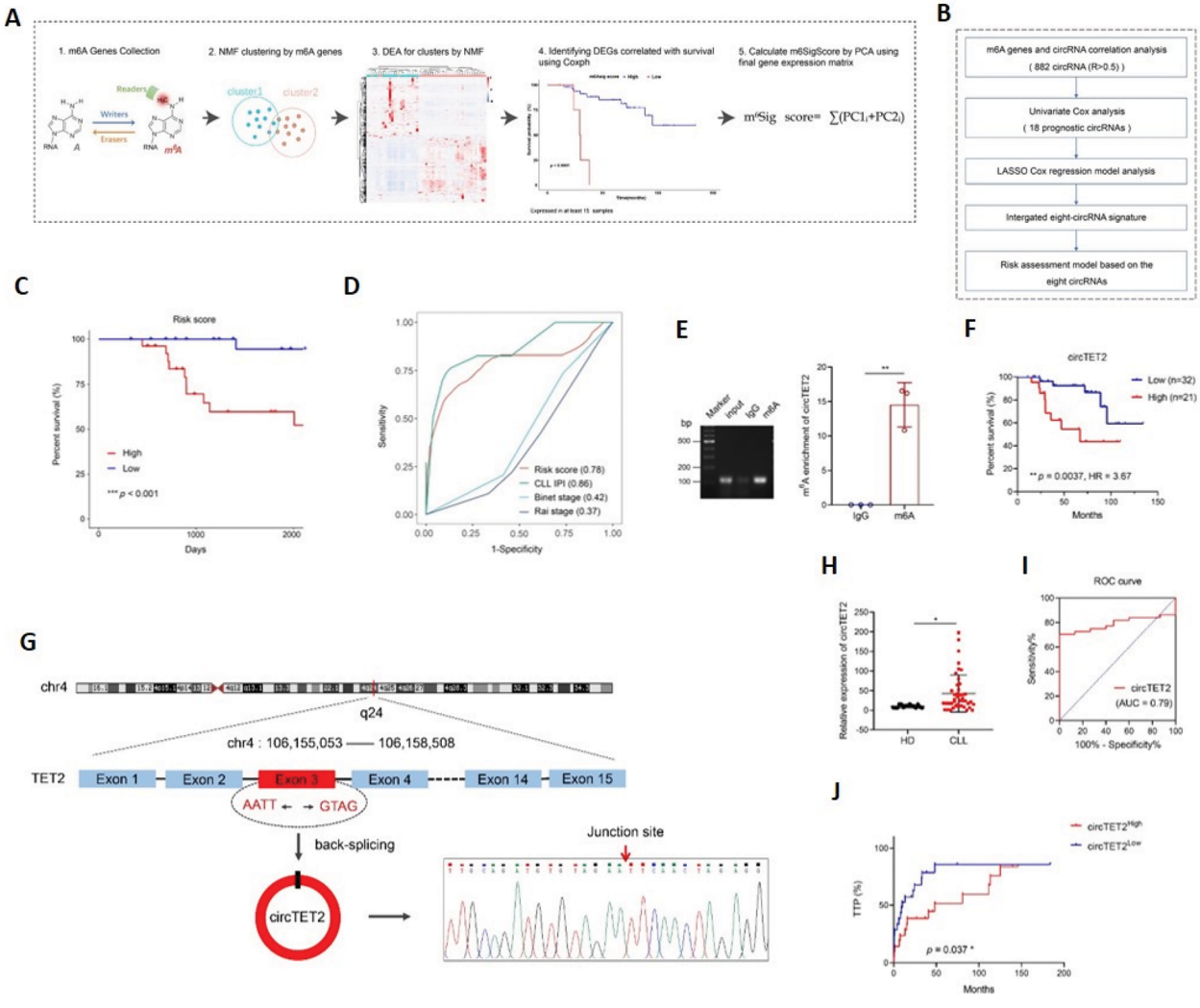

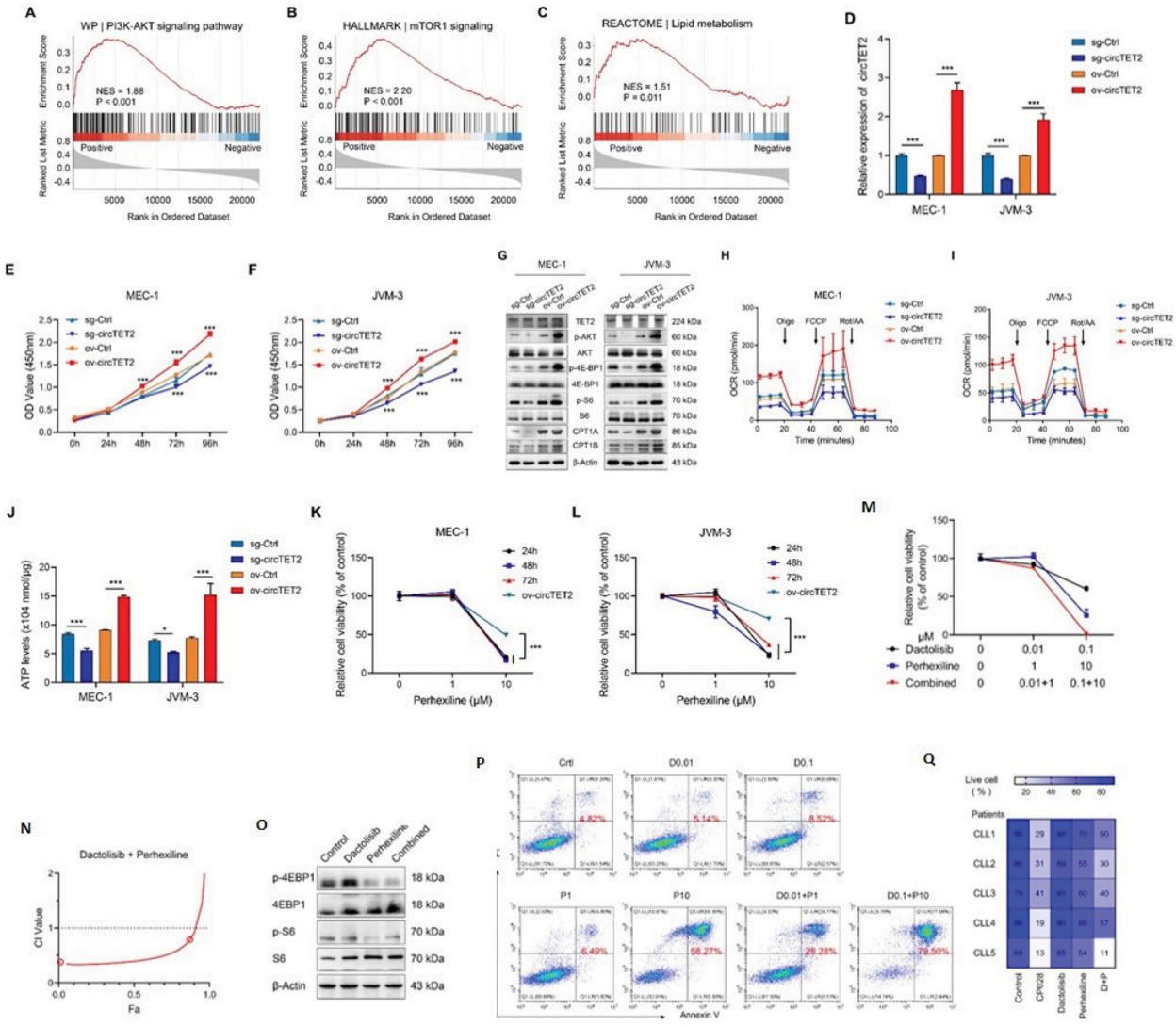

Results: Herein, we established an m6A-related circRNA prognostic signature and identified circTET2 with a higher risk score and higher level of m6A modification that is a potential prognostic biomarker for CLL. By interacting with the RNA-binding protein (RBP) heterogeneous nuclear ribonucleoprotein C (HNRNPC), circTET2 is involved in the regulation of FAO and the mTORC1 signaling pathway to fulfill the energy demands and promote the proliferation of CLL cells. The mTOR inhibitor dactolisib and FAO inhibitor perhexiline exert a synergistic effect on CLL cells. In addition, the biogenesis of circTET2 can be affected by the splicing process and RBPs. CP028, a splicing inhibitor, modulates the expression of circTET2 and shows pronounced inhibitory effects.

Conclusion: In summary, we identified m6A-modified circTET2 as a prognostic marker in CLL. CircTET2 that was upregulated in CLL was modulated by the splicing factors RBMX and YTHDC1, and that circTET2 interacted with HNRNPC, occupying a vital role in the modulation of lipid metabolism and cell proliferation of CLL. The data generated by this study collectively provide new evidence for a role and underlying mechanism for circRNAs in CLL lipid metabolism, and this may engender novel potential targets in clinical treatment.

Abstract ID: 1551967

Title: Refining the phenotypic and functional intraclonal complexity in chronic lymphocytic leukemia B cells uncovers a discrepancy between surface membrane IG levels and time since birth supporting the requirement for multifactorial activation and different subclonal sensitivities to treatment

Authors: Andrea Mazzarello, Mark Fitch, Martina Cardillo, Anita Ng, Sabreen Bhuiya, Esha Sharma, Chiara Salvetti, Jonathan E. Kolitz, Steven L. Allen, Kanti R. Rai, Joanna Rhodes, Marc K. Hellerstein and Nicholas Chiorazzi

Chronic lymphocytic leukemia (CLL) clones can be divided into subsets based on time since last cell division. This can be determined by patients drinking deuterated water (2H2O)

and then using flow cytometry to identify intraclonal subpopulations with reciprocal surface levels of CXCR4 and CD5. This approach distinguishes fractions enriched in recently divided 'proliferative' (PF; CXCR4DimCD5Bright); 'intermediate' (IF; CXCR4IntCD5Int) and 'resting' (RF; CXCR4BrightCD5Dim) cells. This 3-subpopulation model proposes that CLL cells, dividing in tissue proliferation centers, upregulate surface membrane (sm) CD5 and reduce smCXCR4, allowing cells to detach from the stroma and emigrate into the blood as the PF. Over time, cells of the PF transition to IF and then RF. Aging cells with higher smCXCR4 levels re-acquire the ability to migrate in the secondary lymphoid organs and some can be stimulated again and be re-born, perpetuating the cycle. However, this model does not consider all fractions based on CXCR4/CD5 expression and how they transition from one to another. For example, the model assumes a linear and concomitant transition of smCXCR4 and smCD5 and the stimulants required to generate the 'youngest' CLL cells are not clearly defined. Also, the model does not discriminate changes in smIG levels that can affect antigenic responsiveness. We redefine the kinetics of CLL fractions and provide novel insights about their functional dynamics. Unmanipulated *ex vivo* CLL cells from 10 patients who drank 2H2O for 4 weeks were sorted by CXCR4/CD5 relative densities, isolating PF, IF, RF, and two previously uncharacterized fractions, 'Double Dim' (DDF: CXCR4DimCD5Dim) and 'Double Bright' (DBF; CXCR4BrightCD5Bright). For each fraction, the amount of deuterium incorporated into cellular DNA in vivo was measured. The PF contained more 2H-labeled DNA than the RF and IF. The DDF also contained more 2H-DNA than RF. The DBF contained more 2H-DNA than the RF, but less than the PF. Hence, using 2H-DNA as determinant of age, a unidirectional path of phenotypic change could be defined, with the PF transitioning to DDF or IF or DBF, with the latter three moving to the RF directly or indirectly through the IF. Since BCR signaling is fundamental for CLL proliferation, we analyzed the densities of smIgM, smIgD (smIGs) and smCD19 for each subpopulation, finding higher smIGs and smCD19 densities on fractions with higher 2H-DNA incorporation. Accordingly, we measured 2H-DNA in fractions with low, intermediate, and high levels of smIGs, confirming that intraclonal subpopulations with high smIGs/CD19 divided more recently. Notably, these findings are not consistent with cell division being uniquely initiated by BCR engagement since that lowers smIGs levels. Therefore, we tested if engagement of TLR9 or CD40L would affect mIG densities on CLL cells. After stimulation of 32 CLL clones via TLR9 or CD40L or smIGs pathways, an increase in smIGs and CD19 was observed for the former two, while the latter led to their downregulation. Interestingly, chronological combinations of stimuli via TLR9 and smIGs showed that increased IG density required TLR9 stimulation before or concurrently with the latter. Thus, recently-divided cells might have experienced multifactorial stimulation in defined chronologies. Finally, the 5 intraclonal fractions sorted from CLL patients, before and during ibrutinib treatment in vivo, displayed diverse intraclonal changes in smIG densities and metabolic activation, with 2H-enriched and higher smIG density cells being more affected. These data define additional CXCR4/CD5 subpopulations of divergent ages, phenotypes, and sensitivities to treatment, suggesting that CLL B-cell kinetics are more complex than the current model describes. This complexity originates in secondary lymphoid organs, where serial stimulation delivered by the BCR and other pathways generates the young PF and possibly the DDF that, once in the blood, continues to age to the quiescent RF fraction. Combining CXCR4/CD5 with smIG/CD19 densities might better resolve the complexity of the time from last cell division in leukemic cells, thereby allowing better understanding of the underlyng biological mechanisms that give rise to subpopulations differing in biologic function and susceptibility to therapies. Since each cell within a clone appears to traverse these stages, the unique biologic features at each phase might represent novel processes for potential therapeutic targeting, alone or in combination.

Abstract ID: 1552406

Title: Sequencing of circulating tumour DNA reveals additional driver mutations in Richter transformation

Authors: Niamh Appleby, Sitara Akbar, Anthony Cutts, Hélène Dreau, Thomas Wenban-Smith, Melinda Kormany, Kieran Howard, Grigore-Aristide Gafencu, Kate Ridout, Dimitris Vavoulis, Rebecca Boucher, Nicola Jackson, Joseph A. Rogers, Francesca Yates, Aimee Jackson, Sonia Fox, Toby A. Eyre and Anna Schuh

Richter Transformation (RT, formerly Richter syndrome) is an aggressive, chemotherapy resistant high-grade B-cell lymphoma arising in CLL [1]. Highly sensitive sequencing of circulating tumour DNA (ctDNA) promises to allow representative detection of genomic features across nodal disease. As ctDNA captures tumour derived fragments from all sites of disease it offers the potential for simultaneous assessment of bone marrow, lymph node and circulating blood compartments in RT. Accurate measurements of disease bulk informs clinical prognosis, response assessment and treatment decisions. Quantification of ctDNA burden (measured as human genome equivalents) correlates with metabolic tumour volume by PET-CT in primary CNS lymphoma [2], classical HL [3], follicular lymphoma [4], mantle cell lymphoma [5] and DLBCL [6–8]. Pre-treatment ctDNA burden correlates with International Prognostic Index (IPI) in DLBCL [6,8], M-IPI in mantle cell lymphoma [9], and the German Hodgkin Study Group score in HL [3]. Significantly, pre-treatment ctDNA burden predicts clinical response to chemoimmunotherapy in DLBCL and HL [3,6–8]. Circulating tumour DNA remains underexplored in RT. The UK NCRI STELLAR trial is a prospective randomised trial for newly diagnosed DLBCL-type RT [9] The combination of acalabrutinib with R-CHOP in STELLAR is designed to obtain rapid disease control in this clinically aggressive lymphoma. The primary objective of the randomised study is comparison of progression free survival (PFS) between R-CHOP and R-CHOP plus acalabrutinib arms. The study includes two additional platforms for studying RT after chemoimmunotherapy (Cohort 1) and RT arising on BTKi treatment (Cohort 2). The primary outcome is ORR (complete response (CR) or partial response (PR)) for both platform cohorts. Plasma samples for ctDNA analysis are collected at enrolment, following each treatment cycle and for up to 72 weeks of follow-up. To date, forty patients (24M; 16F) provided plasma samples for ctDNA sequencing (Table 1). In this exploratory study, we interrogated pre-treatment tumour and plasma cell-free DNA from RT patients enrolled in STELLAR using a customised targeted next-generation

Table 1: Baseline features of the STELLAR participants (n=40)		
Demographics	Gender	24 Male
		16 Female
	Age (median, range)	71.5 years (39-84 years)
Clinical Stage	Stage I	1
	Stage II	8
	Stage III	5
	Stage IV	22
	Data missing	4
Blood parameters	Hb	122g/L (72-161g/L)
	Lymphocytes	$2.5x10^{\wedge}9$/L ($0.3-187x10^{\wedge}9$/L)
	Platelets	$140x10^{\wedge}9$/L ($24-760x10^{\wedge}9$/L)
Other parameters	Known to be *TP53* deleted/mutated at trial screening	7/40 (17.5%)
	B-symptoms	15/40 (37.5%)
	Bulky disease	16/40 (40%)

Figure 1: Circulating tumour DNA variants detected at baseline in STELLAR participants

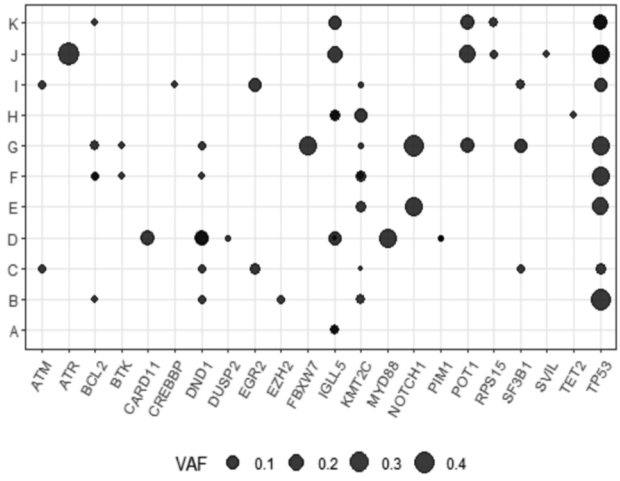

Legend: Plasma ctDNA variants detected at baseline by gene (x-axis) on a per participant basis (y-axis). The variant allele frequency (VAF) is illustrated by the size of the circle. Trial IDs are withheld as individual level participant data cannot be shared publicly for this ongoing trial.

sequencing panel enriched for CLL-driver genes. Tumour libraries and cell-free DNA libraries were sequenced to mean deduplicated depth of 139X (IQR 78.5–165X) and of 893X (IQR 331–1050X), respectively. Data analysis was performed using a custom bioinformatics pipelines developed at the Oxford Molecular Diagnostics Centre. Plasma ctDNA burden was calculated by multiplying the total plasma cell-free DNA concentration (pg/ml) by the median allele fraction of the variants detected on a per patient basis and reported on a log10 scale. Based on the pre-treatment samples from STELLAR001-STELLAR018, no relationship between ctDNA burden and presence of B-symptoms (wilcoxon, $p=0.8$), extranodal disease (wilcoxon, $p=0.19$), ECOG performance status (kruskal-wallis, $p=0.2$) and clinical stage (Kruskal–Wallis, $p=0.2$) was observed. Ten TP53 variants were detected in the ctDNA of eight STELLAR patients (2 patients had 2 mutations each). Two of these 8 participants were known to be TP53 mutated at screening. As STELLAR is an ongoing trial, data on baseline parameters only were provided by the Clinical Trials Research Unit, University of Birmingham. Further ctDNA sequencing is ongoing and results of the baseline ctDNA analysis of participants STELLAR019-STELLAR040 will be presented at IWCLL 2023.

Abstract ID: 1551047

Title: Single-cell RNA sequencing reveals the spatial heterogeneity in BTKi-resistant Richter transformation patients

Authors: Yeqin Sha, Shuchao Qin, Yi Miao, Yi Xia, Xiao Lu, Luomengjia Dai, Tonglu Qiu, Wei Wu, Lei Fan, Wei Xu, Hui Jin, Jianyong Li and Huayuan Zhu

Introduction: Richter transformation (RT) remains a clinical challenge with poor prognosis to standard treatment. The underlying mechanisms has not been fully disclosed yet, especially the spatial heterogeneity of tumor cells and immune microenvironment when progressed after novel targeted agents like Bruton's Tyrosine Kinase inhibitors (BTKi). Methods Single-cell RNA sequencing (scRNA-seq) of paired lymph node (LN) and peripheral blood (PB) was performed among 4 CLL patients and bioinformatics analysis was conducted. Patient 1 and Patient 2 were treated with BTKi (P1 ibrutinib for 3 months and P2 zanubrutinib for 19 months) and then progressed to RT. Patient 3 were initially diagnosed as aCLL and Patient 4 were treated with zanubrutinib for 54 months and then progressed to accelerated CLL (aCLL).

Results: 1. BTKi-resistant RT showed MYC targeted pathways activation and metabolic reprogramming, high proliferative cells enriched in LN showed downregulation of MHC class I. GSVA analysis showed significant activation of MYC targeted pathways and oxidative phosphorylation (OXPHOS) in RT. Trajectories of tumor cells were constructed and cells from PB were mainly distributed in the front of trajectories with the enrichment of G1 phase cells, while cells from LNs were mainly distributed in the terminal with S and G2M cells, indicating that the BTKi-resistant aggressive LNs were evolved from PB indolent CLL cells. The expression of MHC genes were displayed in these trajectories and showed gradual downregulation of MHC class I genes including HLA-A, HLA-B, HLA-C and HLA-E in those high proliferative cells, indicating that those BTKi-resistant proliferative cells escape from immune surveillance by the downregulation of MHC class I. 2. BTKi-resistant RT showed strengthened crosstalk between tumor and T cells, the activation of CD70-CD27 and LGALS9 (galectin-9)-HAVCR2 (TIM3) contributed to the enrichment of exhausted T cells in LN. Distribution of T cell subsets between PB and LN showed great spatial heterogeneity, especially in RT after BTKi progression. PB of all four patients showed relatively similar T cells distribution, with CD4+ naïve T cells and CD8+ effector memory T cells being two dominant clusters. However, LN of two RT patients displayed significant enrichment of CD8+ exhausted T cells while CD4+ naïve T cells were dominant cluster in LN of treatment-naïve CLL. Construction of cell-cell interaction displayed that RT showed significantly higher number of interactions with T cell subsets than treatment-naïve CLL, especially the interactions with CD8+ effective and exhausted T cells. Further analysis of

receptor-ligand interactions between T cell subsets and tumor cells were conducted and activation of CD70–CD27 and LGALS9 (galectin-9)-HAVCR2 (TIM3) were found between BTKi-resistant tumor cells and CD8+ effective and exhausted T cells, indicating the underlying mechanism contributing to immune escape of RT. 3. Spatial distribution of CD8+ exhausted T cells showed great heterogeneity, with terminally enhausted T cells specifically enriched in LN. Monocle 2 analysis showed the evolutionary trajectories of T cells subsets. CD8+ naïve T cells were distributed in the initial point of the evolutionary trajectories while CD8+ exhausted T cells showed heterogeneous evolution, with two different evolutionary trajectories in the terminal points. The heterogeneity of CD8+ exhausted T cells were further explored and we found four clusters of exhausted T cells manifesting heterogeneous characteristics. Herein, exhausted CD8+ T cells in PB were mostly Cluster 1, showing highest cytotoxicity and lowest exhausted feature. Cluster 2 was distributed scantly in PB while mostly in LN, showing highest cycling and proliferation score. Cluster 3 was LN specific exhausted T cells, showing highest exhausted score and lowest cytotoxicity score, indicating its terminally exhausted characters.

Conclusion: This study disclosed the spatial heterogeneity of tumor and immune microenvironment between PB and LN among BTKi-resistant RT patients. High proliferative tumor cells enriched in LN showed downregulation of MHC class I and strengthened crosstalk with T cells, contributing to T cell exhaustion and immune escape through the activation of CD70-CD27 and LGALS9-HAVCR2 crosstalk. In summary, we proposed the possible immune escape mechanism of proliferative LN progression under BTKi-resistant treatment and provide novel treatment targets to overcome the drug resistance.

Abstract ID: 1551637

Title: T cell type abundance and gene expression patterns in the context of clinical progression of treatment-naïve CLL/MBL patients from the OxPLoreD study

Authors: Grigore-Aristide Gafencu, Niamh Appleby, Charlotte Rich-Griffin, Kyla Dooley, Holm Uhlig, Calliope Dendrou, Dimitris Vavoulis and Anna Schuh

Background: Chronic lymphocytic leukaemia (CLL) is a B-cell neoplasm preceded by an asymptomatic precursor phase, monoclonal B-cell lymphocytosis (MBL). The Oxford Premalignant Lymphoproliferative Disorders (OxPLoreD) study (REC 19/SC/0065; NCT04023747) is a national prospective study of people with MBL/Stage A CLL or high-risk MGUS exploring the genomic and immunological features of progression to cancer. Malignancy progression may be mediated by the expansion of one or more subclones with distinct gene expression and/or mutation profile [1] as well as non-tumour cells in the peripheral blood [2].

Methods: Through a joint venture between OxPLoreD and the CARTOGRAPHY strategic collaboration between Oxford

Fig.1 A

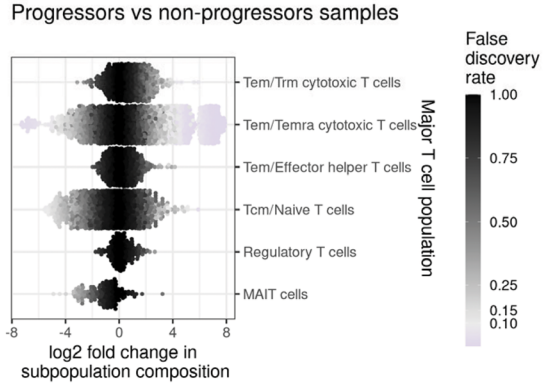

Fig.1 B

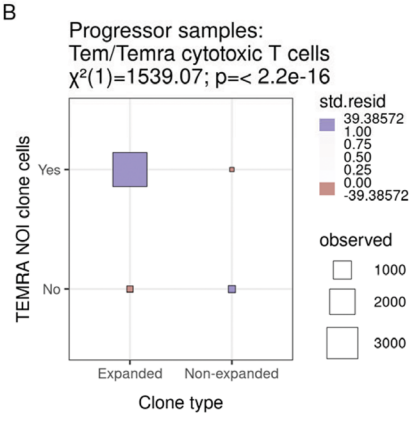

Fig.2 A

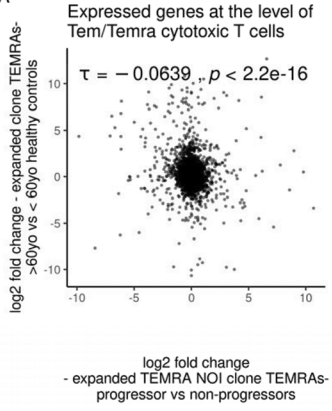

Fig.2 B

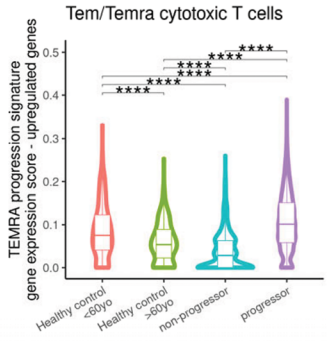

Fig.2 C

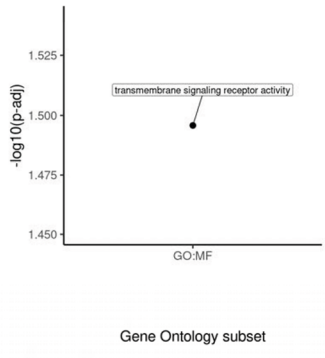

University and Janssen Immunology, the peripheral blood of six OxPLoreD early MBL/CLL patients as well as three aged matched (>60yo) and three younger (median age 24) healthy control samples from the CARTOGRAPHY project was analysed using combined cellular indexing of transcriptomes and epitopes by sequencing (CITE-seq) [3], and single cell B-cell (BCR) & T-cell (TCR) receptor sequencing, as implemented by 10× Genomics. We provide a proof-of-concept of this type of single cell, multi-omic profiling in this disease and investigate the gene expression & clonality patterns that are associated with clinical progression of pre-malignancy.

Results: Preliminary results of the CITE-seq data analysis revealed terminally differentiated T effector memory cells (TEMRAs) subpopulations or cellular neighbourhoods of interest (NOI) in the lower dimensionality gene expression space of the CITE-seq dataset T cell-rich subset that were more abundant in cells from the peripheral blood samples of individuals with treatment naïve MBL/CLL taken up to 2 years prior to clinical progression compared to their non-progressing counterparts (Figure 1(A)). An ongoing analysis of the TCR repertoire in MBL/Stage A CLL shows that at the level of the TEMRAs of progressors, clones that contain TEMRAs from the previously highlighted populations (TEMRA NOI clones) are expanded more frequently than clones containing other TEMRA subpopulations (Figure 1(B)). The gene expression patterns observed while comparing TEMRAs of expanded TEMRA NOI clones from progressors versus non-progressors were not strongly correlated with the ones observed while investigating TEMRAs part of expanded clones from aged-matched vs. younger healthy control samples (Figure 2(A)). A TEMRA CLL/MBL progression gene expression signature (Figure 2(B)) was derived from studying the TEMRAs of the TEMRA NOI clones in the context of both CLL/MBL and healthy aged-matched samples with elements of this signature being broadly associated with transmembrane signalling receptor activity (Figure 2(C)).

Conclusions: These initial results hint at TEMRAs as a population that could be directly or indirectly involved in the clinical progression of pre-malignancy. Though TEMRAs have been associated with the process of immunological ageing [4], the TEMRAs from individuals with MBL/Stage A CLL who subsequently progressed to needing treatment have a distinct transcriptomic profile from those of aged-matched healthy elderly controls, particularly at the level of the expanded clones. Further analysis of TCR repertoires of additional individuals is needed and could potentially elucidate if there is a CLL-directed T cell response and how this relates to CLL prognosis.

Abstract ID: 1546705

Title: The PKCβ inhibitor MS-553 displays pre-clinical efficacy in BTK inhibitor resistant chronic lymphocytic leukemia

Authors: Britten Gordon, Elizabeth Muhowski, Janani Ravikrishnan, Shanmugapriya Thangavadivel, Samon Benrashid, Alexander He, Shrilekha Misra, Tzung-Huei Lai, Alexander Marr, Brandi Walker, Elizabeth Perry, Nicole Grieselhuber, Kerry Rogers, James Blachly, Adam Kittai, Seema Bhat, John Byrd, Michael Niesman, Kai Zhang, Deepa Sampath and Jennifer Woyach

Background: Treatment of chronic lymphocytic leukemia (CLL) has been revolutionized through usage of targeted therapies against the B-cell receptor (BCR) signaling cascade, specifically BTK. However, resistance to BTK inhibition has occurred through acquisition of various mutations in BTK or its immediate downstream signaling partner, PLCγ2 [1,2]. Clinical outcomes for these patients are quite poor, emphasizing the need for alternative therapeutics. Despite the presence of these mutations, BCR signaling remains intact, suggesting that targeting molecules downstream of BTK may be effective. Protein kinase C-β (PKCβ) is a downstream component of the BCR pathway that has been shown to be over-expressed in CLL. Moreover, PKCβ has been shown to be essential to the development of CLL in the Eμ-TCL1 mouse model and its expression in stromal cells to be required for the survival of leukemic B-cells [3–5]. This suggests that signaling through PKCβ, in both CLL cells and cells in the microenvironment, is essential to promote leukemogenesis. MS-553 is a potent, ATP competitive, reversible inhibitor of multiple PKC isoforms including PKCβ.

Methods: Primary CLL cells were isolated by negative selection and treated with up to 5 μM MS-553. Cell viability was assessed via Annexin V/PI with and without HS-5 stromal cell co-culture. BCR and canonical WNT signaling changes were evaluated by change in target protein phosphorylation or total protein by immunoblot following drugging. Changes in downstream NFκB and WNT signaling were interrogated by RT-qPCR. Using genetically modified TMD8 cells that express only C481S or T474I mutated BTK, we determined MS-553's effect on cell-viability and BCR signaling. *In vivo* survival studies were performed using the Eμ-MTCP1 mouse model, which is an aggressive model of CLL, with subsequent randomization into vehicle or MS-553 treatment arms [6]

Results: Following 72 hours of drugging, 5 μM MS-553 displayed modest cytotoxicity against primary CLL cells both alone ($p<0.0001$, $n=8$) and in the presence of HS-5 stromal cells ($p=0.0008$, $n=8$). At 24 hours, 5 μM MS-553 inhibited downstream BCR and WNT signaling in primary CLL cells,

Figure 1

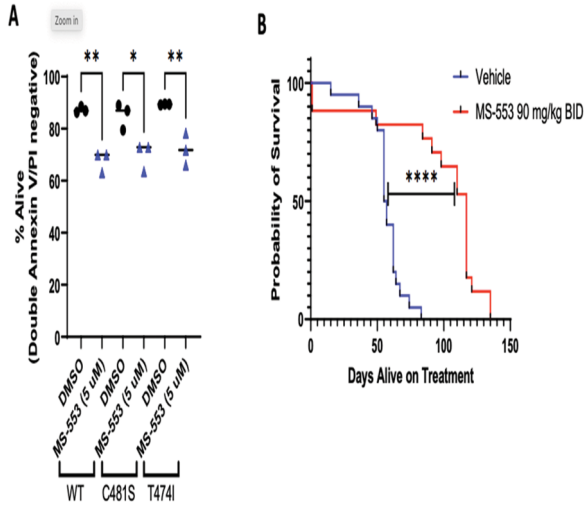

demonstrated by reduced phosphorylation of PKC-β ($p=0.0024$, $n=15$) and several of its downstream targets including pGSK3β ($p<0.0001$, $n=15$), pIκBα ($p<0.0001$, $n=15$), and pERK ($p=0.0301$, $n=15$), and reduced total protein of β-Catenin ($p<0.0001$, $n=9$), Cyclin D2 ($p=0.0375$, $n=9$), and cMyc ($p=0.0031$, $n=9$) compared to vehicle treated, stimulated samples. In patient samples, mRNA expression of WNT pathway targets BCL-2, OCT-2, BFL-1, MYC, CD40, Cyclin D1, and Cyclin D2 were all decreased after 48 hours of treatment with 1 or 5 μM MS-553. MS-553 also showed efficacy in the presence of BTK mutations: viability in TMD8 cells was reduced following 72-hour drugging with MS-553 regardless of BTK mutational status ($p<0.05$) (Figure 1(A)): *0.05 ≥ p ≥ 0.01: **0.01≥p ≥ 0.001). Inflammatory cytokine production by CLL cells is inhibited by MS-553 through its ability to decrease CCL3 and CCL4 cytokine expression in WT and mutant BTK-harboring TMD8 cells ($p<0.001$, $n=3$). As proof of concept, we examined MS-553's efficacy *in vivo*, and found a significant reduction in disease progression and increase in survival (median 117 days) when compared to vehicle control (median 56 days, $p<0.0001$) (Figure 1(B)).

Conclusion: Our data demonstrate the efficacy of the PKCβ inhibitor MS-553 in preclinical models of CLL, including BTK inhibitor resistant disease. These findings support continued preclinical and clinical investigation of MS-553 in CLL, and the phase 1 trial of this agent is currently underway (NCT03492125) [7].

Abstract ID: 1552680

Title: Toll-like receptor 9 signalling in CLL: a resistance mechanism to B-cell receptor-targeted treatments, and a potential tool for therapeutic stratification

Authors: Emma Kennedy, Lauren Stott, Eleanor Jayawant, Rosalynd Johnston, John Jones, Eleni Ladikou, Iona Ashworth, Valter Gattei, Antonella Zucchetto, Simon Mitchell, Chris Pepper and Andrea Pepper

Background: CLL cell trafficking to secondary lymphoid tissues is fundamental to disease progression, since within these protective niches, CLL cells encounter an abundance of activating, pro-proliferative and pro-survival signals. The primary mechanism of CLL cell activation is via the B-cell receptor (BCR)-signalling pathway, and BCR-targeted treatments are extremely effective at releasing tissue-resident cells into the peripheral blood and inducing apoptosis. Despite these successes, currently available agents fail to achieve complete tumour clearance, and CLL remains incurable. Toll-like receptor 9 (TLR9) is an intracellular pattern recognition receptor, which responds to unmethylated CpG motifs in bacterial/viral/mitochondrial DNA. We recently showed unmethylated DNA levels are 28-fold higher in CLL patient plasma relative to healthy controls, and that TLR9-ligation induces an NF-κB and STAT3-driven activation/migratory phenotype in primary CLL cells [1]. We hypothesise TLR9 signalling is a BCR-independent contributor to CLL homing and potential resistance mechanism to BCR-targeted agents.

Results: In a cohort of 74 primary CLL samples, a dichotomous migratory response was observed in response to the TLR9 agonist ODN 2006. 53% showed an increase in CLL cell migration (categorised as 'Responders'[R]), whilst 47% showed either no change or a decrease (categorised as 'Non/Reverse Responders'[NR/RR]). There was a significant (but not exclusive), correlation with mutational status, with 71 vs. 33% of M-CLL vs. U-CLL samples being categorised as R, respectively ($p=0.03$, $n=48$), and no correlation was found between CD49d + ve vs. CD49d-ve or CD38 + ve vs. CD38-ve samples. Surprisingly, there was no significant difference in total TLR9 expression between R and NR/RR samples ($p=0.23$, $n=45$), and ODN 2006 stimulation induced TLR9 signalling in both subgroups. Post-stimulation, IRAK1 and IκBα were degraded in R ($n=4$) and NR/RR ($n=3$) and the activation marker CD69 was equally upregulated in each subgroup ($p<0.0001$, $n=34$ and $p<0.0001$, $n=28$, respectively). This indicates the observed dichotomous migratory response is due to downstream signalling divergence, as opposed to a complete lack of response to stimulation. Previous studies have shown constitutive BCR activation to be heterogeneous in CLL, and generally elevated in U-CLL relative to M-CLL [2]. We hypothesised that the most basally activated CLL cells may reach their maximal activation/migratory capacity through BCR-signalling-alone, rendering them non-responsive to further external stimuli. This is supported by our finding that NR/RR have significantly lower basal CD5 ($p=0.02$, $n=54$), and significantly higher NF-κB p-p65 ($p<0.01$, $n=12$) and MCL-1 ($p=0.03$, $n=16$). Using *in-silico* modelling, we simulated TLR9 activation in states of low/high basal BCR activity, using canonical NF-κB activity as a functional read-out. Our model showed cells with low basal activation responded strongly to TLR9 stimulation, whilst cells with high basal activation were unresponsive. These results were verified *in-vitro* as basal p-BTK and p-p65 (representative of constitutive BCR activation) showed negative correlation with the migratory response to ODN 2006 in the NR/RR subgroup ($p<0.01$, $R=-0.91$, $n=8$ and $p=0.02$, $R=-0.93$, $n=5$, respectively); these data indicate constitutive signalling impairs the ability of NR/RR samples to respond to alternative stimuli. Interestingly, we found responsiveness to ODN 2006 (migration) correlated strongly with responsiveness to IgM (p-BTK expression) ($p=0.03$, $R^2=0.33$, $n=14$), signifying that this trend is not TLR9-specific, but extends to other microenvironmental interactions. Importantly, when simulating NR/RR treatment with a BTK inhibitor *in-silico*, we observed a renewed responsiveness to TLR9 activation, which was later verified *in-vitro*. In the presence of the BTK-inhibitor ibrutinib, we found a subset of previously non-responsive NR/RR samples became 'sensitised' to TLR9 activation, showing an increase in CLL cell migration in response to stimulation with ODN 2006. This suggests a switch from BCR to TLR9 signalling in some NR/RR samples and implicates TLR9 signalling as a tumour escape mechanism following BTKi therapy. We hypothesise that TLR9 'responder' and 'sensitised' subgroups may benefit from BCR/TLR dual targeted therapy. We are currently investigating NF-κB as a potential therapeutic target to simultaneously inhibit BCR/TLR9 signalling. Whilst pan NF-κB inhibitors have proven extremely toxic (*in-vivo*), we are opting for a more streamlined subunit-specific approach. We are working to create patient-specific NF-κB 'fingerprints' (i.e. subunit expression profiles), to ascertain whether different subgroups show targetable differences in NF-κB subunit expression. Early analyses suggest fingerprints to be distinct between R and NR/RR samples, rendering this technique a potential tool for personalising future NF-κB-targeted therapies.

Abstract ID: 1549277

Title: Transcription factor FoxO1 mediates adaptive increase in Akt activity and cell survival during BCR inhibitor therapy in CLL

Authors: Marek Mraz, Laura Ondrisova, Vaclav Seda, Eva Hoferkova, Giorgia Chiodin, Krystof Hlavac, Lenka Kostalova, Gabriela Mladonicka Pavlasova, Daniel Filip, Pedro Faria Zeni, Jan Oppelt, Anna Panovska, Karla Plevova, Sarka Pospisilova, Martin Šimkovič, Filip Vrbacký, Daniel Lysak, Stacey Fernandes, Matthew Davids, Alba Maiques-Diaz, Stella Charalampopoulou, Jose Martin-Subero, Jennifer Brown, Michael Doubek, Francesco Forconi and Jiri Mayer

Background: Genetic resistance mechanisms to BCR inhibitors in CLL have been extensively described, but it remains unclear whether non-genetic adaptation might exist in CLL cells allowing for lasting lymphocytosis or resistance. We focused on the possible role of the Akt pathway in adapting to BCR inhibitors since, in mouse models, PI3K-Akt activation is the only known factor that rescues the apoptosis induced by BCR deletion in mature B cells [1].

Methods: We performed transcriptome profiling (Illumina) and analyzed samples obtained from CLL patients before and during ibrutinib or idelalisib therapy ($n=70$) and performed gene editing in MEC1 cells to reveal the FoxO1/Rictor functional role.

Results: We observed that Akt phosphorylation (S473) is induced above pre-therapy levels in ~70% of CLL patients treated with ibrutinib within the first 3 months of therapy ($n=31$; $p=0.016$; Figure 1(A)), and an additional 10% of patients had stable pAkt[S473] levels. Similarly, pAkt[S473] increased in 55% of patients treated with single-agent idelalisib ($n=11$). pAkt[S473] was also restored in ibrutinib-treated MEC1 cells, where after an initial drop in Akt phosphorylation, its levels were induced by >10 folds ($p<0.05$). Importantly, CLL cases with pAkt[S473] induction had a significantly higher lymphocytosis on ibrutinib *in vivo* (month 1 and 3, $p<0.05$), and cells obtained during ibrutinib therapy were highly sensitive to Akt inhibitor MK2206 (80% apoptosis, Figure 1(B)). To decipher mechanisms leading to Akt activation, we performed RNA profiling of paired CLL samples obtained before and during ibrutinib ($n=22$) or single-agent idelalisib ($n=18$) therapy. This identified 16 differentially expressed mRNAs (overlap of both drugs) involved in the PI3K-Akt pathway. Rictor induction was particularly notable since it is an essential assembly protein for mTORC2, which phosphorylates Akt on S473 [2]. Rictor was also increased on protein level ($n=39$, $p=0.02$ for

Figure 1

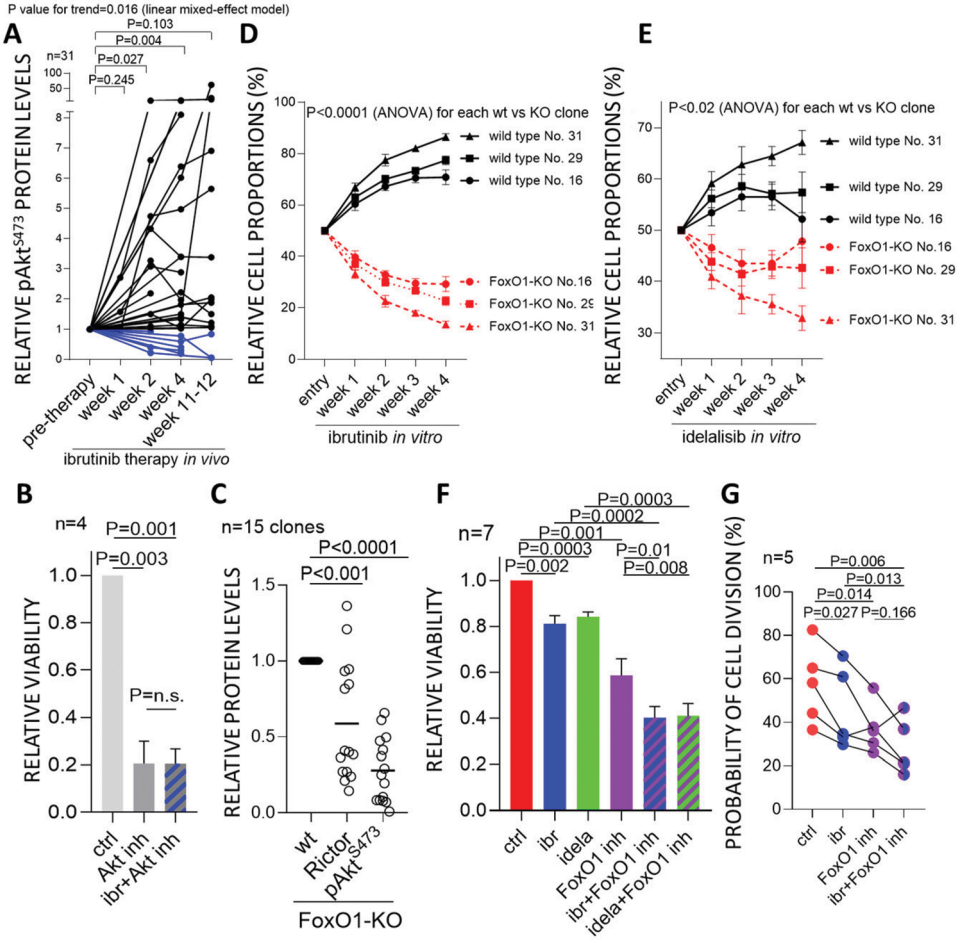

Figure 2

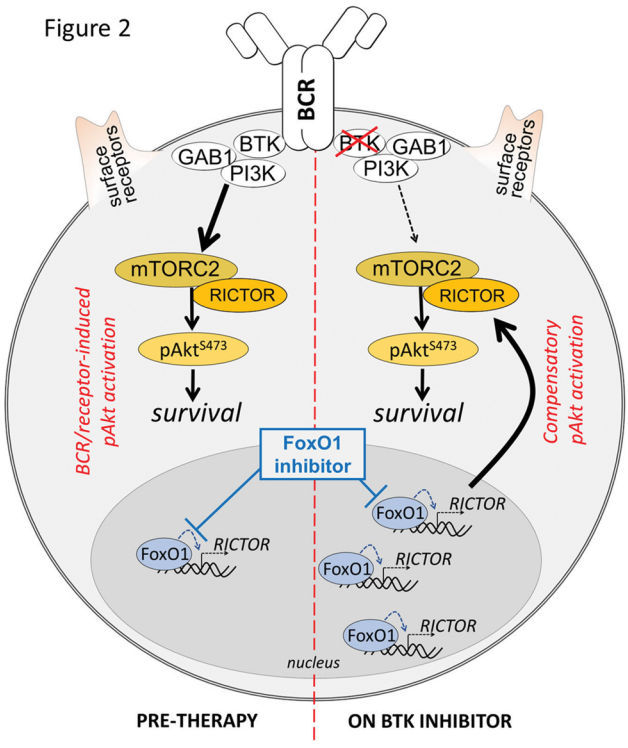

ibrutinib; $n=9$, $p=0.027$ for idelalisib). RICTOR knock-out in MEC1 or inhibition of mTOR led to a dramatic decrease in basal pAkt[S473] levels as well as ibrutinib-induced pAkt[S473]. RNA sequencing of primary samples obtained during therapy revealed that levels of transcription factor FoxO1 were upregulated during BCR inhibitor treatment ($n=31$, $p=0.005$ for ibrutinib; $n=9$, $p=0.002$ for idelalisib), which attracted our attention since FoxO1 has been previously shown to activate Rictor in renal cells. Analysis of genome-wide FoxO1 binding (Cut&Run) revealed a clearly increased binding to RICTOR promotor in ibrutinib-treated MEC1 cells, and overall increased binding across the genome (1,190 FoxO1-bound regions in vehicle-treated cells vs. 3,354 regions in ibrutinib-treated cells). Genome-editing experiments and treatment with FoxO1 inhibitor (AS1842856, 0.5 μM) revealed that transcription factor FoxO1 is directly responsible for Rictor/pAkt[S473] activation during ibrutinib and idelalisib treatment. Knock-out of FoxO1 in the MEC1 cell line in 15 independent FoxO1 knock-out MEC1 clones led to a 70% decrease in pAkt[S473] levels ($p<0.0001$) and a 40% decrease in Rictor levels ($p<0.001$; Figure 1(C)). Moreover, FoxO1 knock-out cells had a growth disadvantage in a competitive growth assay in the presence of ibrutinib or idelalisib (Figure 1(D,E)). This suggests that the FoxO1-Rictor-pAkt[S473] axis does not require BTK or PI3Kδ activity. FoxO1 inhibitor decreased basal, anti-IgM-induced, and ibrutinib-induced pAkt[S473] levels. Furthermore, FoxO1 inhibitor (0.5 μM) induced apoptosis alone (~40% CLL cell killing) or more potently in combination with ibrutinib or idelalisib (~60% apoptosis; $n=7$, Figure 1(F)). FoxO1 inhibitor also blocked the proliferation of primary CLL cells induced by T-cell factors in vitro (CD40L + IL21 + IL4), and the effect was even more potent in combination with ibrutinib (Figure 1(G)).

Conclusion: Overall, we describe for the first time that the FoxO1-Rictor-pAkt[S473] axis is involved in acute non-genetic adaptation to BCR inhibitors and CLL lymphocytosis during therapy (Figure 2) and suggest that FoxO1 is a potential novel therapeutic target. It has been previously shown that Akt activity is a driver of Richter transformation [3]. It is plausible that increased pAkt[S473] levels during that BCR inhibitor therapy might accelerate the transformation, and this is the subject of ongoing experimental work.

Abstract ID: 1498877

Title: XPO1 mutations identify early stage CLL characterized by shorter time to first treatment and enhanced BCR signaling

Authors: Riccardo Moia, Donatella Talotta, Lodovico Terzi di Bergamo, Riccardo Bomben, Gabriela Forestieri, Valeria Spina, Alessio Bruscaggin, Chiara Cosentino, Mohammad Almasri, Riccardo Dondolin, Tamara Bittolo, Antonella Zucchetto, Stefano Baldoni, Ilaria del Giudice, Francesca Romana Mauro, Rossana Maffei, Annalisa Chiarenza, Agostino Tafuri, Roberta Laureana, Maria Ilaria del Principe, Francesco Zaja, Giovanni D'Arena, Jacopo Olivieri, Silvia Rasi, Abdurraouf Mahmoud, Wael Al Essa, Bassel Awikeh, Sreekar Kogila, Matteo Bellia, Samir Mouhssine, Paolo Sportoletti, Roberto Marasca, Lydia Scarfò, Paolo Ghia, Valter Gattei, Robin Foà, Davide Rossi and Gianluca Gaidano

Background: The XPO1 gene, which codes for a nuclear exportin responsible for the partitioning of macromolecules essential for cell homeostasis, represents one of the chronic lymphocytic leukemia (CLL) driver genes. In cases of XPO1 mutations a negatively charged glutamic acid at position E571 is substituted with a positively charged lysine, thus promoting XPO1 interaction with proteins bearing a negatively charged nuclear export signals (NES). Most of newly diagnosed CLL patients do not require therapy initially and are managed with a watch and wait strategy. CLL is characterized by a high grade of molecular heterogeneity and the analysis of gene mutations may further improve the stratification of time to first treatment (TTFT).

Aims: To evaluate the transcriptomic and the epigenomic profile of XPO1 mutant CLL and the correlation of XPO1 mutations with TTFT.

Methods: CAPP-seq mutational analysis was performed targeting the most frequently mutated genes in CLL. Results were correlated with TTFT. CD19+/CD5+ tumoral cells from 8 XPO1 mutated patients were sorted for RNA-seq and ATAC-seq. Fifteen XPO1 wild type cases, matched for IGHV status, TP53 status and FISH karyotype, were analyzed for comparative purposes.

Results: By principal component analysis of ATAC-seq, XPO1 mutated CLL showed a distinct chromatin accessibility compared to wild type cases. Chromatin regions more accessible in XPO1 mutated CLL were enriched in binding sites for transcription factors downstream to the B cell receptor (BCR), including NF-kB signaling, p38-JNK, RAS-RAF-MEK-ERK (Figure 1(A)). By RNA-seq, 236 genes were

upregulated, and 296 genes were downregulated in XPO1 mutated CLL compared to wild type cases. Upregulated pathways included immediate early response, TGFβ and EGF-EGFR signaling, FOSB gene expression and MAPK regulation through DUSP. By combining epigenomic and transcriptomic data, MIR155HG, the miR-155 host gene, and MYB, the transcription factor that positively regulates MIR155HG, were upregulated by RNA-seq and their promoters were more accessible by ATAC-seq. MYB induces miR-155 expression that, in turns, inhibits SHIP1 thus potentially enhancing the BCR cascade. Consistently, an inverse correlation was found between MIR155HG and SHIP1 levels (Figure 1(B)). As XPO1 mutated CLL are conceivably characterized by a high proliferative behavior, we asked if XPO1 mutated CLL patients are characterized by a more aggressive clinical course in terms of TTFT. A training validation design was used for the analysis. In the training cohort (Nf276 Rai 0/I patients), XPO1 mutations associated with shorter TTFT (at 10 years 0% in XPO1 mutated and 69.8% in wild type patients $p<0.0001$) (Figure 1(C)). Superimposable results were observed in two independent cohorts composed of 286 Binet A patients (at 6 years 25.0% in XPO1 mutated and 61.3% in wild type patients, p value =0.025) (Figure1(D)) and 395 Rai 0 patients (at 7 years of 0% in XPO1 mutated patients and 73.4% in wild type patients, p value <0.0001) (Figure1(E)). In addition, XPO1 mutations maintained their prognostic value independently of IGHV status and of variables that build the prognostic models predicting TTFT in early stage CLL, namely IPS-E (Table 1) and Rai 0 prognostic model (Table 2).

Conclusions: These data suggest that XPO1 mutations, conceivably through increased miR-155 levels, may enhance

Table 1. Multivariate analysis for *XPO1* mutations and IPS-E variables

Variable	HR	95% C.I.	p value
Unmutated IGHV	3.60	2.18-5.96	<0.0001
Palpable lymph nodes	2.71	1.63-4.70	<0.001
Lymphocyte >15,000/μL	2.49	1.50-4.11	<0.001
XPO1 mutations	2.79	1.16-6.71	0.022

HR, Hazard Ratio; CI, Confidence Interval; IGHV, immunoglobulin heavy chain variable

Table 2. Multivariate analysis for *XPO1* mutations and Rai 0 prognostic score variables

Variable	HR	95% C.I.	p value
WBC > 32,000/μL	2.73	1.08-6.38	0.033
Unmutated IGHV	4.00	2.37-6.76	<0.0001
Del 17p	1.63	0.49-5.42	0.493
Tris 12	1.68	0.89-3.13	0.104
Del 11q	0.78	0.28-2.20	0.641
XPO1 mutations	3.56	1.48-8.59	0.005

HR, Hazard Ratio; CI, Confidence Interval; WBC, white blood cells; IGHV, immunoglobulin heavy chain variable

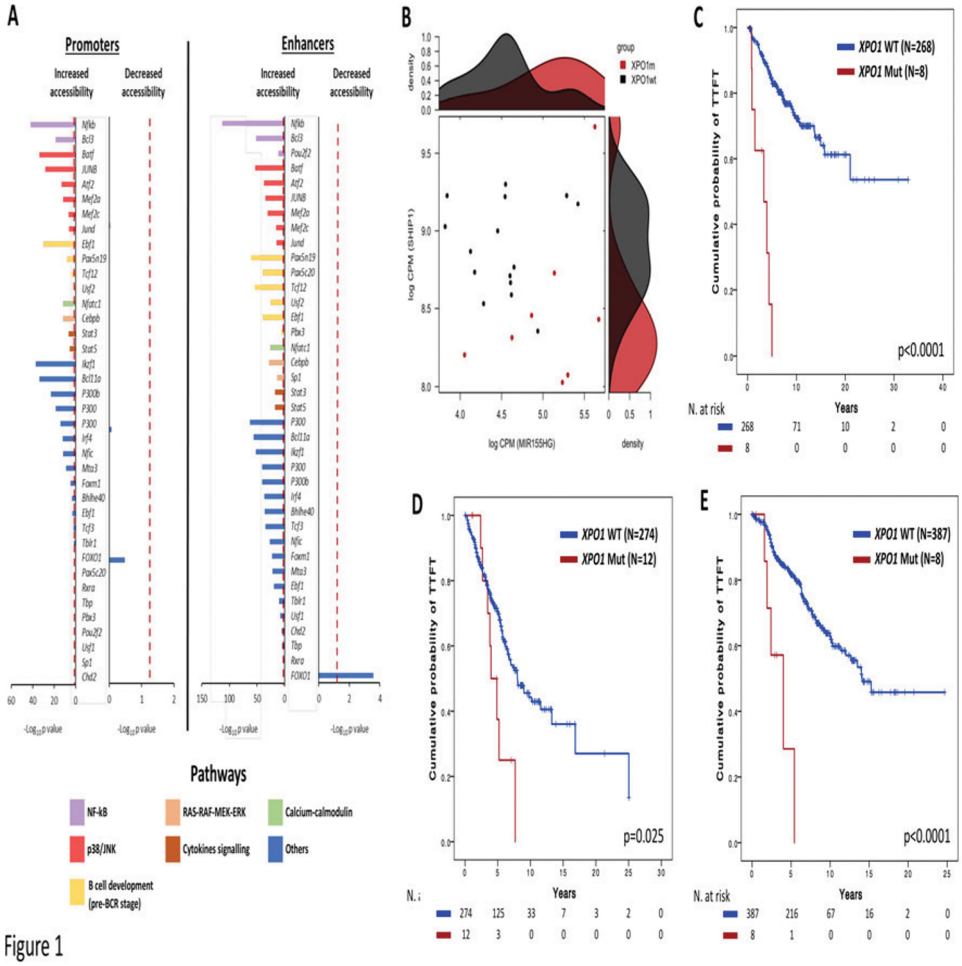

Figure 1

BCR signaling leading to higher proliferation and shorter TTFT in early stage CLL.

Abstract ID: 1549217

Title: Non-hematological autoimmune disorders are frequent in CLL, but are they clinically related? Data from a single-center real-life cohort

Authors: Miguel Arguello-Tomas, Nil Albiol, Paola Jara, Alba Mora, Jordi Sierra, Esther Moga and Carol Moreno

Background: Chronic lymphocytic leukemia (CLL) is marked by severe immune dysfunction, which results in an increased risk of autoimmune disorders (AID). The association of autoimmune cytopenia (AIC) with CLL has been extensively studied. However, there is little information about its relationship with other non-hematologic autoimmune complications.

Aims: To describe the prevalence and characteristics of patients with CLL spectrum (CLL, small lymphocytic lymphoma, and monoclonal B-cell lymphocytosis) and non-hematologic AID. The secondary objective was to ascertain differences in clinical and prognostic features between AIC and non-hematologic AID groups.

Methods: We included 712 patients with CLL from the historical database of our center. The medical records were retrospectively reviewed to identify any AID diagnosis. AID were categorized based on the American Autoimmune

Table 1. Characteristics of patients with chronic lymphocytic leukemia and autoimmune disorders. Quantitative variables are presented as median (range). Qualitative variables are shown as n (%). CLL = chronic lymphocytic leukemia; SLL= Small lymphocytic lymphoma; MBL= Monoclonal B-cell lymphocytosis; AID= Autoimmune disorder. FISH, fluorescence in situ hybridization; SCT, stem cell transplantation; ns = not significative; BTKi Bruton's tyrosine kinase inhibitors; BCL2i BCL2 inhibitors.

	AIC (n=45)	Non-hematologic AID (n=87)	P *
Age at CLL diagnosis, years (range)	67 (47.3-93.9)	69.5 (43.8-95.8)	ns
Age at AID diagnosis, years (range)	71.4 (54.2-93.6)	68 (15.2-97.5)	ns
Sex, male	31 (55.4%)	34 (39.1%)	0.001
Diagnoses: CLL; SLL; MBL	48 (85.7%); 4 (7.1%); 4 (7.1%)	72 (82.8%); 8 (9.2%); 7 (8%)	Ns
Rai stage at diagnosis			
0	38 (67.9%)	63 (72.4%)	Ns
I-II	12 (21.4%)	17 (19.5%)	
III-IV	6 (10.8%)	7 (8%)	
Binet stage at diagnosis			Ns
A	40 (71.4%)	74 (85.1%)	
B	9 (16.1%)	6 (6.9%)	
C	7 (12.5%)	7 (8%)	
IGHV unmutated, n (%)	25/45 (55.6%)	22/61 (36.1%)	0.02
FISH Alterations n (%)			Ns
del(11q)	7/49 (14.3%)	6/71 (6.9%)	
+12	13/49 (26.5%)	16/71 (18.4%)	
del(13q)	18/49 (36.7%)	29/72 (33.3%)	
del(17p)	6/49 (12.2%)	9/72 (12.5%)	
Complex karyotype	5/23 (21.7%)	11/50 (22%)	Ns
***TP53* mutated, n(%)**	1/21 (4.8%)	1/46 (1.1%)	Ns
Temporal relationship between diagnoses and AID			Ns
CLL diagnosis prior to AID	37/56 (66.1%)	38/87 (43.9%)	
Concomitant	18/56 (33.9%)	3/87 (3.5%)	
AID prior to CLL	1/56 (1.8%)	46/87 (52.6%)	
Need therapy for AID	56/56 (100%)	66/87 (75.9%)	Ns
Use of corticosteroids, n(%)	34/56 (60.7%)	15/66 (22.7%)	-
Need therapy for CLL	40/56 (82.1%)	32/87 (36.8%)	0.01
Treatment for CLL, type			Ns
Alkylating agents	10/40 (25%)	14/32 (43.8%)	
Purine analogues	7/40 (17.5%)	13/32 (40.6%)	
Chemoimmunotherapy	13/40 (32.5%)	23/32 (71.9%)	
Targeted therapies	13/40 (32.5%)	12/32 (37.5%)	

Figure 1. Overall survival of patients with CLL without AID (green), non-hemic AID (red), and AIC (blue). CLL = chronic lymphocytic leukemia; AID= Autoimmune disorder; AIC= Autoimmune cytopenia, OS = Overall survival.

Median OS: AIC 10.9 y (8.9-12.8); Non-hemic AID 13.9 y (12.9-14.8); No AID 13.9 years (12.8-15).

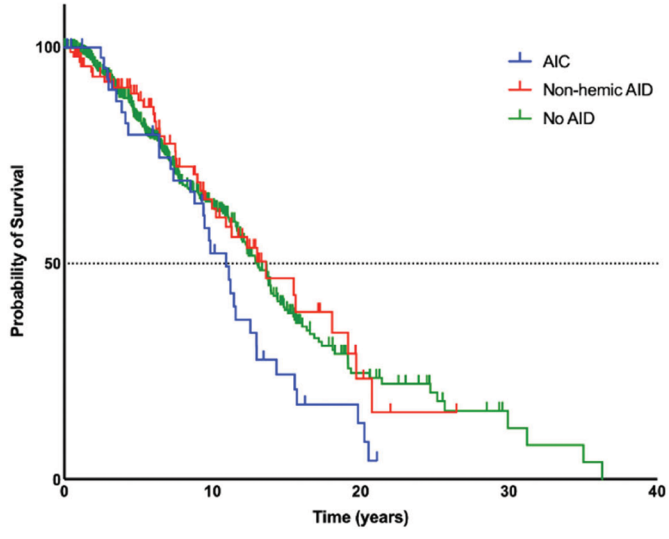

No AID	580	350	183	106	44	23	14	8	3	2	1
Non-hemic AID	87	66	41	24	11	5	2	1	0	0	0
AIC	45	34	27	13	6	4	1	0	0	0	0

Related Diseases Association classification. Those patients with both AIC and non-hematologic AID were included into the AIC group.

Results: The main characteristics of patients with CLL and AID are shown in Table 1. After a median follow-up of 6.4 years (0.1–36.4), 87/712 (12.2%) presented non-hematologic AID, and 45/712 (6.3%) showed AIC; 11/712 (1.5%) had both AIC and a non-hematologic AID. In the non-hematologic AID group, endocrine disorders were the most frequent (48.3%; 42/87), followed by dermatological AID (33.3%; 29/87; including 5 patients with paraneoplastic pemphigus), and other AID such as rheumatoid arthritis (6.9%; 6/87), vasculitis (5.7%; 5/87), and neuromuscular syndromes (6.9%; 6/87). As diseases, the most observed non-hematologic AID were autoimmune hypothyroidism ($n=41$), psoriasis ($n=17$), rheumatic polymyalgia ($n=7$), rheumatoid arthritis ($n=6$), and pemphigus ($n=5$). Most patients (51/87; 58.6%) presented the non-hematologic AID before CLL diagnosis, with a median time of - 1.3 years (−45.8 – 15.9). We found a significant association between AIC and the presence of poor biological variables (e.g. unmutated IGHV), and anti-CLL therapy. In contrast, female gender was the only variable significantly associated with non-hematologic AID. Prognostically, patients with CLL and AIC had shorter OS than those with non-hematologic AID (median 10.9 vs. 13.9 years; $p=0.002$) (Figure 1).

Conclusion: In our series, 12.2% of patients with CLL presented non-hematologic AID, the endocrine disorders being the most frequent. The presence of non-hematologic AID was not associated with CLL adverse features and these patients had the same prognosis as those with CLL without autoimmunity. In contrast, AIC was linked to the presence of poor biological features and had a negative impact on patients' outcomes. Moreover. non-hematologic autoimmune disorders do not appear to be more frequent in CLL than in the general population, albeit the challenges they can pose in the management of patients with CLL should not be dismissed.

Abstract ID: 1509035

Title: XPO1 inhibitor selinexor induces heme oxygenase-1 mediated p53-dependent ferroptosis in chronic lymphocytic leukemia

Authors: Jiazhu Wu, Bihui Pan, Zhangdi Xu, Jiale Zhang, Yue Li, Jinhua Liang, Li Wang, Jianyong Li and Wei Xu

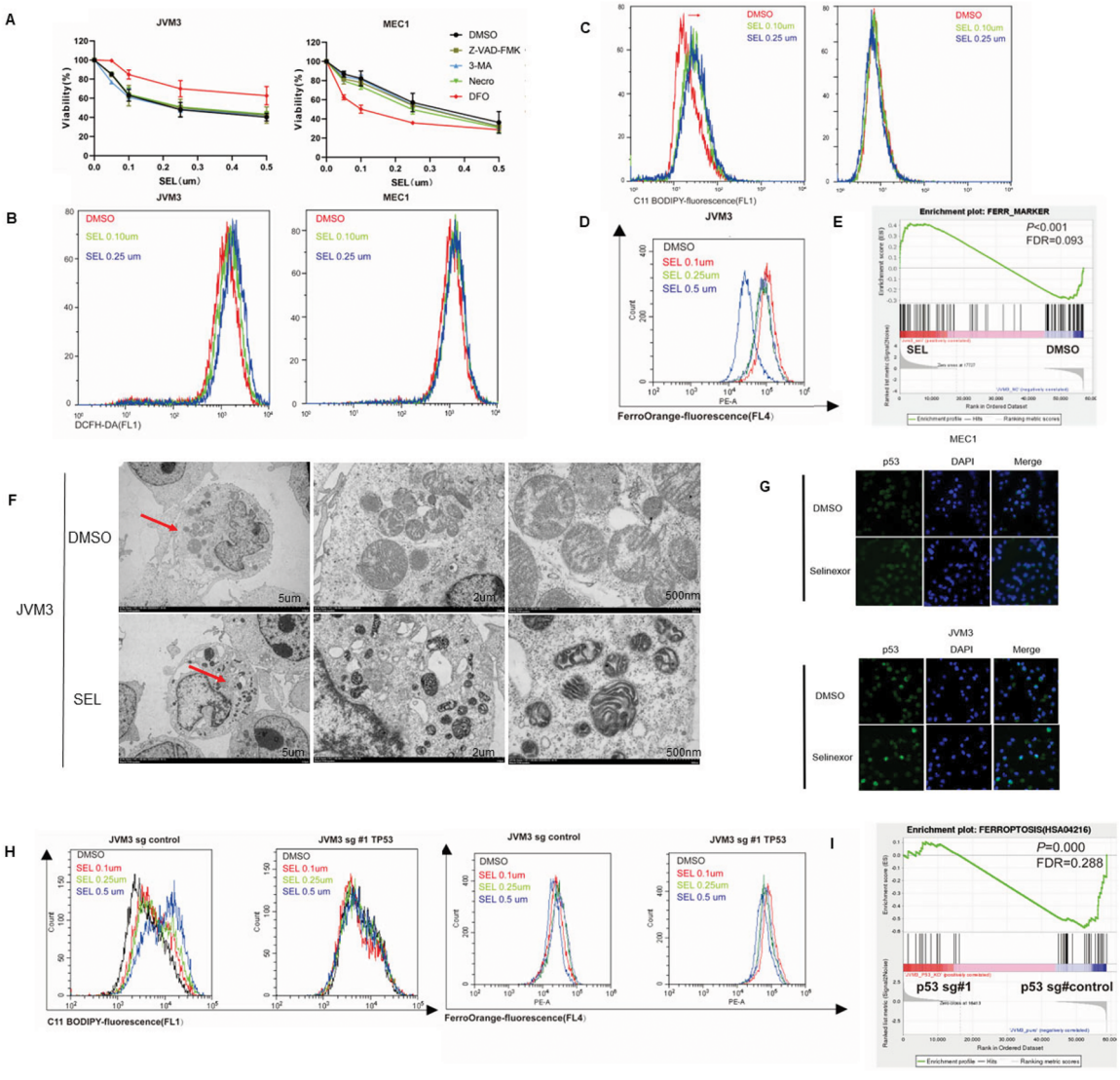

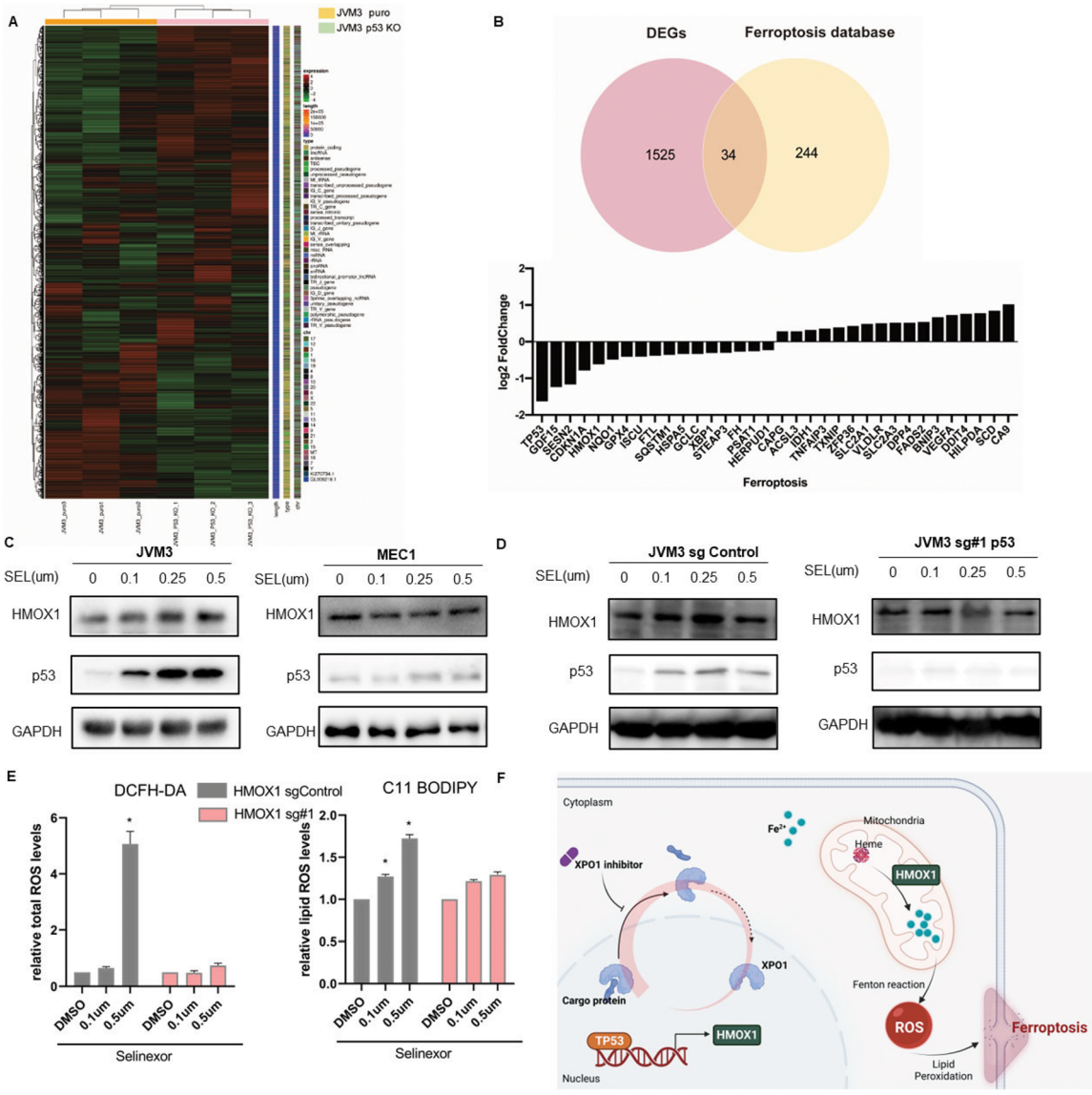

Chronic lymphocytic leukemia (CLL) is a chronic disease resulting from B-cells clonal proliferation. In recent years, CLL treatment has entered the era of non-chemotherapy, and exploring new treatment targets and strategies has important value. Exportin-1 (XPO1) is a critical nuclear-cytoplasmic transport protein in cells that is responsible for the unidirectional export of cargo proteins (including tumor suppressors) from the nucleus to the cytoplasm, and is closely related to the occurrence, development, and drug resistance of various tumors. In previous studies, we found high expression of XPO1 is associated with poor prognosis and showed the effect of Selinexor on proliferation inhibition, cell cycle arrest, and apoptosis, and observed effective inhibition of the NF-κB pathway and up-regulation of the FOXO pathway in CLL [1]. In our previous study, we found that the results of CCK8 were not consistent with the flow cytometry results of apoptosis when treating CLL cells with a relatively low concentration of Selinexor. This suggested that there may be other pathways of cell death activated. Therefore, we used a variety of cell death inhibitors, including Z-VAD-FMK (an apoptosis inhibitor), Necrosulfonamide (a necrosis inhibitor), 3-MA (an autophagy inhibitor), and the iron chelator DFO (a ferroptosis inhibitor), to treat CLL cell lines. We compared the effects of each inhibitor on the drug activity of Selinexor before and after treatment and found that only the ferroptosis inhibitor DFO could significantly reverse the inhibitory activity of Selinexor on p53 wild-type JVM3 cells (Figure 1(A)). This suggested that the drug activity of Selinexor can be exerted through the ferroptosis pathway. After detecting the total ROS and lipid peroxidation levels in cells after Selinexor treatment, we found that the lipid ROS level increased significantly in JVM3 cells (Figure 1(B,C)). Overproduction of Fe2+ was also detected in JVM3 cells after treatment (Figure 1(D)). Then, we used RNA-Seq to perform high-throughput sequencing on JVM3 cells before and after Selinexor treatment and conducted GSEA enrichment analysis on the expression profile data (Figure 1(E)). The results showed that the ferroptosis-related gene pathway was activated in JVM3, suggesting that Selinexor could induce ferroptosis. We observed the mitochondrial morphology changes in JVM3 cells treated with Selinexor at a concentration of 0.5 μmol/L for 24 hours using transmission electron microscopy. We found that the mitochondria were reduced in size, the mitochondrial cristae were reduced, the outer membrane was ruptured and shrunk, and the double-layer membrane density was increased (Figure 1(F)).

This indicated that Selinexor can induce ferroptosis in p53 wild-type JVM3 cells. Selinexor can also cause p53 nuclear retention (Figure 1(G)). RNAseq analysis revealed that Selinexor activated the p53 pathway in JVM3 cells. To further investigate whether Selinexor exerts its effects through the TP53 gene, we used CRISPR Cas9 technology to knock out TP53 in the JVM3 cell line. After treating p53 wild-type and knockout cells with Selinexor, we found that the total ROS and lipid ROS levels increased significantly in p53 wild-type JVM3 cell lines, while there was no significant change in the ROS levels in p53 knockout cells (Figure 1(H)). These results suggested that Selinexor-induced ferroptosis depends on the normal function of p53. GSEA enrichment analysis showed the ferroptosis-related pathway was also significantly enriched in p53 wild-type JVM3 cells (Figure 1(I)). We then combined the differentially expressed genes (DEGs) from the two groups with the ferroptosis database and identified 34 potential ferroptosis target genes (Figure 2(A,B)). After analyzing the expression and relationship with ferroptosis of the potential target genes, we speculated Heme Oxygenase 1 (HMOX1) as the bridge to connect p53 and ferroptosis. HMOX1 degrades heme and releases free iron to generate oxidized lipids in the mitochondria membrane to induce ferroptosis [2]. The expression of HMOX-1 is regulated by p53 [3]. XPO1 inhibitor treatment increased HMOX1 expression in a dose-dependent manner in JVM3 cells (Figure 2(C,D)). It was found that the levels of p53 and HMOX1 increased significantly in wild-type cells. Silencing HMOX1 decreased lipid ROS levels in CLL cells after Selinexor treatment (Figure 2(E)). Our data thus indicated that targeting XPO1 by Selinexor increased HMOX1 expression in a p53-dependent pathway and upregulated the lipid ROS to trigger ferroptosis in CLL (Figure 2(F)).

Abstract ID: 1521808

Title: Zanubrutinib and venetoclax as initial therapy for CLL with obinutuzumab triplet consolidation in patients with minimal residual disease positivity (BruVenG)

Authors: John Allan, Daniel Helbig, Sarah Rutherford, Erin Mulvey, Katie Greig, Sandra Stewart, Melissa LaPinta, Leslie Rudolph, Orel Agami, Melanie Bernstein, Jia Ruan, John Leonard, Peter Martin and Richard Furman

Background: Bruton's tyrosine kinase inhibitors (BTKi), anti-CD20 antibodies, and B cell lymphoma 2 inhibitors (BCL-2i) are essential therapeutic drug classes in the treatment of chronic lymphocytic leukemia/small lymphocytic lymphoma (CLL/SLL). Current evidence demonstrates clinical synergy between BTKi and BCL-2i, which allows for an all-oral regimen, that can be safely administered in a clinic setting for most patients [1,2]. This combination can achieve high rates of minimal residual disease (MRD) negativity and offer a fixed duration therapeutic approach [3]. Still, it remains uncertain if anti-CD20 therapy meaningfully adds to the effectiveness of oral combination therapy. Recent reports of triplet regimens demonstrate modest improvement in MRD negativity with similar overall response rates when compared to oral doublets [4–6]. Additionally, anti-CD20 antibody use causes significant B cell depletion resulting in prolonged immune suppression. Lastly, evidence suggests BTKi use may impair clinical activity of anti-CD20 antibodies when used early in combination with BTKi. This is mitigated by using more selective BTKi or incorporating anti-CD20 later in the treatment course with lower disease burden [7–10]. Therefore, anti-CD20 therapy may not be required for all patients and could be best utilized within a response-adapted strategy. This trial has been developed to assess efficacy of a response adapted consolidative treatment approach utilizing obinutuzumab triplet consolidation in CLL/SLL patients who remain MRD positive after completion of an oral doublet fixed duration treatment with zanubrutinib and venetoclax. This strategy has the potential to minimize obinutuzumab use, spare toxicity, while maximizing MRD negativity. This study will utilize once daily zanubrutinib for which there is limited data in regard to safety and efficacy particularly in combination with venetoclax. Study Design and Endpoints: We will conduct a single center, open label, phase II, investigator initiated clinical trial enrolling 50 subjects evaluating the safety and efficacy of zanubrutinib and venetoclax with obinutuzumab triplet consolidation in subjects who remain MRD positive (BruVenG). Eligible patients must have treatment naïve CLL/SLL and confirmed treatment indications per International Workshop on CLL 2018 guidelines. Subjects with Richter's transformation are excluded. Treatment will consist of lead-in, combination, and consolidation phases. All subjects will be treated with a 3-cycle lead-in of 320mg, oral, once daily zanubrutinib monotherapy. Venetoclax will be incorporated at cycle 4, per the standard prescriber insert ramp-up schedule. A final dose of 400mg oral, once daily venetoclax, in combination with 320mg oral, once daily zanubrutinib will be used in all subsequent cycles after ramp-up. At cycle 16, MRD will be assessed in the peripheral blood (PB) and bone marrow (BM) via clonoSEQ (Adaptive Biotechnologies). Subjects who are MRD negative ($<1\times10^{-4}$) in both compartments will stop therapy. Subjects who are MRD positive in PB or BM will continue zanubrutinib and venetoclax for an additional 6 cycles. Obinutuzumab will be added to the oral doublet starting at cycle 17. Standard intravenous obinutuzumab lead-in will occur during cycle 17, followed by standard monthly intravenous dosing of 1000mg through cycle 22. Depending on MRD status, subjects will be treated for 16 or 22 cycles. All subjects who receive consolidation will stop treatment at cycle 23 regardless of end of treatment MRD

Figure 1. Study Schema

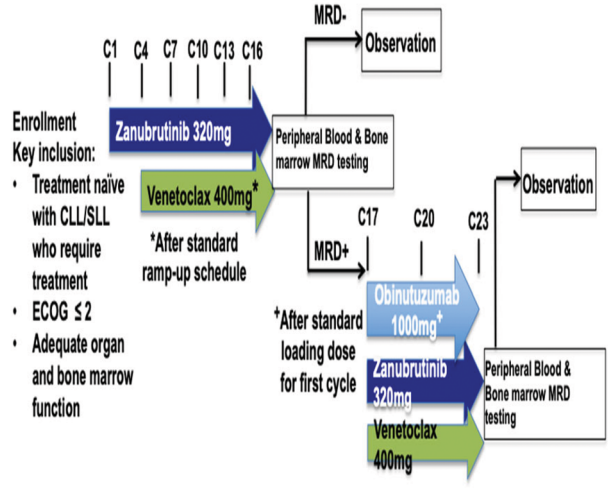

status. The primary endpoint is cycle 16 PB and BM MRD negativity rates. A co-primary endpoint will be cycle 23 PB and BM MRD negativity rates in subjects who were MRD positive at C16 and who went on to receive at least 1 dose of obinutuzumab. Key secondary endpoints will include cycle 16 overall response rate, 36-month progression free survival, 36-month overall survival, 36-month time to next treatment, 24- and 36-month PB MRD negativity rates, tumor lysis risk reduction rates, and safety. Exploratory endpoints will assess the positive predicative value of the Δ400 biomarker [5] on MRD negativity at cycle 16. This biomarker will be assessed between cycle 4 and 6. The MRD negative rates at cycle 16 and cycle 23 will be estimated with a 90% confidence interval using the Clopper-Pearson method based on exact binomial distribution. Enrollment: Begins May 2023 Clinical Trials Registry #: NCT05650723

Abstract ID: 1527398

Title: Safety and effectiveness in CLL patients treated with venetoclax monotherapy in Austria, Germany, and Switzerland - long term follow up data

Authors: Ingo Schwaner, Holger Hebart, Christoph Losem, Thomas Wolff, Burkhard Schmidt, Davide Rossi, Caroline Lehmann, Julia Benzel, Johannes Huelsenbeck and Petra Pichler

Background: In clinical trials, treatment of chronic lymphocytic leukemia (CLL) with venetoclax (Ven) has shown promising efficacy and good tolerability. However, patients treated in clinical trials often represent a selected group and prospective real-world data are limited.
Aim: We conduct a prospective non-interventional observational study assessing effectiveness, safety, and quality of life in patients treated with Ven in Austria, Germany, and Switzerland. The population enrolled is representative for patients treated with Ven according to local label2. This report focuses on patients treated with Ven monotherapy.
Methods: Adult patients with CLL requiring therapy treated with Ven according to local label are eligible for the study. Patient's visits are scheduled at the physician's discretion and according to clinical practice. Study documentation is possible at baseline, weekly during ramp-up, monthly until the end of 6 months and 3-monthly afterwards up to a maximum of 2 years. Response assessment according to iwCLL criteria can be documented at the end of ramp-up, after 3, 12, and 24 months.
Results: The study started in November 2017. Until 4 November 2022, 89 patients receiving Ven monotherapy were enrolled, 84 had received at least one dose of Ven (= safety population), and for 66 treatment response had been documented at least once (=effectiveness population). Median age at therapy start was 75 years, 59.6% of patients were male, 76.4% had at least one comorbidity, most commonly cardiovascular (56.2%), 67.4% received comedication. Patients were heavily pre-treated with a median of 2 (range 1–10) lines of therapy, i.e. chemoimmunotherapy (67.4%) and therapy with B-cell receptor inhibitors (66.3%). Del(17p), TP53 mutation, and presence of unmutated IGHV had been diagnosed in 43.8, 40.4, and 33.7%, respectively (excl. missing data: 49.4, 48.6, 63.8%). With a median observation time of 461 (range 1–1131) days, 91.7% of patients experienced at least one AE, 61.9% experienced CTCAE grade ≥3 AEs, SAEs were reported in 42.9%. Most common AEs were diarrhoea, thrombocytopenia, neutropenia (17.9%/16.7%/14.3%). 16 patients died. Tumour lysis syndrome (TLS) was reported in 9 patients (3 clinical TLS). This rather high rate may in part be due to advanced age of patients and/or incomplete laboratory monitoring, e.g. full laboratory values at 24 h post first dose of Ven were reported in only 49.4% of patients. Furthermore, only 72.6% of patients received hyperuricemic prophylaxis. Out of the 9 patients with reported or suspected TLS, 8 completed ramp-up, 1 patient discontinued the therapy. The median for progression-free survival (PFS) and overall survival (OS) has not been reached, the 24-month estimates were 76.0% (PFS) and 75.7% (OS). The reported best overall response at 24 months was 80.3% (CR + CRi 42.4%; PR: 37.9%). Remissions appeared to deepen with longer treatment duration.

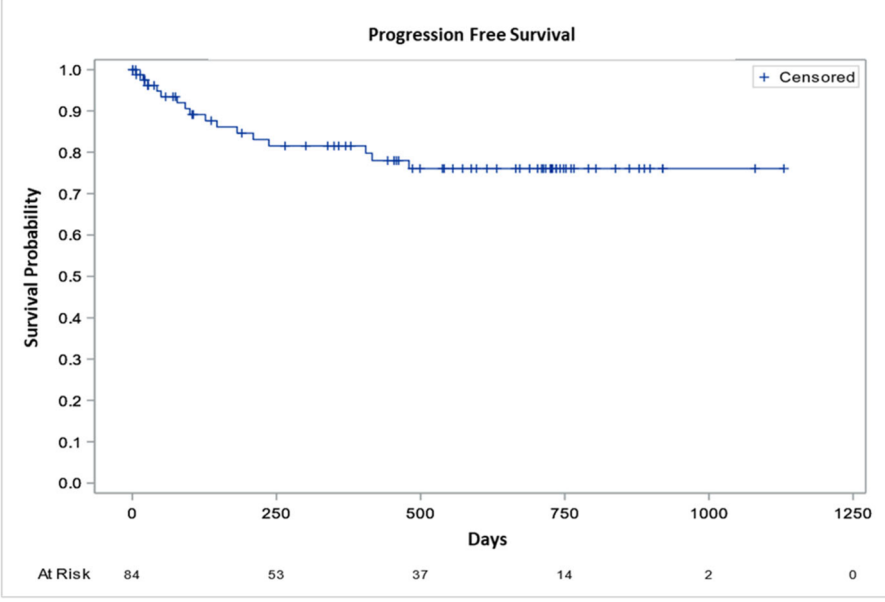

Conclusion: Under real-world conditions, Ven monotherapy is used in heavily pre-treated elderly patients. The treatment was well tolerated. TLS monitoring deviated from recommended lab monitoring procedures as specified in the Ven label. Despite the difficult-to-treat patient population, the response rate was high. Our study confirms findings from Ven Phase-II-studies in patients treated under real-world conditions.

Abstract ID: 1529308

Title: Clinical relevance of the recommended intensive laboratory monitoring during the standard ramp-up at time of venetoclax initiation for CLL: a real-world experience

Authors: Grace Baek, Ivan Huang, Jonathan Cohen, Sirin Khajaviyan, Stephanie Louie, Laura Samples, Stephen Smith, Brian Till, Edus Warren, Ajay Gopal, Christina Poh, Ryan Lynch, Chaitra Ujjani and Mazyar Shadman

Introduction: Venetoclax-based treatments are standard of care for treatment of CLL. The requirements for intensive monitoring, which require frequent patient visits, is a limiting factor that has contributed to the relatively low utilization of this effective drug. The clinical relevance of such intensive monitoring strategy in clinical practice, especially in patients with low or medium risk for tumor lysis syndrome (TLS), is unknown. We hypothesized that most of the monitoring labs and visits beyond the first week of the standard 5-week ramp-up [1] do not result in significant clinical findings or interventions. The aim of this study was to determine the clinical significance of laboratory monitoring for TLS during the standard ramp-up period as indicated by the approved prescription information. The primary endpoint was the incidence of laboratory and clinical TLS and clinical interventions that were done based on the laboratory findings during the ramp-up.
Methods: We included patients who started venetoclax in the outpatient setting for patients with CLL/SLL from 2016 to 2022. Laboratory and clinical information were reviewed for each dosing during the 5-week ramp-up. Patients with non-standard (escalated) ramp-up, those on clinical trials, or those on concurrent BTK inhibitors were excluded. TLS was defined by Cairo-Bishop criteria [2]; laboratory abnormalities were documented based on absolute threshold. Clinical interventions based on the laboratory or clinical findings were documented. The study was approved by the institutional IRB.
Results: A total of 56 patients (25% female) with median age 64 years old (range 39–81) met study criteria. TLS risk categories included 42 low-risk (75%), 13 medium-risk (23%), and 1 high-risk (2%). The majority (59%) received venetoclax in the first-line setting. Forty-six patients (82%) received prior debulking with an anti-CD20 antibody (obinutuzumab 46%, rituximab 54%). At venetoclax initiation, all patients received either allopurinol (98%) or febuxostat (2%). Throughout the ramp-up process, patients received preemptive intravenous fluids (73% week 1, 55% week 2, 34% week 3, and 20% weeks 4 and 5). Overall, no incidence of clinical TLS (neurotoxicity, cardiotoxicity, or renal toxicity) was noted. Criteria for laboratory TLS were met with 1 patient (1.8%) overall. A patient who met laboratory TLS criteria with

Clinical Relevance of the Recommended Intensive Laboratory Monitoring during the Standard Ramp-up at Time of Venetoclax Initiation for CLL: A Real-World Experience

Table 1:

n=56	Week 1		Week 2	Week 3	Week 4	Week 5	Total Events
	Day 1$^{\Delta}$	Day 2					
Lab TLS , n (%)	1 (1.8%)	0	0	0	0	0	1
Clinical TLS , n (%)*	0	0	0	0	0	0	0
Any clinical intervention	1 (1.8%)	1 (1.8%)	2 (3.6%)	1 (1.8%)	1 (1.8%)	0	6 (across 3 patients)
IV fluids (therapeutic)	0	0	0	0	1 (1.8%)	0	1
Clinical intervention other than IV fluids	1 (1.8%)*	1 (1.8%)*	2 (3.6%)*,**	1 (1.8%)*	0	0	5 (across 2 patients)
Hospitalization	0	0	0	0	0	0	0

Abbreviations: IV, intravenous; TLS, tumor lysis syndrome

$^{\Delta}$ *On day 1, after initiating venetoclax ramp-up*
**Received phosphate-lowering intervention*
***Received calcium supplementation*

hyperphosphatemia and hypocalcemia in week 5 was excluded; the patient was on dialysis throughout ramp-up, and there was concern with compliance with nephrologist-directed sevelamer therapy. Three patients exhibited laboratory deviations from normal limits that did not meet Cairo-Bishop criteria [patient 1: day 1 (after venetoclax initiation), week 3, and week 4; patient 2: week 2; and patient 3: week 2]. No patient required anti-hyperuricemic therapy (e.g. rasburicase) nor hospitalization. Only 2 patients (3.6%) received interventions for hyperphosphatemia (weeks 1–3) or hypocalcemia (week 2). Only 1.8% of patients required addition of intravenous fluids during ramp-up for serum creatinine elevation (one during week 4).
Conclusion: Intensive laboratory monitoring during the 5-week ramp-up in CLL/SLL patients with low or medium-risk TLS resulted in very low rates of laboratory and clinical TLS or clinical interventions. Strategies to modify such requirements need to be considered and can potentially increase the utilization of venetoclax.

Abstract ID: 1532047

Title: Mechanisms of differential response to BTKi targeted therapy in patients with chronic lymphocytic leukemia

Authors: Zhenshu Xu, Peixia Tang, Wenjie Zhang, Guangyao Guo, Jinlan Long, Jie Lin, Liping Liu and Xi Chen

Introduction: Clinical findings have shown that the response of patients with chronic lymphocytic leukemia (CLL) to treatment with BTKi is either fast or slow. The peripheral blood clonal B cells of patients sensitive to BTKi increase rapidly in the early stage of treatment, and these patients easily obtain a complete response (CR). Patients insensitive to BTKi therapy do not respond until several months of BTKi treatment, and the reason for the difference is unknown.

According to the therapeutic response to BTKi, the patients with CLL can be divided into two groups, early responders (ER) and late responders (LR), who may have different characteristics and underlying molecular mechanisms for responding to BTKi. In this study, we begin exploring the differences between ER and LR patients and the underlying molecular mechanisms affecting the difference. When we understand molecular mechanisms, will be able to improve our future clinical treatment, and further optimize the strategy for treatment of patients with CLL.

Materials and methods: The clinical characteristics and treatment response of 32 newly diagnosed patients with CLL treated with single-agent BTKi (zanubrutinib 19, ibrutinib 11 and orelabrutinib 2) were analyzed. Early Responders (ER) refers to a 50% increase in lymphocytes at 3-months of BTKi treatment and/or a complete response at 12 months of treatment, otherwise patients were categorized as LR. Microchips and principal component analysis (PCA) were used to analyze differentially expressed genes in both groups. Immunohistochemistry, PCR, Western Blotting, and other methods were used to analyze the expression of the related molecules of the leukemia cells. Mass spectrometry and CHiP were used to analyze the phosphorylation level of key regulatory molecules.

Results: (1) There were 14 patients in the ER group and 18 in the LR group. The mean age of the patients in the two groups was 63.6 and 69.6 years, respectively. In the ER group, 57% of patients were high risk of CLL-IPI, while 72% were high risk in the LR group. The proportion of ER between different BTKi treatments is roughly the same. All 14 patients with ER showed a rapid rise of early lymphocytes, and eight of them achieved complete remission after 12 months of treatment. (2) Compared with the LR group, the expression of IL-2, IL-6, CCL3, CCL4, and CCL17 in the ER group decreased significantly after BTKi treatment. Gene expression profile (GEP) showed that there were significantly different molecular expression patterns in the two groups, and the phosphorylation level of the transcription factor Ikaros in the ER group was significantly higher than that in the LR group. (3) The nuclear localization and transcriptional activity of Ikaros depends on BTK-mediated phosphorylation of pSer442 residues, and the function of BTKi in the regulation of Ikaros was significantly different in the ER group than in the LR group. After the treatment with BTKi, the gene and protein expression of MYC (Ikaros activator) in the ER group was significantly down-regulated, while the expression of the YES1 (Ikaros inhibitor) gene and protein was significantly upregulated. Changes of MYC and YES1 in the LR group were not significant.

Discussion and conclusions: The difference in the treatment response to BTKi in patients with treatment naïve CLL was related to the level of Ikaros phosphorylation. For those with an ER the immune response of the tumor microenvironment is enhanced, and inflammatory factors are inhibited, which is conducive to immune reconstruction after BTKi treatment. On the other hand, BTKi can inhibit the proliferation of cloned cells by reducing the ikaros function through upregulating YES1 expression and downregulating MYC expression. The research conclusions reveal the key molecules affecting the response of CLL cells to BTKi therapy and provide a basis for formulating precise treatment strategies for patients with treatment naïve CLL. Of course, because the number of cases included in this study is small and the observation time is not long, it is difficult to infer that ER patients have a better and longer survival advantage. These are subjects of follow-up experiments and observations.

Abstract ID: 1539453

Title: A phase 1 study evaluating PRT2527, a potent and highly selective CDK9 inhibitor, in patients with select relapsed/refractory B-cell malignancies

Authors: Bruce Cheson, Sarit Assouline, Talha Munir, Petra Langerbeins, Constantine S. Tam, Gareth Gregory, Franck Morschhauser, Wojciech Jurczak, Michael Choi, Geoffrey Shouse, Monica Tani, Gina Paris, William Sun, Siminder Atwal, Wan-Jen Hong and Clémentine Sarkozy

Aim: PRT2527 is an investigational, potent and highly selective cyclin-dependent kinase 9 (CDK9) inhibitor. CDK9 is a key regulator of transcription elongation and has been studied as a potential target for therapy in transcriptionally addicted cancers that are dependent on oncogenic drivers with short half-lives. Although most of these drivers do not respond to direct inhibition, studies suggest that a subset of drivers with short half-lives such as MYC, MYB, and MCL-1 may be targeted indirectly through CDK9 inhibition in select hematological malignancies and solid tumors. Preclinical data with PRT2527 have demonstrated evidence of on-target inhibition of MYC, MYB, and MCL-1, as well as induced apoptosis, as measured by cleaved caspase 3 in cell lines and translational models (e.g. patient-derived xenograft models; [1].

Methods: PRT2527-02 is a phase 1, open-label, multicenter, dose-finding study to evaluate the safety, tolerability, recommended phase 2 dose (R2PD), and preliminary efficacy of PRT2527 in patients with select B-cell malignancies such as aggressive B-cell lymphoma subtypes, mantle cell lymphoma, and chronic lymphocytic lymphoma/small lymphocytic lymphoma including Richter syndrome. Aggressive B-cell lymphoma subtypes, including diffuse large B-cell lymphoma not otherwise specified, gray zone lymphoma, follicular lymphoma grade 3b, high-grade B-cell lymphoma with or without translocations, and primary mediastinal large B-cell lymphoma or large B-cell lymphoma transformed from indolent B-cell lymphoma, are eligible to enroll. Patients must have relapsed or be refractory to or ineligible for standard-of-care therapy. Other key eligibility criteria include measurable disease or requirement for treatment in accordance with standard disease-specific criteria for the hematologic malignancies under study, Eastern Cooperative Oncology Group performance status of 0–1, and adequate bone marrow, renal, and liver function. The study consists of dose escalation with successive cohorts of patients receiving escalating doses of intravenous PRT2527 once weekly in a 21-day cycle. PRT2527 treatment will continue until disease progression or unacceptable toxicity, whichever comes first. Dose escalation and de-escalation decisions will be guided by the Bayesian optimal interval design method based on the number of patients with dose-limiting toxicities (DLTs) observed at the dose level under evaluation until a maximum tolerated dose and R2PD have been determined. The primary endpoints include safety, tolerability, DLTs, and RP2D of PRT2527. Secondary endpoints include objective response rate, duration of response, duration of complete response, and pharmacokinetic profile of PRT2527. The study is open to enrollment and registered at ClinicalTrials.gov, NCT05665530.

Abstract ID: 1541600

Title: Health-related quality of life in patients with relapsed or refractory chronic lymphocytic leukemia or small lymphocytic lymphoma treated with liso-cel in TRANSCEND CLL 004

Authors: David G. Maloney, Tanya Siddiqi, Bita Fakhri, Shuo Ma, Nirav Shah, Peter A. Riedell, Stephen J. Schuster, Laurie Eliason, Lin Wang, Sherilyn A. Tuazon, San-San Ou, Ling Shi, Xiaomei Ye and Saad Kenderian

Introduction: Patients with relapsed or refractory (R/R) chronic lymphocytic leukemia (CLL)/small lymphocytic lymphoma (SLL), especially those with progression on Bruton tyrosine kinase inhibitors (BTKi) and venetoclax failure, have limited treatment options and poor patient-reported outcomes (PRO)/health-related quality of life (HRQOL). The CD19-directed chimeric antigen receptor T cell therapy lisocabtagene maraleucel (liso-cel) is being evaluated in R/R CLL/SLL in the phase 1/2 TRANSCEND CLL 004 study (NCT03331198). Here, we report PRO/HRQOL for patients in the phase 2 part of TRANSCEND CLL 004.

Methods: Patients completed the European Organisation for Research and Treatment of Cancer Quality of Life Questionnaire (EORTC QLQ)-30 items (C30), EORTC QLQ-17 items for CLL (CLL17), and EQ-5D-5L at baseline (≤7 days before lymphodepletion), preinfusion on the day of liso-cel infusion (Day 1), and 30, 60, 90, 180, 270, 365, 455, 545, and 730 days after infusion. The primary domains of interest were EORTC QLQ-C30 global health status (GHS)/quality of life (QOL), physical functioning, role functioning, cognitive functioning, and fatigue and EORTC QLQ-CLL17 symptom burden and physical condition/fatigue. The PRO-evaluable population was defined as patients with baseline and ≥1 postbaseline PRO assessment, among all patients who received leukapheresis in the phase 2 portion. Observed scores and mean changes from baseline were calculated across postbaseline visits. Intra-patient meaningful changes from baseline were calculated using prespecified change thresholds.

Results: Of 112 patients in the PRO-evaluable population and 70 in the BTKi progressed/venetoclax failure subset, baseline completion rates were 61% in both populations, with rates of 40–70% across most visits for all measures. The main reasons for not completing PROs were COVID-19–related restrictions. Outcomes were similar in both populations. Mean baseline scores were worse than those of the United States general population for many domains. After initial deterioration in HRQOL after liso-cel infusion, the observed mean changes from baseline showed improvement starting at Day 60 for all primary domains (representative domains shown in Figure) except for cognitive functioning score, which was comparable with the general population at baseline and maintained over time. The proportion of patients with meaningful improvement increased over time for multiple domains, including fatigue-related domains and GHS/QOL on the EORTC QLQ-C30 and EORTC QLQ-CLL17. From Day 90 through Day 730, the proportions of patients with meaningful improvement or no change on the primary domains exceeded the proportion with meaningful deterioration.

Conclusions: Liso-cel either improved or maintained HRQOL from baseline in patients with heavily pretreated R/R CLL/SLL. Meaningful improvements were achieved in the key CLL symptom of fatigue and overall QOL.

Figure. Observed mean changes from baseline in select primary domains of (A) EORTC QLQ-C30 GHS/QOL and (B) fatigue

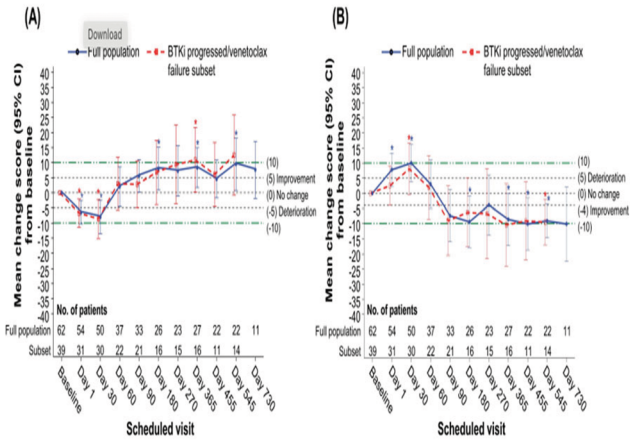

Higher score for GHS/QOL (A) indicates better overall HRQOL, while higher score for symptom domain (fatigue [B]) indicates worse symptoms. Dashed lines represent minimally important difference thresholds.
*Observed change from baseline was statistically significant based on nominal $P < 0.05$.
CI, confidence interval.

Abstract ID: 1542397

Title: Immunogenetics and antigen reactivity profiling contribute to unravelling the ontogeny of CLL stereotyped subset #4

Authors: Anastasia Iatrou, Electra Sofou, Eleni Kotroni, Lesley Ann Sutton, Michela Frenquelli, Raphael Sandaltzopoulos, Ioanna Sakellari, Niki Stavroyianni, Fotis Psomopoulos, Paolo Ghia, Richard Rosenquist Brandell, Andreas Agathangelidis, Anastasia Chatzidimitriou and Kostas Stamatopoulos

Introduction: CLL subset #4 (IGHV4-34/IGKV3-20) is the largest stereotyped subset with somatically hypermutated clonotypic B cell receptor immunoglobulin (BcR IG) and a prototype for indolent disease. The variable heavy complementarity determining region 3 (VH CDR3) of the clonotypic BcR IG is long and enriched in positively charged residues, reminiscent of pathogenic anti-DNA antibodies and contains a (K/R)RYY motif that has been demonstrated to be 'CLL-biased' and exclusive to subset #4. Additionally, subset #4 BcR IG are capable of specific homotypic interactions which induce cellular activation. Critical structural determinants mediating such interactions are provided by the gamma constant domain, offering a plausible functional explanation for the ubiquitous expression of IgG-switched BcR IG in subset #4. Subset #4 BcR IG have also been reported to display intense intraclonal diversification in the context of ongoing SHM, suggestive of active, ongoing interaction with antigen(s). Thus far, the immunogenetic characterization of subset #4 has relied on low-throughput sequencing approaches that are inherently limited, precluding comprehensive assessment of antigenic impact on (sub)clonal composition. In this study,

we sought to overcome this limitation by performing next-generation sequencing (NGS) of heavy (HC) and light (LC) chains of 6 subset #4 patients and explore whether/how (auto)antigens could drive the clonal evolution by comparing the reactivity profile of the clonotypic BcR IG with those detected at subclonal level.

Methods: We studied longitudinal samples from 6 subset #4 and 6 non-subset #4 IGHV4-34-expressing M-CLL cases. Clonotypic HC and LC gene rearrangements were analyzed by NGS. The clonotype accounting for the majority of NGS reads in a given sample was defined as dominant; related clonotypes expressing the same IGHV/IGKV gene and VH CDR3 amino acid (aa) sequence yet differing in the aa sequence of the VH and/or VK domains were defined as subclonotypes. The dominant clonotypes of all cases as well as 32 subclonotypes of subset #4 cases were expressed as recombinant monoclonal antibodies (rmAbs) and screened for antigen reactivity using ELISA and flow cytometry.

Results: NGS revealed two distinct patterns of subclonal architecture in the IGH repertoire of subset #4. The first was characterized by the presence of a single dominant clonotype (4 cases) whereas the second by the co-existence of 2 significantly expanded clonotypes with comparable frequencies (2 cases). Turning to the IGK repertoire, 5/6 cases carried a single dominant clonotype, while 1 case carried more than 1 expanded clonotypes. In contrast, a single dominant clonotype was detected in all non-subset #4 cases for both HC and LC. Longitudinal analysis revealed significantly ($p < 0.05$) more pronounced subclonal drift (changing relative frequencies) of the expanded clonotypes in subset #4 vs non-subset #4 cases, particularly for the HC. Surprisingly, in all subset #4 cases we identified clonotypic IgG transcripts (same IGH gene and VH CDR3 length, high VH CDR3 aa sequence identity) with 100% germline IGHV identity ('truly unmutated'), present at low frequency (median: 0.003%, range: 0.0003–0.03%). Prompted by this, we produced rmAbs for both the dominant, somatically hypermutated BcR IG clonotype of all 6 subset #4 cases, as well as 32 truly unmutated subclonotypes (from all studied subset #4 cases) and compared their antigen reactivity profiles. We report consistent, significantly ($p < 0.05$) stronger reactivity of the truly unmutated, subclonotypic BcR IG compared to the mutated BcR IG expressed by the dominant CLL #4 clone. With few exceptions, all subclonotypic truly unmutated BcR IG displayed more intense recognition of dsDNA and lipopolysaccharides, antigenic agents from CMV, Influenza A and Mycoplasma pneumoniae as well as viable HEK293 and Jurkat T cells.

Conclusions: Our findings support that SHM in CLL subset #4 is functionally driven by persistent selection by (auto) antigens, ultimately leading to a significant redemption from autoreactivity. The identification of truly unmutated clonotypic IgG gene transcripts likely reflects a complex trajectory of clonal evolution, offering hints about the precise timing of SHM in relation to class switch recombination in the natural history of CLL subset #4.

Abstract ID: 1542401

Title: Uncovering the immune-related challenges facing people with chronic lymphocytic leukaemia

Authors: Yasmine Hassan, Nick York, Paul Moss, Pierre Aumont, Rita Christensen, Lea Koren, Jan Rynne, Raymond Vles and Clemens Wendtner

Introduction: Infections are a leading cause of mortality and affect the management of their day-to-day activities for individuals with chronic lymphocytic leukaemia (CLL) [1]. COVID-19 has highlighted the immune-related difficulties faced by individuals with CLL, which increases their vulnerability to COVID-19 infection and negatively impacts their daily lives. During the initial wave of COVID-19, individuals with CLL had fatality rates up to 16.5 times higher than the global median rate [2]. Lymphoma Coalition's 2020 Global Patient Survey completed by 9,179 patients and 2,699 caregivers from over 90 countries said 19% were affected by frequent infections [3]. In contrast, a comprehensive literature review of available data and clinical guidelines on the management and support of individuals with CLL showed that data related to the risk and management of immune challenges remains limited. To address the gaps in guidelines and data available, a multidisciplinary steering committee comprising of leading clinicians, patient representatives and patient advocacy groups (PAGs) was established to formulate recommendations aimed at enhancing the management of immune challenges experienced by people with CLL.

Methodology: The steering committee was brought together at one virtual working group meeting to discuss evidence around the impact of immune challenges on individuals, best practice management and immune-related support. The working group comprised of leading clinicians, patient representatives, and patient advocacy groups (PAGs) who were able to share expert insights and information along with the views of their respective patient members. To inform discussion and associated recommendations, a comprehensive literature review of published data across a timeframe of 2017–2022 focussed on chronic lymphocytic leukaemia and immune challenges was undertaken, including published data from PAG-initiated patient surveys and testimonials. It excluded non-English language publications and articles specifically focussing on COVID-19 vaccination (Table 1). To accompany the findings from the literature review and better qualify the impact of immune challenges, a patient survey was completed by representatives from four

Table 1. Immune challenges themes identified through the literature review.

Immune challenge's theme(s)	Number of publications covering theme
Risk of infection due to intrinsic CLL-related immunosuppression	18 Publications
Risk of infection as a consequence of CLL therapy	17 Publications
Diagnostic tests to determine pathogen type	1 Publication
Prophylactic strategies	1 Publication
Autoimmune hemolytic anaemia	5 Publications
Immunoglobulin therapy	5 Publications
Secondary cancer risk	1 Publication
Richter transformation	5 Publications
Infection prophylaxis	7 Publications
Risk of infection due to intrinsic CLL-related immunosuppression vs constitutional susceptibility	1 Publication
Immune thrombocytopenia (ITP)	1 Publication
Autoimmune thrombocytopenic purpura (ATP)	2 Publications
Shingles	3 Publications
Post-herpetic neuralgia	1 Publication
Second malignancy	10 Publications
Venous thromboembolism (VTE)	1 Publication
COVID-19	5 Publications

Table 2. Recommendations to address immune challenges in CLL.

Build a stronger evidence base regarding immune challenges facing individuals with CLL by:
1. Establishing the impact of vaccination status on CLL outcomes
2. Quantifying and assessing the impact of opportunistic infections that are unrelated to treatment
3. Identifying research needs to advise on planning and clarification of protective measures for immunocompromised people
4. Understanding the social and mental health impact of immune-related challenges on individuals with CLL
5. Prioritizing research and surveys that focus on immune challenges in CLL, whether related to clinical research or patient experiences
Support HCPs to optimally manage individuals with CLL facing immune challenges by:
1. Developing global clinical guidelines for monitoring and managing immunosuppression for individuals with CLL
2. Ensuring that immunocompromised status is flagged within patient health records of individuals with CLL
3. Developing and implementing educational and awareness campaigns among HCPs, particularly primary care physicians.
4. Promoting shared decision-making and personalized approaches in the management and care of CLL patients
Provide Individuals with CLL support with a range of information and resources to feel empowered, regardless of any immune challenges that they may be facing. This could be addressed by:
1. Creating and disseminating resources to educate and empower CLL patients, including holistic self-assessments or information about how certain lifestyle choices impact infection risk.

countries. The survey focused on the real-life experiences of immunocompromised individuals with CLL including how it affects their day-to-day lives and what challenges they experience in their care. The meeting discussions, patient survey, and associated testimonials, alongside the themes established after the literature review were considered to formulate recommendations that were agreed and ratified by the steering committee.

Results: Discussion focussed on the evidence base for the impact of immune challenges on people with CLL, particularly gaps in existing care and published data. It covered immune-related best practice management for people with CLL, as well as the role of HCPs in ensuring individuals receive specific immune-related care and support (Table 2). Based on the combined experience of committee representatives, a consensus was reached that immune challenges in haematological cancers, particularly regarding a patient's quality of life, can be worse than other cancers. Patient testimony found that doctors focus on the cancer treatment and do not discuss infection risk and prevention. COVID-19 was identified as a catalyst that has enabled immune-related challenges to be increasingly discussed in the clinical assessment and management of CLL. However, there remains a need to support HCPs to optimally manage immune challenges; and provide individuals with a range of information and resources on immune challenges to feel empowered. Consensus was reached that establishing the impact of vaccination status on CLL outcomes and understanding the social and mental health impact and prioritizing research are important tools to build a stronger evidence base on immune challenges. It was agreed that developing global clinical guidelines for monitoring and managing immunosuppression; ensuring that patient health records flag immunocompromised status and promoting shared decision-making and personalized approaches in CLL management would support HCPs to optimally manage individuals. The steering committee highlighted that disseminating resources focused on immune-related challenges to educate individuals would enable better infection prevention.

Conclusion: The literature review and discussions highlight the significant immune-related challenges individuals with CLL face. The vulnerability to infections, including COVID-19, has emphasized the urgent need for improved management and support. The recommendations address key areas, including establishing a robust evidence base, supporting HCPs to manage immune challenges, and access to information. It is important for stakeholders to embrace these recommendations and collaborate to optimize healthcare delivery so that CLL patients receive the comprehensive immune-related management and care they deserve.

Abstract ID: 1543495

Title: The interplay between BcR signaling and the p53 pathway upon DNA damage in primary CLL cells

Authors: Michaela Pesova, Jitka Malcikova, Sarka Pavlova, Veronika Mancikova, Robert Helma, Anna Panovska, Yvona Brychtova, Tomas Arpas, Michael Doubek and Sarka Pospisilova

Background: In the clinical management of chronic lymphocytic leukemia (CLL), inhibitors targeting the B-cell receptor (BcR) are considered to act independently of the p53 pathway. However, different frequencies of TP53 gene defects in CLL subgroups harboring distinct antigen receptors suggested a potential interplay between BcR signaling and p53. We aimed to study whether the therapeutical inhibition of BcR signaling may affect this interplay and whether potential off-target effects of BTK kinase inhibitors affect p53 phosphorylation and function.

Methods: To explore the potential BcR-p53 crosstalk, we performed *in-silico* differential expression analysis after BcR activation using publicly available transcriptomic data (PMID: 33833385). Subsequently, we examined the effect of BcR signaling inhibitors (ibrutinib, idelalisib) in combination with DNA damage agents (doxorubicin, fludarabine) on p53 protein level by western blot analysis in 37 primary CLL cell samples with wild-type TP53 locus. In addition to monitoring p53 level, we analyzed the p53 phosphorylation pattern by Zn(II)Phos-Tag method followed by western blots. The transcriptional activity of p53 was assessed using qPCR focused on the expression of four p53 targets: BAX, BBC3, CDKN1A, and GADD45A.

Results: *In-silico* analysis of publicly available data showed that activated BcR signaling led to significant changes (FDR <0.05; logFC≥|2|) in the expression of 13 out of 116 typical p53 targets. Next, we investigated the effect of BcR signaling inhibition on the p53 protein stabilized with DNA-damaging drugs in wt-TP53 primary CLL cells. While idelalisib showed a heterogeneous effect on the p53 level with either of DNA damaging drugs, ibrutinib combined with doxorubicin led to a significant and homogeneous decrease in the p53 level compared to a DNA-damaging drug alone. As the stability of p53 is dependent on its phosphorylation, we further explored whether ibrutinib affects the p53 phosphorylation pattern,

and we found that the p53 phosphorylation pattern remained unchanged. Next, we used qPCR to evaluate whether decreased p53 level affected the expression of p53 target genes (BAX, BBC3, CDKN1A, and GADD45A). As expected, p53 activation by doxorubicin led to a significant increase in the expression of four target genes. However, samples treated with the combination of doxorubicin and ibrutinib showed either no significant difference in the expression level (CDKN1A, BBC3) or exhibited a higher expression of p53 target genes (BAX, GADD45A) compared to doxorubicin alone. **Conclusion:** We documented the interplay between BcR signaling and the p53 pathway in primary CLL cells. While BTK inhibition in DNA-damaging conditions led to the reduction of p53 level, the expression of p53 target genes remained stable. It suggests that p53 target genes were either activated via compensatory mechanisms involving alternative p53-independent pathways or that strong activation by upstream signaling cannot be overcome solely by reducing p53 levels in the presence of persistent DNA damage.

Abstract ID: 1544055

Title: Real world treatment patterns, reasons for discontinuation, and survival outcomes among patients with chronic lymphocytic leukemia/ small lymphocytic lymphoma (CLL/SLL) receiving second or later lines of therapy in a contemporary population treated in the United States

Authors: Matthew Davids, Jacob Ambrose, Enrico de Nigris, Jennifer Prescott, Siyang Leng, Mohammed Farooqui, Shravanthi R. Gandra, Christina Zettler, Laura L. Fernandes and Ching-Kun Wang

Introduction: The development of targeted agents has transformed the treatment paradigm both in the first-line (1L) setting and for previously treated patients with CLL/SLL. This study examines the characteristics, treatment patterns, and outcomes of a large cohort of real-world patients receiving 2L or later lines of therapy (LOTs) by LOT.
Methods: Patients meeting the following criteria were identified from the COTA real-world database: aged ≥18 years at diagnosis with a confirmed CLL/SLL diagnosis who initiated 2L therapy between 1 January 2014 and 30 June 2021. Patients were ineligible if they had a documented diagnosis of a concurrent primary malignancy or transformation at the time of CLL/SLL diagnosis or a history of other primary malignancies, excluding benign skin cancers, within 3 years prior to CLL/SLL diagnosis. The initial index date for the study was the date of initiation of 2L therapy and was updated to the start of each subsequent LOT for LOT-specific analyses. The observation period was defined as the duration of time from index date to the date of patient death or last visit date (if date of death was not available). Patient and clinical characteristics and treatment patterns were summarized as appropriate using means, medians, and/or patient counts and percentages. Clopper-Pearson exact method was used for presenting confidence intervals for proportions. Time to event outcomes, including real-world progression-free survival (rwPFS) and real-world overall survival (rwOS), were assessed for the study population and by LOT using the Kaplan–Meier method.

Table 1: Patient and Clinical Characteristics by Line of Therapy

Characteristics	2L (N= 1102)	3L (N= 468)	4L (N= 201)	5L (N= 75)	6L (N=25)
Age at initiation of LOT, n (%)					
<65 years	560 (50.8)	126 (26.9)	52 (25.9)	24 (32.0)	6 (4.0)
≥65 years	542 (49.2)	342 (73.1)	149 (74.1)	51 (68.0)	19 (76.0)
Age at initiation of LOT, median [IQR]	70.00 [63.00, 78.00]	71.00 [64.00, 79.00]	72.00 [64.00, 79.00]	70.00 [64.00, 78.50]	74.00 [69.00, 82.00]
Sex, n (%)					
Female	431 (39.1)	192 (41.0)	77 (38.3)	22 (29.3)	4 (16.0)
Race, n (%)					
Black or African American	84 (7.6)	43 (9.2)	22 (10.9)	8 (10.7)	3 (12.0)
Asian	10 (0.9)	5 (1.1)	2 (1.0)	1 (1.3)	0 (0.0)
Other Race	70 (6.4)	35 (7.5)	15 (7.5)	6 (8.0)	1 (4.0)
White	915 (83.0)	369 (78.8)	158 (78.6)	59 (78.7)	20 (80.0)
Unknown	23 (2.1)	16 (3.4)	4 (2.0)	1 (1.3)	1 (4.0)
Ethnicity, n (%)					
Hispanic	96 (8.7)	38 (8.1)	19 (9.5)	8 (10.7)	3 (12.0)
Non-Hispanic	954 (86.6)	406 (86.8)	172 (85.6)	65 (86.7)	21 (84.0)
Unknown	52 (4.7)	24 (5.1)	10 (5.0)	2 (2.7)	1 (4.0)
Practice Type, n (%)					
Academic	131 (11.9)	66 (14.1)	32 (15.9)	11 (14.7)	3 (12.0)
Community	971 (88.1)	402 (85.9)	169 (84.1)	64 (85.3)	22 (88.0)
Previous LOT Category, n (%)					
BTKi	165 (15.0)	178 (38.0)	80 (39.8)	27 (36.0)	5 (20.0)
BCL2 inhibitor	7 (0.6)	20 (4.3)	17 (8.5)	11 (14.7)	7 (28.0)
PI3Kδ inhibitor	1 (0.1)	13 (2.8)	16 (8.0)	7 (9.3)	3 (12.0)
CD20	781 (70.9)	255 (54.5)	89 (44.3)	39 (52.0)	17 (68.0)
Chemotherapy	719 (65.2)	185 (39.5)	57 (28.4)	23 (30.7)	6 (24.0)
Investigational	61 (5.5)	28 (6.0)	11 (5.5)	4 (5.3)	1 (4.0)
HSCT	1 (0.1)	1 (0.2)	1 (0.5)	0 (0.0)	0 (0.0)
Other	734 (66.6)	189 (40.4)	63 (31.3)	24 (32.0)	6 (24.0)
Year of Initial Diagnosis					
≤2014	817 (74.1)	368 (78.6)	168 (83.6)	61 (81.3)	22 (88.0)
2015-2019	275 (25.0)	98 (20.9)	32 (15.9)	14 (18.7)	3 (12.0)
2020+	10 (0.9)	2 (0.4)	1 (0.5)	0 (0.0)	0 (0.0)
Follow-up Time From Initial Diagnosis (months), median [IQR]	101.46 [67.06, 142.33]	112.31 [78.26, 153.20]	118.32 [82.92, 154.65]	121.25 [85.50, 154.75]	132.30 [88.47, 152.42]
Time from Initial Diagnosis to R/R (months), median [IQR]	61.48 [33.07, 99.86]	59.18 [31.36, 100.05]	57.50 [33.73, 94.98]	50.50 [30.28, 92.43]	50.04 [37.71, 76.73]
Follow-up Time From R/R (months), median [IQR]	35.05 [18.45, 56.61]	48.10 [31.22, 65.55]	53.39 [39.16, 74.27]	63.72 [48.35, 79.99]	69.37 [63.72, 83.41]
ECOG Status, n (%)					
0-1	753 (68.3)	291 (62.2)	122 (60.7)	44 (58.7)	12 (48.0)
2+	42 (3.8)	19 (4.1)	6 (3.0)	4 (5.3)	1 (4.0)
Unknown	307 (27.9)	158 (33.8)	73 (36.3)	27 (36.0)	12 (48.0)
Rai Stage, n (%)					
0	294 (26.7)	121 (25.9)	52 (25.9)	23 (30.7)	6 (24.0)
I	231 (21.0)	93 (19.9)	33 (16.4)	15 (20.0)	4 (16.0)
II	105 (9.5)	40 (8.5)	12 (6.0)	6 (8.0)	3 (12.0)
III/IV	190 (17.2)	84 (17.9)	41 (20.4)	12 (16.0)	3 (12.0)
Unknown	282 (25.6)	130 (27.8)	63 (31.3)	19 (25.3)	9 (36.0)
Cytogenetic Risk*, n (%)					
Low Risk	37 (3.4)	14 (3.0)	3 (1.5)	0 (0.0)	0 (0.0)
High Risk	230 (20.9)	116 (24.8)	52 (25.9)	21 (28.0)	10 (40.0)
Unknown	835 (75.8)	338 (72.2)	146 (72.6)	54 (72.0)	15 (60.0)
Bulky Disease, n (%)**					
Presence	84 (7.6)	37 (7.9)	19 (9.5)	6 (8.0)	2 (8.0)
Absence	131 (11.9)	61 (13.0)	21 (10.4)	6 (8.0)	3 (12.0)
Unknown	887 (80.5)	370 (79.1)	161 (80.1)	63 (84.0)	20 (80.0)

*High Cytogenetic Risk defined as at least one of: del (17p) and/or TP53 mutation and/or IGHV unmutated; Low Cytogenetic Risk defined as none of: del (17p) and/or TP53 mutation and/or IGHV unmutated; and unknown defined as at least one unknown test result and none of: del (17p) and/or TP53 mutation and/or IGHV unmutated
**Bulky Disease is reported as documented in the EHR by the treating physician.

Figure 1: 2L Treatment Regimens

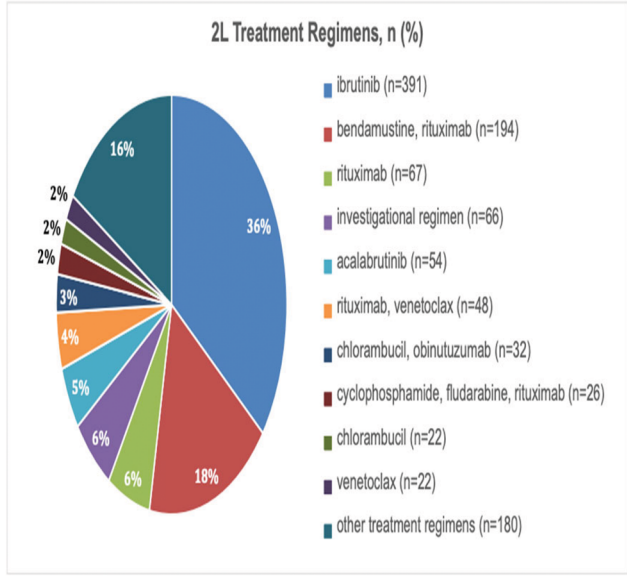

Results: A real-world population of 1,102 eligible patients with the following characteristics were included in the study: median age at diagnosis of 64 years (IQR: 57, 72), median age at 2L initiation of 70 years (IQR: 63, 78), male (60.9%), Caucasian (83.0%), and treated in the community setting (88.1%) (Table 1). Patients were most commonly diagnosed in 2014 or earlier (74.1%). Among patients with test results for the given molecular marker, marker positivity included: 59% (Nf314/536) del(13q), 35% (Nf135/385) del(11q), 23.1% (Nf86/372) del(17p), 20.6% (Nf102/496) TP53, and 32.3% (Nf70/217) IGHV mutated. The most common treatments among patients receiving 2L therapy were ibrutinib, bendamustine + rituximab (BR), rituximab, acalabrutinib, and investigational regimen (Figure 1). In 3L, the most common regimens were ibrutinib (26.1%, Nf122), acalabrutinib (10.7%, Nf50), and BR (10.0%, Nf47), and among patients who received 4L, common regimens included ibrutinib (21.9%, Nf44), rituximab + venetoclax (10.4%, Nf21), and acalabrutinib (9.5%,

Nf19). Utilization of BTK and BCL2 inhibitors and anti-CD20 antibodies increased from 2014 (39.9, 0.0, and 9.2%, respectively) to 2022 (48.9, 34.0, and 25.5%, respectively), while utilization of chemoimmunotherapy decreased markedly over the same time period (from 37.9 to 6.4%). Regarding reasons for treatment discontinuation, patients receiving 2L BTKi therapy discontinued therapy primarily due to toxicity (47.3% [Nf115/243] among patients receiving ibrutinib and 40.0% [Nf8/20] among patients receiving acalabrutinib) or death (14.0% [Nf34/243] among patients receiving ibrutinib and 20.0% [Nf4/20] among patients receiving acalabrutinib). CLL disease progression and doctor preference were also common reasons for treatment discontinuation in 2L. Approximately 17% of patients died after initiating 2L and prior to initiating 3L, and 25.5% of patients died prior to initiation of 4L. Among the study population, median rwPFS from initiation of 2L was 31.4 months (95% CI: 28.6, 35.5) and median rwOS from initiation of 2L was 79.0 months (95% CI: 68.9, 85.3).

Conclusions: Although targeted therapies have improved the outcomes of patients with CLL/SLL, these analyses suggest that there is still an unmet need with a high proportion of patients discontinuing treatments due to progression or toxicity. Furthermore, 2L+ patients continue to experience poor survival outcomes. Innovative treatment options and novel mechanisms of action are needed to improve CLL patient outcomes.

Abstract ID: 1544928

Title: An ongoing first-in-human phase 1 trial of NX-5948, an oral Bruton's tyrosine kinase (BTK) degrader, in patients with relapsed/refractory B cell malignancies, including chronic lymphocytic leukemia (CLL)

Authors: Francesco Forconi, Graham Collins, Emma Searle, Dima El-Sharkawi, David Lewis, Mary Gleeson, John Riches, Pam McKay, Jeanette Doorduijn, Rogier Mous, Wendy Stevens, Sarah Injac and Kim Linton

Background: BTK plays a central role in the B cell receptor (BCR) signaling pathway and is involved in the pathogenesis of several B cell malignancies. In various B cell malignancies, including CLL, BTK mutations confer broad resistance to both covalent and non-covalent BTK inhibitors, limiting their utility in later lines of therapy. Surprisingly, some of these mutations render BTK 'kinase dead' while preserving enhanced oncogenic BCR signaling, pointing to a scaffolding function of BTK. Novel therapeutics that can overcome emerging resistance mutations may represent an alternative treatment option for patients with CLL who have developed resistance to BTK inhibitors or in B cell indications where treatment with BTK inhibitors has been less effective [1]. NX-5948 is a novel, orally administered small molecule that induces BTK degradation via recruitment of the cereblon E3 ubiquitin ligase complex, without inducing degradation of other cereblon neo-substrates. NX-5948 induces sub-nanomolar potency degradation of both wild-type and known mutant forms of BTK *in vitro* [2], demonstrating rapid *in vivo* degradation in mouse and non-human primate B cells within two hours of oral administration [3]. In addition to efficacy in subcutaneous tumor models, NX-5948 can cross the blood-brain barrier and degrade BTK intracranially, translating to preclinical efficacy in mouse brain lymphoma disease models [3](Robbins et al. ASH 2021). This abstract describes the design and status of an ongoing phase 1 trial of NX-5948 in patients with relapsed/refractory B cell malignancies, including CLL.

Methods: NX-5948-301 is a first-in-human, dose-escalation (phase 1a) and cohort-expansion (phase 1b) study designed to evaluate the safety, tolerability, and preliminary efficacy of NX-5948 in adult patients with relapsed/refractory B cell malignancies, including CLL (NCT05131022; see Figure 1). Phase 1a will evaluate safety and tolerability of NX-5948 in patients with relapsed/refractory CLL, small lymphocytic lymphoma (SLL), non-germinal center B-cell (non-GCB) diffuse large B-cell lymphoma (DLBCL), follicular lymphoma (FL), mantle cell lymphoma (MCL), marginal zone lymphoma (MZL), and Waldenström macroglobulinemia (WM), including those with secondary central nervous system (CNS) involvement in any disease indication listed or primary CNS lymphoma (PCNSL). Phase 1b will investigate longer-term safety and anti-tumor activity of NX-5948 at the recommended dose(s) selected in phase 1a in patients with relapsed/refractory B cell malignancies across four cohorts. Key eligibility criteria include: ≥two prior lines of therapy; measurable disease per indication-specific response criteria; and an Eastern Cooperative Oncology Group (ECOG) score

Figure 1. NX-5948-301 study design

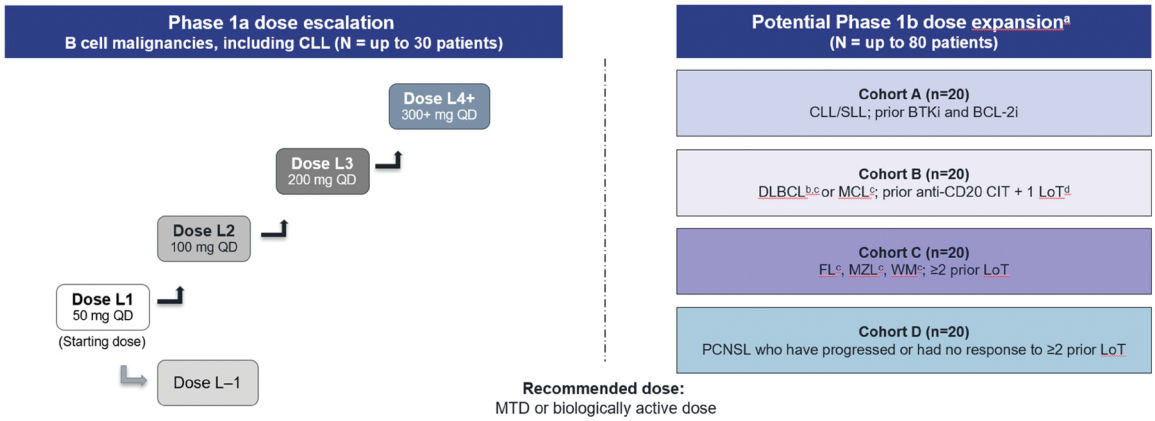

[a]Potential dose-expansion cohorts are expected to open in the second half of 2023; [b]Subtypes include: transformed indolent lymphoma (e.g. grade 3b/transformed FL), Richter-transformed DLBCL, high-grade B-cell lymphoma with MYC and BCL-2 and/or BCL-6 rearrangements, high-grade B-cell lymphomas NOS; [c]Includes patients with secondary CNS involvement; [d]Additional lines of therapy include anthracycline for non-GCB DLBCL and BTKi for MCL; [d]Grade 1–3a; eEMZL, MALT, NMZL, and SMZL.

of 0–2. NX-5948 is given orally, once daily, with dose escalation according to a standard 3 + 3 design. Dose-limiting toxicities will be assessed following the first cycle (28 days) of therapy. The recommended phase 1b dose(s) will be determined following assessment of PK/PD, safety, and anti-tumor activity. Approximately 110 patients (30 in phase 1a, 80 in phase 1b) may be enrolled and treated until confirmed progression or unacceptable toxicity. Enrollment in the phase 1a portion of this study is underway in the UK and the US, and is anticipated to begin in the Netherlands in 2023.

Abstract ID: 1545014

Title: Systematic literature review (SLR) of treatments and outcomes in patients with relapsed or refractory (R/R) chronic lymphocytic leukemia (CLL)/small lymphocytic lymphoma (SLL) previously treated with Bruton tyrosine kinase inhibitors (BTKi) and venetoclax

Authors: Lin Wang, Louise Hartley, Emma Hawe, Teresa Kangappaden, Alyshia Laidlaw and Jeff Sharman

Introduction: CLL/SLL remains incurable, despite the introduction of targeted agents such as BTKi and the B-cell lymphoma 2 inhibitor (BCL2i) venetoclax. Patients with R/R CLL/SLL require multiple lines of therapy, and outcomes are poor in these patients. Thus, an SLR was conducted to understand the efficacy of treatments for patients with R/R CLL/SLL who have failed ≥2 prior lines of therapy (i.e. third-line or later [3L+] R/R CLL/SLL), especially those previously treated with a BTKi and venetoclax.

Methods: Searches of the following sources were conducted: bibliographic databases (Medline, Embase, Cochrane Library) from inception to September 2022; trial registries; regulatory/health technology assessment agency websites from inception to October 2022; and conference proceedings from January 2020 to February 2023. Moreover, bibliographies of included SLRs were hand searched. Identified records were screened using the Population, Intervention, Comparator, Outcome, and Study design framework. Selection criteria targeted English language publications, reporting on studies of phase 2+ or observational study design, investigating all available treatments for adult patients with R/R CLL/SLL. Data extracted included study description, treatment information, baseline patient and disease characteristics, and efficacy outcomes. Where available, reported efficacy outcomes were classified according to either individual pharmacologic classes or class groupings, such as conventional systemic therapies (e.g. BTKi, BCL2i/venetoclax, phosphoinositide 3-kinase inhibitors [PI3Ki], chemoimmunotherapy, or combinations of the aforementioned), allogeneic stem cell transplantation (alloSCT), noncovalent BTKi, and chimeric antigen receptor (CAR) T cell therapy.

Results: Of the 643 studies included in the SLR, 41 trials and 25 observational studies reported outcomes data specifically in patients with 3L + R/R CLL/SLL. Of those, only 6 (2 trials and 4 observational studies) reported data in patients previously treated with BTKi and venetoclax. The 2 trials were phase 1/2 and investigated outcomes with noncovalent BTKi (nemtabrutinib and pirtobrutinib) as 3L + treatments (Table 1). The complete response (CR) rate was 0% in both trials, whereas objective response rate (ORR) was 58 and 79%, and median progression-free survival (PFS) was 10.1 and 16.8 months, for nemtabrutinib and pirtobrutinib, respectively. Neither trial reported overall survival (OS) data. Across the 4 observational studies (Table 2) where efficacy outcomes were reported for conventional systemic therapies, the CR rate ranged from 5.9% for PI3Ki therapy to 10.0% for BTKi, ORR ranged from 31.8% for chemoimmunotherapy to 53.4% for BTKi, median PFS ranged from 3 months for chemoimmunotherapy to 12 months for BTKi, and median OS ranged from 3.6 to 16.6 months for any conventional systemic therapy. For observational studies reporting data for alloSCT, ORR was 76.5%, and median PFS was 11 months; for noncovalent BTKi, ORR was 75.0%, and median PFS was not reached at a median follow-up of 9 months; for CAR T cell therapy, CR rate was 33.3%, ORR was 66.6–85.7%, and median PFS was 4–9 months. Among the 6 included studies

Table 1. Outcome data for trials

Reference	Treatment received in 3L/ population reporting outcomes	CR rate, %	ORR, %	Median (95% CI) PFS, months	Median (95% CI) OS, months
Woyach 2022[1]	Nemtabrutinib				
	Overall (n = 57)	4.0	56.0	26.3 (10.1–NE)	NA
	After BTKi + V (n = 24)	0	58.0	10.1 (7.4–15.9)	NA
Mato 2022[2]	Pirtobrutinib				
	Overall (n = 247)	1.6	82.2	19.6 (16.9–22.1)	NA
	After BTKi + V (n = 100)	0	79.0	16.8 (13.2–18.7)	NA

3L, third line; BTKi, Bruton tyrosine kinase inhibitors; CI, confidence interval; CR, complete response; NA, not available; NE, not estimable; ORR, overall response rate; OS, overall survival; PFS, progression-free survival; V, venetoclax.

1. Woyach JA, et al. *Blood* 2022;140(suppl 1):7004–7006.
2. Mato AR, et al. ASH 2022; Oral presentation 961.

Table 2. Outcome data for observational studies

Reference	Treatment received in 3L/ population reporting outcomes	CR rate, %	ORR, %	Median (95% CI) PFS, months	Median (95% CI) OS, months
Awan 2022[1]	Conventional systemic therapies				
	After BTKi + other (n = 405)	NA	NA	NA	33.1 (28.3–40.0)
	After BTKi + V (n = 57)	NA	NA	NA	16.6 (11.0–27.5)
Lew 2021[2]	Conventional systemic therapies or noncovalent BTKi				
	After BTKi + V (n = 17)	NA	NA	NA	3.6 (2.0–11.0)
Thompson 2021[3]	Conventional systemic therapies, alloSCT, noncovalent BTKi, or CAR T cell				
	After BTKi + V (CIT; n = 23)	NA	31.8	3	NA
	After BTKi + V (PI3Ki; n = 24)	NA	40.9	5	NA
	After BTKi + V (alloSCT; n = 17)	NA	76.5	11	NA
	After BTKi + V (noncovalent BTKi; n = 45)	NA	75.0	NR	NA
	After BTKi + V (CAR T cell; n = 9)	NA	85.7	4	NA
Mato 2020[4]	BTKi, PI3Ki, or CAR T cell				
	After BTKi + V (BTKi; n = 30)	10.0	53.4	12	NA
	After BTKi + V (PI3Ki; n = 17)	5.9	46.9	5	NA
	After BTKi + V (CAR T cell; n = 18)	33.3	66.6	9	NA

3L, third line; alloSCT, allogeneic stem cell transplantation; BTKi, Bruton tyrosine kinase inhibitors; CAR, chimeric antigen receptor; CI, confidence interval; CIT, chemoimmunotherapy; CR, complete response; NA, not available; NR, not reached; ORR, overall response rate; OS, overall survival; PFS, progression-free survival; PI3Ki, phosphoinositide 3-kinase inhibitors V, venetoclax.

1. Awan FT, et al. *Blood* 2022;140(suppl 1):7028–7029.
2. Lew TE, et al. *Blood Adv* 2021;5:4054–4058.
3. Thompson MC, et al. *Blood* 2021;138(suppl 1):2628.
4. Mato AR, et al. *Clin Cancer Res* 2020;26:3589–3596.

that reported on patients previously treated with BTKi and venetoclax, duration of response (DOR) was only reported in the nemtabrutinib trial, where the medium DOR was 8.5 months (95% confidence interval, 2.7–not estimable).

Conclusions: There remains a high unmet medical need for patients with 3L+R/R CLL/SLL previously treated with BTKi and venetoclax, with poor outcomes associated with conventional systemic therapies. Novel therapies such as CAR T cell therapy and noncovalent BTKi may provide better efficacy outcomes; however, no CR was observed with noncovalent BTKi in the included trials.

Abstract ID: 1545480

Title: Immune-profiling of ibrutinib-treated CLL patients revealed TMBIM6 as a potential target for CLL and its high expression as an independent variable associated with poor prognosis

Authors: Daniel Medina Gil, Laura Palomo, Víctor Navarro, Oriol Castells, Belén Sánchez, Pau Marc Muñoz Torres, Carlota Pagès, Cristina Hernández, Gemma Pujadas, Christelle Ferrà, Miguel Alcoceba, María José Terol, Rafael Andreu, Francesc Bosch, Pau Abrisqueta and Marta Crespo

CLL is distinguished by a marked T-cell disfunction that aggravates at disease progression. Ibrutinib treatment is commonly used in first-line and relapsed/refractory CLL. Discontinuations due to adverse effects, progression/Richter transformation and secondary resistances are current limitations. Identifying potential adaptive mechanisms to ibrutinib may help to overcome these limitations. Additionally, although there are some discrepancies between in-patient and in vitro studies, ibrutinib has been reported to improve T-cell function. Our study aimed to longitudinally assess the immune profile of ibrutinib-treated CLL patients to evaluate its effect in T-cell function and to identify

Figure 2

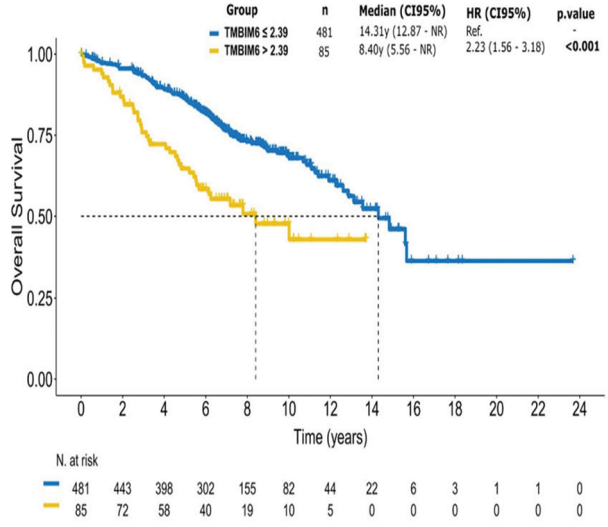

Figure 1

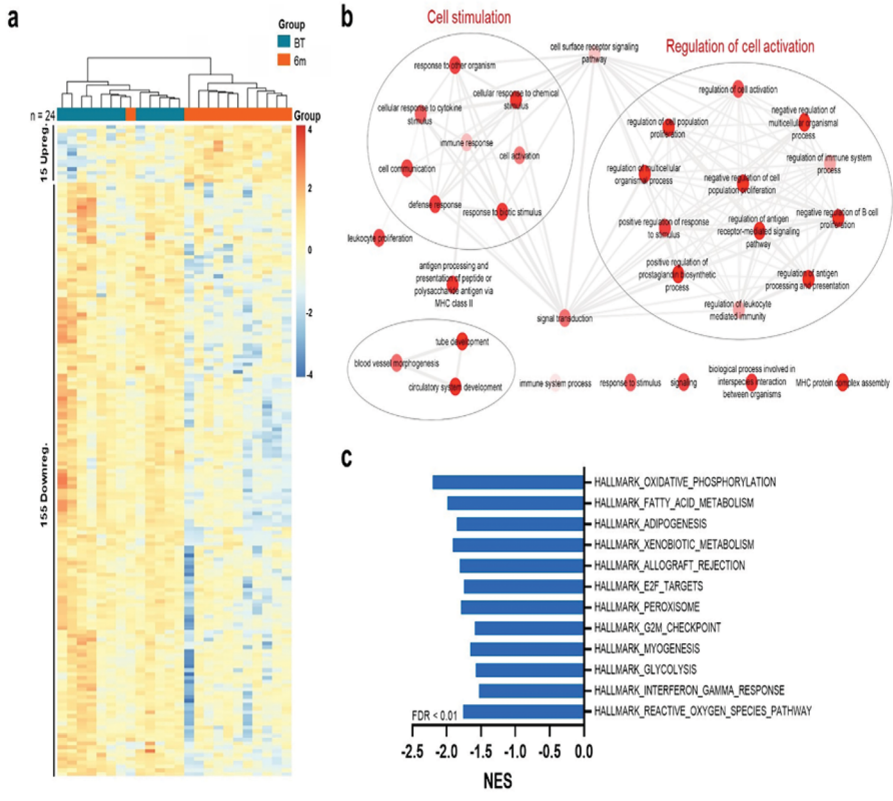

potential adaptive mechanisms. To do so, blood samples from 28 patients from GELLC7 trial (NCT03280160) were collected, at least, at two timepoints, including before treatment (BT), at 1, 3, 6 and 12 months during the first year of single-agent ibrutinib treatment. Peripheral blood mononuclear cells and plasma were isolated and stored to perform flow cytometry, RNA/DNAseq, migration assays, and cytokine determination. T-cell immunophenotyping revealed a decrease of CD4+ and CD8+ T cells expressing PD1 and CD244 upon ibrutinib treatment. The immunosuppressive/supportive subpopulations of T-regulatory cells and T-follicular helper cells were also reduced. Bulk-RNAseq of purified T cells revealed 170 differential expressed genes (DEG) upon 6 months of ibrutinib treatment. These genes participate in biological processes (Gene Ontology) related to cell stimulation and regulation of cell activation. Gene set enrichment analysis (GSEA) showed a downregulation of oxidative metabolism, proliferation, and activation pathways, indicating a reduction of the CLL inflammatory burden (Figure 1). Furthermore, there was a significant decrease of several inflammatory/migration chemokines (CCL2/CCL3/CCL4/CXCL10/CXCL12/CXCL13/CCL19) in plasma at 6 months. CLL-cell immunophenotyping showed a decreased expression of markers related to adhesion (CD44/CD62L), immunosuppression (CD200/BTLA), and migration (CXCR5/CCR7) at 6 months of ibrutinib treatment. However, CXCR4 expression increased upon ibrutinib treatment, and the proliferative CXCR4dimCD5br population was reduced. We investigated CXCR4-mediated migration as a potential mechanism of CLL-cell adaptation to ibrutinib. To this end, we evaluated the CXCL12-migratory capacity of CLL cells from 14 patients at BT and upon 6 months of BTK inhibition. We observed a reduced CXCL12-migratory capacity, but still some CLL cells were able to migrate under BTK inhibition. To characterize CLL cells that retained migratory capacity under BTK inhibition, we compared the recurrent genetic alterations and gene expression profiling of migrated cells from BT and after 6 months of ibrutinib. Targeted-DNAseq of migrated cells from the two timepoints revealed that, in 6 out of 12 patients, there was an alteration of the subclonal composition of CLL cells that retained migratory capacity under BTK inhibition with a recurrent enrichment of subclones harboring mutations in ATM and a NF-kB gene (NFKBIE or IKBKB). BTK or PLCG2 mutations were not observed at any timepoint. GSEA showed an upregulation of mTORC1 and Myc pathways in cells that retained migratory capacity under BTK inhibition. Among the DEG, TMBIM6 was the most significantly upregulated gene (FDR <0.05). TMBIM6 gene is related to apoptosis and mTOR-Akt axis and associated with poor prognosis in several solid tumors. We evaluated the prognostic impact of TMBIM6 expression using public clinical data from the CLL-map portal. TMBIM6 high expression was associated with poor overall survival in the univariable analysis (HR:2.23, *p*-value <0.001) (Figure 2), and in the multivariate analysis including age, gender, IGHV status and recurrent genetic alterations. We targeted TMBIM6 with BIA, an TMBIM6 antagonist, to assess its impact in CLL viability [1]. BIA induced CLL-cell apoptosis in suspension and co-cultured with a bone marrow stromal cell line plus CD40L and CpG ODN. Moreover, ibrutinib addition to BIA treatment enhanced the apoptotic effect of BIA. Collectively, these results indicate that TMBIM6 may be a potential novel target for CLL. Further experiments describing the molecular effects of BIA should be performed. In conclusion, ibrutinib treatment impacted on T cells from CLL patients by reducing the expression of exhaustion markers and the frequency of T-regulatory/follicular helper subpopulations. In CLL cells, we observed a downregulation of markers related to adhesion, immunosuppression, and migration, and an overexpression of TMBIM6 in CLL cells that retained migrative capacity towards CXCL12 under ibrutinib. Furthermore, we identified TMBIM6 high expression as an independent poor prognostic variable and demonstrated that BIA induces apoptosis of CLL cells *ex vivo* revealing TMBIM6 as a potential novel target for CLL.

Abstract ID: 1545577

Title: COVALENT-101: Phase I Study of BMF-219, a Covalent Menin Inhibitor, in adult patients with AML, ALL (with KMT2A/ MLL1r, NPM1 Mutations), DLBCL, MM, and CLL/SLL (NCT05153330)

Authors: Brian Hill, Jacqueline Barrientos, Juan Miguel Bergua Burgues, John Byrd, Jimena Cannata, Catherine C. Coombs, Herbert Eradat, Pau Montesinos, Daniel Morillo, Lawrence Morris, Olalekan Oluwole, Ricardo Parrondo, Javier Pinilla-Ibarz, Joseph Tuscano, Alex Cacovean, Courtney Follit, Mona Vimal, Steve Morris, Thomas Butler and William Wierda

Introduction: Menin, a protein involved in transcriptional regulation, impacting cell cycle control, apoptosis, and DNA damage repair, plays a direct role in oncogenic signaling in multiple cancers. Inhibition of menin is therefore a novel approach to cancer treatment. Preclinical data of BMF-219, a highly selective, orally bioavailable, small-molecule covalent inhibitor of menin, show sustained potent abrogation of menin-dependent oncogenic signaling *in vitro* and *in vivo*. BMF-219 exhibited a strong anti-proliferative effect on various menin-dependent acute myeloid leukemia (AML) cell lines, diffuse large B-cell lymphoma (DLBCL) cell lines representing Double/Triple Hit Lymphoma (DHL/THL) & Double Expressor Lymphoma (DEL), multiple myeloma (MM) cell lines with diverse mutational backgrounds. BMF-219 also exhibits high

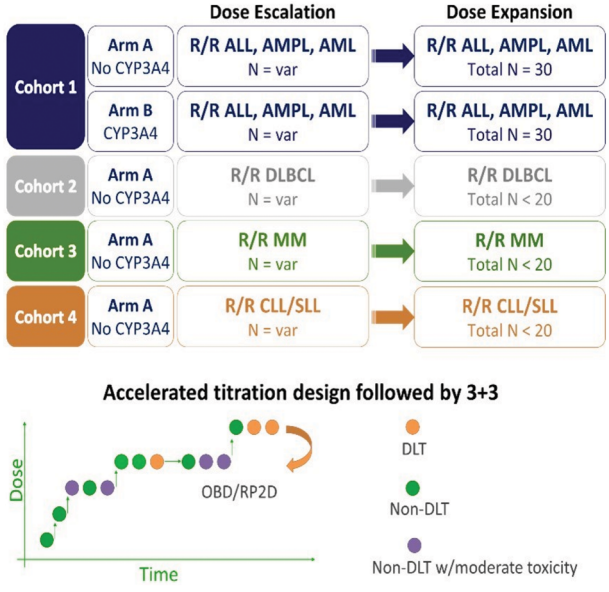

potency *ex vivo* in patient samples from MLL-rearranged and NPM1-mutant AML, THL and MYC-amplified DLBCL, bone marrow mononuclear cells from treatment-naive and R/R MM, and a collection of CLL patient specimens with various cytogenetic backgrounds including TP53 and NOTCH1 mutations, & previous BTK inhibitor therapy.

Aims: COVALENT-101 (NCT05153330) is a prospective, open-label, multi-cohort, non-randomized, multicenter Phase I study evaluating the safety, tolerability, and clinical activity of escalating doses of daily oral BMF-219 in patients with relapsed or refractory (R/R) acute leukemia (AL), DLBCL, MM and CLL who have received standard therapy. The primary objective of the study is to determine independently for each cohort/indication, the optimal biological dose (OBD)/ recommended Phase 2 dose (RP2D) of BMF-219 oral monotherapy. Key secondary objectives include further evaluation of safety and tolerability, characterization of the pharmacodynamics and pharmacokinetics of BMF-219, and assessment of its antitumor activity based on best overall response rate (ORR), duration of response (DOR), progression-free survival (PFS), and time to progression (TTP) per disease-specific response criteria as assessed by the investigator. Food-effect studies will be performed at certain dose levels.

Methods: Utilizing an accelerated titration design, doses of BMF-219 will be escalated in single-subject cohorts independently for each indication until 1 subject experiences either a ≥ Grade 2 related adverse event or dose limiting toxicity (DLT). At that point, the cohort will switch to a classical '3 + 3' design. Treatment will continue in 28-day cycles until progression or intolerability. Expansion cohorts for each indication will enroll patients to obtain further safety and efficacy data. Patients with R/R AL, DLBCL who received at least 2 prior therapies, MM who received at least 3 prior therapies, CLL/SLL who received at least 2 prior therapies and have either failed or are ineligible for any standard therapies are eligible. Patients must have ECOG PS ≤2, and adequate organ function. Key exclusion criteria include known CNS disease involvement, and clinically significant cardiovascular disease.

Results: As of 20 May 2023, the study is currently enrolling at 16 sites in the United States, Spain, and the Netherlands. Other European sites in Greece, Italy and France are in startup.

Conclusion: Enrollment commenced in January 2022 in the United States and in May 2023 in Europe.

Abstract ID: 1545879

Title: A phase 2 study of minimal residual disease-guided, time-limited, first-line therapy of chronic lymphocytic leukemia with pirtobrutinib and venetoclax (MIRACLE)

Authors: Yucai Wang, Wei Ding, Betsy LaPlant, Paul Hampel, Saad Kenderian, Eli Muchtar, Min Shi, Amber Koehler, Amy Behnken, Casey Aitken, Chandra Hutchens, Rachel Bubik, Neil Kay and Sameer Parikh

Background and significance: The current standard of care for first-line therapy of chronic lymphocytic leukemia (CLL) is continuous therapy with a covalent Bruton's tyrosine kinase inhibitor (BTKi), with or without an anti-CD20 monoclonal antibody, or fixed-duration therapy with venetoclax plus obinutuzumab. Indefinite therapy with a BTKi comes with long-term toxicities and inevitable development of resistance, while fixed-duration venetoclax-based therapy might be insufficient for a subset of high-risk diseases (e.g. with TP53 deletion or mutation). Combination therapy with a covalent BTKi and venetoclax is being studied in several clinical trials, but the optimal strategy, especially the optimal duration of therapy, remains unclear. We developed an investigator-initiated study to evaluate time-limited first-line CLL therapy with pirtobrutinib and venetoclax, in which the duration of therapy will be guided by minimal residual disease (MRD) status. Pirtobrutinib is an orally available, highly selective, noncovalent, reversible inhibitor of BTK, which has demonstrated excellent efficacy and safety in CLL and mantle cell lymphoma, including in patients with prior covalent BTKi exposure and BTK C481 mutation, a key mechanism of resistance to covalent BTKi in CLL. The rationale for combining pirtobrutinib and venetoclax include their distinct mechanisms of action, potential synergy, significant single-agent activities, and the potential for achieving undetectable MRD (uMRD) with time-limited therapy. The rationale for MRD-guided therapy include (1) MRD status is prognostic for progression-free survival (PFS) and overall survival (OS) in CLL and achieving uMRD is an important milestone in CLL treatment; and (2) the MRD-guided approach can tailor individualized duration of therapy based on the depth of response and may result in less toxicities and longer remissions.

Study design and methods: This is a single center, open label, phase 2 study. A total of 45 patients will be enrolled at Mayo Clinic (Rochester, MN). The main inclusion criteria include confirmed diagnosis of CLL or small lymphocytic lymphoma (SLL), presence of an indication for treatment according to iwCLL 2018 guidelines, ECOG performance status 0–2, adequate blood counts and hepatorenal function (e.g. CrCl ≥40 ml/min). The main exclusion criteria include prior CLL/ SLL-directed therapy, Richter transformation, CNS involvement, major comorbidities (e.g. cardiac, pulmonary, infectious), a bleeding disorder, major surgery within 4 weeks, and other active primary malignancy requiring treatment or limiting expected survival to ≤2 years. Eligible patients will receive time-limited combination therapy with pirtobrutinib and venetoclax, and the duration of therapy will be guided by MRD results. Treatment consists of a

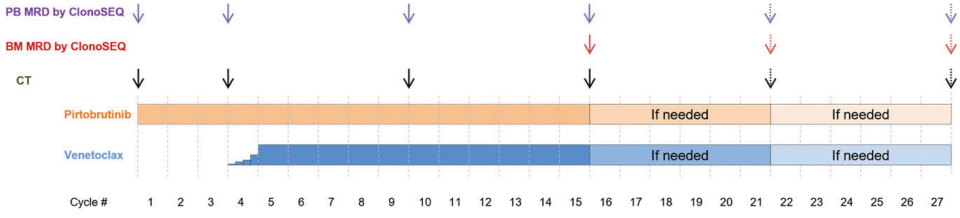

Fig 1. Trial schema including treatment cycles and response assessment schedule

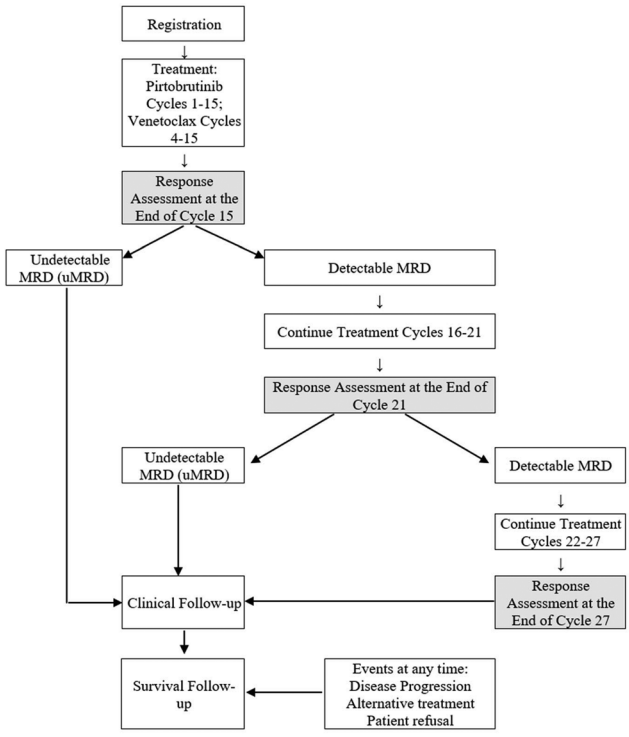

Fig 2. MRD-guided decision on duration of treatment

3-cycle lead-in with pirtobrutinib alone, followed by 12–24 cycles of pirtobrutinib-venetoclax combination therapy (with standard venetoclax dose ramp-up in Cycle 4). MRD status in peripheral blood (PB) and bone marrow (BM) will be monitored using the ClonoSEQ assay at key timepoints (Figure 1). Patients can discontinue therapy if they achieve uMRD (<1/10^4) in both PB and BM after Cycle 15 or Cycle 21. Patients who do not achieve uMRD by Cycle 21 will continue therapy for 6 more cycles and discontinue therapy after Cycle 27, regardless of MRD results (Figure 2). After completion of therapy, PB MRD will be monitored by ClonoSEQ every 6 months for 3 years. Research samples will be collected at key clinical response assessment timepoints for correlative research. The primary endpoint is the rate of uMRD in both PB and BM after Cycle 15. The secondary endpoints include PB uMRD rate, BM uMRD rate, complete response (CR) rate, objective response rate (ORR), duration of response (DOR), PFS, time to next treatment, OS, and adverse event incidences (measured per NCI-CTCAE version 5.0). With a one-stage binomial design, a sample size of 41 evaluable patients will have 10% Type I error and 90% power to detect an effective treatment, if the true proportion of patients who achieve uMRD in both PB and BM after Cycle 15 is at least 60% versus the null hypothesis that the true proportion is at most 40%. Four additional patients will be enrolled to account for ineligibility or drop out, for a total sample size of 45. This study is registered with ClinicalTrial.gov (NCT05677919). The trial is currently open to accrual at Mayo Clinic in Rochester, MN, and we anticipate to complete accrual by early 2024.

Abstract ID: 1546087

Title: Impact of nucleotide metabolism on CLL B-cell pathobiology and CLL disease progression

Authors: Sutapa Sinha, Weiguo Han, Zhiquan Wang, Kari Rabe, Susan Slager, Chantal McCabe, Daniel O'brien, Sameer Parikh, Esteban Braggio and Neil Kay

It has become increasingly clear that external signals from the leukemic microenvironment make pivotal contributions to disease progression in CLL. Multiple studies including ours have demonstrated that bone marrow stromal cells (BMSCs) promote CLL B-cell survival and protect these cells from the cytotoxic effects of therapy, but the complete nature of this interaction is still under studied. To further uncover the mechanism of this interaction, we performed RNA-seq in paired CLL B-cells isolated from untreated blood and bone marrow (BM) ($n=6$) and in untreated CLL B-cells ($n=4$) cultured alone or co-cultured with primary BMSCs derived from normal individuals ($n=2$) or CLL patients ($n=2$). We found upregulation of 232 and 917 genes in CLL B-cells from BM and in co-cultured CLL B-cells compared to CLL B-cells from the same patient's blood and CLL B-cells cultured alone respectively ($p<0.05$, fold change >1.5). However, we found only 13 genes overlapped between BM CLL B-cells and co-cultured CLL B-cells (Figure 1). To explore the functional importance of these 13 genes, we analyzed the expression of these genes in CLL blood B-cells from an additional 162 untreated patients by RNA-seq and compared them with their clinical outcomes. We found a positive relationship between 4 of these 13 genes (PNP, C16orf54, MOB3A, CDK2AP2) with CLL patient's clinical outcomes including overall survival (OS), progression-free survival (PFS), and time to first treatment (TTFT) (Figure 1) using Cox multivariable proportional hazard model (MCPHR $p<0.05$). Out of these 4 genes, purine nucleotide phosphorylase (PNP) an enzyme in the purine salvage pathway, showed the most significant association for patient's OS, PFS, and TTFT using MCPHR [hazard ratio (HR) {HR (95% CI)}: 2.2 (1.4–3.7), 2.2 (1.5–3.2), 2.5 (1.7–3.7) respectively, $p<0.005$]. We also observed an increase in PNP protein levels in CLL B-cells co-cultured with BMSCs or from BM using Western blot (WB) analysis but only when baseline PNP protein is low. Additionally, untargeted metabolomic profiling (LC-MS + GC-MS) showed an increased level of purine salvage pathway metabolites adenosine, inosine, and hypoxanthine in CLL B-cells when co-cultured with BMSCs. When we treated high and low PNP expressing CLL B-cells from untreated patients with drugs known to be active in CLL, interestingly we found high PNP expressing CLL B-cells are sensitive to Bcl2 inhibitor venetoclax and AXL kinase inhibitor TP-0903 versus low PNP expressing CLL B-cells. These results suggest purine metabolism plays an important role in CLL B-cell survival and /or drug resistance. Consistent with this altered purine nucleotide metabolism data, we also found increased pyrimidine pathway enzyme thymidylate synthase (TYMS) at both RNA and protein levels in co-cultured CLL B-cells and in CLL B-cells isolated from BM. We further analyzed the RNA-seq data generated from the 162 CLL patient cohort and found a positive association of TYMS gene with their TTFT (Figure 1) using MCPHR [HR: 1.4, 95% CI (1–1.8), $p<0.05$]. However treatment of CLL B-cells from untreated patients cultured alone or co-cultured with BMSCs with TYMS inhibitor raltitrexed did not show any killing indicating an alternate role of TYMS in BMSC cultured CLL B-cells. To that end we have detected increased expression of epithelial to mesenchymal (EMT) markers with increased TYMS expression in co-cultured CLL B-cells compared to CLL B-cells cultured alone by WB analysis. In conclusion, these results indicate that active purine and pyrimidine metabolism in CLL B-cells augmented by the BM

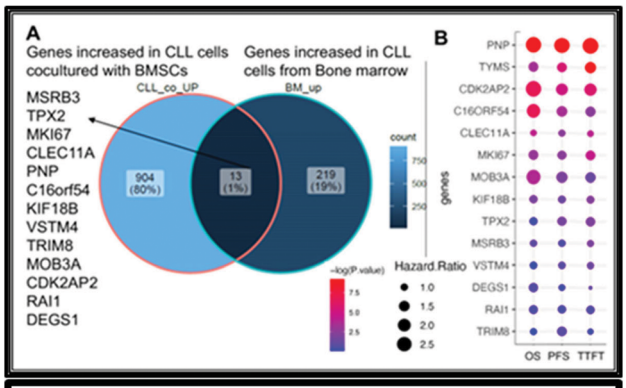

Figure 1. A. Venn Diagram showing the overlapped genes upregulated in both CLL B-cells after co-cultured with BMSCs and CLL B-cells isolated from BM. **B.** The clinical outcomes with the expression of the indicated genes. OS= overall survival, PFS= progression-free survival and TTFT= time to first treatment.

environment can support CLL B-cell survival and drug resistance and possible induction of EMT components. Future studies are underway to understand the role and regulation of PNP and TYMS in CLL disease progression and drug resistance for both untreated and treated CLL patients.

Abstract ID: 1547449

Title: Immunophenotyping of chronic lymphocytic leukemia in Yemen

Author: Saleh Abohadi

Background: Immunophenotyping is an essential component for the diagnosis of chronic lymphoproliferative disorders. This assessment is required by the WHO for disease classification and is a financial burden for resource-constrained countries. In Yemen there are also major logistical problems due to ongoing civil unrest. Objectives: We aimed to establish and assess 3-color flow cytometry to assist in the diagnostic assessment of chronic lymphocytic disorders (CLL) in Yemen. **Methods:** The immunophenotypic profile of 346 cases with the morphology of chronic lymphocytic leukemia that presented over a six years period was determined using a single laser FACSCalibur flow cytometer. CD45/Side scatter gating was used to identify the leukemic cells. Antibodies used were to surface and intracellular antigens including CD45, CD34, CD10, CD19, CD20, CD79a, CD22, CD23, CD5, FMC7, CD11c, CD25, CD38, Kappa and Lambda. Antibodies were conjugated with FITC, PE or PerCP fluorophores. **Results:** The patients aged in range from 22-90 (median 60) years, with a male: female ratio of 1.6:1 and the leucocyte counts 11-543×109/L. Flow cytometry was successful in all cases. CD19 was positive in all, along with other B-cell antigens CD20 (98%), CD79a (94%), CD23 (87%) with 75% of cases kappa and 25% lambda light chain restricted. CD5 was positive in 96% of cases, CD38 (52%), CD11c (43%), CD25 (89%) and FMC7 (34%). CD10 and CD34 were negative. **Conclusion:** Despite the geopolitical conditions faced flow cytometry was able to be performed. The antigen expression patterns were in keeping with the WHO definition for CLL. However, there was higher expression of CD25 and CD11c, and half the cases in Yemen expressed CD38 antigen, known to be associated with a poorer prognosis. Key Words: Flow cytometry, chronic lymphoproliferative disorders, Immunophenotyping.

Abstract ID: 1547566

Title: Pericardial effusion in patients with chronic lymphocytic leukemia treated with Bruton's tyrosine kinase inhibitors

Authors: Liron Hofstetter, Shai Shimoni, Pia Raanani and Gilad Itchaki

Introduction: Burton tyrosine kinase inhibitor (BTKI) has revolutionized the treatment of chronic lymphocytic leukemia (CLL). While more effective than common chemoimmunotherapy (CIT) regimens, they have a unique safety profile, including rare yet reported life-threatening adverse events (AEs) such as hemorrhage, ventricular arrhythmia, and sudden death. Next-generation BTKIs such as acalabrutinib and zanubrutinib are more specific and associated with fewer AEs. Pericardial effusion or tamponade (PE/T) related to BTKI treatment is an underrecognized AE with only a few cases reported to date. Putative mechanisms may be related to on- or off-target effect of BTKI. We present our institutional experience with ibrutinib-associated pericardial effusion, estimate its prevalence from a national registry, and estimate its incidence from published randomized control trials (RCTs).
Methods: We used two computerized databases: an institutional, and a national registry from the largest public medical organization in Israel (Kupat Cholim Clalit), to detect cases of PE/T in patients with CLL according to their exposure to BTKIs. Diagnoses of pericarditis and other pericardial pathologies were excluded. We assessed the prevalence of this AE and the relative risk associated with BTKI treatment. We further assessed its relative incidence from published RCTs where BTKI-containing regiments were compared with non-BTKI, usually CIT regimens. This study was done in accordance with the institutional Helsinki Committee.
Results: At our institute, we found 4 CLL patients who developed PE/T while on treatment with ibrutinib. Details regarding the cases are listed in Table 1. All patients received full-dose of ibrutinib. Time from start of treatment to effusion development varied between 1 and 26 months. Three patients suffered from atrial fibrillation (AF) along with PE/T. Three patients had accompanying pleural effusion. The pericardial effusion was drained in all patients; two had bloody pericardial fluid, all had exudative markers, and cytology was negative for malignant cells in all cases. Only one patient had taken aspirin before the event. Ibrutinib was discontinued in all patients, while it was reintroduced in 1 without further events. All patients received additional treatment with prednisone and/or colchicine. PE/T did not recur in any of them. According to our institution database, out of 750 CLL patients, 154 received BTKIs (mostly ibrutinib), 5 developed PE/T, 4 of whom were on ibrutinib at the time, and 1 was without therapy. The calculated prevalence of PE/T in CLL patients under BTKI was 2.6% (95%CI: 0.71–6.52%) with a relative risk (RR) of 15.48 (95%CI 1.74–137.5; Fisher Exact test, *p*-value =0.0072). In the national HMO registry of 5917 CLL patients, of whom 770 were treated with BTKIs, we identified 19 cases of PE/T: 6 after the administration of BTKI, and 13 in patients who did not receive BTKI. The estimated prevalence in this larger cohort was 0.78% in patients under BTKI with a RR of 3.09 (95%CI

Table 1. Cases of pericardial tamponade under ibrutinib in our institute.

Pt	Time from start of Ibrutinib	Dosing	AF	Treatment of tamponade	Pleural effusion drainage	Effusion type	Treatment following pericardial effusion	Predisposing event	Anticoagulation treatment/ Anti-aggregation treatment	Effusion reoccurred
1	26 Months	420 mg	No	Drainage + prednisone + colchicine	Yes	ExudateSero-bloody	Ibrutinib stopped	No	No	No
2	41 Months	420 mg	Yes	Drainage + colchicine	Yes	Exudate	Ibrutinib stopped for one month and then restarted	No	No	No
3	6 Months	420 mg	Yes	Drainage + colchicine + NSAIDS	Yes	ExudateClear fluid	Ibrutinib stopped	No	Aspirin	No
4	1 Month	420 mg	Yes	Drainage + prednisone	No	Bloody fluid	Ibrutinib stopped	URTI	No	No

Table 2. RCTs of BTKI vs. CIT reporting PE/T.

Study	Design	BTKi arm		Control arm		Median follow up (months)
		N. of patients	Events	*N.* of patients	Events	
RESONATE-2 (1)	IB vs. Chl	136	1	133	0	18.4
HELIOS (2)	IB + BR vs. BR + placebo	289	0	289	2	34.8
E1912 (3)	IB + R vs. FCR	354	2	174	0	33.6
ALLIANCE (4)	IB+/−R vs. BR	364	5	183	0	38
FLAIR (5)	IB + R vs. FCR	386	1	385	0	53
SEQUOIA (6)	Zan vs. BR	352	2	238	0	26.2
ELEVATE TN (7)	Acal+/−O vs. Chl-O	358	2	177	0	28.3

Abbreviations: IB: ibrutinib; Chl: chlorambucil; R: rituximab; FCR: fludarabine, cyclophosphamide, rituximab; BR: bendamustine, rituximab; Zan: zanubrutinib; Acal: acalabrutinib; O: obinutuzumab. Ref. 1. Byrd et al, NEJM 2014; 2. Chanan-Khan et al, Lancet Oncol 2016; 3. Shanafelt et al, NEJM 2019; 4. Woyach et al, NEJM 2018; 5. Hillmen et al, Lancet Oncol 2023; 6. Tam et al, Lancet Oncol 2022; 7. Sharman et al, Lancet 2020.

1.18–8.1), *p*-value =0.029). Since data is anonymized, we do not have further information on these patients. In an analysis of RCTs comparing BTKI-containing regimens with non-BTKI-containing regimens in CLL, we found 7 relevant studies that reported on PE/T specifically. Studies that reported on 'other cardiac toxicity' without specifications were excluded from analysis. Details are summarized in Table 2. Twelve cases (out of 2239 patients) of PE/T were reported in the investigational arm vs. 2 cases (out of 1580) in the non-BTKI containing arm. The calculated weighted average incidence of PE/T, according to the median exposure time on BTKI in each trial, was 216.2 cases/100,00 patient-years (PY). According to intention to treat analysis and based on median follow-up at each reported study, the incidence RR for developing PE/T in the BTKI arm was 5.91 (95%CI 4.11–8.50, *p*-value <0.0001) compared with the control arm, with a number needed to harm of 599 (95%CI 730–507).

Conclusion: BTKIs are associated with an increased risk for pericardial effusion or tamponade. Further studies are needed to appreciate its incidence in next-generation BTKIs and understand the involved mechanism.

Abstract ID: 1548126

Title: Chronic obstructive pulmonary disease and previous infections have impact on infectious complications in patients with chronic lymphocytic leukemia treated with venetoclax: a multicentre SEIFEM study.

Authors: Francesco Autore, Andrea Visentin, Marina Deodato, Candida Vitale, Eugenio Galli, Alberto Fresa, Rita Fazzi, Alessandro Sanna, Jacopo Olivieri, Ilaria Scortechini, Maria Ilaria del Principe, Paolo Sportoletti, Luana Schiattone, Nilla Maschio, Davide Facchinelli, Marta Coscia, Alessandra Tedeschi, Livio Trentin, Idanna Innocenti, Anna Candoni, Alessandro Busca, Livio Pagano and Luca Laurenti

Introduction: Infections are a major source of morbidity and mortality in patients with Chronic Lymphocytic Leukemia (CLL). The development of targeted agents decreased the rate of these complications in comparison to standard chemoimmunotherapy regimens. However, these patients often elderly, with other comorbidities, heavily treated, experienced serious infections. The aim of our study was to evaluate the incidence of clinically or microbiologically documented bacterial, fungal and viral infectious complications in CLL patients treated with venetoclax.

Methods: The retrospective multicenter study included CLL patients treated since 2017 with venetoclax single agent until progression or toxicity or venetoclax plus antiCD20 antibody (mainly rituximab as part of VR protocol for 24 months or obinutuzumab as part of VO protocol for 12 months).

Results: A total of 287 patients with CLL received venetoclax during the study period from 16 different institutions: 151 patients (52.6%) as monotherapy and 136 (47.4%) associated to antiCD20 antibody. Basal characteristics of the whole population and of the two groups are summarized in Table 1. Patients of the first group were older, more frequently had del17/TP53mut, renal impairment and lower basal levels of IgG. They also showed more previous infections in the 12 months before the beginning of the treatment with venetoclax. We registered 284 infections of any grade. When

comparing time of first infection of any grade between the patients treated with venetoclax and those treated with venetoclax plus antiCD20 antibody, we registered a trend toward a higher rate of infection in the latter group after the first year ($p=0.066$). This difference was not confirmed when we focused on infections of grade 3-4 ($p=0.521$). One-hundred eighty-one infections of grade 1–2 developed in 114 patients (39.7%) during the study. Most of the infections involved the respiratory tract (106 events, 58.6%), followed by genitourinary tract (23, 12.7%) and gastrointestinal one (16, 8.8%). Pathogens implicated in the infections were isolated only in 57 (31.5%) cases: 36 viral, 18 bacterial and 3 fungal. We recorded 103 episodes of infections of grade 3–4, occurred in 73 patients (25.4%). The most common site of infection involved the respiratory tract (71 events, 68.9%), then we registered sepsis (13, 12.6%) and gastrointestinal tract infections (7 events, 6.8%). Of 103 severe infections, 64 (62.1%) were microbiologically proven, of whom 40 were viral, 21 bacterial and 3 fungal. When comparing patients with and without infection, COPD ($p<0.001$, OR 3.75), previous infections in the last 12 months ($p<0.001$, OR 3.15), renal impairment CrCl <70 ($p=0.049$, OR 1.62), previous treatments ($p=0.023$; OR 1.196) and stage A ($p=0.001$; OR 0.2) were more frequently associated with infection in univariate analysis. In multivariate analysis COPD ($p<0.001$, OR 5.39) and previous infections ($p=0.001$, OR 2.57) resulted significant. Stratifying patients according to COPD and previous infections in the last 12 months we obtained 3 groups significantly different in terms of risk for infections ($p<0.001$; Figure 1). When considering only grade 3–4 infections, risk factors significant in the univariate analysis were COPD ($p<0.001$, OR 3.23), smoke ($p=0.033$, OR 1.98) and previous infections ($p=0.020$, OR 1.91). COPD was the unique significant variable in multivariate analysis ($p=0.008$, OR 2.62). Treatment was withdrawn for infections in 80 patients (27.9%): in 58 (20.2%) treatment was temporarily discontinued, while in 22 (7.7%) discontinuation was permanent. The temporary withdrawals had median length of 20 days (range 3–200), in 35 cases hospitalization was necessary. The infections that caused definitive withdrawals were mainly pneumonia (12 cases, 6 of whom from SarS-CoV2 infection) and sepsis (8 cases, 5 of whom after a SarS-CoV2 infection). A total of 83 patients (28.9%) died and the median

Figure 1. Stratification of patients according to the two risk factors for infections COPD and previous infections in the last 12 months: none risk factor (group 0), one of the two risk factors (group 1), both the risk factors (group 2), p <0.001.

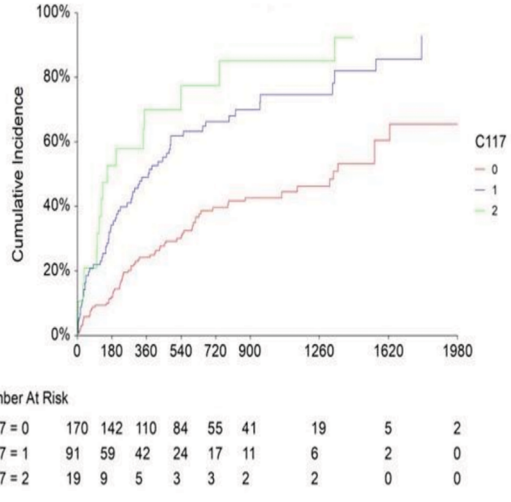

Table 1. Patients' characteristics with subdivision in the two subgroups (venetoclax single agent and venetoclax plus antiCD20 antibody) with significant differences between them.

		GENERAL 287 pts	VEN 151 pts	VEN plus antiCD20 136 pts	p value
Age	med	70	72	68	**0,002**
Gender	F/M	84/203	43/108	41/95	0,756
CIRS	≤6 / >6	209/78	110/41	99/37	0,991
Smoking	no/yes	233/54	125/26	108/28	0,447
Diabetes	no/yes	254/34	137/14	116/20	0,156
COPD	no/yes	247/40	131/20	116/20	0,721
CrCl <70	no/yes	170/117	80/71	90/46	**0,023**
IgG	med (mg/dL)	585	552	618	**0,038**
Binet	A/B/C	33/121/133	18/68/65	15/53/68	0,504
Del13	yes	97	56	41	0,273
+12	yes	37	20	17	0,899
Del11	yes	66	34	32	0,744
Del17	yes	82	54	28	**0,005**
TP53 mut	yes	85	56	29	**0,001**
Previous PCT	med	2	2	1	**<0,001**
Lymphocytes	med (x 10^9/L)	27	17	35	0.104
Neutrophils	med (x 10^9/L)	3.1	3	3.2	0,267
Platelets	med (x 10^9/L)	129	130	128	0,730
Hemoglobin	med (g/dL)	11.7	11.8	11.6	0,692
Previous infection	no/yes	193/94	88/63	105/31	**<0,001**
Previous pneumonia	no/yes	257/30	130/21	127/9	0,108

OS was 55 months. The main causes of death were CLL progression (36 cases) and infection (22 cases).

Conclusions: This is a real-life study on 287 patients affected by LLC treated with venetoclax with the aim to describe the infectious complications in such population in routine clinical practice. The analysis found a significant rate of infections, most of grade 1–2: 39.7% of the patients experienced a grade 1–2 infection; 25.4% a grade 3–4 infection. The identification of additional infectious risk factors found a role of comorbidities such as COPD and previous infections; COPD resulted a risk factor also for infections of grade 3–4 (Figure 2).

Abstract ID: 1548190

Title: Real-world characteristics and outcomes of patients with chronic lymphocytic leukemia/small lymphocytic lymphoma treated with long-term ibrutinib: results from the prospective, observational informCLL Registry

Authors: Nilanjan Ghosh, Jacqueline Barrientos, Meghan Gutierrez, Zaina Qureshi, Wasiulla Khan, Anat Raz, Vincent Girardi, Gabriel Krigsfeld and Jeff Sharman

Introduction: Recent analyses from the phase 3 RESONATE-2 study in patients with previously untreated chronic lymphocytic leukemia (CLL)/small lymphocytic lymphoma (SLL) showed that more than half of patients treated with ibrutinib continued to benefit from long-term ibrutinib therapy regardless of baseline characteristics, with sustained efficacy benefits [1]. Limited data are available on patient characteristics associated with long-term ibrutinib treatment in the real-world setting. The informCLL registry is a large, US-based, prospective, observational registry of patients who initiated FDA-approved treatment for CLL/SLL in the era after approval of ibrutinib and represents an opportunity to explore real-world outcomes in patients treated primarily in community-based practices. Here, we present the real-world characteristics and outcomes of previously untreated patients with CLL who received long-term (≥3 years) first-line (1L) treatment with ibrutinib on informCLL.

Methods: Patients with CLL/SLL who initiated FDA-approved treatment (within ±45 days of enrollment) were enrolled between October 2015 and June 2019. For this analysis, we evaluated the baseline demographics and characteristics, time to next treatment (TTNT), OS, and safety among the cohort of patients treated with 1L ibrutinib for ≥3 years. Multivariate logistic regression analysis was performed to determine baseline factors associated with the likelihood of receiving long-term ibrutinib (variables included time from initial diagnosis to 1L therapy, age, sex, race, insurance type, geographic region, ECOG status, Rai stage, comorbidity burden, other prior malignancy, FISH testing, del[17p]) by evaluating patients with 1L ibrutinib for ≥3 years compared to all others. TTNT and OS were estimated by Kaplan–Meier methods. Safety was assessed by rates of serious adverse events (AEs) and AEs leading to treatment discontinuation.

Results: A total of 1459 eligible patients were enrolled to informCLL; 854 patients were treated in the 1L setting, including 383 who received 1L ibrutinib therapy. Median duration of 1L ibrutinib was 24.0 months (range, 0.2 – 61.1) with a median follow-up of 31.4 months (range, 1.2 – 66.1); 42% of patients were receiving ongoing ibrutinib at study exit, including 82 patients who exited the study prior to 3 years of treatment due to study closure. Overall, 100 patients received ≥3 years of ibrutinib therapy, with a median treatment duration of 43.7 months. Baseline characteristics were largely similar between patients who received ≥3 years and those who received <3 years of ibrutinib (Table 1). In univariate analysis, there was a trend toward patients with high comorbidity burden (CCI ≥2) being less likely to receive ibrutinib for ≥3 years, although these findings were not statistically significant. In both univariate and multivariate analyses, no factors were significantly associated with likelihood of receiving ≥3 years of ibrutinib. With a median follow-up of 47.2 months in patients who received ibrutinib for ≥3 years, the estimated rate without next-line therapy was 93.9% at 48 months and 90.8% at 54 months; estimated OS rate was 96.5% at 48 months and 94.0% at 54 months. In patients treated with ≥3 years of ibrutinib, serious AEs occurred in 32 patients (32%); the most common serious AEs (reported in >3 patients) included pneumonia ($n = 5$) and atrial fibrillation ($n = 4$). AEs leading to ibrutinib treatment discontinuation occurred in 7 patients (7%) and included mucosal inflammation, increased hepatic enzyme, myalgia, Richter syndrome, confusional state, and palmar-plantar erythrodysesthesia syndrome ($n = 1$ each). AEs led to ibrutinib dose modification in 19 patients (19%), most commonly due to fatigue ($n = 6$). Among these 19 patients, AEs leading to first dose reduction tended to occur within the first year of ibrutinib, with a median treatment duration of at least 3 years after first dose reduction and 74% (14/19 patients) remaining on treatment at end of study (Table 2).

Conclusion: Analyses from informCLL show sustained TTNT and OS benefits in patients treated with ≥3 years of ibrutinib, with low rates of AEs leading to treatment discontinuation beyond 3 years and no new AEs observed. Baseline characteristics were similar between patients treated with 1L ibrutinib for ≥3 and those treated for <3 years. Consistent with the recent findings from the RESONATE-2 study, patients with dose modifications were also able to receive long-term therapy with 1L ibrutinib in this real-world registry. Together, these results suggest that patients with CLL representing a broad range of baseline characteristics can receive and benefit from long-term therapy with 1L ibrutinib in the real-world setting.

Table 1. Baseline demographics and patient characteristics by duration of ibrutinib therapy

Characteristic	Time on Ibrutinib			
	≥3 years n=100	<3 years due to study exit n=82*	<3 years due to non-exit reasons n=201*	Total N=383
Median age (range), years	70 (40–90)	70 (45–87)	74 (41–89)	72 (40–90)
Age ≥65 years, n (%)	70 (70)	58 (71)	156 (78)	284 (74)
Age ≥75 years, n (%)	33 (33)	25 (30)	89 (44)	147 (38)
Male, n (%)	59 (59)	51 (62)	123 (61)	233 (61)
Median time from initial diagnosis to treatment at registry enrollment (range), months	21.9 (0.2–241.2)	19.5 (0.2 –398.4)	21.3 (<0.1–471.3)	21.3 (<0.1–471.3)
Race, n (%)				
White	90 (90)	72 (88)	184 (92)	346 (90)
Black/African American	9 (9)	6 (7)	14 (7)	29 (8)
American Indian/Alaskan Native	0	0	2 (1)	2 (<1)
Unknown/not available	1 (1)	4 (5)	1 (<1)	6 (2)
ECOG performance status, n (%)				
0	45 (45)	48 (59)	86 (43)	179 (47)
1	49 (49)	30 (37)	100 (50)	179 (47)
≥2	2 (2)	3 (4)	13 (6)	20 (5)
Rai stage III/IV, n/N (%)	33/64 (52)	28/62 (45)	58/131 (44)	119/257 (46)
del(17p), n/N (%)	16/57 (28)	12/51 (24)	21/103 (20)	49/211 (23)
History of other malignancy, n (%)	25 (25)	17 (21)	58 (29)	100 (26)
Median CCI score (range)	1 (0–4)	1 (0–7)	1 (0–6)	1 (0–7)
CCI score ≥2, n (%)	22 (22)	20 (24)	66 (33)	108 (28)
Institution/site type, number of sites (%)	62 sites	57 sites	102 sites	132 sites
Community	59/62 (95)	51/57 (89)	93/102 (91)	122/132 (92)
Academic	3/62 (5)	6/57 (11)	9/102 (9)	10/132 (8)

*Given that baseline characteristics were largely similar between the patient subgroups treated with <3 years of ibrutinib due to study exit (N=82) and non-study exit reasons (N=201), these subgroups were combined as the <3 years treatment group (N=283).

Table 2. Time to first dose reduction and duration of ibrutinib treatment in patients with dose modification due to AEs

	N=19*
Median time to first dose reduction (range), months	7.9 (0.2–41.0)
Patient outcome post-dose reduction, n Patients continuing on treatment until end of study Patients discontinuing treatment	 14 5
Median time from first dose reduction to end of treatment or end of study** (range), months	37.6 (6.0–55.7)

*3 of 19 patients with dose reductions due to AEs were subsequently re-escalated to 420 mg dose.
**14 of 19 patients were receiving ongoing ibrutinib at end of study.

Abstract ID: 1548199

Title: Real-world duration of venetoclax treatment for chronic lymphocytic leukemia and small lymphocytic lymphoma

Authors: Anna Teschemaker, Shweta Hakre, Jenny Tse, Nazneen Fatima Shaikh, Yifan Gu and Aimee Near

Introduction: Venetoclax (V) is an approved fixed-duration treatment for patients with chronic lymphocytic leukemia and small lymphocytic lymphoma (CLL/SLL), either as a 12-cycle regimen (~12 months) in combination with obinutuzumab (O) in the first-line (1L) setting or as a 24-cycle regimen (~24 months) in combination with rituximab (R) in the relapsed/refractory (R/R) setting. Our objective was to analyze real-world treatment patterns of V+O in 1L and V+R in R/R settings in patients with CLL/SLL in the United States.

Table. Index treatment cycles among 1L cohort with V+O only and ≥12 months of follow-up (n=55) and R/R cohort with V+R only and ≥24 months of follow-up (n=39)

Measures	1L cohort with V+O and ≥12 months of follow-up (n=55)	R/R cohort with V+R and ≥24 months of follow-up (n=39)
Index treatment duration relative to fixed duration,[a] n (%)		
Treated for fixed duration[a]	5 (9.1)	2 (5.1)
Treated beyond fixed duration[b]	29 (52.7)	19 (48.7)
Median duration of index treatment regimen beyond fixed cycles, months (Q1, Q3)	1.3 (0.7, 2.6)	1.8 (0.5, 10.8)
Mean duration of index treatment regimen beyond fixed cycles, months (SD)	2.6 (3.4)	5.1 (6.7)
Early treatment discontinuation[c]	21 (38.2)	18 (46.2)
Median duration of index treatment regimen, months (Q1, Q3)	4.6 (2.3, 8.3)	7.1 (3.4, 11.1)
Mean duration of index treatment regimen, months (SD)	5.1 (3.5)	8.4 (5.7)

O, obinutuzumab; Q1, quartile 1; Q3, quartile 3; R, rituximab; SD, standard deviation; V, venetoclax.

Analyses were conducted among patients with sufficient follow-up (ie, ≥12 months for 1L cohort and ≥24 months for R/R cohort) to assess the proportion of patients meeting the definition of fixed-duration treatment, and with only V+O in the 1L or V+R in the R/R setting and no other treatments in the index treatment regimen.

[a]Fixed index treatment duration was defined as 336–364 days for V+O in the 1L setting or 707–735 days for V+R in the R/R setting, based on the 12- or 24-cycle dosing schedule (1 cycle = 28 days) and the tumor debulking phase, plus 28 days to allow for small gaps between V prescription fills. In the 1L cohort, the 12 cycles of V+O include the 5 weeks of V dose ramp-up because cycle 1 starts with O and V is added at day 22 of cycle 1. In the R/R cohort, the 24 cycles of V+R begin after the 5 weeks of V dose ramp-up, thus adding an extra 35 days.

[b]Treated beyond fixed duration was defined as index treatment duration >364 days in the 1L setting and >735 days in the R/R setting.

[c]Early treatment discontinuation was defined as index treatment duration of <336 days in the 1L setting or <707 days in the R/R setting with evidence of ≥60-day gap in V prescription refills.

Methods: A retrospective cohort analysis was conducted using the IQVIA PharMetrics® Plus database to identify patients aged ≥18 years treated with V+O (1L cohort; May 2019 to September 2021) or V+R (R/R cohort; June 2018 to September 2021). The start of the treatment regimen was defined as the index date. All patients were required to have ≥1 diagnosis code for CLL/SLL, 12 months of continuous enrollment (CE) prior to the index date, and ≥3 months of CE after the index date. Duration of treatment (DoT) was defined as time from index date to the earliest of either treatment discontinuation (defined as a ≥60-day gap in V prescription refills) or censoring (defined as end of follow-up). Fixed-duration treatment cycle was defined as 12- or 24-cycle dosing, corresponding to days 336–364 for the 1L setting and days 707–735 for the R/R setting, based on the dosing schedule plus 28 days. Kaplan–Meier analysis was used to estimate the probability of remaining on treatment for the 1L and R/R cohorts.

Results: A total of 116 patients in 1L setting (mean age, 62.3 years; 73.3% male) and 145 patients in R/R setting (mean age, 64.2 years; 73.8% male) were identified; 48.3% of patients in the R/R cohort had prior targeted therapy. The median (95% CI) DoT in patients treated with V+O ($n=115$) was 12.4 (11.5, 13.4) months over a median follow-up of 11.4 months; the probability of remaining on treatment at 6, 12, and 18 months was 80.6, 56.4, and 20.2%, respectively. The median (95% CI) DoT in patients treated with V+R ($n=133$) was 24.5 (13.4, 25.2) months over a median follow-up of 15.5 months; the probability of remaining on treatment at 12, 24, and 36 months was 66.0, 53.8, and 19.0%, respectively. Among patients treated with V+O, 47.8% (55/115) of patients had ≥12 months of follow-up (Table 1). Of the 55 patients with ≥12 months of follow-up, 9.1% had fixed cycles and 38.2% discontinued early (median DoT: 4.6 months; mean DoT: 5.1 months). Among patients treated with V+R, 29.3% (39/133) of patients had ≥24 months of follow-up. Of the 39 patients with ≥24 months of follow-up, 5.1% had fixed cycles and 46.2% discontinued early (median DoT: 7.1 months; mean DoT: 8.4 months). Among the patients treated for <12 months with V+O ($n=30$) and <24 months with V+R (n=48), the DoT was much shorter than the fixed-dosing schedule (mean DoT [SD]: 4.9 [3.2] and 6.8 [4.8] months, respectively) over a median follow-up of 17.8 and 17.9 months, respectively. Among the patients treated for >12 months with V+O (n=29) and >24 months with V+R ($n=19$), the DoT was slightly longer than the fixed-dosing schedule (mean DoT [SD]: 14.7 [3.4] and 29.6 [6.7] months, respectively) over a median follow-up of 20.0 and 35.3 months, respectively.

Conclusion: While the median DoT was approximately 12 months for patients treated with V+O and 24 months for patients treated with V+R in the 1L and R/R settings, respectively, more than 50% of patients in both cohorts either discontinued treatment sooner or continued to receive treatment beyond the approved fixed-dosing schedule. For patients treated for less than the fixed-dosing schedules, the mean DoT was <5 months in those treated with V+O and <7 months in those treated with V+R. Patients treated beyond the fixed-dosing schedules continued treatment for approximately 3 more months with V+O and 6 more months with V+R. This study provides evidence that a V-based approach may not be suitable for all patients with CLL/SLL. Future studies should include additional follow-up with a larger sample, reasons for treatment discontinuation, and patient molecular genetic profile.

Abstract ID: 1548582

Title: In-depth molecular analysis using a multi-gene lymphoma NGS panel in lymphomas with lymphoplasmacytic differentiation may provide more precise diagnosis, differentiation of entities and may optimize rational treatment allocations

Authors: Ella Willenbacher, Wolfgang Willenbacher and Andrea Brunner

Aims: To enable a more precise diagnosis and to describe potentially prognostic and therapeutic relevant mutations a refined molecular analysis of formalin-fixed paraffin embedded and decalcified bone marrow trephine biopsies at time of primary diagnoses, as well as follow-up of 41 patients with lymphomas with lymphoplasmacytic differentiation (LPLs) was performed.
Material and methods: Analysis was performed by means of a commercially available Lymphoma Panel (Lymphoma Solution, SophiaGenetics). Results were correlated with clinical and pathological parameters including pathological diagnosis, immune phenotype, volume of infiltration, infiltration pattern, and number of mast cells.
Results: Our group finally covered a spectrum of lymphomas with plasmacytic differentiation ranging from Waldenstroems macroglobulinaemia (WM), comprising the largest group, to small-B-cell lymphomas with plasmacytic differentiation (SBCL-PC) to IgM myeloma (MM). The most helpful diagnostic criteria were a combination of morphology including infiltration pattern and mast cell count, and immune phenotypes. The prototycical MYD88 L265P mutation was present in nearly all cases of WM but also in 50% of the SBCL-PC. Only MM were consistently negative for the mutation. We found that known oncogenic mutations, such as TP53 are already detectable early in the course of the disease and were associated with a significantly shorter PFS. In addition, we report on a novel BIRC3 frameshift mutation in a case of a progressive WM.
Conclusion: Our data indicate that patients with LPL might benefit from a thorough pathological work-up and a detailed molecular analysis in terms of a precise diagnosis and a more targeted treatment allocation.

Abstract ID: 1548590

Title: Rituximab maintenance after chemoimmunotherapy induction in 1st and 2nd line improves progression free survival: long term follow up of the international randomized AGMT-CLL8/a Mabtenance Trial

Authors: Alexander Egle, Petra Obrtlíková, Lukáš Smolej, Tomáš Kozák, Jan-Paul Bohn, Johannes Andel, Josef Thaler, Eva Mikušková, Liana Gercheva, Thomas Nösslinger, Miriam Ladická, Michael Girschikofsky, Mikuláš Hrubiško, Ulrich Jaeger, Clemens A. Schmitt, Martin Pecherstorfer, Eva Králiková, Cristina Burcoveanu, Emil Spassov, Jana Jurkovikova, Andreas L. Petzer, Georgi G. Mihaylov, Julian Raynov, Horst Oexle, August F. Zabernigg, Emília Flochová, Stanislav Palášthy, Thomas Melchardt, Jiří Mayer and Richard Greil

Introduction: Results of Rituximab maintenance after chemoimmunotherapy induction in 1st or 2nd line for 263 patients from the AGMT-CLL8/a Mabtenance trial NCT01118234 (Lancet Haematol. 2016) had been previously presented with a median follow up (FU) of 33.4 months and had shown a PFS benefit. We present an updated FU of 87.3 months, including analyses of MRD endpoints and salvage treatment results.
Results: The primary endpoint PFS benefit of maintenance remained stable and significant over time with an increase in median PFS from 35.6 to 47.5 months in the maintenance population compared to observation ($p=0.012$). PFS at median FU was 31.1 vs 20.2% in maintenance vs observation patients, respectively. The median time to next treatment increased from 53.3 in the observation arm to 78.7 months in the maintenance arm ($p=0.01$). The trial was not powered for analysis of OS. We observed no significant benefit in OS with 62.6% in the observation arm vs 68.4% in the maintenance arm alive at the median FU ($p=0.24$). In exploratory analyses MRD parameters (MRD from PB or BM, quantitative MRD subgroups) and BMI (as previously published) remained significant predictors of PFS with longer FU. The effect of rituximab maintenance was more pronounced in patients with detectable MRD after induction. MRD-parameters were also highly significant predictors of OS. A novel parameter of dynamic assessment of MRD in the first 6 months of observation (or maintenance) was a predictor of PFS independent of MRD strata. An analysis of retreatment outcomes in 144 retreated patients to date showed that the inclusion of novel drugs (any BTKi, Venetoclax or PI3K) in retreatment at any time ($n=85$ or 59% of retreated patients) led to a highly significant increase in OS ($p<0.0001$) for the group salvaged with novel drugs in any line of salvage. Patients in the maintenance arm had a somewhat higher percentage of novel drug treatment (66 vs. 53% in the observation arm) – likely due to the 25.4 months longer time to next treatment in a sensitive period for access to the novel drugs. Despite this small, but observable difference in usage of or access to novel drugs, no significant OS benefit was observed for maintained patients, likely because a majority of retreated patients had received novel drugs in both arms.
Conclusions: We present longer FU of a trial of rituximab maintenance after remission induction in the chemoimmunetherapy era. With longer FU we observe stable and meaningful benefits for maintenance in PFS and TTNT. We can validate MRD endpoints for PFS and OS prediction in long follow up and show novel dynamic MRD endpoints. Finally, we observe an enormous increase in OS for the trial group receiving novel drugs in any line of salvage, suggesting that OS benefits may no longer be attainable in trials due to effective salvage options in the current treatment paradigms.

Abstract ID: 1548596

Title: BRUIN CLL-314: A phase 3, open-label, randomized study of pirtobrutinib versus ibrutinib in patients with chronic lymphocytic leukemia/small lymphocytic lymphoma (trial in progress)

Authors: Maricer Escalón, Jennifer Woyach, Catherine C. Coombs, Katharine L. Lewis, Matteo Ceccarelli, Qiang Zhang, Yuanyuan Faith Bian and William Wierda

Background: Covalent (c) Bruton tyrosine kinase inhibitors (BTKi) have transformed the management of chronic lymphocytic leukemia/small lymphocytic lymphoma (CLL/

SLL), but these agents are not curative. cBTKi share pharmacologic liabilities such as low oral bioavailability and a short half-life that may lead to suboptimal BTK target coverage, especially in rapidly proliferating tumors with high BTK protein turnover, such as accelerating CLL/SLL, which can manifest as acquired resistance to cBTKi. Novel therapeutic agents addressing both intolerance and resistance while also improving efficacy are needed. Pirtobrutinib, a highly selective, non-covalent (reversible) BTKi, inhibits both wildtype and C481-mutant BTK with equal low nM potency and has favorable oral pharmacology that enables continuous BTK inhibition throughout the dosing interval regardless of intrinsic rate of BTK turnover. In the phase 1/2 BRUIN study, pirtobrutinib demonstrated promising durable overall response rates (ORR) and was well tolerated in patients with CLL/SLL irrespective of prior therapy (including cBTKi), number of prior lines of therapy, BTK C481 mutation status, or reason for prior cBTKi discontinuation. The objective of this study is to compare efficacy and tolerability of pirtobrutinib versus ibrutinib in patients with CLL/SLL.

Methods: BRUIN CLL-314 (NCT05254743) is a global, phase 3, open-label, randomized study comparing pirtobrutinib with ibrutinib. Approximately 650 BTKi-naïve patients, either treatment-naïve (approximately 30%) or previously treated with other non-BTKi agents, will be randomized 1:1 to receive daily 200 mg pirtobrutinib once daily or 420 mg ibrutinib as continuous monotherapy. Randomization will be stratified by del(17p) status (yes/no) and number of prior lines of therapy (0 vs. 1 vs. ≥2). Enrollment for this study is ongoing. Adults with CLL/SLL who require therapy per iwCLL 2018 criteria are eligible. Key exclusion criteria include prior exposure to any BTKi, use of some concomitant therapies including anticoagulants, such as warfarin and other vitamin K antagonists, significant cardiovascular disease, active infections, and other clinically significant conditions. The primary objective is to establish non-inferiority of pirtobrutinib versus ibrutinib by comparing the ORR per iwCLL guidelines assessed by an independent review committee. Superiority of pirtobrutinib versus ibrutinib in progression-free survival is a key secondary outcome. Other endpoints include duration of response, overall survival, time-to-next treatment, tolerability, and patient-reported outcomes. Trial efficacy and safety will be monitored by an independent data monitoring committee.

Abstract ID: 1548631

Title: Pharmacokinetics of idelalisib and outcomes

Authors: Loic Ysebaert, Fabien Despas, Etienne Chatelut, Sandra De Barros and Protin Caroline

Background: Idelalisib, a phosphoinositide 3-kinase (PI3K) delta inhibitor, has shown high efficacy as an oral drug in the treatment of B-lymphoproliferative disorders. Due to safety concerns, the FDA terminated postmarketing registry trials, leading to the ultimate withdrawal of the drug from the market in 2022. Surprisingly, excluding initial phase 1 trials, little information is available concerning the pharmacokinetics (PK) of idelalisib and its relationship with patient outcome. The study reported here was designed to investigate the relationship between PK (assessed after one month of treatment) and the occurrence of adverse events and outcomes.

Patients and methods: This open, prospective, non-randomized study was carried over two years (registered at clinicaltrials as NCT02824159) in Toulouse (France) University Hospital between April 2016 and April 2019. The study had planned a cohort of 57 patients, but, due to the safety alerts mentioned above, ultimately included 15 patients with CLL, 11 with FL and 1 with Waldenström macroglobulinemia (total $n=27$). At month 1 of treatment, when drug levels become stable, a one-day PK study was performed, with plasma collection before idelalisib intake, then at 30 minutes, 1, 2, 4 and 6 hours for 26 patients. Plasma concentration was assessed using a validated (according to FDA and EMA guidelines) U-HPLC-MS/MS method (chromatography plus mass spectrometry as detector). The parameters measured were (i) trough (Cmin) and Cmax and (ii) area under the curve (AUC) reflecting drug exposure.

Results: There were 12 women and 15 men, with a mean age of 68-year-old, all had been previously treated for a median of 3 lines (range 1–6). Idelalisib was prescribed at the classical dosage of 150 mg twice daily. Of the 27 patients, 74% interrupted treatment before the end of the first year, because of adverse event (AE) for 10, progression/relapse for 6 and death for 3. Over the first year of treatment, 169 AE were recorded in the 27 patients. Of them, 56 were clinically significant adverse events (CSAE: serious AE and/or CTCAE grade ≥3 and/or leading to dose concession) observed in 19 patients. They were mostly gastro-intestinal (35%), hepatic (28%) or hematological (18%). Of note, very little were respiratory (2%). PK analyses: an important inter-individual variation was observed with mean (+SD) values of 1077 + 416 ng/mL for SSC, 2886 + 900 ng/mL for Cmax and 13307 + 5152 ng/mL for AUC. As shown in Table 1, no difference in these parameters appeared to be associated with CSAE. No significant difference was observed either in PK values between patients who responded to idelalisib therapy ($n=17$) and those who did not ($n=8$). However, considering the median AUC as cutoff, interesting differences were observed in outcome. Indeed, the hazard ratio (HR) for progression-free survival was 2.65 (95% confidence interval [CI] 1.08–6.52), yielding a statistically significant difference ($p=0.003$) in favor or AUC below the median. This trend translated into a potential improvement in overall survival ($p=0.06$) for the group with lower AUC values, characterized by a higher HR of 3.09 (95% CI 0.94–10.1). Alltogether, this study demonstrates

Table 1. Pharmacokinetics of idelalisib according to the occurrence of CSAE (Mean ± SD).

PK parameters	Whole cohort N=26	CSAE N=18	No CSAE N=8	P value
Trough ng/mL	1077 ± 416	1138 ± 475	939 ± 199	0.4
Cmax ng/mL	2886 ± 900	2820 ± 956	3033 ± 796	0.8
AUC ng/mL	13307 ± 5152	13652 ± 5697	12530 ± 3872	0.8

Cmax: maximal concentration, AUC (τ ss): area under the curve

that lower overall exposure to idelalisib results in better outcomes.

Conclusions: Available data, including those presented in this study, plead in favor of a controlled assessment of idelalisib PK that would allow to pursue therapy with this drug. This therapeutic drug monitoring approach could be accompanied by appropriate individual dose adjustment to improve PFS/OS with this class of inhibitors, with clinical activity but unwanted toxicities.

Abstract ID: 1548777

Title: A phase 2 study of zanubrutinib in previously treated B-cell malignancies intolerant to ibrutinib and/or acalabrutinib: preliminary results for patients with CLL/SLL

Authors: Mazyar Shadman, John M. Burke, Syed F. Zafar, Jamal Misleh, Subramanya S. Rao, Charles M. Farber, Aileen Cohen, Rocco Crescenzo, Kunthel By, Ian Flinn and Jeff Sharman

Introduction: Patients with chronic lymphocytic leukemia/small lymphocytic lymphoma (CLL/SLL) treated with Bruton tyrosine kinase inhibitors (BTKi) often have adverse events (AEs) that lead to treatment discontinuation. Interim data from BGB-3111-215 (NCT04116437) suggest that zanubrutinib, a next-generation BTKi, is well tolerated in patients with B-cell malignancies who are intolerant of ibrutinib or acalabrutinib. Preliminary safety and efficacy results in patients with CLL/SLL treated with zanubrutinib after intolerance of ibrutinib or acalabrutinib are presented here.

Methods: Patients with CLL/SLL who were intolerant of ibrutinib, acalabrutinib, or both (without progression on prior BTKi) were given zanubrutinib monotherapy (160 mg twice daily [BID] or 320 mg once daily [QD]). Safety, including recurrence of AEs that led to intolerance of ibrutinib and/or acalabrutinib, and efficacy were assessed.

Results: As of Jan 3, 2023 (median follow-up, 25.6 mo), 61 patients with CLL/SLL (44 intolerant of only ibrutinib; 17 intolerant of acalabrutinib [9 intolerant of acalabrutinib only; 8 intolerant of acalabrutinib and ibrutinib]) were enrolled and received ≥1 zanubrutinib dose (160 mg BID, 43 [70%]; 320 mg QD, 18 [30%]). Median age was 71 y (range, 49–91 y); median duration of zanubrutinib treatment was 23.7 mo (range, 0.5–36.2 mo). The most common prior BTKi-intolerance AEs were fatigue ($n = 12$ events), rash ($n = 11$), and atrial fibrillation ($n = 10$). With zanubrutinib, 61% of patients did not experience recurrence of any prior BTKi-related intolerance AE. At the event level, 68% (65/95) of ibrutinib- and 71% (15/21) of acalabrutinib-intolerance AEs did not recur with zanubrutinib (Figure 1). Of the ibrutinib-intolerance AEs that did recur, 73% (22/30) recurred at a lower grade and 27% (8/30) recurred at the same grade. Of the acalabrutinib-intolerance AEs that did recur, 33% (2/6) recurred at a lower grade and 67% (4/6) recurred at the same grade. No intolerance AEs recurred at a higher grade. At data cutoff, 41 patients remained on treatment; 20 discontinued treatment (progressive disease, 6; AEs, 5; other, 9) and 12 discontinued the study (death, 6; patient withdrawal, 4; lost to follow-up, 2). The most common treatment-emergent AEs (TEAEs) were fatigue ($n = 18$ [30%]), COVID-19 ($n = 14$ [23%]), contusion ($n = 13$ [21%]), diarrhea ($n = 12$ [20%]), arthralgia, myalgia, and cough ($n = 10$ each [16%]). Grade ≥3 TEAEs were reported in 31 patients (51%); the most common grade ≥3 TEAE was neutropenia ($n = 7$ [11%]). Serious TEAEs were reported in 16 patients (26%), TEAEs requiring dose interruption in 30 (49%), and TEAEs leading to dose reduction in 15 (25%). One patient experienced a TEAE (COVID-19 pneumonia) that led to death. In 57 efficacy-evaluable patients, the disease control and overall response rates were 95% ($n = 54$) and 72% ($n = 41$), respectively. Progression-free survival rates at 6 and 12 mo were 95 and 88%, respectively.

Conclusions: AEs that previously caused patients to discontinue ibrutinib or acalabrutinib treatment were unlikely to recur with zanubrutinib, and their disease continued to be controlled, suggesting that patients intolerant of ibrutinib or acalabrutinib are likely to continue receiving clinical benefit by switching to zanubrutinib.

Figure. Recurrence and Change in Severity of Intolerance Adverse Events From Prior Ibrutinib or Acalabrutinib Exposure During Zanubrutinib Treatment in Patients With CLL/SLL

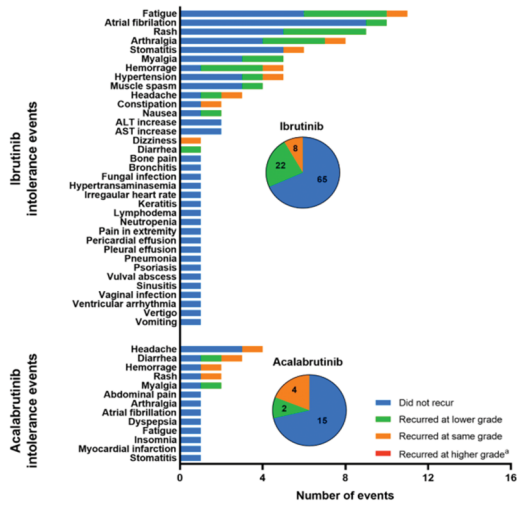

[a] No intolerance adverse events recurred at a higher grade.
ALT, alanine aminotransferase; AST, aspartate aminotransferase; CLL, chronic lymphocytic leukemia; SLL, small lymphocytic lymphoma.

Abstract ID: 1548812

Title: Zanubrutinib vs. bendamustine + rituximab (BR) in patients with treatment-naive chronic lymphocytic leukemia/small lymphocytic lymphoma: extended follow-up of the SEQUOIA Study

Authors: Jennifer Brown, Talha Munir, Mazyar Shadman, Tadeusz Robak, Brad S. Kahl, Paolo Ghia, Krzysztof Giannopoulos, Martin Šimkovič, Anders Österborg, Luca Laurenti, Patricia Walker, Stephen Opat, Hanna Ciepluch, Richard Greil, Merit Hanna, Monica Tani, Marek Trněný, Danielle Brander, Ian Flinn, Sebastian Grosicki, Emma Verner,

Alessandra Tedeschi, Sophie De Guibert, Gayane Tumyan, Kamel Laribi, José A. García-Marco, Jianyong Li, Tian Tian, Vanitha Ramakrishnan, Yu Liu, Andy Szeto, Jason Paik, Aileen Cohen, Constantine S. Tam and Wojciech Jurczak

Introduction: Zanubrutinib is a next-generation Bruton tyrosine kinase (BTK) inhibitor designed to minimize off-target binding and limit associated side effects that is approved in the US and EU for chronic lymphocytic leukemia/small lymphocytic lymphoma (CLL/SLL). Results from the SEQUOIA study (NCT03336333), at a median follow-up of 26.2 months, demonstrated superior progression-free survival (PFS) by independent review for zanubrutinib vs BR in patients with treatment-naive CLL/SLL without del(17p); patients with del(17p) treated with zanubrutinib in a separate cohort had similar outcomes to patients without del(17p). We report updated efficacy and safety results from the SEQUOIA study after approximately 18 months of additional follow-up.

Methods: Patients without del(17p) were randomized to receive zanubrutinib or BR. Patients with del(17p) were assigned to zanubrutinib monotherapy. Investigator-assessed (INV) PFS, overall survival (OS), overall response rate (ORR), and safety/tolerability were evaluated. Adverse events (AEs) were recorded until disease progression or start of next-line therapy.

Results: As of 31 October 2022, a total of 479 patients without del(17p) were randomized to receive zanubrutinib ($n=241$) or BR ($n=238$). At a median follow-up of 43.7 months (range, 0–60 months), median PFS was not reached with zanubrutinib; however, median PFS with BR was 42.2 months (HR, 0.30; 95% CI, 0.21–0.43; Figure 1). At 42 months, the estimated PFS rate was 82.4% with zanubrutinib. With additional follow-up, PFS with zanubrutinib vs BR was improved for patients with mutated IGHV (HR, 0.35; 95% CI, 0.19–0.64) and was sustained in patients with unmutated IGHV (HR, 0.23; 95% CI, 0.14–0.37) or del(11q) (HR, 0.26; 95% CI, 0.13–0.51). Complete response/complete response with incomplete hematologic recovery (CR/CRi) rates in patients without del(17p) were 17.4% and 21.8% with zanubrutinib and BR, respectively. While median OS was not reached in either arm, the HR for OS was 0.87 (95% CI, 0.50–1.48) with zanubrutinib vs BR and the estimated 42-month OS rates were 89.4 and 88.3%, respectively. For 110 patients with del(17p) assigned to zanubrutinib monotherapy, after a median follow-up of 47.9 months, the estimated 42-month PFS and OS rates were 79.4 and 89.5%, respectively. In this population, the CR/CRi rate was 14.5%. As of 31 Oct 2022, zanubrutinib treatment was ongoing in 74.7% patients without del(17p) and 70.3% patients with del(17p). The most common causes for treatment discontinuation were AEs and progressive disease for both patients without del(17p) (14.9, 5.8%, respectively) and with del(17p) (13.5, 13.5%). AEs of interest (AEI), using pooled terms, were as expected for the class in patients without del(17p) (zanubrutinib vs BR). AEI included any-grade atrial fibrillation/flutter (5.0 vs. 2.6%), hypertension (17.5 vs. 13.7%), bleeding (48.8 vs. 12.3%), infection (72.9 vs. 62.6%), anemia (7.1 vs. 20.7%), thrombocytopenia (6.3 vs. 18.1%), and neutropenia (16.7 vs. 56.8%). Additionally, grade ≥3 AEI included bleeding (5.8 vs. 1.8%), infection (23.8 vs. 22.0%), anemia (0.4 vs 2.2%), thrombocytopenia (2.1 vs 7.9%), and neutropenia (12.5 vs 51.1%).

Conclusions: Extended follow-up SEQUOIA data demonstrated that the efficacy of zanubrutinib was maintained in patients without del(17p) with a safety profile aligned with long-term follow-up for the BTK inhibitor class. Longer follow-up showed benefit in patients with mutated IGHV. Patients with del(17p) continue to demonstrate PFS benefits consistent with the randomized cohort. Zanubrutinib continues to be well tolerated with low rates of treatment discontinuation and remains a valuable frontline treatment option for CLL/SLL.

Figure: Progression-Free Survival by Investigator Assessment

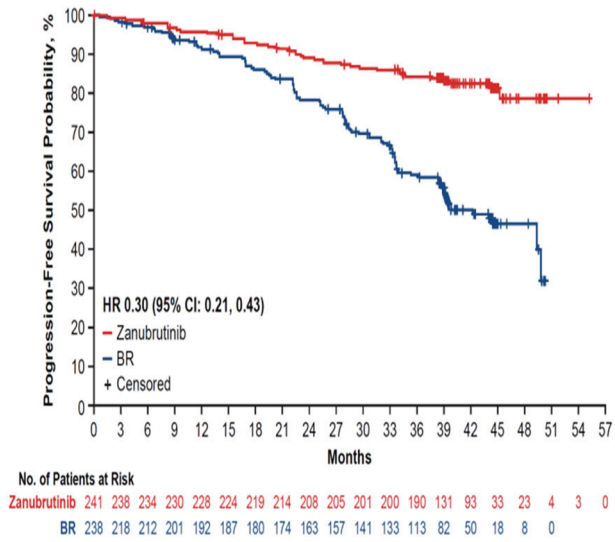

Abstract ID: 1549155

Title: Venetoclax consolidation after BTKi based therapy for patients with CLL

Authors: Benjamin Heyman, Michael Choi and Thomas Kipps

Background: Bruton Tyrosine Kinase Inhibitors (BTKi) can yield long-term disease control for patients (pts) with chronic lymphocytic leukemia (CLL) but requires indefinite therapy that can lead to cumulative side effects, especially cardiovascular [1]. Venetoclax (Ven) is a BCL-2 inhibitor that produces deep responses with high rates of undetectable minimal residual disease (uMRD) for pts with CLL, thus allowing for fixed duration therapy [2]. We performed a single institution retrospective analysis of pts treated ven regimen following BTKi evaluating feasibility, efficacy, and safety.

Methods: 19 Pts treated between the years of 2015 and 2023 were evaluated. Pts were initially treated with a BTKi but stopped therapy either due to intolerance or personal preference. Pts who had progression on BTKi were excluded. Ven based treatment consisted of single agent ven or in combination with obinutuzumab, with standard ven dose ramp up to a maximum dose of 400mg daily. Obinutuzumab was administered per FDA standard dosing. Response assessment was performed using iwCLL criteria. Minimal residual disease (MRD) was assessed by multi- parametric peripheral blood flow cytometry with a sensitivity of 10^{-4}.

Results: The pts had a median age of 64 years (range; 41–82). Rai stage at time of treatment (Tx) initiation with

BTKi: I 10.5%; II 47.4%; III 5.3%; Stage IV 26.3%. 73.6% of Pts were previously treated. The median number of previous Txs was 1 (range; 0–5). One patient was previously treated with ven. Pts harbored the following cytogenetic abnormalities: del(13q) 52.6%; del(11q) 36.8%; trisomy 12 21.1%; normal 15.8%; del(17p) 10.5%; and complex in 10.5%. 61.5% of pts harbored an unmutated immunoglobulin heavy chain. 78.9% of pts were treated with ibrutinib and 21.1% of patients were treated with acalabrutinib. Reasons for stopping BTKi included: atrial fibrillation 26.3%; desired for fixed duration therapy 21.1%; diarrhea 15.8%; completion of planned treatment 15.8%; infection 10.5%; arthralgia 5.3%; and hemorrhage 5.3%. Tumor lysis risk (TLS) prior to starting BTKi was low 63.2%; intermediate 26.3%; and high 10.5%. The median number of months on BTKi therapy prior to ven was 29.3 (range; 1.3–70.3). 15.8% of pts underwent dose reduction of BTKi prior to switching to ven. Response to BTKi therapy was partial response (PR) in 89.5% of pts and stable disease (SD) in 10.5% of pts. Tumor lysis risk prior to starting ven was low 94.7% and intermediate 5.3%. 68.4% of pts received ven monotherapy, and 31.6% of pts received ven plus obinutuzumab. The median number of months of ven based treatment was 13 (range; 0.2–63.2). 42% of pts currently remain on ven based therapy. 13 pts we assessable for MRD. The best peripheral blood MRD response was: uMRD 76.9% and low MRD 23.1%. The best MRD response for pts on ven monotherapy was uMRD 77.8% and low MRD 22.2%. The best MRD response for pts on ven plus obinutuzumab was uMRD 75% and low MRD 25%. One pt had progression after ven based therapy. Four pts required dose reductions of ven, secondary to neutropenia and diarrhea. Eight pts currently remain on ven. The median progression free survival (PFS) and time to next treatment (TTNT) after ven was 67.3 and 50.7 months, respectively.

Conclusions: We found that CLL pts treated with ven after BTKi discontinuation due to intolerance/patient preference is a feasible treatment strategy, with high uMRD rates. There has been increasing focus on investigating the combination BTKi and ven. However, combination therapy does increase the risk of hematologic and gastrointestinal side effects, which can lead to dose reduction or drug discontinuation [3]. In our analysis we found high rates of uMRD irrespective of the type of ven based therapy. Thus, initial BTKi administration may facilitate sufficient debulking of CLL to facilitate administration of single agent ven, avoiding the use of an anti-CD20 monoclonal antibody which can increase toxicity. This was evident in our cohort, as all but one pt had low-risk TLS prior to initiation of ven. Moreover, sequential therapy of a BTKi followed by single agent ven may lower the incidence of adverse events related to combination therapy. Our analysis demonstrates that sequential ven after BTKi is a feasible and effective treatment strategy for pts with CLL that deserves further evaluation in prospective clinical trials.

Table 1: Results

Median Number of Months of BTKi Treatment	29.3 (1.3 – 70.3)
Dose Reduction of BTKi Prior to Switch	
Yes	3 (15.8)
No	16 (84.2)
Response after BTKi	
PR	17 (89.5)
SD	2 (10.5)
TLS Risk After Stopping BTKi	
Low	18 (94.7)
Intermediate	1 (5.3)
Venetoclax Based Treatment	
Venetoclax Monotherapy	13 (68.4)
Venetoclax + Obinutuzumab	6 (31.6)
Median Number of Months of Venetoclax Based Treatment	13 (0.2 – 63.2)
Median Dose of Venetoclax	400mg (200-400)
Currently Remain on Venetoclax	8 (42)
Best MRD Response	
uMRD	10 (76.9)
Low MRD	3 (23.1)
High MRD	0
Best MRD Response Based on Treatment	
Ven Mono	
uMRD	7 (77.8)
Low MRD	2 (22.2)
Ven + Obinutuzumab	
uMRD	3 (75)
Low MRD	1 (25)
Progression After Venetoclax	
Yes	1 (5.3)
No	18 (94.7)
Subsequent Treatment after Venetoclax	
Yes	3 (23.1)
No	16 (76.9)
Toxicity From Venetoclax	
Neutropenia	2 (10.5)
Diarrhea	4 (21.5)

Figure 1: Survival

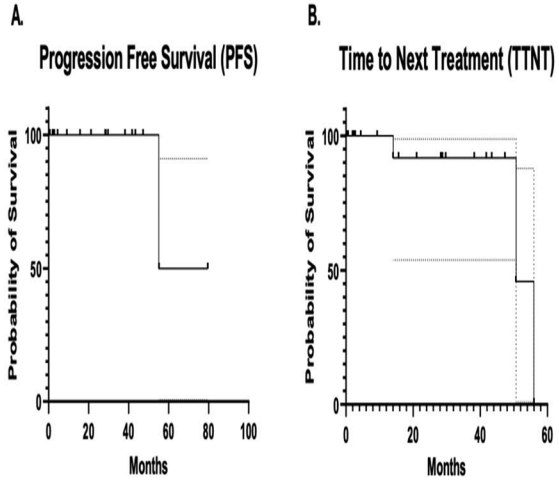

Abstract ID: 1549201

Title: Safety profile in patients with chronic lymphocytic leukemia undergoing treatment with 1st and 2nd generation Bruton tyrosine kinase inhibitors: multicentric real-world experience

Authors: Alberto Lopez-Garcia, Alfonso García, Ester Macias, Daniel Morillo, Carolina Miranda, Laura Bermejo, Maria Yuste, Pilar Llamas and Raul Cordoba

Introduction: Chronic lymphocytic leukemia (CLL) is the most frequent leukemia, being more frequent in older adults. Bruton's tyrosinkinase inhibitors (BTKi) have revolutionized the treatment, displacing immunochemotherapy treatment in all patient profiles. The selectivity profile in the action of these drugs means that the toxicity of first and second generation BTKi is different, resulting in higher rates of atrial fibrillation and arterial hypertension, mainly in patients treated in the second line or later, while maintaining their efficacy. Real-life studies are needed to be able to demonstrate the effects in first-line treatment in a more heterogeneous patient profile, without the strict exclusion and inclusion criteria used in clinical trials.

Methods: An observational, retrospective, multicenter, retrospective study was performed. Patients with in treatment with Ibrutinib or Acalabrutinib in first line or later were

	Acalabrutinib N (%) N=25	Ibrutinib N (%) N=66	P
Sex (Male)	16 (64.0%)	44 (66.7%)	1.000
ECOG >2	1 (4.0%)	1 (1.5%)	0.476
RAI Stage			0.043
0	0 (0.0%)	5 (7.6%)	
1	9 (36.0%)	13 (19.7%)	
2	9 (36.0%)	21 (31.8%)	
3	6 (24.0%)	9 (13.6%)	
4	1 (4.0%)	18 (27.3%)	
BINET Stage			0.937
A	7 (28.0%)	21 (31.8%)	
B	11 (44.0%)	27 (40.9%)	
C	7 (28.0%)	18 (27.3%)	
CGA			0.475
1	3 (12.0%)	12 (18.2%)	
2	4 (16.0%)	4 (6.1%)	
3	2 (8.0%)	6 (9.1%)	
Comorbidity index >6	13 (52.0%)	36 (54.5%)	1.000
Treatment			0.013
Frontline	21 (84.0%)	32 (48.5%)	
2nd	4 (16.0%)	25 (37.9%)	
3nd	0 (0%)	7 (10.6%)	
4nd	0 (0%)	2 (3.0%)	
Anticoagulant use	8 (32.0%)	15 (22.7%)	0.523
Antiagregant use	1 (4.0%)	7 (10.6%)	0.563
Antiarrhymic use	7 (28.0%)	12 (18.2%)	0.459
Antihypertensive use	10 (40.0%)	30 (45.5%)	0.817
Unmutated IgHV	23 (92.0%)	58 (87.9%)	0.853
Mut TP53	6 (24.0%)	14 (21.2%)	0.998
del17p	3 (12.0%)	9 (13.6%)	1.000
del11q	4 (16.0%)	10 (15.2%)	1.000
tri12	5 (20.0%)	16 (24.2%)	0.881
del13q	15 (60.0%)	26 (39.4%)	0.127
Other alterations	1 (4.0%)	5 (7.6%)	0.888
Hypetension	12 (48.0%)	35 (53.0%)	0.846
Diabetes	7 (28.0%)	16 (24.2%)	0.922
Dyslipemia	5 (20.0%)	25 (37.9%)	0.171
Obesity	5 (20.0%)	6 (9.1%)	0.287
Smoking	7 (28.0%)	11 (16.7%)	0.359

Hypertension	0 (0.0%)	14 (21.2%)	0.029
Infection	6 (24.0%)	19 (28.8%)	0.846
Cardiac toxicity	3 (12.0%)	16 (24.2%)	0.320
Bleeding	5 (20.0%)	20 (30.3%)	0.472
Hematological	11 (44.0%)	30 (45.5%)	1.000
Gastrointestinal toxicity	4 (16.0%)	18 (27.3%)	0.397
Other toxicity	6 (24.0%)	17 (25.8%)	1.000
Global toxicity	20 (80.0%)	58 (87.9%)	0.533

included. Demographic data, comorbidity, cytogenetic and mutational disease data, adverse effect profile, comprehensive geriatric assessment (if applicable) and treatment response evaluation data are collected.

Results: A total of 91 patients were included with a median age of 73.22 years SD 11.06. Fifty-three (58.2%) were male. Fifty-three (58.2%) were treated in frontline, 31.9% (29) in second line and 9.9% (9) in subsequent lines. Acalabrutinib was used in 25 (27.5%) patients and Ibrutinib in 66 (72.5%). Patient characteristics are shown in Table 1. Differences were revealed between these two BTKis in terms of line of treatment, with the majority being treated first ($p = 0.006$) and Rai stage, with Rai II predominating ($p = 0.014$). No differences were found between the two BTKis according to the rest of the characteristics. In terms of toxicity, 14 (15.4%) of patients treated with Ibrutinib developed arterial hypertension, compared to no patients in the Acalabrutinib arm ($p = 0.009$). With respect to the development of cardiac toxicity, 19 (20.9%) patients suffered some cardiotoxic event, 3 (3.3%) in patients on acalabrutinb and 16 (17.6%) on ibrutinib, with no significant differences found between the two drugs ($p = 0.2$). No significant differences were found with respect to other toxicities (hematologic, digestive, bleeding and infections) (Table 2). No differences were found in terms of progression-free survival or overall survival.

Conclusions: The iBTKs have changed the treatment of CLL, although the second-generation iBTKs have a safer cardiovascular profile and are just as effective in our cohort, even in the frontline.

Abstract ID: 1549212

Title: Evolution in the frontline treatment of patients with chronic lymphocytic leukemia: experience from one European Center

Authors: Miguel Arguello-Tomas, Nil Albiol, Paola Jara, Josep Nomdedéu, Jordi Sierra, Alba Mora and Carol Moreno

Treatment of chronic lymphocytic leukemia (CLL) has dramatically evolved over the last decades thanks to the introduction of targeted therapies. Chemoimmunotherapy was a big step forward in CLL therapy, and since 2014 several small molecules inhibiting different pathways have been introduced in the CLL treatment algorithms. International guidelines [1,2] recommend targeted therapies including covalent BTK inhibitors (cBTKi; ibrutinib, acalabrutinib, zanubrutinib) and BCL2 inhibitors (BCL2i; venetoclax) combinations as preferred regimens for most treatment naïve CLL patients. The main objective of this study was to describe the evolution in the patterns of frontline therapies in CLL patients from a single referral institution. As a secondary objective, we aimed to evaluate the impact of the targeted therapies on time to next treatment (TTNT) and overall survival (OS) in our cohort. This is a retrospective, single-center, and non-interventional study. We included patients treated in clinical trials and in routine clinical practice. Front-line treatment was classified into 5 groups: (1) alkylating agents, (2) purine analogs, (3) chemoimmunotherapy, (4) targeted therapies, and (5) other therapies. TTNT and OS were defined from the date of starting therapy to the event (next treatment or death, respectively), or loss to follow-up. We included 780 patients with a diagnosis of CLL. After a median of 6.4 years (0.1–36.4) of follow-up from diagnosis, 323 of 780 CLL patients (41.4%) required frontline therapy. The median age at the time of treatment was 69.8 years (32.2–92.4). IGHV genes were unmutated in 59% (138/234), del(11q) in 17.7% (46/260), and TP53 alterations (del(17p) and/or TP53 mutations) in 13.7% (36/262) of patients. As first-line therapy, 120 patients received alkylating agents (37.2%), 43 purine analogs (13.3%), 101 chemoimmunotherapy regimens (31.3%), 53 targeted therapies (16.4%), and 6 other treatments (1.9%). Before 2012 alkylating agents in monotherapy (chlorambucil) were the therapy most frequently used, and from that year onwards, chemoimmunotherapy (FCR, R-Bendamustine) was particularly given (Figure 1). Since 2018, targeted therapies

Figure 1. Historical evolution in the selection of first-line treatment for chronic lymphocytic leukemia patients in our institution.

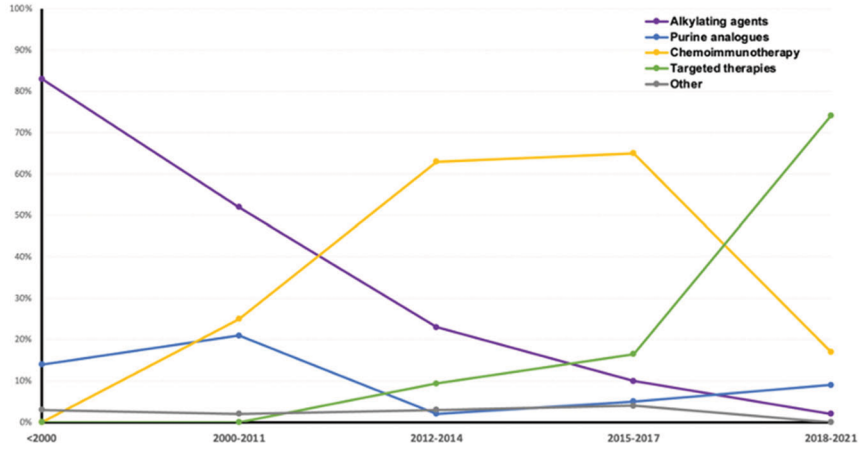

	Alkylating agents	Purine analogues	Chemoimmunotherapy	Targeted therapies	Other
<2000	83%	14%	0%	0%	3%
2000-2011	52%	21%	25%	0%	2%
2012-2014	23%	2%	63%	9.4%	3%
2015-2017	10%	5%	65%	16.5%	4%
2018-2021	2%	9%	17%	74.1%	0%

have been those most frequently employed, namely Ibrutinib, (29/55, 53.7%), and Venetoclax-based therapies (11/55, 20.4%). After a median time of 2.4 years (0–14.2), 168/323 patients (52%) received second-line therapy. Targeted therapies (Figure 2), chemoimmunotherapy, and mutated IGHV were related to a longer TTNT in the multivariant analysis. At the time of the closure of the study, 216/323 patients (66.9%) had died. The median OS was 7.5 years (0.2–35.1). The median OS was not reached in patients treated with targeted therapies, and it was 5.9 years (CI 95% 4.8–7) for the rest of the patients ($p = 0.36$). In the multivariant analysis, age younger than 65 years, female sex, and mutated IGHV were related to better OS. In summary, our data confirm that targeted therapies have become the most used treatment as frontline therapy in CLL, emphasizing the need for treatment algorithms including best sequential treatments and optimal treatment duration.

Figure 2. Time to next treatment (TTNT) (3A) and overall survival (OS) (3B) in patients with chronic lymphocytic leukemia treated at frontline with targeted therapies vs other therapies.

(3A)

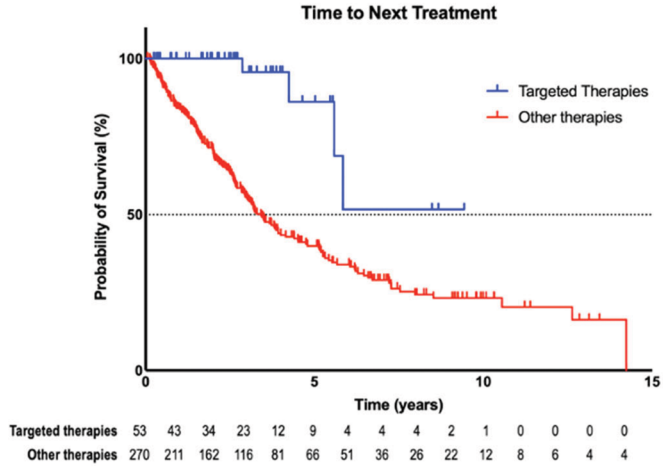

(3B)

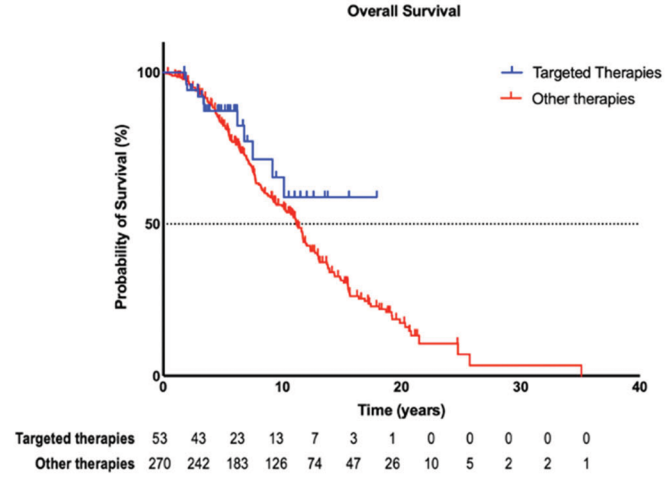

Abstract ID: 1549218

Title: Similar discriminatory values of IPS-E, AIPSE, and CR0 scores predicting time to first treatment in a large series of unselected patients with early-stage CLL

Authors: Miguel Arguello-Tomas, Santiago Osorio, Miguel López-Esteban, Patricia Font, Nil Albiol, Jordi Sierra, Carolina Martinez-Laperche and Carol Moreno

In Western countries, most patients with chronic lymphocytic leukemia (CLL) are diagnosed in early phases of the disease. Although overall their prognosis is good, there are patients who progress and require therapy shortly after diagnosis. Identifying these latter at diagnosis may be useful to decide the frequency of clinical controls as well as their setting (i.e. academic center versus general practice) to monitor the pace of the disease and to include patients at high risk of disease progression in clinical trials. To date, several scores including IPS-E, AIPS-E, and CR0 scores, have been designed to predict to first treatment (TTFT) in patients with early-stage CLL. We conducted a retrospective, and non-interventional study performed in two Spanish centers: Hospital General Universitario Gregorio Marañón (HGUGM, Madrid), and Hospital de la Santa Creu I Sant Pau (HSCSP, Barcelona). The primary objective was to compare the discriminatory value of each score for detecting patients with CLL at an early stage with a high-risk of progression using Harrell's Comparison Index (C index). As secondary objectives, the discriminatory value was also calculated with Receiver Operating Characteristics (ROC) curves, and the concordance between scores was measured with Cohen's kappa coefficient

test. Patients with early-stage CLL (Binet A and Rai 0), and without indication for treatment at diagnosis were included. 354 patients (Table 1) with a diagnosis of CLL in early stage were included: 66 (18.6%) from HGUGM and 288 patients (81.4%) from HSCSP. The median follow-up was 6.9 years (0.13–29.5). The median age at diagnosis was 67.3 years (28.9–93), and 180 were male (50.8%). As high-risk biomarkers at diagnosis, IGHV genes were unmutated in 37.3% of patients (132/354), del(17p) in 5.9% (21/354), and del(11q) in 8.2% (29/354). 140 patients (39.5%) started first-line treatment, with a median TTFT of 5.7 years (0.1–24.9). The 3 scores were successfully validated in our cohort (Figure 1) and identified low, medium, and high-risk progression groups. According to the C index, all the scores presented a good-discriminatory value (c = 0.71 for IPS-E, c = 0.71 for AIPS-E, and c = 0.7 for CR0) for detecting high-risk patients, with no significant differences between the scores ($p = 0.46$). The discriminatory value of the scores was also high according to the AUC with ROC (AUC =0.73 for IPS-E, AUC =0.72 for AIPS-E, and AUC =0.71 for CR0). The concordance between the scores for categorizing high-risk patients was analyzed, finding a substantial agreement between AIPS-E and IPS-E scores ($k = 0.68$), and AIPS-E and CR0 scores ($k = 0.69$), but it was moderate for IPS-E and CR0 scores ($k = 0.41$). The percentage of patients classified as high-risk was not significantly different between the three scores (IPS-E 15.5% vs. AIPS-E 19.2% vs. CR0 21.5%; $p = 0.64$). According to the data from this study, IPS-E, AIPS-E, and CR0 scores identify a similar group of patients with early stage with low, intermediate- and high-risk of disease progression most likely reflecting the items included in the different scores. The scores had a similar discriminatory value according to the C-index ($c = 0.71$, $c = 0.71$, and $c = 0.7$, respectively). Although the c-value is high, there is an uncertainty level of 30% whichever the score. This is a drawback in selecting patients for clinical trils.

Table 1. Characteristics of patients with CLL at diagnosis.

n=354	
Median age, years (range)	67.3 (28.9-93)
Male gender –- no. (%)	180 (50.4%)
Palpable lymph nodes, no. (%)	30 (8.5%)
LDH elevated (>ULV), n (%)	31/324 (9.6%)
FISH cytogenetics,	
del (11q), no. (%)	29 (8.2%)
+12, no. (%)	56 (15.8%)
del (17p) –- no. (%)	21 (5.9%)
IGHV mutational status–- no. (%)	
Mutated	222 (62.7%)
Unmutated	132 (37.3%)
Initiation of treatment – no (%)	140 (39.5%)
Time to first treatment (median, range), years	5.7 (0.1-24.9)
Follow-up (median, range), years	6.9 (0.13-29.5)
IPS-E score	
Low risk	170/354 (48%)
Intermediate risk	129/354 (36.4%)
High risk	55/354 (15.5%)
AIPS-E score	
Low risk	169/354 (47.7%)
Intermediate risk	117/354 (33.1%)
High risk	68/354 (19.2%)
CR0 score	
Low risk	168/354 (47.5%)
Intermediate risk	110/354 (31.1%)
High risk	76/354 (21.5%)

Abstract ID: 1549371

Title: Treatment strategies and outcomes for double refractory chronic lymphocytic leukemia; a single center experience

Authors: Mohammad Ammad Ud Din, Todd Knepper, Julio Chavez, Lisa Nodzon, Sameh Gaballah, Hayder Saeed, Lobomir Sokol, Ning Dong, Leidy Isenalumhe, Celeste Bello, Bijal Shah and Javier Pinilla-Ibarz

Background: There remains an unmet need for patients with aggressive disease refractory to both Bruton Tyrosine Kinase inhibitors (BTKi) and Venetoclax. We conducted a single-center retrospective study to identify the treatment strategies and outcomes for these 'double refractory' patients.

Figure 1. Time to first treatment (TTFT) for IPSE (a), AIPS-E (b) and CR0 (c) scores in early-stage patients.

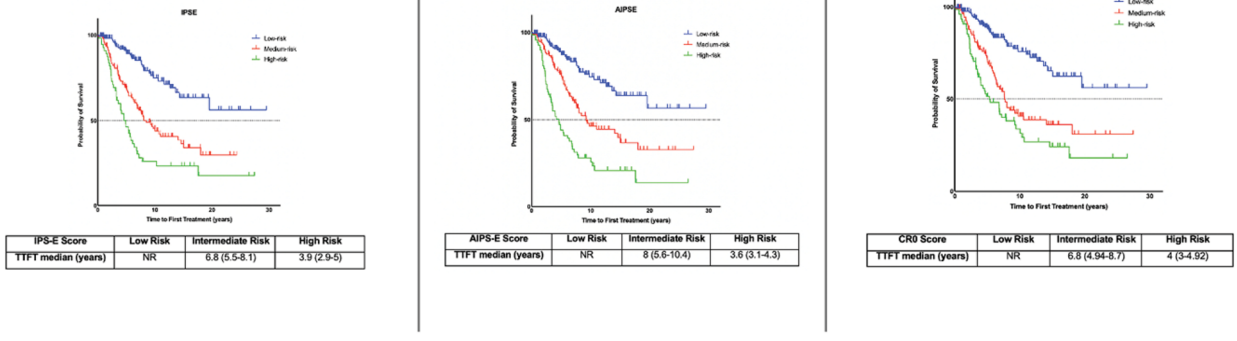

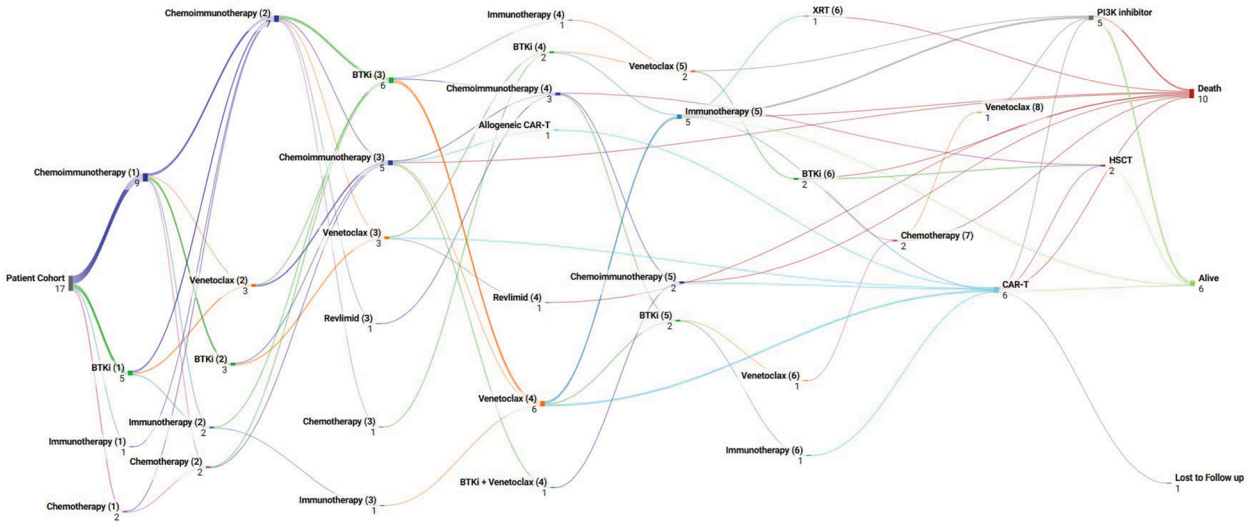

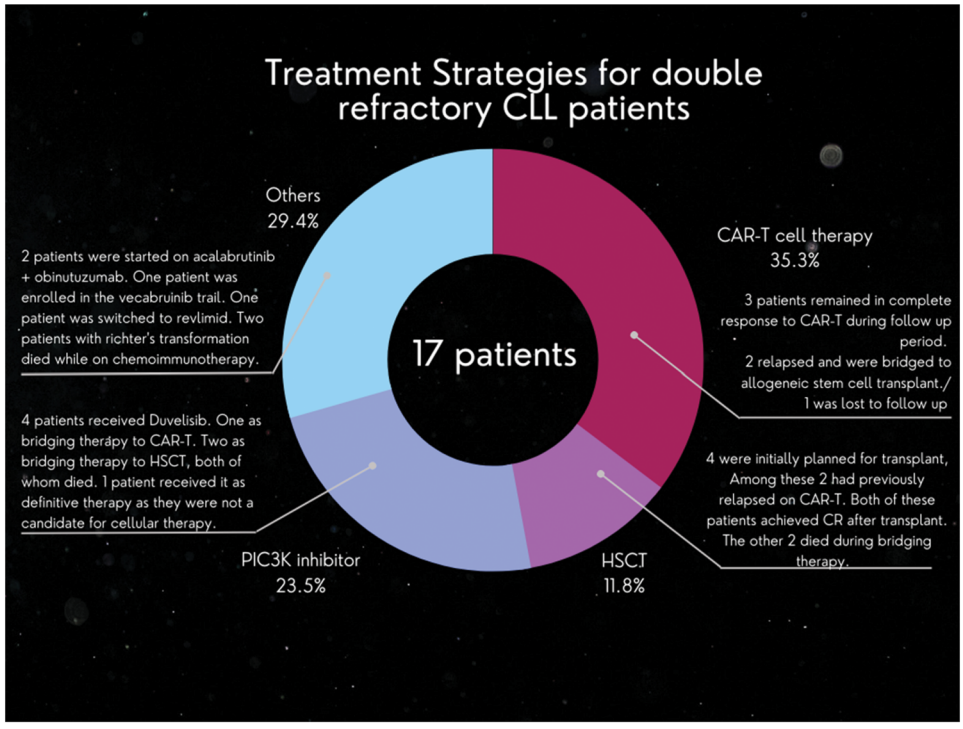

Methods: The data was gathered using the pharmacy dispensing records from H Lee Moffitt Cancer and Research Institute. All patients with chronic lymphocytic leukemia (CLL) that filled a Venetoclax prescription from the in-house pharmacy from 2016 to 2021 were identified. The medical record charts of these patients were accessed to determine double-refractory patients who had progression of disease (POD) while on BTKi followed by Venetoclax-based therapy or vice-versa. Only patients with POD were selected. Patients who had their treatment regimen changed due to intolerance or adverse effects were not included. The patient's charts were followed till 1 January 2023. The Mantel-Cox test was used to determine differences in survival outcomes among various cohorts. A p-value of ≤0.05 was considered significant.
Results: A total of 17 double refractory CLL patients were identified between 2016 and 2021. The median age was 66 years (range 47–80 years), and 10 (58.8%) patients were female. At the time of double refractory status, 15 (88.2%) patients had unmutated IgHV disease, 11 (64.7%) had 17p deletion, while 9 (52.9%) had complex karyotype identified on the CLL fluorescence in situ hybridization (FISH) test. Next-generation gene sequencing identified a BTK mutation in 7 (41.2%) of the patients. All patients progressed on a BTKi before receiving one venetoclax except for one. The median lines of therapies prior to Venetoclax was 3 (range 1–7) (Figure 1). Seven (41.2%) patients had Richter's transformation during their disease course. There was no survival difference among patients with 17p deletion or Richter's transformation compared to those with neither ($p=0.75$ and 0.48, respectively). The overall survival at 1 year of follow-up was 58.8%. Six patients (35.3%) were bridged to chimeric T cell therapy (CAR-T) following double refractory status. Among these, 2 patients relapsed and eventually needed to be bridged to HSCT. The overall survival of patients that received

CAR-T cell therapy was significantly better (median 33 versus 6 months, $p=0.05$). Overall, 3 patients had a complete response as the best response to CAR-T. Four patients (23.5%) were started on phosphoinositide 3 kinase (PI3-K) inhibitor, 1 as definitive therapy, 1 as successful bridging therapy to CAR-T, and 2 as bridging therapy for an allogeneic stem cell transplant (HSCT) but died prior to receiving a transplant. Overall, 4 patients were considered for an HSCT, however, only two patients were able to receive it while the other two died due to complications during the bridging therapy. Both patients that received HSCT had previously relapsed on CAR-T cell therapy. Two patients received acalabrutinib and obinutuzumab, one patient had a sustained partial response while the other died due to POD. One patient was started on vecabrutinib and died due to POD. Two patients died while on chemotherapy, while one patient was started on lenalidomide and died during the follow-up period. (Figure 2).

Abstract ID: 1549389

Title: Single-cell RNA-seq analysis reveals distinct tumor and immunosuppressive T cell phenotypes in CLL patients treated with ibrutinib

Authors: Shanmugapriya Thangavadivel, Shrilekha Misra, Samon Benrashid, Britten Gordon, Alexander He, Tzung-Huei Lai, Kerry Rogers, Seema Bhat, Adam Kittai, John Byrd, James Blachly, Jennifer Woyach and Bradley Blaser

Introduction: The development of Bruton tyrosine kinase inhibitors (BTKIs) and their introduction into clinical practice represents a major advance in the treatment of chronic lymphocytic leukemia (CLL). Monotherapy with ibrutinib or other BTKIs generally do not induce complete remissions or undetectable minimal residual disease (uMRD) even with extended therapy. The reason why some patients relapse, and some have minimal residual disease is unknown. Therefore, there is a need to understand the differences between ibrutinib sensitive and resistant CLL cells along with the immune microenvironment to identify novel therapeutic targets.

Methods: Here, we investigate the cellular heterogeneity of peripheral blood mononuclear cells from patients with CLL treated with ibrutinib using single-cell RNA sequencing. To understand ibrutinib resistance mechanisms, samples were collected from 8 patients at baseline (before treatment) (1), where BTK C481S is present with low variant allele frequency (VAF) (2) and at time of relapse (3). Data from these were compared to ibrutinib sensitive patient samples at baseline (1) (before treatment), 3yr (2) and 5yr (3) on treatment timepoints. Single cells were isolated using the 10X Genomics 5′ immune profiling kit. Data were processed with CellRanger v3.1.0. Poor quality cells were filtered out based on a high proportion of mitochondrial reads and low overall feature count. Sample variation was reduced using Batchelor to aid clustering. Clustering was performed using the partitioning and Leiden methods. Cluster top markers were calculated using functions from monocle3. Identity mapping was performed using Seurat and a published PBMC reference dataset.

Results: Single-cell RNA sequencing revealed transcriptional heterogeneity within the B cell cluster (Figure 1(A)). Three subpopulations of B cells were defined based on differential representation in the ibrutinib-sensitive and resistant

Figure 1:

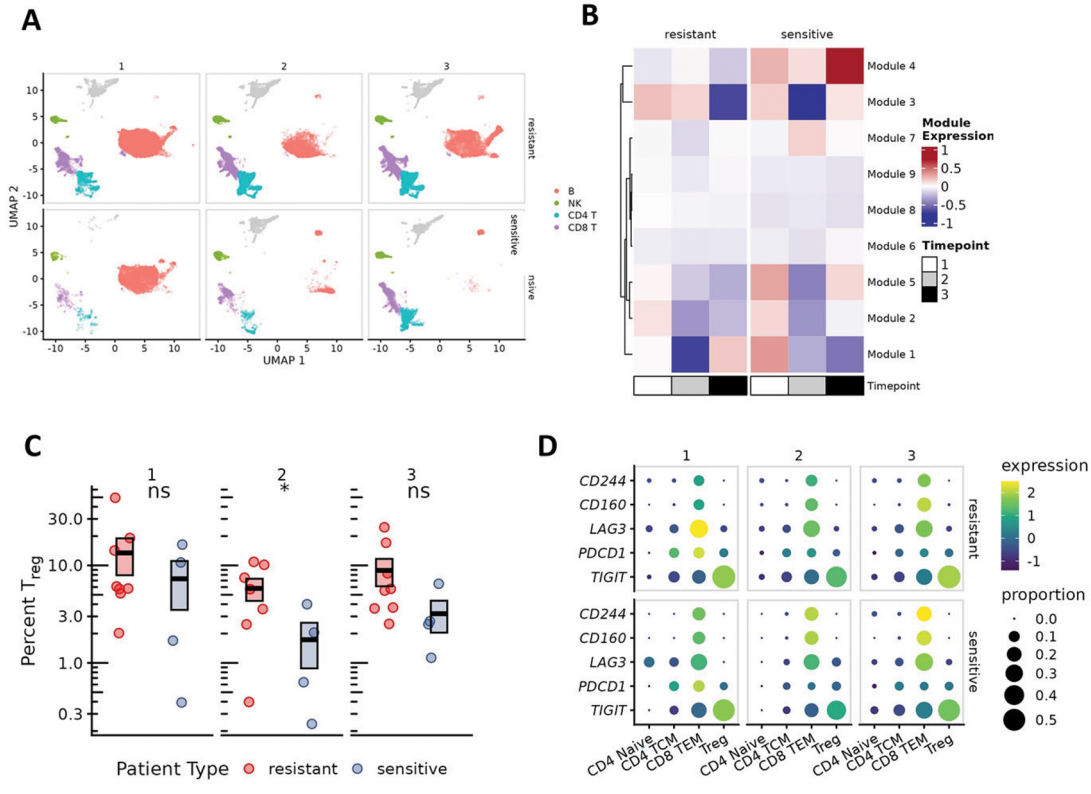

patients. Ibrutinib sensitive cells showed enrichment of B cell populations with upregulation of MHC I molecules and TNF family members. We also identified that inflammatory response and metabolic-related pathways were decreased, whereas cellular response to stress and DNA repair programs were increased in the ibrutinib resistance samples. Gene module analysis showed that ibrutinib sensitive samples had an increase in T cell activation, RNA splicing, cell adhesion and migration programs during therapy (Figure 1(B)). We hypothesized that the emergence of BTK C481S mutation in ibrutinib-resistant cells would lead to a distinct transcriptional profile. Long-read sequencing was performed using Oxford Nanopore technology. BTK-mutant cells were identified based on the presence of two or more unique RNA molecules detected with the C481S mutation and these were predominantly identified in the low-VAF and relapse samples. However, there was no significant difference between BTK-mutant cells and the remaining B cells. To see if T cell phenotypes reflected the differences observed in B cell transcriptional state, we characterized and quantified T cell populations according to ibrutinib response and investigated the changes in the T cell population. Ibrutinib markedly increased CD4+ and CD8+ T cell numbers in both resistant and sensitive CLL patients. However, there was a significant ($p < 0.05$) enrichment of Tregs in the ibrutinib-resistant samples Figure (1C). We found a connection between the immunosuppressive phenotype in the microenvironment demonstrating tumor's intrinsic immunological reactive program with exhausted T cells. Also, we found significant difference in the expression of checkpoint molecules and suppressive genes in T cells (Figure 1(D)) and NK cells.

Conclusion: Our findings demonstrate that the B cell population in ibrutinib-resistant and ibrutinib sensitive CLL patients exhibit distinct transcriptional states. At the single-cell level, our findings demonstrate a systematic picture of diverse malignancy and microenvironmental changes in CLL. Overall, these findings provide an insight into the complex molecular and cellular interactions of CLL that may have a crucial role in BTKI resistance.

Abstract ID: 1549416

Title: Safety of concomitant delivery of radiotherapy for second primary malignancy in patients with chronic lymphocytic leukemia treated with continuous novel agents

Authors: Samuel Kosydar, Sameer Parikh, Scott Lester, Kari Rabe, Wei Ding, Saad Kenderian, Yucai Wang, Eli Muchtar, Amber Koehler, Susan Schwager, Susan Slager, Neil Kay, Timothy Call, William Breen and Paul Hampel

Background: Patients with chronic lymphocytic leukemia (CLL) are at elevated risk of developing non-hematologic malignancies. Radiation therapy (RT) is a critical component of management in localized solid organ malignancies. With the advent of novel agents for CLL, such as Bruton tyrosine kinase inhibitors (BTKi) and the BCL-2 inhibitor venetoclax, patients with CLL are often receiving continuous daily therapy. Unnecessary BTKi dose interruptions are avoided as these holds can result in immediate morbidity in the form of disease flare and have also been associated with worse survival outcomes. However, safety data are lacking to guide the concurrent administration of radiation therapy for a second cancer in patients receiving ongoing CLL novel agent treatment.

Methods: After IRB approval, we identified patients treated concurrently with novel agents for CLL and RT for second primary malignancy at Mayo Clinic from 2014 to 2022. Adverse events within 3 months of RT were evaluated using the International Workshop on Chronic Lymphocytic Leukemia (iwCLL) criteria for hematological toxicity and the Common Terminology Criteria for Adverse Events (CTCAE) version 5 for non-hematological toxicity. Patients without seamless, concurrent treatment with novel agent therapy and RT were excluded; sequential therapy was not considered. The Wilcoxon signed-rank test was used to assess the median difference before and after radiation.

Results: Twenty-six patients were included in the study. Most patients were male ($n = 24$, 92.3%) and the average age at start of concurrent radiation treatment was 68 years (range: 51–85 years). Four patients had del(17p) and 18 patients had unmutated IGHV. The median number of prior CLL-directed therapies was 1 (range: 0–4) and 20 patients had received prior chemotherapy. Concurrent CLL-directed treatment consisted of ibrutinib ($n = 23$), acalabrutinib ($n = 2$), and venetoclax ($n = 1$) (Table 1); 58% of patients were receiving a reduced dose prior to RT start. There were no reports of dose reduction in anticipation of radiation therapy. The most common second primary malignancies were prostate ($n = 9$), head/neck ($n = 8$), and lung ($n = 3$) (Table 1). The most common conventionally fractionated prescriptions (cGy/fx) were 6000/30 ($n = 6$) and >6000–7020/20–33 ($n = 7$). SBRT ranged from 3300/5 to 5400/3 ($n = 8$). Five patients received other, varied RT prescriptions. Median follow up time since RT completion was 1.5 years. Median hemoglobin pre- and post-radiation were 13.3 and 12.4 g/dL ($p = 0.001$), respectively (Table 2). Per CTCAE criteria, two cases of grade 3 anemia were identified. At baseline, both of these patients had grade 1 anemia. There were no cases of grade 3 or 4 anemia using iwCLL criteria. Median platelet count before radiation was 175.5 × 109/L and after treatment was 140.5 × 109/L, ($p = 0.004$; Table 2). There was one case each of grade 3 and grade 4 thrombocytopenia per CTCAE (Table 2; Patient 2 and 1). Prior to radiation, Patient 1 had a baseline grade 1 thrombocytopenia. Using iwCLL criteria there were two cases of grade 4 thrombocytopenia. Median neutrophil count pre- and post-radiation were 4.4 × 109/L and 3.4 × 109/L ($p < 0.001$), respectively (Table 2). One case each of grade 3 (Table 2; Patient 3, baseline grade 1) and grade 4 (Table 2; Patient 1, baseline grade 1) neutropenia was reported with both CTCAE and iwCLL criteria. We did not find any evidence of major hemorrhage. There were no reports of tumor lysis syndrome, malignant hypertension, or severe cardiac arrhythmias. Grade ≥3 non-hematological toxicities occurred in two patients that required hospitalization for critical illness, including one patient with grade 5 respiratory failure 2 months after RT. The most common side effects documented were grade 1 fatigue ($n = 7$, 26.9%) and grade 1 radiation dermatitis ($n = 5$, 19.2%). Every patient completed their course of radiation and there were no cases of dose reduction for radiation.

Conclusion: This study provides the first assessment of patients with CLL on novel agents who were concurrently treated with radiotherapy for a subsequent solid organ malignancy. Our study found limited CLL-treatment related adverse events. Radiation side effects did not appear to be heightened. Our results suggest that concurrent treatment should be a shared decision-making discussion regarding

Novel Agent	N=26
ibrutinib	23 (88.5%)
140 mg daily	6 (23.1%)
140 mg every 3 days	1 (3.8%)
280 mg daily	6 (23.1%)
420 mg daily	10 (38.5%)
venetoclax	1 (3.8%)
200 mg daily	
acalabrutinib	2 (7.7%)
100 mg twice daily	1 (3.8%)
100 mg daily	1 (3.8%)
Prior Therapies	
Number of CLL therapies prior to NA	
0	6 (23.1%)
1	9 (34.6%)
2	6 (23.1%)
3	3 (11.5%)
4	2 (7.7%)
Number of CLL therapies prior to NA	
Mean (SD)	1.5 (1.2)
Median	1
Range	(0.0-4.0)

Secondary Malignancy	
adenocarcinoma prostate	9 (34.6%)
head/neck carcinoma	8 (30.8%)
NSCLC	3 (11.5%)
glioblastoma	1 (3.8%)
IDC breast	1 (3.8%)
plasmacytoma	1 (3.8%)
melanoma	1 (3.8%)
RCC	1 (3.8%)
thymoma	1 (3.8%)
Radiation	
Radiation Type	
Photon	18 (69.2%)
Proton	7 (26.9%)
Both	1 (3.8%)
Radiation Sensitizing Agent	
Yes	2 (7.7%)
No	24 (92.3%)
Radiation Location	
pelvis	8 (30.8%)
head/neck	8 (30.8%)
Lung	4 (15.4%)
brain	1 (3.8%)
chest wall	2 (7.7%)
mediastinum	1 (3.8%)
pelvis+lung	1 (3.8%)
renal	1 (3.8%)
Radiation Intent	
Palliative	1 (3.8%)
Neoadjuvant	0
Adjuvant	10 (38.5%)
Definitive	15 (57.7%)

Hematological adverse events

	Pre Radiation	Post Radiation	P value	CTCAE Criteria	CTCAE Attribution	iwCLL Criteria
Hemoglobin, median(range) g/dL	13.3(10.1-18.6)	12.4(5.9-17.4)	0.001	not applicable: 8 (30.8%) grade 1: 13 (50.0%) grade 2: 3 (11.5%) grade 3: 2 (7.7%) grade 4: 0 grade 5: 0	not applicable: 8 (30.8%) unrelated: 8 (30.8%) unlikely: 1 (3.8%) possibly: 7 (26.9%) probably: 2 (7.7%)	grade 0: 17 (65.4 %) grade 1: 6 (23.1%) grade 2: 3 (11.5%) grade 3: 0 grade 4: 0
Platelet Count, median(range) x10^9/L	175.5(78.0-373.0)	140.5(10.0-287.0)	0.004	not applicable: 15 (57.7%) grade 1: 8 (30.8%) grade 2: 1 (3.8%) grade 3: 1 (3.8%) grade 4: 1 (3.8%)	not applicable: 15 (57.7%) unrelated: 3 (11.5%) unlikely: 1 (3.8%) possibly: 5 (19.2%) probably: 2 (7.7%)	grade 0: 19 (73.1%) grade 1: 3 (11.5%) grade 2: 2 (7.7%) grade 3: 0 grade 4: 2 (7.7%)
Neutrophil Count, median(range) 10^9/L	4.4(1.2-19.3)	3.4(0-6.6)	<0.001	not applicable: 21 (80.8%) grade 1: 1 (3.8%) grade 2: 2 (7.7%) grade 3: 1 (3.8%) grade 4: 1 (3.8%)	not applicable: 19 (73.1%) unrelated: 1 (3.8%) unlikely: 0 possibly: 4 (15.4%) probably: 2 (7.7%)	grade 0: 19 (73.1%) grade 1: 5 (19.2%) grade 2: 0 grade 3: 1 (3.8%) grade 4: 1 (3.8%)

Frequency of grade 3 and 4 toxicities per patient

Patient	Novel Agent	Second Primary Malignancy	RT cGy/ fraction	Grade 3/4 Adverse Events*
1	ibrutinib	head/neck cancer	6000/30 with weekly cisplatin	grade 4 thrombocytopenia grade 4 neutropenia grade 4 febrile neutropenia grade 4 lung infection grade 3 acute kidney injury grade 3 mucositis oral
2	ibrutinib	head/neck cancer	6600/33	grade 4 thrombocytopenia grade 4 acute kidney injury grade 4 sepsis grade 5 respiratory failure
3	ibrutinib	head/neck cancer	6600/33	grade 3 neutropenia

*iwCLL used for hematological adverse events

potential harms versus benefits. A comprehensive clinical evaluation that accounts for the patient's medical comorbidities and personal risk factors should inform the discussion.

Abstract ID: 1549882

Title: First-in-human open-label study of lisaftoclax (APG-2575), a novel BCL-2 inhibitor, in patients with relapsed/refractory chronic lymphocytic leukemia and other hematologic malignancies

Authors: Sikander Ailawadhi, Zi Chen, Bo Huang, Aneel Paulus, Mary Collins, Lei Fu, Mingyu Li, Mohammad Ahmad, Lichuang Men, Hengbang Wang, Matthew Davids, Eric Liang, Divya Mekala, Zhicong He, Masa Lasica, Costas Yannakou, Ricardo Parrondo, Laura Glass, Dajun Yang, Asher Chanan-Khan and Yifan Zhai

Background: Many B-cell malignancies evade apoptosis by overexpressing BCL-2 proteins. The BCL-2 inhibitor venetoclax is active in certain hematologic malignancies but can increase the risk of tumor lysis syndrome, requiring a 5-week dose ramp-up for patients with chronic lymphocytic leukemia (CLL). Cases of severe neutropenia with venetoclax treatment have also been reported. Investigational lisaftoclax (APG-2575) is a novel, potent, selective BCL-2 inhibitor that is active against hematologic malignancies and is under clinical development [1]

Methods: This first-in-human global phase 1 dose escalation and expansion study assessed the safety, pharmacokinetics, pharmacodynamics, efficacy, and maximum tolerated or recommended phase 2 dose of lisaftoclax in patients with relapsed/refractory CLL and other hematologic malignancies. Lisaftoclax was orally administered daily in a 28-day cycle. Patients with CLL or intermediate-high tumor lysis syndrome risk were initiated on a daily ramp-up schedule until the assigned dose was reached.

Results: As of 22 October 2022, 52 patients were enrolled and treated with lisaftoclax at doses ranging from 20 to 1,200 mg, with a median (range) of 2 (1–13) prior lines of treatment. Patients had diagnoses of relapsed/refractory CLL or small lymphocytic lymphoma (SLL; $n=23$), non-Hodgkin lymphoma ($n=14$), multiple myeloma ($n=11$), and either acute myeloid leukemia, myelodysplastic syndrome, hairy cell leukemia, or Castleman disease ($n=1$ each). No dose-limiting toxicity was observed even at 1,200 mg, the highest treatment dose. The maximum tolerated dose was not reached, and no laboratory or clinical tumor lysis syndrome was reported. The median (range) of treatment duration was 7 (1–43) cycles. Any grade treatment-emergent adverse events (TEAEs) in ≥20% of patients included anemia (28.8%), thrombocytopenia (28.8%), neutropenia (26.9%; hematologic), diarrhea (48.1%), fatigue (34.6%), nausea (30.8%), constipation (25.0%), vomiting (23.1%), and headache (21.2%; nonhematologic). Grade 3–4 TEAEs in ≥5% of patients included neutropenia (21.2%), thrombocytopenia (13.5%), and anemia (9.6%). In patients with CLL/SLL, grade 3–4 TEAEs included neutropenia (26.1%), increased lipase (13.0%), and thrombocytopenia (8.7%), which did not cause treatment-related discontinuation. Of 22 evaluable patients with relapsed/refractory CLL/SLL, 14 achieved partial responses, for an overall response rate of 63.6% (95% CI: [41, 83%]) and median (range) time to response of 2 (2–8) cycles. Among 28 evaluable patients without CLL/SLL, clinical benefit was observed in 14 (50.0%). The pharmacokinetic profile showed that exposures increased with lisaftoclax doses from 20 to 1,200 mg (average half-life: 3–5 hours). BH3 profiling demonstrated that lisaftoclax rapidly induced changes in BCL-2 complex and triggered cytochrome c release in CLL/SLL patient samples, which were consistent with rapid clinical reductions in absolute lymphocyte counts.

Conclusions: Lisaftoclax was well tolerated up to 1,200 mg/day. No tumor lysis syndrome was observed even with the daily ramp-up schedule. There were no significant new or unmanageable safety findings, and the overall response rate in patients with relapsed/refractory CLL/SLL was 63.6%. Grade 3–4 TEAEs were infrequent even at dose levels of 800 mg and above. Thus, the BCL-2 inhibitor lisaftoclax offers a potential treatment alternative for patients with relapsed/

refractory CLL/SLL and other hematologic malignancies, with a daily ramp-up schedule that may be more patient 'user friendly' and a favorable preliminary safety profile. Internal study identifier: APG-2575-001; clinical trial registration: NCT03537482.

Abstract ID: 1549935

Title: BRUIN CLL-322: a phase 3 open-label, randomized study of fixed duration pirtobrutinib plus venetoclax and rituximab versus venetoclax and rituximab in previously treated chronic lymphocytic leukemia/small lymphocytic lymphoma (trial in progress)

Authors: Ching Ching Leow, Toby A. Eyre, Phillip Thompson, William Wierda, Martin Šimkovič, Sebastian Grosicki, Wojciech Jurczak, Yucai Wang, Heidi Mocikova, Pier Luigi Zinzani, Constantine S. Tam, Matthew Davids, Amy E. Chang, Joana M. Oliveira, Yi Lu, Lindsey Roeker and Jennifer Woyach

Background: Covalent (c) Bruton tyrosine kinase inhibitors (BTKi) have reshaped the treatment landscape for chronic lymphocytic leukemia/small lymphocytic lymphoma (CLL/SLL) and are now often used as initial therapy. The MURANO study established 2-year fixed duration venetoclax plus rituximab as a standard of care regimen for patients with relapsed or refractory CLL/SLL. However, its efficacy has not been formally assessed in CLL/SLL patients treated with a cBTKi, a common setting where this regimen is used in contemporary practice. Pirtobrutinib, a highly selective, non-covalent (reversible) BTKi, inhibits both wildtype and C481-mutant BTK with equal low nM potency, and has favorable oral pharmacology that enables continuous BTK inhibition throughout the dosing interval regardless of intrinsic rate of BTK turnover. In the phase 1/2 BRUIN study, pirtobrutinib demonstrated promising durable overall response rates (ORR) and was well tolerated in patients with pre-treated CLL/SLL regardless of prior therapy (including cBTKi), number of prior lines of therapy, BTK C481 mutation status, or reason for prior cBTKi discontinuation. The study's objective is to assess the superiority of adding time-limited pirtobrutinib to the MURANO regimen, hypothesized to prolong disease control in a largely BTKi-pretreated population.
Methods: BRUIN CLL-322 (NCT04965493) is a randomized, open-label, global, phase 3 study comparing time-limited pirtobrutinib (200mg QD) plus venetoclax and rituximab versus venetoclax and rituximab in previously treated CLL/SLL patients. Approximately 600 patients, 80% who have been previously treated with cBTKi, will be randomized 1:1 and stratified by del(17p) status (yes/no) and prior BTKi experience (discontinuation due to progressive disease vs due to other reasons vs. no prior BTKi exposure). Eligible patients are adults diagnosed with CLL/SLL and require therapy per iwCLL 2018 criteria who have received prior therapy that may or may not include a cBTKi. There are no restrictions on the number of lines of prior therapy. Key exclusion criteria include CNS involvement by CLL/SLL, Richter transformation at any time, prior BCL2 inhibitor or non-covalent BTK inhibitor, or a history of either allogeneic or autologous stem cell transplant, or chimeric antigen receptor T-cell therapy within 60 days prior to randomization. The primary endpoint is progression-free survival (PFS) per iwCLL criteria assessed by an independent review committee. Secondary endpoints include investigator assessed PFS, ORR, overall survival, time to next treatment, event-free survival, safety and tolerability, and patient-reported outcomes. Enrollment is ongoing for patients previously treated with BTKi and completed for BTKi naïve patients.

Abstract ID: 1549942

Title: Long-term safety with ≥12 months of pirtobrutinib in relapsed/refractory (R/R) B-cell malignancies

Authors: Catherine E. Muehlenbein, Catherine C. Coombs, Nirav Shah, Wojciech Jurczak, Jennifer Woyach, Chan Y. Cheah, Krish Patel, Kami Maddocks, Yucai Wang, Chunxiao Wang, Sarang Abhyankar, Donald E. Tsai and Toby A. Eyre

Introduction: While Bruton tyrosine kinase inhibitors (BTKi) can induce sustained remissions, ongoing response requires continuous treatment and thus long-term safety/tolerability is critical for adherence, maintaining dose intensity, and delivering maximum efficacy. Pirtobrutinib is a highly selective, non-covalent (reversible) BTKi approved by the FDA in January 2023 for R/R mantle cell lymphoma after 2 prior lines of therapy including a BTKi. Pirtobrutinib has demonstrated promising efficacy with low discontinuation and dose reduction rates in patients (pts) with multiple subtypes of R/R B-cell malignancies. However, the long-term safety and tolerability of pirtobrutinib has not yet been reported. Here we report the clinical safety in pts with long-term (≥12 months) pirtobrutinib treatment from the phase 1/2 BRUIN trial.
Methods: Pts with R/R B-cell malignancies who received ≥12 months of pirtobrutinib were included. Median time to onset, dose reduction, discontinuation, and cumulative incidence rates were determined for treatment emergent adverse event (TEAE) that occurred in ≥20% of pts and select AE of interest associated with BTKi.
Results: As of 29 July 2022, 773 pts were enrolled, and 326 (42%) pts received treatment for ≥12 months. Among these 326 pts, median time on treatment was 19 months (IQR: 16,25), with 231 (71%) remaining on pirtobrutinib. The most common TEAE (all grade, regardless of attribution) in this long-term 326 pt cohort were fatigue (32%), diarrhea (31%), Covid-19 (29%), contusion (26%), cough (25%), and back pain (21%). TEAE leading to dose reduction or discontinuation occurred in 23 (7%) and 11 (3%) pts, respectively. Four (1%) pts discontinued due to a treatment-related AE, and 1 pt had a fatal treatment-related AE (Covid-19 pneumonia). Select AE of interest for the long-term pts are shown in the Table 1. Comprehensive safety analyses describing the frequency of TEAE over time will be presented.
Conclusion: Prolonged pirtobrutinib therapy continues to demonstrate a safety profile amenable to long-term administration at the recommended dose without evidence of new or worsening toxicity signals. The safety and tolerability observed in pts on therapy for ≥12 months was similar to previously published safety analyses on all pts enrolled regardless of follow-up.

Select AE of interest associated with BTKi in pts with ≥12 months exposure (N=326)

AE	Any-Grade TEAE %	Grade ≥3 TEAE %	Median time (months) to first occurrence (Q1, Q3)	Leading to dose reduction %	Leading to drug discontinuation %	Cumulative incidence rate (6, 12, 24 months) %
Bruising[a]	31	0	1.8 (0.5, 5.6)	<1	0	23, 27, 29
Arthralgia	21	1	7.4 (2.9, 12.0)	0	0	9, 16, 20
Rash[a]	20	<1	2.4 (0.7, 9.1)	0	0	13, 15, 18
Hemorrhage/ Hematoma[a]	17	2	5.8 (1.9, 13.7)	0	0	9, 11, 16
Hypertension	16	3	6.9 (2.1, 11.6)	<1	0	7, 12, 16
Atrial fibrillation/ flutter[a]	3	1	10.2 (3.8, 15.0)	0	0	1, 2, 2

[a]Consolidated Terms.

Abstract ID: 1549945

Title: Matching-adjusted indirect comparison of pirtobrutinib vs. venetoclax continuous monotherapy in patients with relapsed/refractory CLL previously treated with a covalent BTK inhibitor

Authors: Matthew Davids, Othman Al-Sawaf, Min-Hua Jen, Lisa M Hess, Jiewen Zhang, Benjamin Goebel, John M Pagel and Toby A. Eyre

Background: Venetoclax-based therapy is a standard option for patients with relapsed/refractory (R/R) chronic lymphocytic leukemia (CLL) previously treated with a covalent BTK inhibitor (cBTKi). However, nearly all prospective data on venetoclax efficacy in the post-cBTKi setting were generated from a subgroup analysis within a single-arm study of venetoclax administered as continuous monotherapy. Pirtobrutinib is a highly selective, non-covalent (reversible) BTKi that was designed to overcome the pharmacologic limitations of cBTKi and restore BTK inhibition. Pirtobrutinib has demonstrated marked efficacy and a favorable safety profile in patients with CLL previously treated with a cBTKi.
Aims: This unanchored MAIC was designed to estimate the treatment effect of pirtobrutinib (BRUIN, NCT03740529) versus venetoclax continuous monotherapy (NCT02141282) in patients with R/R CLL previously treated with a cBTKi.
Methods: Data from patients with R/R CLL previously treated with at least one cBTKi and without prior venetoclax exposure who received pirtobrutinib were analyzed ($n=146$). Only one prospective trial of venetoclax (administered as a continuous monotherapy) for patients previously treated with a cBTKi ($n=91$) was identified [1]. Progression-free survival (PFS), overall survival (OS), investigator-assessed overall response rate (ORR), and grade ≥3 treatment-emergent adverse events (TEAEs) regardless of attribution were evaluated. Patient level data from the pirtobrutinib cohort were re-weighted to match the venetoclax cohort using method of moments approach, adjusting for well-established prognostic factors reported in both studies (age, IGHV mutation status, TP53 aberrancy, del(17p), del(11q); number of prior lines of therapy, and reason for prior cBTKi discontinuation). Kaplan Meier PFS and OS curves from the venetoclax trial were digitized (using WebPlotDigitizer) for time-to-event analyses. Fishers exact test was used to compare proportional outcomes (ORR, TEAEs); time to event outcomes (PFS, OS) were compared using Cox regression model and log-rank test.
Results: After adjustment, the median age in the pirtobrutinib and venetoclax cohorts was 66.5 and 66.0 years, respectively; all other prognostic factors were similarly well matched in both cohorts. Median follow-up was 21.3 and 14 months for the pirtobrutinib and venetoclax cohorts, respectively. PFS and OS were comparable with no significant differences noted for pirtobrutinib versus venetoclax (both $p>0.05$; Figure 1). ORR was 80% for pirtobrutinib (inclusive of PR-L) vs. 65% for venetoclax ($p=0.01$). Grade ≥3 TEAEs reported in both trials indicated that febrile neutropenia, neutropenia, anemia, and thrombocytopenia were significantly lower for pirtobrutinib vs. venetoclax in adjusted analyses (all $p<0.01$). No differences were observed for pneumonia ($p=0.06$) or for discontinuation due to TEAEs (3 vs. 7%, $p=0.32$) in adjusted analyses. Unadjusted results were consistent with the adjusted analyses.
Summary/Conclusions: The efficacy of pirtobrutinib was comparable to continuously administered venetoclax monotherapy in patients with R/R CLL previously treated with a cBTKi. Pirtobrutinib was associated with improved ORR and favorable overall safety profile for most TEAEs compared to venetoclax. This study raises questions regarding optimal treatment sequencing of pirtobrutinib and venetoclax in cBTKi treated CLL, but the lack of prospective direct comparisons and limited long-term follow-up preclude definitive conclusions. Multiple randomized Phase 3 studies of pirtobrutinib in patients with CLL remain ongoing.

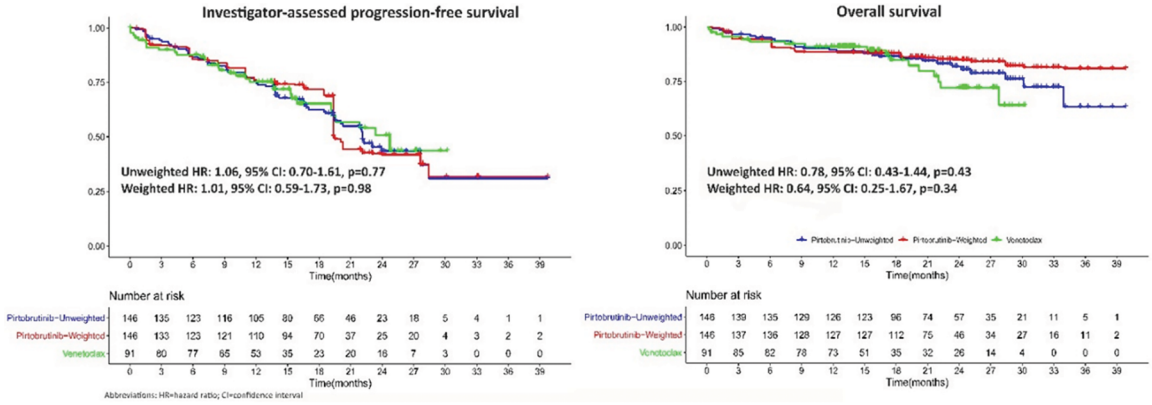

Abstract ID: 1549996

Title: Lisaftoclax (APG-2575) is a novel BCL-2 inhibitor with robust antitumor activity in preclinical models of hematologic malignancy

Authors: Aneel Paulus, Alak Manna, Hengbang Wang, Jianyong Chen, Ping Min, Yan Yin, Navnita Dutta, Nabanita Halder, Gina Ciccio, John Copland, Bing Han, Longchuan Bai, Liu Liu, Mi Wang, Donna McEachern, Sally Przybranowski, Chao-Yie Yang, Jeanne Stuckey, Depei Wu, Caixia Li, Jeremy Ryan, Anthony Letai, Sikander Ailawadhi, Dajun Yang, Shaomeng Wang, Asher Chanan-Khan and Yifan Zhai

Introduction: Unique challenges in drug design have largely constrained successful development of BCL-2-specific inhibitors because of BCL-2 homology domain 3– (BH3–) shared homology between BCL-2 family members and the shallow surface of their protein-protein interactions. This study reports discovery and extensive preclinical investigation of BCL-2 inhibitor lisaftoclax (APG-2575).
Methods: Lead compounds were developed using computational modeling, and the selectivity and potency of lisaftoclax were determined using biochemical binding, mitochondrial BH3 profiling, and cell-based viability or apoptosis assays. The antitumor effects of lisaftoclax were also assessed in several xenograft models.
Results: Lisaftoclax selectively bound BCL-2 (Ki <0.1 nM), disrupted BCL-2:BIM complexes, and compromised mitochondrial outer membrane potential with BAX/BAK-dependent, caspase-mediated apoptosis. It also exerted strong antitumor activity in hematologic malignancy cell lines and tumor cells from patients with chronic lymphocytic leukemia, multiple myeloma, or Waldenström macroglobulinemia. Lisaftoclax treatment increased the expression of prodeath BCL-2 family proteins BIM and Noxa, and BIM translocated from the cytosol into the mitochondria. In line with these proapoptotic effects, lisaftoclax entered malignant cells rapidly, reached a plateau at 2 hours, and significantly downregulated mitochondrial respiratory function and production of ATP. Lisaftoclax also inhibited tumor growth in xenograft models, correlating with caspase activation and PARP-1 cleavage (a hallmark of apoptosis). Tumor growth inhibition by lisaftoclax furthermore corresponded with its pharmacokinetic profile, which included a short plasma elimination half-life (~6 hours), a longer half-life in tumors (13–48 hours), and a rapid attainment of maximum concentration to drive apoptosis. It has been suggested that BH3-mimetic BCL-2 inhibitors need to attain a mitochondrial threshold rapidly to trigger apoptosis, with their effects being driven by the rate of cell penetration and maximum concentration. *In vivo*, lisaftoclax combined with rituximab or bendamustine plus rituximab enhanced antitumor activity.
Conclusions: Lisaftoclax is a novel, orally bioavailable BH3 mimetic BCL-2-selective inhibitor with considerable potential in the treatment of certain hematologic malignancies. These preliminarily encouraging findings support ongoing clinical trials, including a phase 1, first-in-human study [1] and phase 2 trial evaluating lisaftoclax alone or combined with Bruton tyrosine kinase inhibitors acalabrutinib or rituximab [2].

Abstract ID: 1550086

Title: Zanubrutinib vs ibrutinib in relapsed/refractory chronic lymphocytic leukemia and small lymphocytic lymphoma (R/R CLL/SLL): impact on health-related quality of life (HRQoL)

Authors: Jennifer Brown, Susan M. O'Brien, Constantine S. Tam, Barbara Eichhorst, Lugui Qiu, Keri Yang, Ken Wu, Tommi Salmi, Gisoo Barnes and Nicole Lamanna

Introduction: Zanubrutinib is a potent and highly selective next-generation Bruton tyrosine kinase (BTK) inhibitor designed to maximize BTK occupancy and minimize off-target effects. In the ALPINE study (NCT03734016), zanubrutinib was compared head-to-head with ibrutinib as treatment for R/R CLL/SLL, where it demonstrated superiority to ibrutinib in both progression-free survival and overall response rate and a more favorable safety profile. The purpose of this analysis was to assess HRQoL in patients treated with zanubrutinib and ibrutinib. Results from the data cutoff (8 August 2022) related to recent progression-free survival analysis are reported here.
Methods: HRQoL was measured by EORTC QLQ-C30 and EQ-5D-5L at baseline, Cycle 1, and then every third 28-day cycle until end of treatment. Key patient-reported outcome (PRO) endpoints included global health status (GHS), physical

and role functions, fatigue, pain, diarrhea, and nausea/vomiting. Descriptive analysis was conducted on all the scales; a mixed models for repeated measures analysis using key PRO endpoints at the key clinical cycles of Cycles 7 (6 months) and 13 (12 months) was performed. Adjusted completion rates were defined as the number of patients who completed the questionnaires at each cycle divided by the number of patients still on treatment. Clinically meaningful was defined as a ≥5% mean change difference from baseline.

Results: A total of 652 patients were randomized to receive zanubrutinib ($n=327$) or ibrutinib ($n=325$); baseline characteristics were generally similar between arms, although the zanubrutinib arm had fewer males than the ibrutinib arm (65.1 vs. 71.4%). At baseline, GHS, functional, and symptom scale scores were similar between arms. Although more ibrutinib-treated patients discontinued treatment due to adverse events than zanubrutinib-treated patients (22.2 vs. 15.4%), adjusted PRO completion rates were high at Cycles 7 and 13 in both the zanubrutinib arm (89.6 and 94.3%) and ibrutinib arm (87.7 and 92.3%), respectively. By Cycle 7, GHS scores were improved with zanubrutinib vs. ibrutinib (least-squares mean change difference, 3.0 [95% CI: 0.23, 5.77]; nominal p=.0338). By Cycle 13, the difference in GHS scores from baseline was no longer significant (least-squares mean change difference, 1.34 [95% CI: −1.37, 4.06]; nominal p=.3304) (Table 1). Patients in the zanubrutinib arm experienced clinically meaningful improvements in physical and role functioning as well as pain and fatigue at Cycles 7 and 13, but the difference between the arms was not significant. Although patients in the zanubrutinib arm reported lower diarrhea scores, the difference between treatments was not significant. Nausea/vomiting scores were maintained in both arms with no measurable difference. VAS scores showed greater improvement from baseline at both Cycles 7 (7.92 vs. 3.44) and 13 (7.75 vs. 3.92) with zanubrutinib vs ibrutinib treatment, respectively.

Conclusions: In ALPINE, patients with R/R CLL/SLL treated with zanubrutinib demonstrated improvement over those treated with ibrutinib in the QLQ-30 GHS/QoL scale at Cycle 7 (6 months). Other endpoints continued to improve, suggesting treatment with zanubrutinib positively affected HRQoL and that HRQoL improved over time. As expected, given the generally good HRQoL at baseline in both arms, the differences between the arms were small and not significant.

Table: Least-Squares Mean Differences (95% CI) From Baseline Within and Between Treatment Arms

	Cycle 7 (6 months)			Cycle 13 (12 months)		
	Zanubrutinib n=327	Ibrutinib n=325		Zanubrutinib n=327	Ibrutinib n=325	
	Difference Within the Arm	Difference Within the Arm	Difference Between the Arms	Difference Within the Arm	Difference Within the Arm	Difference Between the Arms
Global Health Status	8.18 (6.25, 10.12)	5.18 (3.20, 7.17)	**3.00 (0.23, 5.77)***	7.28 (5.41, 9.15)	5.93 (3.97, 7.89)	1.34 (−1.37, 4.06)
Physical functioning	6.55 (4.96, 8.15)	4.73 (3.08, 6.38)	1.82 (−0.47, 4.12)	5.46 (3.87, 7.04)	4.31 (2.65, 5.97)	1.15 (−1.15, 3.44)
Role functioning	6.95 (4.85, 9.06)	6.32 (4.14, 8.50)	0.63 (−2.40, 3.66)	6.81 (4.61, 9.02)	5.01 (2.69, 7.33)	1.80 (−1.40, 5.00)
Fatigue†	−12.54 (−14.47, −10.60)	−10.63 (−12.63, −8.62)	−1.91 (−4.70, 0.87)	−11.13 (−13.19, −9.08)	−10.78 (−12.93, −8.63)	−0.35 (−3.32, 2.62)
Nausea/vomiting†	−1.21 (−2.03, −0.38)	−0.92 (−1.77, −0.07)	−0.29 (−1.48, 0.89)	−0.92 (−1.94, 0.10)	−0.40 (−1.47, 0.66)	−0.51 (−1.99, 0.96)
Pain†	−5.06 (−7.21, −2.91)	−3.63 (−5.85, −1.42)	−1.43 (−4.51, 1.66)	−5.18 (−7.38, −2.97)	−2.75 (−5.06, −0.44)	−2.43 (−5.62, 0.77)
Diarrhea†	−2.11 (−3.80, −0.42)	−0.52 (−2.27, 1.22)	−1.59 (−4.01, 0.84)	−3.23 (−4.79, −1.66)	−1.38 (−3.03, 0.27)	−1.85 (−4.12, 0.43)

Data cutoff: 8 August 2022.

*Nominal P-value <.05.

†Negative values indicate improvement.

Abstract ID: 1550093

Title: High-dimensional single-cell characterisation of the chronic lymphocytic leukaemia tumour microenvironment using imaging mass cytometry

Authors: Timothy Woo, Paul Buckley, Hanna Mohamed, Julie Chan, Cynthia Bishop, Liron Barnea Slonim and Piers Patten

Introduction: In chronic lymphocytic leukaemia (CLL), the lymphoid tumour microenvironment (TME) can drive disease progression. Cellular and molecular interplay skews the TME towards a pro-survival and proliferative milieu, culminating in progressive accumulation of CD5+ B-cell clones. A systematic evaluation of the CLL TME may enable improved diagnostic, prognostic and therapeutic patient stratification. Imaging mass cytometry (IMC) permits the simultaneous multiplexed assessment of over 40 antigens across multiple cells on a single tissue slide, superseding the limitations of conventional immunohistochemistry. Applying IMC, we aimed to evaluate the CLL TME landscape with single-cell resolution to facilitate deep phenotyping and characterisation of its cellular composition, with the intention of exploring how spatially resolved features associate with clinical outcome.

Methods: Archival formalin-fixed paraffin-embedded lymph node tissue slides were obtained from patients with CLL ($n=7$). Non-malignant lymph node specimens ($n=2$) were available for comparison. Tissue slides were stained with a previously optimised panel of primary metal isotope-conjugated antibodies designed to identify lineage-specific cell subsets, functional status and stromal elements. Images were acquired using the Fluidigm Hyperion Imaging System. Following extraction of raw data, automated, deep-learning based cell segmentation was employed to identify single-cells. A mixed strategy of marker-based cell characterisation (ASTIR) and consensus clustering was employed to categorise cell populations. For clustered populations, cell identities were assigned manually based on canonical marker expression. Computational and statistical analyses were performed using R or Python.

Results: After segmenting a total of 163,212 cells from IMC images, we profiled the landscape of the CLL TME. We identified a diversity of cell populations including B-cells, T-cell subsets, monocytes, macrophages, dendritic cells, NK-like-cells, and other stromal components. Compared with non-malignant lymph node data we observed that CLL considerably alters the TME. Indeed, across CLL tissues, we observed substantial heterogeneity regarding the presence of cellular populations. In CLL, the median relative frequency of malignant cells was 66.4% (13.4–85.1%). CLL B-cells expressing Ki67, indicative of a proliferative state, comprised 0.2–8.4% (median, 2.1%) of the tumour bulk. During preliminary statistical analyses, we found that the frequencies of CLL B-cells per sample were negatively associated with macrophage proportions (Spearman; $R=-0.84$, $p=0.024$), although up-scaling of our sample size and careful statistical analysis to eliminate technical artefacts are needed. Through subclustering key parent lineages, we uncovered heterogeneous cellular subpopulations including previously-described CD4+ CD45RO+T-cells as well as, interestingly, CD45RAhi and CD57+ CLL B-cells which to our knowledge have not been commonly characterised. Taken together, these findings highlight the diversity of the CLL TME and will guide further phenotypic and spatial analyses using IMC.

Conclusions: IMC has previously been utilised to spatially characterise the anatomy of solid tumours and haematologic neoplasms such as diffuse large B-cell lymphoma at a cellular level, but to our knowledge has not yet been applied in CLL. Our work thus far has confirmed the feasibility of highly multiplexed analysis of the CLL TME composition using IMC. Furthermore, we have demonstrated a diversity of cellular populations, of which preliminary analysis suggests a substantially altered composition compared with normal lymph node. These data are consistent with the premise that CLL can shape the TME. We have additionally uncovered inter-patient variability which mirrors the characteristically heterogeneous clinical course and genomic paradigm of the disease. In future, we will perform an in-depth characterisation of the spatial context of cellular neighbourhoods to gain insights into interactions between proliferating tumour cells and their microenvironment. Therefore, we aim to derive meaningful clinical correlates associated to outcome that can be ultimately translated into practice.

Abstract ID: 1550097

Title: Patients with unmutated IgHV_1-69; 1-02; 3-30; 4-39 and high expression of AID enzyme need earlier treatment

Authors: Pablo Oppezzo, Ana Inés Landoni, Jorge Souto, Victoria Remedi, Gimena Dos Santos, Sabrina Ranero, Cecilia Guillermo, Carolina Oliver, Victoria Irigoín, Lilian Diaz, Rita Uría, Eugenia Payque, Juliana Querol Rivas, Maria Elena Marquez, Jorge González-Puelma, Irma Slavutsky, Carmen Stanganelli, Guillermo Dighiero, Hugo Naya, Marcelo A. Navarrete, Raul Gabus and Florencia L. Palacios

Clinical and molecular heterogeneity is a hallmark of chronic lymphocytic leukemia (CLL). This point is even more complex considering that leukemic cells continuously interact with cells and/or soluble factors from their microenvironment constantly modifying the evolution of the disease. The practical problem of this heterogeneous landscape is that leukemia progression cannot be predicted and it still remains an important unmet clinical need. Among different prognostic tools validated in CLL the mutational IgHV status is recognized as the most reliable molecular prognostic factor. Patients expressing mutated IgHV (M-CLL) develop a more indolent disease, whereas unmutated IgHV (U-CLL) patients display a more aggressive one, often unresponsive to treatment. Despite this categorization and a myriad of other molecules proposed as prognostic markers (CD38, Zap-70, CD49d, CXCL3/4, LPL and others) disease progression and/or treatment requirement still cannot be accurately predicted in many patients. We and others have described that activation-induced cytidine deaminase (AID) is over-expressed in peripheral blood (PB) of patients with poor clinical outcome and that it is predominantly expressed in U-CLL. Despite AID expression in CLL cells has been linked with disease progression, the role of AID in this leukemia and how its expression is involved during disease evolution remains controversial. To deepen into this question we studied AID expression in relationship with specific IgVH rearrangements that may contribute as prognostic markers. In a cohort of 270 CLL patients diagnosed according to IWCLL diagnostic criteria we analyzed the mutational IgHV status, the fluorescence *in-situ* hybridization (FISH) abnormalities and AID's mRNA expression by TaqMan Quantitative-PCR in the PB at diagnosis. Finally, we assessed the prognostic impact of IgHV rearrangements and AID expression levels in time to first treatment (TTFT). Of 270 patients, 172 were men and 98 women, (male-female ratio =1.75). From these, 153 (57%) were Binet's stage A, 60 (22%) stage B and 57 (21%) were stage C. IgHV gene status was mutated in 53%, whereas typical cytogenetic aberrations were found in 68%: del(13q14) in 36%, trisomy 12 in 15%, del(11q22) in 10% and del(17p13) in 7%. Median age at diagnosis was 67 years old and median of follow up was 5 years. Our first observation was that positive AID patients in the unmutated group mostly express the rearrangements IgHV_1-02; 1-69; 3-30 and 4-39. However, negative AID U-CLL as well as the M-CLL counterpart (expressing AID or not), remain distributed among the different IgHV rearrangements without any significant selection in the use of a specific IgHV/D/J genes. Prompted by these findings, and also considering previous reports describing the poorest clinical outcome for U-CLL expressing IgHV_1-69, we focused on these 4 unmutated IgHV rearrangements (1-02; 1-69; 3-30 and 4-39, hereafter, Sub-group_1) and compared the prognostic impact on TTFT with those U-CLL, expressing AID or not, but carrying different IgHV rearrangements of the Sub-group_1, (hereafter, mentioned as Sub-group 2). Forest plot of the hazard ratio assessed for association with TTFT by univariate and multivariate analysis were performed. Our results showed that U-CLL group expressing AID with BCR rearrangements corresponding to Sub-group_1 maintained the highest hazard ratio in the final model even after being included in the multivariable analyses del(17p) or Trisomy12. Next, we performed Kaplan–Meier curves analyzing TTFT among the different groups (U-CLL/AIDpos/Sub-group_1; U-CLL/AIDneg/Sub-group_1; U-CLL/AIDpos/Sub-group_2; U-CLL/AIDneg/Sub-group_2). Our results showed statistically significant differences comparing TFTT between the different sub-groups of patients indicating that: U-CLL/AIDpos/Sub-group_1 needed earlier treatment (χ TFTT= 7 months, $n=44$), compared with: U-CLL/AIDpos/Sub-group_2, (χ TFTT= 26 months, $n=27$, p=*); U-CLL/AIDneg/Sub-group_2, (χ

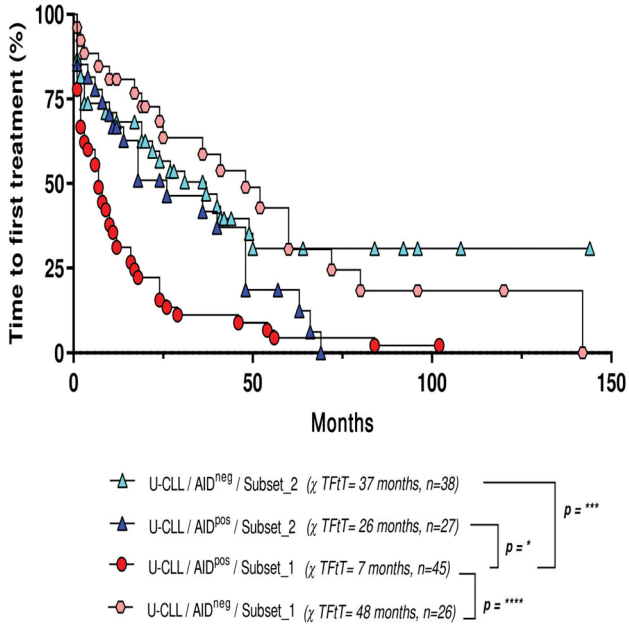

TFTT= 37 months, $n=39$, p=***), and U-CLL/AIDneg/Sub-group_1, (χ TFTT= 48 months, $n=26$, p=****), Log-rank (Mantel-Cox) test. In conclusion, our results highlight the relevance of assessing AID expression in PB of CLL patients in relationship with the mutational IgHV profile with the final goal of identifying the U-CLL/AIDpos/Sub-group_1. Considering our previous study analyzing the South American cohort, $n=900$ [1], the percentage of patients corresponding to the sub-group_1 is 27%. Hence, we can assume that the new entity described here (U-CLL/AIDpos/Sub-group_1) represents ~15% of the total CLL population, thus, accurate prediction of this sub-group could result in a useful tool to be incorporated in clinical practice after validation.

Abstract ID: 1550098

Title: A matching-adjusted indirect comparison of ELEVATE-TN versus SEQUOIA: acalabrutinib with and without obinutuzumab versus zanubrutinib in treatment-naïve chronic lymphocytic leukemia

Authors: Adam Kittai, John Allan, Dan James, Helen Bridge, Miguel Miranda, Alan Yong, Fady Fam, Jack Roos, Vikram Shetty, Alan Skarbnik and Matthew Davids

Introduction: The second-generation Bruton tyrosine kinase inhibitors acalabrutinib and zanubrutinib have not been compared with each other in a head-to-head randomized controlled trial (RCT). Acalabrutinib with and without obinutuzumab was evaluated in the ELEVATE-TN RCT in treatment-naïve chronic lymphocytic leukemia (CLL) and zanubrutinib was evaluated in treatment-naïve patients with CLL/small lymphocytic leukemia (SLL) without del(17p) in the SEQUOIA RCT. We used unanchored matching-adjusted indirect comparison (MAIC) to compare the efficacy and safety of acalabrutinib with and without obinutuzumab versus zanubrutinib in patients with treatment-naïve CLL/SLL using individual patient data (IPD) from ELEVATE-TN and published aggregate data from SEQUOIA.

Methods: In this unanchored MAIC, we weighted IPD for the acalabrutinib plus obinutuzumab and acalabrutinib monotherapy arms from ELEVATE-TN to match zanubrutinib baseline data from SEQUOIA. We included patients without del(17p) in ELEVATE-TN to ensure the patient population was similar to the SEQUOIA population. The efficacy analysis evaluated investigator-assessed progression-free survival (INV-PFS) in randomized patients with baseline data (acalabrutinib + obinutuzumab, $n=162$; acalabrutinib monotherapy, $n=163$; zanubrutinib, $n=241$) using the October 2021 data cut-off (DCO) for ELEVATE-TN and the May 2021 DCO for SEQUOIA. Patients were matched based on variables considered prognostic/predictive of INV-PFS in an exploratory multivariate Cox-regression analysis of ELEVATE-TN. These were age, ECOG status, Binet stage, bulky disease, cytopenia, del(11q), trisomy 12, IGHV status, and TP53 mutation. Pseudo-IPD for INV-PFS for zanubrutinib were obtained from Kaplan–Meier curves. The safety analysis assessed odds ratios (ORs) of adverse events (AEs) in treated patients with baseline data (acalabrutinib + obinutuzumab, $n=162$; acalabrutinib monotherapy, $n=162$; zanubrutinib, $n=240$). Patients were matched based on characteristics considered relevant by clinical experts, which were age, ECOG score, and cytopenia. To compare the incidence of AEs, the ELEVATE-TN February 2019 DCO was used to match the median treatment exposure from the SEQUOIA May 2021 DCO. Confidence intervals (CI) of 95% were used in both analyses.

Results: In the efficacy analysis, the acalabrutinib + obinutuzumab and acalabrutinib monotherapy effective sample sizes (ESSs) post-matching were 124 (76%) and 105 (64%), respectively. Matching had little impact on acalabrutinib + obinutuzumab and acalabrutinib monotherapy INV-PFS (Figure 1). Post-matching, 24-month INV-PFS was 96% (CI: 91–98) with acalabrutinib + obinutuzumab, which was higher than that with zanubrutinib (88%; CI: 82–92). The MAIC-weighted Cox hazard ratio (HR) showed INV-PFS to be superior with acalabrutinib + obinutuzumab versus zanubrutinib (HR: 0.33; 0.15–0.71; Figure 1(A)). Acalabrutinib monotherapy post-matching had a similar 24-month INV-PFS (92%; CI:

Figure 1. Kaplan–Meier curve showing INV-PFS for acalabrutinib+obinutuzumab (A) and acalabrutinib monotherapy (B) before and after matching versus zanubrutinib

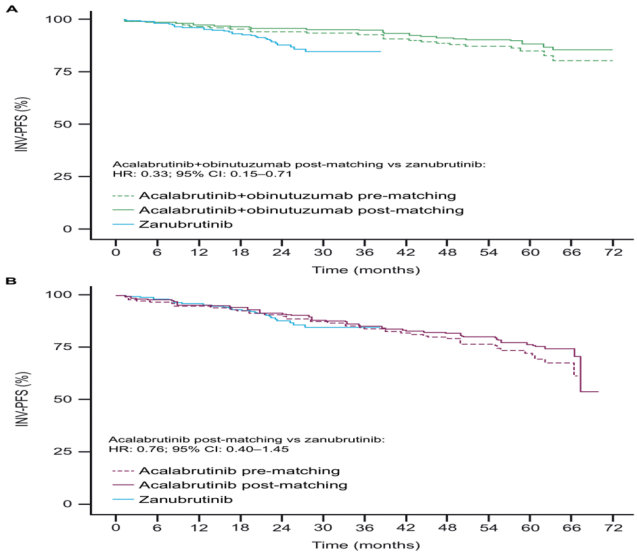

CI, confidence interval; HR, hazard ratio; INV-PFS, investigator-assessed progression-free survival

Figure 2. Forest plot of odds ratios of adverse events with acalabrutinib+obinutuzumab (A) and acalabrutinib monotherapy (B) after matching

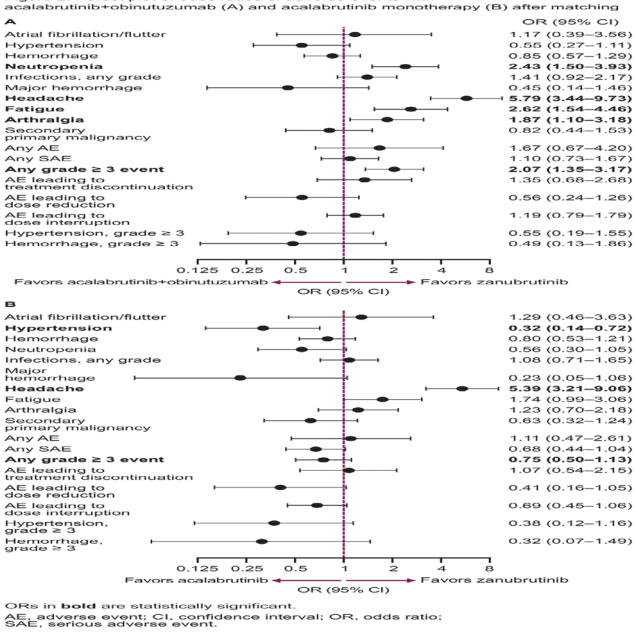

ORs in **bold** are statistically significant.
AE, adverse event; CI, confidence interval; OR, odds ratio; SAE, serious adverse event.

85–96) to zanubrutinib (88%; CI: 82–92) and no differences in the MAIC-weighted Cox HR were observed versus zanubrutinib (0.76; CI: 0.40–1.45) (Figure 1(B)). In the safety analysis, the median treatment exposure was similar between acalabrutinib + obinutuzumab and acalabrutinib monotherapy (both 28 months) and zanubrutinib (26 months). The acalabrutinib + obinutuzumab and acalabrutinib monotherapy ESSs post-matching were 154 (95%) and 157 (97%), respectively. With acalabrutinib + obinutuzumab, there were no significant differences versus zanubrutinib in the odds of having any AE, any serious AE, atrial fibrillation/flutter, hypertension, and hemorrhage (Figure 2(A)). However, acalabrutinib + obinutuzumab was associated with higher odds versus zanubrutinib of having any grade ≥3 event (OR: 2.07; CI: 1.35–3.17), headache (OR: 5.79; CI: 3.44–9.73), fatigue (OR: 2.62; CI: 1.54–4.46), neutropenia (OR: 2.43; CI: 1.50–3.93), and arthralgia (OR: 1.87; CI: 1.10–3.18). Acalabrutinib monotherapy also showed no significant differences versus zanubrutinib in the odds of having any AE, any SAE, atrial fibrillation/flutter and hemorrhage. However, the odds of having hypertension were significantly lower (OR: 0.32; CI: 0.14–0.72) while the odds of having headache were higher (OR: 5.39; CI: 3.21–9.06) with acalabrutinib monotherapy versus zanubrutinib (Figure 2(B)).

Conclusions: In this MAIC of ELEVATE-TN and SEQUOIA, acalabrutinib + obinutuzumab had a superior efficacy in terms of INV-PFS versus zanubrutinib, while acalabrutinib monotherapy and zanubrutinib had similar efficacies in patients with treatment-naïve CLL/SLL without del(17p). Acalabrutinib + obinutuzumab and acalabrutinib monotherapy generally had similar safety profiles to zanubrutinib; however, acalabrutinib + obinutuzumab was associated with higher odds of grade ≥3 AEs, headache, fatigue, neutropenia, and arthralgia, versus zanubrutinib. Acalabrutinib monotherapy was associated with higher odds of headache but lower odds of hypertension versus zanubrutinib. Our results systematically compare common regimens where randomized, prospective data are not available. Limitations of MAIC analyses mean the results should be viewed as hypothesis-generating.

Abstract ID: 1550104

Title: Characterization of the safety/tolerability profile of zanubrutinib and comparison with the profile of ibrutinib in patients with B-cell malignancies: post hoc analysis of a large clinical trial safety database

Authors: Jennifer Brown, Barbara Eichhorst, Paolo Ghia, Wojciech Jurczak, Brad S. Kahl, Nicole Lamanna, Tadeusz Robak, Mazyar Shadman, Constantine S. Tam, Lugui Qiu, Aileen Cohen, Meng Zhang, Tommi Salmi, Jason Paik, Liping Wang, Jun Zhang, Han Ma and Alessandra Tedeschi

Introduction: Bruton tyrosine kinase (BTK) is an important regulator of cell proliferation and cell survival in various B-cell malignancies. BTK inhibitors block B-cell receptor–induced BTK activation and its downstream signaling, leading to growth inhibition and cell death in malignant B cells. The first-generation BTK inhibitor, ibrutinib, revolutionized treatment; however, inhibition of off-target kinases such as EGFR, HER2, TEC, and CSK may be associated with toxicities, including gastrointestinal side effects, rash, and atrial fibrillation, that limit its use. Zanubrutinib, a potent and selective next-generation BTK inhibitor, was designed to maximize BTK occupancy and minimize off-target effects. Here, we characterize the overall safety and tolerability of zanubrutinib in patients with B-cell malignancies and compare its profile with ibrutinib.

Methods: In the *post hoc* analyses, safety data were pooled from 10 zanubrutinib monotherapy clinical trials in patients with chronic lymphocytic leukemia/small lymphocytic lymphoma, mantle cell lymphoma, marginal zone lymphoma, Waldenström macroglobulinemia, follicular lymphoma, and other B-cell malignancies (Nf1550), including 2 (ASPEN, ALPINE) that compared zanubrutinib head-to-head with ibrutinib. Incidence rates and exposure-adjusted incidence rates (EAIRs) of treatment-emergent adverse events (TEAEs; summarized in MedDRA preferred terms) and adverse events of special interest (AESIs; defined in grouped terms) were assessed.

Results: Median zanubrutinib exposure was 34.4 months. The most common nonhematologic any-grade TEAEs with zanubrutinib were upper respiratory tract infection (29.7%), diarrhea (21.1%), contusion (19.5%), cough (18.1%), and rash (16.6%). Grade ≥3 TEAEs in ≥5% of patients included pneumonia (8.4%) and hypertension (8.1%). The only serious TEAE in ≥5% of patients was pneumonia (8.2%). In ASPEN/ALPINE, patients treated with zanubrutinib had lower rates of discontinuation (14.1 vs. 22.0%), dose reduction (13.9 vs. 19.2%), and death (8.7 vs. 10.2%) due to TEAEs than those treated with ibrutinib. EAIRs of AESIs were numerically lower with zanubrutinib vs. ibrutinib, except for neutropenia (Table 1). With longer follow-up, the prevalence of AESIs with zanubrutinib generally remained constant or decreased.

Conclusions: These pooled safety analyses in patients with B-cell malignancies showed that zanubrutinib is well tolerated, with generally mild to moderate TEAEs and low discontinuation rates due to TEAEs. The prevalence of AESIs generally decreased over time, with no new safety signals emerging. Due to the continuous dosing of BTK inhibitors in most B-cell malignancies, long-term tolerability and low treatment discontinuation rates with BTK inhibitors are important. These analyses support zanubrutinib as an appropriate long-term treatment option for patients with B-cell malignancies.

Table. Exposure-Adjusted Incidence Rates for Adverse Events of Special Interest

		ASPEN/ALPINE[a]	
	Zanubrutinib (N=1550)	Zanubrutinib (n=425)	Ibrutinib (N=422)
Median exposure, mo	34.4	32.6	25.7
Exposure-adjusted incidence rate, persons/100 person-months			
Infections	6.01	5.40	6.64
Opportunistic infections	0.07	0.07	0.13
Hemorrhage	3.00	2.49	3.00
Major hemorrhage	0.17	0.17	0.24
Neutropenia	1.21	1.32	1.05
Thrombocytopenia	0.59	0.49	0.65
Hypertension	0.57	0.82	1.08
Anemia	0.51	0.57	0.75
Second primary malignancies	0.52	0.47	0.58
Skin cancers	0.30	0.27	0.38
Atrial fibrillation/flutter	0.15	0.20	0.64

[a] Head-to-head trials of zanubrutinib vs ibrutinib.

Abstract ID: 1550290

Title: Treatment patterns and outcomes of patients with TP53-mutated chronic lymphocytic leukemia

Authors: Steven Hwang, Yucai Wang, Kari Rabe, Marquise Williams-Watley, Saad Kenderian, Eli Muchtar, Paul Hampel, Neil Kay, Amber Koehler, Amy Behnken, Jose Leis, Esteban Braggio, Min Shi, David Viswanatha, Daniel Van Dyke, Susan Slager, Sameer Parikh, Rong He and Wei Ding

Background: TP53 alterations are associated with inferior outcomes in chronic lymphocytic leukemia (CLL). However, the heterogeneity of TP53 alterations and the impact of single-hit vs. multi-hit TP53 alterations on treatment outcomes are understudied. We present a descriptive analysis of outcomes of CLL patients with TP53 alterations treated at Mayo Clinic, including mutation profiles and the potential impact of single-hit versus multi-hit TP53 alterations.

Methods: Patients with CLL and TP53 mutation(s) detected by Sanger sequencing between June 2014 and April 2021 were identified. Patient demographics, clinical/pathologic characteristics, treatment, and follow-up data were abstracted from the Mayo Clinic CLL database and by chart review. We defined multi-hit TP53 status as presence of multiple TP53 mutations or both TP53 mutation(s) and del17p. Event-free survival (EFS) and overall survival (OS) were calculated from start of treatment after TP53 sequencing.

Results: A total of 145 patients with TP53 mutation(s) were identified (70% male). At time of TP53 mutation testing, median age was 69 years (range: 44–92), 39% of patients had Rai stage III–IV, 77% had unmutated IGHV, 53% had del17p, and 62% had ≥3 cytogenetic abnormalities. A TP53 mutation was identified prior to CLL treatment in 63 patients (Group 1) and after at least one prior line of treatment in 82 patients (Group 2). Del17p by FISH was present at time of TP53 mutation identification in 54% of patients in Group 1 and 52% in Group 2. We identified a total of 170 TP53 mutations in 145 patients (74 in untreated, 54 in those who had previously received a novel agent, and 42 in those who had previously received chemoimmunotherapy [CIT] only) (Figure 1(A)). Of the 170 mutations, 102 (60%) were identified only once, suggesting that most of the mutations were unique to each patient. Overall, 55 patients had single-hit TP53 disruption and 90 had multi-hit TP53 disruption. Collectively, patients with single-hit and multi-hit TP53 disruption had a median EFS of 26.4 (95% CI 8.4–NE) and 26.3 months (95% CI 16.6–NE, $p=0.76$), respectively, and a median OS of NE (95% CI 40.3–NE) and 61.8 months (95% CI 47.1–NE, $p=0.87$), respectively. In Group 1 ($n=63$), 46 patients had initiated first-line treatment (39 BTKi-based, 3 BCL2i ± BTKi-based, 4 CIT). The median time from TP53 testing to treatment initiation was 1.2 months (95% CI 0.2–34.3). The median EFS following treatment initiation was 53.7 months (95% CI 29.9–NE), and the median OS was not reached (median follow-up 26 months after treatment initiation). Patients with single-hit

Figure 1

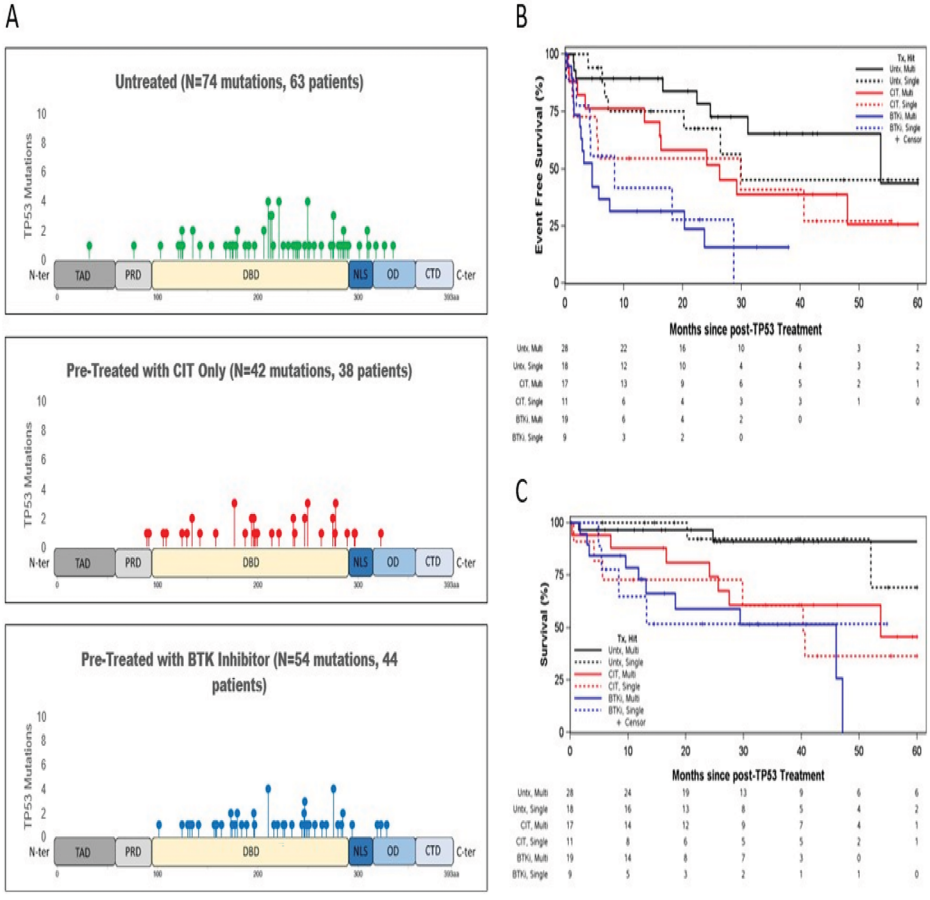

($n=18$) and multi-hit ($n=28$) TP53 alterations had a median EFS of 29.9 months (95% CI 20.2–NE) and 53.7 months (95% CI 31.1–NE, $p=0.46$), respectively (Figure 1(B_). In Group 2 ($n=82$), the median number of prior lines of therapy was 2 (range 1–16). Prior treatment exposure included novel agent therapy ($n=44$, 54%) and CIT only ($n=38$, 46%). The median time from TP53 mutation detection to subsequent treatment initiation was 1.2 months (95% CI 0.0–44.5) among the 56 patients who were treated. For 38 patients previously treated with CIT only, 28 had initiated subsequent treatment. The median EFS and OS from subsequent treatment initiation was 26.3 months (95% CI 13.5–NE) and 40.6 months (95% CI 27.5–NE), respectively. Patients with single-hit ($n=11$) and multi-hit ($n=17$) TP53 alterations had a median EFS of 29.8 months (95% CI 5.4–NE) and 26.3 months (95% CI 16.1–NE, $p=0.69$), respectively (Figure 1(B)), and a median OS of 40.3 months (95% CI 29.8–NE) and 53.7 months (95% CI 25.6–NE, $p=0.52$), respectively (Figure 1(C)). For 44 patients previously treated with BTKi, 28 had initiated subsequent treatment. The median EFS and OS from subsequent treatment initiation was 4.6 months (95% CI 2.9–23.7) and 46.0 months (95% CI 13.2–NE), respectively. Patients with single-hit ($n=9$) and multi-hit ($n=19$) TP53 alterations had a median EFS of 8.4 months (95% CI 4.2–NE) and 4.6 months (95% CI 2.7–NE, $p=0.76$), respectively (Figure 1(B)), and a median OS of NE (95% CI 8.4–NE) and 46.0 months (95% CI 13.1–NE, $p=0.81$), respectively (Figure 1(C)).

Conclusions: Specific sites of TP53 mutations in our cohort were heterogeneous without clear differences in patients with or without prior treatment. Treatment outcomes did not differ significantly between patients with single-hit versus multi-hit TP53 alterations stratified by prior treatment status.

Abstract ID: 1550392

Title: Anti-CD19 chimeric antigen receptor T-cell therapy for Richter's transformation: a multicenter retrospective study

Authors: Adam Kittai, David Bond, Ying Huang, Seema Bhat, Emily Blyth, John Byrd, Julio Chavez, Matthew Davids, Jamie Dela Cruz, Mark Dowling, Caitlyn Duffy, Carrie Ho, Caron Jacobson, Samantha Jaglowski, Nitin Jain, Kevin Lin, Christine McCarthy, Erin Parry, Manoj Rai, Kerry Rogers, Aditi Saha, Levanto Schachter, Hamish Scott, Mazyar Shadman, Tanya Siddiqi, Deborah M. Stephens, Vinay Vanguru, William Wierda, Omer Zulfa, Jennifer Woyach and Phillip Thompson

Background: Aggressive lymphoma, most commonly large B-cell lymphoma (LBCL), arising in the setting of chronic lymphocytic leukemia (CLL) is known as Richter's transformation (RT), and is associated with poor outcomes. Anti-CD19 Chimeric Antigen Receptor T-cell therapy (CART) has revolutionized the treatment of LBCL, with impressive durable responses for patients with relapsed/refractory disease. Patients with RT have been excluded from most major anti-CD19 CART clinical trials. Therefore, there are minimal available data describing outcomes of RT following anti-CD19 CART.

Methods: We conducted a multicenter retrospective analysis of patients with RT who received anti-CD19 CART currently approved for hematologic malignancies at 7 academic centers in the United States. RT was defined as patients with LBCL with preceding or concurrently diagnosed CLL. We collected patient, disease, and treatment characteristics. Progression-free survival (PFS) and overall survival (OS) were measured from date of anti-CD19 CART infusion and estimated using the Kaplan–Meier method. Cox regression model was used to associate prognostic factors with PFS and OS. Response was assessed by Lugano criteria by individual investigators.

Results: Fifty-five patients were included. Median age at the time of anti-CD19 CART infusion was 64 years (range: 27–78). Median prior lines of therapy for CLL or RT were both 2 (CLL range: 0–10, RT range: 0–7). Forty-nine (89.1%) patients previously received a Bruton tyrosine kinase inhibitor (BTKi) or BCL2 inhibitor (BCL2i) for CLL or RT. Median Ki-67 on pathology sample was 80% (range: 40–100), median SUV on brightest lymph node (LN) on PET-CT was 14.5 (range: 3–50.6), median size of largest LN was 4.1cm (range: 0-16), and median LDH prior to anti-CD19 CART was 249 (range: 140–2828). Median time from apheresis to anti-CD19 CART infusion was 33 days (range: 24–100), and 45 (81.8%) patients received bridging therapy. 35 (63.6%), 13 (23.6%), 6 (10.9%), and 1 (1.8%) patients received axi-cel (axicabtagene ciloleucel), tisagenlecleucel (tisa-cel), lisocabtagene maraleucel (liso-cel), and brexucabtagene autoleucel (brexu-cel), respectively. Overall response rate was 61.9%, with 25 (45.5%) and 9 (16.4%) patients attaining complete response (CR) and partial response, respectively. After a median follow up of 27.5 months from anti-CD19 CART infusion, the median PFS was 3.45 months (95% CI: 1.81–6.94), and median OS was 8.5 months (95% CI: 4.80–25.4) (Figure 1). Among 34 patients who died, twenty-four (70.6%) died due to progression of disease, and 10 (29.4%) died for other reasons including 7 infections (4 COVID), 1 septic shock, 1 stroke, and 1 respiratory failure. The cumulative incidence of non-relapse mortality at 12-months was 17.1% (95% CI: 8.3–28.6). Three patients in a CR underwent allogeneic stem cell transplantation, two were alive at last known follow up (3.9 and 24.2 months post-transplant), and 1 patient died from progression of disease 21 months post-transplant. Forty-eight (87%) patients had CRS, with 9 (16.3%) grade ≥3 events. Thirty-seven (67.2%) patients had ICANS, with 22 (40%) grade ≥3 events. On univariable analysis, increasing Ki-67 and LDH were found to be associated with higher risk of progression and death. On multivariable analysis, increasing Ki-67, increasing LDH, and greater number of prior lines of therapy for RT were independent prognostic variables for worse PFS and OS. All other variables, including type of anti-CD19 CART product received, were not correlated with PFS or OS (Table 1).

Conclusions: We report the largest cohort of patients with RT who received anti-CD19 CART. This was a heavily pretreated cohort with a median prior lines of therapy for CLL or RT of 2, and 89% of patients were exposed to either BTKi or BCL2i agents. RT remains a disease of unmet need, as the median OS was 8.5 months in this study. However, there is some progress made as historically the median OS for patients with RT previously treated with BTKi is 4 months [1]. Given higher number of prior therapies is associated with worse OS, earlier use of anti-CD19 CART in the RT disease course may be warranted. Our data support the use of anti-CD19 CART for patients with RT, with durable disease control in a subset of patients. Given observed high response rate to anti-CD19 CART, along with most patients experiencing early relapse, allogeneic stem cell transplantation at response should be considered. Prospective clinical trials evaluating anti-CD19 CART with novel agents, including BTKi, for RT are currently ongoing.

Figure. Progression-free Survival and Overall Survival of patients receiving anti-CD19 CART for RT.

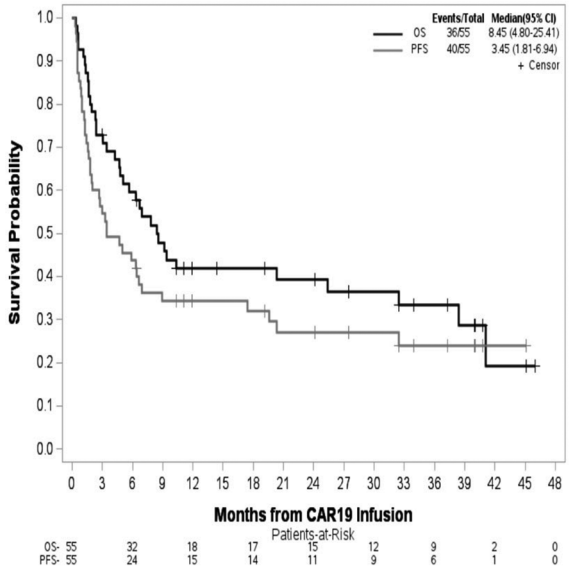

Table. Univariable and Multivariable Cox Model for Overall Survival

	Univariable Models		Multivariable Model	
	HR (95% CI)	p-value	HR (95% CI)	p-value
Age at anti-CD19 CART infusion, 5-years older	1.01 (0.87-1.19)	0.87	-	-
# prior lines of therapy for CLL prior to RT	1.09 (0.91-1.31)	0.34	-	-
# prior lines of therapy for RT prior to CART	1.30 (0.99-1.70)	0.06	1.59 (1.19-2.11)	0.0014
Total prior lines of therapy	1.15 (1.00-1.33)	0.06	-	-
Ever received prior BTKi or Ven for CLL or RT	1.80 (0.53-6.18)	0.35	-	-
Ki-67, 10% higher	1.45 (1.11-1.88)	0.0060	1.66 (1.27-2.17)	0.0002
LDH, 2-fold increase	1.85 (1.31-2.61)	0.0005	1.75 (1.17-2.61)	0.0064
SUV, 1-unit increase	1.02 (0.99-1.05)	0.16	-	-
Size of LN, 1-cm increase	0.98 (0.89-1.08)	0.66	-	-
Received BTKi concurrently with RT*	0.83 (0.43-1.61)	0.59	-	-
Days from apheresis to anti-CD19 CART, 5 more days	1.02 (0.89-1.16)	0.78	-	-
Received bridging therapy	1.35 (0.52-3.49)	0.53	-	-
Types of anti-CD19 CART therapy, vs Brexu-cel or Liso-cel				
Axi-cel	0.93 (0.32-2.72)	0.90	-	-
Tisa-cel	0.78 (0.24-2.53)	0.67	-	-

* Received BTKi as part of the most recent therapy prior to apheresis, or as part of the bridging treatment or concurrently with anti-CD19 CART.

Abstract ID: 1550634

Title: The HEALTH4CLL study: optimization of behavioral interventions for patients with chronic lymphocytic leukemia

Authors: Alessandra Ferrajoli, Che Young Lee, Max Gordon, Melissa Markofski, Emily LaVoy, Susan Peterson, Liang Li, Miranda Bauma, Margaret Pace, Danielle Walsh and Karen Basen-Engquista

Introduction: Chronic lymphocytic leukemia (CLL) is the most prevalent leukemia in the United States, and advanced age and comorbidities increase the risk of cancer-related fatigue in patients with CLL. Exercise reduces fatigue, but optimal health behavior intervention methods for patients with CLL are unknown. We conducted a pilot study of digital diet and physical activity intervention tools (HEALTH4CLL) designed to reduce fatigue in patients with CLL.

Materials and methods: The HEALTH4CLL study used a randomized factorial design based on the multiphase optimization strategy (MOST). All patients received diet, exercise, and weight management instructional materials plus a Fitbit and were randomized to undergo one of sixteen combinations of four evidence-based intervention strategies over sixteen weeks: telephone versus email coaching, text message reminders versus no reminders, daily versus weekly self-monitoring, and aerobic plus resistance exercise versus aerobic exercise alone. Patients' fatigue, physical function, health-related quality of life, behavioral changes, and program satisfaction and retention were assessed. Paired *t*-tests were used to examine changes in outcomes from baseline to follow-up among all patients. Factorial analysis of variance was used to examine effective intervention components and their combinations regarding improvement in fatigue and physical function scores.

Results: Thirty-one patients completed the interventions and follow-up assessment. We observed significant improvements in fatigue score ($p = 0.001$), physical function score ($p = 0.01$), sit to stand test results ($p = 0.046$), arm curl test results (right, $p = 0.03$; left, $p = 0.041$), and grip strength (right, $p = 0.013$; left, $p = 0.003$) at follow-up. The combination of resistance and aerobic exercise with daily self-monitoring was associated with improved fatigue scores ($p = 0.027$). Analysis of the individual components of the MOST design demonstrated greater improvement in the physical function score with resistance plus aerobic exercise than with aerobic exercise alone ($p = 0.048$). We identified telephone coaching, text message reminders, and Fitbit use as feasible interventions.

Discussion: These findings demonstrated the feasibility and effectiveness of behavioral interventions in reducing fatigue and improving physical function in patients with CLL. Combined aerobic and resistance exercise, daily self-monitoring, and remote coaching were associated with improved physical function and reduced fatigue.

Abstract ID: 1550655

Title: Venetoclax retreatment after MRD-guided venetoclax +/– ibrutinib: the improve study cohort

Authors: Lydia Scarfò, Silvia Heltai, Elisa Albi, Eloise Scarano, Luana Schiattone, Lucia Farina, Riccardo Moia, Marina Deodato, Andrea Ferrario, Marina Motta, Alessandro Noto, Rosaria Sancetta, Marta Coscia, Paolo Rivela, Luca Laurenti, Marzia Varettoni, Eleonora Perotta, Antonella Capasso, Pamela Ranghetti and Paolo Ghia

Background: The efficacy and tolerability of venetoclax retreatment in patients with chronic lymphocytic leukemia (CLL) relapsing after venetoclax-based fixed-duration regimens is not yet fully elucidated. Data derived from small cohorts suggest that venetoclax retreatment can be effective and well tolerated, thus it is worth exploring in larger cohorts of well-characterized patients with CLL.

Aims: We analyzed the efficacy and safety of venetoclax retreatment in patients with relapsed/refractory CLL enrolled in our clinical trial IMPROVE (NCT04754035).

Methods: Patients enrolled into the study were treated with venetoclax single-agent for 12 months; those with undetectable measurable residual disease (uMRD) discontinued therapy while those with detectable MRD received the combination of ibrutinib and venetoclax until uMRD, toxicity or for up to 12 months. Patients with detectable MRD at the end the combination therapy stopped venetoclax and continued with ibrutinib only. In patients experiencing relapse requiring treatment (PD), venetoclax was restarted according to the standard schedule with an initial 5-week dose escalation ramp-up and continued until PD or unacceptable toxicity. MRD was tested every 3 months in peripheral blood using the 8-color flow cytometry panel validated by the ERIC (European Research Initiative on CLL) including CD45/CD5/CD19/CD20/CD43/CD79b/CD81/ROR1.

Results: After a median follow-up of 54 months (5–62) from C1D1, 17/38 (44.5%) patients experienced PD requiring treatment after discontinuing therapy, including 16 after having reached confirmed uMRD (9 treated with venetoclax single-agent, 7 with the combination of venetoclax and ibrutinib), 1 who discontinued both venetoclax and ibrutinib in response with detectable MRD due to an unrelated adverse event. Two out of 17 had Richter transformation (RT), 2 developed autoimmune hemolytic anemia, and all 4 went off study. The remaining 13 pts (6 uMRD with venetoclax monotherapy, 6 uMRD with the combination of venetoclax and ibrutinib, 1 MRD+on venetoclax+ibrutinib) received venetoclax retreatment at a median of 32 months (12–41) after the end of initial therapy (Table 1). Median progression-free survival (PFS) from the end of initial venetoclax +/– ibrutinib treatment was 23 months and the median PFS2 (from C1D1 of venetoclax +/– ibrutinib) 54 months (range 39–60). The 12 uMRD patients experienced MRD relapse at a median of 5 months (0–41) after stopping treatment, while the median time between MRD relapse and disease progression requiring treatment was 27 (0–37) months. The only patient who stopped treatment in PR with detectable MRD, due to an unrelated adverse event, restarted venetoclax after 13 months. At the time of venetoclax initiation tumor lysis syndrome (TLS) risk was high in 6, medium in 3, low in 4. Best overall response rate in 10 evaluable patients was partial response (8/10, 80%), and 2 stable disease. With a median time on treatment of 9.5 months, 2 patients achieved uMRD after 3 and 6 months, the second one maintained uMRD for 6 months and then became MRD positive again (Figure 1). Four out of 13 patients progressed after 7, 12 ($n=2$), and 14 months on venetoclax retreatment, 3/4 received next-line treatment with ibrutinib and achieved a partial response. At last follow-up 11/13 patients undergoing venetoclax retreatment were alive (1 death due to RT on ibrutinib, 1 due to CLL progression on non-covalent BTK inhibitor). Progression-free survival from venetoclax restart to PD on venetoclax retreatment, last follow-up or death was 14 months (0–23). Venetoclax retreatment was very well tolerated with no patients experiencing clinical or laboratory TLS, 5/13 having grade 3–4 neutropenia, 3/13 infections (2 grade 3, 1 grade 2). Only one patient discontinued venetoclax due to persistent grade 3–4 neutropenia.

Conclusion: Venetoclax retreatment was effective and well-tolerated in a cohort of patients with relapsed/refractory CLL who have previously received MRD-guided treatment with venetoclax+/– ibrutinib. MRD relapse occurred at a median of about 2 years before clinical progression requiring treatment. Updated results with longer follow-up will be presented at the meeting.

Table 1. Baseline characteristics at baseline and at the time of venetoclax retreatment.

Characteristic	Venetoclax +/- ibrutinib (n=38)	Venetoclax retreatment (n=13)
Age at treatment initiation (median, range)	64 (47-81)	65 (51-82)
Male gender no./total (%)	25/38 (66)	8/13 (62)
Prior lines of therapy (median, range)	1 (1-7)	2 (1-7)
del(17p) no./total (%)	7/33 (21)	1/11 (9)
TP53 mutation no./total (%)	9/31 (29)	3/11 (27)
Unmutated IGHV no./total (%)	27/34 (79)	10/12 (83)
Venetoclax mono	-	6
Venetoclax + ibrutinib	-	7
TLS risk before venetoclax no./total (%)		
High	14/38 (37)	6
Medium	18/38 (47)	3
Low	6/38 (16)	4
Best overall response rate no./total (%)	36/38 (95)	8/10 (80)
Best PR	10/38 (26)	8 (80)
Best CR	26/38 (68)	0 (0)
Stable disease	0	2
PD	1	0

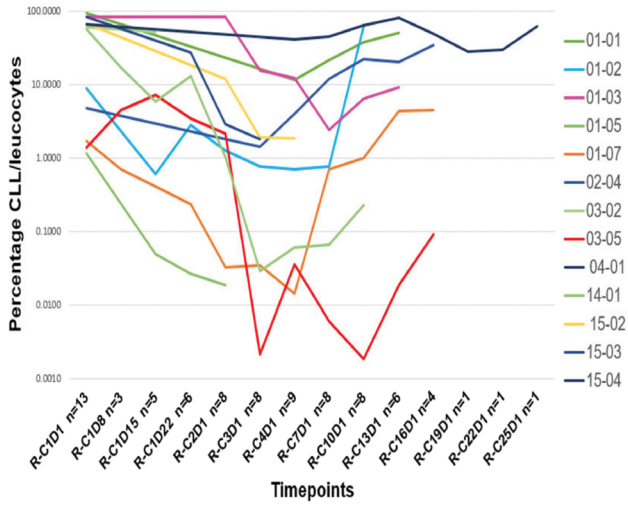

Figure 1

Abstract ID: 1550759

Title: Efficacy and toxicity of ibrutinib in CLL – Croatian experience. A non-interventional, real world study of KroHem

Authors: Igor Aurer, Nikola Bulj, Barbara Dreta, Inga Mandac-Smoljanovic, Antonija Miljak, Fran Petricevic, Marija Ivic, Sandra Basic-Kinda, Viktor Zatezalo, Martina Madunic, Dubravka Carzavec, Jasminka Sincic-Petricevic, Dragana Grohovac, Ozren Jaksic, Ivan Krecak, Martina Moric-Peric, Bozena Coha, Petra Bernes, Neno Zivkovic and Vlatko Pejsa

Ibrutinib has revolutionized the treatment of CLL. Despite being a targeted agent, it does cause off-target toxicities, most notably cardiac and hemorrhagic. Factors affecting the risk of adverse outcomes are incompletely understood and the type and extent of pretreatment evaluation needed to identify patients at an increased risk of serious cardiovascular side effects unknown. In order to evaluate the efficacy and toxicity of ibrutinib treatment and risk factors for adverse outcomes KroHem collected data on Croatian patients starting treatment between the time the drug became reimbursable in 2015 until 31 December 2021. We identified 436 patients fulfilling entry criteria (Table 1); 404 (92.7%) responded to treatment. 312 patients (71.6%) are alive, 263 of these (60.3%) progression-free and 233 (53.4%) still on therapy. 34 patients (7.8%) died after progression, 18 (4.1%) suddenly or of cardiovascular causes, 4 (0.9%) of bleeding, 13 (3.0%) of other tumors, 16 (3.7%) of COVID19, 20 (4.6%) of other infections, 2 frail elderly (0.5%) after general deterioration, and in 17 (3.9%) the cause of death is unknown. 60 (13.8%) patients stopped treatment for insufficient response or progression, of whom 19 with Richter's syndrome; 75 (17.2%) due to intercurrent death; 55 (12.6%) for toxicity: cardiovascular 26, bleeding 8, gastrointestinal 5, cutaneous 5, neurologic 3, hematologic 3, infections 3 and pneumonitis and ocular 1 each; 7 (1.6%) for patient decision; and 6 (1.4%) for treatment of another disease. Cardiovascular side effects occurred in 25.0% of patients and hemorrhagic in 15.6%. The dose of ibrutinib was permanently reduced in 22.2% of patients. Median follow-up of the cohort was 29 mo, range 1–95 mo; estimated median overall survival (OS) 75 mo, progression-free survival (PFS) 54 mo and time on treatment (TT) 44 mo (Figure 1). Factors significantly related to OS in multivariate analysis were stage (Binet A median OS not reached, B 75 mo, C 55 mo, $p=0.009$); treatment line (1st line median not reached, 2nd 75 mo, ≥3rd 54 mo, $p=0.036$) and age (≤68 y median not reached, 68–75 y 55 mo, >75 y 42 mo, $p<0.0001$). Factors significantly related to PFS in multivariate analysis were treatment line (1st line median 67mo, 2nd 54 mo, ≥3rd 40 mo, p = 0.023), age (≤68 y median 64 mo, 68–75 y 43 mo, >75 y 37 mo, $p<0.0001$), and pretreatment history or ECG finding of cardiac arrhythmia (no 54 mo, yes 39 mo, $p=0.001$). Factors significantly related to TT in multivariate analysis were age (≤68 y median 56 mo, 68–75 y 41 mo, >75 y 25 mo, $p<0.0001$), pretreatment cardiac arrhythmia (no 51 mo, yes 24 mo, $p<0.0001$) and need for permanent ibrutinib dose reduction (no median 51 mo, yes 27 mo, $p<0.0001$). Sex, FISH and presence of arterial hypertension were not independently significantly related to any of these outcomes. Pretreatment cardiologic consultation did not improve TT, PFS, OS, risk of stopping treatment due to cardiovascular side effects or risk of cardiovascular or sudden death neither in the whole cohort nor in the subgroup of patients without pretreatment cardiac arrhythmia. Our analysis confirms the efficacy of ibrutinib in treatment of CLL. Outcome, especially of front-line patients, seems inferior to that reported in clinical trials. A possible explanation is that the drug was first approved only for patients with del 17p and in early relapse, which therefore comprise an extraordinarily high proportion of our cohort. Another possible explanation is the adverse effect of the COVID19 pandemics. Age was the most important prognostic factor, those older than 75 did significantly less well. Patients with cardiac arrhythmias are at an increased risk of having to stop treatment early. Del 17p did not appear to be a significant negative prognostic factor, possibly due to the number of high-risk patients in our cohort and a relatively short follow-up. Around 4% of patients die of cardiovascular side effects and additional 6% have to stop ibrutinib for same reasons. Routine pretreatment cardiologic consultation is insufficient to reduce this risk. Additional studies are needed to improve early identification of these patients for whom alternative treatments might be more suitable.

Characteristic	N (%)
Gender M/F	268 (61.5%) / 168 (38.5%)
Age (median/range)	68 y / 36-87 y
Binet stage (A/B/C)*	46 (10.6%) / 209 (43.3%) / 176 (40.6%)
FISH: not done	85
normal	112 (31.0%)
del 11	49 (13.6%)
+12	22 (6.1%)
del 13	62 (17.2%)
del 17	116 (32.1%)
IgHv mutational status: not done	378
mutated / unmutated	10 (17%) / 48 (83%)
Treatment line: 1st	216 (49.5%)
2nd	116 (26.6%)
≥3rd / median, range	104 (23.9%) / 3, 3-11
Pretreatment cardiac consultation (yes / no)**	132 (30.3%) / 303 (69.7%)
History or pretreatment ECG with cardiac arrhythmia (yes / no)**	54 (12.4%) / 381 (87.6%)
Pretreatment arterial hypertension (yes / no)	223 (51.1%) / 213 (48.9%)

*unknown for 3 patients

**unknown for 1 patient

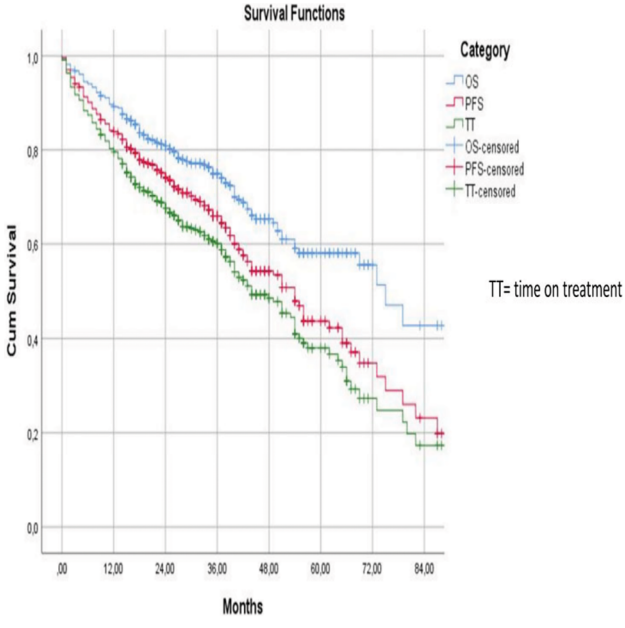

Abstract ID: 1550795

Title: The role of artificial intelligence in differential diagnosis and prognostic significance of small B-cell lymphoma

Authors: Zizhu Tian, Hongling Peng, Yi Jiang and Zeyu Deng

Objective: To obtain quantitative pathological immunohistochemistry (IHC) data using artificial intelligence (AI) technology to investigate the differential diagnosis and prognostic significance of immunophenotypic expression in MCL and CLL/SLL.

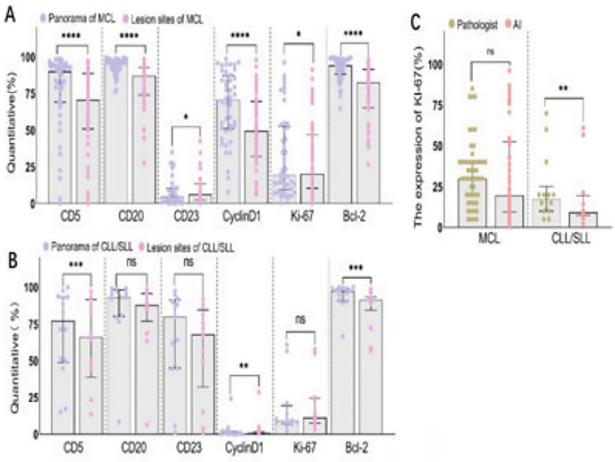

Figure 1. Comparison of Ki-67 expression in MCL and CLL/SLL as interpreted by pathologists and artificial intelligence (A), and of the two diseases in terms of immunohistochemical expression in the panorama and at the site of the lesion (B-C). ns, P>0.05; *, P≤0.05; **, P≤0.01; ***, P≤0.001; ****, P≤0.0001, significance is determined at p < 0.05.

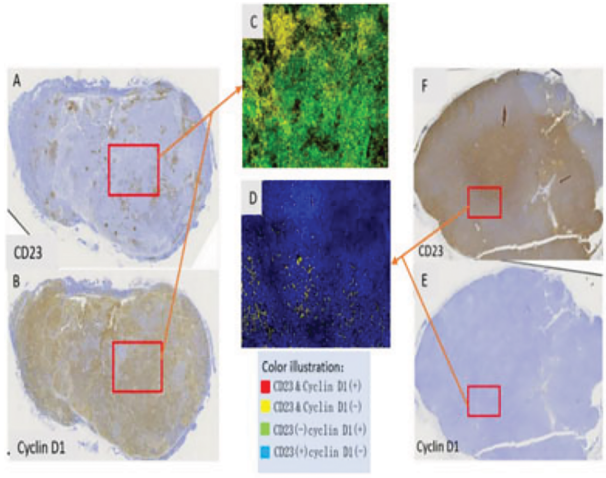

Figure 2 Pathological immunohistochemistry (AB, EF) of 1 case of MCL and 1 case of CLL/SLL and their pseudo-color images (C, D). A-C is from the same MCL patient, and D-F is from the same CLL/SLL patient.

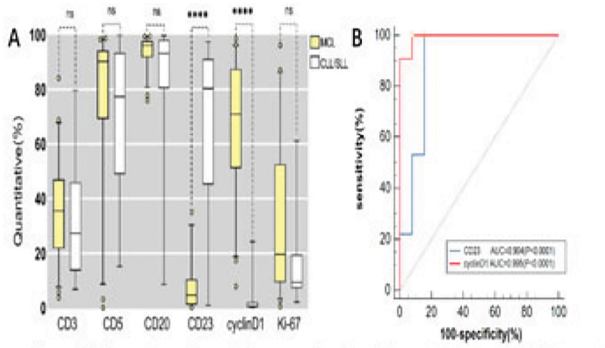

Figure 3. Comparison of quantitative expression of each immunohistochemistry in 51 cases of MCL and 14 cases of CLL/SLL(A). ROC curve based on CD23 and Cyclin D1 quantification for differentiating MCL and CLL/SLL. ns, P>0.05; ****, P≤0.0001; Significance is determined at p< 0.05.

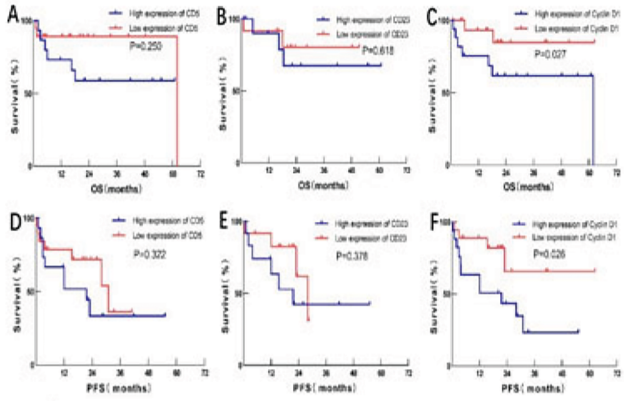

Figure 4. Overall survival (A-C) versus progression-free survival (D-F) curves for each immunohistochemical expression subgroup in MCL patients. A, D: CD5; B, E: CD23; C, F: Cyclin D1.

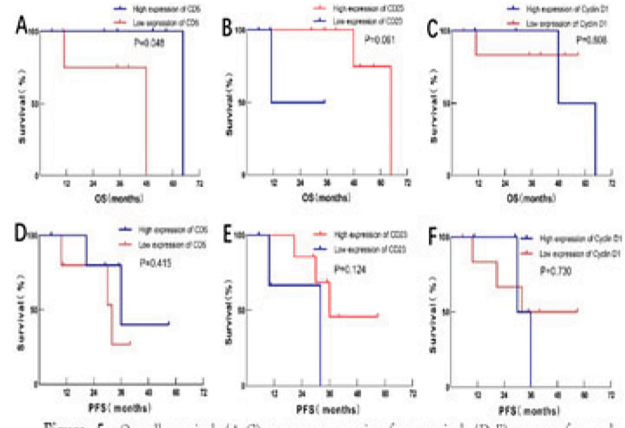

Figure 5. Overall survival (A-C) versus progression-free survival (D-F) curves for each immunohistochemical expression grouping in CLL/SLL patients. A, D: CD5; B, E: CD23; C, F: Cyclin D1.

Methods: Retrospective collection of pathological sections of 52 cases with a pathological diagnosis of MCL and 14 instances of SLL at our hospital from April 2017 to April 2022, together with the data of patients. The Kaplan–Meier method was used for survival function estimation.

Results: A cut-off value of ≤35.02% for CD23 (AUC =0.904; p<0.0001) and >24.26% for Cyclin D1 (AUC =0.995; p<0.0001) was favored for the diagnosis of MCL. The model consisting of CD20, CD5, CD23, and Cyclin D1 was used to diagnose MCL or CLL/SLL with 100% accuracy. Among MCL patients, the 3-year overall survival (OS) rates were (90.0 ± 9.5)% and (60.2 ± 11.8)% (p = 0.027), and the 3-year progression-free survival (PFS: rates were (64.5 ± 19.9)% and (23.6 ± 12.7)% (p = 0.026) in the Cyclin D1 low and high expression groups, respectively. The OS was prolonged in the CD5 high expression group compared to the low expression group in SLL patients (64.7 months vs. 48.0 months, p = 0.048).

Conclusion: The application of AI in IHC helps to identify MCL and CLL/SLL more accurately and efficiently. The newly identified risk factors are expected to guide better the treatment and prognosis of MCL and CLL/SLL.

Abstract ID: 1550829

Title: Frequent monitoring in chronic lymphocytic leukemia clinical trials: what is the true value?

Authors: Agnes Mattsson, Jeanette Lundin, Tom Mulder, Sandra Eketorp Sylvan, Marzia Palma, Lotta Hansson and Anders Österborg

Background: Industry-initiated clinical trial protocols on new precision therapeutics designed for chronic lymphocytic leukemia (CLL) require not only frequent admissions and blood analyses but also repeated computerized tomography (CT) examinations. The value of such intense monitoring has not been systematically analyzed and is in bright contrast to recommendations issued by the iwCLL guidelines.
Methods: This retrospective analysis included patients who participated in industry-initiated clinical trials. Descriptive analyses were performed on number of admissions, blood tests and CT examinations where the patients served as their own controls, i.e. were analyzed twice, once as specified in the study protocol and once hypothetically according to iwCLL guidelines. Time to response (TTR) and time to progression (TTP) as well as objective response rate (ORR) was also compared.
Results: Forty-two patients with CLL who participated in 7 pharma conducted phase 2 or 3 clinical trials at one single center between February 2013 and December 2020 were included in the study. The median age at study start was 73 years (range 52–87) and 43% received their study medication as first-line therapy. The most common regimen was zanubrutinib monotherapy (38%) followed by ibrutinib monotherapy (24%) and rituximab-bendamustine (12%). The median follow-up time was 38 months (range 2–108). The median numbers of outpatient visits per protocol and hypothetically according to iwCLL guidelines were 18 (range 3–34) and 10 (range 1–18), respectively ($p<0.0001$). The corresponding median number of blood tests were 29.5 (range 3–73) and 18 (range 1–45), respectively ($p<0.0001$). The median number of CT examinations performed during treatment and follow-up according to study protocols were 10 (range 2–17) with an estimated median total radiation dose of 100 mSv (range 16 to 136–187), compared to zero CT examinations according to iwCLL guidelines ($p<0.0001$). ORR was 90% per protocol and 93% when analyzed according to iwCLL guidelines (not significant). The median TTR and TTP were not significantly different per protocol vs. per iwCLL guidelines: 5.62 vs. 4.57 months, respectively, for TTR (Figure 1), and not reached for TTP (Figure 2).
Conclusion: We conclude that participation in a clinical trial results in a considerable number of extra admissions and examinations for patients. The value of such intense monitoring appears to be limited since there was no significant difference in time to response or progression between the excessive monitoring as per protocol and the more restricted hypothetically reconstructed monitoring as per iwCLL guidelines. The cumulative radiation dose from CT examinations was, in many patients, higher than recommended in recent national radiation protection guidelines, especially if conducted early in the disease course. Harmonization of the monitoring requirements, especially regarding CT examinations, between CLL clinical trial protocols and iwCLL guidelines, is warranted.

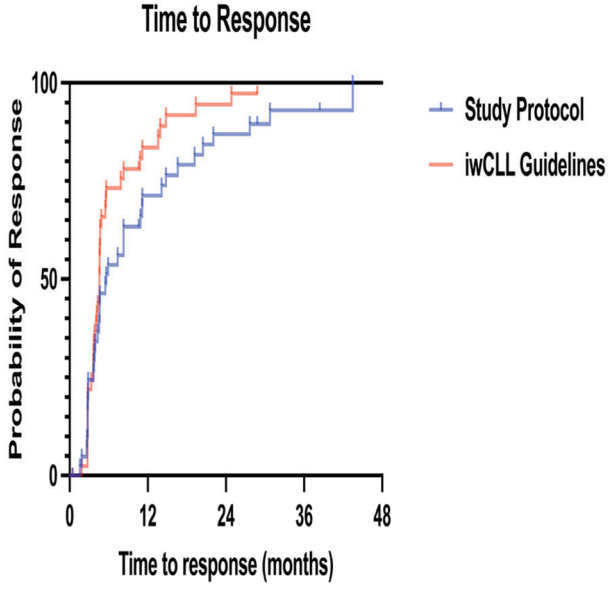

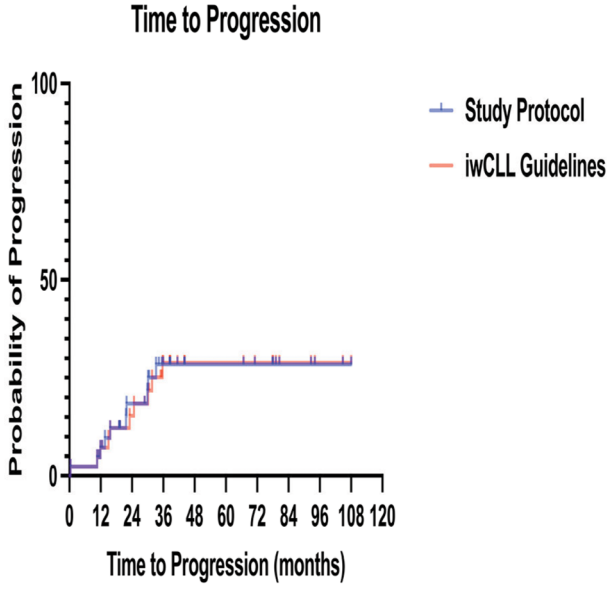

Abstract ID: 1550929

Title: Significance of sIL-2R and LD in predicting time to first treatment in Japanese CLL patients with early asymptomatic disease

Authors: Jun Takizawa, Ritsuro Suzuki, Koji Izutsu, Atae Utsunomiya, Kengo Takeuchi, Naoya Nakamura, Koichi Ohshima, Sadao Aoki and Junji Suzumiya

Purpose: A prospective nationwide registry study (CLLRSG-01) was conducted to determine the clinical status of chronic lymphocytic leukemia (CLL) and related diseases, which are rare in Japan. Our previous reports in the iwCLL held in 2015, 2017, 2019, and 2021 have provided insights into the characteristics and prognosis of CLL in the Japanese population. As part of this research, we evaluated the effectiveness of the international prognostic score for predicting the time to first treatment (TTFT) in CLL patients

TTFT of patients with CLL based on serum sIL-2R levels above or below 1,000 U/mL

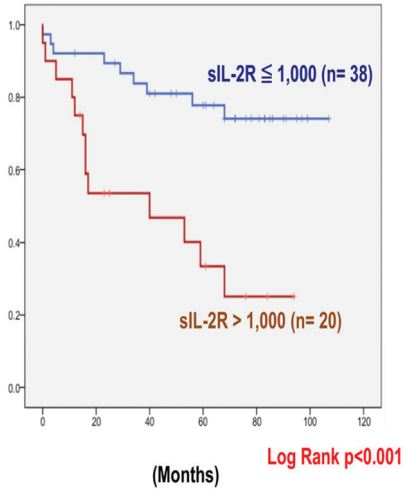

Cox regression analysis of TTFT

Characteristic	Univariate analysis		Multivariate analysis	
	HR (95% CI)	*P*-value	HR (95% CI)	*P*-value
sIL-2R>1,000	4.24 (1.79-10.02)	0.001	2.71 (1.03-7.17)	0.044
palpable LN	3.49 (1.45-8.40)	0.005	2.08 (0.75-5.81)	0.162
unmutaed *IGHV*	3.62 (1.46-8.92)	0.006	3.63 (1.24-10.62)	0.018
Ly>15,000	1.49 (0.65-3.46)	0.349		
Age>65	0.69 (0.29-1.64)	0.399		
Male	0.97 (0.42-2.28)	0.946		
PS>0	0.05 (0.00-1269.91)	0.556		
LDH>ULN	5.36 (1.88-15.29)	0.002	4.92 (1.49-16.27)	0.009
CD38(+)	4.20 (1.68-10.51)	0.002		
ZAP70(+)	2.92 (1.11-7.67)	0.030		
MYD88 mutation	1.36 (0.18-10.11)	0.766		
β2MG>3.5	1.24 (0.28-5.36)	0.773		
del(17p)	3.03 (0.70-13.07)	0.137		
del(11q)	5.47 (1.24-24.17)	0.025		
del(11q) or del(17p)	4.31 (1.43-13.00)	0.009		
del(13q)	0.53 (0.23-1.25)	0.532		
+12	3.19 (1.01-10.12)	0.049		

with early, asymptomatic disease, known as the 'International Prognostic Score for Early-stage CLL (IPS-E)' [1]. Additionally, we investigated other factors that could serve as prognostic indicators in this patient population.

Methods: The study included 58 patients with Binet stage A CLL from the CLLRSG-01 trial, who were divided into three IPS-E risk groups. The IPS-E model was used to calculate the risk scores by assigning points based on the absolute lymphocyte count (ALC) > 15 × 109/L, unmutated immunoglobulin heavy-chain variable-region (IGHV) gene, and the presence of palpable lymph nodes. Patients were categorized as low-risk (score 0), intermediate-risk (score 1), or high-risk (score2–3). Kaplan–Meier survival curves were used to estimate the TTFT, defined as the time from enrollment to the initiation of CLL treatment due to progression to symptomatic disease as per the iwCLL guidelines. The log-rank test was used to assess differences in the TTFT among the risk groups. Furthermore, univariate and multivariate Cox regression analyses were performed to identify independent correlations of outcome variables, including lactate dehydrogenase (LD) and soluble interleukin 2 receptor (sIL-2R).

Results: The patients had a median age of 65 years (range: 34–84 years), and 34 of the 58 patients were males (59%). After a median follow-up of 59.5 months (range, 0–107 months), 22 patients (38%) underwent treatment. Based on the IPS-E, 31 patients were classified as low-risk, 17 as intermediate-risk, and 10 as high-risk. The scoring system revealed that the 5-year cumulative risk of treatment initiation was 19% for low-risk patients, 42% for intermediate-risk patients, and 75% for high-risk patients. However, no significant differences were observed between the intermediate- and high-risk groups ($p = 0.097$). Hence, univariate analyses were performed for the patients in this study; however, the ALC was not a significant factor associated with TTFT (Table). Multivariate analyses were performed using 17 baseline factors, and three covariates were independently correlated with TTFT: unmutated IGHV gene, LD (>upper limit of normal range), and sIL-2R (>1,000 U/mL) (Table 1). Patients with sIL-2R <1,000 U/mL (median not reached) exhibited significantly longer TTFT compared to those with sIL-2R ≥1,000 U/mL (median 40 months, $p<0.001$) (Figure 1). Similarly, CLL patients with LD within the normal range (median not reached) experienced significantly longer TTFT compared to those with LD above the upper limit of the normal range (median 12 months, $p<0.001$).

Conclusions: Our results suggest that sIL-2R and LD might serve as robust novel biomarkers for predicting the likelihood of treatment necessity among patients with early-stage CLL. However, further validation using a larger dataset is necessary to substantiate these findings.

Abstract ID: 1550933

Title: Clonal architecture and single-cell transcriptome landscape in Richter's syndrome

Authors: Heng Li, Lingli Yuan, Peilong Wang, Zheng Fu and Hongling Peng

Richter's syndrome (RS) is an uncommon clinicopathological condition in which chronic lymphocytic leukemia (CLL) evolves into aggressive lymphoma, the mechanism of which still remains difficult to elucidate. To dissect the precise molecular mechanism of RS, paired samples of peripheral blood mononuclear cells and the lymphonodus tissue of the patient were analyzed by single-cell RNA-seq, and lymphoma-related gene mutations were examined by targeted next-generation sequencing. An inferred branched revolutionary architecture from CLL clones to RS clones was shown in Figure 1(A). Overall, 27,058 single-cell transcriptomes were integrated into a two-dimensional map using the Uniform Manifold Approximation and Projection (UMAP) method. Four major cell types were identified, namely, B cells, mononuclear phagocytes, T cells and neutrophils. Compared to CLL, the cell composition and expression landscape of RS were significantly different. Nine clusters of B cells were identified using UMAP analysis. CLL cells were mostly mapped to Clusters 1, 5, 6, 7 and 8; RS B cells were mostly mapped to Clusters 2, 3 and 4; and Cluster 9 was mutually harbored by CLL and RS samples. Gene sets of downstream targets of MYC were significantly enriched in Cluster 4 and Cluster 9, indicating the potential therapeutic targets. PySCENIC analysis was used to identify master regulators of B cell clusters. The transcription factors BACH2 and JUNB were most associated with RS B cells. The upregulated RGS2 was the downstream target gene of BACH2 and JUNB. IRF9 was most associated with RS B cells, which could modulate the expression of PRDX1. GO enrichment analysis showed that differentially overexpressed

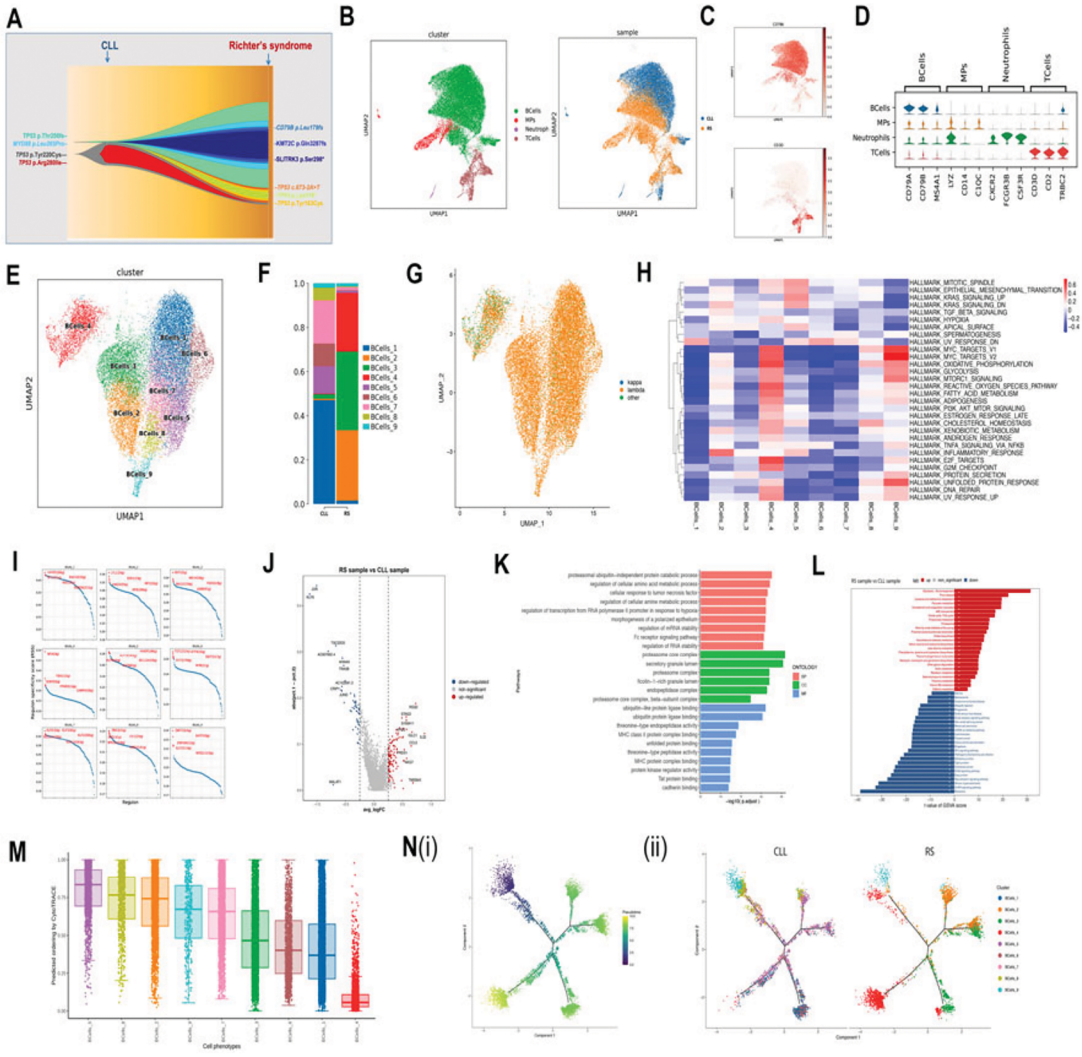

genes of RS B cells were enriched in the proteasomal ubiquitin-independent protein catabolic process and regulation of cellular amino acid metabolic process, while scGSVA analysis also demonstrated that the proteasome pathway and amino acid metabolism pathway were enriched in the RS sample. CytoTRACE was used to predict the differentiation status of B-cell clusters. Cluster 4 was predicted to have lower capacity of differentiation. Subsequently, Monocle2 was used to perform pseudotime analysis on malignant B cells. Notably, proliferating cells were enriched at the end of Cluster 4 pseudotime trajectories. The immune cell composition was remarkably changed between the CLL and RS samples. T cells were reclustered into six distinct populations by UMAP analysis: CD4+ naïve T cells, CD4+ regulatory T cells (Treg), CD8+ effector T cells (Teff), CD8+ exhausted T cells (Tex), CD8+ effector memory T cells (Tem), and natural killer cells (NK). In the RS sample, CD4+ naïve T cells, CD8+ Tex and Treg cells were significantly increased, while NK and CD8+ Tem cells were decreased. A volcano plot was created to show differentially expressed genes of T cell subtypes between CLL and RS samples. The upregulated genes of CD8+ Tex in the RS sample included ALOX5AP, which contributes to inflammation, and ABCG1, which is involved in T cell activation and apoptosis. CytoTRACE revealed the differentiation potential, and the exhausted T cells were predicted to have the least differentiation ability. In the RS sample, T cells deviated from the normal path. Meanwhile, more exhausted T cell subsets were observed in RS sample, which were also enriched at the end of the pseudotime trajectory. Genes correlated with exhaustion, toxicity or inflammation were mapped to T cell populations, which were measured by their uniform score (U-score). The exhaustion U-score was significantly higher and the toxicity U-score was significantly decreased in the T cell population of the RS sample, implying the possible contribution of T cell defects to the mechanism of RS. Meanwhile, we used CellPhoneDB to predict ligand-receptor interactions between malignant cells and immune cells. The cell-to-cell interactions were predicted to be impaired between Cluster 4 and T cell subtypes, suggesting that tumor progression may be attributed to immune escape. Furthermore, we observed that PDCD1/FAM3C, PTPRC/CD22, and CCL4/CNR2 were commonly enriched between B cells of the RS sample and CD8+ Tex, as well as CD8+ Teff cells. These interactions suggest that blocking these axes may affect the interaction of malignant B cells with surrounding immune cells and could be an effective strategy to treat RS. In conclusion, we have demonstrated the clonal architecture and single-cell transcriptome landscape of RS using single-cell transcriptomics and bulk somatic mutation analyses, which is helpful to understand the potential molecular mechanisms of RS.

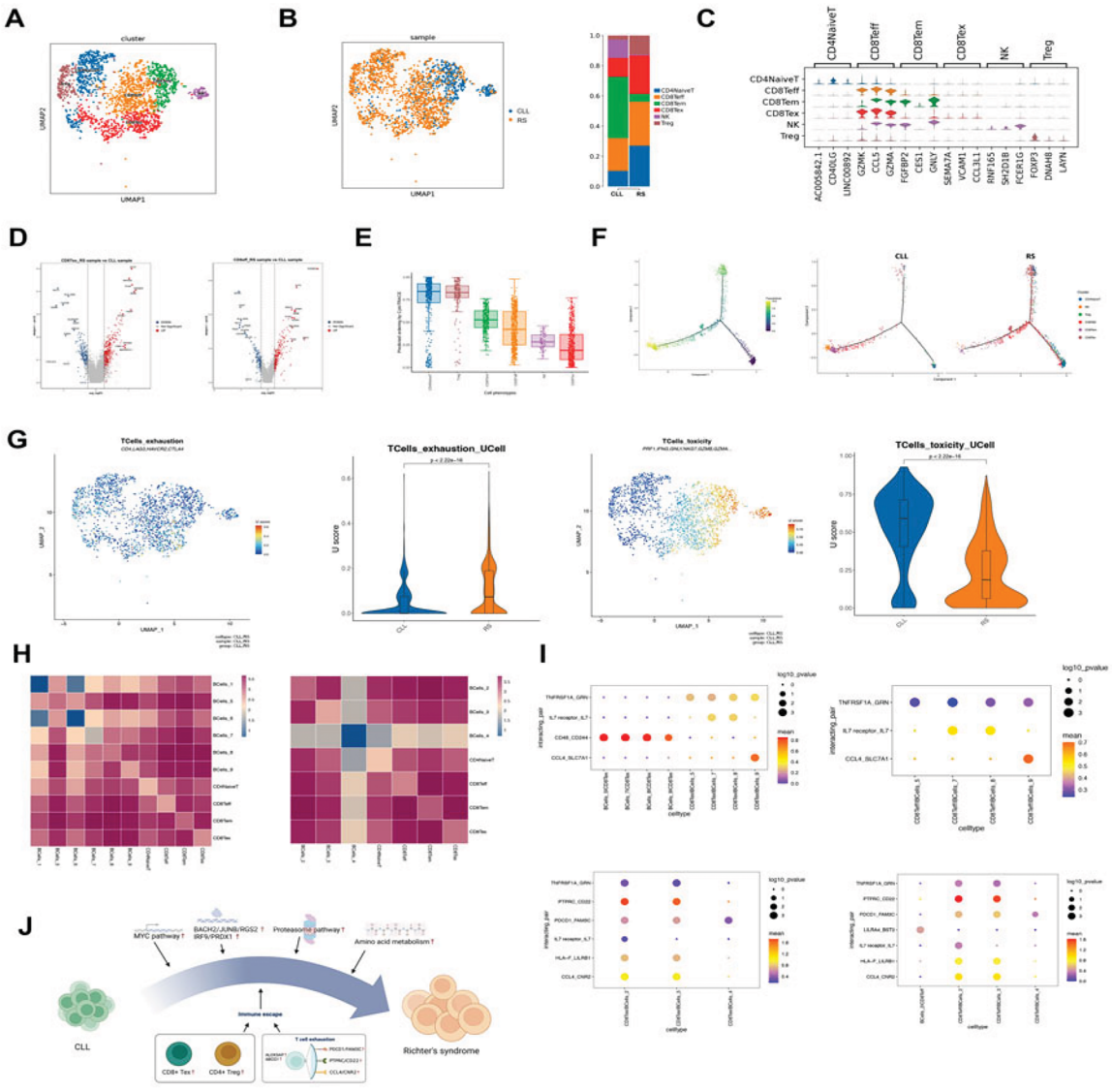

Abstract ID: 1550939

Title: Ibrutinib plus fludarabine, cyclophosphamide and rituximab (iFCR) as initial treatment in chronic lymphocytic leukemia/small lymphocytic leukemia with or without TP53 aberrations: a prospective real-world study in Chinese cohort

Authors: Huayuan Zhu, Yi Miao, Yeqin Sha, Yi Xia, Shuchao Qin, Rui Jiang, Luomengjia Dai, Hui Shen, Tonglu Qiu, Wei Wu, Chongyang Ding, Yujie Wu, Lei Fan, Wei Xu and Jianyong Li

Background: Bruton tyrosine kinase inhibitors (BTKi) monotherapy has introduced the concept of continuous treatment in chronic lymphocytic leukemia/small lymphocytic leukemia (CLL/SLL) until disease progression, leading to several concerns like lack of deep remission, increasing risk of toxic effects and substantial cost. Therefore, time-limited treatment strategies as first line treatment of CLL/SLL were comprehensively explored and BTKi combined with chemoimmunotherapy (CIT) was one of these options, which could induce durable responses in young fit patients.

Methods: CLL/SLL patients who were treated with iFCR as initial therapy in the First Affiliated Hospital of Nanjing Medical University (Jiangsu Province Hospital) were included without any genomic restrictions. Ibrutinib (420 mg daily) was given continuously for 2 years and intravenously rituximab (375 mg/m^2 in day 0 of cycle 1; 500 mg/m^2 in day 0 of cycle 2–6), fludarabine (25 mg/m^2, days 1–3) and cyclophosphamide (250 mg/m^2, days 1–3) were administered every 28-day cycle, up to maximal 6 cycles. Patients who achieved complete remission or complete remission with incomplete recovery (CR/CRi) and bone marrow (BM) undetectable minimal residual disease (uMRD) 2 years after iFCR initiation were feasible to discontinue ibrutinib maintenance.

Results: Thirty-four previously untreated, young fit CLL/SLL patients who received iFCR regimen between January 2019 and Match 2021 were retrospectively included in our cohort. The median age was 55 years (IQR: 48–56). IGHV was

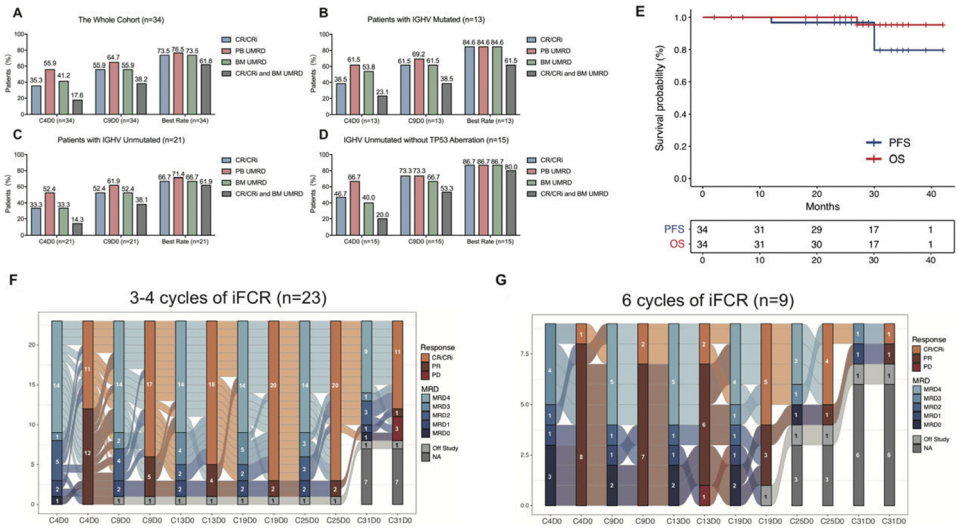

unmutated in 21 of 34 (61.8%) patients; complex karyotype was present in 11 of 34 (32.4%) patients; TP53 mutation or del(17p) was detected in 6 of 34 (17.6%) patients. CR/CRi rate and BM uMRD rate was 35.3% (12/34) and 41.2% (14/34) after 3 cycles of iFCR and increased to 55.9% (19/34) 2 months after 6 cycles in both patients who received 3 or 4 and 6 cycles of iFCR. The best CR/CRi and BM uMRD rate were both 73.5% (25/34). With the median follow-up of 33 months (range 7–42 months), the 3-year PFS and OS rate was 80.0 and 95.5%, respectively. CR/CRi rate and BM uMRD rate was comparable between patients with IGHV mutated and unmutated status without TP53 aberration, while all patients with TP53 aberration failed to achieve sustainable CR/CRi or BM uMRD. Patients who achieved MRD 10–6 negative post 3 cycles of iFCR sustained remission and discontinued ibrutinib maintenance. The most common hematological adverse events were neutropenia (25/34, 73.5%) and thrombocytopenia (24/34, 70.6%), grade 3–4 neutropenia and thrombocytopenia occurred in 67.6% (23/34) and 35.3% (12/34) patients respectively. The most common non-hematological adverse events were nausea (21/34, 61.8%), fatigue (16/34, 47.1%) and vomiting (15/34, 44.1%). 35.3% (12/34) patients experienced at least one dose FC regimen reduction and 47.1% (16/34) patients experienced at least once ibrutinib dose-hold with a median duration of 7 days.

Conclusion: The iFCR regimen could achieve high response rate and proportion of uMRD as initial treatment for young fit CLL/SLL patient without TP53 aberrations with acceptable tolerability. MRD-guided iFCR courses adjustment in patients who achieved early phase remission could achieved sustainable response and reduced toxicity.

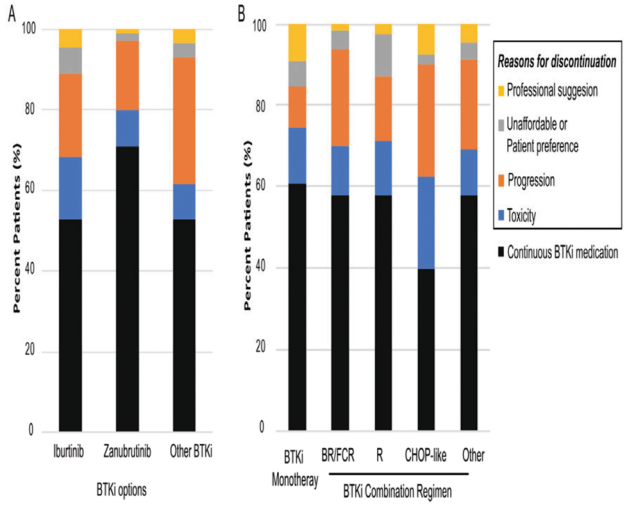

Abstract ID: 1550994

Title: Real-world treatment patterns, discontinuation and clinical outcomes in patients with B-cell lymphoproliferative diseases treated with BTK inhibitors in China

Authors: Yuting Yan, Rui Lv, Tingyu Wang, Ying Yu, Yanshan Huang, Wenjie Xiong, Gang An, Dehui Zou, Lugui Qiu and Shuhua Yi

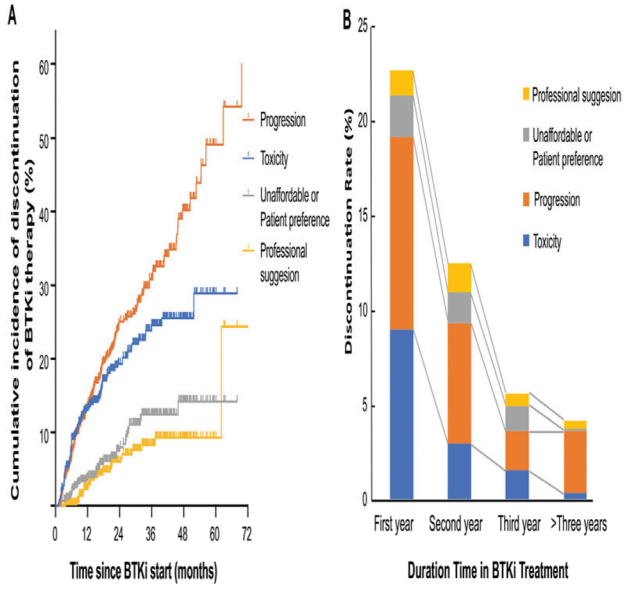

Bruton tyrosine kinase inhibitor (BTKi) has demonstrated substantial efficacy in treating B-cell lymphoproliferative diseases (BLPD). Nonetheless, the significant discontinuation rates due to toxicity or financial reasons cannot be overlooked. In China, empirical evidence on the usage of BTKi remains scarce. To address this, a retrospective cohort study was conducted focused on 673 Chinese patients with BLPD who underwent at least one month of BTKi therapy. Median age at BTKi initiation was 60 years. The median duration on BTKi treatment of the whole cohort was 36.4 months. The median post-BTK survival was not reach. BTKi-based treatment was permanently discontinued in 288 (43.8%) patients during follow-up, mostly attributed to progressive disease. Within the first 6 months of BTKi treatment, 76 patients (26.3%) had early treatment discontinuation. Patients with early discontinuation had extreme worse outcome with a median post-discontinuation survival of only 6.9 months. On multivariate analysis, withdrawal BTKi by toxicity and withdrawal BTKi within 6 months retained to be independent predictors of post-BTK survival, after taking account of the response depth, lines of therapy and baseline cytogenetics including 17p deletion. The decision between BTKi monotherapy and combination therapy, along with the preference for first or second-generation BTKi, exerted no significant impact on survival. These observations contribute valuable real-world insights into the utilization of BTKi in China. We concluded that BTKi is an effective and well-tolerated treatment for long-term use in Chinese patient population. However, it is imperative to stress that a proportion of patients discontinue BTKi early, leading to suboptimal outcomes. This study underscores the importance of adherence to BTKi therapy for improved clinical outcomes in real-world patients.

Abstract ID: 1551042

Title: Coupled effect of a miR-155 deficiency and hypoxia conditions leads to the upregulation of SLC2A1 (GLUT1), SLC2A3 (GLUT3) and EGLN1 genes in the leukemic B-cells

Authors: Elena Golovina, Karina Savvulidi Vargova, Tomas Heizer, Lenka Daumova and Martin Bajecny

Hypoxia represents one of the key factors that stimulate the growth of leukemic cells in their niche. Hypoxia forces the leukemic cells to reprogram their original transcriptome, miRNome, and metabolome. It is still not fully known how the microRNAs (miRNAs)/mRNAs coupling enables the emergence of a leukemic state. Generally, miRNAs regulate practically all cells' biological processes and play a crucial role in leukemia development and progression. In the present study, we aimed to uncover the impact of hsa-miR-155-5p (miR-155, MIR155HG) on the metabolism, proliferation, and mRNA/miRNA network of human chronic lymphocytic leukemia cells (CLL) in hypoxia conditions. In this project, we used the human MEC-1 cell line, as a model of CLL, where we deleted mature miR-155 with the CRISPR/Cas9 tool. However, hypoxia increases the proliferation of MEC-1 cells; the miR-155 deficiency overall reduces cell proliferation. The miR-155 deficiency under hypoxia condition was accompanied by a level-up of apoptosis. Besides the common hypoxia-related genes (HIF1α, EGLN1, VHL, HK1, and HK2) we also examined glucose-transporters genes SLC2A1 (GLUT1) and SLC2A3 (GLUT3) by qRT-PCR. The hypoxic, miR-155 deficient MEC-1 cells significantly raised the expression of EGLN1, GLUT3, and GLUT1 genes, which points out possible novel targets of miR-155 in CLL. In addition to this, we detected considerable overexpression of hsa-miR-210-5p, a well-known hypoxamiRNA, in MEC-1 cells in hypoxia. Subsequently, the qRT-PCR and the metabolic assays showed the significant influence of miR-155 on glucose and lactate metabolism. Decreased glucose uptake and increased lactate support our hypothesis that miR-155 deficiency and hypoxia transform leukemic cell metabolism. To conclude, the coupled effect of miR-155 deficiency and hypoxia affects glucose and lactate metabolism that stimulates the expression of GLUT1, GLUT3, and EGLN1 genes in MEC-1 CLL cells. Effective inhibition of key metabolites in the leukemic cells could be one of the novel options in the current treatment of CLL.

Abstract ID: 1551086

Title: Defactinib affects chronic lymphocytic leukemia cell survival with additive effect in combination with BTK inhibitors

Authors: Nayla Mouawad, Guido Capasso, Edoardo Ruggeri, Andrea Visentin, Filippo Severin, Valentina Trimarco, Alessia Tonini, Stefano Pravato, Monica Facco, Federica Frezzato and Livio Trentin

Introduction: The emergence of BTK inhibitors (BTKi) has improved the outcomes of patients with chronic lymphocytic leukemia (CLL). The pioneering bruton tyrosine kinase (BTK) inhibitor, ibrutinib along with the second-generation inhibitors acalabrutinib and zanubrutinib, have displayed remarkable therapeutic efficacy in patients with CLL. Despite the effectiveness of these agents, resistance and severe side effects can arise, resulting in treatment failure, highlighting the need for alternative treatments. Research on molecules involved in the increased survival and drug resistance of leukemic B cells, may unveil novel therapies for a successful outcome in CLL that can be employed clinically alone or in combination with the currently approved BTKi. Focal adhesion kinase (FAK) is a 125 kDa protein, which upon phosphorylation on tyrosine (Y) 397, is activated and can recruit numerous signalling proteins controlling several cellular processes such as adhesion, migration, apoptosis and proliferation, especially in solid tumors. Consequently, several inhibitors have been developed to target FAK phosphorylation at Y397 or its kinase activity. One such inhibitor is defactinib that has demonstrated safety and efficacy in clinical trials for solid tumors. However, limited efforts are made on investigating the effects of defactinib specifically on CLL. Based on this knowledge, we hypothesized that defactinib may exert a significant effect on the survival of CLL cells, and that its combination with BTKi may improve their cytotoxic effects, thereby enhancing their *in vitro* activity.
Methods: B lymphocytes were isolated from eight CLL patients and then were treated with either 5uM of ibrutinib, acalabrutinib, zanubrutinib alone, or in combination with defactinib at a 1:1 ratio. Parallel experiments were performed where these cells were co-cultured with the human bone marrow stromal HS5 cell line, applying the same treatments. After 24 and 48 hours of treatment, apoptosis was evaluated through two methods: PARP cleavage analysis by western

blot and Annexin V/Propidium iodide assay by flow cytometry. The expression level of FAK phosphorylation on Y397 representing its kinase activity, was examined using western blot analysis.

Results: We demonstrated that defactinib alone exhibits greater apoptosis-inducing effects compared to BTKi alone. In particular, when defactinib was combined with BTKi, an increase in PARP cleavage was observed using western blot analysis, indicating that defactinib enhances BTKi activity. This finding was further supported by the Annexin V/Propidium iodide assay, where leukemic B cells exhibited a significant reduction in their viability when co-treated with both agents compared to treatment with either agent alone. Interestingly, the phosphorylation of FAK was not affected by BTKi alone. However, samples treated only with defactinib or in combination with BTKi showed a reduction in FAK phosphorylation. This suggests that the enhanced apoptosis observed in the co-treated conditions is specifically due to the selective inhibition of FAK activation. Furthermore, when CLL B cells were cultured with HS5 stromal cells, which are known to enhance CLL cell survival in vivo, co-treatment of defactinib and BTKi prevented the protective effect of HS5 cells and instead resulted in higher levels of apoptosis. This effect may be attributed to the alteration of FAK in the HS5 cell line upon treatment.

Conclusions: In summary, our findings demonstrate that defactinib, by inhibiting FAK activation, exhibits greater capability as an apoptotic agent compared to BTKi. Moreover, defactinib enhances the cytotoxic effects of BTKi in vitro and counteracts the protective effect of HS5 stromal cells on CLL cell survival. These results highlight FAK as a promising target for developing of novel therapeutic approaches in CLL. Furthermore, the combination of FAK inhibitors with BTKi may enhance their therapeutic efficacy, leading to deeper treatment responses and better outcomes for CLL patients. These findings suggest the potential clinical relevance of targeting FAK and warrant further investigation in clinical settings.

Abstract ID: 1551130

Title: The evolution of treatments and outcome of patients with chronic lymphocytic leukemia treated at Fondazione Policlinico Universitario Agostino Gemelli IRCCS: a monocentric experience of the last 30 years.

Authors: Idanna Innocenti, Alberto Fresa, Annamaria Tomasso, Michela Tarnani, Eugenio Galli, Diana Giannarelli, Francesco Autore and Luca Laurenti

The covalent Bruton's Tyrosine Kinase inhibitors (cBTKi) and B-Cell Lymphoma-2 inhibitor (BCL2i) have changed the treatment approach into the chronic lymphocytic leukemia (CLL) over the last 10 years. This Italian monocentric retrospective observational study describes the treatment patterns and outcomes of patients (pts) with CLL, to better understand the impact of treatment sequencing in the novel targeted-agents era. CLL patients treated between 1992 and 2022 and prospectively registered in the institution's electronic database were included. Time-to-event outcomes were evaluated using Kaplan Meier method. Time to next treatment (TTNT) was defined as time from treatment start to the start of subsequent therapy or death. Time to next treatment failure or death (TTNTF) was defined as time from treatment discontinuation to the discontinuation of subsequent therapy or death. Of 637 registered CLL patients, 318 (49.9%) received treatment (characteristics in Figure). Of 318 treated patients, cBTKi-exposed were 157 (49.4%). Patients BCL2-exposed, but cBTKi-naïve, were 34 (10.7%). Patients who received both a cBTKi and BCL2i +/− antiCD20 (double-exposed) were 26 (8.2%). Seventeen patients (5.3%) received chemoimmunotherapy, cBTKi, and BCL2i. Patients cBTKi- and BCL2i-naïve were 127 (39.9%). Of 157 patients, 77 (49%) received cBKTi frontline, 55 (35%) in second line, 28 (17.8%) after >2 lines of treatment. Need for a subsequent treatment or death after cBTKi therapy was 10.4% ($n=8$) after frontline cBTKi, 41.8% ($n=23$) after second line, 67.9% ($n=19$) after >2 lines of treatment; collectively, it was 30.6% (48/157). Deaths during BTKi were 16 (10.2%). Four patients were retreated with cBTKi. For the 34 BCL2i-exposed cBTKi-naïve patients, BCL2i was administered frontline in 13 (38.2%), in second line in 12 (35.3%), after >2 lines of treatment in 11 (32.3%). Need for a subsequent treatment or

Figure 1. Patients' characteristics and time to next treatment in BTKi-exposed and BCL2i-exposed patients according to the line of treatment.

Patients' characteristic	n=318
Male/Female (%)	201/117 (63.2%/36.8%)
Median age at first treatment (range)	68 years (61-74)
Median time from diagnosis to first treatment (range)	24 months (7-51)
Del17p (%) not available = 39	28/279 (10.0%)
TP53 mut (%) not available = 86	42/232 (18.1%)
IGHV unmutated (%) not available = 63	137/255 (53.7%)
cBTKi-exposed (%)	157 (49.4%)
BCL2i-exposed (%)	60 (18.9%)
BCL2i-exposed cBTKi-naive (%)	34 (10.7%)
cBTKi- and BCL2i-exposed (%)	26 (8.2%)
CIT-, cBTKi- and BCL2i-exposed (%)	17 (5.3%)
cBTKi- and BCL2i- naïve (%)	127 (39.9%)

cBTKi = covalent Bruton's Tyrosine Kinase inhibitors;
BCL2i = B-Cell Lymphoma-2 inhibitor;
CIT = chemoimmunotherapy

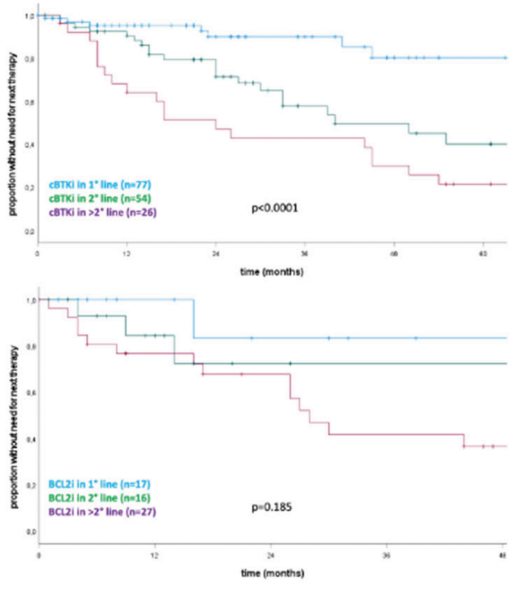

Figure 2. Sankey plot of therapies of the whole cohort, before and after cBTKi/BCL2i.

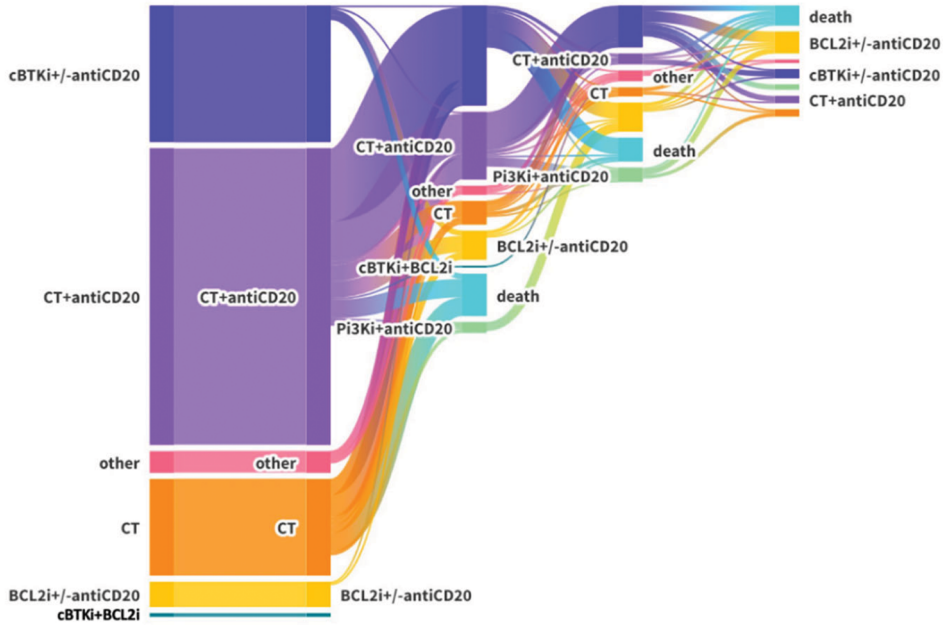

death after BCL2i therapy in this group was 7.7% ($n=1$) after frontline BCL2i, 25% ($n=3$) after second line, 27.3% ($n=3$) after >2 lines of treatment; collectively, it was 17.6% (6/34). Deaths during BTKi were 7 (11.7%). Four patients were retreated with BCL2i. For the 26 double-exposed patients, 96.1% ($n=25$) received BCL2i after cBTKi. Collectively, the need for subsequent treatment or death was 38.5% (10/26). Deaths in double-exposed were 4 (15.4%). Five-year TTNT in cBTKi-exposed patients were 80% (median not reached), 40% (median 40 months), 21% (median 24 months) months in first, second and subsequent lines respectively ($p<0.0001$). Five-year TTNT in BCL2i-exposed patients were 83% (median not reached), 72% (median not reached), 12% (median 28 months) in first, second and subsequent lines respectively ($p=0.185$). Stratifying BCL2i-exposed patients in first line and relapsed/refractory, 5-year TTNT were 83% (median not reached) and 42.5% (median 30 months) ($p=0.089$). Kaplan Meier curves are shown in Figure 1. The treatment sequence of the entire cohort is shown in the Sankey plot in Figure 2. Median TTNTF was 9 months (range 1–87) for all patients who discontinued the cBTKi independently of the line of treatment, and 17 months (range 8–49) for those who discontinued both a cBTKi and BCL2i. Our results were superimposable with previous experiences for patients relapsing after cBTKi, while they were slightly higher in double-exposed patients. Mato et al. reported TTNTF after frontline BTKi 11.3 months and after second line 7.8 months, and our cohort was mostly composed of patients taking cBTKi in first or second line [1]. Eyre et al. reported a median time to progression or death of 9.2 months [2]. TTNTF in double-exposed patients reported by Mato et al. was inferior (5.5 months) compared to our cohort (median TTNTF 17 months) probably for two main reasons: firstly 4 out of 6 patients in this group underwent HSCT for high-risk CLL features or Richter's transformation; secondly patients treated with BCL2i have a shorter observation time because of the later approval in Italy. Nevertheless, these data reinforce the idea that, considering the worsening outcome after multiple targeted agents, patients in the condition to receive treatment urgently need new viable alternatives after current treatments have been exhausted. Despite its limitations, this study shows how anticipating target therapy improved the outcome of CLL patients. Nonetheless, the poor outcomes in advanced lines of therapy also highlight the need for even more effective treatments, especially for younger and high-risk patients.

Abstract ID: 1551150

Title: Single-center study of COVID-19 infection in patients with chronic lymphocytic leukemia

Authors: Huayuan Zhu, Xiao Lu, Tonglu Qiu, Luomengjia Dai, Yeqin Sha, Siqi Qian, Ziyuan Zhou, Yi Miao, Shuchao Qin, Yi Xia, Lei Fan, Wei Xu and Jianyong Li

Objective: To report the vaccination status, oncology treatment, and characteristics of COVID-19 infections in CLL in China.

Methods: The COVID-19 infection of CLL patients attending the Department of Hematology of Jiangsu Provincial People's Hospital since December 2022 was investigated by questionnaire and telephone follow-up, which included basic information, treatment, and characteristics of COVID-19 infection.

Results: A total of 414 CLL patients were followed up in this study, 343 were confirmed with COVID-19 infection during December 2022 to May 2023. Among these patients, median age was 60 years (range 24–87), Of which 18.95% (65/343) were over 70 years old. And with male preponderance (64.43%,221/343). Most patients (93.29%,320/343) were symptomatic at COVID-19 diagnosis. 74.34% (255/343) in mild cases and 25.66% (88/343) in severe cases, and hospital admission was required in all severe cases. More patients were in treatment-free observation period (39.22 vs. 25.00%, $p=0.016$) and received more than one dose of COVID-19 vaccination (41.18 vs. 32.95%, $p=0.173$) in Mild cases as compared to severe cases. In contrast, compared to mild

cases, severe cases have more proportion of patients over than 70 years of age or older(23.86 vs.12.94%, $p=0.015$), with ≥3 comorbidities(9.09 vs.5.49%, $p=0.235$), ≥2 prior CLL treatment (26.14 vs. 17.25%, $p=0.07$), and in the progressive stage of CLL(14.77 vs. 3.92%, $p<0.001$). The proportion of patients with severe cases who had received anti-CD20-based treatments, BTK inhibitors treatments, and Bcl-2 inhibitors treatments within the last 12 months was 29.55% (26/88), 50.00% (44/88), and 14.77% (13/88), respectively, higher than that of patients with mild cases (12.94% [33/255], 45.49% [116/255], and 10.20% [26/255]). (Anti-CD20-based: $p<0.001$; BTKi: $p=0.465$; Bcl-2 inhibitors: $p=0.244$). Similarly, a significantly higher proportion of patients with severe cases had received anti-CD20-based treatments within the last 6 months and within the last 3 months compared to patients with mild cases (Last 6 months:26.14 vs. 9.02%, $p<0.001$; Last 3 months:19.32 vs. 7.06%, $p=0.001$). In addition, 10.23% (9/88) of severe cases were treated at ICU level, of which 44.44% (4/9) died of respiratory failure due to COVID-19 infection.

Conclusions: CLL patients have a low rate of COVID-19 vaccination and a high rate of severe cases. High proportion of severe cases were confirmed in patients with active disease, previous multiple lines of therapy, advanced age, and multiple comorbidities. In addition, anti-CD20-based treatments within the last 12 months may be a risk factor for exacerbating COVID-19 infection.

Abstract ID: 1551157

Title: NOTCH pathway mutation contributes to inferior prognosis in HBV-infected chronic lymphocytic leukemia

Authors: Yue Li, Chunyu Shang, Jiazhu Wu, Jinhua Liang, Li Wang and Wei Xu

Backgrouds: Chronic lymphocytic leukemia (CLL) patients with hepatitis B virus (HBV) infection have a poor prognosis, underlying mechanism remains unclear. NOTCH mutations are frequent in CLL and associated with disease progression and drug resistance. It is also reported to be associated with hepatitis infection in lymphoid malignancies.

Aims: In order to investigate the relation between NOTCH pathway and HBV-associated CLL, we studied 98 previously untreated HBV positive CLL patients and 244 HBV-negative CLL.

Methods: A total of 342 treatment naïve patients diagnosed with CLL at the First Affiliated Hospital of Nanjing Medical University from 01 Jan 2010 to 31 Oct 2021 were enrolled in our study. The mutation hotspots of NOTCH pathway genes were analyzed by Next Generation Sequencing (NGS) of DNA that used PCR for the identification of genomic mutation. Fisher exact and χ^2 tests were used to assess the correlation between HBV infection and clinical, demographic factors in CLL patients. Survival curves were generated by Graphpad 9.5.

Results: NOTCH mutations were more frequent in HBV positive CLL subgroup (17.3 vs. 7.4%, $p=0.033$). By survival analysis, HBV infection was associated with disease progression and poor survival [$p=0.0099$ for overall survival (OS) and $p=0.0446$ for time-to-treatment (TTT)]. Any lesions of the NOTCH pathway (NOTCH1, NOTCH2 and SPEN) aggravated prognosis. In multivariate analysis, NOTCH mutation retained an independent significance for HBV-infected patients ($p=0.016$ for OS and $p=0.023$ for TTT). However, HBV positive with NOTCH unmutated had no statistical difference in prognosis compared with HBV negative patients ($p=0.1706$ for OS and $p=0.2387$ for TTT), which indicated that NOTCH pathway mutation contributed to inferior prognosis in HBV-infected CLL.

Summary: In conclusion, a cohort of CLL patients with HBV positive displayed a worse clinical outcome and the status of NOTCH signaling pathway might play a crucial role.

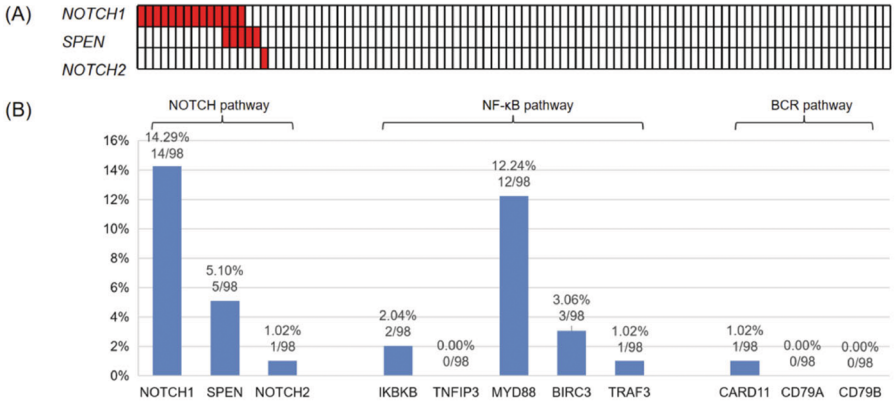

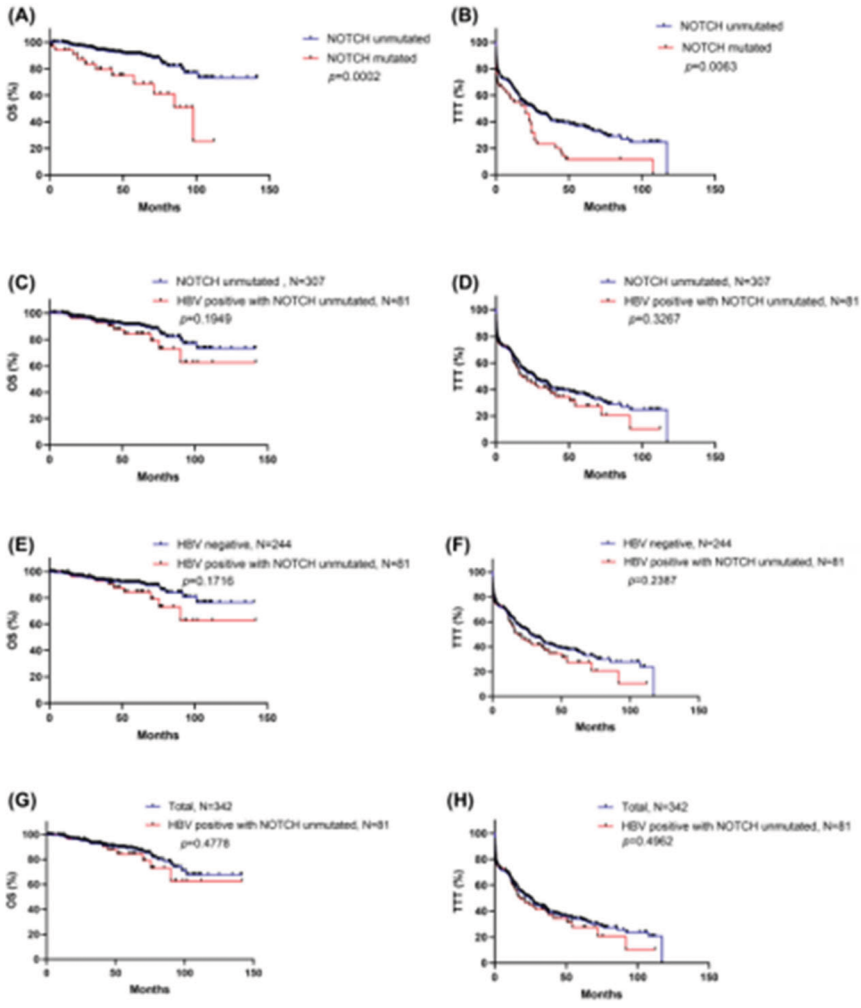

Abstract ID: 1551206

Title: Incidence and clinical correlates of non-immune cytopenia at diagnosis of chronic lymphocytic leukemia

Authors: Nil Albiol, Miguel Arguello-Tomas, Paola Jara, Josep Nomdedéu, Esther Moga, Alba Mora, Jordi Sierra and Carol Moreno

Introduction: Cytopenias due to bone marrow infiltration define Rai stages III–IV and Binet C in chronic lymphocytic leukemia (CLL) and are usually associated with poor outcomes and, consequently, the need for therapy. We aimed at ascertaining the incidence of cytopenia in a large series of unselected patients with CLL, its origin, clinical correlates, and outcome.

Methods: In our single-center database of 781 patients with CLL diagnosed between 1979 and 2022, we identified those who presented with anemia (Hb <11 g/dL) and/or thrombocytopenia (platelets under 100×109/L) at diagnosis. The main aims were to describe their prevalence, clinical and biological characteristics, as well as their impact on progression-free survival (PFS) and overall survival (OS).

Results: Patient characteristics and incidence Among 781 patients with CLL we identified 81 with anemia and/or

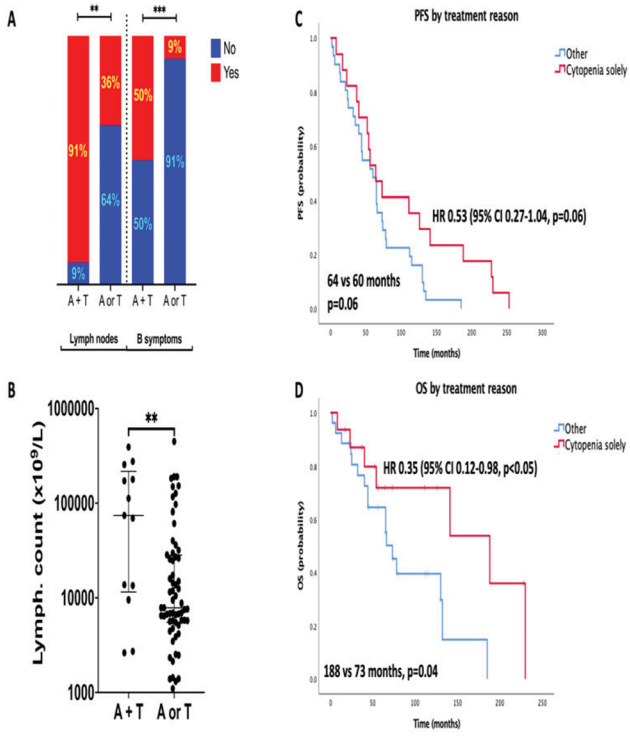

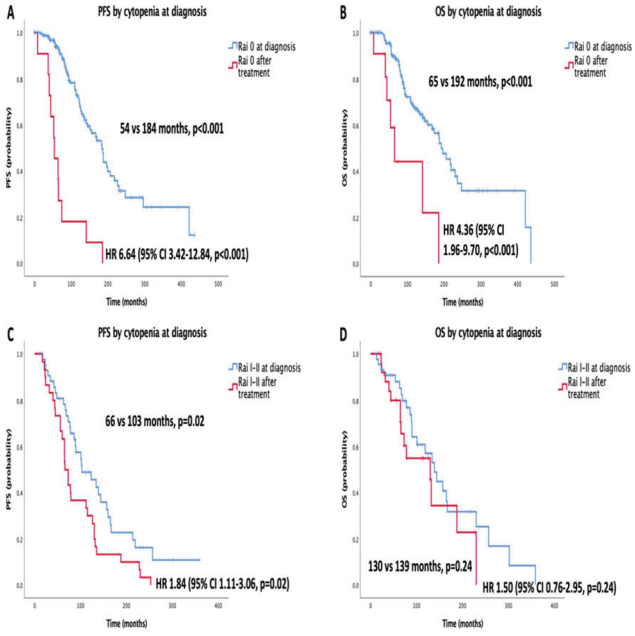

thrombocytopenia at diagnosis (10.3%): forty-three (5.5%) had only anemia, 22 (2.8%) only thrombocytopenia, and 16 (2%) both anemia and thrombocytopenia. All cases were due to bone marrow infiltration but seven: five had autoimmune hemolytic anemia (AIHA) and two immune thrombocytopenia (ITP). These latter cases were not included in the survival analysis. The median follow-up was 53 months (range, 0–275). The median age of the patients was 73 years. Patients who presented both anemia and thrombocytopenia were younger than those with either anemia or thrombocytopenia (median age 58 vs. 75 years, $p=0.04$), had a higher incidence of lymphadenopathy (91 vs. 36%, $p<0.01$), presented B symptoms more frequently (50 vs 9%, $p<0.001$), and had a higher median lymphocyte count (75.000 vs 7.925×106/L, $p<0.01$), see Figure 1(A,B). Prognosis The 74 patients with non-immune cytopenia at diagnosis were analyzed for survival data. Patients with both anemia and thrombocytopenia presented a shorter time to first treatment –TTFT- [median 0 months (95% CI 0–2 months)] when compared to patients with only anemia [median 3 months (95% CI 0–10 months)] or thrombocytopenia [median 10 (95% CI 0–30 months)], $p<0.001$. However, no differences were observed in PFS or OS. Overall, 49 of 74 patients received upfront treatment. The patients in which cytopenia was the only treatment criterion ($n=17$) presented a longer PFS and OS compared to those with more than one criterion to start therapy ($n=32$): median PFS, 64 vs. 60 months ($p=0.06$); median OS, 188 vs 73 months, $p=0.04$ (Figure 1(C,D)). After initial treatment, 13 patients dropped from Rai III–IV to Rai 0, and 36 from Rai III–IV to Rai I–II. In an exploratory analysis, we compared the survival of the patients who shifted to Rai 0 to another cohort of patients with CLL from our database who presented Rai 0 stage at diagnosis and required treatment ($n=170$). The analysis showed a shorter PFS (median 54 vs. 184 months, $p<0.001$) and OS (median 65 vs. 192 months, $p<0.001$) for the patients who had cytopenia at diagnosis that was resolved after therapy (downstaged to Rai 0) versus those who had Rai 0 at diagnosis (Figure 2(A,B)). Similarly, patients who dropped to Rai I–II were compared with patients Rai I–II at diagnosis ($n=45$). Patients downstaged to Rai I–II presented a shorter PFS (median 66 vs. 103 months, $p=0.02$) with no differences in OS (Figure 2(C,D)).

Conclusions: In our single-center series of 781 patients with CLL, around 10% presented with any non-immune cytopenia at the time of diagnosis (53% only had anemia, 28% only thrombocytopenia, and 19% both). While some patients with isolated non-immune thrombocytopenia could be closely followed without requiring upfront treatment (most likely because of the variety of mechanisms accounting for thrombocytopenia), those who have anemia or both cytopenia at diagnosis usually require immediate treatment (median TTFT 0 months). However, no differences were observed in PFS or OS. Importantly, patients with CLL with cytopenia at diagnosis had an adverse prognosis even if the cytopenia resolved upon initial therapy, a concept that warrants further consideration because of its implication when planning the treatment strategy.

Abstract ID: 1551210

Title: Prolonged treatment with ibrutinib modulates phenotypic and functional features of immune cell compartments in chronic lymphocytic leukemia

Authors: Valentina Griggio, Rebecca Jones, Francesca Perutelli, Candida Vitale, Francesca Romana Mauro, Chiara Salvetti, Elia Boccellato, Lorenzo Comba, Daniela Pietrasanta, Iolanda Donatella Vincelli, Paolo Ghia, Giovanni Del Poeta, Gianluca Gaidano, Valter Gattei, Robin Foà and Marta Coscia

Introduction: CLL is characterized by a wide range of immune alterations, responsible for the increased susceptibility to infections, the occurrence of autoimmunity and the failure to control disease progression. Besides its direct anti-tumor activity, ibrutinib has shown to exert immunomodulatory effects. The aim of this study was to analyze immune changes occurring in CLL patients treated with ibrutinib.
Materials and methods: Thirty-one patients with progressive CLL and the indication to start ibrutinib therapy were included. Peripheral blood samples were collected before and after 1, 6, 12 and 24 months of ibrutinib treatment. Fifteen additional patients with early-phase disease (ES-CLL) and 10 healthy donors (HD) were analyzed. Immune cell counts, the expression of surface markers and functional assays were performed by flow cytometry. Clinical response was assessed according to the IWCLL guidelines.
Results and discussion: At the 6-month timepoint, we observed a significantly lower value in the number of CLL cells, which persisted after 12 and 24 months of ibrutinib treatment. We detected a significant reduction of CD3+ and CD4+ T-cell counts at month 12, and a decrease of CD8+ T-cell number already at month 6 of therapy. Regarding γδ T-cell compartment, the count of Vδ1 T cells – but not Vγ9Vδ2 T cells – significantly decreased by 12 months of treatment. A prolonged (i.e. 24-month) therapy with ibrutinib also favored the normalization of Tregs, NK and NKT-cell counts. Before treatment, we found a higher expression of the activation marker CD69 on T cells from pre-treatment compared to ES-CLL and HD, which normalized after 6 months of therapy. Phenotypic analysis revealed that PD-1 expression on CD8+ T cells was significantly lowered by 6 and 12 months of ibrutinib treatment. Ibrutinib also induced a significant downmodulation of other inhibitory checkpoints expressed on T cells: CTLA-4, CD96, Tim-3 and TIGIT. Of

note, TIGIT expression was reduced on Tregs at 12 months of therapy. Similar to T cells, CD69, CD96, TIGIT and Tim-3 were significantly decreased overtime by ibrutinib therapy on NK and NKT cells. Functional data showed that, besides a positive phenotypic modulation, 12 months of ibrutinib treatment enhanced Vγ9Vδ2 T-cell cytotoxicity and NK-cell-mediated ADCC of obinutuzumab towards MEC-1 cell line. An improvement in the proliferation of both CD4+ and CD8+ T cells was also detected at month 24. The correlation of phenotypic changes with clinical response at 12 months demonstrated that the positive immunomodulatory effects of ibrutinib were mainly observed in patients achieving a partial ($n=21$) or complete ($n=2$) response and not in patients with a stable disease ($n=8$).

Conclusions: Our results show that ibrutinib exerts a wide range of immune-modulating effects, which are mainly associated with the achievement of a clinical response to therapy.

Abstract ID: 1551335

Title: Vertebral fractures in patients with B-cell chronic lymphocytic leukemia before and after ibrutinib treatment

Authors: Vlatka Pandzic Jaksic, Ena Soric, Jelena Andric, Jelena Jaksic, Renata Huzjan Korunic, Zdravko Mitrovic and Ozren Jaksic

In population-based analysis before the era of targeted agents B-cell chronic lymphocytic leukemia (B-CLL) has been associated with increased risk of vertebral and axial fractures. This fracture risk may be due to intrinsic factors of the disease but also to the treatment with steroids or chemotherapy. The direct impact of novel targeted agents on bone fragility in these patients has not been recognized yet. Previous experimental studies suggested that ibrutinib may inhibit osteoclast differentiation and function so it was supposed that it might be used in the treatment of osteoclast-related diseases, such as osteoporosis and rheumatoid arthritis. However, recent retrospective studies found a higher incidence of vertebral fractures in patients treated with ibrutinib. In order to evaluate incidence of fractures in relation to ibrutinib treatment we designed a retrospective study. All B-CLL patients treated with ibrutinib in our center were evaluated. We included patients with CT scan immediately before the introduction of ibrutinib in the pretreatment work-up and with follow-up CT scan that was done for the evaluation of response. Total of 57 patients out of 97 met the criteria for inclusion in this study. In our group, there were 35 males and 22 females. Median age at diagnosis was 64.5 years (range 46–84 years), median age at ibrutinib start was 71 years (range 53–86 years), while median duration of B-CLL before ibrutinib was 5.5 years (0–16 years). Ibrutinib was first line treatment in 16 patients (28.1%) while 41 (71.9%) were previously treated. Total of 35 patients received glucocorticoids (18 as a part of therapeutic protocols, 17 as premedication with anti-CD20 antibody). There were 24 patients with Rai III/IV or Binet C clinical stage, while 23 patients had lymphoma like tumor distribution (TD), median total tumor mass (TTM) was 11.28. Patients were followed for 344.9 patient-years from diagnosis. On pre-treatment CT scan 7 patients had at least one vertebral fracture (range 1–3) while 50 patients had no vertebral fractures. None of patients with fractures had them detected by the time of diagnosis thus making incidence rate up to 0.02 per patient-year (95% CI 0.01–0.043). All

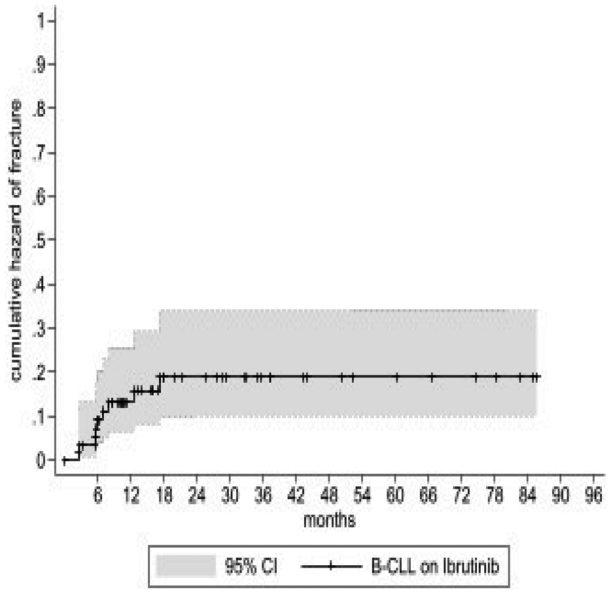

patients in this cohort had CT for evaluation of response and these patients were followed for 132.6 patient years while on ibrutinib. Total of 9 patients had new vertebral fractures (6 with no previous fractures and 3 with new additional fractures) making incidence rate at least 0.068 per patient year (95% CI 0.035–0.13). This is significantly higher than before ibrutinib treatment ($p<0.05$). Since all new fractures were detected in the initial 1.5 years of ibrutinib treatment, incidence rate was calculated at first 6, 12 and 18 months and compared to pretreatment incidence rate. The highest incidence rate was observed in the first 6 months with incidence rate ratio compared to pre-ibrutinib of 8.95 (95% CI 2.24–32.75). Patients on ibrutinib were also evaluated for the presence of standard fracture risk factors including previous steroid use and other fractures, sex, secondary causes of osteoporosis, smoking and alcohol use. Bone mineral density measurement was mostly not available as it was usually not performed before ibrutinib therapy. Only female sex was significantly associated with early vertebral fractures ($p<0.05$). We also evaluated factors associated with B-CLL. We compared previous treatments, stages, lymphocytosis, lymph nodes and spleen size, bone marrow infiltration, TTM and TD, as well as response to therapy with special emphasis on marrow changes and redistribution of tumor mass. None of these factors were found to be related except a trend for lower pretreatment hemoglobin in patients who developed new fractures after ibrutinib initiation. In conclusion, until recently ibrutinib has not been regarded as a drug that could significantly impair bone health, but latest observations recorded signals of a possible increase of fractures associated with ibrutinib therapy. Although we cannot establish a causal relationship, the occurrence of multiple osteoporotic vertebral fractures shortly after the initiation of the ibrutinib suggests that this drug might play a role in bone fragility and requires further analysis with prospective studies.

Abstract ID: 1551414

Title: Fatty acid metabolism fingerprints predict prognosis and regulate immunophenotype in chronic lymphocytic leukemia

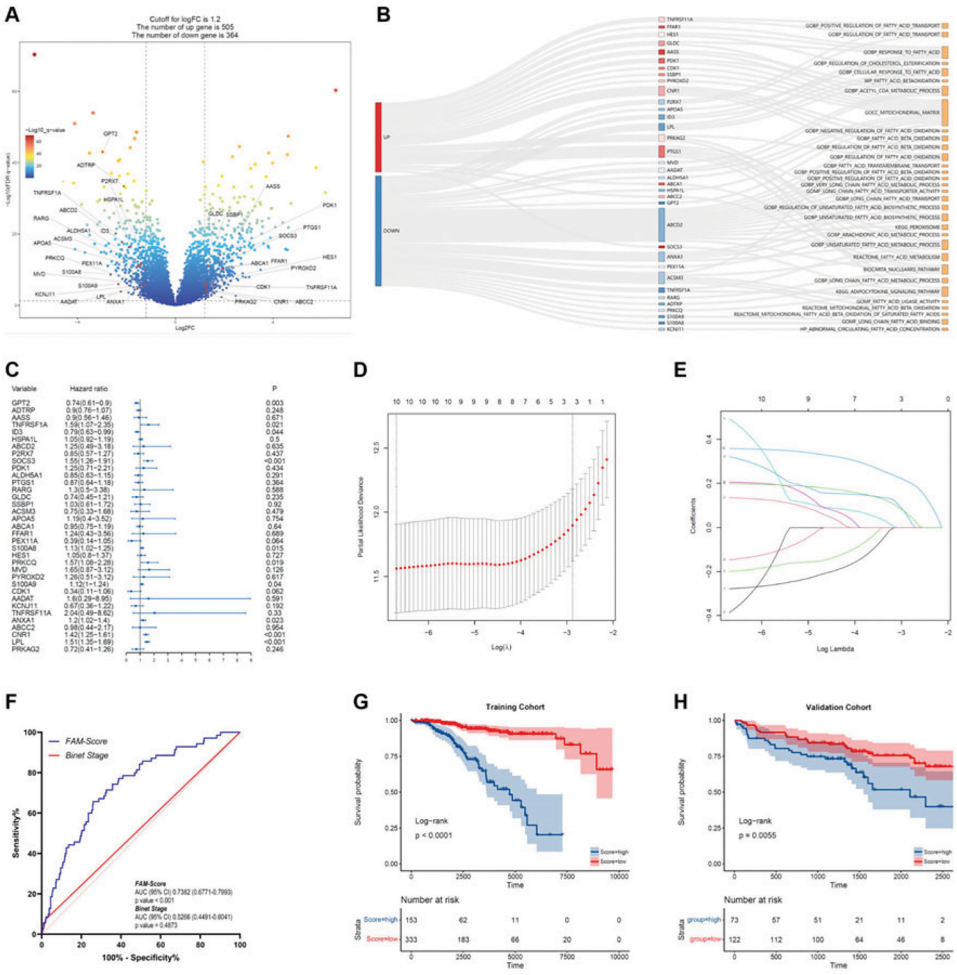

Authors: Ya Zhang, Yang Zhang, Xinting Hu, Zheng Tian, Hua Wang, Xin Zhang and Xin Wang

Introduction: Fatty acid is an essential source of energy for tumor cells during chronic lymphocytic leukemia (CLL) progression. CLL is characterized by immune dysfunction and potentially reprogrammed by fatty acid metabolism (FAM). However, it is currently unclear how FAM regulates immune function in CLL. Hence, the aim of the present study was to determine FAM characteristics, develop FAM associated prognostic score, and investigate the mechanism of CLL immune regulation by FAM.

Methods: In this study, 3 RNA sequencing dataset with a total of 870 CLL patients and 32 healthy donors. The FAM-related geneset was obtained from the Molecular Signatures Database. The risk score based on FAM-related genes was constructed in the training cohort of 487 CLL patients by Cox-LASSO regression analyses and validated in the independent cohort of 195 CLL patients. Moreover, the immune infiltrates in CLL patients were assessed in the training cohort. The single-cell RNA sequencing datasets were accessed from a male CLL patient aged 40 with IGHV mutated status. Then the reciprocal molecules of the FAM-related genes were identified. Functional enrichment analysis was performed using the Gene Ontology (GO) database.

Results: The present study identified 864 DEGs between CLL patients and healthy donors, of which 35 genes were related to FAM (|logFC >1.2|, $p<0.05$; Figure 1(A,B)). Through Cox-LASSO regression analysis, 3 genes (LPL, SOCS3, CNR1) with independent prognostic significance were selected to construct the FAM associated risk score named FAM-Score (Figure 1(C–E)). The ROC analysis showed better specificity and sensitivity of FAM-Score (AUC =0.738, $p<0.001$) than Binet stage (AUC =0.527, $p=0.487$; Figure 1(F)). The Kaplan–Meier curves suggested a significant association between high-risk subgroup and undesirable overall survival in CLL patients ($p<0.001$; Figure 1(G)). Consistent with these results, the overall survival of high-risk subgroup decreased significantly in the independent validation cohort ($p=0.006$; Figure 1(H)). Comparison of risk scores of CLL patients with different clinical characteristics revealed that the high-risk subgroup was significantly associated with IGHV unmutated status, advanced Binet stage, and disease progression. To further investigate the role of the FAM-Score in CLL immune microenvironment, the immune infiltrates between two subgroups were quantified as abundance of 22 immune cell types for comparison. The results showed significant differences in T cells, NK cells, and macrophages, suggesting the impact of FAM on CLL immunophenotype (Figure 2(A)). In an attempt to further explore the role of FAM in CLL immune regulation, the expression characteristics of LPL, SOCS3, and CNR1 at the single-cell level were analyzed in CLL patient samples before and after ibrutinib treatment. The UMAP profiles revealed the cell subpopulation specificity in the expression of key genes in CLL: LPL and CNR1 were mainly expressed in B and NK cells, while SOCS3 tended to be more expressed in T cells (Figure 2(B–E)), suggesting that FAM potentially induces differences between immune cell

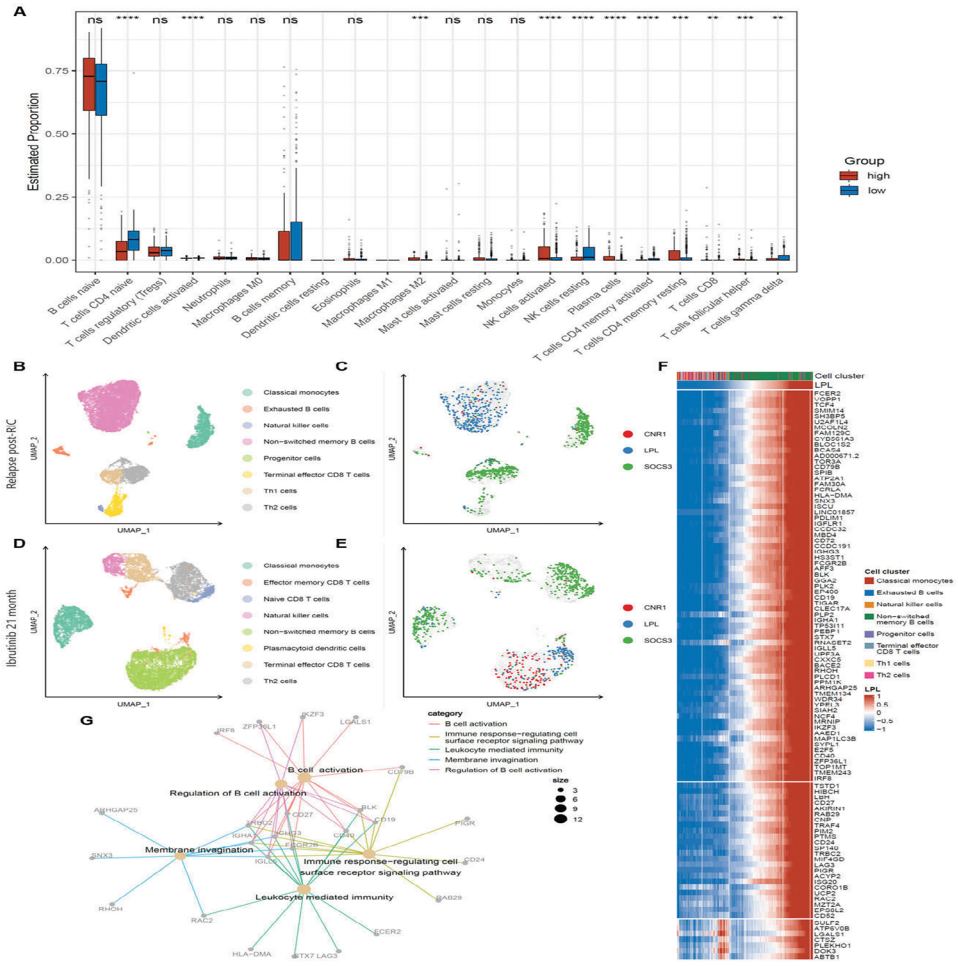

types. To investigate the mechanism of FAM-induced differences of CLL immunophenotype, the reciprocal molecules of the key genes were identified. The top 100 reciprocal genes of LPL were shown in Figure 2(F). Finally, the results of functional analysis demonstrated that LPL drives CLL genesis and progression potentially through mediating B-cell activation and cell surface receptor expression pathways (Figure 2(G)).

Conclusions: The present study identified a novel prognosis risk score based on FAM associated genes and revealed the immunophenotypic differences in CLL related to FAM-Score. The function of LPL in immune response pathways demonstrates that FAM is an integral part of CLL immune regulation. Though the underlying mechanisms of fatty acid metabolic reprogramming to modulate CLL immunophenotype remain to be elucidated, FAM constitute promising targets to augment the efficacy of immunotherapy against CLL.

Abstract ID: 1551459

Title: Long-term follow-up of multicenter phase II trial of zanubrutinib, obinutuzumab, and venetoclax (BOVen) in previously untreated patients with chronic lymphocytic leukemia: impact of early MRD kinetics on posttreatment outcomes

Authors: Jacob Soumerai, Ahmet Dogan, Venkatraman Seshan, Kelsey Flaherty, Jason Carter, Ephraim Hochberg, Jeffrey Barnes, Jeremy Abramson, Audrey Hamilton, Ariela Noy, Colette Owens, M. Lia Palomba, Anita Kumar, Lindsey Roeker, Meghan Thompson, Ronald Takvorian, Zachary Epstein-Peterson, Mark Geyer, Walter Ramos-Amador, Neena Mahajan, Rosalba Martignetti, Sean Plummer, Joanna Mi, Julia Lynch, Brianne McGree, Maryanne Sherburne, Emily Patterson, Natalie Slupe, Maria Chabowska, Alyssa Labarre, Morgan Choma, Grace McCambridge, Hailey Kelly, Mary Devlin, Madeline Puccio, Rayna Garcia, Clare Grieve, Aileen Cohen, Juliana Biondo, Allison Jacob, Omar Abdel-Wahab and Andrew Zelenetz

Background: Venetoclax plus obinutuzumab induces durable undetectable MRD (median time from end-of-therapy (EOT) to MRD conversion $\geq 10^{-4}$ of 21 months) in previously untreated CLL [1] and zanubrutinib is a second-generation BTK inhibitor with a favorable safety profile and superior progression-free survival compared with ibrutinib [2]. BOVen appeared well-tolerated and achieved frequent uMRD in CLL [3]. However, longer follow-up was needed to evaluate the MRD-driven treatment strategy. Herein, we present the initial report on long-term follow-up of BOVen in CLL.

Methods: In this multicenter, phase 2 trial (NCT03824483), eligible patients had CLL/SLL requiring first-line treatment per

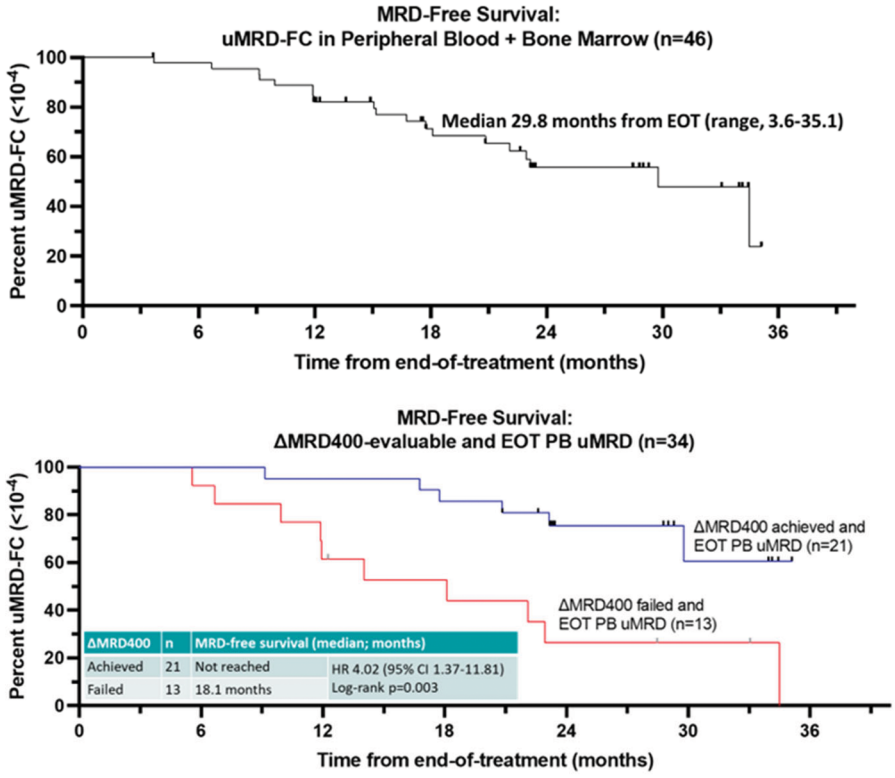

iwCLL 2018 guidelines, ECOG performance status ≤2, absolute neutrophil count (ANC) ≥ 1,000/ul and platelet (PLT) count ≥75,000/ul (PLT ≥20,000 and no ANC requirement if due to CLL). Informed consent was obtained from all patients. BOVen was administered in 28-day cycles: Zanubrutinib 160 mg by mouth (PO) twice daily starting D1; Obinutuzumab was administered at 1000 mg intravenously (IV) on days 1 (split days 1–2 if lymphocyte count ≥25,000/ul or LN ≥5 centimeters), 8, and 15 of cycle 1, and day 1 of cycles 2-8; Venetoclax ramp up was initiated on cycle 3 day 1 (target 400 mg PO daily). MRD was evaluated by flow cytometry (MRD-FC) with uMRD defined as $\leq 10^{-4}$ for the primary endpoint. ΔMRD400 was evaluated by immunosequencing in 35 of the first 39 patients enrolled (pending in final 13 pending) and defined as ≥400-fold reduction in the peripheral blood (PB) MRD level from baseline to cycle 5 day 1. Treatment consisted of 8-24 cycles with duration determined by prespecified MRD-FC criteria. Beginning on cycle 7 day 1 then every 2 cycles, patients with PB uMRD-FC underwent bone marrow (BM) within 14 days. If BM uMRD-FC was confirmed, PB MRD-FC was repeated after 2 additional cycles. Patients with confirmed uMRD-FC in both PB and BM discontinued therapy. All-cause adverse events (AE) were assessed per CTCAE v5. Median time to MRD-FC conversion ($\geq 10^{-4}$) was calculated from EOT (Kaplan–Meier method).

Results: The study accrued 52 pts (3/19–10/19; 7/20–4/21): median age 62 (range, 23–77), 75% (39/52) male, 71% (37/52) IGHV unmutated, 17% (9/52) del17p/TP53M. All patients are evaluable for safety and 50 are evaluable for efficacy. With median follow up of 40 months (4.1–47.4) and treatment duration of 10 cycles (interquartile range [IQR] 8–14), 96% (48/50) were uMRD-FC in PB, and 92% (46/50) were uMRD in PB and BM after a median of 8 months (IQR 6–11.5). The most common AEs were thrombocytopenia (55.8%), fatigue (55.8%), neutropenia (53.8%), diarrhea (46.2%), bruising (44.2%), infusion related reaction (36.5%). The most common grade ≥3 AE were neutropenia (23.1%), thrombocytopenia (7.7%), lung infection (5.8%). No laboratory or clinical TLS occurred (Howard criteria). Of 46 patients meeting MRD-FC criteria to end treatment, MRD-FC free survival was 29.8 months (3.6–35.1; Figure 1). Of patients with EOT PB uMRD-FC who were evaluable for ΔMRD400, MRD-FC free survival was longer in ΔMRD400 achievers (NR vs. 18.1 mo, log-rank $p = 0.003$; Figure 2) despite fewer median cycles of therapy (8 vs. 13, $p < 0.001$).

Conclusion: Long-term follow up of BOVen demonstrate high rates of durable uMRD-FC. A phase II trial of BOVen with ΔMRD400-directed treatment duration is planned, and we hypothesize that longer duration of therapy for pts who fail ΔMRD400 (24 vs. 10 mo) will further improve uMRD duration in these pts.

Abstract ID: 1551462

Title: Performance of a novel 8-color flow cytometry panel in the detection of minimal residual disease assessment of chronic lymphocytic leukemia

Authors: Yujie Wu, Xiao Chen, Sishu Zhao, Yu Shi, Ninghan Zhang, Zhen Guo, Chun Qiao, Huimin Jin, Liying Zhu, Huayuan Zhu and Jianyong Li

Background: The status of minimal residual disease (MRD) has been established as an important prognostic indicator in chronic lymphocytic leukemia (CLL).

Methods: Owing to the requirements of high accuracy, reproducibility and comparability of MRD, this study investigated the performance of a flow cytometric approach (CD45-ROR1 panel) in the MRD detection of CLL patients, with European Research Initiative on CLL (ERIC) 8-color panel as the 'gold standard'.

Results: The sensitivity, specificity and concordance rate of CD45-ROR1 panel in the MRD assessment of CLL were 100% (87/87), 88.5% (23/26) and 97.3% (110/113), respectively. Two of the 3 non-consistent samples were further verified by the next-generation sequencing. In addition, the MRD results obtained from the CD45-ROR1 panel were positively associated with ERIC 8-color results for MRD assessment ($R=0.98$, $p<0.0001$). MRD detection at low levels (≤1.0%) demonstrated a smaller difference between the two methods (bias, −0.11; 95% CI, −0.90–0.68) as compared with that at high levels (0.1%). For the reproducibility assessment, the bias was smaller at three datapoints in the CD45-ROR1 panel as compared with that of ERIC 8-color panel. Moreover, MRD level detected using the CD45-ROR1 panel for the same samples between different laboratories showed a strong statistical correlation ($R=0.99$, $p<0.0001$) with a trivial inter-laboratory variation (bias, 0.135; 95% CI, −0.439–0.709). Interesingly, the MRD level detected in the lymph nodes samples were significantly higher than that of the peripheral blood and bone marrow samples ($p=0.029$).
Conclusions: Collectively, this study demonstrates that the CD45-ROR1 panel is a reliable method for the MRD assessment of CLL, with high sensitivity, reproducibility, and reliability.

Abstract ID: 1551488

Title: A Phase II study of intermittent duvelisib dosing in patients with chronic lymphocytic leukemia/small lymphocytic lymphoma (CLL/SLL)

Authors: Geoffrey Shouse, Lu Chen, Tanya Siddiqi, Alex Muir, Jennifer Brown, Stephen Spurgeon and Alexey Danilov

Background: Targeting phosphatidylinositol 3-kinase (PI3K) has emerged as an efficacious approach for treatment of chronic lymphocytic leukemia (CLL) and non-Hodgkin lymphoma (NHL). However, toxicities of the PI3K inhibitors are an important concern limiting their use. Duvelisib is a potent oral inhibitor of both the PI3K-δ and PI3K-γ isoforms with proven efficacy in CLL/SLL. Here we report the results of a phase 2 study evaluating efficacy and safety of duvelisib with intermittent dosing in patients with relapsed/refractory CLL/SLL
Methods: This open-label, single arm, phase 2 study enrolled patients with CLL/SLL treated with at least 1 prior line of therapy with active disease as defined by the iWCLL 2008 criteria. Duvelisib was given at a dose of 25 mg PO BID for 28-day cycles for a total of 12 weeks during the induction phase, followed by 75 mg PO BID 2 days on and 5 days off for repeated 28-day cycles during the maintenance phase until death, intolerance or disease progression. The primary endpoint was progression free survival (PFS) at 12 months; secondary endpoints were safety and clinical benefit. The trial was originally planned to enroll 27 patients but was stopped early due to difficulties with enrollment following changing FDA guidance for the use of PI3K inhibitors.
Results: Fifteen patients were enrolled. Median age was 74 (59–82) years, 8/15 (53%) were female; patients were primarily Caucasian (13/15; 87%); performance status was 0–1, with 27% (4/15) ECOG 0 and 73% (11/15) ECOG 1. This was a heavily pre-treated patient population with a median of 3 prior lines of therapy (1–6). Among patients where results were available, 79% (11/14) had abnormal FISH results including 36% with TP53 gene loss, 27% del(13q), and 18% del(11q). Sixty-seven percent (8/12) had unmutated IGHV. Of the 15 patients treated, 4 were not evaluable for efficacy due to coming off study early for toxicity (2), development of MDS unrelated to study drug (1) or death due to complications from COVID-19 infection (1). Among the 11 efficacy-evaluable patients, 82% achieved PR, and 18% had stable disease. The 12-month PFS was 43% (95%CI: 18–66%) and the median PFS was 9.9 months (95% CI: 5.5–NA). Among the 9 responders, the median duration of response (DOR) was 5.3 months (95%CI: 1.9–NA) and 12-month DOR was 22% (95%CI:3–51%). Five patients (33%) discontinued therapy due to adverse events, which occurred during the induction phase in 4/5 of the patients. Five patients (33%) discontinued due to progressive disease – all during the maintenance phase of treatment. Additionally, 2 patients discontinued due to MD decision; one patient developed

Figure 1. PFS among all patients (n=15). Median PFS: 9.9 months (95% CI: 5.5-NA). 12-month PFS: 43% (95% CI: 18%-66%).

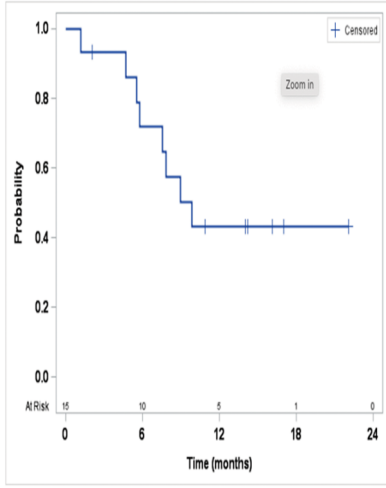

Table 1. Adverse events of all grade (>10% frequency) and grade 3-4, considered at least possibly related to duvelisib.

Adverse Event	N (%)
All Grades	
Fatigue	5 (33%)
Leukocytosis	4 (27%)
Vomiting	4 (27%)
ALT increased	4 (27%)
AST increased	4 (27%)
Diarrhea	4 (27%)
Alkaline phosphatase increased	4 (27%)
Lymphocyte count increased	3 (20%)
Nausea	3 (20%)
Abdominal pain	3 (20%)
Platelet count decreased	3 (20%)
Chills	2 (13%)
Blood bilirubin increased	2 (13%)
Neutrophil count decreased	2 (13%)
Colitis	2 (13%)
Mucositis oral	2 (13%)
Hypertension	2 (13%)
Arthralgia	2 (13%)
Rash maculopapular	2 (13%)
Grade 3-4	
Leukocytosis	3 (20%)
Alanine aminotransferase increased	2 (13%)
Aspartate aminotransferase increased	2 (13%)
Colitis	2 (13%)
Mucositis Oral	2 (13%)
Heart Failure	1 (7%)
Lymphocyte count increased	1 (7%)
Anemia	1 (7%)
Neutrophil count decreased	1 (7%)
Febrile neutropenia	1 (7%)
Thrombotic thrombocytopenic purpura	1 (7%)
Abdominal pain	1 (7%)
Diarrhea	1 (7%)
Nausea	1 (7%)
Vomiting	1 (7%)
Platelet count decreased	1 (7%)
Pancreatitis	1 (7%)
Alkaline phosphatase increased	1 (7%)

MDS which was unrelated to duvelisib; one patient died during treatment due to complications from COVID-19. Treatment was generally well tolerated with the most common grade 3 or higher adverse events being leukocytosis (20%), alanine aminotransferase (ALT) increase (13%), aspartate aminotransferase (AST) increase (13%), oral mucositis (13%) and colitis (13%). The adverse events leading to treatment discontinuation occurred primarily during induction. The most common adverse events of any grade included fatigue in 5 patients (33%), leukocytosis, vomiting, ALT increase, AST increase, diarrhea, and elevation of alkaline phosphatase, which occurred in 4 patients each (27%).

Conclusions: We report the results of an open-label, phase 2 study utilizing a continuous dosing induction phase followed by an intermittent dosing maintenance phase of the PI3K inhibitor duvelisib in patients with relapsed/refractory CLL/SLL. Patients who received duvelisib on an intermittent schedule achieved some clinical benefit, however, the desired 12-month PFS goal of 50% was not reached. Adverse events in general were manageable and mainly related to gastrointestinal and liver toxicity, and patient died during treatment from complications from COVID-19 pneumonia. After an initial 12 weeks of continuous duvelisib treatment, the incorporation of intermittent dosing appears to be a viable option for patients with previously treated CLL/SLL.

Abstract ID: 1551541

Title: Chemokine receptor and adhesion molecule profile on B-cell chronic lymphocytic leukemia (B-CLL) lymphocytes in different lymphoid compartments and changes during BTK inhibitor therapy

Authors: Marija Ivic, Branimir Gizdic, Ena Soric, Anamarija Vrkljan, Ozana Jaksic, Zdravko Mitrovic, Vlatko Pejsa and Ozren Jaksic

B-cell chronic lymphocytic leukemia (B-CLL) is a lymphoproliferative disorder characterized by circulation of B lymphocytes between bone marrow, peripheral blood, and lymphoid organs. Homing, proliferation, and apoptosis of lymphocytes is a consequence of the interaction with tumor microenvironment. Bruton's tyrosine kinase (BTK) inhibitors (ibrutinib, acalabrutinib, etc.) in addition to inhibition B-cell receptor signaling also significantly influence interactions with the microenvironment. Along reduction of tumor mass ibrutinib may induce a significant redistribution of B lymphocytes from lymphoid organs to the peripheral blood. We have designed the study to evaluate relationship of chemokine receptor and adhesion molecules profile on B-CLL lymphocytes in different lymphoid compartments with tumor mass distribution and redistribution in B-CLL patients treated with BTK inhibitors. Patients with B-CLL who started BTK inhibitor monotherapy (ibrutinib or acalabrutinib) were included in this prospective, longitudinal, observational study. Both untreated and previously treated patients were included. Patients receiving other active agents for CLL (steroids, anti-CD20 antibodies, bcl2 antagonist or chemotherapy) or other malignancy were excluded from the study. Patients were followed for six months after BTK inhibitor treatment start. Time points are the beginning of the treatment, the third and the sixth month after start of BTK inhibitor treatment. Methods include complete blood count, computed tomography (CT) of the neck, the thorax, the abdomen and the pelvis and flow cytometry with determination of expression levels of CXCR3, CXCR4, CXCR5, CCR7, CD38 and CD49d on malignant CD5+/CD19+ lymphocytes from peripheral blood (PB), bone marrow (BM) and lymph nodes (LN) at the start and from peripheral blood during follow-up. We have evaluated 25 patients (10 female, 15 male) who completed follow-up, median age was 73 years. Ibrutinib have received 20 patients and acalabrutinib 5 patients. Median TTM at the beginning of treatment was 10.4 and at the end of six month of treatment 4.0. Median of TD at the beginning of the treatment was 0.62 and 1 at the end of sixth months of treatment. Redistribution lymphocytosis during first 6 months was observed in 76% patients. Profile of CXCR4 showed higher expression in PB compared to BM and LN contrary to CXCR3, CCR7 and CD38 showing higher expression in LN ($p<0.05$). CXCR5 showed lower expression in LN ($p<0.05$). There was no significant difference between compartments for CD49d. There were changes in expression pattern of analyzed molecules (higher CXCR4 and lower CXCR3, CXCR5, CCR7) on PB lymphocytes during BTK inhibitor treatment in patients with significant tumor redistribution (differences are smaller and less significant than between compartments before treatment). When analyzed relationship with lymphoid compartment involvement CXCR4 in PB and BM and CXCR3 in BM were positively associated with TTM and lymphocytosis, CXCR3, CXCR4 and CCR7 in LN were negatively associated with LN size, and CXCR4 in BM was positively associated with spleen size ($p<0.05$). After 6-months no significant relationships were observed due to significant reduction of tumor mass. BTK inhibitors induce the significant redistribution of B-CLL lymphocytes from lymphoid organs and BM to PB in the first months of the treatment. Tumor distribution is related to different chemokine receptor and adhesion molecule patterns observed by significant intraclonal heterogeneity between B-CLL lymphocytes in lymphoid compartments. Changes of surface molecules CXCR3, CXCR4, CXCR5, CCR7, CD38 and CD49d expression during ibrutinib treatment and consequent impact on interactions with microenvironment may play an important role in the disease pathogenesis, drug resistance and may reveal new treatment strategies. Current study is ongoing evaluating other molecules involved in interactions within microenvironment and with development of model for tumor distribution and redistribution.

Abstract ID: 1551543

Title: The mechanical properties of CLL cells are linked to the actin cytoskeleton and are target of BTK inhibitors

Authors: Cristina Scielzo, Marta Sampietro, Valeria Cassina, Federica Barbaglio, Riccardo Campanile, Domenico Salerno, Lydia Scarfò, Paolo Ghia, Oliver Otto, Francesco Mantegazza and Valeria Caiolfa

Chronic lymphocytic leukemia (CLL) is an incurable leukemia characterized by an intense trafficking of the leukemic cells between the peripheral blood and lymphoid tissues. The ability to recirculate between tissues depends on the capacity of those cells to modify and rearrange their cytoskeleton, and adapt to external cues, however not much is known about the differences occurring between CLL and healthy B cells during these processes. Nowadays new target

therapies are emerging, in particular the BTK inhibitors, as effective therapies leading to sustained responses, though patients may become resistant and relapse. BTK inhibitors promotes CLL cells mobilization from tissue to peripheral blood, where cells eventually undergo apoptosis, however, what really occurs in the tissues, and which are the processes regulating CLL cells dynamics and resistance to therapy remains to be elucidated. In the present work we demonstrated that CLL cells at nanoscale resolution, have a specific actomyosin complex organization with longer and more branched actin filaments and altered mechanical properties in comparison to their healthy counterpart. By super resolution microscopy on single cells we observed a low level of colocalization of actin and myosin suggesting that CLLs have a less contractile actomyosin complex, which correlates with a softer cellular cortical stiffness, measured by atomic force microscopy (AFM). On the contrary healthy B cells (HBs) are more contractile and stiffer (CLL $n=19$, HB $n=9$). To evaluate the clinical relevance of our findings we treated CLL cells with the BTK inhibitors ibrutinib and acalabrutinib. We observed a significant rescue of the physiological heathy phenotype upon treatment, characterized by stiffening of the cellular cortex by AFM (before and after treatment: p value <0.0001), and activation of the actomyosin complex by increasing myosin phosphorylation and colocalization with actin. We further validate our findings also *in vivo* on CLL cells isolated from patients undergoing ibrutinib treatment (CLL $n=4$), confirming our conclusion (p value <0.0001). Moreover, we were preliminary able to show that CLL cells fail to restore the healthy phenotypes in case of resistance to ibrutinib. Furthermore, by measuring the cortical stiffness of tissue resident CLL cells (CLL from bone marrow $n=2$, CLL from lymph node $n=3$), we observed a persistent stiffening, confirming a possible regulation of CLL cell's life cycle via BTK inhibition, by impairing the reentry of CLL cells into the tissues during treatment. Our results suggest that CLL cells' mechanical properties are linked to their actin cytoskeleton organization and might be involved in novel mechanisms of drug resistance thus becoming a new potential therapeutic target aiming at the normalization of the mechanical fingerprints of the leukemic cells.

Abstract ID: 1551561

Title: Very low COVID mortality and hospitalization rates in CLL and MBL with repeated vaccination to maximum antibody response

Authors: Stephen Mulligan, Yandong Shen, Jane Freeman, Ian Kerridge, Paul Downe, Kartik Naidu and Juliette Holland

Introduction: Patients with chronic lymphocytic leukemia (CLL) and monoclonal B-lymphocytosis (MBL) have impaired immunity and high risk of severe COVID infection, hospitalization, and death. The current dominant Omicron variants XBB are now resistant to the prophylactic monoclonal antibodies tixagevimab and cilgavimab (T+C). Hence vaccination, and anti-viral therapy, are the only remaining measures against severe infection. Australia had very low COVID infection numbers from January 2020 until December 2021 when border closures and quarantine measures were removed, by which time community vaccination rates exceeded 95%. For CLL and MBL patients with impaired vaccine responses, we adopted an approach of measuring anti-spike antibody (Ab) response using multiple COVID vaccine doses to achieve the optimum individual response, which significantly increased seroconversion and anti-spike Ab levels [1,2]. We evaluated the effectiveness of this multiple vaccination strategy against severe COVID infection in CLL and MBL patients.

Methods: Medical and COVID history was assessed in routine consultations, questionnaire and medical records from January 2020 to April 2023 at Royal North Shore Hospital, and Sydney Adventist Hospital, Sydney, Australia with informed consent. Anti-SARS-CoV-2 spike antibody (quantitative) and anti-nucleocapsid (NC) antibody (qualitative) levels were measured as previously reported (Abbott Diagnostics). Vaccination commenced in March 2020, and the first CLL patient developed COVID infection in December 2021.

Results: In this study, there were 296 patients with CLL (241) and MBL (55) with up to 8 (median 4) vaccine doses included. COVID infection rates were 53.9% (129/241) in CLL and 40.0% (22/55) in MBL patients. 7 CLL patients had a second episode of infection. These rates of infection are significantly lower than the incidence of infection in the general Australian community (>90%), and those aged >65 years (>70%). Hospitalization was required in 8 (of 129) CLL patients (6.2%) with 1 death (0.8%) from beginning of the pandemic in January 2020 until April 2023. The duration of admission ranged from 3 to 8 weeks; none required ventilation or ICU admission. Three were on active CLL treatment (2 ibrutinib, 1 venetoclax), but did not correlate to higher risk of hospitalization. There was 1 COVID-related death (1/129, 0.8%) due to acute anuric renal failure at 4 weeks (with concurrently diagnosed refractory metastatic melanoma). No MBL patient was hospitalised or died. There were 61 (of 129, 47.3%) CLL patients treated with anti-viral therapy; 33 received nirmatrelvir+ritonavir (54.1%), 23 molnupiravir (37.7%), and 5 remdesivir (8.2%). Of the 8 hospitalized CLL patients, 5 received remdesivir only, 1 molnupiravir and 2 no anti-viral therapy. Of the total 23 COVID infected MBL patients, 15 (68.2%) received no medication and 7 (31.8%) received antiviral therapy; 4 nirmatrelvir+ritonavir (57.1%) and 3 molnupiravir (43.9%). Positive anti-spike levels (>50AU/mL) were documented in 90.6% CLL (106/117) and 100%

Table 1. Patient summary

	Total	*CLL*	*MBL*
Number of patients	296	241	55
Age (min-max)	74 (23-95)	74 (23-95)	75 (50-94)
Male	164 (55.4%)	138 (57.3%)	27 (47.3%)
Number of infected (n, %)	151 (51.0%)	129 (53.9%)	22 (40.0%)
Age (min-max)	72 (38-92)	71 (38-92)	73.5 (54-86)
Infected male	87 (57.6%)	77 (59.7%)	10 (45.5%)
Hospitalization	8 (5.3%)	8 (6.2%)	0 (0%)
Death	1 (0.7%)	1 (0.8%)	0 (0%)
Type of treatment for COVID	Total (151)	CLL (129)	MBL (22)
None	76 (50.3%)	61 (47.3%)	15 (68.2%)
Symptoms relief only	7 (4.6%)	7 (5.4%)	0 (0%)
Anti-viral	68 (45.0%)	61 (47.3%)	7 (31.8%)
▪ Nirmatrelvir + ritonavir	37 (54.4%)	33 (54.1%)	4 (57.1%)
▪ Molnupiravir	26 (38.2%)	23 (37.7%)	3 (43.9%)
▪ Remdesivir	5 (7.4%)	5 (8.2%)	0 (0%)
Duration of COVID *	Total (70)	CLL (59)	MBL (11)
<3 days	4 (5.7%)	2 (3.4%)	2 (18.2%)
3-7 days	28 (40.0%)	23 (39.0%)	5 (45.5%)
7-14 days	21 (30.0%)	18 (30.5%)	3 (27.3%)
>14 days	17 (24.3%)	16 (27.1%)	2 (18.2%)
Anti-NC levels post COVID **	Total (57)	CLL (48)	MBL (9)
Detectable within 2 months	17 (29.8%)	12 (25.0%)	5 (55.6%)
Followed >6 months	Total (19)	CLL (14)	MBL (5)
Detectable after 6 months	10 (17.5%)	9 (18.8%)	1 (11.1%)

**Only included data where detailed questionnaire feedback from patients was received (70 patients)*
***Only included data where anti-nucleocapsid antibody level was measured (57 patients).*

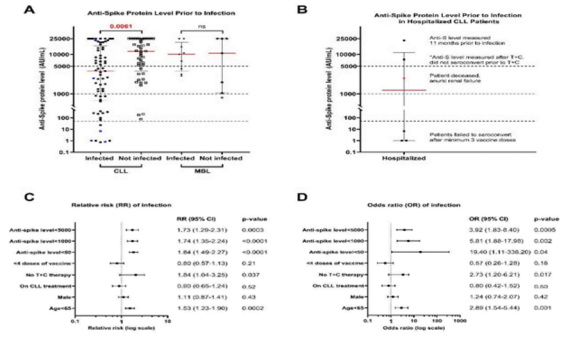

Figure 1. Anti-spike protein levels prior to infection and relative risk (RR) and odds ratio (OR) of infection. (A) Anti-spike protein levels in CLL and MBL patients with and without infection. Red line indicates median anti-spike levels and blue dots indicates hospitalised patients. Dotted lines indicate positive/negative threshold of measuring assay at 50AU/mL; positive neutralization threshold against D614G and Delta COVID variants at 1000AU/mL; and positive neutralization threshold against Omicron BA.1 at 5000AU/mL. (B) anti-spike protein levels in hospitalised CLL patients (n=8). The majority of hospitalized patients had no endogenous antibody response to vaccination. Anti-spike levels were not recorded for 2 out of 8 hospitalised patients, hence 6 data points. Red dot indicates the deceased patient. (C) Relative risk (RR) of COVID infection in CLL patients. (D) Odd ratio (OR) of COVID infection in CLL patients. T+C: prophylactic monoclonal antibodies therapy tixagevimab and cilgavimab; CLL patients who received T+C post infection were excluded. P-values of RR and OR were calculated using the formulae described by *Tenny et al. (2023)*, and *Altman et al. (2011)*, $p<0.05$ was considered as statistically significant. *This patient was excluded from statistical analysis as the anti-spike level was measured after T+C.

MBL patients (20/20). The median anti-spike levels in CLL patients who developed COVID infection (3778.8 AU/mL) were significantly lower compared to those who, to date, have not (13486.8 AU/mL) ($p=0.0061$) (Figure 1(A,B)). In MBL, there was no difference in anti-spike levels. CLL patients with low anti-spike levels and younger patients had a higher risk COVID infection (Figure 1(C,D)). Anti-nucleocapsid antibody (anti-NC Ab) post-COVID infection were detected in 12 of 48 CLL (25.0%) and 5 of 9 MBL (55.6%) within 2 months. Among patients followed >6 months, only 9 of 12 CLL patients (18.8% of 48) and 1 of 5 MBL patients (11.1% of 9) still had detectable anti-NC antibodies (Table 1). Hence, anti-NC Ab is not a reliable marker of COVID infection in CLL populations. Despite only 9 patients being administered T+C prior to COVID infection, these had a lower risk of infection (Figure 1(C,D)); 1 required hospitalization due to COVID 5 months after T+C (Figure 1(B)). The currently dominant Omicron XBB variants (NSW respiratory surveillance reports 2023), are now resistant to prophylactic T+C highlighting that the optimum stimulation of endogenous immune response remain very important.

Conclusion: CLL and MBL patients have impaired immune response to vaccination, leading to slower and lower levels of anti-spike response. A multiple vaccine doses strategy to optimal response resulted in very low mortality (0.8%) and hospitalization rates (6.2%).

Abstract ID: 1551571

Title: Transcriptional correlation analysis of the CD180/MD-1 complex and toll-like receptors and signaling lymphocyte activation family receptors in chronic lymphocytic leukemia.

Authors: Kurtis Edwards, Emanuela V. Volpi, Nicholas Chiorazzi, Peter M. Lydyard and Nino Porakishvili

Introduction: CD180 is a toll-like receptor (TLR) which is highly co-expressed with the satellite molecule MD-1 on surface of normal B cells and heterogeneously on the surface of CLL cells [1]. The natural ligand for CD180 is presently unknown although evidence suggests that CD180/MD-1 signals in concert with other surface receptors including signaling lymphocyte activation receptor 1 (SLAMF1) in CLL [2] and TLR9 in healthy B cells' [3]. Little is known however about the interactions between CD180/MD-1 and TLRs and other members of the SLAMF family in CLL. We therefore set out to identify novel signaling partners for CD180/MD-1 by analyzing the co-expression CD180 and MD-1 relative to TLRs and SLAMF receptor genes at the transcriptional level.

Methods: We accessed dataset GSE126595 [4] from the gene expression omnibus which contained normalized gene expression for 726 CLL patients (untreated =337; relapsed =389). We screened for the transcriptional expression of TLRs and SLAMF receptors. We considered the receptor to be expressed by CLL cells if the mRNA expression was higher than the CD3G gene which is exclusively expressed by T cells. The CD19 gene, which is known to be highly expressed by CLL cells, was used as a positive control. Pearson's correlation was applied to measure relationships between CD180/MD-1 and TLR/SLAMF gene expression.

Results: CD180 and MD-1 mRNA were found to be highly expressed compared to CD19 (Figure 1(a)). Among the classical TLR genes, TLR7 was the most highly expressed followed by TLR9, TLR6 and TLR10. TLR2, TLR4 and the TLR4-associated satellite molecule MD-2 were all expressed at very low levels (Figure 1(a)). TLR3 and TLR8 were not expressed by CLL cells (Figure 1(a)). SLAMF2 was the most highly expressed by CLL cells followed by SLAMF3, SLAMF6 and SLAMF5. SLAMF1, SLAMF3, SLAMF5 and SLAMF6 genes were highly expressed by CLL cells (Figure 1(b)). SLAMF1 was also expressed albeit at lower levels (Figure 1(b)). The remaining SLAMF receptor genes were found to be negative or marginally positive and were therefore excluded from the correlation analysis. CD180/MD-1 mRNA was found to be highly correlated with TLR1 and TLR6 mRNA (Table 1) which code for surface TLRs. Given that CD180/MD-1 is expressed on the cell surface, it is possible that the complex may dimerise with TLR1 or TLR6 the cell surface to detect pathogen-associated ligands. TLR1 and TLR6 are therefore rational novel targets for studying receptors which topologically associate with CD180/MD-1 for ligand detection. As expected, there was a negative correlation between CD180/MD-1 and TLR4 given that human B cells do not express this receptor, but a positive correlation with MD-2 (Table 1), the satellite molecule which is co-expressed with TLR4 [5]. The reasons for this are presently unclear however, it is hypothesised that MD-1 and MD-2 are evolved from a common ancestral molecule which appeared during the

Table 1. The correlation between *CD180* and *MD-1* genes and *TLRs* and *SLAMF* receptors. All permutations were determined as significant ($p<0.001$) except where indicated (^{NS} – Non-significant).

	CD180 Vs	*MD-1* Vs
TLRs Pearson's r		
TLR1	0.468	0.29
TLR2	0.151	0.184
TLR4	-0.507	-0.298
MD-2	0.783	0.55
TLR6	0.743	0.475
TLR7	0.813	0.512
TLR8	0.257	0.179
TLR9	0.535	0.259
TLR10	0.853	0.617
SLAMFs Pearson's r		
SLAMF1	0.317	0.166
SLAMF2	0.708	0.542
SLAMF3	0.205	0.023^{ns}
SLAMF5	0.685	0.384
SLAMF6	0.823	0.584

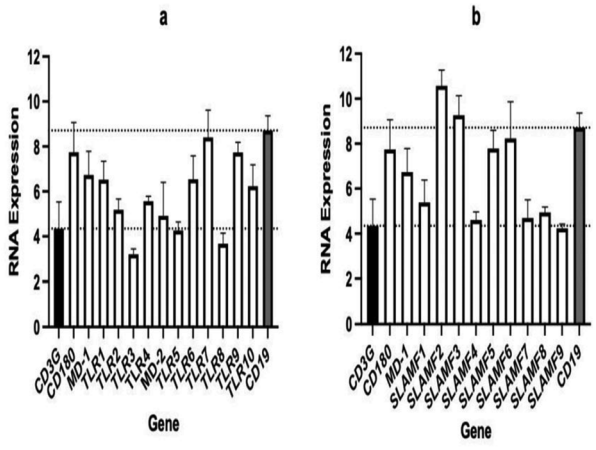

Figure 1. The expression of *TLRs* (a) and *SLAMF* (b) receptors in CLL cells. Levels of normalised mRNA gene expression were extracted from GEO under accession number GSE126595.

early development of vertebrates [6]. This could therefore mean that the same transcriptional regulation pathways exist for both MD-1/CD180 and MD-2 resulting strong corelations of the two genes. Studies should be conducted to determine if there is aberrant expression of MD-2 protein by CLL cells which may be of biological relevance. CD180/MD-1 were also both found to be highly correlated with TLR7, TLR9, and TLR10 which code for TLRs expressed in the endosomes (Table 1). This indicates potential role for CD180/MD-1 in modulating immune responses to intracellular pathogens in CLL. SLAMF2, which serves as a ligand for CD2 and SLAMF4 [7], was highly correlated with CD180/MD-1 indicating a potential role for the complex in modulating the interactions between CLL cells and various other haematopoietic cell types. There was also a high correlation between CD180/MD-1 and SLAMF6 and SLAMF5.

Conclusions: Co-expression analysis of CD180/MD-1 at the transcriptional level has revealed potential novel signaling partners for this TLR complex, providing rationale for further phenotypic and functional studies in CLL. Since CD180 can rewire IgM-mediated signaling to a pro-apoptotic pathway in CLL [8], it will be important to determine if CD180/MD-1 has synergistic or antagonistic effects on the signaling partners proposed here. The high correlation between CD180/MD-1 and TLR10 and SLAMF6 mRNA suggest these receptors as rational starting points for such studies.

Abstract ID: 1551588

Title: The role of 18F-FDG PET-CT in Richter transformation and accelerated CLL

Authors: Ziyuan Zhou, Siqi Qian, Xiao Lu, Tonglu Qiu, Luomengjia Dai, Yeqin Sha, Yi Miao, Shuchao Qin, Yi Xia, Lei Fan, Wei Xu, Jianyong Li and Huayuan Zhu

Objective: To investigate the diagnostic and prognostic value of 18F-FDG PET-CT in Richter transformation (RT) and accelerated CLL (aCLL).

Methods: A total of 35 RT patients and 12 aCLL patients who had undergone 18F-FDG PET-CT at Department of Hematology of Jiangsu Provincial People's Hospital were retrospectively examined. The analysis involves the imaging characteristics of 18F-FDG PET-CT, measuring metabolic parameters, including maximum standard uptake value (SUVmax), tumor metabolic volume (MTV), total lesion glycolysis (TLG), maximum lesion distance (Dmax) and etc., with clinical, genetic and molecular biological data at the time of RT and aCLL diagnosis to investigate the diagnostic and prognostic value of 18F-FDG PET-CT in RT and aCLL.

Results: RT patients have higher SUVmax (13.2 vs. 7.9 in RT vs. aCLL patients, $p<0.001$) and TLG (1651.9 vs. 527.1 in RT vs. aCLL, $p<0.01$). Multivariate analysis results suggest that SUVmax is a significant predictor for RT. A SUVmax cutoff value ≥10 (lesions with SUVmax ≥10 highly suspicious for transformation) shows a sensitivity, specificity, negative and positive predictive value of 74.3, 92.3, 57.1, and 96.3%, respectively. In comparison to aCLL, RT has a poorer prognosis, with a median overall survival (OS) of 13.5 months. Univariate COX analysis indicates that high MTV, high TLG, high Dmax, high β2-microglobulin, and complex karyotype (≥3 chromosomal abnormalities or structural abnormalities) are adverse prognostic factors for OS. In multivariate COX analysis, high TLG and complex karyotype are independently associated with shorter OS.

Conclusion: 18F-FDG PET-CT is a useful diagnostic and prognostic tool for CLL/SLL patients with clinical suspicion of RT or aCLL. SUVmax is a significant predictor for RT, and lesions with SUVmax ≥10 should be highly suspected of transformation, warranting pathological biopsy or aspiration for confirmation. RT has a poorer prognosis, with high TLG and complex karyotype being independent associated with shorter OS.

Abstract ID: 1551592

Title: COVID-19 infection in chronic lymphocytic leukemia (CLL) patients treated with venetoclax: a Danish single-center experience

Authors: Sophie Thau, Christian Bjørn Poulsen and Lars Møller Pedersen

Introduction: Patients with chronic lymphocytic leukemia (CLL) or small lymphocytic lymphoma (SLL) have shown to be at high risk of developing severe COVID-19 disease and studies have reported COVID-19 mortality rates at approximately 30% [1–3] Many CLL patients present with dysfunction of the innate and adaptive immune system and are frequently treated with immunosuppressants. Venetoclax blocks the interaction between the ACE2 receptor and the SARS-CoV-2 spike (S) glycoprotein *in vitro* [3] and may have a protective role against COVID-19 in CLL patients. However, the American Society of Hematology recommended that venetoclax treatment should be avoided during the COVID-19 pandemic due to a high number of clinical visits and lab testing. We performed an observational single-center study of CLL patients treated with venetoclax in a real-world setting during the COVID-19 pandemic. The primary aim was to elucidate morbidity and mortality of COVID-19 infections. The extensive Danish testing strategy and the access to nationwide registries made it possible to present a large collection of COVID-19 data among CLL patients treated with venetoclax.

Methods: The cohort consisted of 108 patients with CLL/SLL treated with venetoclax at the Department of Hematology,

Table 1 – COVID-19 outcome

COVID-19 outcomes	COVID-19 cohort (n=48), (n(%))
COVID-19 severity	
Asymptomatic or mild COVID-19 disease	36 (75)
Severe or critical COVID-19 disease	12 (25)
COVID-19 morbidity	
Hospitalization	22 (46)
Pulmonary infiltrates on X-ray	13 (27)
SpO2 < 90%	8 (17)
ICU admission	0
Mortality	2 (4)

Table 2 – COVID-19 treatment

COVID-19 treatments	COVID-19 cohort (n=48), (n(%))
Glucocorticoids	10 (21)
Anticoagulants	11 (23)
Antiviral antibodies (sotrovimab, evusheld, REGN-COV-2)	34 (71)
Other antivirals (remdesivir, paxlovid)	15 (31)
Treated with oxygen supplements	10 (21)
Antibiotic treatment related to COVID-19	21 (44)
No treatments	12 (25)

Zealand University Hospital, Denmark. Patients were treated with venetoclax according to national guidelines including a five week ramp up schedule and a steady state dose of 400 mg. Venetoclax was used in combinations with anti-CD20 (84.3%), BTK inhibitors (10.2%) or as monotherapy (8.3%). The Danish mass testing strategy identified positive SARS-COV-2 real-time reverse transcription-PCR (qRT-PCR) tests in 48 (44%) of the cohort. We collected data from patients with COVID-19 prior to and during the Danish Omicron era (cut off point January 2022). Our primary outcome was 30-day COVID-19 mortality. Secondary outcomes were COVID-19 severity (according to Wu & McGoogan's criteria), hospitalization rate and treatment with antiviral drugs. All clinical data was collected from electronic records and from the Danish Pathology Data Registry. The study was approved by the regional Data Protection Agency (ID: EMN-2022-11057 and EMN-2022-11065).

Results: Mean age was 71 years and 71% were male. Median (range) lines of therapy prior to venetoclax were 1 (0–6). Median (range) length of venetoclax treatment was 13 months (1–36). The majority of patients (92%) had received more than four COVID-19 vaccines. Most patients presented with asymptomatic/mild COVID-19 (75%) and only two deaths (4%) were registered within 30 days from positive SARS-COV-2 PCR test (Table 1). The causes of death were Richter transformation in a patient with mild COVID-19 and both pulmonary cancer and COVID-19 in a patient with critical COVID-19. The hospitalization rate was 46% with no ICU admissions (Table 1). Thrombocytopenia prior to venetoclax treatment ($p<0.01$) and high CIRS scores ($p<0.02$) were identified as risk factors for developing severe COVID-19 disease. In five patients (10%), a reactivation of the same SARS-COV-2 origin was detected within 2 months after a negative PCR test. COVID-19 treatment characteristics are outlined in Table 2. COVID-19 severity, morbidity and mortality were similar before and in the Omicron era. Patients with COVID-19 during active treatment with venetoclax received more intensive treatment with antiviral antibodies ($p=0.03$), anticoagulants ($p=0.03$), Piperacillin/Tazobactam ($p<0.01$) and antiviral drugs ($p=0.02$) compared to patients with COVID-19 after the end of venetoclax treatment.

Conclusions: Our results suggest that CLL/SLL patients treated with venetoclax generally present with mild COVID-19 and low mortality rates compared to data from studies of general CLL populations. COVID-19 morbidity and mortality are highly associated with other comorbidities. The results point to venetoclax having a potential protective effect against severe COVID-19.

Abstract ID: 1551601

Title: FOXO4 is required for the promotion of CLL growth and survival

Authors: Jamie Lees, Alison Michie, Michael Moles and Jodie Hay

Chronic lymphocytic leukaemia (CLL) pathogenesis is supported in part by 'tonic' B-cell receptor (BCR) signalling, through activation of oncogenic signalling pathways such as the phosphoinositide-3-kinase (PI3K)-AKT/mTOR pathway. This pathway is critical in regulating a plethora of cell functions ranging from cell size to oxidative damage, with increased activity promoting cell survival and proliferation via AKT-mediated negative regulation of the Forkhead Box (FOX) class O (FOXO) transcription factor family. This is achieved via AKT-mediated phosphorylation of FOXO at conserved sites, negating DNA binding via cytoplasmic relocalisation. FOXO family members (FOXO1, FOXO3, FOXO4 and FOXO6) are implicated in the regulation of numerous cellular processes, however it is their primary role in cell cycle arrest and apoptosis that has depicted FOXOs as 'bona fide' tumour suppressors. This can be achieved via FOXO-mediated upregulation of pro-apoptotic and anti-proliferative target genes such as BCL2L11 (BIM) and CDK1NB (p27kip1) respectively. However, FOXOs also regulate processes such as DNA and oxidative damage responses and thus exhibit 'bimodal' characteristics, either promoting or preventing cell survival in a context-dependent manner. This behaviour is mimicked in B-cell malignancies, where FOXO activity can hinder or promote lymphomagenesis in a disease-specific context. Nevertheless, the strong tumour suppressive effects induced by FOXO activity demonstrate clinical relevance in utilising FOXO activity as a novel therapeutic target for CLL

treatment. We previously demonstrated that while FOXO1 expression is upregulated and inactive (cytoplasm sequestered) in primary CLL patient samples, treatment of cells with the dual mTOR inhibitor AZD8055 resulted in FOXO1 nuclear accumulation and activation resulting in cell cycle arrest and cell death. We now demonstrate that pharmacological inhibition of FOXO1 nuclear accumulation using a selective FOXO1 inhibitor (AS1842856) attenuates an AZD8055-mediated proliferative block and cell kill, further demonstrating that FOXO1 behaves in a tumour suppressive manner in CLL. FOXO3 activity has also been reported to be anti-tumourigenic in CLL; microenvironmental chemokines (e.g. CCL19, CCL21) promote CLL cell survival through PI3K-AKT-mediated FOXO3 inactivation, indicating that the CLL tumour microenvironment can promote CLL proliferation and survival in part through AKT-mediated FOXO inactivation. However, no clear role has been identified for FOXO4 in CLL proliferation and survival. Initial investigations revealed upregulated FOXO4 expression compared to healthy B-cell donor samples, suggesting a potential role for FOXO4 in CLL. We generated a bulk RNA-seq dataset profiling 5 primary CLL patient samples co-cultured on a pro-proliferative co-culture (NTL-CD40L/IL4; 24 hr) in the presence or absence of AZD8055, ibrutinib (BTKi), or a combination. One striking feature of the dataset was that primary CLL cells treated with AZD8055 exhibit significant increases in FOXO4 expression (2.5 fold), likely due to AKT inhibition and subsequent FOXO-mediated upregulation of FOXO4. This finding was supported in AZD8055-treated MEC1 and HG3 cell lines, both exhibiting significant FOXO4 upregulation. As pharmacological mTOR inhibition also increases the activity of FOXO1 and FOXO3, we generated shRNA-mediated FOXO4 depletion in the MEC1 cell line to investigate distinct FOXO4-mediated processes. Proliferation (CellTrace Violet) analysis revealed a significant reduction in proliferative capacity in cells with depleted FOXO4, while apoptosis (Annexin/7-AAD) analysis showed significant increases in AZD8055/Ibrutinib-induced cell death, coinciding with significant increases in the pro-apoptotic FOXO target gene BCL2L11. These data suggest FOXO4 is required for CLL cell survival and chemoresistance. The importance of FOXO4 in CLL homeostasis is supported by investigation of the DNA damage response. Initial gene profiling showed a significant downregulation of GADD45A expression in FOXO4 depleted cells, suggesting a role for FOXO4 in the DNA damage response. Further investigation via intracellular staining revealed that p-γH2AX - a phosphorylated histone crucial for forming repair foci at sites of dsDNA breaks - is significantly upregulated following AZD8055/Ibrutinib treatment, further supporting FOXO4 as a mediator of DNA damage repair and chemoresistance. There is also significant upregulation of SESN3 in FOXO4-depleted cells, suggesting a role for FOXO4 in maintaining intracellular ROS levels. Further investigation of the role of FOXO4 in the oxidative damage response, as well as investigation into the role of FOXO4 in primary patient samples, are currently ongoing. Collectively, these findings demonstrate the opposing roles of individual FOXO family members and indicate a putative role for FOXO4 in promoting CLL cell survival, proliferation and the cellular response to intracellular damage.

Abstract ID: 1551683

Title: Venetoclax as an alternative and effective treatment in central nervous system involvement of chronic lymphocytic leukemia: monocentric experience

Authors: Luca Inchiappa, Anne Calleja, Pierre Durozard, Robin Noel, Mariela Catalina, Montes De Oca, Joseph Ciccolini and Thérèse Aurran

Introduction: Central nervous system (CSN) involvement in chronic lymphocytic leukemia (CLL) is rare, making diagnosis challenging. Presence of CLL-type cells in the cerebrospinal fluid (CSF) alone is insufficient for diagnosis, and CLL is rarely the cause of neurological symptoms. Differential diagnosis includes other inflammatory neurological disorders, agressive lymphoma among others. The optimal treatment for CLL patients with CNS involvement is yet to be standardized. However, ibrutinib is commonly used in this context. Recent research has highlighted the penetration of venetoclax into the cerebral compartment. Here, we report two cases of CLL patients with CNS involvement who were treated with a venetoclax-based regimen in our center Case 1: A 57-year-old male had an history of visual loss starting in July 2019. Cerebral MRI confirmed optic neuropathy, ruling out autoimmune and infectious causes. CSF analysis were unremarkable. Corticosteroid therapy resulted in a partial response. Subsequently, CLL monoclonal B lymphocytosis was diagnosed, and a PET scan showed normal results. The patient developed progressive paresthesia in both legs starting in February 2021. Cerebrospinal and medullary MRI showed features of multilevel myelitis. Lumbar puncture revealed 100 white blood cells (80% CLL-type cells). Further laboratory investigations showed normal white blood cell count with 5.5 G/l lymphocytes, as well as normal LDH and B2M levels. CLL characteristics included unmutated IGHV gene, del 13q, absence of TP53 dysfunction, and no pathogenic mutations in NGS analysis. Ibrutinib treatment was initiated, but after 1 month, the patient experienced worsening paresthesia despite decreased lymphocytes in the CSF. A subsequent spinal MRI showed partial regression of the myelitis lesions, and ibrutinib was pursued. In September 2021, the patient presented a complete sensory-motor deficit in the legs. Cerebral and spinal MRI revealed new lesions. A cord spinal biopsy confirmed CLL cells infiltration. The patient received one cycle of high-dose methotrexate, followed by the administration of venetoclax plus rituximab (according to the Murano study). Venetoclax was rapidly escalated over 10 days without toxicity. After three months of treatment, significant neurological improvement was observed, with recovery of the walk. CSF analysis at month 9 showed few CLL-type elements, while the concentration of venetoclax in the CSF was 24.7 ng/ml consistent with literature findings. At month 12, MRI did not show any lesions left. The patient is currently in his 21st month of venetoclax treatment, with complete regression of all neurological symptoms. Case 2: A 77-year-old male was diagnosed with Binet stage A CLL in 2005 and initially opted for therapeutic abstention. FISH analysis at the time did not show any dismal prognostic features. After three years, the patient progressed to stage B disease and the patients received four cycles of FCR achieving complete remission. In 2014, treatment with ibrutinib was initiated after progression stage B disease with del17p deletion. In 2019 patient progressed and was given 3rd line treatment with venetoclax-rituximab, which was discontinued after 21 months due to hepatic cytolysis. However, the patient showed negative MRD at the end of treatment. After 16 moths the patient experienced numb chin syndrome, and the CSF analysis confirmed presence of CLL cells , with normal blood counts, MRD positive at 1.3%, and normal total body scan and cerebral MRI results. Genetic analysis of CSF revealed pathogenic variations in the TP53 gene, while no acquired Bcl2 mutations were found. The patient promptly resumed treatment with venetoclax-rituximab, with rapid

dose escalation over 10 days, and demonstrated good tolerance. Currently, the patient is in the 10th month of venetoclax treatment and showing a complete neurological clinical response.

Conclusion: This report highlights the successful use of a venetoclax-based regimen in CLL patients with CNS involvement. It presents a case of primary ibrutinib-resistant CNS involvement in CLL, responding to second-line therapy with venetoclax-rituximab. Additionally, it discusses a case of CNS relapse after venetoclax treatment discontinuation, with a response to resuming venetoclax. Based on these results and other reported cases, venetoclax-based regimens should be considered as a therapeutic alternative for CLL patients with CNS involvement and as a treatment option for those progressing after BTK inhibitor therapy. Rapid ramp-up is considered a safe and potentially effective approach to attain therapeutic concentrations of venetoclax in CSF, but the optimal treatment duration and combination with monoclonal antibodies remain subjects of debate.

Abstract ID: 1551686

Title: High deletion burden identified by whole genome sequencing is associated with enhanced risk in del17p CLL patients

Authors: Preeti Trisal, Esteban Braggio, Nicholas Stong, Kay Medina, Sameer Parikh, Daniel Van Dyke, Zhiquan Wang, C. Chris Huang, Anita Gandhi and Neil Kay

Introduction: Presence of deletion17p (del17p) in frontline (1L) and relapsed/refractory (R/R) CLL has been associated with shorter time to treatment initiation, early relapse after therapy and inferior overall survival (OS) [1,2]. However, there exists notable clinical heterogeneity in terms of outcome within this group [3–5]. Previous reports in 1L and R/R CLL have identified percentage of del17p nuclei by fluorescence in situ hybridization (FISH), having TP53 mutations on the second allele, copy number alterations and complex karyotype (CK) as additional risk factors within the del17p population [4,6–8]). Here we profile a cohort of wait and watch (W&W, $n=14$), 1L treated ($n=36$) and R/R CLL ($n=3$) patients by whole genome sequencing (WGS) and RNA sequencing (RNAseq) to gain insights into genomic factors and gene expression pathways contributing to the high-risk nature of del17p across the spectrum of CLL patients.

Methods: Using the Mayo Clinic CLL Database, we identified 53 patients with del17p (identified by FISH testing in routine clinical practice at diagnosis) who had stored peripheral blood mononuclear cells (PBMCs) available. RNA and DNA from matched peripheral blood (tumor) and DNA from CD19- (germline) samples at diagnosis ($n=50$) and relapse ($n=3$) was extracted using Qiagen RNeasy (RNA) and Purene (DNA) kits and subjected to RNAseq and WGS respectively. Additional FISH assays (del11q, trisomy 12, del13q) and CK by chromosomal banding analysis (CBA) were performed. Baseline clinical characteristics, time to first treatment, types of treatment, and survival were abstracted from the CLL Database. The Mayo Clinic IRB approved this study.

Results: Copy number analysis identified deletions in 3p, 4p, 8p, 9p, 9q and gains in 2p, 8q, 15q and 17q chromosomal lesions occurring in patients. We explored the association of clinical and genetic factors, and genomic instability signatures with survival to identify high-risk features in del17p patients. Both total number of deletions by WGS and number of chromosomal aberrations by CBA as a continuous variable were significantly associated with unfavorable OS in the entire cohort ($n=53$) in a univariate analysis (Hazard ratio, HR= 2.29, $p=0.00054$ and HR= 2.33, $p=0.0054$, respectively). However, there was no significant association of number of gained genes by WGS or aneuploidy scores with survival (HR =0.74, $p=0.37$). In patients with CK data ($n=41$), deletion burden, but not gains, were highly correlated to chromosomal aberrations by CBA. Using cutpointr package for identifying deletion threshold corresponding to CK ≥3, we defined patients with deletion burden ≥514 as enhanced-high risk (EHR; median OS =4.83 years) compared to the group with high-risk (HR; median OS =9.94 years) ($p=0.025$). There was no significant difference in number of deleted genes between WW and treated patients. The EHR group is enriched in patients with high clonal cell fraction of del17p by FISH, unmutated IGHV and CK≥ 3. The EHR group remains significant in a multi-variable analysis with IGHV-mutation status, ZAP70, and age (HR: 5.16, 95% CI: 1.04 – 25.6, $p=0.04$). Mutational analysis identified 35 known CLL driver mutations with TP53 (86%), ATM (15%), NOTCH1(13%), MGA (13%), CHD2 and MED12(11%) as the top mutated genes. Total number of driver genes mutated was not significantly different between EHR and HR subgroups, but the EHR subset was significantly enriched with mutations in NOTCH1 (21%), and MGA (21%) as compared to no mutations in the HR group in these genes. Deleted genes (≥514) was prognostic in bi-allelic TP53 aberration patients as well ($p=0.021$) Differential expression gene-set enrichment analysis indicated a significant enrichment of DNA repair, cellular response to DNA damage and downregulation of inflammatory responses in the EHR group.

Conclusions: CK is a known prognostic marker which includes both chromosomal losses and gains. In this small cohort of del17p we were able to show the prognostic value of deletions only, but not gains, as captured by WGS. Using genome wide sequencing, we identify increasing genomic deletions as a

A. Forest plot of univariate analysis for determinants of overall survival

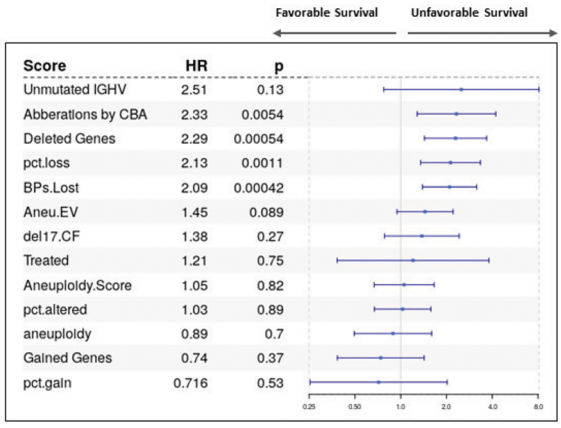

B. Del17p CLL OS

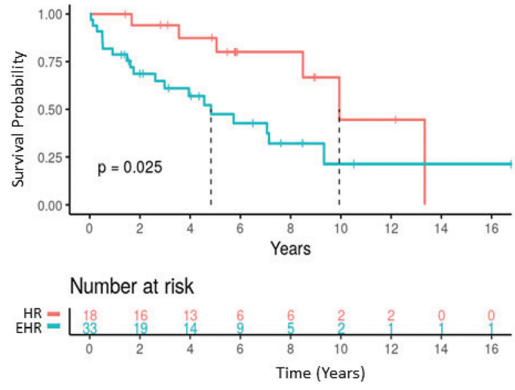

feature of enhanced-high risk del17p. While deletion burden cut-offs identified here are specific to our research method and require further validation in additional independent cohorts, EHR subgroup remained significant after adjusting for other known prognostic variables.

Abstract ID: 1551689

Title: Venetoclax-obinutuzumab for previously untreated chronic lymphocytic leukemia: 6-year results of the randomized CLL14 study

Authors: Othman Al-Sawaf, Sandra Robrecht, Can Zhang, Stefano Olivieri, Naomi Chang, Anna Fink, Eugen Tausch, Matthias Ritgen, Karl Kreuzer, Lilly Sivcheva, Carsten Niemann, Anthony Schwarer, Javier Loscertales, Robert Weinkove, Dirk Strumberg, Allanah Kilfoyle, Eva Runkel, Barbara Eichhorst, Stephan Stilgenbauer, Yanwen Jiang, Michael Hallek and Kirsten Fischer

Background: One-year fixed-duration venetoclax-obinutuzumab (Ven-Obi) is a standard-of-care for patients with previously untreated chronic lymphocytic leukemia (CLL). The CLL14 study previously demonstrated feasibility and high efficacy of Ven-Obi in patients with CLL and coexisting conditions. Due to the ongoing study follow-up of clinical data and data on minimal residual disease (MRD), the CLL14 study provides unique insights into the long-term outcome. Here we present data with particular interest on outcomes after Ven-Obi treatment completion. The aim of this report is to provide updated efficacy, safety, and MRD data from the ongoing follow-up of the CLL14 study, all patients being off study treatment for ≥5 years.

Methods: Patients with previously untreated CLL and coexisting conditions were randomized 1:1 to 12 cycles of venetoclax with 6 cycles of obinutuzumab, or 12 cycles of chlorambucil with 6 cycles of obinutuzumab (Clb-Obi). The primary endpoint was investigator-assessed progression-free survival (PFS). Secondary endpoints included safety, rates of MRD, time to next treatment (TTNT) and overall survival (OS). Follow-up is ongoing. Samples of peripheral blood were assessed every 6 months and were analysed for MRD by next generation sequencing (NGS).

Results: Of the 432 enrolled patients, 216 were randomly assigned to receive Ven-Obi and 216 to receive Clb-Obi. At a median follow-up of 76.4 months (interquartile range 52.5–80.5) median age of the patient population was 77 years. PFS remained superior for Ven-Obi compared to Clb-Obi (median 76.2 vs. 36.4 months; hazard ratio [HR] 0.40 [95% CI 0.31–0.52], $p<0.0001$). At 6 years after randomization, the estimated investigator-assessed PFS rate was 53.1% after Ven-Obi, and 21.7% after Clb-Obi. Progressive disease (PD) occurred in 67 cases in the Ven-Obi arm with 39 second-line treatment initiations, and in 141 cases in the Clb-Obi arm (with 103 second-line treatments). TTNT was significantly longer after Ven-Obi (6-year TTNT 65.2 vs. 37.1%; HR 0.44 [95% CI 0.33–0.58], $p<0.0001$). In both arms, the most frequent second-line treatments were BTK inhibitors (59.0% in the Ven-Obi arm, 53.4% in the Clb-Obi arm). The PFS and TTNT difference between the two arms was maintained across all risk groups, including patients with TP53 mutation/deletion (median PFS 51.9 vs. 20.8 months; median TTNT 57.3 vs. 29.0 months) and unmutated IGHV status (median PFS 64.8 vs. 26.9 months; median TTNT 85.4 vs. 40.6 months). Multivariate analysis identified TP53 deletion/mutation, unmutated IGHV and lymph node size ≥5 cm as independent negative prognostic factors for PFS in patients treated with Ven-Obi. Five years after treatment completion, 17 (7.9% of the intention-to-treat population) patients in the Ven-Obi arm still had uMRD ($<10^{-4}$ by NGS in peripheral blood), 22 (10.2%) had low (L)-MRD ($\geq 10^{-4}$ and $<10^{-2}$) and 23 (10.6%) high (H)-MRD ($\geq 10^{-2}$), compared to 4 (1.9%) uMRD, 9 (4.2%) L-MRD and 18 (8.3%) H-MRD in the Clb-Obi arm. Overall, 48 deaths were reported in the Ven-Obi arm (9 PD related) and 70 in the Clb-Obi arm (26 PD related); at 6-year-OS rate was 78.7% in the Ven-Obi and 69.2% in the Clb-Obi arm (HR 0.69 [95% CI 0.48–1.01], $p=0.052$). Second primary malignancies were reported in 30 patients in the Ven-Obi and 18 in the Clb-Obi arm; cumulative incidences 6 years after randomization were 14.2 and 8.5%, respectively ($p=0.071$). Two Richter transformations were reported in the Ven-Obi arm and four in the Clb-Obi arm. No new safety signals were observed.

Conclusion: These long-term data confirm a continued PFS benefit of fixed-duration Ven-Obi treatment compared to Clb-Obi, including patients with high-risk CLL. Five years after cessation of Ven-Obi, over half of the patients of this elderly patient population remained in remission, 8% still had uMRD and over 60% had not required second-line treatment. The 1-year Ven-Obi regimen is an effective fixed-duration option for patients with CLL and coexisting conditions.

Abstract ID: 1551697

Title: Implementing the data-driven CLL-TIM algorithm into an EPIC-based EHR: proof of concept for automated decision support models

Authors: Rudi Agius, Anders C. Riis-Jensen, Bettina Wimmer, Daniel Dawson Murray, Marianne B. Bertelsen, Jens Lundgren, Henning Langberg and Carsten Niemann

Background: Implementing large predictive models in routine clinical practice requires proof-of-concept examples of how such research algorithms, and their results, can be integrated safely and successfully in clinical practice. While Electronic Health Records (EHR) have increased the availability of health data for training predictive machine learning (ML) algorithms, the algorithms implemented in EHR are often rule-based models with few variables and lack continuous performance monitoring. This simplicity compromises prediction accuracy and fails to capture the complexity of patient-disease dynamics. Moreover, there is currently no proof-of-concept example of all the necessary processes and stakeholders involved in implementing complex decision-making algorithms in clinical practice. We here describe such a system exemplified by our implementation of an algorithm for Chronic Lymphocytic Leukemia (CLL) implemented as a stand-alone platform into a Danish EHR.
Aim: To implement a complex prognostic model into EHR and detail the steps and challenges required for such an implementation.
Methods: The CLL Treatment and Infection Model (CLL-TIM) was developed to identify high-risk CLL patients who may experience severe infections or require treatment within two years of diagnosis. CLL-TIM is currently being used to select patients for the PreVent-ACaLL clinical trial. We implemented CLL-TIM on a Python platform within the EHR system that extracts relevant data from the EHR on a daily basis. The platform provides CLL-TIM predictions, including individual patient risk factors and prediction confidence, as a view within the EHR. We present the process of data harmonization, validation between research and production environment data, benchmarking of predictions, architecture for automating predictions and the proposed setup for automatic monitoring of the algorithm. Findings: To ascertain the success of the implementation, we benchmarked the implemented version of CLL-TIM on a blinded test set of CLL patients diagnosed with CLL after 2018. Compared to results obtained in the research environment, CLL-TIM demonstrated similar performance within the real-time production environment, achieving an MCC (Matthews correlation coefficient) of 0.64 under similar missing data conditions. Implementing CLL-TIM into clinical practice posed significant challenges particularly in the areas of (1) data validation and harmonization between research and production environments, (2) technical integration with the EHR, (3) strategic negotiation for presenting results within the patient context and (4) obtaining approval under the EU-based Medical Device Regulation. Interpretation: Having highly accurate and trustworthy machine learning algorithms in clinical practice requires moving beyond simple rule-based models. In this study, we present a proof-of-concept with detailed steps involved in implementing a complex prognostic model as a standalone platform integrated with the EHR. Retrospective validation, continuous monitoring, and personalized predictions for all patients, regardless of missing data, were included, providing a pathway for others interested in implementing similar data-driven machine learning algorithms in clinical practice.

Abstract ID: 1551702

Title: Targeting NF-κB-inducing kinase (NIK) in chronic lymphocytic leukaemia

Authors: Iona Ashworth, Thomas Burley, Emma Kennedy, Eleni Ladikou, Lauren Stott, Christopher West, Christopher Fegan, Rosalynd Johnston, Simon Mitchell, Andrea Pepper and Chris Pepper

Background: Aberrant NF-κB signalling appears to play a key role in the pathogenesis of CLL, including several recurrent genetic mutations in NF-κB-activating genes[1–3]. Constitutive NF-κB activity is associated with a more aggressive disease [1,4] and is implicated in the development of resistance to both ibrutinib and venetoclax [5]. Inhibiting NF-κB signalling is therefore a potential therapeutic approach. However, given the key role of canonical NF-κB signalling on multiple cellular processes, direct pharmacological targeting of NF-κB (e.g. through IKKβ inhibitors) has so far failed due to associated toxicities. We investigated the potential for targeting NF-κB inducing kinase (NIK), the central kinase regulating non-canonical NF-κB signalling, in CLL. We evaluated three NIK inhibitors, CW15337, Amgen16 and BO22, in the MEC-1 cell line and in primary CLL cells. Given that NIK expression levels are very low under physiological conditions, and constitutive activation is usually only present in pathological contexts [6], NIK may represent a tumour-selective therapeutic target. We hypothesised that NIK inhibition may represent a promising strategy in the treatment of CLL by targeting CLL cells in the lymphoid tissue environment where they are particularly reliant on non-canonical NF-κB signalling.
Results: All three NIK inhibitors caused a dose-dependent G1 arrest in the cell cycle in the MEC-1 cell line. Mean proportion of MEC-1 cells in G1 with no drug =48%, whilst at the highest drug concentration =69, 68 and 66% for CW15337, Amgen16 and BO22, respectively. All three agents were cytotoxic in both in the MEC-1 cell line (LC50 = 1.63, 30 and 19.3μM for CW15337, Amgen16 and BO22, respectively) and in primary samples (LC50 = 2.05, 15.23and 14.4μM for CW15337, Amgen16 and BO22, respectively). CW15337 was the most potent drug in both MEC-1 and primary samples. Nuclear expression of the non-canonical NF-κB subunit, p52, was correlated with sensitivity to CW15337 ($p = 0.01$; $r^2 = 0.39$). When co-cultured with CD40L-expressing fibroblasts, as a model of the lymphoid niche, NIK inhibitors were able to overcome this cytoprotective environment and cause cell death. This was seen with both MEC-1 and primary samples. Furthermore, all three agents significantly inhibited MEC-1 cell migration against a chemokine gradient ($p < 0.001$) in a dose-dependent manner. Co-culture on CD40L-expressing cells induced both canonical and non-canonical subunit expression in nuclear extracts, which promoted in vitro resistance against fludarabine and ABT-199 (venetoclax) but not CW15337. Furthermore, the combination of CW15337 with fludarabine or ABT-199 showed cytotoxic synergy. Mechanistically, CW15337 caused the selective inhibition of non-canonical NF-κB subunits and the transcriptional repression of BCL2L1, BCL2A1 and MCL1 anti-apoptotic gene transcription. Taken together, these data suggest that the NIK inhibitor, CW15337, exerts its effects via

suppression of the non-canonical NF-κB signalling pathway, and reverses venetoclax resistance in the context of CD40L stimulation through repression of BCL2 family proteins. In conclusion, NIK inhibitors can overcome the cytoprotective environment conferred by co-culture, suggesting that they could be effective at targeting disease in lymphoid tissues, where CLL cells are more reliant on NF-κB signalling. The inhibition of MEC-1 migration suggests that NIK inhibitors could block re-entry of CLL cells to the lymph node microenvironment. Furthermore, they may be effective in targeting residual disease in the lymph node by suppressing the non-canonical NF-κB signalling pathway, which resensitises CLL cells to venetoclax.

Abstract ID: 1551711

Title: Predictive modeling of treatment outcomes in chronic lymphocytic leukemia based on functional profiles at baseline

Authors: Sigrid Skånland, Johanne Hermansen, Weikaixin Kong, Yanping Yin, Haifeng Xu, Liye He, Andrea Brodersen, Aleksandra Urban, Rebecca Teglgaard, Christian Brieghel, Sabina Kersting, Geir Tjønnfjord, Mark-David Levin, Hoa Tran, Mattias Mattsson, Juha Ranti, Gerrit-Jan Veldhuis, Caspar da Cunha-Bang, Rogier Mous, Julie Dubois, Jorrit Enserink, Jennifer Brown, Anthony Mato, Arnon Kater, Carsten Niemann and Tero Aittokallio

Background: Although targeted therapies have revolutionized the management of chronic lymphocytic leukemia (CLL), treatment efficacy varies from patient to patient and no treatment is given with curative intent. To avoid short treatment durations or toxicities of therapy, there is a need to identify biomarkers that can guide optimal treatment decisions for the individual patient.
Aim: To develop computational models that predict treatment outcomes in CLL patients based on functional analyses performed on primary CLL cells sampled before treatment start.
Methods: Peripheral blood mononuclear cells (PBMCs) were collected at baseline from relapsed/refractory CLL patients enrolled in three phase 2 clinical trials [NCT03226301 (ibrutinib + venetoclax cohort; $n = 186$), NCT02742090 (umbralisib cohort; $n = 55$), and NCT04624633 (umbralisib + acalabrutinib cohort; $n = 12$)]. Multi-color flow cytometry with fluorescent cell barcoding was applied to the PBMCs for (phospho)protein profiling (31 proteins) of resting CLL cells. Two computational models were developed to predict treatment outcomes on the clinical trials. Model 1 used (phospho)protein profiles from the ibrutinib + venetoclax cohort to predict MRD level in peripheral blood at cycle 15. The cohort was divided into a training set ($n = 139$; 75%) and a test set ($n = 47$; 25%), stratified based on MRD level, IGHV mutational status, and TP53 aberration status. After 15 cycles of ibrutinib + venetoclax treatment, 63, 44, and 7 patients in the training set had obtained an undetectable ($<10^{-4}$, i.e. less than 1 CLL cell detected in 10000 leukocytes by flow cytometry), intermediate (10^{-4} to 10^{-2}), or high MRD ($>10^{-2}$) status, respectively. MRD sample or (phospho)protein profile was missing for the remaining 25 patients. Model 2 used (phospho)protein profiles from the umbralisib cohort (training set) to predict tumor objective response rate (ORR). The umbralisib + acalabrutinib cohort was used as an independent test set. Patients who achieved partial response (PR) or complete response (CR) to umbralisib were classified as responders ($n = 15$). Patients who achieved stable disease (SD) or progressive disease (PD) were classified as non-responders ($n = 40$). Statistical associations between the (phospho)protein profiles and treatment outcomes were assessed with Wilcoxon non-parametric test.
Results: Patients with high MRD after 15 cycles of ibrutinib + venetoclax therapy showed significantly higher (phospho)protein levels than patients with intermediate or undetectable MRD for 8 proteins in the training set ($p<0.05$), including Bim, ERK1/2 (pT202/Y204), and STAT3 (pY705). There were no significant differences in (phospho)protein profiles between intermediate and undetectable MRD groups. In the umbralisib cohort, the (phospho)protein levels were significantly higher in CLL cells from responders than from non-responders for 8 proteins ($p<0.05$), including MEK1 (pS298), mTOR (pS2448), and p90 RSK (pS380). The (phospho) protein profiles from the two training sets were used as input data to construct two independent LASSO logistic models with leave-one-out cross validation to predict patients with either high MRD (ibrutinib + venetoclax cohort; Model 1) or objective response (umbralisib cohort; Model 2). In the test sets, we obtained ROC-AUC (Receiver Operating Characteristic/Area Under the Curve) scores of 0.70 and 0.82 for Model 1 and Model 2, respectively. The proportion of the positive (responders) class in the umbralisib cohort (15/55; 0.27) was used as cut-off for the probability to predict a responder. The model correctly predicted all patients in the test set (umbralisib + acalabrutinib cohort) to be responders (median probability of 0.52, range =0.33–0.86), suggesting that it is feasible to predict treatment outcomes in CLL based on functional profiles at baseline.
Summary/Outlook: We present a novel approach to model treatment outcomes for CLL patients based on functional analyses and show that baseline (phospho)protein profiles of CLL cells have predictive value in independent CLL cohorts treated with targeted therapies. To further increase the robustness of the models, we will include additional types of functional data (immune phenotyping and drug sensitivity screening data), as well as clinical data. These analyses will be presented. A parallel strategy will be to expand the training set by combining input data from various patient cohorts. The goal is to develop a robust model and apply it in a biomarker-driven clinical trial to guide individual treatment selection.

Abstract ID: 1551727

Title: The proto-oncogene TCL1A deregulates cell cycle and genomic stability in CLL

Authors: Johanna Stachelscheid, Qu Jiang, Christoph Aszyk, Kathrin Warner, Nadine Bley, Olga Vydzhak, Konstantinos Symeonidis, Giuliano Crispatzu, Stuart James Blakemore, Gudrun Goehring, Sebastian Newrzela, Stephanie Hippler, Sandra Robrecht, Karl

Kreuzer, Christian Pallasch, Marcus Krueger, Axel Lechner, Kirsten Fischer, Stephan Stilgenbauer, Dirk Beutner, Michael Hallek, Daniel Auguin, Stefan Hüttelmaier, Johannes Bloehdorn, Elena Vasyutina and Marco Herling

The oncoprotein T-cell leukemia/lymphoma 1A (TCL1A) is a 14 kDa adapter protein that is causally implicated in various B-cell and T-cell malignancies. TCL1A was initially discovered in T-prolymphocytic leukemia (T-PLL), where chromosomal abnormalities cause an increase in TCL1A expression, considered the initiating event in this aggressive disease. In chronic lymphocytic leukemia (CLL), TCL1A is overexpressed in the majority of patients, and high expression correlates with aggressive disease features and inferior clinical outcomes. Despite extensive research on TCL1A's oncogenic functions in stemness, survival, and signaling pathways (e.g. enhancing the activity of the serine/threonine kinase AKT), its full spectrum of effector functions and the molecular concept of TCL1A-mediated leukemogenesis remain unclear. Therefore, we aimed to systematically characterize undiscovered TCL1A effector molecules, affected pathways, and their influence on TCL1A-induced CLL pathogenesis. We observed in mouse models of subcellular-site specific TCL1A-induced lymphomagenesis, that TCL1A exerts a strong transforming impact via nuclear topography. In proteomic screens of TCL1A-bound molecules in CLL cells and B-cell-lymphoma lines, we identified regulators of cell cycle and DNA repair pathways as novel TCL1A interactors, particularly enriched under induced DNA damage and mitosis. We identified as a novel TCL1A interactor the mitotic checkpoint protein CDC20, which is crucial in the regulation of timely separation of the sister chromatids during mitosis. CDC20 functions as a coactivator of the anaphase-promoting complex/cyclosome (APC/C), thereby driving mitotic exit, but is also part of the mitotic checkpoint complex (MCC), inhibiting the APC/C. Via *in-silico* modeling and experimental validations, we defined the crucial domains mediating the direct TCL1A-CDC20 interaction and identified an abrogating effect of TCL1A on the engagement of CDC20 with the MCC protein MAD2. According to a regulatory impact of TCL1A on the activity of the CDC20-containing mitotic checkpoint and anaphase-promoting complexes during mitotic progression, TCL1A overexpression accelerated cell-cycle transition in B-cell-lymphoma lines, impaired apoptotic damage responses in association with pronounced chromosome mis-segregation and caused cellular aneuploidy in Eμ-TCL1A mice. Interestingly, among hematopoietic cancers, CDC20 levels seem particularly low in CLL. CDC20 expression negatively correlated with TCL1A, and lower expression marked more aggressive and genomically instable disease and cellular phenotypes. Importantly, knock-down of Cdc20 in TCL1A-initiated murine CLL promoted aneuploidy and leukemic acceleration. Taken together, our data give significant novel insights into the molecular mechanisms of TCL1A-induced leukemogenesis. We propose that the cross-talks between enhanced survival signaling, and deregulation of the DNA damage response and the cell cycle checkpoints, drive genomic instability and malignant transformation. Through this comprehensive characterization of TCL1A's function, we gained a deeper understanding of the mechanisms involved in CLL pathogenesis, which could also potentially be applied to other malignancies harboring TCL1A overexpression. It will also help uncover potential vulnerabilities that could be exploited for more targeted treatment approaches.

Abstract ID: 1551756

Title: Impaired mitochondrial metabolism drives T-cell dysfunction in chronic lymphocytic leukemia

Authors: Nienke Goedhart, Jaco A. C. Van Bruggen, Eric F. Eldering, Helga Simon-Molas and Arnon Kater

Background: Chronic lymphocytic leukemia (CLL) remains incurable despite implementation of novel targeted therapies. Successful autologous cell-based anti-cancer therapies require functionality and longevity of effector cells, features that highly depend on complex metabolic processes. Our group previously demonstrated a disease-specific dysfunction in CLL T-cells including signs of impaired metabolic plasticity [1]. However, in-depth analysis of the metabolic phenotype of CLL T cells and mechanisms underlying the dysfunction are lacking, preventing development of therapeutic strategies aiming to overcome dysfunction by metabolic reprogramming.
Methods: In this study, we assessed mitochondrial and glycolytic activity of T cells from CLL patients and age-matched healthy controls (HD) upon T cell receptor stimulation *in-vitro* (αCD3/28) by extracellular flux analysis. Concurrently, we measured the expression of key mitochondrial regulators and markers of T cell function by flow cytometry along time after two stimulations separated by a period of 15 days.
Results: Extracellular flux analyses revealed impaired mitochondrial activity in T cells from CLL patients, including reduced spare respiratory capacity, an important indicator of mitochondrial and T cell fitness. The response in glycolysis, a key pathway for early T-cell activation, varied between patients and reflected activation levels (Figure 1). These findings pointed towards mitochondrial dysfunction rather than overall metabolic impairment at the basis of T-cell

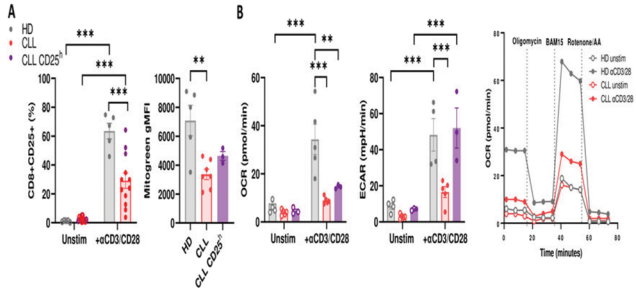

Figure 1. Activation and real-time metabolic activity of T cells from healthy individuals (HD) and CLL patients. PBMCs from HD or CLL patients were stimulated for 48h. A) T-cell activation and mitochondrial mass were measured by CD25 surface expression and MitoTracker Green abundance, respectively, by FACS. B) Extracellular flux analysis was performed on isolated T cells (50.000 cells/well) with the T-cell metabolic profiling test on a Seahorse XF HS. Basal extracellular acidification rate (ECAR) and oxygen consumption rate (OCR) are shown together with a representative measurement of OCR over time. Data are presented as mean ± SEM and differences were analyzed with two-way ANOVA (* p < 0,05; ** p < 0,01; *** p < 0,001).

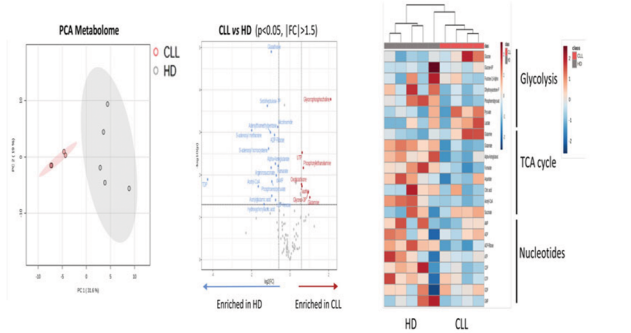

Figure 2. CD4+ and CD8+ cells from HD or CLL PBMCs were FACS-sorted at baseline (n=5 for each group) or upon 2 days of stimulation with αCD3/28 antibodies (HD n=5, CLL n=4) and subjected to metabolomics analysis. Metabolites were analyzed by LC-MS and abundance was normalized by total metabolome pool in each sample. Data were analyzed using Bruker TASQ software version 2.1.22.3 and MetaboAnalyst 5.0. Principal component analysis of total metabolome and heatmap of pathway-specific metabolites are shown.

dysfunction in CLL. 13C-glucose and glutamine isotope tracing revealed that glutamine rather than glucose is the dominant fuel for mitochondrial metabolism. Although metabolic fluxes were conserved in CLL T-cells, metabolomics analyses showed significantly decreased tricarboxylic acid cycle (TCA) intermediates and nucleotides in stimulated T-cells from CLL patients, as well as a high ratio of oxidized/reduced glutathione, indicator of impaired mitochondrial activity and enhanced production of reactive oxygen species (Figure 2). In line with this, we observed a significant increase of mitochondrial depolarization in CLL T cells, which has been previously associated with mitochondrial damage and loss of T-cell effector function. Accordingly, CLL T cells showed delayed expression of activation markers, impaired proliferation and were almost completely unresponsive to re-stimulation. Mitochondrial function is primarily regulated by the expression of Peroxisome proliferator-activated receptor Gamma Coactivator 1-alpha (PGC1α) and Mitochondrial Transcription factor A (TFAM). Upregulation of both PGC1a and TFAM upon stimulation was delayed in CLL T cells compared to healthy T cells, and especially impaired after the second stimulation.

Conclusion: These results pinpoint to defects at the core of mitochondrial regulation as potential causes of T cell dysfunction in CLL. Specifically, we identified impaired expression of mitochondrial regulators in these cells, providing possible targets to improve T-cell based therapies in CLL

Abstract ID: 1551781

Title: Over-time monitoring of CXCR4dim/CD5bright proliferative fraction anticipates relapse in ibrutinib-treated CLL : a reservoir for BTK mutations?

Authors: Federico Pozzo, Gabriela Forestieri, Filippo Vit, Erika Tissino, Tamara Bittolo, Robel Papotti, Lodovico Terzi di Bergamo, Agostino Steffan, Roberta Laureana, Agostino Tafuri, Annalisa Chiarenza, Francesco Di

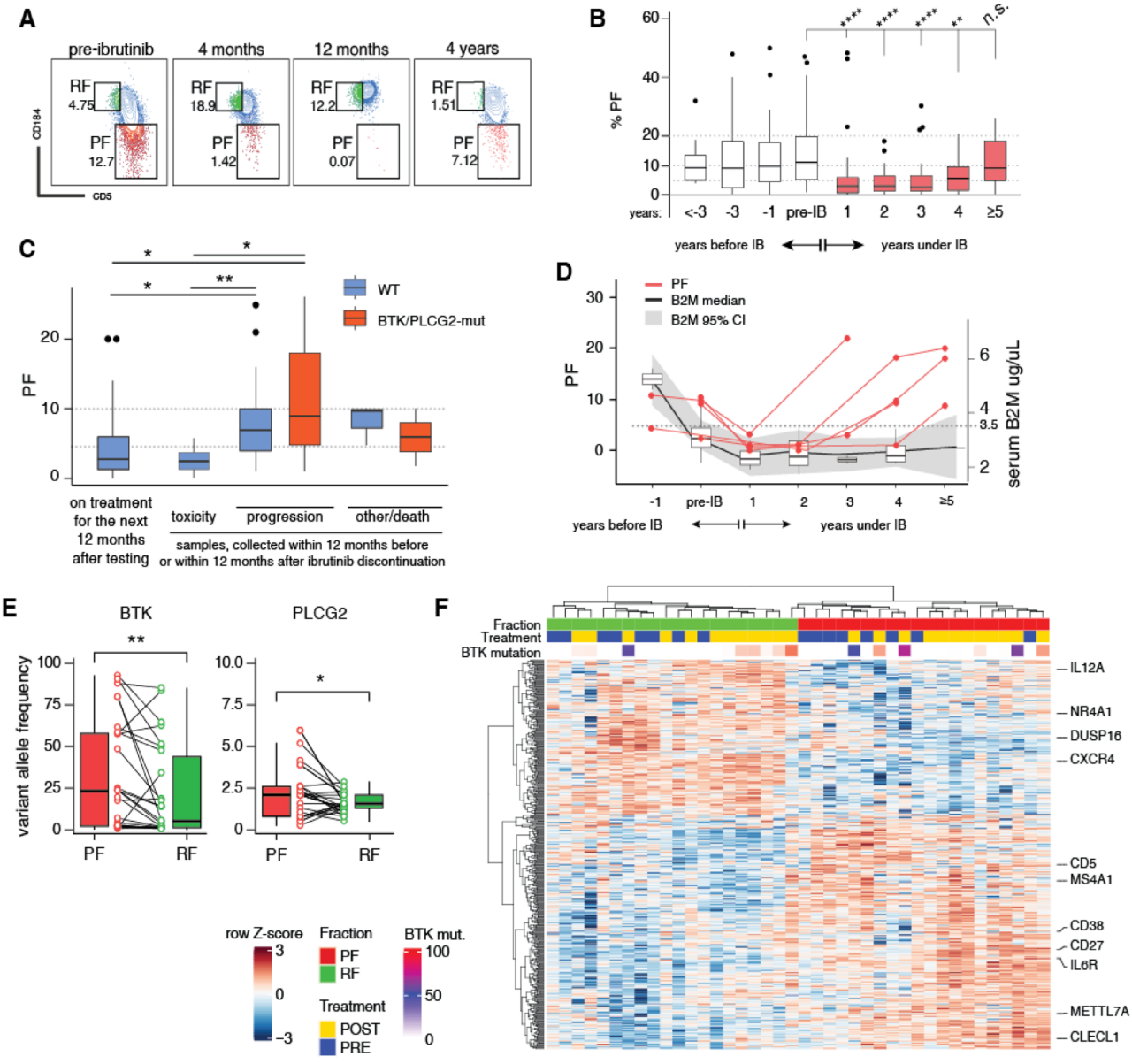

Raimondo, Jacopo Olivieri, Francesco Zaja, Luca Laurenti, Maria Ilaria del Principe, Riccardo Bomben, Antonella Zucchetto, Davide Rossi and Valter Gattei

Reciprocal expression of CXCR4 and CD5 on the surface of chronic lymphocytic leukemia (CLL) cells can discriminate the proliferative fraction (CD5high/CXCR4dim, PF), recently egressed from the lymph node, from the resting fraction (CXCR4high/CD5dim, RF) of older, quiescent cells. BTK inhibitors affect the proliferative capacity of CLL cells and cause their redistribution from nodal compartments to the blood stream. Little is known about the impact of long-term ibrutinib (IBR) treatment on the PF/RF phenotype. Therefore, we monitored the PF dynamics in two cohorts of IBR-treated CLL cases with long-term follow-up, and correlated with the emergence of IBR resistance. Peripheral blood samples were collected from CLL patients who either entered the IOSI-EMA-001 study (NCT02827617) or were referred to our institution for routine immunogenetic analyses. Immunophenotypic analyses were performed using a FACSCanto II flow cytometer (BD Bioscience). DNA sequencing was performed with targeted amplicons, while RNA-seq was performed with the mRNA Library prep Kit on a Nextseq instrument (Illumina) and analyzed with R package DESeq2. Longitudinal analysis of the PF under IBR in 31 CLL cases (IOSI-EMA-001) with sequential samplings (156 samples, median 6 samples/case) showed a depletion of the PF over time, from 17.7% at pre-treatment to 4.75, 0.4, 1.5, 0.6, 1.5% at later timepoints (0.5, 6, 12, 18, 24 months; $p<0.001$, *U* test), along with loss of proliferative potential by Ki67 expression. We then retrospectively analyzed the PF from a wider cohort of 100 IBR-treated CLL cases from the real world, referred for routine immunophenotyping (296 samples, median 3 samples/case; Figure 1(A,B)). Median PF of pre-IBR samples was 12.0% (range 0.7–50), with a significant drop to 2.7% within one year of treatment and to 1.0% in the second year ($p<0.001$, *U* test). Out of 100 cases, 71 discontinued IBR within 5 years (17 toxicity, 46 progression, 8 other/death). Mutations of BTK/PLCG2 were detected in 29/100 cases (29%); among these, 24 (64.2%) discontinued IBR due to progression/relapse (23/24) or toxicity (1/24). To correlate the reappearance of the PF with cause of IBR discontinuation and with presence of BTK/PLCG2 mutations, we focused on 59 samples collected within 12 months before/after IBR discontinuation due to toxicity ($n=11$), progression ($n=43$) or other/death ($n=5$), and compared with 26 samples still on treatment for the next 12 months after testing. Mutations were present in 22/43 progressing cases, with a PF higher than wild-type (WT) cases discontinuing for toxicity (8.9 vs. 2.4%; $p=0.012$) or still on treatment (2.8%, $p=0.015$; Figure 1(E) upper comparisons). Notably, the 21 WT progressing cases also showed higher PF compared to cases discontinuing for toxicity (6.9 vs. 2.4%; $p=0.004$) or to cases still on treatment (6.9 vs. 2.8%; $p=0.024$; Figure 1(C) lower comparisons). Sequential dosages of plasmatic B2M in progressing cases ($n=5$) revealed steady levels below the 3.5 ug/mL threshold, despite the PF increase (median PF 18%; Figure 1(D)). We then isolated the PF/RF fractions from 10 cases, who developed BTK mutations and with PF reappearance after prolonged IBR treatment (median 50.7 months). Sequencing revealed 27 BTK mutations (mean 1.7 mutations per sample, range 1–4), with a median VAF higher in the PF (23.0%, 0.3–92.3) than in the RF (5.2%, 0.1–84.8; $p=0.003$, paired rank test); overall, the PF VAF was on average 2.8 times larger than the RF (0.01–38). A similar trend was present for PLCG2 mutations (median PF VAF: 2.0%, 0.1–6.2; RF VAF: 1.35%, 0.4–2.8; $p=0.014$) (Figure 1(E)). We performed mRNA-seq on 20 cases, with matching PF/RF fractions from samples at pre-IBR and progression, the latter enriched in BTK mutations. Differential expression signature of pre-IBR PF vs. RF, concordant with published gene sets, drove co-clustering of post-IBR PF/RF with their respective counterparts (Figure 1(F)), indicating that PF at progression functionally resembles its pre-treatment counterpart. To conclude, here we report: (i) that IBR treatment abrogates the PF fraction within 1 year of treatment, expanding previous short-term observations; (ii) its reconstitution after long-term treatment often predates clinical progression; (iii) the enrichment of BTK/PLCG2 mutations in the reconstituted PF suggests the presence of active clonal selection dynamics, bona fide taking place within the lymph node microenvironment. Clinically, longitudinal monitoring of the CXCR4/CD5 fractions by flow cytometry may provide a simple tool helping to intercept CLL progression under IBR therapy.

Abstract ID: 1551807

Title: Curcumin enhances ibrutinib induced killing effect against TP53-mutated chronic lymphocytic leukemia cells *in vitro*

Authors: Yunxia Zhang, Xutao Guo, Ru Feng, Xiaolei Wei, Yongqiang Wei and Haohao Lei

Introduction: TP53 mutation and del (17p) are the most important poor prognostic factors in patients with Chronic Lymphocytic Leukemia (CLL).Patients with deletion 17p or TP53 mutations tend to have lower response rates to standard first-line chemoimmunotherapy and a more aggressive clinical course [1]. RESONATE-2 study long-term follow-up showing that ibrutinib continues to demonstrate significant and durable clinical benefit in older patients, including those with TP53 mutation [2]. However, CLL bearing del(17p) showed inferior OS and time to next treatment compared to non-del(17p) [3]. A significant proportion of patients treated with single-agent ibrutinib experienced CLL progression.BTK and/or PLCG2 mutations were present in 80.0% of patients progressing with CLL, confirming prior reports on the high prevalence of these mutations in patients with ibrutinib-resistant CLL [4]. Curcumin is a bioactive natural polyphenol compound extracted from the Curcuma longa(Zingiberaceae plant). Curcumin has anti-tumor effect and can induce apoptosis and inhibit the proliferation of a series of tumor cells [5]. Curcumin may limit the development of therapy-related toxicity and reduce the financial burden of treatment. In this study, we found that Curcumin inhibits TP53-mutated CLL cells, and eliciting a strong synergistic cytotoxic effect in combination with ibrutinib.

Research objective: The human CLL cell line MEC1 with TP53 mutation was used as the research object to explore whether curcumin could increase the killing effect of ibrutinib on CLL cells with TP53 mutation in vitro and explore its potential mechanism.

Contents and methods: (1)The inhibitory effect of ibrutinib combined with curcumin on the proliferation of TP53-mutated Chronic Lymphocytic Leukemia cells was detected by CCK8, and the apoptosis of TP53-mutated CLL cells induced by ibrutinib combined with curcumin was detected by flow cytometry; (2) the differences of gene and signal pathway expression among different treatment groups were analyzed by RNA-seq ; (3) using Western blot technology to verify the expression of related pathway proteins and explore the mechanism of curcumin increasing

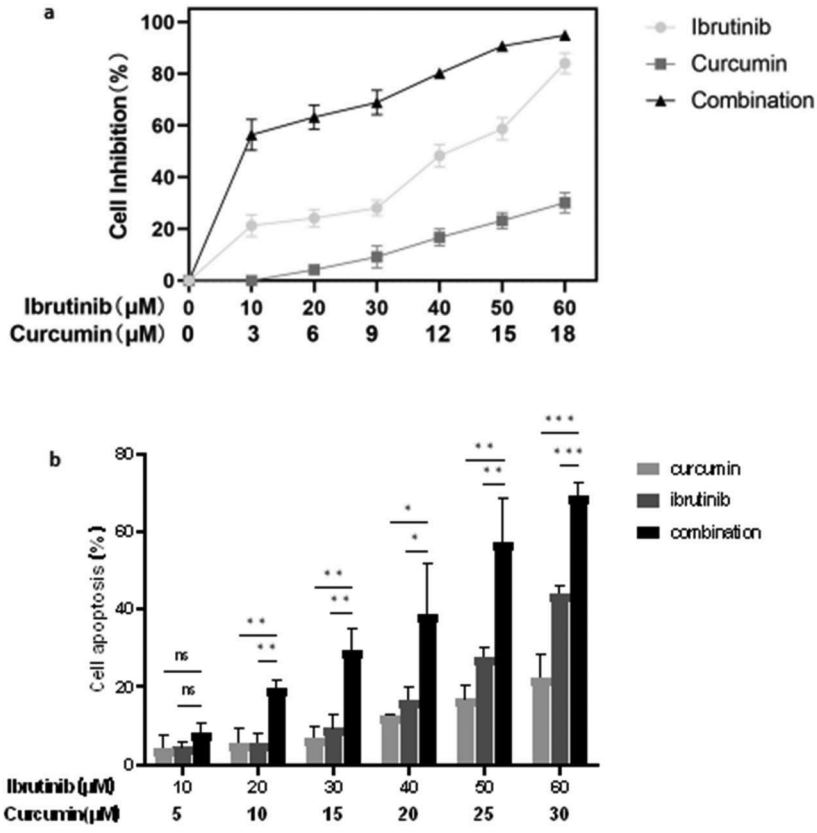

Figure1 a:Cell Inhibition of MEC-1 cell line that were exposed to various drug concentration of Curcumin combine with Ibrutinib for 24h;b:Cell apoptosis of MEC-1 cell line that were exposed to various group for 24h.

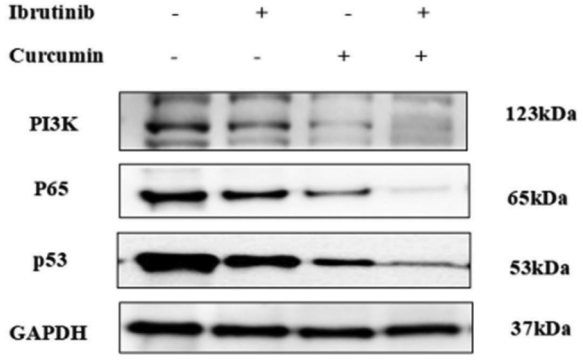

Figure2 The expression of PI3K、p53 and P65 after the treatment of Ibrutinib and Curcumin for 24h.

the killing effect of ibrutinib against TP53-mutated Chronic Lymphocytic Leukemia cells.

Results: (1) The CCK8 results showed that the IC50 of ibrutinib for 24 hours was 40.61±2.35μM, while the IC50 of curcumin for 24 hours was 26.6±0.94μM. The IC50 of ibrutinib for 48 h was 14.6±0.8307μM, and the IC50 of curcumin for 48 h was 15.7±2.53μM. The CI of ibrutinib combined with curcumin at 24 hours and 48 hours was calculated by CompuSyn software. The results showed that the CI values of ibrutinib combined with curcumin were less than 1 at 24 and 48 h, suggesting that ibrutinib combined with curcumin has a synergistic killing effect on CLL cells with TP53 mutation; (2) Flow cytometry showed that the IC50 of ibrutinib for 24 hours was 67.20±2.86μM, while the IC50 of curcumin for 24 hours was 144±6.6 μM. The CI value of ibrutinib combined with curcumin was less than 1 at 24 h, suggesting that ibrutinib combined with curcumin has a synergistic promoting apoptosis on CLL cells with TP53 mutation; (3) RNA-seq analysis and KEGG analysis of down-regulated genes of combination group compared with the control group were mainly enrich in PI3K/AKT, Cytokine-Cytokine Recptor signal pathway and so on. (4) The results of Western blot showed that the protein expression levels of P65, PI3K and p53 in the single drug group and the combination group were down-regulated in varying degrees, especially in the combination group.

Conclusion: (1) Ibrutinib combined with curcumin has synergistic killing effect on TP53- mutated CLL cells; (2) Curcumin increases the killing effect of ibrutinib on TP53-mutated CLL cells by inhibiting PI3K and NFκB pathway, and degrading p53mt protein.

Abstract ID: 1551868

Title: Serum monoclonal immunoglobulin predicts inferior prognosis in patients treated for chronic lymphocytic leukemia

Authors: Martin Šimkovič, Filip Vyskočil, Pavel Vodárek, Dominika Écsiová and Lukáš Smolej

Introduction: The prognostic significance of monoclonal immunoglobulins/paraproteins in patients with chronic lymphocytic leukemia (CLL) remains incompletely understood. Previous studies have primarily focused on the importance of paraprotein at the time of CLL diagnosis. In a recent Italian study, Corbigni et al. [1] found that the presence of serum monoclonal immunoglobulin (MIg) at CLL diagnosis was linked to a worsened prognosis. However, the prognostic significance of MIg in patients at the time of initiation of therapy has not been investigated. Objectives: This single-centre, retrospective study aimed to examine the presence and prognostic relevance of serum MIg in patients with CLL. We included all patients diagnosed with CLL fulfilling the IWCLL criteria with available result of MIg testing at the beginning of their CLL treatment. Serum paraprotein detection was performed using automated serum protein and immunofixation electrophoresis. We performed statistical analyses with the R software (version 4.2.1, www.r-project.org). Differences in proportion were determined using the chi-squared test. Survival curves were constructed using the Kaplan–Meier method, and differences in survival were compared via the log-rank test. Independent predictors of time to event were determined by Cox regression analysis.

Results: A total of 220 consecutive patients treated for CLL between 1996 and 2022 were included in this study. Among the patients, 42 (19%) exhibited detectable serum MIg, with 23 (55%) having IgM paraprotein and 19 (45%) having IgG paraprotein. Full details of baseline demographic and clinical characteristics are presented in Table 1. The median follow-up period was 102 months, the estimated overall survival from the start of first-line treatment was 92 months (95% Confidence interval [CI], 65–119) in patients without the presence of MIg vs. 78 months (95% CI, 61–94) in those with detectable MIg (Figure 1). In univariate analysis, the presence of paraprotein was associated with a shortened overall survival from first-line treatment (hazard ratio [HR] of 1.48 (95% CI 1.02–2.17; $p=0.04$). Additionally, shorter overall survival was shown in patients treated with chemoimmunotherapy who did not receive targeted inhibitors during their clinical course (HR 1.72 (95% CI 1.08–2.74; $p=0.02$), in participants aged >65 years (HR 2.69, 95% CI 1.80–4.02; $p<0.001$). Treatment without oral kinase inhibitors and age over 65 maintained their importance in multivariate analysis. Moreover, TP53 deletion/mutation was associated with inferior outcomes (HR 2.95, 95% CI 1.01–8.59, $p=0.05$) in multivariate analysis.

Conclusion: The presence of serum paraprotein in patients with chronic lymphocytic leukemia emerged as a negative prognostic marker for patients initiating first-line therapy. Further studies are needed to confirm these findings.

Table 1. Characteristics of Patients Treated for CLL Based on Monoclonal Immunoglobulin (MIg) Presence

Characteristics	MIg positive CLL	MIg negative CLL	*P*
Number of patients	42 (19%)	178 (81%)	
Age at CLL diagnosis in years, median	63	60	0.035
Age at administration of 1st line treatment in years, median	66	64	0.099
Male gender	24 (57%)	116 (65%)	NS
Median follow-up in months	131	162	NS
Time to first CLL treatment in months	33	36	NS
Prognostic markers			
Unmutated IGHV genes	27/39 (69%)	113/151 (75%)	NS
Del17p and/or *TP53* mutation	2/42 (5%)	10/178 (6%)	NS
Del11q	13/39 (33%)	53/167 (32%)	NS
Tris12	12/39 (39%)	21/173 (16%)	0.005
Del13q	20/39 (51%)	85/164 (52%)	NS
Complex karyotype	5/24 (21%)	20/119 (17%)	NS
Rai modified risk			
Low	4 (10%)	5 (1%)	0.049
Intermediate	7 (10%)	18 (10%)	NS
High	24 (35%)	66 (26%)	0.124
Treated with oral tyrosine kinase inhibitor	16 (38%)	90 (51%)	0.137
BCL-2 inhibitor	5 (12%)	28 (16%)	NS
PI3K inhibitor	4 (10%)	29 (16%)	NS
BTK inhibitor	12 (17%)	63 (35%)	NS

Abbreviations: CLL, chronic lymphocytic leukemia, MIg, monoclonal immunoglobulin, IGHV immunoglobulin heavy chain variable region, *TP53*, tumour protein p53, BCL-2, B-cell lymphoma 2, BTK, Bruton tyrosine kinase, PI3K, phosphatidyl inositol 3-kinase, NS, not significant

Figure 1. Overall Survival From Start of First-Line Therapy: Impact of Monoclonal Immunoglobulin Presence

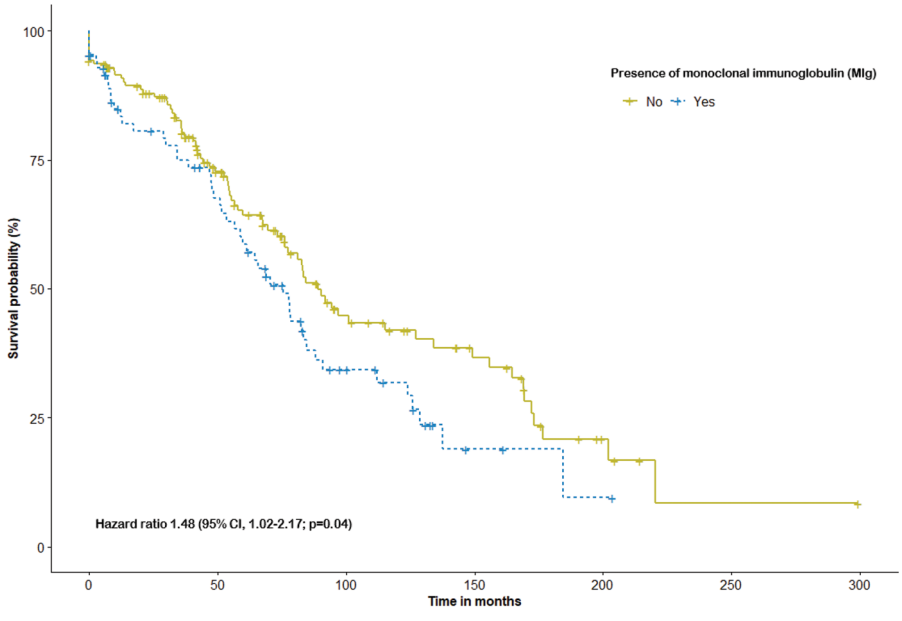

Abstract ID: 1551878

Title: Targeting the pro-inflammatory protein S100-A9 in chronic lymphocytic leukemia

Authors: Angimar Uriepero, Melanie Mediavilla-Varela, Kamira Maharaj, Wael Gamal, Maria Elena Marquez, Eugenia Payque, John Powers, Mohammad Ahmmad-Ud-Din, Vishaal Kunta, Eva Sahakian, Pablo Oppezzo and Javier Pinilla-Ibarz

Background: During Chronic Lymphocytic Leukemia (CLL) progression, pro-inflammatory pathways are activated, providing leukemic B lymphocytes with survival signals. Recently, our group described the presence of S100-A9 protein in exosomes derived from CLL patients during disease progression. S100-A9 is a potent mediator of inflammation, tumor invasion, and metastasis. This protein plays an important role in the myeloid compartment, where high expression of S100-A9 is associated with the suppressive activity of myeloid-derived suppressor cells (MDSCs). In addition, S100-A9 inhibitors have shown immunomodulatory properties and are currently being evaluated in early-phase clinical trials for multiple myeloma and prostate cancer. We hypothesize that S100-A9 provides B-CLL cells with a survival advantage by activating inflammatory pathways and modulating the tumor microenvironment.
Methods: *In vitro* stimulation of peripheral blood mononuclear cells (PBMCs) from CLL patients with IL-4/CD40L or IL-4/S100-A9 was made for 72 hours. S100-A9 and Ki-67 expression were assessed by flow cytometry. We generated a new Eμ-TCL1/S100A9/ murine model by crossing Eμ-TCL1 and S100A9−/ mice. Adoptive transfer (AT) into NOD-scid IL2Rgammanul (NSG) mice was performed using B-CLL isolated from aged Eμ-TCL1 or Eμ-TCL1/S100A9/. To evaluate the in vivo effect of S100-A9 inhibitors, we use C57BL/6 mice with adoptively transfer splenocytes from Eμ-TCL1 mice. Paquinimod (PaQ) and Tasquinimod (TasQ) were administered at a dosage of 25 mg/Kg in drinking water ad libitum for 4 weeks. Once the treatment was completed the animals were euthanized for tissue collection. Fluorescence-activated cell sorting (BD FACS Aria II) was used to isolate CD19+ for the Nanostring study. All immunophenotyping analysis was performed using a BD FACSymphony or a BD LSR II cytometer.
Results: S100-A9 expression in B cells from CLL patients increases after stimulation with IL-4/CD40L, likewise IL-4 in combination with rhS100-A9 promotes activation of Ki-67 in primary CLL cells. We also found that CD19+CD5+ lymphocytes from Eμ-TCL1 mice express high levels of S100-A9 protein in comparison with normal B cells from C57BL/6 mice. To better understand the role of S100-A9 in CLL, we developed a novel Eμ-TCL1/S100A9-/- mouse model. Eμ-TCL1/S100A9/ mice do not show structural abnormalities and develop a CLL phenotype characterized by the accumulation of CD19+/CD5+ cells in PB, BM, and secondary lymphoid tissues. However, these mice show a longer survival rate compared to Eμ-TCL1. Since the Eμ-TCL1/S100A9/ model is a global knock-out, we aimed to confirm whether the survival advantage was attributed to the deficiency of S100-A9 in the B-CLL cells. We, therefore, isolated CD19+/CD5+ B-CLL cells from Eu-TCL1 and Eu-TCL1/S100A9/ mouse spleens and adoptively transferred them into NSG mice. Our results show that the S100A9/ B-CLL cells grow slower than those from Eu-TCL1 mice. Moreover, NSG mice from the Eu-TCL1/S100A9/ group show accumulation of fewer tumor cells in the spleen and bone marrow. Longer survival was also observed in these mice compared to the Eu-TCL1 controls. Next, we evaluated the in vivo response to the S100-A9 inhibitors PaQ and TasQ. A significantly lower tumor burden and longer survival were found in mice treated with PaQ or TasQ compared to the vehicle group. Interestingly, S100-A9 inhibitors reduced the expression of PD-L1 and impaired the production of IL-10 and IL-6 by B-CLL cells. We also observed a reduction in the total number of patrolling monocytes and MDSCs after the treatment. T cells show a predominantly naïve and central memory phenotype with lower expression of exhaustion markers after being exposed in vivo to S100-A9 inhibitors. To dive deeper into the mechanism of how S100-A9 inhibition impairs CLL progression, we performed a Nanostring PanCancer immune profiling. Our data demonstrated significant downregulation in transcription factors (Fos, Jun, and Egr1) downstream to the MAPK pathway in S100A9/ B-CLL cells as well as PaQ-treated CD19+ cells.
Conclusion: Genetic and pharmacological targeting of S100-A9 impairs CLL cell growth *in vivo*, probably through a MAPK pathway-dependent mechanism. This data demonstrates for the first time the significance of targeting S100-A9 as a novel therapeutic approach in CLL.

Abstract ID: 1551883

Title: B cell receptor-mediated signals modulate rapid FOXO1 upregulation in chronic lymphocytic leukaemia: a role for deubiquitinate proteins?

Authors: Hassan Almuhanna, Jodie Hay, Michael Moles and Alison Michie

B cell receptor (BCR) engagement of CLL cells is vital for disease progression, driving cell survival, proliferation, and chemo-resistance. Forkhead box protein, subgroup O-1 (FOXO1), a transcription factor widely regarded as a tumour suppressor in B cell malignancies, is inactivated downstream of BCR activation. Previously, we demonstrated that the expression of FOXO1 is significantly upregulated in lymph node biopsies of poor prognostic patients and that FOXO1 activation induces chemosensitivity of BCR-targeted drug activity, positively regulating apoptosis, indicating that FOXO1 possesses a tumour suppressive function in CLL cells. We now demonstrate that FOXO1 expression is rapidly and significantly upregulated within 30 minutes of BCR crosslinking, with upregulation sustained for up to 2 hr; the BTK inhibitor ibrutinib inhibited BCR-mediated FOXO1 upregulation. Due to the rapid changes of FOXO1 protein expression upon BCR crosslinking and the known role of deubiquitinase (DUB) enzymes in regulating its function, we investigated whether DUB proteins were involved in the regulation of FOXO1 expression in CLL cells, with a view to identifying potential novel drug targets that could enhance current CLL treatment. Little is known about the role of individual DUB family members in CLL. Our analysis revealed dysregulated expression of DUB family members USP7, USP8, USP9x, USP10, and USP14 in freshly isolated CLL cells compared to healthy B-cells, all showing significant upregulation in CLL cells. Stratification of CLL patient samples by Binet stage also revealed that these DUB family

members were upregulated in poor prognostic (Stage C) patients compared with Stage A patients, suggesting that DUB proteins may represent a novel biomarker for CLL progression. Treatment of the CLL cell line MEC1 and primary CLL patient samples with DUB inhibitors including PR-619 (pan-DUBi), P5091 (USP7i) and HBX19818 (USP7i) alone reduces the phosphorylation of AKTS437 and FOXO1T24, indicating that DUBs play a role in inhibiting FOXO1 activity. These effects of DUBi were further enhanced upon combination with ibrutinib treatment, indicating a potential benefit of combining DUB inhibition with current ibrutinib therapy. Furthermore, we demonstrated that the DUBi/ibrutinib combination was synergistic in terms of inducing a 10% enhancement in apoptosis compared with single treatments, and significantly reduced proliferation in MEC1 cells at 72hr. USP7 has previously been shown to regulate a number of proteins including p53 and PTEN in CLL cells, and has been demonstrated to influence sub-cellular localisation of FOXO family members in melanoma. To define the relationship between FOXO1 and USP7, we performed co-immunoprecipitation assays and demonstrated a direct interaction between FOXO1 and USP7, an interaction that was increased upon BCR crosslinking. To elucidate a role for USP7 in CLL cells, we performed lentiviral-shRNA technology to selectively knockdown (KD) USP7 in MEC1, achieving 68% reduction in USP7 expression. Cells targeted with sh-USP7 showed downregulation of p-FOXO1T24 and total FOXO1 at protein levels, and significant increase in the gene expression of FOXO1. Furthermore, the expression of FOXO1 gene targets were altered, including a significant upregulation of Sestrin3 (SESN3), Bcl-2-like protein 11 (BCL2L11) and cyclin-dependent kinase inhibitor 1A (CDKN1A), and a significant downregulation of cyclin D2 (CCND2) and cyclin G2 (CCNG2). These data suggest that silencing USP7 increases FOXO1 functions, indicating that USP7 is responsible for the reduction of FOXO1 activities. As cellular localisation of FOXO1 dictates its DNA binding activity, we performed cellular fractionation on MEC1 and primary CLL cells in the presence and absence of ibrutinib and/or DUBi, and sh-USP7 KD MEC1 cells. These studies revealed a significant upregulation of FOXO1 in the nuclear fraction and upon ibrutinib treatment, which was further enhanced in the USP7 KD cells, or the combination with DUBi. Indeed, USP7 KD sensitised MEC1 cells to ibrutinib treatment leading to increase in FOXO1 nuclear localisation. Additionally, FOXO1 activity studies demonstrated significant activation of FOXO1 upon ibrutinib treatment, which was further enhanced in the USP7 KD and combination with USP7i. These studies suggest that selective DUBs play a role in BCR-mediated signalling to aid in the promotion of CLL cell survival and chemo-resistance through FOXO1 inhibition, and targeting these DUBs enhance FOXO1 activity leading to cell cycle arrest and apoptosis.

Abstract ID: 1551973

Title: Peripheral blood CXCR4hiCD5hi chronic lymphocytic leukaemia cells are primed for returning to the lymph nodes for further activation and proliferation

Authors: Robbert Hoogeboom, Friedman Daniel, Jennifer Vidler and Piers Patten

Chronic Lymphocytic Leukaemia (CLL) cells proliferate in the lymph nodes, where the microenvironment promotes activation, proliferation, and drug resistance of malignant cells. Following activation and proliferation in lymph nodes, CLL cells may migrate into the periphery as CXCR4loCD5hi cells and thought to transform into CXCR4hiCD5lo cells that remain quiescent until they return to the lymph nodes for further proliferation and activation. However, we poorly understand which peripheral blood CLL cells are able to return to the lymph nodes for re-activation. To identify which cells are most likely to return to the lymph nodes, we fractionated CD19+CD5+ cells of 22 CLL patients based on CXCR4 and CD5 densities and analysed their phenotype and functionality. Surprisingly, we found that the CXCR4hiCD5hi fraction of peripheral blood CLL cells is enriched for Ki67+ proliferating cells and high expression of the activation marker AID, demonstrating that CXCR4loCD5hi cells are not the only proliferating and activated fraction in the blood. Flow microscopy confirmed that the CXCR4hiCD5hi fraction contained proliferating cells. Analysis of blood and tissues of 10 Emu-Tcl1-transgenic mice revealed that murine CXCR4hiCD5hi CLL cells also expressed high levels of Ki67. Moreover, we found CXCR4hiCD5hi CLL cells were expanded in the spleens of Emu-Tcl1-transgenic mice and in the cervical lymph node of a CLL patient with mutated TP53 and de novo progressive disease. The peripheral blood CXCR4hiCD5hi fraction displayed high surface expression levels of the chemokine receptors CCR7 and CXCR5, which – together with CXCR4 – facilitate homing to lymph nodes. To investigate if CXCR4hiCD5hi CLL cells are primed for migration to lymphoid tissue, we stimulated peripheral blood CLL cells with CCL21, the ligand of CCR7, and found that the CXCR4hiCD5hi fraction was most efficient at migrating through transwells. CXCR4hiCD5hi CLL cells expressed high levels of surface IgM and had low basal nuclear localisation of Nuclear Factor of Activated T cells (NFAT), implicating that these cells are B cell receptor (BCR) responsive. In contrast, quiescent CXCR4hiCD5lo CLL cells had a pre-dominantly nuclear localisation of NFAT. To mimic stimulation in lymph nodes, we cultured peripheral blood CLL cells on CD40L-expressing fibroblasts in the presence of interleukin (IL)-4 and IL-21, inducing extensive proliferation of CXCR4hiCD5hi and CXCR4loCD5hi CLL cells after six days, while CXCR4hiCD5lo CLL cells remained quiescent. Peripheral blood CXCR4hiCD5hi CLL cells persisted BTK inhibition *in vi*tro, whereas the CXCR4loCD5hi fraction was effectively diminished by ibrutinib. Importantly, the CXCR4hiCD5hi cell fraction was expanded in patients that relapsed while on therapy, expressing higher levels of ki67, AID and chemokine receptors than before relapse. In conclusion, we have identified CXCR4hiCD5hi CLL cells as a potentially dangerous fraction of CLL cells that is primed for migration to tissue, receipt of BCR signals and proliferation. We provide evidence that these cells may give rise to proliferating cell phenotypes in tissues and anticipate this cell fraction may represent critical targets for therapeutic intervention.

Abstract ID: 1552075

Title: Deubiquitinase PSMD14 promotes progression of chronic lymphocytic leukemia by stabilizing CSDE1

Authors: Xin Wang, Xin Zhang, Ya Zhang, Xinting Hu, Yang Han, Hua Wang, Zheng Tian and Tiange Lu

Figure 1

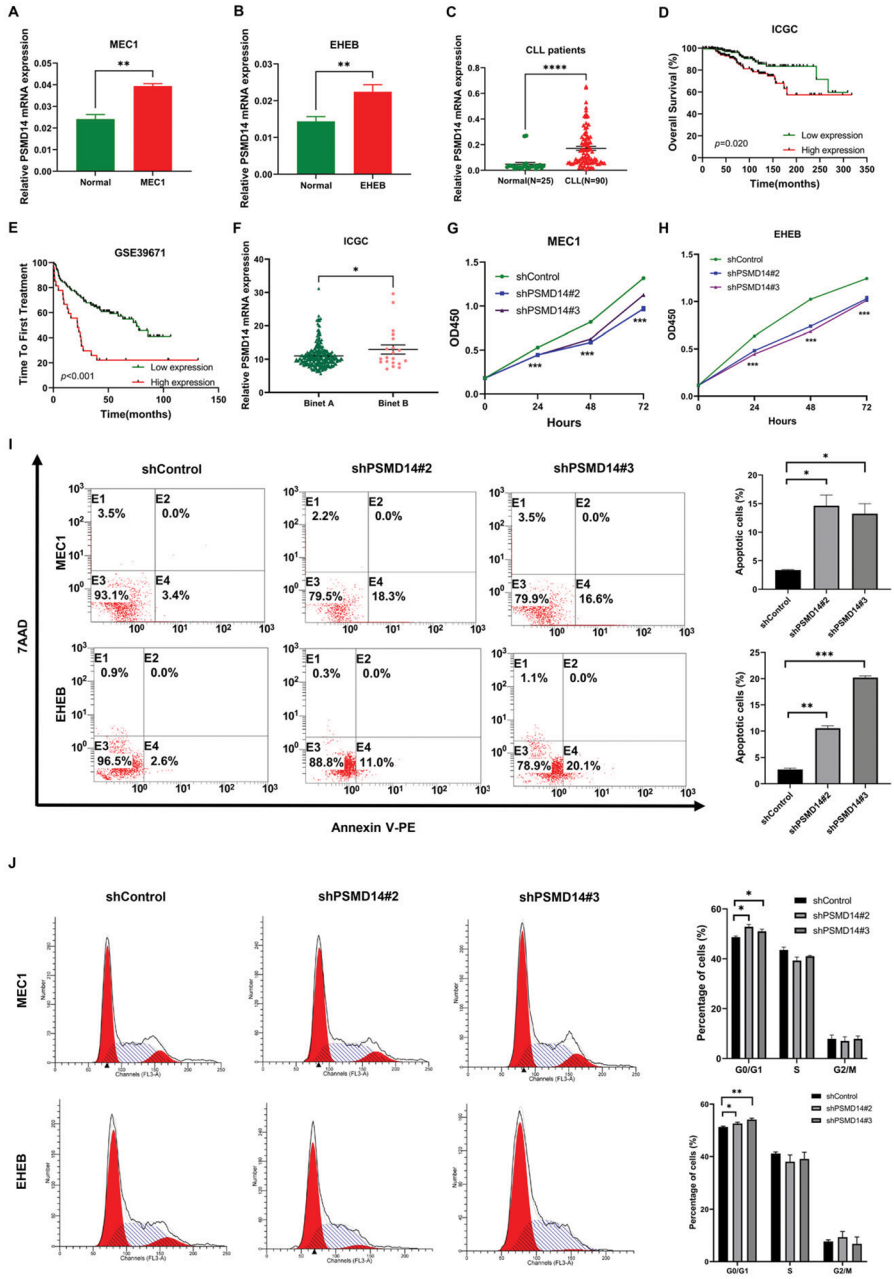

Introduction: Chronic lymphocytic leukemia (CLL) is a heterogeneous B-cell malignancy that lacks specific biomarkers and drug targets. The deubiquitinating enzyme 26S proteasome non-ATPase regulatory subunit 14 (PSMD14) has been reported to act as an oncogene in several human cancers. However, the roles and mechanisms of PSMD14 in CLL is not yet elucidated. Methods Quantitative real-time polymerase chain reaction was used to identify the expression of PSMD14 in CLL cell lines and CLL patients. CCK-8 assays were used to detect cell proliferation viability. The effect of PSMD14 on CLL cell apoptosis and cell cycle was analyzed by cell apoptosis and cell cycle assays. Ubiquitinated 4D-Label free quantitative proteome analysis was employed to probe the molecular mechanism of PSMD14. Deubiquitination assay was performed for explore the regulatory mechanism between PSMD14 and CSDE1.

Results': In this study, our results demonstrated that PSMD14 was significantly up-regulated in CLL cell lines and primary CLL specimens (Figure 1(A–C)). The up-regulation of PSMD14 expression predicted shorter overall survival and time to first treatment in patients with CLL (Figure 1(D,E)). Moreover, the overexpression of PSMD14 was correlated with Binet stage of CLL patients (Figure 1(F)). Knockdown of PSMD14 inhibited cell proliferation, promoted apoptosis and blocked the cell cycle in the G1/S phase (Figure 1(G–J)). Furthermore, pharmacological inhibition of PSMD14 with thiolutin (THL) suppressed the malignant behavior of CLL cells. Interestingly, the combination of THL and ibrutinib improves the sensitivity of CLL cells to ibrutinib. Mechanistically, we identified PSMD14 as a novel post-translational regulator of CSDE1. PSMD14 interacted with CSDE1 and inhibited degradation of CSDE1 via deubiquitinating this oncoprotein in CLL cells

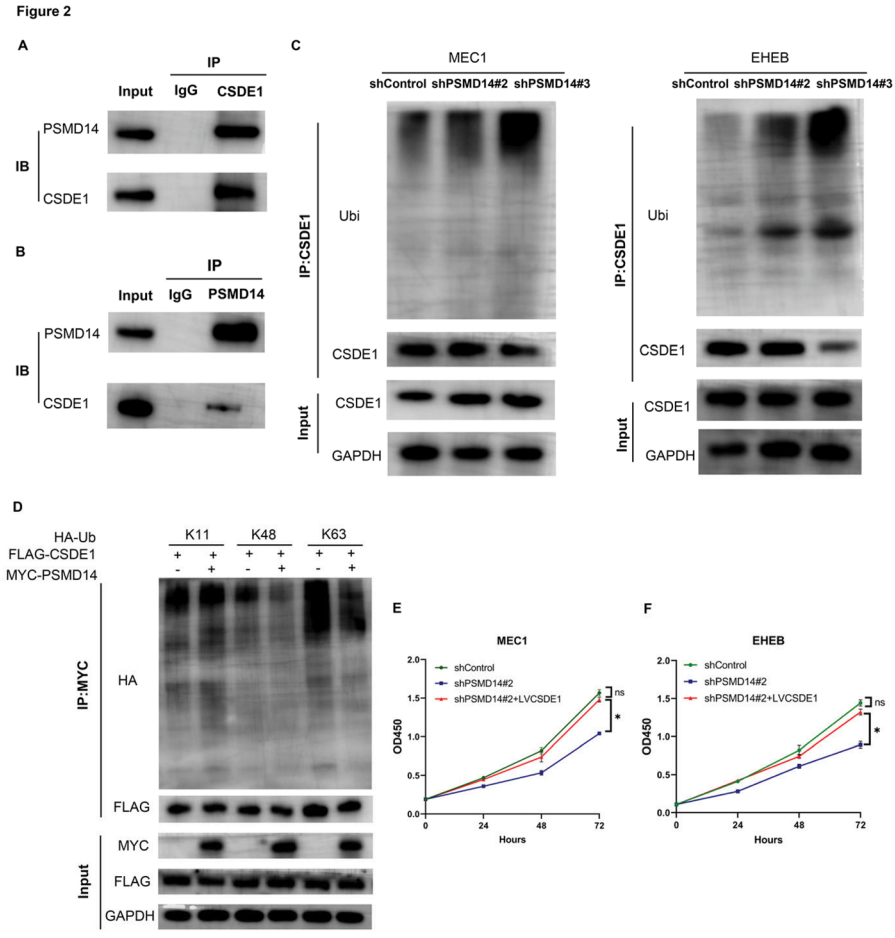

(Figure 2(A–C)). We also found that PSMD14 regulated K48 and K63 ubiquitination of CSDE1 (Figure 2(D)). Furthermore, rescue of CSDE1 expression was able to reverse the biological effects of PSAMD knockdown (Figure 2(E,F)), suggesting that PSMD14 exerts oncogenic effects through CSDE1. In addition, PSMD14 knockdown also attenuated the DNA repair potential in CLL. The PSMD14 knockdown groups were noted to have increased levels of phosphorylated ATM, CHK2 and H2AX.

Conclusion: In conclusion, our findings suggest that PSMD14 could serve as a promising therapeutic candidate for CLL. THL exhibits potent anti-tumor activities in CLL cells, highlighting a novel molecule-based strategy for CLL.

Abstract ID: 1552149

Title: Immunophenotypic characterization of richter syndrome diffuse large B-cell lymphoma type and comparison with the original chronic lymphocytic leukemia

Authors: Juan Marquet-Palomanes, Fernando Martin-Moro, Miguel Piris-Villaespesa, Jesus Villarubia, Eulalia Rodriguez-Martin, Ernesto Roldan, Mónica García-Cosío and Francisco Javier lópez-Jiménez

Introduction: Biological mechanisms undergoing Richter Syndrome diffuse large B-cell lymphoma type (DLBCL-RS) from a previous chronic lymphocytic leukemia (CLL) arouse great scientific interest, but the pattern of markers expressed in DLBCL-RS cases has been scarcely studied. Our aim was to immunophenotypically characterize DLBCL-RS and compare it with the prior CLL population.

Methods: Retrospective unicenter study of patients histologically diagnosed with DLBCL-RS (DLBCL not otherwise specified subtype) from a prior or concomitant CLL (Nf12). Multiparametric flow cytometry (FCM) and immunohistochemistry (IHC) were used to cluster cases according to their expression level for each marker: bright or moderate (positive), low (dim), or absent (negative). Comparisons were made between CLL and DLBCL-RS in available tissues (lymph node, blood, bone marrow, and others).

Results: Median age at DLBCL-RS diagnosis was 74 years (IQR 65–79) and 42% were males. Three cases were concomitantly diagnosed with CLL and DLBCL-RS; the median time of transformation in the remaining 9/12 was 76 months (IQR 51–112), and all of them had received at least 1 therapeutic line for the CLL (median 2). Clonal relationship was demonstrated in 9/10 cases with available information. Figure 1 shows the most relevant phenotypic comparisons between CLL and DLBCL-RS populations. Although phenotypic variability was seen for all antigens, some of them showed tendency to increase or decrease their pattern of expression. CD19, CD20, CD5, CD79b, and CD200 tended to lose expression in the DLBCL-RS phase (3/5 DLBCL-RS CD20 negative cases had received anti-CD20 therapy during

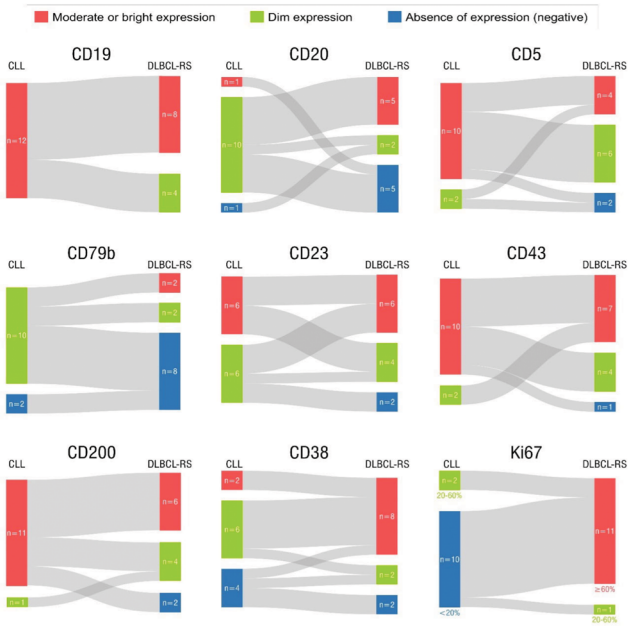

the 12-month period prior to transformation). On contrary, CD38 and Ki67 were constant in the increasing of expression. Other markers such as CD23, CD43, CD22, and CD11c presented higher variability. One case showed CD10 dim expression of the DLBCL-RS, while it remained negative in the other 11/12. The light-chain restriction was the same in 10/12 (κ/λ ratio of 1.5:1); 1/12 presented a switch from κ to λ, and 1/12 DLBCL-RS showed negativity for κ/λ, when κ was restricted in the CLL phase. p53 expression was available in 7 cases, being negative in CLL tissue in all of them: 3/7 retained p53 negativity in the DLBCL-RS, while 4/7 showed p53 overexpression after transformation. Treatment for the DLBCL-RS was initiated in 8/12 cases, being 92% death at data cut-off date (median follow-up 6.5 months from DLBCL-RS diagnosis, IQR 2.4–9.7).

Conclusions: As far as the authors know here is presented the largest series which compares the phenotype between CLL and its DLBCL-RS. The markers CD19, CD20, CD5, CD79b, CD38, Ki67, and p53 showed relevant changes at the moment of histological transformation. This research enhances the importance of validating reproducible assays to follow hematological malignancies with potential of transformation to more aggressive diseases.

Abstract ID: 1552185

Title: Targeted agents in chronic lymphocytic leukemia (CLL): data on outcomes and subsequent therapies of patients observed within the German CLL Study Group (GCLLSG) registry

Authors: Nadine Kutsch, Rudy Ligtvoet, Sandra Robrecht, Hartmut Linde, Thomas Illmer, Steffen Doerfel, Jörg Lipke, Ali Aldaout, Rudolf Schlag, Jolanta Dengler, Othman Al-Sawaf, Petra Langerbeins, Paula Cramer, Barbara Eichhorst, Michael Hallek, Kirsten Fischer and Anna Fink

Introduction: BCL2-inhibitors (BCL2i) and BTK-inhibitors (BTKi) have profoundly improved the outcome of patients (pts) with chronic lymphocytic leukemia (CLL) and are considered standard treatment. However, the translation from novel treatments evaluated within clinical trials into routine clinical practice can be complex. The German CLL Study Group Registry provides real world data of pts with CLL on therapy choices outside of clinical trials in Germany. We here present data on efficacy and subsequent therapies of a large cohort of pts treated with either BCL2i or BTKi.

Methods: Patients with confirmed diagnosis of CLL and with at least one documented first-line CLL treatment between July 1st 2014 and January 30th 2023 were included in this analysis. Treatments were categorized according to the backbone of therapy and pts were allocated to either the venetoclax or the BTKi cohort depending on their first treatment with targeted agents. Treatment sequences were visualized with a sankey-diagram. Time to next treatment (TTNT), event-free survival (EFS) and overall survival (OS) were analyzed using Kaplan-Meier methods.

Results: A total of 274 pts were treated with a venetoclax-based regimen while 915 pts were treated with a BTKi as first therapy using targeted agents. Median observation time from the first documented treatment in the venetoclax cohort was 26 months (range 0 – 296) and 78 months (range 0–266) for BTKi treatment. For the venetoclax cohort, the median age at the time of first venetoclax treatment was 71 years (range 32–87) with 172 pts (62.8%) being male. Median CIRS score was 2 (range 0–13) and 12 pts (7.5%) had an ECOG performance status >1. Among 57 pts with known molecular genetics, 32 pts (56.1%) had an unmutated IGHV status and 9 out of 51 evaluable pts (17.6%) had a deletion and/or mutation TP53 as high-risk feature. Applying the CLL-IPI, 11 out of 58 evaluable pts (19.0%) were in the very high-risk group. In the BTKi treated cohort, median age at time of first BTKi treatment was 72 (range 32–92), with 628 pts (68.6%) being male. Median CIRS score was 3 (range 0–17) and 45 pts (9.5%) had an ECOG performance status >1. Among 162 pts with available data, 108 pts (66.7%) had an unmutated IGHV status and 59 out of 130 evaluable pts (45.4%) had a deletion and/or mutation TP53. According to the CLL-IPI, 46 out of 145 evaluable pts (31.7%) were in the very high-risk group. 152 of 274 pts (55.5%) received venetoclax as firstline treatment (median prior treatments: 0, range 0–9) and 352 of 915 pts (38.5%) were treated with a BTKi in the first line (median prior number of treatments: 1; range 0–12). Among all 222 administered treatments prior to venetoclax and 1090 treatments administered prior to BTKi, chemoimmunotherapy (70.3 and 68.3%, respectively) and chemotherapy (10.4 and 17.8%, respectively) were the most frequent. Following the first venetoclax or BTKi treatment, pts were mainly treated with targeted agent regimens. In the venetoclax cohort, 37 subsequent treatments were documented in 26 pts, 10 of the subsequent treatments (27.0%) were a venetoclax-containing regimen and 13 (35.1%) a BTKi-containing regimen. Within the BTKi-based cohort, 393 subsequent treatments were administered in 264 pts, 146 (37.2%) included venetoclax and 106 (27.0%) a BTKi. Median EFS from the start of the first venetoclax treatment was 31.8 months, with a 2-year EFS rate of 66.6%. For the BTKi cohort, median EFS was 23.2 months, with a 2-year survival rate of 48.6%. Median TTNT was 63.7 months in the venetoclax cohort and 68.4 months for the BTKi cohort. Median OS was 96.5 months for the venetoclax cohort and 85.9 months for the BTKi cohort with a 2-year OS of 89.5 and 84.9%, respectively.

Conclusion: In our dataset of patients being treated within the GCLLSG registry between 2014 and 2023, targeted therapies

Figure 1: Sankey plot of last previous treatments (before) first Ven/BTKi regimen and first subsequent treatments (after) first Ven/BTKi regimen

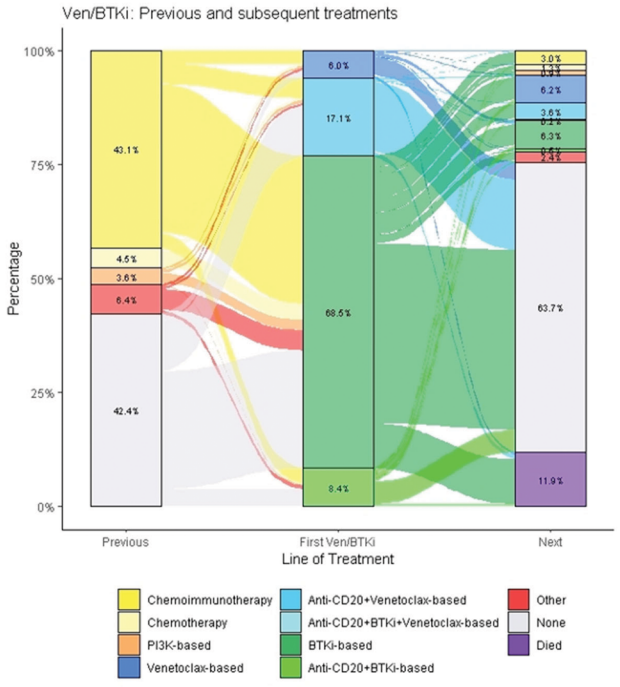

The last column shows (from top to bottom): Chemoimmunotherapy (3.0%), Chemotherapy (1.3%), BI3K-based (0.9%), Venetoclax-based (6.2%), Anti-CD20+Venetoclax-based (3.6%), Anti-CD20+BTKi+Venetoclax-based (0.2%), BTKi-based (6.3), Anti-CD20+BTKi-based (0.5%), Other (2.4%), None (63.7), and patients died (11.9%).

with venetoclax were administered as firstline treatment in 152 of 274 pts (55.5%) while 352 of 915 pts (38.5%) were treated with a BTKi. If prior treatments were given, the majority of pts still received chemo(immuno)therapy. EFS, TTNT and OS were comparable between the venetoclax and BTKi-based treatment cohort.

Abstract ID: 1552204

Title: Exploring the impact of germline ATM mutations in cancer susceptibility and inheritance in chronic lymphocytic leukemia

Authors: Francesca Morelli, Roberta Santos Azevedo, Kiyomi Mashima, Rayan Fardoun, Stacey Fernandes, Samantha Shupe, Marissa Terra, Anisha Patel, Joseph Yu and Jennifer Brown

Background: Chronic lymphocytic leukemia (CLL) patients have an increased, but still poorly defined, risk of secondary neoplasms [1]. Also, CLL has a strong inherited susceptibility, much of which has not been explained by common variants identified by GWAS [2]. Germline Ataxia-telangiectasia mutated (ATM) mutations are among the most common hereditary cancer risk mutations in CLL and other cancers [3]. Rare germline ATM variants are present in 24% of CLL patients, greater than other hematologic neoplasms [4] or the general population [5]. In CLL cases, loss of ATM heterozygosity through 11q23 deletion is associated with adverse prognosis and short progression-free survival following chemotherapy [6]. Whether these ATM variants predispose to other malignancies among CLL patients is unknown and could have implications for cancer screening in patients and their families. To evaluate this potential risk, we undertook a single-center retrospective study to analyze the impact of germline ATM in the predisposition to secondary neoplasm or other ATM-related syndromes in CLL patients and their relatives.

Methods: Five hundred and eighty-five patients seen at Dana-Farber Cancer Institute and who had NGS performed to evaluate germline ATM status, either through direct germline sequencing of saliva or by inference according to the hierarchical algorithm we recently published (Lampson, 2022), were mailed a questionnaire between April 2022 and May 2023. Of these, 320 patients (55%) replied. The questionnaire investigated: demographics; personal and family history of any cancer; non-medical radiation and Agent Orange exposure; ataxia-telangiectasia syndrome. European descendance was categorized based on the United Nations geoscheme [7], one of the systems used to classify countries into subregional groups. Information collected from our Database included FISH and IGHV status. Patients were stratified into four groups, based on ATM mutational status and del(11q), to analyze clinical and demographic characteristics: Group-1, ATM germline mutation alone ($N=61$) Group-2, ATM germline with somatic ATM mutation and/or del(11q)($N=23$) Group-3, ATM somatic aberration alone (including del(11q)) ($N=43$) and Group-4, no ATM aberration ($N=195$) (Figure 1). The patients were stratified into two groups based on the presence or absence of ATM germline mutation to analyze the cancer incidence (groups 1–2 vs. 3–4). All patients had provided written informed consent prior to sample and data collection.

Results: Out of the 320 patients in our cohort, demographic and clinical characteristics among the 4 groups were balanced at baseline, except for unmutated IGHV status. Eighteen (86%) and 37 (86%) patients of groups 2 and 3 had this feature compared to 21 (34%) and 72 (37%) of groups 1 and 4, respectively ($p<0.01$) (Table 1). A total of 211 cancers were reported in the 159 patients (50%) who had a history of another malignant neoplasm before or after CLL diagnosis. This incidence was reduced to 30% (97 patients) excluding patients with only non-melanoma skin cancers. When comparing the patients with germline ATM mutation present (82 patients) with germline ATM absent (238 patients), the incidence of colon cancer was slightly higher in patients with germline aberrations (3 patients, 4% versus 1, 0.4%, $p=0.05$). Two hundred and seventy-three patients (85%) reported at least one relative, including first, second and third-degree, with a cancer history, with a median of 2 relatives affected (1–16). The incidence of familial CLL was significantly higher ($p=0.04$) in patients with germline ATM present ($N=20$, 24%) compared to germline ATM absent ($N=35$, 15%). No difference in the incidence of other hematologic and solid malignancies was found between the relatives in the two groups. No group had an increased number of first-degree relatives with cancer, compared to the other. No patient reported familial or personal history of Ataxia Telangiectasia syndrome.

Conclusions: Germline ATM variants in CLL lead to an earlier diagnosis and an increased likelihood of del11q or somatic ATM mutation, leading to more rapid disease progression. These mutations have been previously associated with increased risk of developing other cancers, such as breast and gastrointestinal [8]; however, a certain role in the development of colon cancer is still unclear. Our results suggest a higher incidence of CLL inheritance, and a slightly

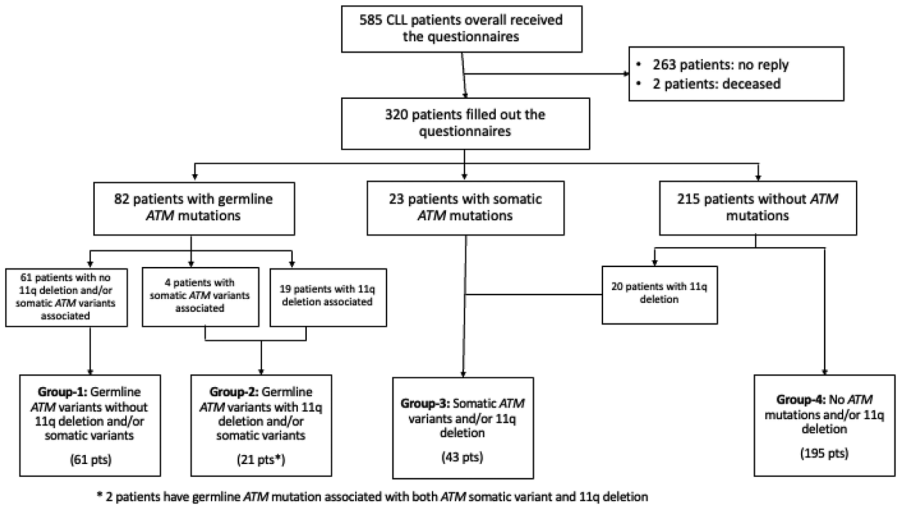

* 2 patients have germline *ATM* mutation associated with both *ATM* somatic variant and 11q deletion

Characteristic*	Patients (N 320)	Characteristic*	Patients (N 320)
Age at diagnosis		**Agent Orange exposure – n (%)**	
Median (range) – years	60 (28-89)	Yes	7 (2%)
Distribution – no (%)		No	311 (97%)
≤ 55 years	111 (35%)	Unknown	2 (1%)
> 55 years	209 (65%)	**European Descendance – n (%)**	
Sex – n (%)		Yes	198 (62%)
Male	185 (58%)	No	122 (38%)
Female	135 (42%)	**European Descendance – n (%)**	
Race – n (%)		Northern Europe	61 (31%)
White	316 (98%)	Northern and Western Europe	37 (18%)
Black or African American	2 (1%)	Southern Europe	29 (15%)
Asian	1 (0.5%)	Western Europe	23 (12%)
Native Hawaiian/Pacific Island	1 (0.5%)	Eastern Europe	23 (12%)
Ethnicity – n (%)		Northern and Southern Europe	13 (6%)
Not hispanic or latino	315 (98%)	Northern and Eastern Europe	9 (4%)
Hispanic or latino	3 (1%)	Western and Eastern Europe	3 (2%)
Unknown	2 (1%)	**Richter's transformation-n (%)**	
Ashkenazi Jewish descendance- n (%)		Yes	9 (3%)
Yes	22 (7%)	No	311 (97%)
No	293 (91%)	**IGHV status – n (%)**	
Unknown	5 (2%)	Mutated	140 (44%)
Non-medical radiation exposure – n (%)		Unmutated	148 (46%)
Yes	19 (6%)	Unknown	32 (10%)
No	299 (93%)	**17p deletion and/or TP53 aberration – n (%)**	
Unknown	2 (1%)	Yes	45 (14%)
		No	273 (85%)
		Unknown	2 (1%)

*All demographics are patients' self-reported. Patients categorized as "*no European descendance*" self-reported themselves as Americans.

increased incidence of colon cancer, in CLL patients who carry germline ATM mutation. Our study is limited by the relatively small sample size which we hope to further expand to explore this question more fully.

Abstract ID: 1552208

Title: An examination of health literacy amongst patients with chronic lymphocytic leukemia- a study from the lymphoma coalition global patient survey 2022.

Authors: Steve Kalloger, Shawn Sajkowski, Amanda Watson and Lorna Warwick

Introduction: Health literacy is a key aspect of efficient and meaningful communication between patients and physicians. Chronic cancer's such as chronic lymphocytic leukemia (CLL) can have a disease course that spans 10 years or longer. The length of this course allows patients to have the opportunity to engage in shared decision-making with their primary lymphoma care providers. We sought to quantify heath literacy using nine key terms relevant to those with CLL and examine if core survey demographics were predictors of poor health literacy.

Methods: The Lymphoma Coalition Global Patient Survey was deployed in 2022. Patients with CLL were asked if they understood the following terms: Stable disease, Indolent disease, Progressive disease, Tumor load, Clonal evolution, Treatment duration, Treatment holiday, Minimum residual disease (MRD) and No evidence of disease (NED). Responses were categorized into completely and partially understand vs. no understanding. Frequency distributions were used to

enumerate responses. Associations with core demographics were performed with contingency analysis and quantified with the Likelihood Chi Square or Fisher's Exact Test as appropriate.

Results: The average rate of response for all questions was 676 and ranged between 668 and 687. The respondents had a mean age of 64 years and ranged from [26 to 97]. Forty-seven percent were female. Sixty-three percent had not experienced a relapse while 23% and 14% had experienced one or more than one relapse respectively. The frequencies of comprehension across the 9 terms are shown in Table 1. The examination of associations with core demographics demonstrated that females had significantly better comprehension than males for the terms: Progressive Disease (OR =1.7 [95%CI =1.1–2.7]); Clonal Evolution (OR =1.5 [95%CI =1.1–2.1]); and Minimal Residual Disease (MRD) (OR =1.5 [95%CI =1.03–1.9]). Receiving post-secondary or higher education resulted in increased comprehension of: Treatment Duration, Minimal Residual Disease (MRD), and Indolent Disease ($p <= 0.008$). Examination of Household Status, Age and Area of Residence revealed very mild associations with comprehension of the terms of interest. Regional differences did exist and are displayed in Table 2, with North America having an average rate of comprehension across the 9 terms of 72.8% followed by Europe and Asia-Pacific with 69.8 and 65.2%, respectively.

Conclusion: The results suggest that there is significant heterogeneity in the comprehension of terms common to the CLL experience. While it can be expected that terms such as Treatment Duration and Stable Disease to exhibit almost universal understanding, the lack of familiarity with the last five terms in Table 1 may indicate a blind spot with regard to awareness of the long term prognosis of the disease. While it is difficult to say whether this stems from the patient not wanting to know, from primary lymphoma care providers using other terminology or actively withholding such information, a lack of comprehension will make shared decision making more challenging. A limitation of our study is that the terms we selected to reflect health literacy may not reflect the medical vernacular of various geographic regions. As expected, those with higher educational levels exhibited improved comprehension. Surprisingly, although we expected to find no differences, females exhibited increased comprehension relative to males for a number of terms. Overall, these results suggest that there is room for improvement in health literacy for patient's with CLL – especially for factors that can influence prognosis of their disease. We feel that good health literacy is one of the necessary components patient's should possess in order to facilitate increased participation in their care.

Table 1. Rate of comprehension for the 9 terms examined in the Lymphoma Coalition Global Patient Survey (2022). These items are ranked from highest to lowest levels of comprehension.

Term	Understood	Not Understood
Treatment Duration	652 (95.3%)	32 (4.7%)
Stable Disease	615 (89.5%)	72 (10.5%)
Progressive Disease	584 (85.8%)	97 (14.2%)
Treatment Holiday	537 (80.3%)	132 (19.7%)
No Evidence of Disease (NED)	429 (64.1%)	240 (35.9%)
Indolent Disease	413 (60.3%)	272 (39.7%)
Tumor Load	400 (59.5%)	272 (40.5%)
Minimum Residual Disease (MRD)	398 (59.4%)	272 (40.6%)
Clonal Evolution	205 (30.7%)	463 (69.3%)

Table 2. Rate of comprehension for the 9 terms examined in the Lymphoma Coalition Global Patient Survey (2022) across geographic regions. NOTE: Middle East & Africa and South America have low response rates and the estimates should be interpreted with caution.

Term	Asia-Pacific	Europe	Middle East and Africa	North America	South America
Stable disease					
No	18 (15.0%)	47 (9.4%)	0 (0.0%)	7 (11.7%)	0 (0.0%)
Yes	102 (85.0%)	454 (90.6%)	2 (100.0%)	53 (88.3%)	4 (100.0%)
Indolent disease					
No	39 (31.7%)	214 (43.3%)	0 (0.0%)	19 (31.7%)	0 (0.0%)
Yes	84 (68.3%)	282 (56.8%)	2 (100.0%)	41 (68.3%)	4 (100.0%)
Progressive disease					
No	17 (14.5%)	72 (14.5%)	0 (0.0%)	8 (13.3%)	0 (0.0%)
Yes	100 (85.5%)	426 (85.5%)	2 (100.0%)	52 (86.7%)	4 (100.0%)
Tumour load					
No	62 (53.0%)	187 (38.3%)	1 (50.0%)	22 (37.3%)	0 (0.0%)
Yes	55 (47.0%)	303 (61.8%)	1 (50.0%)	37 (62.7%)	4 (100.0%)
Clonal evolution					
No	83 (72.3%)	338 (69.1%)	2 (100.0%)	38 (65.5%)	2 (50.0%)
Yes	32 (27.8%)	151 (30.9%)	0 (0.0%)	20 (34.5%)	2 (50.0%)
Treatment duration					
No	13 (10.9%)	16 (3.2%)	0 (0.0%)	3 (5.2%)	0 (0.0%)
Yes	106 (89.1%)	485 (96.8%)	2 (100.0%)	55 (94.8%)	4 (100.0%)
Treatment holiday					
No	54 (46.6%)	60 (12.3%)	1 (50.0%)	17 (29.3%)	0 (0.0%)
Yes	62 (53.4%)	429 (87.7%)	1 (50.0%)	41 (70.7%)	4 (100.0%)
Minimal residual disease (MRD)					
No	45 (38.1%)	210 (43.0%)	2 (100.0%)	15 (25.9%)	0 (0.0%)
Yes	73 (61.9%)	278 (57.0%)	0 (0.0%)	43 (74.1%)	4 (100.0%)
No evidence of disease (NED)					
No	36 (30.8%)	180 (38.7%)	1 (50.0%)	14 (24.1%)	0 (0.0%)
Yes	81 (69.2%)	299 (61.3%)	1 (50.0%)	44 (75.9%)	4 (100.0%)

Abstract ID: 1552217

Title: An investigation into the differences between Western and Chinese population with chronic lymphocytic leukemia

Authors: Shuhua Yi, Jiawen Chen, Tingyu Wang, Yuting Yan, Rui Lv, Qi Wang, Wenjie Xiong, Wei Liu, Gang An, Yan Xu, Zhen Yu, Dehui Zou, Jianxiang Wang and Lugui Qiu

Introduction: The incidence of Chronic Lymphocytic Leukemia (CLL) is notably lower in Asian population, being 10–20-fold less than that in Western population. Previous research has indicated that CLL in China tend to be younger, exhibit more mutated immunoglobulin heavy-chain variable genes (IGHV), and possess a unique mutation landscape. However, there are few large series cohort to systematically illustrate difference of CLL between Chinese and Western population.

Methods: We analyzed clinical data from 2005 CLL patients treated at the Blood Diseases Hospital, Chinese Academy of Medical Sciences, from February 2000 to December 2020. Furthermore, we collected the Immunoglobulin heavy chain variable (IGHV) sequences of 1223 Chinese CLL patients and compared them to sequences from 7424 published CLL patients from Europe and the United States.

Results: The median patient age at diagnosis was 61 years (range 20–92), which is younger than Western CLL patients, who typically are 65–70 years old. Additionally, a larger proportion of our patients had Binet stage B or C at diagnosis (69.3%) compared to Western CLL patients (20–40%). Among 1476 patients with available treatment data, 1191 (80.7%) received treatment, which is a higher proportion than in Western countries. The time from diagnosis to first treatment (TTFT) was shorter than in Western countries, being 7.0 months (95% CI 4.1–9.9). Chemotherapy, immunochemotherapy, and targeted therapy constituted

69.1, 14.4, and 16.5% of first-line treatments, respectively, leading to varying overall response rates (ORR). After a median follow-up period of 76.0 months (95% CI 72.2–79.8), we observed certain progression free survival (PFS) and overall survival (OS) rates. The observed outcomes were similar to those reported in Western studies. As anticipated, patients receiving immunochemotherapy and targeted therapy showed better PFS and OS than those receiving chemotherapy. Regarding cytogenetic abnormalities, we observed a lower proportion of RB1 deletion (20.9%) compared to Western countries, while the frequency of other cytogenetic abnormalities was similar. When compared to Western CLL, Chinese CLL showed a higher proportion of mutated IGHV, higher frequent usage of certain IGHV fragments, and lower frequent usage of others. Additionally, certain IGHD and IGHJ fragments were either more or less frequently used in Chinese CLL. Stereotyped BCR was found in 15.3% of CLL patients, which is less than in Western countries. Furthermore, the frequency of certain subsets was higher or lower in Chinese CLL compared to Western CLL.

Conclusions: This study, the largest real-world investigation involving Eastern CLL to date, provides an essential foundation for future clinical investigations of CLL in China. Despite patients being younger, having advanced stages at diagnosis, the outcomes did not deviate from those reported in Western studies. The biological difference may contribute to the discrepancy.

Abstract ID: 1552244

Title: Efficacy of immune checkpoint inhibitors for the treatment of advanced melanoma (AM) in patients with concomitant chronic lymphocytic leukemia (CLL)

Authors: Samuel Cass, Joshua Tobin, Dave Seo, Georgina Gener-Ricos, Emily Keung, Elizabeth Burton, Michael Davies, Jennifer McQuade, Paul Hampel, Jennifer Wargo and Alessandra Ferrajoli

Introduction: CLL is the most prevalent adult leukemia and is associated with an increased risk of melanoma. CLL alters systemic immunity and can induce T-cell exhaustion, which may limit the efficacy of ICI in patients with CLL. Immune checkpoint inhibitors (ICI) have revolutionized management of AM, but data on ICI effectiveness have largely been restricted to clinical trials, thereby excluding patients with co-existing malignancies. We, therefore, sought to examine the efficacy of ICI for melanoma in patients with concomitant CLL and AM.

Methods: In this international and multicentre retrospective study, review of clinical databases identified patients with concomitant CLL and AM treated with ICI from two US tertiary cancer centers ($n=39$) and an Australian multi-institutional experience (AUS, n=19). Objective response rates (ORR), defined as complete or partial response by RECIST v1.1, and survival outcomes (overall survival, OS, and progression-free survival, PFS) among patients with CLL and AM were assessed. Clinical factors associated with improved ORR and survival were explored. Additionally, ORR and survival outcomes were compared between the Australian CLL/AM cohort ($n=19$) and a control cohort of 148 Australian patients with AM alone.

Results: Between 1997 and 2020, 58 patients with CLL were treated with ICI for concomitant AM. ORRs were comparable between AUS CLL/AM ($n=19$) and AM control cohorts ($n=148$) (53 vs. 48%, $p=0.81$) (Figure 1). PFS and OS from ICI initiation were also comparable between cohorts. Among all CLL/AM patients ($n=58$), ORR was 41%. A majority were untreated for CLL (64%) at the time of ICI. Patients with prior history of treatment for CLL had significantly reduced ORRs (21 vs. 51%, $p=0.04$), PFS (3.6 vs. 14.6 months, $p=0.005$), and OS (7.4 vs. 52.2 months, $p=0.002$), compared to patients on observation for their CLL. Prior treatment with T-lymphocyte depleting chemoimmunotherapy was particularly associated with poor outcomes (median OS of 7.0 months, median PFS of 3.4 months) (Figure 2). On univariate analysis, prior treatment for CLL, high risk CLL 17p deletion, and higher CLL Rai stage were associated with shorter PFS from ICI, though CLL treatment was the only factor independently associated with shorter PFS in the multivariate model (HR 6.5, [CI 2.1–20.3], $p=0.001$]. Overall, 3 patients developed

Figure 1. ICI objective response rates for treatment of advanced melanoma alone (n=19) or advanced melanoma with concomitant CLL (n=148)

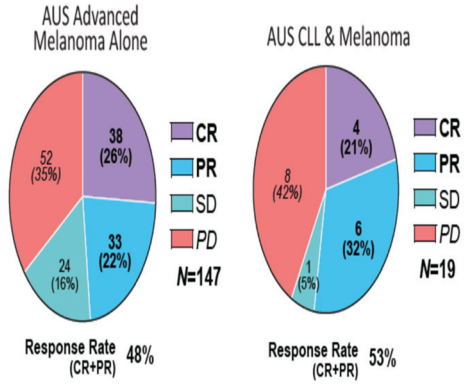

*Objective response defined as complete or partial response by RECIST v1.1.

Abbreviations: CR, complete response; PR, partial response; SD, stable disease; PD, progressive disease

Figure 2. Overall survival (left) and progression-free survival (right) following ICI for advanced melanoma in patients with concomitant CLL, stratified by prior treatment for CLL

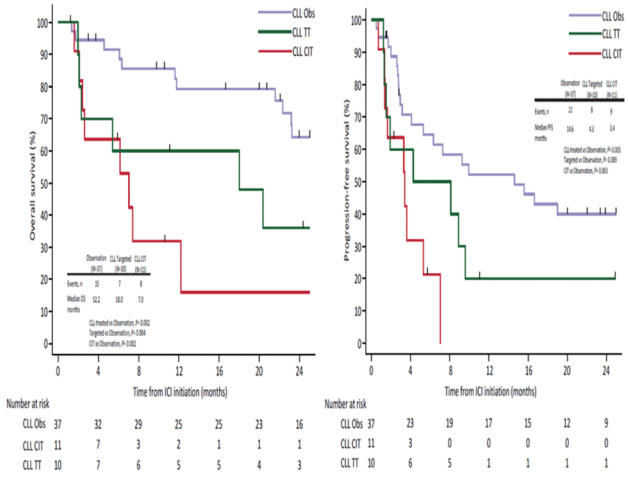

Abbreviations: Obs, observation (no prior or concurrent CLL treatment); TT, targeted therapy; CIT, chemoimmunotherapy; ICI, immune checkpoint inhibition.

CLL progression while on ICI, though in two of these patients, the AM had an objective, durable clinical response to ICI. Overall, immune-related adverse events (irAE) occurred following 38% of ICI and rates of irAE were similar by CLL treatment status.

Conclusions: Our case series of patients with concomitant CLL and melanoma demonstrate frequent, durable clinical responses to ICI However, those with prior chemoimmunotherapy treatment for CLL had significantly worse outcomes. We found that CLL disease course is largely unchanged by treatment with ICI.

Abstract ID: 1552256

Title: Covalent menin inhibitor, BMF-219, impacts key gene signatures and molecular pathways in chronic lymphocytic leukemia patient-derived models

Authors: Priyanka Somanath, Daniel Lu, Mini Balakrishnan and Thomas Butler

Chronic lymphocytic Leukemia (CLL) is the most common type of adult leukemia characterized by clonal proliferation of malignant B-lymphocytes. Although standard-of-care agents are well tolerated in CLL, patients with certain genetic subsets of the disease continue to display poor response to these therapeutic regimens. Menin is an epigenetic protein that drives oncogenic function through transcriptional regulation directed by interactions with various protein partners. In the B-cell maturation pathway, menin regulates a distinct set of genes targets [1]. We previously described the potent activity of BMF-219, a selective covalent oral menin inhibitor, against a diverse panel of CLL patient specimens with various cytogenetic and mutational backgrounds, including TP53 and NOTCH1 mutations. We also reported the ability of BMF-219 to downregulate the anti-apoptotic gene, BCL2, an established major driver of CLL, in acute leukemia cells. Here, we provide insights into the molecular impact of BMF-219 in CLL patient samples, as revealed through gene expression profiling of CLL specimens from BTK-inhibitor experienced patients that represent clinical profiles of TP53 mutated and complex cytogenetic backgrounds (del13q, del6q). BMF-219 displayed on-target activity through dose dependent reduction of the target gene, MEN1, in the treated patient samples. Differential gene expression analysis revealed alteration of additional novel gene targets, including reduction of BCL2 and genes modulated in response to prior BTK-inhibitor treatment. Gene set enrichment analysis highlighted top altered molecular pathways in BMF-219 treated CLL models. Notably, cell adhesion, cytokine receptor signaling, and autoimmune function were top downregulated pathways in BMF-219 treated CLL patient samples. Gene ontology analysis of biological processes and molecular function identified additional novel mechanisms elicited by BMF-219 in these treated CLL models. Furthermore, we provide new data demonstrating the superior potency of BMF-219 and ability to achieve >98% growth inhibition in ex vivo cultured CLL patient specimens when compared to new investigational drugs currently in clinical development and established standard-of-care agents for CLL. Collectively, these data demonstrate the mechanistic impact of BMF-219 on key gene targets and molecular pathways modulated by covalent menin inhibition, further highlighting its potential as a novel therapeutic agent in CLL.

Abstract ID: 1552313

Title: High-risk International Prognostic Score for early asymptomatic CLL (IPS-E) identifies chronic lymphocytic leukaemia at risk of progression to treatment in the OXPLORED study, a prospective observational study for early lymphoproliferative disease

Authors: Georgeta Ciuban, Gagandeep Batth, Hélène Dreau, Thomas Wenban-Smith, Melinda Kormany, Kate Ridout, Pauline Robbe, Grigore-Aristide Gafencu, Dimitris Vavoulis, Clare Freestone, Daniel McAleese, Anna Schuh and Niamh Appleby

Title: High-risk IPS-E identifies CLL at risk of progression to treatment in the OXPLORED study, a prospective observational study for early lymphoproliferative disease Early identification of people with MBL and CLL who will experience disease progression is challenging. Randomised trials of early intervention reported fewer progressors in the untreated arm than predicted by scoring systems [1,2]. Robust tools to delineate CLL prognostic subgroups at diagnosis are needed to enable future trials of targeted treatment. In a large retrospective analysis, the one year risk of requiring treatment was <1, 3 and 14% with a cumulative incidence of treatment at 5 years of 8, 28 and 61% for patients with low-risk, intermediate-risk and high-risk International Prognostic Score for asymptomatic early-stage CLL (IPS-E), respectively [3]. The Oxford Pre-malignant Lympho-proliferative Disorders (OXPLORED) study (REC 19/SC/0065; NCT04023747) offers the opportunity for prospective assessment of these data. OXPLORED is an observational multi-centre study recruiting 800 participants with newly diagnosed MBL and early asymptomatic CLL at 15 sites across England. Participants provide sequential blood, plasma and in selected participants marrow samples over five years and optional informed consent for WGS via the National Genome Research Library (NGRL; REC: 20/EE/0035). 241 participants (137 male; 104 females; median age 67 years (IQR 60–73 years)) enrolled prior to the interim data lock on 30th September 2022. After mean follow-up of 11.4 months, 10/241 MBL/CLL participants had progressed to requiring treatment. To date, paired CD19+ B-cells (tumour) and salivary (germline) have been whole genome sequenced from 165 MBL/CLL participants and IGHV status determined by NGS from an additional 76 participants. So far, IPS-E has been calculated for 85 participants, based on available data. Participants scored 1 for palpable lymphadenopathy, 1 for lymphocytosis >15×109/L and 1 for unmutated IGHV (u-IGHV; baseline on germline homology >98%). The V3-21 #subset 2 rearrangement detected in two participants was considered equivalent to u-IGHV. The sum of the three variables was translated into low-risk (score 0), intermediate-risk (score 1) and high-risk (score 2–3) IPS-E scores. After of 11.4 months follow-up, no participant with low-risk IPS-E progressed, two of 27 (7.4%) intermediate-risk IPS-E and 5/31 (16.1%) high-risk IPS-E participants required treatment. In our prospective study, progression to treatment parallels the cumulative

Table: OXPLORED participants (n=241) recruited prior to 30-Sept-2023		
Blood Parameters		Median, IQR
	Haemoglobin	140g/L (129-148)
	WCC	16.9x10^9/L (12.3-29.6)
	Lymphocytes	11.75x10^9/L (7.24-24.0)
	Platelets	209.5x10^9/L (169-252.5)
	B2microglobulin	2.3mg/L (1.9-3.7)
Diagnosis		Number of participants
	MBL	44
	Early stage CLL	180
	Data missing	17
	Total	241
IGHV-status	Mutated	65*
	Unmutated and/or #subset2	28*
	Pending IGHV-status	148
IPS-E parameters	Lymphocytes > 15x10^9/L	95
	Nodal disease	148
	Unmutated and/or #subset2	28*
*Based on available results 31st May 2023		

incidence of treatment predicted at 1 year by the IPS-E score. The full dataset on all 241 participants will be available for presentation at IWCLL 2023.

Abstract ID: 1552337

Title: Unveiling the spectrum of genetic alterations in relapsed/refractory CLL patients on targeted inhibitors: a prospective unicentric study

Authors: Dominika Écsiová, Pavel Vodárek, Lukáš Smolej, Filip Vrbacký, Kateřina Hrochová, Michaela Řehounková and Martin Šimkovič

Introduction: Next-generation sequencing (NGS) has been instrumental in characterizing the genomic landscape of Chronic Lymphocytic Leukemia (CLL). While a wealth of predictive data has been derived predominantly from large phase 3 trials, comprehending the practical implications of CLL mutational landscape continues to present challenges due to the presence of variants of uncertain significance (VUS) and minor clone presence. Real-world studies that trace clonal evolution can serve as a bridge to this knowledge gap, offering insights into the pathology of CLL. Therefore, our goals were to map genetic mutations, track clonal evolution, specify associated parameters, and uncover their potential associations.

Patients and methods: This prospective unicentric study included patients with relapsed or refractory CLL who were initiating treatment with oral kinase inhibitors between 2019 and 2022 at our hematologic center. CLL cells were isolated using the RosetteSep method. Following cell separation, DNA samples were analyzed using a custom capture-based panel (SureSelect XT HS by Agilent) for CLL-associated genes. This NGS analysis was performed using the Illumina MiSeq platform. Further sample collection after 12 months of therapy and at disease progression was planned.

Results: We studied a cohort of 45 CLL patients with a median age of 72 years, 71% male. A significant proportion 76% of patients had unmutated IGHV, 40% displayed TP53 mutation and/or del17p; del11q was identified in 33% of patients. Complex karyotype was detected in 11% of cases. The median follow–up was 22 months. With regard to treatment, 56% received Brutone tyrosine kinase (BTK) inhibitors, others received Bcl-2 inhibitor venetoclax (31%) or PI3K inhibitor idelalisib (13%). Basic characteristics and prognostic factors are summarized in Table 1. Molecular profiling of the 63 samples from 45 patients revealed a broad spectrum of gene mutations and variants. The most frequent oncogenic mutations were observed in the TP53 gene (40% of cases, $n=25$) and the SF3B1 gene (37% of cases, $n=23$). NOTCH1 and ATM mutations were also notable, each appearing in 19% of instances ($n=12$ each). Oncogenic variants were identified also in the following genes: ASXL1, ATM, BCL2, BCOR, BIRC3, BRAF, BTK, CARD11, DDX41, ETV6, FBXW7, IKZF3, KIT, KRAS, MED12, NFKBIE, NOTCH1, NRAS, PLCG2, POT1, RPS15, SAMHD1, SF3B1, STAG2, TET2, TP53, TRAF2, WT1, XPO1, ZRSR2. Upon further analysis, VUS were found in several genes, including ATM, GATA2, KIT, NOTCH1, RPS15, STAG2, TP53, and ZRSR2. Clonal evolution was assessed in 16 patients, with genomic changes in 15 (94%). New mutations emerged in 11 patients (69%), with observed genes including XPO1, KRAS, BIRC3, TRAF2, NRAS, BRAF, TP53, RPS15, ATM, MED12, SF3B1, TET2, BTK, and NOTCH1. Meanwhile, 5 patients (31%) experienced the disappearance of certain mutations, specifically those in NOTCH1, STAG2, WT1, KIT, KRAS, TP53, IKZF3 and SAMHD1. In one patient, a benign BCL2 mutation was initially detected and followed an oncogenic variant in the same gene in a subsequent sample. Additionally, one patient demonstrated disease progression associated with the emergence of a BTK mutation.

Conclusion: This interim analysis points to the dynamic and complex nature of genomic alterations in CLL, with implications for disease progression and therapeutic responses. Our findings highlight the importance of longitudinal genomic monitoring to uncover evolving mutational profiles and their clinical implications.

Sloupec1	Sloupec2
Table 1. Patient Characteristics and Clinical Data	
Characteristics	**N (%)**
Total number of patients	45
Median age	72 years (range 45-86)
Male patients	32 (71%)
Median follow-up	22 months
Median number of previous treatment lines	3 (range 2-5)
Median ECOG score	1 (range 0-2)
Treatment	
Bcl 2 inhibitor	14 (31%)
BTK inhibitor	25 (56%)
PI3K inhibitor	6 (13%)
Prognostic marker	
Unmutated IGHV	34 (76%)
Del17p and/or TP53 mutation (by Sanger and FISH)	18 (40%)
Del11q	15 (33%)
Del13q	26 (58%)
Trisomy 12	5 (11%)
Complex karyotype	5 (11%)
Data at the start of treatment	
Rai modified risk: low	1 (2%)
Rai modified risk: intermediate	16 (35%)
Rai modified risk: high	29 (63%)
Bulky lymphadenopathy (> 5cm)	16 (36%)
Splenomegaly (> 13 cm in craniocaudal length)	18 (40%)
Thrombocytopenia (< 100 x 10^9/L)	14 (31%)
Anemia (< 100 x 10^9/L)	11 (24%)
B2M over ULN	28 (62%)
LDH over ULN	32 (71%)
Decreased ClCr G-C (< 70mL/min)	31 (69%)

Abbreviations: ECOG, performance status scale, IGHV immunoglobulin heavy chain variable region, TP53, tumour protein p53, BCL-2, B-cell lymphoma 2, BTK, Bruton tyrosine kinase, PI3K, phosphatidyl inositol 3-kinase, LDH, lactate dehydrogenase, ClCr G-C, creatinine clearance the Cockcroft and Gault formula, N, number, B2M, β2 microglobulin, ULN, upper limit of mormal

Figure 1. Heatmap of Genetic Mutation Distribution in the Studied Cohort (pre-treatment samples)

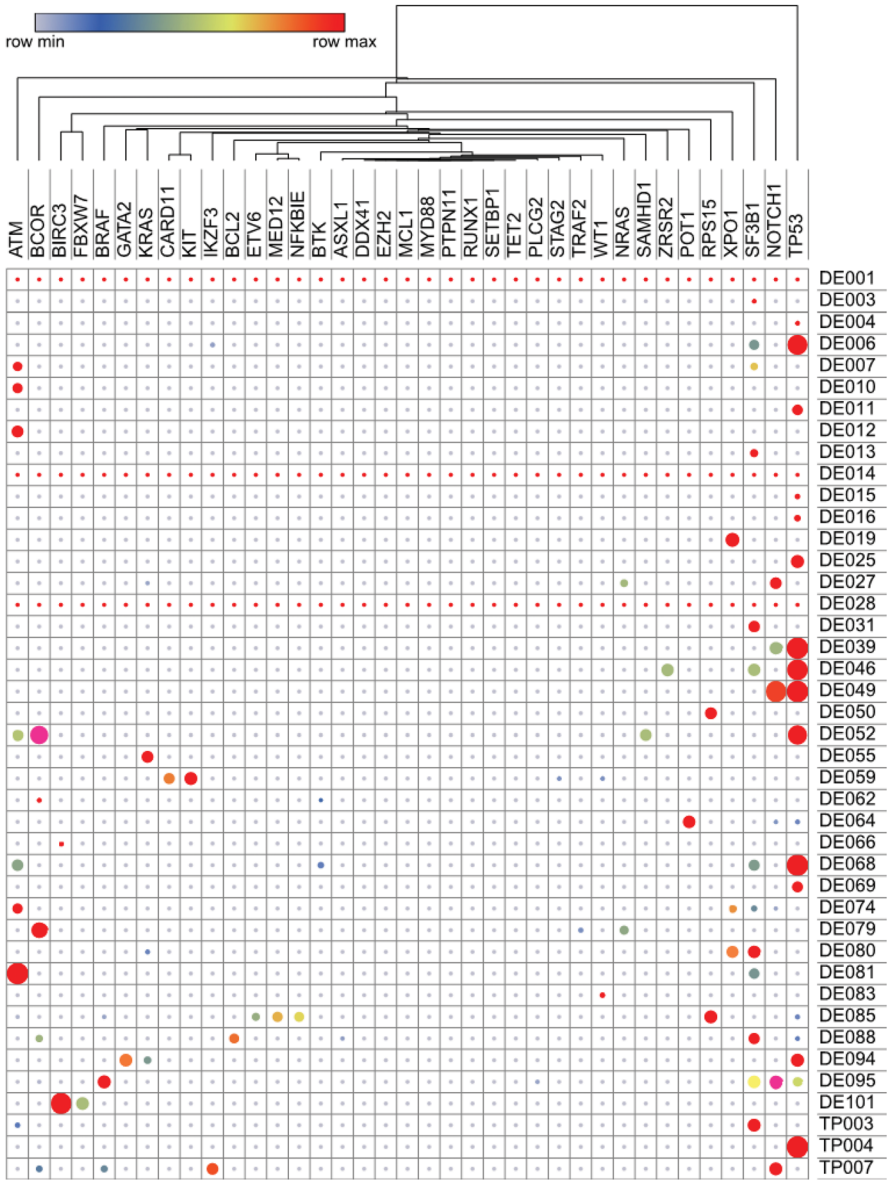

Abstract ID: 1552343

Title: Characterizing specificities of chronic lymphoid leukemia harboring a BCL2 rearrangement, an update from the FILO group

Authors: Charles Herbaux, Rayane Berrahouane, Loic Ysebaert, Agnes Daudignon, Romain Guieze, Hugo Navarro, Liam Hackett, Stephen Chong, Kamel Laribi, Alain J. Delmer, Florence Cymbalista, Florence Nguyen-Khac, Jennifer R. Brown, Matthew S. Davids and Stephanie Poulain

Introduction: Although survival dependence on BCL2 is a well-known aspect of the pathophysiology of chronic lymphocytic leukemia (CLL), the mechanisms of BCL-2 dysregulation are incompletely understood. Recurrent translocations involving BCL2 and immunoglobulin genes, including t(14;18)(q32;q21) and variants such as t(2;18) or t(18;22), are classically observed in follicular lymphoma or germinal center diffuse large B-cell lymphoma (GC DLBCL), but are uncommon (<5%) in CLL and usually associated with an indolent clinical course. Here, we characterize the mutational landscape and the functional BCL-2 family dependencies of BH3 proteins in BCL-2-rearranged (BCL2-R) CLL.

Methods: Clinically annotated primary samples from BCL2-R CLL patients identified by karyotype were obtained from the French Innovative Leukemia Organization network and Dana-Farber Cancer Institute. Primary samples from CLL without BCL2 rearrangement were used as a control (ctrl CLL). Next generation sequencing (NGS) was performed using a custom-designed panel of 60 genes, including among others: BCL2, BIRC3, NOTCH1, FBXW7, MLL2, RAS pathway, SF3B1 and TP53. The mean coverage obtained was 2000×(limit of detection (LOD): 1%). Digital droplet PCR (ddPCR) was used to quantify NOTCH1 c.7544_7545delCT (LOD: 0.025%). Protein

expression (Bcl2, Mcl1, Bim) was assessed by Western blot. Baseline BH3 profiling was performed as per Ryan et al.[1]. To mimic the lymph node microenvironment, viability assays were performed in co-culture with the stromal cell line NK.tert. Viability was assessed by AnnexinV/Hoechst staining. Ex vivo drug treatments included: BCL2i (inhibitor): venetoclax; MCL-1i: AZD5991, S63845 and BCLXLi: A133. Statistical analyses were by unpaired and paired t-test with a two-tailed nominal $p \leq 0.05$ considered as significant.

Results: In our cohort of 118 patients, the median age at diagnosis was 62 yrs., and 79.5% were male. Forty-six of them never received any treatment for CLL. BCL2-R were t(14;18) in 77.2%, t(18;22) in 16.3% and t(2;18) in 6.3% of patients. The translocation involving BCL2 gene was isolated in 23.6% of cases, and was associated with trisomy 12 in 45.4% of patients. IgVH was hypermuted in 69% of cases. The most frequently mutated genes in this cohort were in the NOTCH pathway (NOTCH1 mutation: 43.6 %, mostly subclonal (mean of variant allelic frequency: 6.1%) and FBXW7: 4.5%)) and RAS pathway (KRAS, NRAS, BRAF: 9.1%). BCL2 mutations were observed in 14.6% of cases. No mutation previously described in venetoclax resistant CLL, such as F104L or G101V variant, were observed. Furthermore, MLL2 mutations were observed in 14.5% cases and were significantly associated with complex karyotype ($p=0.01$) and trisomy 12 ($p=0.04$). Others mutated genes were: BIRC3 (5.4%), TP53 (3.6%), SF3B1 (1%) and MYD88 L265P (1%). No mutations in EZH2, CREBBP or EP300 were found. In 15 CLL representative samples from each group (BCL2-R and ctrl), Bcl2 protein expression was significantly higher in BCL2-R CLL (ratio Bcl2/actin 0.94 vs 0.74, $p=0.009$) as was expression of the pro-apoptotic protein Bim (ratio Bim/actin: 2.059 vs 1.524, $p=0.007$). BH3 profiling demonstrated that BCL2-R CLL and ctrl CLL samples ($n=23$ in each group) had comparable overall priming (cyto-C release 66.1 vs. 63.3%, ns) and Bcl-2 dependence (cyto-C release 75.4 vs. 76.3%, ns). Both also had low dependence on Bcl-xL (cyto-C release 8.2 vs. 8.8%, ns). In contrast, Mcl-1 dependence was found to be significantly lower in BCL2-R CLL (cyto-C release 15.6 vs. 37.4%, $p<0.0001$). Consistent with our BH3 profiling results, the activity of venetoclax and the Bcl-xLi A133 did not differ significantly between the 2 groups ($n=15$). In contrast, both Mcl-1i were less active in the BCL2-R group: average viabilities after 24h treatment with AZD5991 were 76.4 vs. 56.3% ($p=0.006$) and with S63845 77.3 vs. 62.9% ($p=0.02$) in the BCL2-R vs ctrl group, respectively.

Conclusion: The genomic landscape of BCL2-R CLL is characterized by a high frequency of trisomy 12, subclonal NOTCH and RAS pathway mutations, as well as BCL2 and MLL2 mutations. Protein expression, BH3 profiling and viability assays data are consistent with nearly exclusive dependence on Bcl-2.

Abstract ID: 1552424

Title: Sex bias in mutational landscape of chronic lymphocytic leukemia: analysis of clinical sequencing data

Authors: Mariia Mikhaleva, Svitlana Tyekucheva, Kiyomi Mashima, Stacey Fernandes and Jennifer Brown

Background: Chronic lymphocytic leukemia (CLL) is more common in males and associated with worse outcomes in males, although the reasons for this remain poorly understood, despite well-established molecular markers defining prognostic impact in CLL. This study aimed to identify potential sex-based differences in genomic data and their prognostic impact on time to first treatment (TTFT) as a primary clinical endpoint in an untreated CLL cohort.

Methods: A clinical targeted next-generation sequencing panel, called The Rapid Heme Panel (RHP), was implemented by BWH, and covered all or hotspot exons of 95 genes. The RHP was performed on a consecutive cohort of 795 treatment-naïve patients with CLL. The cohort included 475 males (59.7%) and 320 females (40.3%). All cases were diagnosed based on iwCLL guidelines. Whole blood ($n=690$) or bone marrow ($n=105$) was studied. The earliest collected sample was selected for analysis if multiple samples had been studied on a given patient. The median time from diagnosis to RHP analysis was 6.6 months (26.50–33.27, 95% CI). Sex-based risk and association were analyzed via Cox proportional-hazards regression. TTFT was defined as the time from diagnosis to initial treatment.

Results: The median age at diagnosis was 61 (range 20–88) years and displayed no differences between males and females ($p=0.262$; Table 1). Males were more often diagnosed at Rai stage 3–4 compared to females, albeit still infrequently (M 7.5 vs. F 3.7%, $p=0.015$). Males had a significantly higher incidence of ß2-microglobulin (B2M) level >3.5 mg/L ($p=0.005$). Unmutated IGHV (UM-IGHV), del17p and complex karyotype (CK) defined as either 3+ or 5+ abnormalities had similar incidence between males and females, while del11q had a significantly higher incidence in males (M 14.5 vs. F 9.2%, $p=0.032$). About half of the patients harbored unfavorable ZAP70 (ZAP70+) status, with no differences by sex. The most commonly mutated (≥10%) genes in the whole cohort were ATM (24.9%), followed by NOTCH1 (18.0%), TP53 (13.6%), and SF3B1 (12.7%). Thirty additional genes had a mutation prevalence of ≥1% and <10%, with MYD88 and SF3B1 mutations more common in male patients: M 5.3% vs. F 1.9% ($p=0.016$) and M 14.3% vs. F 9.4% (p = 0.038), respectively. FANCL and SH2B3 mutations were more common in female patients: M 0.4% vs. F 3.1% ($p=0.002$) and M 0.8 vs. F 2.8% ($p=0.032$). We analyzed patients with a higher mutational burden (≥2 distinct mutated genes) for co-occurrence and mutual exclusivity patterns using Fisher's exact test ($p<0.05$). For example, in males, co-occurrence was found between NOTCH1 and BCOR; as well as del17p, TP53 and CREBBP. In females, co-occurrence patterns were different: NOTCH1 and NRAS; del17p, TP53 and ASXL1. In contrast, mutual exclusivity of gene mutations between ATM and FANCL ($p=0.014$), and MYD88 and NOTCH1 ($p=0.026$) was observed only in males. The median follow-up time for all patients was 3.91 years (range 0 – 42.8). 36.6% of males received at least first-line treatment, with a median TTFT of 7.83 yrs (6.54 – 8.81, 95% CI). In contrast, only 28.1% of females were treated, with a median TTFT of 8.62 yrs (7.96 – 13.76, 95% CI), $p=0.013$. In univariable (UV) analyses, male sex ($p=0.041$), age >65 ($p=0.022$), UM-IGHV ($p<2.0E-16$), CK3 ($p=7.0e-10$), each of del17p, del11q, and tri12 ($p<0.001$), as well as positive ZAP70 ($p=0.00012$) were associated with shorter TTFT. Mutations in ASXL1 ($p=0.00086$), ATM ($p=0.00042$), BCOR ($p=0.0016$), IKZF3 ($p=0.012$), NOTCH1 ($p=0.000036$), RUNX1 ($p=0.035$), SF3B1 ($p=0.000013$), TP53 ($p=0.00004$), and XPO1 ($p=0.00016$) were also associated with shorter TTFT. Mutated MYD88 ($p=0.029$) and del13q ($p=7.10e-06$) were associated with prolonged TTFT in UV. In multivariable (MV) analysis evaluating factors with $p<0.05$ in the UV analysis, factors identified as independently worsening TTFT include mutated

Table 1. Characteristics of studied cohort.

	Male n=475	Female n=320	Total cases n=795	*p*-value [1]
Age at diagnosis (years)				
Median (IQR)	61 (53, 68)	62 (55, 69)	61 (53, 68)	0.262
Range	23 – 88	20 – 88	20 – 88	
Age > 65	154 (32%)	114 (36%)	268 (33.7%)	0.349
Rai stage				**0.004**
0	191 (40.2%)	158 (49.4%)	349 (43.9%)	
1-2	249 (52.4%)	151 (47.2%)	400 (50.3%)	
3-4	35 (7.3%)	11 (3.4%)	46 (5.7%)	
IGHV				0.541
Mutated	221 (46.5%)	161 (50.3%)	382 (48.1%)	
Unmutated	222 (46.7%)	137 (42.8%)	359 (45.2%)	
Unknown [a]	32	22	54	
Chromosomal aberration				
del(11q)	66 (13.9%)	28 (8.8%)	94 (11.8%)	**0.028**
del(13q)	238 (50.1%)	179 (55.9%)	417 (52.5%)	0.106
del(17p)	53 (11.2%)	26 (8.1%)	79 (9.9%)	0.161
tri12	99 (20.4%)	67 (20.9%)	166 (20.6%)	0.722
no abnormalities	113 (23.8%)	61 (19.1%)	174 (21.9%)	
FISH prognostic groups				**0.006**
Favorable	165 (34.7%)	142 (44.4%)	307 (38.6%)	
Intermediate	195 (41.1%)	125 (39.1%)	320 (40.3%)	
Unfavorable	115 (24.2%)	53 (16.6%)	168 (21.1%)	
Karyotype				0.330
Normal	260 (54.7%)	178 (55.6%)	438 (55.1%)	
Sole / Two abnormalities	132 (27.8%)	98 (30.6%)	230 (28.9%)	
Complex ≥ 3	83 (17.5%)	44 (13.8%)	127 (16%)	
ZAP-70				0.069
Favorable	245 (51.6%)	186 (58.1%)	431 (54.2%)	
Unfavorable	230 (48.4%)	134 (41.9%)	364 (45.8%)	
ß2 microglobulin				**0.005**
≤3.5 mg/L	362 (76.2%)	269 (84.1%)	631 (79.4%)	
>3.5 mg/L	111 (23.4%)	47 (14.7%)	158 (19.9%)	
Unknown [b]	2	4	6	
Treatment status [c]				**0.013**
Treatment-naïve	301 (63.4%)	230 (71.9%)	531 (66.8%)	
Treated	174 (36.6%)	90 (28.1%)	264 (33.2%)	
Vital status [c]				0.858
Alive	456 (96%)	308 (96.2%)	774 (96.1%)	
Deceased	19 (4%)	12 (3.8%)	31 (3.9%)	
Mutated genes[d]				
ATM	115 (24.2%)	84 (26.2%)	199 (25%)	0.515
NOTCH1	94 (19.8%)	47 (14.7%)	141 (17.7%)	0.065
TP53	65 (13.7%)	40 (12.5%)	105 (13.2%)	0.629
SF3B1	68 (14.3%)	30 (9.4%)	98 (12.3%)	**0.038**
MYD88	25 (5.3%)	6 (1.9%)	31 (3.9%)	**0.016**
SH2B3	4 (0.8%)	9 (2.8%)	13 (1.6%)	**0.032**
FANCL	2 (0.4%)	10 (3.1%)	12 (1.5%)	**0.002**

1 – Pearson's Chi-squared test.
a – Analysis of *IGHV* mutational status was failed or was not done.
b – ß2 microglobulin level was not tested.
c – Status at timepoint of last follow-up.
d – Shown are the most commonly mutated (≥10%) genes and those differing by sex.

TP53 +/– del17p (HR 1.90, $p=0.0012$), UM-IGHV (HR 2.42, $p<5.43E-08$), CK (HR 1.65, $p=0.003$), del11q (HR 1.51, $p=0.191$), SF3B1 (HR 1.65, $p=0.0023$), ASXL1 (HR 2.60, $p=0.00013$), and IKZF3 (HR 2.47, $p=0.037$).

Conclusion: In this study we distinguish a shorter TTFT in males vs females, but males also have more advanced disease at diagnosis (stage, B2M) and sex is not a significant predictor of TTFT in MV analysis. Among significant factors identified in MV analysis, small sex differences were found in del11q ($p=0.028$) and SF3B1 ($p=0.038$), with higher prevalence in males.

Abstract ID: 1552457

Title: Longitudinal review of cardiac events with acalabrutinib in the treatment of chronic lymphocytic leukemia (CLL) using data from 3 phase 3 randomized controlled trials (RCTs)

Authors: Rupal O'Quinn, Anthony J. Corry, Naghmana Bajwa, Suman Jannuru, Hong Chen, Katherine Stewart and Jennifer Brown

Introduction: The first-generation Bruton tyrosine kinase inhibitor (BTKi) ibrutinib has demonstrated notable efficacy in CLL; however, it is associated with significant cardiac toxicity, including cardiac arrhythmias (eg, atrial fibrillation), cardiac failure, and sudden death. Acalabrutinib is a selective next-generation BTKi for the treatment of CLL with a more favorable cardiovascular (CV) safety profile with fewer atrial fibrillation events versus ibrutinib. The CLL population is at higher risk for cardiac events due to advanced age, polypharmacy, significant comorbidities, and pre-existing cardiac disorders, thereby necessitating comprehensive assessment of cardiac toxicities with CLL therapies. We performed a comprehensive analysis of cardiac outcomes with acalabrutinib versus active comparators, including ibrutinib, in patients with and without CV disorders at baseline to assess the impact of CLL therapies.

Methods: Safety data were extracted from 3 phase 3 RCTs in CLL (ELEVATE-RR, ELEVATE-TN, ASCEND) utilizing 19 Standardized MedDRA Queries (SMQs; Table 1) yielding ~2400 preferred terms (PTs); a subset of specific PTs pertaining to baseline CV disorders and treatment-emergent adverse events (TEAEs) was utilized for further assessments. Exposure-adjusted incidence rates (EAIR; events/100 person-months) were reported for system organ class (SOC) 'cardiac disorders' in patients overall and by number of baseline CV disorders. EAIRs for SOC 'cardiac disorders' were also reported pre- and post-crossover for patients who crossed over from comparator arms (chlorambucil + obinutuzumab [ELEVATE-TN]; idelalisib + rituximab [IR] or bendamustine + rituximab [BR] [ASCEND]) to acalabrutinib monotherapy. EAIRs were also reported for SOC 'cardiac disorders' overall and by number of baseline CV disorders for pooled acalabrutinib monotherapy and pooled comparator groups across the 3 RCTs.

Results: In total, 1362 patients with 3672 TEAEs were retrieved from the clinical trial database utilizing 19 SMQs. Of the 1362 patients, 404 (29.7%) had ≥1 baseline CV disorder (data by study provided in Table 1). The distribution of baseline CV disorders was similar in the acalabrutinib and comparator arms across studies. The EAIR of cardiac disorder events for each treatment arm in each study overall and by number of baseline CV disorders is shown in Table 1. In the 3 RCTs, the overall EAIR of any-grade cardiac disorder events was numerically lower in the acalabrutinib arm versus comparator arms, with no specific trend seen among patients with ≥1 baseline CV disorder. In ELEVATE-RR, the EAIR of de novo cardiac disorder events of any grade among patients without baseline CV disorders with ibrutinib was twice as high compared with acalabrutinib (0.67 vs. 0.34) (Table 1). In ELEVATE-TN, EAIR of de novo cardiac disorder events of any grade was also numerically lower for acalabrutinib + obinutuzumab (0.28) and acalabrutinib monotherapy (0.25) versus chlorambucil + obinutuzumab (0.59) (Table 1). Similarly, in ASCEND, the EAIR of de novo cardiac disorder events of any grade was numerically lower for acalabrutinib (0.28) versus IR (0.44) and BR (0.54) (Table 1). In crossover patients in ELEVATE-TN ($n=72$), the EAIR of any-grade cardiac disorder events was lower during the post-crossover period with acalabrutinib (0.62) versus the pre-crossover period with comparator treatment (1.11). In crossover patients in ASCEND ($n=80$), the EAIR of any-grade cardiac disorder events was low before (0.29) and after (0.36) crossover to acalabrutinib. Based on pooled data across the 3 trials, the EAIR of cardiac disorder events overall and in patients with no baseline CV disorders was numerically lower for acalabrutinib (0.55 and 0.29) versus comparator (0.95 and 0.62) (Table 2). EAIR of fatal events was 3 to 4 times higher in the pooled comparator arms versus pooled acalabrutinib arms overall and in patients with no baseline CV disorders; the EAIR of fatal events did not increase in patients with ≥1 baseline CV disorder versus no baseline CV disorders and was low overall (Table 2).

Conclusion: The incidence of overall cardiac TEAEs across 3 phase 3 RCTs was numerically low overall with acalabrutinib compared with comparators. The current analysis does not suggest an increased risk of cardiac TEAEs and outcomes in patients treated with acalabrutinib, regardless of the presence of baseline CV disorders. The cardiac safety profile of acalabrutinib is consistent across groups with and without

Table 1. Baseline Cardiovascular Disorders and EAIR of Treatment-Emergent Cardiac Disorders (SOC) in Phase 3 Trials

	ELEVATE-RR		ELEVATE-TN			ASCEND		
	Acala (N=266)	Ibr (N=263)	Acala + Obin (N=178)	Acala (N=179)	Obin + Chl (N=169)	Acala (N=154)	Idela + Ritux (N=118)	Benda + Ritux (N=35)
Treatment duration	Median 38.3 mos	Median 35.5 mos	Median 58 mos	Median 58 mos	6 cycles (max)	Median 44.2 mos	Idela: median 11.5 mos Ritux: median 5.5 mos	Benda: 6 cycles (max) Ritux: median 5.5 mos
Number of CV Disorders at Baseline, Number of patients (%)								
0	190 (71.4)	195 (74.1)	119 (66.9)	125 (69.8)	113 (66.9)	111 (72.1)	84 (71.2)	21 (60.0)
1	47 (17.7)	43 (16.3)	40 (22.5)	39 (21.8)	35 (20.7)	25 (16.2)	20 (17.0)	9 (25.7)
2	15 (5.6)	15 (5.7)	12 (6.7)	5 (2.8)	12 (7.1)	8 (5.2)	9 (7.6)	3 (8.6)
≥3	14 (5.3)	10 (3.8)	7 (3.9)	10 (5.6)	9 (5.3)	10 (6.5)	5 (4.2)	2 (5.7)

Cardiac TEAEs (SOC=Cardiac Disorders), Number of events (EAIR) [EAIR ratio of acala monotherapy vs comparator]																
	Any Grade	Grade ≥3[a]	Any Grade	Grade ≥3[a]	Any Grade	Grade ≥3[b]	Any Grade	Grade ≥3[b]	Any Grade	Grade ≥3[b]	Any Grade	Grade ≥3[c]	Any Grade	Grade ≥3[c]	Any Grade	Grade ≥3[c]
Overall	64 (0.71) [0.72]	23 (0.26) [0.82]	79 (0.98)	25 (0.31)	43 (0.47)	17 (0.18)	39 (0.44) [0.95][d] [0.35][e]	18 (0.20) [1.11][d] [0.69][e]	13 (1.28)	3 (0.30)	24 (0.44) [0.76][f] [0.27][g]	8 (0.15) [0.50][f] [0.09][g]	12 (0.58)	6 (0.29)	3 (1.61)	3 (1.61)
By number of CV disorders at baseline (PMH)[h]																
0	31 (0.34)	5 (0.06)	54 (0.67)	16 (0.20)	26 (0.28)	10 (0.11)	22 (0.25)	6 (0.07)	6 (0.59)	1 (0.10)	15 (0.28)	4 (0.07)	9 (0.44)	4 (0.19)	1 (0.54)	1 (0.54)
1	20 (0.22)	11 (0.12)	17 (0.21)	6 (0.07)	10 (0.11)	3 (0.03)	10 (0.11)	7 (0.08)	6 (0.59)	2 (0.20)	7 (0.13)	3 (0.06)	0	0	2 (1.08)	2 (1.08)
2	9 (0.10)	4 (0.04)	5 (0.06)	2 (0.02)	4 (0.04)	3 (0.03)	1 (0.01)	1 (0.01)	1 (0.10)	0	1 (0.02)	1 (0.02)	2 (0.10)	2 (0.10)	0	0
≥3	4 (0.04)	3 (0.03)	3 (0.03)	1 (0.01)	3 (0.03)	1 (0.01)	6 (0.07)	4 (0.04)	0	0	1 (0.02)	0	1 (0.05)	0	0	0

Acala, acalabrutinib; Benda, bendamustine; Chl, chlorambucil; CV, cardiovascular; EAIR, exposure-adjusted incidence rate; Ibr, ibrutinib; mos, months; Obin, obinutuzumab; PMH, past medical history; Ritux, rituximab; SMQ, Standardized MedDRA Query; SOC, system organ class; TEAE, treatment-emergent adverse event.
[a]Fatal events included 2 for acala and 3 for ibr.
[b]Fatal events included 0 for acala + obin, 1 for acala, and 1 for obin + chl.
[c]Fatal events included 2 for acala, 4 for idela + ritux, and 1 for benda + ritux.
[d]Ratio of acala monotherapy to acala + obin.
[e]Ratio of acala monotherapy to obin + chl.
[f]Ratio of acala monotherapy to idela + ritux.
[g]Ratio of acala monotherapy to benda + ritux.
[h]Number of CV disorders at baseline were based on 19 SMQs for cardiac disorders from PMH (SMQ terms: Cardiac arrhythmias; Cardiac arrhythmia terms (including bradyarrhythmias and tachyarrhythmias); Cardiac failure; Cardiomyopathy; Chronic kidney disease; Congenital and neonatal arrhythmias; Dyslipidemia; Embolic and thrombotic events; Embolic and thrombotic events, venous; Embolic and thrombotic events, vessel type unspecified and mixed arterial and venous; Hemorrhage laboratory terms; Pulmonary hypertension; Hyperglycemia/new onset diabetes mellitus; Hemorrhage terms (excluding laboratory terms); Hypertension; Ischemic heart disease; Other ischemic heart disease; Ischemic central nervous system vascular conditions; and Noninfectious myocarditis/pericarditis.
Each subject/event is counted only once under maximum grade.

Table 2. EAIR of Treatment-Emergent Cardiac Disorders (SOC) for Pooled Acalabrutinib and Comparator Data (ELEVATE-RR, ELEVATE-TN, ASCEND)

	Acalabrutinib Pooled (N=598)			Comparator Pooled (N=585)		
Cardiac TEAEs (SOC=Cardiac Disorders) Number of events (EAIR) [EAIR ratio of acalabrutinib monotherapy vs comparator]	Any Grade	Grade ≥3	Fatal	Any Grade	Grade ≥3	Fatal
Overall	127 (0.55) [0.58]	49 (0.21) [0.64]	5 (0.02) [0.27]	107 (0.95)	37 (0.33)	9 (0.08)
By number of CV disorders at baseline (PMH)[a]						
0	68 (0.29)	15 (0.06)	4 (0.02)	70 (0.62)	22 (0.19)	7 (0.06)
1	37 (0.16)	21 (0.09)	0	25 (0.22)	10 (0.09)	1 (0.01)
2	11 (0.05)	6 (0.03)	1 (0.00)	8 (0.07)	4 (0.04)	1 (0.01)
≥3	11 (0.05)	7 (0.03)	0	4 (0.04)	1 (0.01)	0
Most Frequent (EAIR ≥0.04) Cardiac Disorder Preferred Terms Number of events (EAIR)						
Atrial fibrillation	47 (0.20)	16 (0.07)	0	46 (0.41)	10 (0.09)	0
Palpitations	19 (0.08)	0	0	13 (0.12)	0	0
Cardiac failure	10 (0.04)	7 (0.03)	0	9 (0.08)	7 (0.06)	1 (0.01)
Angina pectoris	13 (0.06)	4 (0.02)	0	6 (0.05)	2 (0.02)	0
Cardiac failure chronic	2 (0.01)	1 (0.00)	0	5 (0.04)	3 (0.03)	1 (0.01)
Myocardial ischemia	3 (0.01)	1 (0.00)	0	4 (0.04)	2 (0.02)	0

CV, cardiovascular; EAIR, exposure-adjusted incidence rate; PMH, past medical history; SMQ, Standardized MedDRA Query; SOC, system organ class; TEAE, treatment-emergent adverse event.
[a]Number of CV disorders at baseline was based on 19 SMQs for cardiac disorders from PMH (terms provided in footnote h in Table 1).
Each subject/event is counted only once under maximum grade.

CV disorders at baseline and in line with acalabrutinib's known positive safety profile.

Abstract ID: 1552496

Title: Global perspectives through multi stakeholder mapping of lived experience with CLL – insights to improve equity, services, and unmet need

Authors: Nick York, Kathryn Huntley, Deborah Baker, Michael Rynne, Nicole Schroeter, Pierre Aumont, Brian Koffman, Felice Bombaci, Jennie Bradley, Lynsey Fenwick, Alina S. Gerrie, Yervand Hakobyan, Versha Banerji, Nicole Lamanna, Paolo Ghia and Norah O. Akinola

Introduction: Chronic lymphocytic leukemia (CLL) is the most common leukemia in the Western world, with patients facing years of monitoring and treatment modalities. Many countries exist without dedicated community or patient groups to support people as they navigate the treatment and holistic impacts of their diagnosis. The CLL Advocates Network (CLLAN) conducted and co-conducted global multiple stakeholder surveys to understand current lived experience and needs of patients and carers and map current gaps and opportunities to address equity, service and unmet need.

Methodology: A comparative analysis was undertaken from the findings of three separate lived experience surveys conducted between 2021 and 2022 with CLL patients, their carers, and support organisations from across the globe. Across the surveys, respondents represented people and organisations from 40 countries. Responses were obtained from 1202 patients, 137 carers and 57 support organisations. Although there was broad global reach, most responses from the patient and carer surveys were from the UK and North America. The surveys were completed online and available in ten languages. Countries were segmented into low-and-middle-income countries (LMIC) and high-income countries (HIC) according to the Organisation for Economic Co-operation and Development (OECD) to understand and

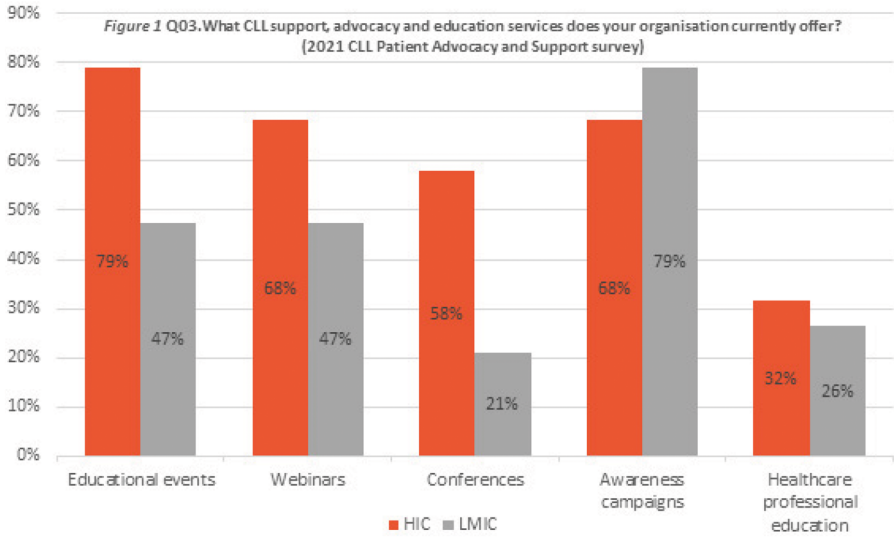

Figure 1 Q03. What CLL support, advocacy and education services does your organisation currently offer? (2021 CLL Patient Advocacy and Support survey)

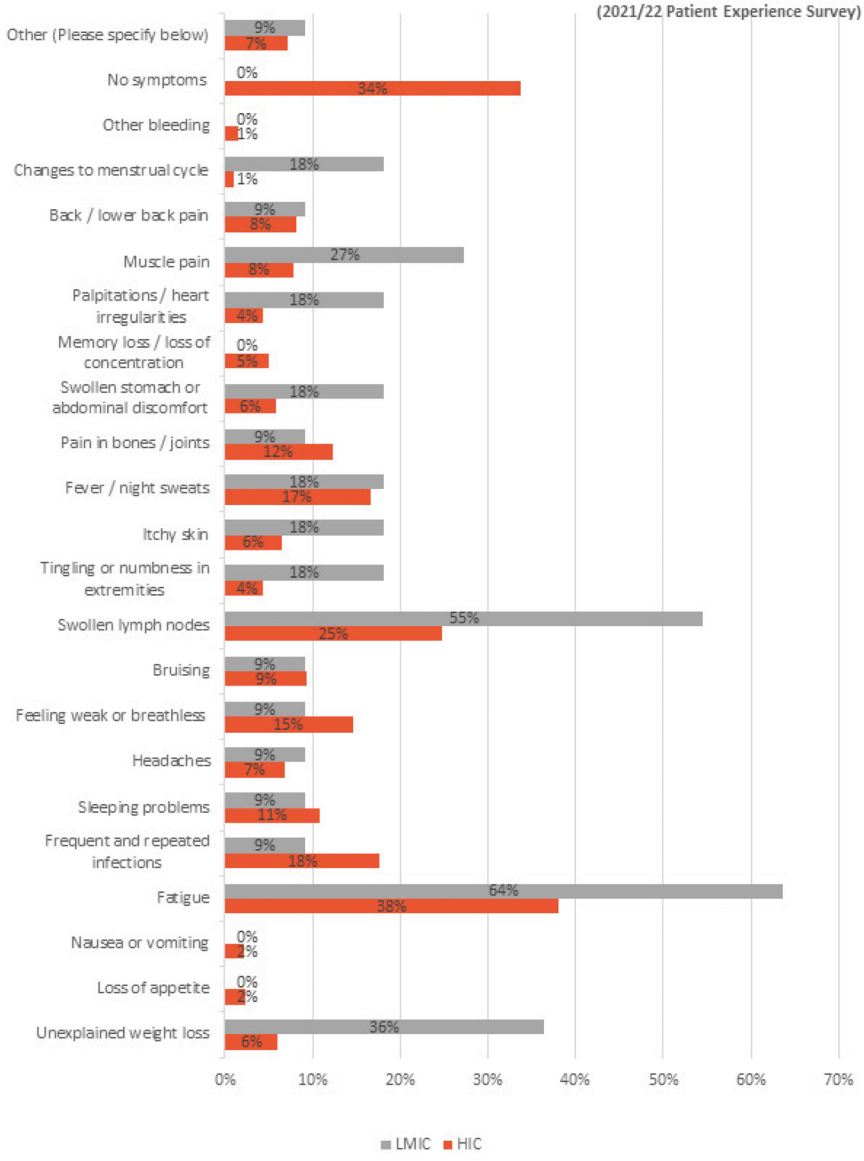

Figure 2 Q14. What symptoms did you encounter before your diagnosis? (2021/22 Patient Experience Survey)

identify geographical impacts on lived experience. As sample populations within the surveys are distinct, the findings are drawn from comparison of overlapping and complementary areas across responses to all three surveys.
Results: Insights from the surveys and analysis have identified differing patient and disease profiles for CLL patients/carers between HIC and LMIC. Key insights can be themed into four distinct areas: Geographical differences for patient outcomes Responses from patients and support organisations suggest that there are geographical disparities for patient outcomes and for support services. Unmet need was higher in LMIC around their CLL diagnosis, treatment and support than those residing in HIC. Patient organisations in HIC are also more likely to provide wider services such as education events and webinars than those from LMIC resulting in further gaps for those in LMIC. Correlation of awareness of CLL and late diagnosis Reduced awareness about CLL correlates with late diagnosis in the survey responses from patients and support organisations. 34% of respondents from HIC reported no symptoms and were diagnosed through routine tests. In contrast, respondents from LMIC all reported some symptoms prior to diagnosis. Patient organisations reported they were less likely to be engaged in healthcare education suggesting a possible opportunity to improve knowledge share between support organisations and healthcare professionals. Unmet need in information and support referrals Respondents reported unmet need around information and support offered to patients across their CLL journey, in particular around diagnosis and 'Watch and Wait'. The surveys reported reduced understanding of the diagnosis (only 35% of patients from HIC and 27% of patients from LMIC reported full understanding), a lack of sensitivity around their diagnosis and advocating greater involvement in their treatment decisions. Availability of clinical trials and treatments Patient organisations reported perceived issues in access to affordable therapies and clinical trials. While these are global issues, results demonstrate that it's more pronounced in LMIC. 84% of organisations from LMIC responded patients weren't able to access clinical trials, opposed to 26% from those countries classed as HIC. Although 54% of CLL patient respondents stated that they were completely involved in their treatment decisions, this was only 30% in LMIC. Almost all patient respondents reported being on at some time a 'Watch and Wait' monitoring plan, the majority also reported they had treatment since diagnosis so access to best practice therapies is vital.
Conclusions: Overall, patients and carers would like to have more choice in their treatment decisions, increased access to clinical trials and better information and support across the whole of their patient journey. Understanding the unique unmet needs and gaps in provision, will help the wider healthcare and support providers to strategically target the development of current services most beneficial to patients and carers. Support particularly targeted at the different patient profiles in different countries will also help to reduce the current disparity across the whole landscape of CLL. There is opportunity globally to improve collaboration and connection between patient organisations and treating teams to address the gaps in need and support the whole life experience of CLL.

Abstract ID: 1552565

Title: Low dose rituximab efficiently clears circulating CLL cells and maintains sensitivity to antibody dependent cellular cytotoxicity (ADCP)

Authors: Clive Zent, Clare Heffernan, Charles Chu, Jennifer Bruno, Christine Herne, Andrea Baran, Ronald Taylor, Paul Barr and Michael Elliott

Introduction: We have recently shown that high frequency (2 × week) low dose (50 mg)(HFLD) rituximab (RTX) and acalabrutinib was highly effective initial therapy for patients ($n = 38$) with progressive CLL (ClinicalTrials.gov identifier NCT03788291, PMID:36689726). The first dose of 50 mg of IV rituximab administered at 25 mg/h decreased the median circulating CLL cell count by 84% from pre-treatment baseline at 1h with no further decrease in the count during the remainder of the infusion (PMID:37003030). During the first hour of infusion, median CLL cell membrane CD20 levels decreased to 65% of baseline and were 41% of baseline at the end of the infusion. Median serum rituximab concentration was 2 mcg/ml at 1h and 10 mcg/ml at the end of the infusion. Median complement (CH50) concentration decreased to 91% of baseline at 1 h and to 81% of baseline at the end of the infusion. The cessation of clearance of CLL cells from the circulation within 1h of starting rituximab therapy is thus unlikely to be caused by low rituximab levels, decrease in CLL cell CD20 expression or low serum complement levels. We and others have previously shown that ADCP is the primary mechanism of clearance of anti-CD20 mAb opsonized B cells in both humans and mice. We hypothesized that clearance of circulating CLL cells decreases because residual circulating CLL cells are resistant to mAb induced ADCP. To test this hypothesis, we measured in vitro ADCP sensitivity of CLL cells sampled from patients before and after treatment with rituximab.
Methods: Blood specimens were collected from 13 patients prior to starting therapy (C1D1_pre), at 1h after start of IV rituximab infusion (C1D1_1h), at end of rituximab infusion (C1D1_post), and 48 h after initiation of therapy (C1D3_pre). Sensitivity of circulating CLL cells to in vitro ADCP was measured using live cell time-lapse high-content microscopy imaging of phagocytosis of CLL cells by human monocyte derived macrophages (hMDM) as previously described (PMID:32005699). Phagocytosis was quantified using a void index and sensitivity of samples was compared using the area under the curve of the 2h void index plot (AUC). Experiments were set up in triplicate with co-cultures of hMDM and CLL cells without mAb as controls. Rituximab (10 mcg/ml) was used to test CD20 mAb mediated ADCP and alemtuzumab (10 mcg/ml) to test non-CD20 mediated ADCP.
Results: Figure 1 (median and 95% confidence intervals) shows that neither rituximab ($p = 0.66$) nor alemtuzumab ($p = 0.58$) induced ex-vivo ADCP was significantly altered by prior *in vivo* exposure of CLL cells to rituximab (Kruskal Wallis Rank test). Discussion: The rapid decrease in circulating CLL cells induced by IV rituximab occurred only during the first hour after initiation of mAb infusion. Based on our measurements, serum rituximab and complement concentrations and CLL cell membrane CD20 levels should be adequate to support additional CLL cell clearance after 1h. We now demonstrate that residual circulating CLL cells remain sensitive to in vitro ADCP by both rituximab and alemtuzumab, suggesting that despite reduced levels of surface antigen, circulating cells remain sensitive to mAb mediated clearance. Alternative explanations for the limited clearance of circulating CLL cells include: (1) Saturation of the limited cytotoxic capacity of the innate immune effector cells (Kupffer cells and splenic macrophages) compatible with our previously reported data on finite macrophage ADCP capacity (PMID:32556153); (2) Mobilization of CLL cells

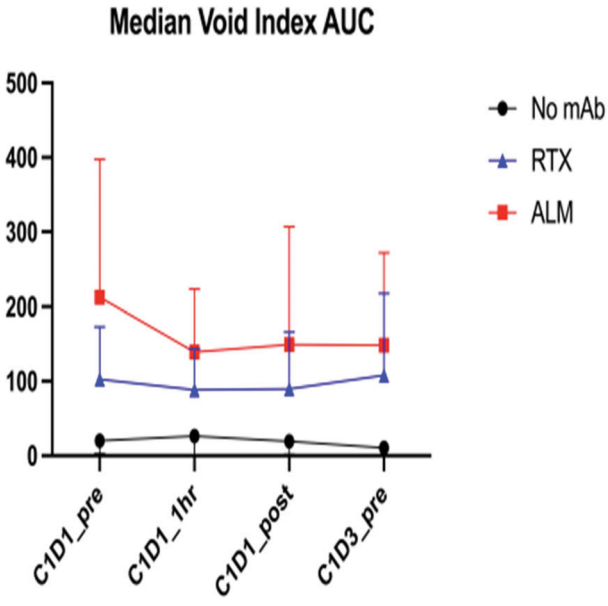

from lymphoid tissue; and 3. Temporary sequestration of rituximab opsonized CLL cells in tissue (e.g. spleen or lungs), which is unlikely because of the observed decrease in lymph node size following initiation of therapy. Ongoing research is testing these hypotheses.

Abstract ID: 1552615

Title: Anti-FcμR antibody drug conjugate as a potential therapeutic agent for the treatment of chronic lymphocytic leukemia

Authors: Amro Fufulan, Dobeen Hwang, Shi Shu, Christoph Rader, Adrian Wiestner and Sivasubramanian Baskar

Historically treatment with naked monoclonal antibodies (mAbs) alone or in combination with standard chemotherapy (e.g. anti-CD52, anti-CD20 plus fludarabine/chlorambucil) have yielded significant clinical response in patients with chronic lymphocytic leukemia (CLL) compared to chemotherapy alone. Later developments include chimeric antigen receptor expressing T cells (CAR-T) targeting cell surface proteins (e.g. CD19, ROR1), small molecule inhibitors such as ibrutinib, idelalisib, venetoclax targeting intracellular proteins (e.g. BTK, PI3Kδ, BCl-2) and combinations thereof have shown excellent clinical activity in patients. However, many patients do not enjoy long-term progression free survival (PFS >5 years) and eradication of the disease is uncommon. Various factors contribute to this failure including disease relapse, treatment intolerance, adverse side effects, unfavorable cytogenetics and treatment-emergent mutations. In this report, we investigate antibody drug conjugates (ADCs) to specifically target CLL cells. An advantage of ADCs is their functional independence of host immune effector mechanisms which are often compromised in patients with CLL. We and others have previously reported over expression of the Fc receptor for IgM (FcμR) in CLL B cells compared to other leukocytes and such over expression of FcμR is an independent indicator of shorter survival in patients with CLL. FcμR binds to human IgM Fc fragment (Fcμ) with high avidity and is rapidly shuttled via clathrin-coated endocytic vesicles into lysosomes. We have also previously demonstrated that IgM derived protein scaffold conjugated to an antimitotic drug could selectively induced cytotoxicity in CLL cells. Commercially available anti-FcμR mAbs failed to internalize. Therefore, we developed recombinant rabbit human chimeric mAbs against FcμR in double variable domain (DVD) formats. The DVD mAbs contain an outer VH domain that targets FcμR on the cell surface and an inner VH domain with an uniquely positioned catalytic (or reactive) lysine residue that allows quick, site-specific conjugation of a cytotoxic drug (e.g. MMAF). We first demonstrated that anti-FcμR-DVDs, both in Fab and IgG formats were able to bind to FcμR positive malignant B cell lines (e.g. Mino, NU-DHL-1) and not to FcμR negative cell lines (Jurkat and HBL-2). Similarly, anti-FcμR-DVDs were able to bind CLL cells, but not other cells present in PBMCs obtained from patients with CLL and in addition did not bind to B cells from healthy donors. Confocal microscopy demonstrated rapid internalization of cell surface bound anti-FcμR-DVDs upon incubation at 370C and their localization to lyzosomes. Anti-FcμR-DVDs conjugated to MMAF induced specific lysis (>80%) of FcμR+cell lines, while a control ADC (H38C2-DVD-IgG-MMAF) failed to do so. The anit FcμR-DVD-IgG-ADC induced dose dependent cytotoxicity of FcuR+cell lines (IC50 0.5 – 33nM) but not of their congeneic FcuR-knock out counterparts. In vitro, we observed that FcμR-DVD-IgG-ADC induced selective cytotoxicity of CLL B cells without affecting the viability of T cells and other mononuclear cells. Together these experiments demonstrated the specificity and potency of anti-FcuR-ADC in vitro, and studies are underway to evaluate its efficacy in vivo using a patient-derived xengograft CLL model. We envisage that anti-FcμR-DVD-ADCs may offer a promising modality for the treatment of CLL.

Abstract ID: 1552675

Title: Time to treatment initiation in 17p-deleted chronic lymphocytic leukemia has no influence on overall survival

Authors: Mayur Narkhede, Sean Patrick Bliven and Randall Davis

Objectives: In chronic lymphocytic leukemia (CLL), chromosome 17 p deletion (del17p) occurs in 8.5% of all newly diagnosed with CLL with an inferior median overall survival (OS) of 2–3 years from time of first-line treatment versus 7–8 years in those without del17p [1]. However, when there are no indications to initiate treatment as per the iwCLL criteria, testing for del17p alters the 'wait and watch' strategy to 'wait and worry'. Despite this understanding, TP53 mutation or chromosome 17p del detection is a part of many standard CLL diagnostic panel testing. Therefore, our objective was to evaluate the testing patterns for del17 by Fluorescence *in situ* hybridization (FISH) and determine the influence of time to treatment initiation (TTTI) in patients (pts) with untreated CLL and del17p on overall survival.
Methods: Data was collected from the nationwide Flatiron Health electronic health record (EHR)-derived de-identified database. The Flatiron Health database is a longitudinal database, comprising de-identified patient-level structured and unstructured data, curated via technology-enabled

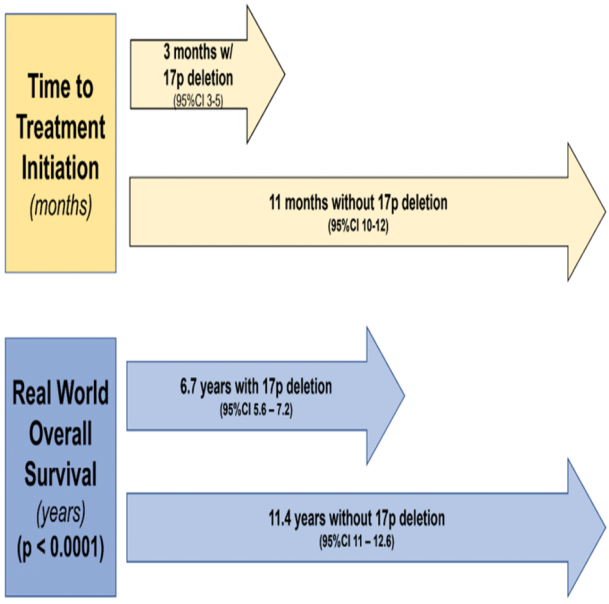

abstraction. During the study period, the de-identified data originated from approximately 280 cancer clinics (~800 sites of care). Inclusion criteria included pts diagnosed with CLL between January 1991 to October 2021 and with a follow up of more than 90 days with at least two visits documented in the EHR. Del17p status was the predictor variable, and the primary endpoint was real-world overall survival (rwOS). TTTI was defined as time from diagnosis to time of first treatment initiation and censored if death prior to treatment. First, Kaplan and Meier method was used to describe the effect of del17p status (del17p v non-del17p) on rwOS and compared using the log rank test from the date of diagnosis to the date of death. Second, to evaluate the influence of del17p status on rwOS adjusted for TTTI, we used the index date as the date of diagnosis with the date of treatment initiation as a time-varying covariate and compared using cox regression model. Lastly, we evaluated the influence of TTTI on rwOS in del17p CLL measured from the time of diagnosis to the time of death with the date of treatment initiation as a time-varying covariate and compared using cox regression model. All patients were followed up until the relevant event of interest (death) or censored at their last structured activity in the EHR, defined as a documented office visit, vital status measurement, or medication administration.

Results: Out of 13,713 patients with CLL who met the inclusion criteria, 9745 (71%) patients had FISH analysis performed. Of these, 5455 (56%) pts had testing done within 3 months of diagnosis. In pts with FISH analysis done within 3 months of diagnosis, 595 pts had del17p present (4079 non-del17p and 781 unk) with a median age at diagnosis of 67 years (IQR 59–74). The median follow-up time by reverse Kaplan Meier method was 6 yrs (IQR 3.5 – 9.4). The median TTTI was 3 months (95%CI 3–5) for del17p and 11 months (95%CI 10 – 12) for non-del17p. The median rwOS for del17p was 6.7 yrs. (95%CI 5.6 – 7.2) compared to 11.4 yrs. (95%CI 11 – 12.6) for non-del17p CLL (p<0.0001). The presence of del17p CLL had inferior rwOS despite adjusting for TTTI compared to non-del17p CLL with HR of 1.99 (95%CI 1.8 – 2.2). In patients with del17p CLL, TTTI had no influence on rwOS with HR of 1.1 (95%CI of 0.58 – 2.19).

Conclusion: Approximately one-third of newly diagnosed CLL patients do not have FISH analysis performed and when done, half of all the FISH analysis are done within the first three months of diagnosis. The presence of del17p confers an inferior survival compared to non-del17p. Pts with del17p have a shorter TTTI however time to treatment initiation does not influence rwOS. Therefore, FISH testing at diagnosis for asymptomatic patients may not aid in guiding treatment decisions and may be considered only when symptomatic or when treatment is indicated.

Abstract ID: 1552730

Title: NX-5948 and NX-2127 potently degrade a broad array of clinically-relevant BTK mutants that display resistance to inhibitors and other BTK degraders

Authors: Mark Noviski, Nivetha Brathaban, Stephanie Yung, Ratul Mukerji, Jordan Ye, Hugo Bousquet, Mateo Sanchez Garcia de los Rios, Brandon Bravo, Jeff Mihalic, Hao Lu, Cristiana Guiducci and Gwenn Hansen

Small molecule kinase inhibitors have revolutionized the treatment of chronic lymphocytic leukemia (CLL) by suppressing signaling pathways essential for tumor cell survival. Bruton's Tyrosine Kinase (BTK) inhibitors are widely used in the clinic for treatment of patients with CLL and other B cell malignancies. Acquired resistance mutations in BTK, however, can reduce or eliminate BTK inhibitor efficacy and represent a growing clinical challenge. Several BTK mutations have been reported in CLL patients. Mutations at C481 dramatically reduce the activity of covalent BTK inhibitors, whereas other clinically-observed mutations such as V416L, T474I, and L528W reduce or eliminate the activity of next-generation non-covalent inhibitors. While some of these mutations, such as V416L and L528W, abolish BTK kinase activity, they retain intact BCR signaling and BTK-dependent growth, indicating that kinase dead BTK mutants can elicit scaffold mediated signaling essential for malignant B cell survival. To assess the impact of resistance mutations on the activity of BTK inhibitors, we generated several DLBCL lines (TMD8) harboring either BTK-C481S, C481R, V416L, T474I, or L528W point mutations. The C481S and C481R mutations eliminated the anti-proliferative effects of covalent inhibitors ibrutinib, acalabrutinib, and zanubrutinib, whereas the V416L, T474I, and L528W mutations had variable effects on the covalent inhibitors. By contrast, the non-covalent inhibitors pirtobrutinib, vecabrutinib, and fenebruitnib maintained activity against C481S but displayed partially reduced potency against the C481R mutation and dramatically reduced potency against the V416L, T474I, and L528W mutations. The variability in mutant sensitivity to BTK inhibitors poses additional challenges to treatment decisions for patients who relapse on BTK inhibitors, creating a therapeutic need for agents that can target resistance mutations more broadly. Targeted protein degradation represents one potentially mutation-agnostic therapeutic option since this modality's event-driven pharmacology requires only transient target interaction to promote elimination of a protein. This contrasts with inhibitors, which require continuous target occupancy to suppress protein activity and pathway activation, making them highly susceptible to point mutations that reduce drug affinity. Here we assessed the activity of several chemically diverse heterobifunctional BTK degrader molecules against clinically observed BTK inhibitor-resistant mutations. All degrader molecules were able to degrade C481S- and

C481R-mutant BTK and suppress proliferation of TMD8 cells harboring these mutations. However, the majority of degrader molecules displayed marked loss of activity against the T474I, V416L, or L528W resistance mutations. By contrast, Nurix clinical stage degraders NX-5948 and NX-2127 were able to broadly target these resistance mutations. To determine the mechanism underlying the anti-mutant activity of our BTK degraders, we used surface plasmon resonance and FRET-based probe displacement assays to evaluate the binding of NX-5948 and NX-2127 to WT and mutant (C481S, C481R, T474I, V416L and L528W) BTK proteins. NX-5948 binds potently to BTK WT, C481S and T474I with single-digit nanomolar affinities, but loses 10-fold or greater binding affinity against the C481R, V416L, and L528W mutants. Furthermore, NX-2127 binds to some mutants with an affinity that would render most non-covalent BTK inhibitors inactive at therapeutically-relevant concentrations. Despite reduced BTK binary binding affinity, NX-5948 and NX-2127 induce potent degradation of all mutant forms of BTK and effectively suppress expression of activation markers and proliferation in TMD8 cells harboring these mutations. We propose that the positive cooperativity induced by NX-5948 and NX-2127 between BTK and the E3 ligase cereblon contributes to their potent and sustained degradation activity against BTK resistance mutants. The exceptional potency and activity of NX-5948 and NX-2127 against emerging BTK point mutations warrant their investigation in indications like CLL that develop diverse resistance to inhibitor molecules. These degrader molecules may also have utility in earlier lines of therapy due to their ability to suppress scaffold-mediated BTK signaling. Phase 1a/b trials of NX-5948 and NX-2127 in patients with relapsed or refractory B-cell malignancies are ongoing (NX-5948: NCT05131022; NX-2127: NCT04830137).

Abstract ID: 1552788

Title: Clonal space assessment in chronic lymphocytic leukemia using an unbiased NGS approach

Authors: Marcelo Navarrete, Jorge González-Puelma, Lindybeth Sarmiento, Julieta Sepulveda-Yañez, Jorge Torres-Almonacid, Diego Alvarez, Angimar Uriepero, Catalina Berca, Maria Elena Marquez, Carolina Perez-Troncoso, Hermy Alvarez, Daniela Cardemil, Roberto Uribe-Paredes and Pablo Oppezzo

Introduction: Chronic Lymphocytic Leukemia (CLL) is characterized by the presence of clonal B-cells in peripheral blood. Leukemic B-cells express a unique VDJ rearrangement, and the somatic hypermutation status and V gene usages serve as prognostic markers. Flow cytometry is the standard method for the identification of clonal B-cells by light chain restriction in the presence of an aberrant immunophenotype. Advances in sequencing technologies enables the detection of the total set of VDJ rearrangement in each sample at a given time point. In this work we evaluate a relatively simple and cost-effective method to obtain information on clonal composition in CLL samples based on immunoglobulin heavy variable genes (IGHV) parallel sequencing. We propose a novel approach that combines balanced amplification and long-read sequencing technology to display the entire B-cell repertoire and distinguish tumoral clonal reads from non-clonal B-cell repertoire reads, thereby defining the clonal space (CS), along with the somatic hypermutation load and characterization of non-clonal B-cell repertoire.

Methods: A total of 47 CLL patients and 13 healthy donors (HD) were processed using by immunoglobulin specific Anchored-PCR and Nanopore sequencing. We developed an error-correction sequencing bioinformatic clustering system to group overexpressed reads. The clonal space was determined by the ratio of overexpressed reads to the non-clonal B-cell repertoire reads. The somatic hypermutation status was assessed in the overexpressed reads to characterize as mutated or unmutated cases. The rearrangement obtained was validated using BIOMED-2 PCR and sanger sequencing, which is considered the gold standard method for determining the IGVH mutational status.

Results: The method allowed for the detection of overexpressed clones in all CLL samples. The average of IGVH reads detected was 123,170, with an average of 96,065 overexpressed clonal reads. Using IGVH data from healthy donors (HD) and clonality data from flow cytometry we established a cut-off value of 0.25 for defining a clonal expansion. The clonal space (CS) had a mean value of 0.68 for CLL samples, with a CS of 0.70 for mutated-CLL (M-CLL) (95% CI 0.58–0.83) and 0.67 for unmutated-CLL (UM-CLL) (95% CI 0.58–0.75). Additionally, biclonality was identified in one sample (VH1-69, CS: 0.63, IGHV5-51, CS: 0.27). The mutational status obtained for each predominant rearrangement had a sensitivity of 91%, specificity of 100% and correlation of 0.8 ($p<0.005$) compared to the gold standard method. No overexpressed sequences were detected in HD. We then analyzed the remaining non clonal B-cell repertoire and found several alterations compared to the immune repertoire of HD; significant abundance of clones as measured by the number of reads composing each clone (reads per clone mean; range: 2.05–10.5), relative expansion of individual rearrangements (5–40% of the repertoire), lower repertoire richness as measured by Hill's index; (1. 178 vs 554 in M-CLL and 651 in UM-CLL), lower repertoire diversity measured by Shannon index (4.48 in M-CLL cases, 4.75 in UM-CLL cases, and 6. 94 in HD), greater inequality measured by Ginís index (0.55 In mutated cases, 0.48 in unmutated cases, and 0.48 in HD), along with altered homogeneity composing predominant rearrangement. We also characterized the CDR3s of the repertoire finding differences in CDR3 sizes (18.2 aa in mutated cases, 19.6 aa in unmutated cases, and 15.8 aa in HD) and in the electrical charge they present (0.75 in mutated, 0.58 in unmutated, and 0.15 in HD).

Conclusion: These findings indicate the feasibility of using IGVH high throughput sequencing for identifying clonal B cells in peripheral blood. The proposed method allows the characterization of the clonal architecture of CLL and highlight the importance of accurate CS assessment. Our approach provides data about the proportion of tumoral reads and intraclonal diversity overcoming economic and technical limitations of assessing clonal architecture and intraclonal diversity by other conventional methods.

Abstract ID: 1552828

Title: Initial anti-CD20 monoclonal antibody therapy in CLL quickly induces cytokine release syndrome with first dose infusion reaction correlating only with high IL-6, IL-8 and IP-10

Authors: Charles Chu, Jeremiah Moore, Paige Bloom, Jennifer Bruno, Sally Quataert, Tim Mosmann, Nydia Jaimes-Delgadillo, Christine Herne, Clare Heffernan, Karl VanDerMeid, Andrea Baran, Derick Peterson, Ronald Taylor, Fatima Rivera-Escalera, Michael Elliott, Lauren Benoodt, John Ashton, Danielle Wallace, Paul Barr and Clive Zent

64% Of CLL patients have a potentially life-threatening first dose infusion reaction (FDIR) within 1–2 h after initiating intravenous (IV) rituximab anti-CD20 monoclonal antibody (mAb) therapy. Once FDIR is observed, the infusion must be interrupted and patient symptoms must be managed before restarting. If FDIR is not treated, serious complications and fatalities may occur. To better understand FDIR, we studied blood samples collected from 37 treatment-naïve CLL patients in our clinical trial NCT03788291 undergoing IV treatment with low dose (50 mg) and slow infusion (25 mg/h) anti-CD20 mAb (rituximab). All human specimen collection and usage was conducted with written informed consent after approval of the University of Rochester Research Subjects Review Board according to the ethical guidelines of the Declaration of Helsinki. We hypothesized that slow infusion of low dose mAb compared to standard infusion and dose (50 mg/h, 375 mg/m^2) may produce fewer FDIRs. We analyzed four time points: baseline (0 h (pre), prior to infusion), 1 h later (during infusion), at the end of infusion (~3 h (post)) and at 48 h (Figure 1). Based on previous reports, we anticipated that CLL counts, CD20 levels and consumption of mAbs/complement would correlate with FDIRs. Furthermore, we expected cytokine release syndrome would be measurable in FDIR sera. 24 (65%) patients had a FDIR as defined by Common Terminology Criteria for Adverse Events version 5 (CTCAE) grade 2 or higher and required intervention within the first two hours. This FDIR frequency is comparable to the rate seen in standard rituximab therapy (64%), implying that dose and infusion rate of anti-CD20 mAb are not key components of FDIR, which further unexpectedly suggests that antigen/antibody levels may not correlate with FDIR. To test this idea, flow cytometry of CLL blood samples was performed to measure CLL cell counts and CD20 levels. We further measured serum rituximab and complement levels. None of these measurements correlated with the occurrence of FDIR in CLL patients. To explore factors outside of antigen/antibody levels, we examined CLL patient characteristics (IGHV mutation, Rai stage, cytogenetic defects/mutations) and none of these correlated with induction of FDIR. Previous studies of rituximab FDIR noticed a cytokine release syndrome, although non-FDIR patients were not examined. In our study, we studied human sera from both FDIR and non-FDIR patients using a Luminex xMAP multiplex assay. We found cytokine release occurred in both types of patients with a ≥4-fold increase in one or more cytokines compared to pre-treatment levels in 95% of patients at the end of infusion (~3 hr (post)). Because overall cytokine induction was similar between patients, we examined specific cytokines for differences in induction that might correlate with FDIR. IL-6, IL-8, and especially IP-10 induction ~3 hr (post) correlated with FDIR. IP-10 (interferon gamma inducible protein-10), also known as CXCL10 (C-X-C motif chemokine ligand 10), is mainly secreted by monocytes and macrophages. To study the source of IP-10, we performed single-cell RNA sequencing on blood samples from two patients with FDIR at three timepoints: baseline (0 h (pre)), at the end of infusion (~3 h (post)) and at 48 h. IP-10 was detected at very low levels only in monocytes and no other

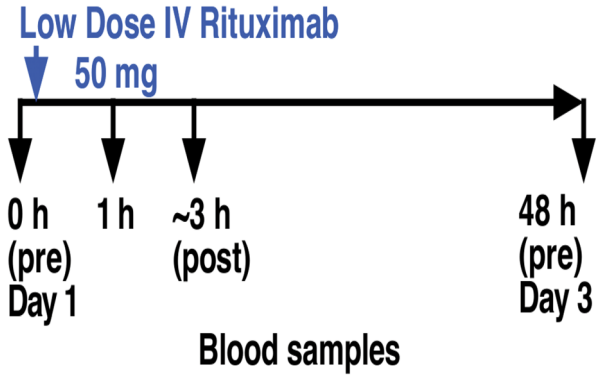

Fig.1. Blood samples were collected in our clinical trial NCT03788291 as shown from treatment-naïve chronic lymphocytic leukemia (CLL) patients (n = 37) undergoing IV infusion with low dose (50 mg) anti-CD20 mAb (rituximab) on Day 1.

cell types. This suggests that IP-10 is produced in tissue-resident cells that are monocytes or derived from monocytes, such as macrophages. To test this, we prepared human monocyte-derived macrophages (hMDM) and added CLL cells opsonized with anti-CD20 mAb. Compared to no mAb, we found that IL-6, IL-8 and IP-10 were induced, although not necessarily at comparable levels. To model FDIR in mice, IV anti-CD20 (5D2 mAb) treatment of C57BL/6 wildtype mice induced IL-6 and IP-10 at 2 h, which decreased at 18 h to levels similar to IgG control. This time course is similar to that seen in FDIR in human patients. In conclusion, FDIR does NOT correlate with anticipated CLL cell characteristics or levels of antigen, antibody, or complement. Infusion of anti-CD20 mAb induces cytokines in most patients, with FDIR correlating with higher levels of IL-6, IL-8, and IP 10. Single cell RNA sequence data suggests tissue resident monocytes or macrophages, are responsible for IP-10 production. Modeling by in vitro assays and a mouse model reproduce mAb induction of cytokines, which is currently under investigation.

Abstract ID: 1552833

Title: Single-cell transcriptome profiling reveals neoplastic effects of exosomal S100A4 in chronic lymphocytic leukemia

Authors: Xin Wang, Zheng Tian, Ya Zhang, Xinting Hu, Xin Zhang, Hua Wang, Liyan Lu and Yang Zhang

Introduction: The crosstalk between chronic lymphocytic leukemia (CLL) cells and immunocytes favors the progression of CLL by promoting the survival of tumor cells and exhaustion of immunocytes. Illustrating the characteristics of CLL cells and immunocytes is an attractive strategy for the treatment of CLL patients. Profiling the peripheral blood mononuclear cells (PBMCs) in CLL patients and healthy donors with single-cell RNA sequencing (scRNA-seq) could provide a detailed molecular and cellular map of PBMCs of CLL patients and healthy donors.

Figure 1

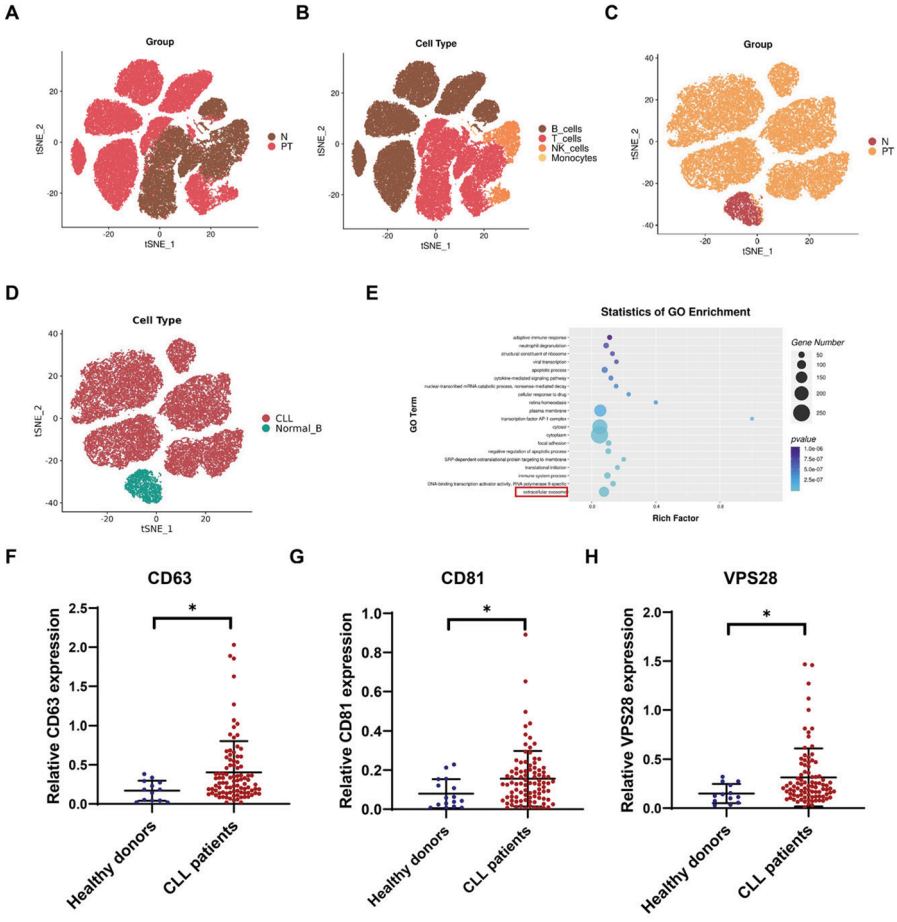

Figure 2

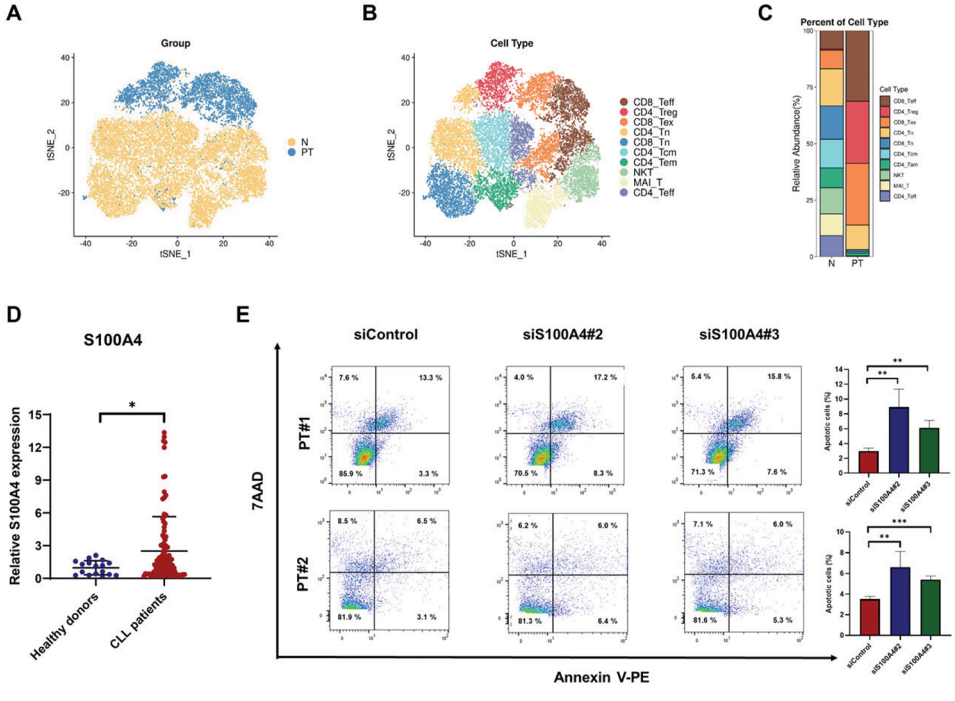

Methods: In the current study, the PBMCs from CLL patients and healthy donors were studied at a single-cell resolution. scRNA-seq was performed on the PBMCs of CLL patients and healthy donors. Flow cytometry assays, and quantitative real-time polymerase chain reaction were performed to verify cellular identity and function.
Results: This study presented a large-scale single-cell transcriptomic atlas of human PBMCs and identified the subclusters of CLL cells, T cells, and natural killer (NK) cells (Figure 1(A–D)). CLL cells exhibited unique genetic markers compared with normal B cells, including cell proliferation, cell cycle progression and extracellular exosome (Figure 1(E)). Genes related to the secretion of exosome including VPS28, CD63 and CD81 were upregulated in CLL cells (Figure 1(F–H)). Exosome inhibitor GW4869 induced cell apoptosis and G0/G1 phase arrest in CLL cells. T cells of CLL patients were investigated to elucidate the molecular mechanisms of T-cell dysfunction in the progression of CLL. T cells of CLL patients presented the hallmarks of exhaustion and the proportion of exhausted CD8+ T cells was upregulated (Figure 2(A–C)). Exosome from CLL cells promoted the exhaustion of T cells. The expression of S100A4 was upregulated in the exosome secreted by CLL cells (Figure 2(D)). Knocking down of S100A4 promoted the apoptosis of CLL cells (Figure 2(E)). Furthermore, knocking down of S100A4 reserved the exhaustion of CD8+ T cells induced by exosome from CLL cells.
Conclusions: The present study revealed the transformation of immune cells during the progression of CLL. The interactions between CLL cells and immune cells were investigated to elucidate the cell communications which accelerated the progression of CLL. Conclusively, this study elucidated the mechanisms of CLL progression through illustrating the characteristics of PBMCs of CLL patients and presenting the cell communications between CLL cells and immunocytes.

Abstract ID: 1552850

Title: Venetoclax resistance induced by activated T cells can be counteracted by sphingosine kinase inhibitors in chronic lymphocytic leukemia

Authors: Valeria Sarapura Martinez, Ana Colado, Chiara Cassarino, Brenda Buonincontro, Juliana Bernatowiez, Gregorio Cordini, Rosario Custidiano, Carolina Mahuad, Miguel Pavlovksy, Fernando R Bezares, Nicolás Favale, Mónica Vermeulen, Mercedes Borge, Mirta Giordano and Romina Gamberale

Introduction: The treatment of CLL patients with venetoclax-based regimens has demonstrated efficacy and a safety profile [1,2], but the emergence of resistant cells and disease progression is a current complication [3–5]. We previously reported that the sphingosine kinase 1 and 2 (SPHK1/2) inhibitor, SKI-II enhanced the *in vitro* cell death triggered by fludarabine, bendamustine or ibrutinib and reduced the activation and proliferation of CLL cells [6]. Since we previously showed that autologous activated T cells (aaT) from CLL patients favor the generation of venetoclax resistance [7,8], we aimed to determine whether SPHK inhibitors could overcome this negative (undesired) effect.
Methods: Peripheral blood mononuclear cells (PBMC) were obtained from twenty-eight unrelated CLL patients that were free from clinically relevant infectious complications and were treatment naïve or without treatment for ≥3 months before the investigation began. To evaluate the effect of SPHK inhibitors on the generation of venetoclax resistance, PBMC were cultured with anti-CD3 antibody (aCD3) in order to induce T cell activation, with or without SKI-II (SPHK1/2 inhibitor) or opaganib (SPHK2 inhibitor) for 72h, in the presence of DMSO (vehicle) or clinically relevant doses of venetoclax (ven, 0,2μM) during the last 24h of culture. CLL cell survival was evaluated by flow cytometry and these values were employed to calculate venetoclax resistance index (VRI) for each patient as follows: VRI = (aCD3 + Ven/aCD3) * (control/Ven). CLL cell proliferation (Ki-67) and activation (CD86, PD-1 and PDL-1) and T cell activation (CD40L) were evaluated by flow cytometry. SPHK1/2, BCL-XL and MCL-1 expression were evaluated by western blot in viable leukemic cells purified with magnetic beads. To assess the effect of SPHK inhibitors on already venetoclax-resistant cells, we first generated resistant cells, which were then cultured with SPHK inhibitors and venetoclax.
Results: We found that both SPHK inhibitors reduced the upregulation of CD86, PD-1, PDL-1 (Figure 1(A)) and Ki-67 (Figure 1(B)) on CLL cells activated by aaT cells. SPHK inhibitors reduced the expression of CD40L induced on CD4+ cells upon CD3 crosslinking (Figure 1(C)) without affecting their survival (Figure 1(D)). More importantly, SKI-II and opaganib prevented the generation of venetoclax-esistance induced by aaT cells (Figure 1(E)) by reducing the upregulation of BCL-XL and/or MCL-1 on malignant cells (Figure 1(F)). In addition, the presence of aaT cells enhanced SPHK2 expression on CLL cells, which was higher in those that survived to venetoclax (Figure 2(A)), while SPHK1 expression was not consistently modified (Figure 2(B)). Moreover, when the public data set RNA-Seq GSE192685 was analyzed, we found that 5 out of 7 CLL samples showed higher SPHK2 expression at progression on venetoclax therapy compared to prior-treatment (Figure 2(C)). Finally, to determine whether SPHK inhibitors can affect the survival of already venetoclax-resistant cells, PBMC from CLL patients were cultured with or without aCD3 for 72h, with DMSO or venetoclax during the last 24h. After that, cells were washed and cultured again with DMSO, SKI-II or opaganib for another 96h, combined with DMSO or venetoclax during the last 24h of culture (Figure 2(D)). Because most of CLL cells die in control cultures with venetoclax (Figure 2(E)), this condition was not assessed. As expected, CLL cells that came from control cultures rapidly died in response to venetoclax and were not affected by SPHK inhibitors (Figure 2(F)). In CLL cells that came from aCD3 + DMSO cultures, as previously, SPHK inhibitors promoted venetoclax-induced cell death (Figure 2(G)). Of note, venetoclax-resistant CLL cells that came from aCD3 + venetoclax cultures died in response to opaganib alone (Figure 2(H)). Moreover, even though 64% of already venetoclax-resistant cells survive to a second drug exposure, 50% of these cells died due to the presence of venetoclax in combination with SKI-II and 75% in combination with opaganib (Figure 2(H), right columns).
Conclusion: Venetoclax-resistant CLL cells express high levels of SPHK2. Both SPHK inhibitors reduce the activation and proliferation of CLL cells, diminish the generation of venetoclax-resistance and re-sensitize already venetoclax-resistant CLL cells to the drug, suggesting that the inhibition of SHPK2 may be involved in this process. Our results highlight the therapeutic potential of SPHK inhibitors in combination with venetoclax as a promising treatment option for the patients.

FIGURE 1

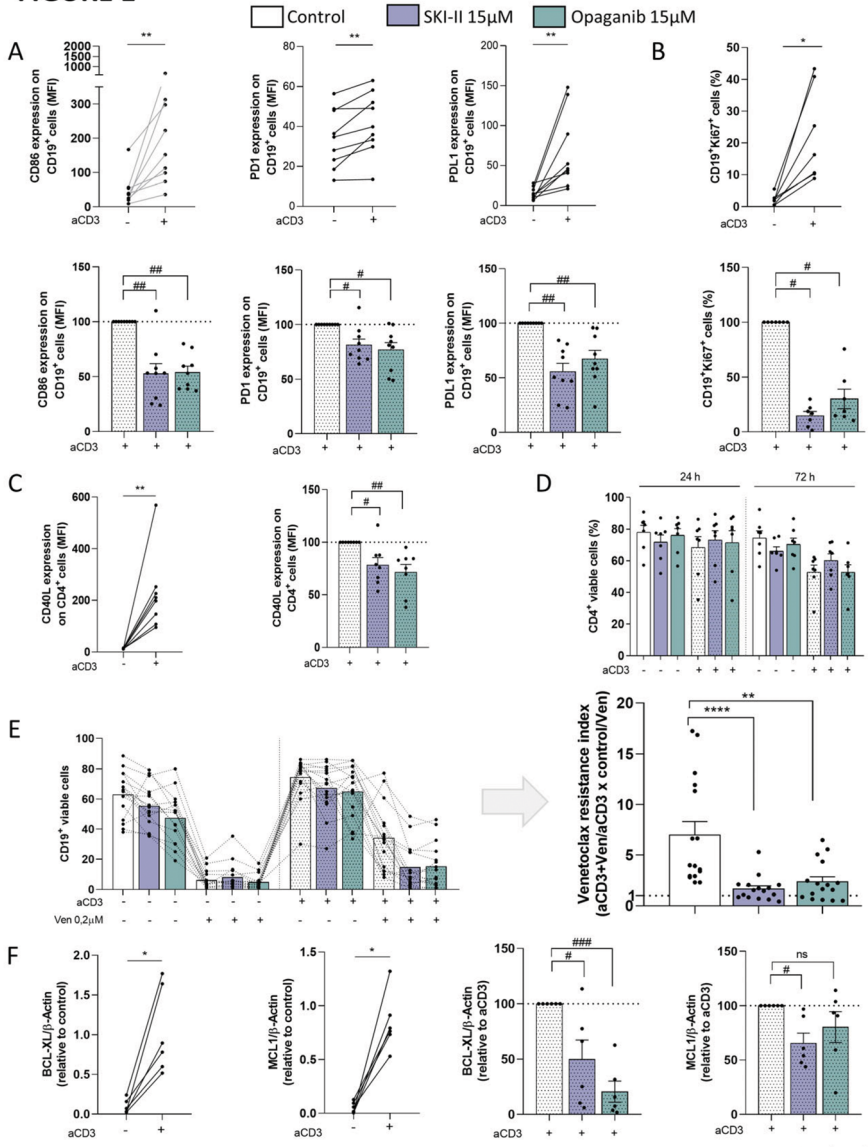

Fig. 1: SKI-II and opaganib prevent venetoclax resistance and CLL activation and proliferation induced by aaT cells. PBMC from CLL patients (4x10^6 cells/ml) were cultured in complete medium with aCD3 or the isotype control with or without SKI-II 15 μM or opaganib 15 μM for 72h, with venetoclax (Ven) 0,2 μM or DMSO during the last 24h. The impact of SPHK inhibitors on: **(A)** CD86, PD-1 and PDL-1 expression on CLL cells at 48h (Wilcoxon matched-pairs signed rank test, ** p<0.01, n=9, Wilcoxon Signed Rank Test, # p< 0.05, ## p<0.01, n=9); **(B)** Ki-67 expression on CLL cells at 7 days (Wilcoxon matched-pairs signed rank test, * p<0.05 n=7; Wilcoxon Signed Rank Test, # p<0.05 n=7); **(C)** CD40L expression on CD4+T cells at 24h (Wilcoxon matched-pairs signed rank test, ** p<0.01, n=8; Right: Wilcoxon Signed Rank Test, # p< 0.05, ## p<0.01, n=8.) and **(D)** CD4+ T cell survival, were evaluated by flow cytometry. **(E)** After 24h of Ven treatment, CLL cell survival was evaluated by flow cytometry and these values were employed to calculate VRI (Friedman test followed by Dunn´s test, ** p<0.01, **** p<0.0001, n=16). **(F)** BCL-XL and MCL-1 expression were determined at 48h by *western blot* in leukemic cells purified with magnetic beads (Left: Wilcoxon matched-pairs signed rank test, * p<0.05, (n=6); Right: Wilcoxon Signed Rank Test, # p< 0.05, ### p<0.001, n=6.)

FIGURE 2

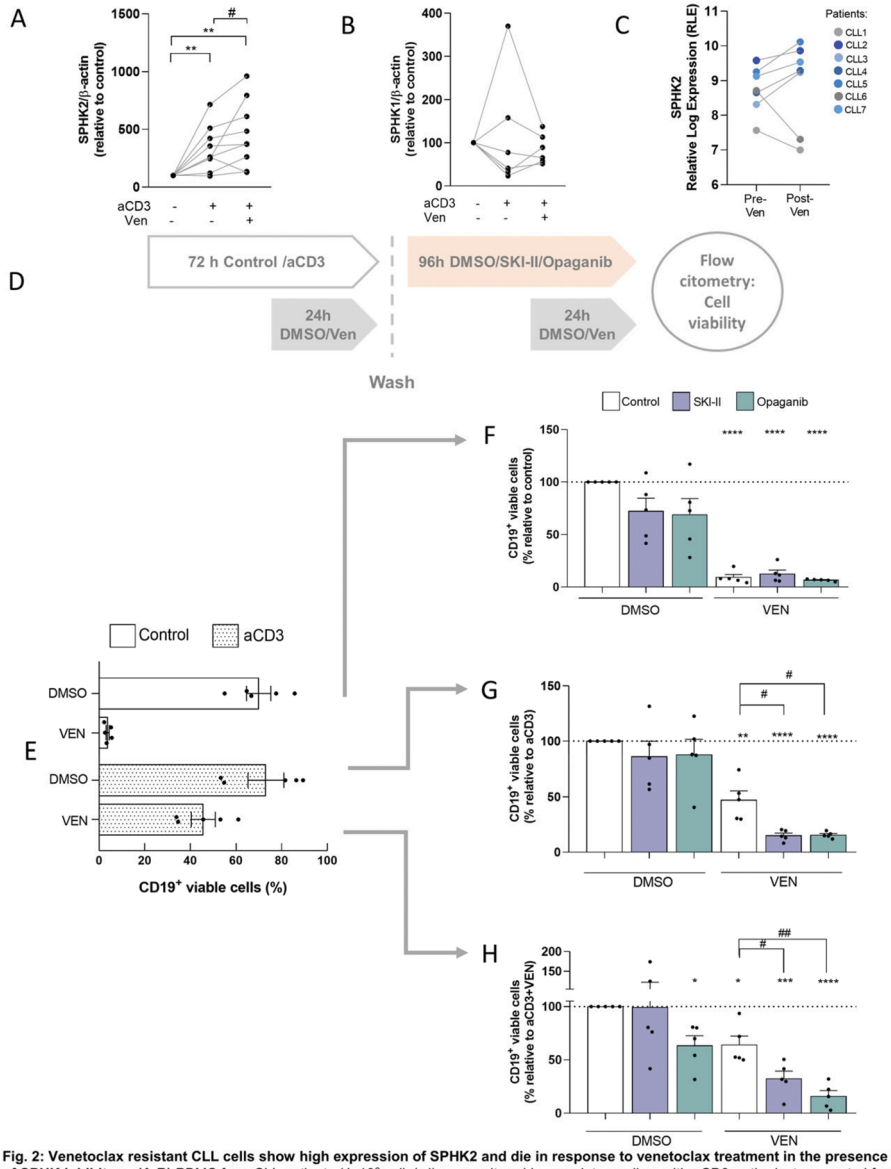

Fig. 2: Venetoclax resistant CLL cells show high expression of SPHK2 and die in response to venetoclax treatment in the presence of SPHK inhibitors. (A-B) PBMC from CLL patients (4x10^6 cells/ml) were cultured in complete medium with aCD3 or the isotype control for 72h in presence of venetoclax (Ven) 0,2 μM or DMSO during the last 24h. Then, viable leukemic cells were purified with magnetic beads to assess for SPHK2 (**A**) and SPHK1 (**B**) expression by western blot. Wilcoxon Signed Rank Test, ** p<0.01 (n=9). Wilcoxon matched-pairs signed rank test, # p<0.05 (n=9) **(C)** SPHK2 expression on CLL cells of 7 CLL patients at progression on venetoclax therapy compared to prior-treatment (public data set RNA-Seq GSE192685) **(D)** Schematic representation of the culture condition of figures E-H. After 24h of Ven treatment CLL cell survival was evaluated by flow cytometry (**E**), and then PBMC from control cultures **(F)**, aCD3 cultures **(G)** and aCD3+VEN cultures **(H)** were washed and cultured with DMSO, SKI-II 15 μM or opaganib 15 μM for 96 h combined with DMSO or Ven during the last 24 h of culture. One sample t test. **** p< 0.0001 (n=5) *** p< 0.001 ** p< 0.01 *p< 0.05 (n=5). RM one-way ANOVA, followed by Holm-Sidak's multiple comparisons test, # p< 0.05 ##p< 0.01 (n= 5).

Abstract ID: 1552871

Title: ENPP2 mediates lipid metabolism and tumorigenesis in chronic lymphocytic leukemia through AMPK signaling pathway

Authors: Xin Wang, Liyan Lu, Ya Zhang, Xinting Hu, Yang Han, Hua Wang, Xin Zhang and Zheng Tian

Introduction: Disorders of lipid metabolism are critical factors in the progression of chronic lymphocytic leukemia (CLL). Ectonucleotide pyrophosphatase/phosphodiesterase 2 (ENPP2), an adipocyte-derived lysophospholipase D, is closely correlated with obesity and disorders of glucolipid metabolism in obese individuals. ENPP2 has been described to be engaged in the progression of several solid neoplasms, but its functional role in CLL remains unclear. Hence, the aim of this study was to investigate the functional mechanism and clinical significance of ENPP2 regulation in CLL.

Methods: In this study, peripheral blood samples of 82 de novo patients diagnosed with CLL were collected at the Department of Hematology in Shandong Provincial Hospital. The mRNA expressions levels of ENPP2 in CLL patients were determined by quantitative RT-PCR. Plasmids were utilized to knockdown and overexpression ENPP2 expression in MEC1 and EHEB CLL cells. ENPP2 targeted inhibitor PF-8380 was used to inhibit ENPP2 impression. RNA-sequencing and functional enrichment analysis were performed. In addition,

Figure 1

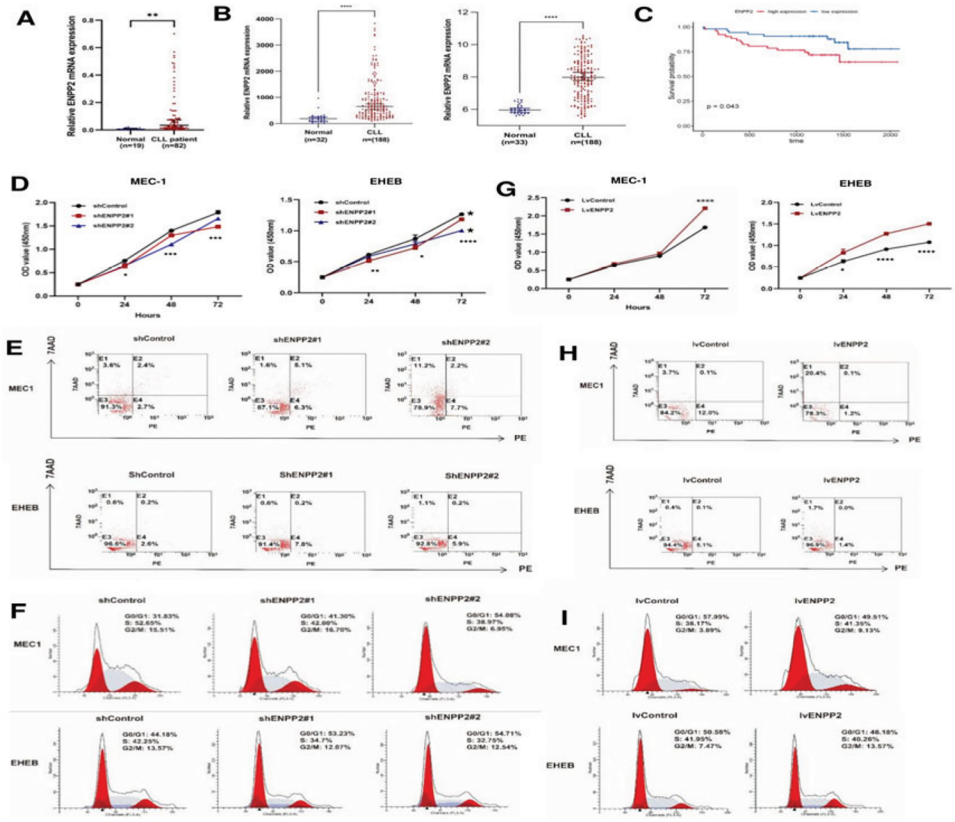

Figure 2

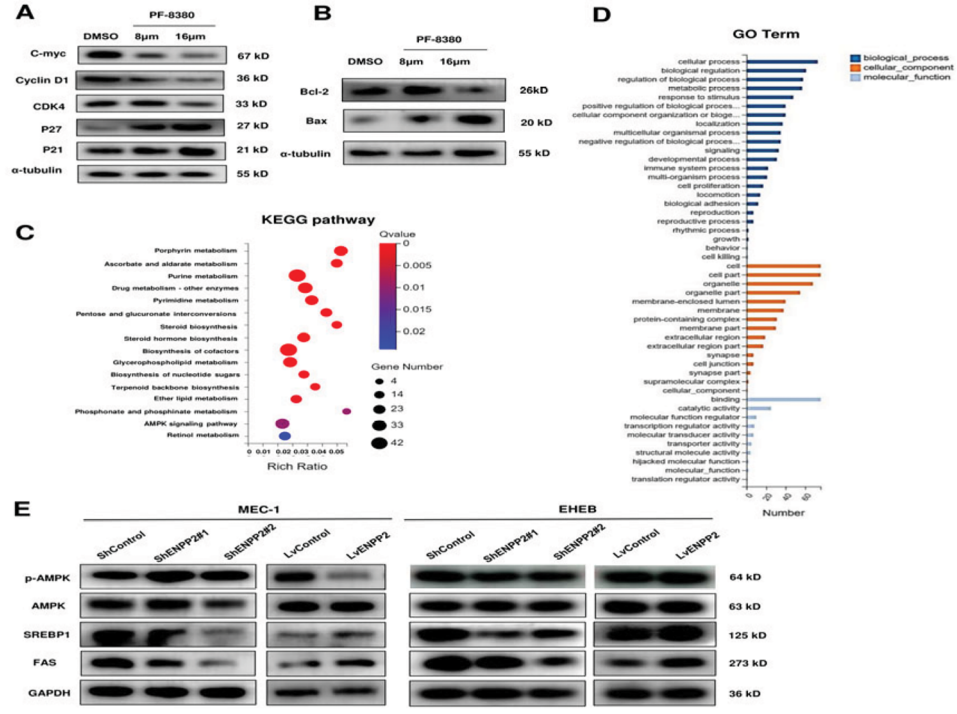

cell viability and apoptosis were assessed by cell counting kit-8 and annexin V-PE/7AAD staining. Bodipy staining was used to explore lipid deposition in CLL cells.

Results: The mRNA expression level of ENPP2 was examined in 82 CLL primary samples from Shandong Provincial Hospital CLL (SPHCLL) database. RT-PCR confirmed the significant

upregulation of ENPP2 in CLL patients compared to normal B cells ($p<0.01$; Figure 1(A)). To validate the altered pattern of ENPP2 expression in CLL patients, we further investigated and found ENPP2 over-expression in CLL patients in two independent microarrays ($p<0.0001$; Figure 1(B)). Kaplan–Meier curves showed higher ENPP2 expression patients were associated with adverse overall survival (HR =2.33, $p<0.043$; Figure 1(C)). To investigate the biological processes of ENPP2 involving in CLL progression, functional assays were performed. CLL cells with ENPP2 knockdown resulted in slow proliferation, G0/G1 phase cell cycle arrest, increased apoptosis and lipid accumulation in CLL cells (Figure 1(D–F)). In contrast, upregulation of ENPP2 produced the opposite effect (Figure 1(G–I)). Similarly, treated with ENPP2 targeted inhibitor PF-8380 exhibited attenuated cell proliferation, increased apoptosis and induced G0/G1 phase arrest. Additionally, the expression of cyclin-related proteins, including C-myc, Cyclin D1, CDK4, P21, and P27 was reduced by treated. The expression of pro-apoptotic proteins Bax was increased, while the expression of anti-apoptotic protein Bcl-2 was reduced (Figure 2(A,B)). To further explore the mechanism of ENPP2 regulation in the tumorigenesis of CLL, RNA-sequencing was implemented between the MEC-1 cells transfected ShControl and ShENPP2#2 respectively. We identified that ENPP2 was concentrated in pathways linked to metabolisms, such as the TCA cycle, AMPK signaling pathway and glycerophospholipid metabolism (Figure 2(C)), through analysis of Kyoto encyclopedia of genes and genomes (KEGG). Gene ontology (GO) analysis implicated that ENPP2 was closely associated with metabolic processes, cellular processes, biological regulation (Figure 2(D)). Accordantly, knockdown of ENPP2 and treated with PF-8380 reduced intracellular lipid deposition. In contrast, intracellular lipid deposition was increased after overexpression of ENPP2. Western blot suggested that ENPP2 was involved in the regulation of lipid metabolism in slow lymphoid cells through participation in the AMPK/SREBP1/FAS signaling pathway (Figure 2(E)).

Conclusion: Taken together, the present study was the first investigation on the role of ENPP2 in the tumorigenesis of CLL. ENPP2 expression was aberrantly increased in CLL cells, and affected cell lipid metabolism through the AMPK pathway. ENPP2 targeted inhibitor PF-8380 inhibited CLL cell proliferation and induced apoptosis, highlighting potent therapeutic potential. Keywords: Chronic lymphocytic leukemia; ENPP2, Lipid metabolism

Abstract ID: 1552961

Title: Randomized, phase III study of early intervention with venetoclax and obinutuzumab (VO) versus delayed therapy with VO in newly diagnosed asymptomatic high-risk patients with chronic lymphocytic leukemia/small lymphocytic lymphoma (CLL/SLL): EVOLVE CLL/SLL Study (SWOG S1925; NCT#04269902)

Authors: Deborah M. Stephens, Anna Moseley, Brian Hill, Mazyar Shadman, Michael Fisch, Alexey Danilov, David Ng, Versha Banerji, Lindsey Roeker, Danielle Brander, Megan Othus, Susan O'Brien and Harry Erba

Background: Currently, asymptomatic patients with chronic lymphocytic leukemia/small lymphocytic lymphoma (CLL/SLL) are observed without treatment until development of CLL/SLL-related symptoms or cytopenias. Historically, early intervention studies in patients with CLL/SLL with non-targeted chemoimmunotherapy agents have not resulted in prolonged overall survival (OS) and have resulted in considerable toxicity. The introduction of targeted therapies, such as venetoclax (an oral BCL2 inhibitor) and obinutuzumab (an intravenous anti-CD20 monoclonal antibody; VO), have provided tolerable and efficacious options for patients with CLL/SLL. In the CLL14 study, symptomatic patients with CLL receiving frontline therapy with VO had longer progression-free survival (PFS) and deeper remissions [more undetectable minimal residual disease (MRDu)] compared with to that seen in patients receiving chlorambucil and obinutuzumab [1]. The CLL-International Prognostic Index (CLL-IPI; Table 1) is a validated prognostic model to predict which patients are at highest risk for a shorter time to first therapy and shorter OS. A CLL-IPI score of ≥4 is considered high-risk on this scale. We aim to use VO as early intervention in asymptomatic, high-risk patients with CLL/SLL to potentially lengthen OS with the goal to alter the natural history of the disease.

Table 1 Calculation of CLL-IPI Score.

Characteristic	Points
Del(17p) or *TP53* mutation	4
β-2-microglobulin ≥3.5mg/L	2
Unmutated IGHV status	2
Rai Stage 1–4	1
Age >65 years	1

Figure 1. SWOG S1925 Study Schema

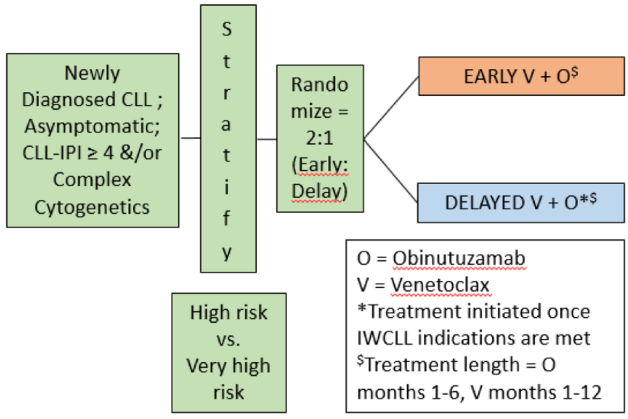

Methods: On 12/14/20, we activated the S1925 study (NCT#04269902) for adult patients with CLL or SLL, diagnosed within 12 months of enrollment. Eligible patients have a CLL-IPI score ≥4 (Table 1) or complex cytogenetics (≥3 cytogenetic abnormalities) and do not meet any criteria for initiation of treatment by the International Working Group for CLL (IWCLL; [2]) guidelines. Enrolled patients are randomized in a 2:1 manner to early versus delayed (at the time IWCLL indication for treatment is met) therapy with VO (Figure 1). Obinutuzumab is given intravenously on Cycle 1 Day 1 (C1D1; 100mg) and 2 (900mg), and at a dose of 1000mg on C1D8, C1D15, and C2-6 D1. Venetoclax is given daily by mouth starting on C1D21 at a dose of 20 mg daily, followed by a weekly ramp up to 50 mg (C2D1), 100 mg (C2D8), 200 mg (C2D15), and 400 mg (C2D21) pending no evidence of tumor lysis syndrome. As tolerated, 400mg daily dosing of venetoclax will be continued through the end of Cycle 12. The VO therapy is provided by the study. The primary endpoint is OS. We hypothesize that early intervention with VO will improve the rate of 6-year OS from 60 to 80%. This design requires 222 eligible patients for 88%

power (2-sided a = 0.05) for the primary comparison. To allow for 10% ineligibility, we will enroll 247 patients. The original estimated accrual time is 4 years. Secondary endpoints include: rates of response, PFS, and relapse-free survival; safety; time to second CLL-directed therapy; and quality of life (assessed by FACT-Leukemia total score). The primary translational objective is to evaluate the association between OS and peripheral blood MRD status by flow cytometry at 15 months after treatment initiation. Additional exploratory objectives include the association of other clinical outcomes, baseline prognostic factors, and IWCLL-defined response with MRD status at multiple timepoints.

Current status: At the time of submission, 67 patients have been registered and randomized per protocol. Accrual is ongoing.

Abstract ID: 1552978

Title: Evolution of natural history and prolongation of overall survival in patients with chronic lymphocytic leukemia: analysis of a long-term follow-up of an unselected cohort in the Hradec Králové district, Czech Republic

Authors: Lukáš Smolej, Martin Dostál, Pavel Vodárek, Dominika Écsiová and Martin Šimkovič

Introduction: One of the fundamental characteristics of chronic lymphocytic leukemia (CLL) is the extreme variability of prognosis: approximately half of patients never require treatment due to an indolent course. Over the last 20 years, there has been a revolution in the therapeutic approach to CLL, from chemotherapy through chemoimmunotherapy to oral targeted inhibitors (especially Bruton tyrosin kinase inhibitors ibrutinib and acalabrutinib and bcl-2 inhibitor venetoclax). However, analyses of the changes in the natural history and overall survival at large specialised centres are hampered by the selection bias from the regional hospitals which usually refer only patients requiring therapy and therefore have a poorer prognosis. Therefore, we eliminated the selection bias by analyzing a large unselected cohort of CLL patients with a long follow – up from a well – defined geographical region (the Hradec Králové district, Czech Republic) where all newly diagnosed cases could be recorded as the 4th Department of Internal Medicine – Hematology at our University Hospital serves as the primary hematology center. The aims of this retrospective study was to evaluate the natural history of the disease and evolution of time to first – line therapy (TTFT) and overall survival (OS) over time. Patients and methods: Between 1999 and 2019, a total of 311 patients were diagnosed in the Hradec Králové district. Basic characteristics and prognostic factors are listed in Table 1. At the median follow-up of 127 months, 44% patients progressed to first-line (1L) therapy and 54% patients died. To compare baseline characteristics and clinical course, we divided our cohort into three subgroups according to the years of diagnosis: Group 1 (1999–2005) included 97 patients, Group 2 (2006–2012) 101 patients and Group 3 (2013–2019) 113 patients. Statistical evaluation was performed using MedCalc v. 20.109 (Medcalc, Mariakerke, Belgium) software, with appropriate nonparametric tests to compare differences in individual variables. Time to first-line treatment and overall survival were assessed using the log-rank test and Kaplan-Meier curves. *p* Values were double – sided and considered significant if <0.05.

Table 1: Basic characteristics and prognostic factors

Total number of patients	311
Median age (range)	69 (31 - 92)
Males, %	59
Performance status ECOG ≥2	5
Binet stage A / B / C, %	86/7/7
Unmutated IGHV, %	44
FISH aberrations 13 / 12 / 11 / 17 / neg., %	41/10/16/5/26
Significant comorbidity, %	45
Second primary malignancy, %	13
Median follow-up, months	127
Treatment for CLL, %	44
Deaths, %	54

Fig. 1a: Overall survival from the initiation of first-line therapy

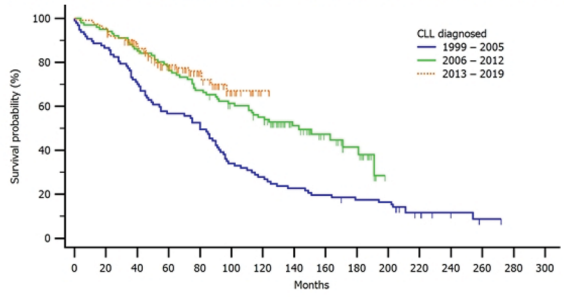

Fig. 1b: Overall survival based on the use of targeted inhibitors

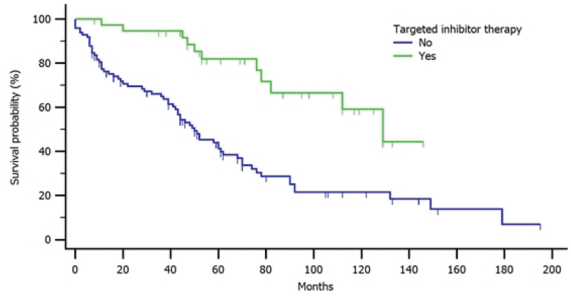

Results: Patients in Group 3 were significantly younger than those in Group 1 (median age 68 vs. 71 years, $p = 0.043$). Regarding time to endpoint variables, there were no significant differences between the 3 regarding TTFT ($p = 0.32$); however, there was a statistically and clinically highly significant increase in overall survival (median 80 vs. 143 months vs. not reached, $p < 0.0001$; Figure 1(a)). We hypothesized that more effective treatment (introduction of chemoimmunotherapy and targeted inhibitors) contributed most significantly to longer overall survival. Indeed, OS from the initiation of 1L treatment was significantly prolonged in Groups 2 and 3 (median 41 vs. 92 months vs. not reached, $p = 0.0001$). Patients who received 1L chemoimmunoterapy had significantly longer OS from the start of treatment than those treated by chemotherapy only (median 112 vs. 43 months, $p < 0.0001$). Similarly, patients who were treated anytime during their course of CLL by targeted oral inhibitors had markedly better OS from initiation of 1L than those who

did not receive such therapy (median 129 vs. 50 months, $p<0.0001$; Figure 1(b)). In addition, the use of chemoimmunotherapy in 1L (hazard ratio [HR], 0.48; 95% confidence interval [CI], 0.30–0.77; $p=0.0025$) and targeted oral inhibitors in R/R disease (HR, 0.40; 95% CI, 0.21–0.79; $p=0.0079$) retained their significance in multivariate analysis.
Conclusion: Analysis of a large, unselected cohort of CLL patients with a long follow – up revealed a significant decrease of age at diagnosis in recently diagnosed patients (Group 3). The key findings were significant prolongation of overall survival both from CLL diagnosis and start of first-line therapy, which was shown to be mainly thanks to introduction of chemoimmunotherapy and targeted oral inhibitors. Supported by programme COOPERATIO (research area ONCO) and DRO MH CZ (UHHK, 00179906).

Abstract ID: 1552997

Title: Pregnancy course of 10 women diagnosed with chronic lymphocytic leukemia

Authors: Tamar Tadmor, Guy Melamed, Hilel Alapi, Sivan Gazit, Tal Patalon and Lior Rokach

Pregnancies following diagnosis of Chronic Lymphocytic Leukemia (CLL) are rare events, mainly because the disease is typically diagnosed in the elderly. Literature on the topic is based only on case reports, and limited data are available on the influence of pregnancy on CLL course. In this retrospective study, we aimed to summarize the clinical and laboratory course of 10 women with CLL who became pregnant. None of the patients had significant changes in blood count during or after pregnancy or had complications as infection, autoimmune phenomenon, or preeclampsia. Four out of 10 pregnancies were terminated with an early miscarriage. Following labor, One patients started anti-CLL treatment due to pre-exciting anemia, but none of the women required therapy during CLL progression during the first two years of follow-up. We conclude that based on our serial; pregnancy doesn't impact negatively on CLL course.

Abstract ID: 1552999

Title: Ibrutinib induces cardiac arrhythmia by targeting CaV1.2 calcium channel

Authors: Juejin Wang, Dongxia Qin, Feiran Liu, Xingyu Song, Ludan Zhang, Pengpeng Li, Wei Hou, Yu Sun, Jianyong Li and Huayuan Zhu

Background: Ibrutinib is a Bruton tyrosine kinase inhibitor that has shown significant efficacy against chronic lymphocytic leukemia (CLL). Clinical studies have found that ibrutinib increases the risk of cardiac arrhythmia, but the underlying molecular mechanisms are still unclear. CaV1.2 calcium channel is indispensable for the cardiac excitations, its dysregulations indeed lead to arrhythmia. However, the associations between ibrutinib and cardiac CaV1.2 channel and calcium-dependent signaling remain unknown.
Methods: We collected clinical history of the CLL patients treated with ibrutinib to analyze possible factors, which might associated with cardiac arrhythmia. Electrophysiological experiments were conducted in the hearts from mouse model and neonatal rat ventricular myocytes (NRVMs) to assess ibrutinib induced arrhythmia. mRNA transcriptomic of cardiac tissue was performed to screen the potential target genes of ibrutinib-induced arrhythmia. The pathogenesis of arrhythmia was further studied at mouse models and cellular experiments.
Results: Clinical data showed that the incidence of cardiac arrhythmia of CLL patients treated with ibrutinib is ~19.2%. At animal model, the mouse treated with ibrutinib (25 mg/kg/d) for 28 days were more likely to develop spontaneous ventricular arrhythmias (46.2%, 6/13) in comparison to the control mice (8.3%, 1/12), and M-mode echocardiography indicated ibrutinib treatment induces systolic dysfunction. The expression levels of CaV1.2 α1C protein and the phosphorylated CaMKII, which were identified by RNA-seq, in mouse hearts and ibrutinib-treated NRVMs were significantly increased. Whole-cell patch clamp showed that the activation kinetics of cardiac CaV1.2 channel of ibrutinib-treated NRVMs shifts towards hyperpolarization, and its current size is also increased. Furthermore, the intracellular calcium concentration that detected with Fluo-4 AM was found to be increased after application with ibrutinib in NRVMs.
Conclusions: These findings suggest that ibrutinib could increase CaV1.2 expression of myocardial cells, and enhance the functions of CaV1.2 channels. Thus, this causes intracellular calcium signaling disturbance and triggering cardiac arrhythmia.

Abstract ID: 1553057

Title: Orelabrutinib combined with bendamustine and obinutuzumab as the first-line treatment for chronic lymphocytic leukemia/small lymphocytic leukemia: a phase II multicenter exploratory study

Authors: Ru Feng, Xutao Guo, Hui Zhou, Hong-xiang Wang, Xiaolei Wei, Yongqiang Wei and Wei Qi

Introduction: Targeted therapy with Bruton's tyrosine kinase inhibitors (BTKis) has emerged as a standardized treatment for patients with previously untreated or relapsed/refractory chronic lymphocytic leukaemia/small lymphocytic lymphoma (CLL/SLL; [1]). Recently, given the increase in adverse events, high dropout rates and drug resistance with long-term continuous administration of BTKi, there has been an increased focus on time-limited BTKi-based regimens and undetectable minimal residual disease (uMRD; [2,3]. Ibrutinib or zanubrutinib combined with bendamustine (B) and rituximab therapy has been confirmed to be associated with promising activity for CLL/SLL through fixed-duration therapy [4]. Compared with rituximab, Obinutuzumab (G) is a type II anti-CD20 antibody with enhanced direct cell killing and antibody-dependent cellular cytotoxicity (ADCC; [5]). Orelabrutinib is a novel BTKi with excellent target selectivity for B-cell lymphoma, combined with rituximab could preserve natural killer-cell-mediated ADCC induced by rituximab and

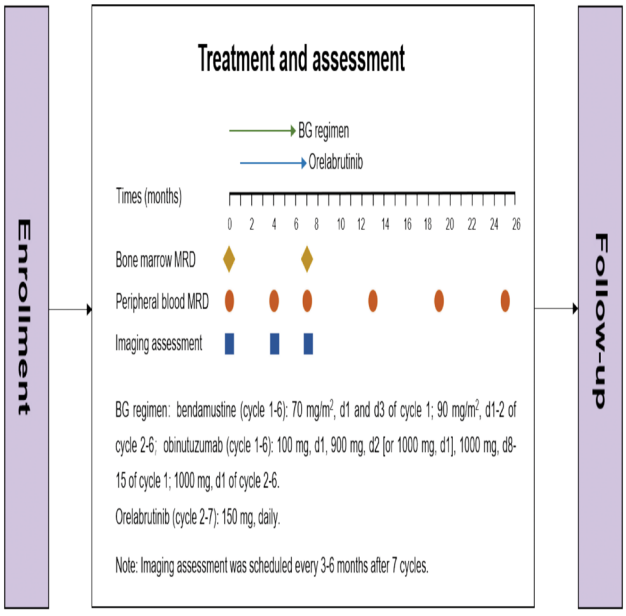

produces synergistic anti-tumor responses [6]. Recent accumulating evidence has demonstrated that orelabrutinib has shown an encouraging anti-tumor activity and favorable safety profile in CLL/SLL [7]. Additionally, taking the CR/CRi with uMRD rate as the primary endpoint would avoid the lack of stability (return to positivity within a short time) and inadequate assessment (residual lesions at other sites) by MRD negativity alone. Here, we present this phase II, multicenter, single-arm trial to investigate the new time-limited orelabrutinib combined with BG regimen in patients with CLL/SLL who are ineligible for intensive chemotherapy and to explore the influence of this time-limited therapy as well as complete response (CR) with MRD negativity on MRD stability by dynamic MRD monitoring.

Methods: Eligible patients will be aged 18–65 years with severe disease (non-CLL Cumulative Illness Rating Scale score ≥6) or >65 years, with histologically/pathologically confirmed CD20 positive CLL/SLL per International Workshop on Chronic Lymphocytic Leukemia (IWCLL) 2008 criteria, and have not received prior systemic therapy for CLL/SLL. Patients are also required to have an Eastern Cooperative Oncology Group performance status score of 0–2, at least one treatment indication according to IWCLL 2008 criteria or Guidelines for the diagnosis and treatment of CLL/SLL in China version 2022, and adequate hematologic, hepatic, and renal function. Patients with chromosome 17p deletion or TP53 mutations are excluded. Patients will receive BG therapy for the first 28-day cycle, followed by orelabrutinib combined with BG for cycle 2–6, and orelabrutinib monotherapy for cycle 7 thereafter (Figure 1). The primary endpoint is CR/CRi with uMRD rate at the end of cycle 7. Secondary endpoints include CR/unconfirmed CR (CRu) with uMRD rate, objective response rate, uMRD rate, progression-free survival, overall survival, duration of response, quality of life, and safety. CRi was defined as CR with incomplete recovery of bone marrow. CRu was defined as CR/CRi with spleen size ≤16 cm. Exploratory endpoints are dynamic monitoring of MRD in the patient's bone marrow (baseline, cycle 7) and peripheral blood (baseline, cycle 4, cycle 7, month 13, month 19, and month 25) using next-generation sequencing assays. This study plans to enroll 24 patients and the clinicaltrials(NCT) registration is ongoing.

Conclusions: This phase II study is expected to provide a treatment option for patients with CLL/SLL who are ineligible for intensive chemotherapy.

Abstract ID: 1553077

Title: Loss of IκBε accelerates disease development in chronic lymphocytic leukemia

Authors: Jessica Bordini, Chiara Lenzi, Michela Frenquelli, Alessia Morabito, Athanasios Pseftogkas, Larry Mansouri, George Tsiolas, Eleonora Perotta, Pamela Ranghetti, Francesca Gandini, Daniel Hägerstrand, Georgios Gavriilidis, Sofoklis Keisaris, Nikolaos Pechlivanis, Riccardo Moia, Frederic Davi, Neil Kay, Anton W. Langerak, Sarka Pospisilova, Lydia Scarfò, Fotis Psomopoulos, Kostas Stamatopoulos, Richard Rosenquist Brandell, Alessandro Campanella and Paolo Ghia

Background: The NF-κB pathway is particularly relevant in the pathophysiology of Chronic lymphocytic leukemia (CLL), as it is activated in patients with CLL as a result of intrinsic and microenvironmental stimuli. Among the few NF-κB pathway genes found altered in CLL, the NFKBIE gene, which encodes the inhibitor IκBε, is mutated in 3–7% of CLL patients. The presence of mutations correlates with an adverse prognosis and an advanced clinical stage, being particularly enriched in clinically aggressive cases and in patients relapsing under the BTK inhibitor ibrutinib treatment, suggesting that a reduced expression of NFKBIE may contribute to CLL aggressiveness through constitutive NF-κB activation and be an alternative pathway of ibrutinib resistance. In this study, we investigated the role of IκBε in controlling NF-κB activity and disease expansion in CLL, inactivating the gene by CRISPR-Cas9 both *in vitro* and *in vivo* disease models.

Materials and methods: We engineered the MEC-1 CLL cell and obtained cell lines with a partial (KO1) or total (KO2) ablation of NFKBIE gene. We studied *in vitro* cell proliferation and migration, gene expression, BcR signaling pathway, and response to treatment with the BTK inhibitor ibrutinib. *In vivo*, we performed xenograft experiments by injecting MEC-1 control and KO cells into RAG2-/-γc-/- recipient mice. We also reproduced the most frequent mutation observed in patients with CLL by generating Nfkbie4bpdel/4bpdel mutated mice and crossed them with Eμ-TCL1 mice to obtain immunocompetent Eμ-TCL1-Nfkbie4bpdel/4bpdel. To thoroughly confirm that NFKBIE mutations play a cell-autonomous role in leukemic cell expansion, we performed adoptive transfer (AT) of Eμ-TCL1 or Eμ-TCL1-Nfkbie4bpdel/4bpdel leukemic cells. In mice, we monitored disease development, dissemination, and ibrutinib sensitivity by following CD19+CD5+ leukemic cells in peripheral blood (PB) at 3, 6, and 9 months of age and in the spleen (SP) and bone marrow (BM) at necropsy. In addition, we performed RNA-sequencing analysis in a cohort of 50 patients with CLL (13 carrying NFKBIE mutations and 37 NFKBIE wildtype CLL cases).

Results: Biochemical analyses in KO cells revealed increased cRel and p50 protein levels and increased p65 phosphorylation, all NF-κB transcription factors, indicating unabated cellular activation. Moreover, NFKBIE KO cells showed higher

proliferative and migratory capacity than control MEC-1 cells at a magnitude directly related to the NFKBIE ablation rate. The effect of NFKBIE manipulation was even more striking evident in vivo. Xenografts, generated with MEC-1 NFKBIE KO cells, showed an increased disease expansion in the SP and BM and shorter survival than mice injected with control MEC-1 cells. Eμ-TCL1 mice carrying the 4bp deletion in the Nfkbie gene showed an increased amount of leukemic cells in the PB than Eμ-TCL1 control mice at 3, 6, and 9 months of age. By necropsy at 6 months of age, we also observed the increase in malignant cells in SP, BM, and PB of Eμ-TCL1 Nfkbie mutated mice compared to Eμ-TCL1 mice at a magnitude directly related to the ploidy of the mutated allele. Adoptive transfer experiments confirmed the cell-autonomous effect of Nfkbie inactivation. *In vitro,* the proliferation of KO cells was less impacted by ibrutinib than MEC-1 control cells, an event particularly evident in the competition experiments in which KO showed an increased advantage over control cells upon ibrutinib exposure. In vivo, ibrutinib treatment reduced disease expansion in SP of MEC-1 xenografts but not in KO xenografts mice. Interestingly, RNA-sequencing analysis of primary CLL samples revealed that functional ablation of NFKBIE is associated with distinct changes in signaling pathways, including activation of the MAPK pathway. This is particularly relevant as it well associates with the increased cell proliferation observed in our models. In addition, it fits with the observation that the activation of the MAPK pathway is associated with the occurrence of resistance to the drug.

Conclusion: Loss of NFKBIE function is associated with more aggressive disease in all CLL models tested, both in vitro and in vivo, accelerating disease progression under pro-tumorigenic CLL conditions. Furthermore, the association with ibrutinib resistance and upregulation of the MAPK pathway highlights the multimodal relevance of the NF-κB pathway in CLL and paves the way for new potential therapeutic strategies with MAPK pathway inhibitors to overcome or prevent drug resistance.

Abstract ID: 1553083

Title: Lenalidomide consolidation improves progression free survival in patients with chronic lymphocytic leukemia following initial FCR chemotherapy – final analysis of CLL6 Residuum Study of the Australian Leukaemia and Lymphoma Group (ALLG) and the French Innovative Leukemia Organization (FILO)

Authors: Thérèse Aurran, Stephen Mulligan, Marie-C Bene, Gavin Cull, Jean-Pierre Vilque, Constantine S. Tam, Sophie De Guibert, Rosemary Harrup, Bernard Drenou, Andrew Grigg, Laurent Voillat, Belinda Butcher, Caroline Dartigeas, Richard Eek, Nicolas Daguindau, Cecily Forsyth, Mourad Tiab, Jenny Curnow, Veronique Leblond, Stephen Larsen, Florence Cymbalista and David Gottlieb

Introduction: Eradication of residual disease after first line chemoimmunotherapy correlates with longer progression-free survival (PFS) in chronic lymphocytic leukemia (CLL) patients.

Table 1 Progressions and Progression Free survivala at 24, 36, 48 and 60 months

	Lenalidomide (N=69)	Observation (N=72)	p-value
Number of Progressions	28	40	
Median (Months)	64.56	42.37	
(95% CI)	(47.67,NR)	(32.28,61.64)	
Log rank test			0.0386
PFS 24 Months	92.1% (82.1%,96.6%)	74.4% (62.4%,83.0%)	
PFS 36 Months	74.5% (61.2%,83.8%)	62.0% (49.3%,72.4%)	
PFS 48 Months	64.2% (50.0%,75.4%)	46.1% (33.3%,57.9%)	
PFS 60 Months	54.4% (39.5%,67.1%)	42.1% (29.5%,54.1%)	

Figure 1: Progression-free (Upper panel) and overall (lower panel) survival CLL6 RESIDUUM Study

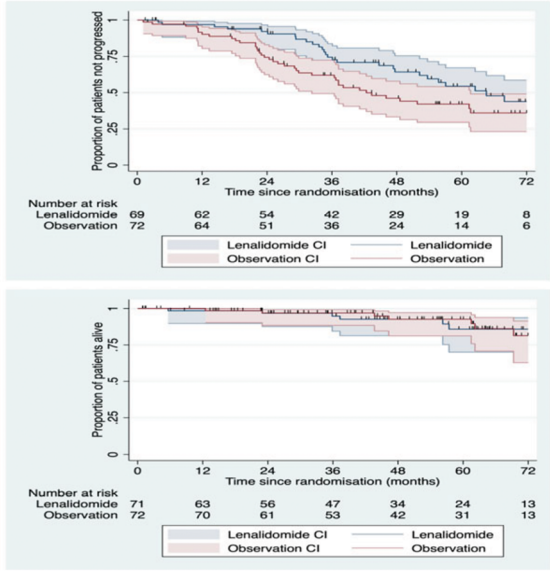

Lenalidomide (LEN) has antiproliferative and immunomodulatory effects in CLL and may be effective in improving response status following chemotherapy [1,2]. Here we report the final analysis of the phase III, randomized, CLL6 RESIDUUM trial, aiming to determine whether lenalidomide is capable of extending remission duration in patients with CLL who have detectable residual disease following induction immunochemotherapy.

Methods: The CLL6 RESIDUUM trial was a joint trial of the Australasian Leukaemia and Lymphoma Group (ALLG) and the French Innovative Leukemia Organization (FILO). CLL patients with CIRS score <6 requiring treatment according to iwCLL criteria received 4 to 6 cycles of fludarabine cyclophosphamide rituximab combination (FCR). Following completion of treatment, patients with clinical, radiological and/or multiparameter flow cytometry evidence of residual CLL in blood or bone marrow were randomized 1:1 to receive 2 years of maintenance treatment with LEN 10 mg daily or observation (OBS). LEN treatment started at 5 mg daily, escalating by

2.5mg every 2 months until a target of 10 mg daily. The primary endpoint of this study was the time to clinical disease progression, or death, from the date of randomization. It was planned to randomize 192 patients in order for the study to be powered to detect a hazard ratio of 1.94, i.e. an increase in the percentage of patients remaining free from progression at 4 years up to 70% in the LEN arm compared with 50% in the OBS arm (two-sided log rank test at alpha =0.05, no competing risks or loss to follow up, power =0.86).

Results: The study closed prematurely because of an acute lymphoblastic leukemia (ALL) warning (3 of 56 patients [5.4%]) in the CLLM1 trial [3,4] Between May 2011 and January 2018, 143 patients were randomized (70 in Australia and 73 in France) to the LEN ($n=71$) or OBS ($n=72$) arms. Their median age was 63 [range 41–78], and 60 [26–79] years in the LEN and OBS arms respectively and 113 patients were males. At the time of evaluation, the median follow-up was 52.56 months (range 44.9–58.97; LEN 49.84 [41.88–57.07], OBS 55.49 [43.95–61.67]). Twenty-four (34%) patients progressed in the LEN arm versus 39 (54%) in the OBS arm (Chi^2 $p=0.01$) and 8 died in each arm. Median PFS was 64.56 (95%CI 47.67–not reached [NR]) months in the LEN arm versus 42.37 (32.28–61.64) months in the OBS arm ($p=0.039$). Multivariate analysis did not identify any predictive factor of relapse. Median overall survival was not reached in the LEN arm and 107.66 (107.55–NR) months in the OBS arm. There were 78 adverse events (AE), 51 in the LEN and 27 in the OBS arms respectively, the main differences being more neutropenia ($n=9$ vs. $n=1$), musculoskeletal ($n=4$ vs. $n=1$), nervous system ($n=5$ vs. $n=1$), respiratory ($n=5$ vs. $n=0$) and vascular ($n=3$ vs. $n=1$) disorders in the LEN arm. Severe adverse events (SAE) were reported in 35 patients (24.5%), 24 in the LEN arm and 11 in OBS. Sixteen secondary malignancies occurred: 9 in the LEN arm; 7 in the OBS arm. Four were of hematological origin (1 Richter transformation in each arm, 1 marginal zone lymphoma in the OBS arm and 1 myelodysplastic syndrome in the LEN arm). No case of ALL occurred.

Conclusion: Overall, the CLL6 RESIDUUM study demonstrates a significant benefit of consolidation therapy with low-dose lenalidomide in CLL patients with residual disease after FCR treatment compared to simple observation. The immunomodulatory effect of lenalidomide translated into a significantly longer PFS, the median of which was not reached at more than 5 years, with no unacceptable toxicity. Specifically, no case of ALL occurred in 69 patients with a minimum 4-year follow-up. This trial was designed and conducted when FCR was gold standard and considered patients who had completed this treatment. However, even with current targeted agents, eradicating minimal residual disease may remain challenging. Some patients could still benefit from such maintenance therapy, expected to control the disease through improved anti-tumoral immune responses in poorer responders.

Abstract ID: 1553084

Title: Regulation of the NF-kB pathway by NEDDylation in chronic lymphocytic leukemia: beyond IkB

Authors: Carlos Pipaón, Víctor Arenas, Jose Luis Castaño, Noelia Ruiz-Alonso and Lucrecia Yáñez

The NF-kB survival pathway is the final effector of many of the alterations found in CLL and is heavily over-activated in CLL. Cells control NF-kB activity by altering the stability of the inhibitor protein of the pathway (IkB) through its phosphorylation and subsequent poly-ubiquitination and degradation at the proteasome and it was assumed that NEDDylation was exclusively modulating the NF-kB pathway through the destabilization of IkB. Indeed, molecules targeting the ubiquitin-proteasome axis have been explored to control CLL. To better understand the role of NEDDylation on the NF-kB pathway, we analyzed samples from CLL patients and healthy donors and the effect of the NEDDylation inhibitor MLN4924 over these samples. When we did a proteomic screening of ubiquitin-like post-translational modifications (UBL-PTM) in CLL cells, we did not find an elevated ubiquitination of IkB. Moreover, when we blocked the proteasome function with bortezomib, MLN4924 scarcely incremented IkBα stability any further, but strongly increased its phosphorylation. This suggested that NEDDylation was modulating IkBα phosphorylation. Our screening in CLL found alterations affecting many UBL-PTMs of upstream members of the NF-kB pathway. B-CLL tumoral cells showed an elevated modification of the IkBα kinase IKKß at lysine 106 that increased even more under the action of MLN4924. Our experiments showed how modulation of the cellular NEDDylation state through chemical and genetic strategies alter the stability of IKKß and consequently the phosphorylation and stability of IkBα. In addition, MLN4924 potentiated the cell death induced by the IKKß inhibitor BAY11-7082. Mutation of IKKß lysine 106 to the non-modificable residue arginine made the protein refractory to destabilization with NEDD8 and affected its kinase activity. NF-kB pathway activates the transcription of its own inhibitor IkBα in a feedback loop to terminate its signaling. Unexpectedly, NFKBIA mRNA levels (coding for IkBα) accumulated in peripheral blood mononuclear cells from CLL patients at a lower level than in those from healthy donors. NFKBIA inhibition through a GSK-3ß-mediated phosphorylation that turns p65/RelA into a transcriptional repressor is a characteristic of senescence cells. We explored whether B-CLL cells may fit into this phenotype. Chemical and genetic inhibition of GSK-3ß reverted the accumulation of NFKBIA in B-CLL cells, leading to an increment in their cell death. GSK-3ß also affected the expression of other inflammatory-related genes, but their pattern of transcription did not support a senescence phenotype of B-CLL cells. We explored whether the general elevated level of UBL-PTMs in B-CLL cells also affected the transcription of NFKBIA. Indeed, in knock out cells for the de-NEDDylation protein NEDP1 that show an increase in basal protein NEDDylation levels, NFKBIA mRNA declined in parallel with a stabilization of GSK-3ß. On the other hand, NEDDylation also modulated the function of p65/RelA, controlling its protein levels, phosphorylation, translocation to the nucleus and DNA binding. In summary, we provide evidence that widens our knowledge of the regulatory action of NEDDylation over the NF-kB pathway in CLL and may help finding new therapeutic targets. Our data indicate that NEDDylation controls the transcription of the NFKBIA gene and the phosphorylation and stability of IkB and RelA/p65. This demonstrates the complexity of this regulation and warns about the general inhibition of NEDDylation that may have contradictory effects on cell biology.

Abstract ID: 1553090

Title: Reduced predictive value of elevated beta-2-microglobulin plasma levels on time to first treatment in newly diagnosed CLL patients with compromised kidney function

Authors: Jan-Paul Bohn, Valentina Stolzlechner, Georg Göbel, Normann Steiner, Markus Pirklbauer and Dominik Wolf

Introduction: The clinical course of newly diagnosed CLL is extremely heterogeneous. Predictive indices, such as the CLL-IPI were developed to help identify patients who require therapy relatively soon after diagnosis. Besides dysfunctional TP53 and unmutated IGHV status, elevated beta-2-microglobulin (B2M) plasma levels were shown to most effectively filter patients at high risk for short time to first therapy (TTFT) in the weighted risk score of the CLL-IPI. However, B2M plasma levels are commonly elevated in patients with chronic kidney disease (CKD) and the CLL-IPI has not been adjusted for compromised kidney function.
Methods: Between 2000 and 2022, newly diagnosed CLL patients not fulfilling criteria for immediate specific treatment were identified from the clinical database at a tertiary care center in Innsbruck, Austria. TTFT was stratified according to the CLL-IPI and CKD (GFR <60 ml/min). B2M plasma levels were compared in CKD and non-CKD patients. In CKD patients with elevated B2M plasma levels (>3.5 mg/L), the CLL-IPI was reviewed to check if elevated B2M plasma levels led to a higher CLL-IPI risk category.
Results: Our cohort included 299 CLL patients with a median age at diagnosis of 66 years (range: 32–88) and a female-to-male ratio of 1:2. CKD was evident in 15% of patients. CLL-IPI risk groups were balanced among patients with and without CKD (low: 34 versus 38%, intermediate: 44 versus 40%, high: 16 versus 12%, very high: 6 versus 10%). With a median follow-up of 98 months (range: 2 – 360 months) 53.5% of patients eventually met criteria for specific CLL treatment. Median TTFT was 154 months in both patients with normal and decreased kidney function, whereas B2M plasma levels were significantly higher in CKD patients (B2M >3.5 mg/L: 35.5 versus 9.3%, $p<0.05$). Elevated B2M plasma levels led to a higher CLL-IPI risk category in 19.4% of CKD patients.
Conclusion: CLL patients with CKD and elevated B2M plasma levels at the time of CLL diagnosis may show similar TTFT as non-CKD patients with normal B2M plasma levels. Our results suggest that the predictive value of B2M plasma levels on TTFT in newly diagnosed CLL patients, particularly as a factor in the CLL-IPI, must be interpreted with caution in those with decreased kidney function.

Abstract ID: 1553104

Title: Past informs the future: outcomes post allogeneic stem cell transplantation in high risk chronic lymphocytic leukaemia (CLL)

Authors: Rory Bennett, Thomas Frawley, Amit Khot, Phillip Thompson, Mary Ann Anderson and David Ritchie

Aim: Emerging immunotherapies for CLL, bispecific antibodies and CAR-T, may challenge the established role of allogeneic stem cell transplantation (alloSCT) for eligible patients. This retrospective study analyzed characteristics and survival outcomes for patients with CLL following alloSCT, including impact of TP53 aberrancy, over a 22-year period. Method: All patients with CLL who underwent first alloSCT between January 2000 and April 2022 (data cut-off 6/12/2022) at Royal Melbourne Hospital (RMH), Australia, were identified from the institutional alloSCT database. Additional patient details were extracted from institutional records. Relapse-free survival (RFS) and overall survival (OS) estimates/comparisons were analyzed by Kaplan–Meier method/log-rank analyses on GraphPad Prism v.9.5.1.
Results: Sixty-two patients, median age 52 (range, 25–75) years, 79% male, were identified for analysis. Patient characteristics are summarized in Table 1. Median two prior lines of therapy were observed in both the pre-novel agent era cohort of 2000–2011 (range 1–4) and 2012–2022 (range 1–9). Eighty-six percent ($n=49$) were purine-analogue-, 15.8% ($n=9$) venetoclax-, 15.8% ($n=9$) Bruton's tyrosine kinase inhibitor (BTKi)-, and 3.5% ($n=2$) PI3 kinase inhibitor-exposed respectively. Two further patients had received alemtuzumab (3.5%). Overall, 26.3% ($n=15$) were treated with a targeted agent immediately prior to alloSCT and 45.6% ($n=26$) with chemoimmunotherapy. All patients who received targeted

	Value (range or %)
Age (years), median (range)	52 (25-75)
Male sex	49 (79%)
History of Richter transformation	17 (27.4%)
Median prior lines of treatment	2 (1-9)
Disease response prior to alloSCT	
CR	17 (28.8%)
PR	21 (35.6%)
SD/PD/untreated	21 (35.6%)
CR/PR uMRD	7 (22.6%)
Adverse genomic lesions*	
CKT (≥3 lesions)	14 (36.8%)
Del(11q)	15 (30.6%)
Del(17p)	16 (35.6%)
TP53 mutation	5 (50%)
Unmutated IGHV	7 (70%)
Peripheral blood HPC	59 (95.2%)
Donor source	
Sibling	38 (61.2%)
Unrelated	23 (37.1%)
Haploidentical	1 (1.6%)
Myeloablative conditioning	18 (29%)
CyTBI	18 (100%)
Non-myeloablative/reduced-intensity conditioning	44 (71%)
FluLDCy+/-TBI	5 (11.4%)
FluHDCy	11 (25%)
FluMel	28 (63.6%)
Median days to neutrophil engraftment, median (range)	18 (10-49)

Table 1. Patient characteristics. *Denominator according to available information. CR – complete response, PR – partial response, SD – stable disease, PD – progressive disease, CKT – complex karyotype, HPC – haematopoietic stem cells, Cy – cyclophosphamide, LD – low-dose, HD – high-dose, TBI – total body irradiation, Flu – fludarabine, Mel – melphalan.

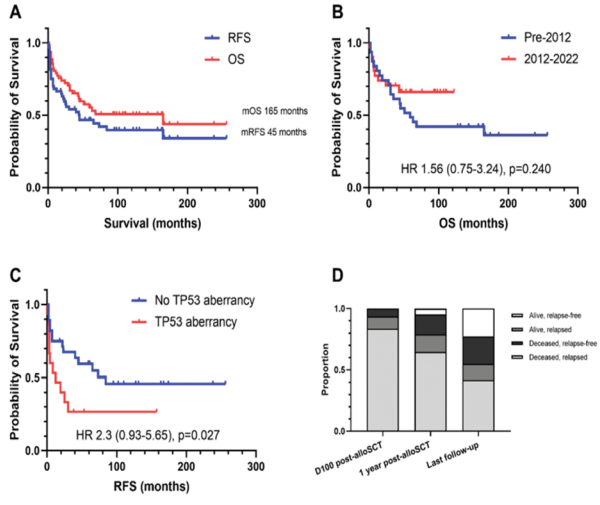

Figure 1. A – Kaplan-Meier estimates of relapse-free and overall survival for cohort. B – Kaplan-Meier estimates of overall survival stratified by year of alloSCT. C – Kaplan-Meier estimates of relapse-free survival as stratified by presence or absence of *TP53* aberrancy. D – Proportions of patients alive or dead with or without disease relapse.

agents before alloSCT underwent alloSCT in 2012 or later. Sixty-four percent ($n=38$) were in partial response (PR) ($n=21$) or CR ($n=17$) prior to alloSCT; 7/31 of whom had peripheral blood/bone marrow undetectable MRD by flow cytometry. The remaining patients had stable or progressive disease as best response to therapy immediately prior to alloSCT ($n=17$), or had untreated progressive disease ($n=4$). Seventeen (27.4%) had prior history of Richter transformation (RT), sixteen of whom received alloSCT in first complete response (CR1). Sixteen (35.6%) patients exhibited del(17p) +/− TP53 mutation (5/10, all del[17p] positive), four of whom had history of RT. Non-myeloablative/reduced-intensity conditioning was used for 71% ($n=44$) patients. Haematopoietic stem cells were obtained from sibling, unrelated, and haploidentical donor sources for 38 (61.2%), 23 (37.1%) and 1 (1.6%) patients, respectively. At a median follow-up of 110 months, median RFS and OS were 45 (range, 0–256) months and 165 (range, 1–256) months respectively following alloSCT (Figure 1). One-year RFS and OS rates were 66.6 and 79.0%, and 5-year RFS and OS rates were 46.5 and 55.5% respectively. Twenty-two patients (35.5%) relapsed during study follow-up, including six (27.3%) with RT, four of whom had prior history of RT. For patients treated with alloSCT prior to 2012, two (20%) received BTKi following subsequent relapse compared with eight (66.7%) from 2012 onwards. At day 100 (median 101, range 71–118) post-alloSCT, 41.2% ($n=21$) demonstrated mixed T-cell chimerism (<95%). One-year non-relapse mortality (NRM) was 16.1% ($n=10$); 4/10 died due to infection, and 3/10 due to complications of GvHD. Overall incidence of grade 3/4 acute GvHD was 21.1% ($n=12$), and chronic GvHD 65.5% ($n=38$). Presence of TP53 aberrancy was associated with inferior mRFS, 12 vs. 84 months (hazard ratio [HR] 2.3 [0.93–5.65], $p=0.027$), but not mOS, 35 months vs. not reached (HR 2.0 [0.76–5.26], $p=0.107$). Response < PR pre-alloSCT, D100 mixed T-cell chimerism, and history of previous RT were not associated with inferior RFS. Treatment with alloSCT pre-2012 was not associated with reduced overall survival; (HR 1.56 [0.75–3.24], $p=0.240$).

Conclusion: RFS, OS, and NRM outcomes for CLL following alloSCT are consistent with other national and international registry data with inferior survival outcomes post-alloSCT for CLL exhibiting TP53 aberrancy. Despite availability of targeted therapies following relapse, post-alloSCT OS was not significantly longer for those receiving alloSCT from 2012 onwards. This is likely to reflect the small numbers of patients included in the study as an expected limitation. These data serve as future comparator for local outcomes following newer immunotherapies.

Abstract ID: 1553145

Title: Chronic lymphocytic leukemia extracellular vesicles induce the differentiation of monocytes into nurse-like cells

Authors: Nathan Dubois, David VanMorckhoven, Laurentijn Tilleman, Filip Van Nieuwerburgh, Dominique Bron, Nathalie Meuleman, Laurence Lagneaux and Basile Stamatopoulos

Background: Bidirectional interactions exist between Chronic Lymphocytic Leukemia (CLL) cells and the cells of their microenvironment (ME): CLL cells indeed received several stimuli such as BCR stimulation but they can also interact with the surrounding cells by the release of extracellular vesicles (EVs). EVs are small double membrane particles (from 100nm to 1µm) carrying proteins, DNA and several types of RNA such as microRNAs. EV exchange is today considered as a new way of cell communication.

Aim: We hypothesize that BCR stimulation could alter EV content and that CLL-EVs could manipulate immune ME cells such as monocytes and stimulate their differentiation into nurse-like cells (NLC), well known in CLL to support leukemic cell survival.

Methods: The microRNA profile of CLL-EVs isolated by ultracentrifugation from leukemic cells cultured with/without BCR stimulation ($n=4$) was performed by NGS and validated by qPCR ($n=25$). CLL-EV integration was monitored using PKH67 and Memglow dyes. After treating purified monocytes with CLL-EVs (Mono + CLL-EVs), the morphology, the cytokine profile, specific microRNA and mRNA expression and their ability to support CLL cell survival were analyzed and compared to those of NLC.

Results: NGS highlighted 31 microRNAs differentially expressed between BCR stimulated/unstimulated conditions and qPCR confirmed the increase of 4 of them ($n=25$): miR-146a-5p (fold: +15.1, $p<0.0001$), miR-132-3p (fold: +42.1, $p<0.0001$), miR-155-5p (fold: +3.3, $p=0.003$) and miR-17-3p (fold: +3.1, $p=0.0135$) in EVs. While the expression of miR-150 was not affected in CLL EVs after BCR stimulation, miR-150-5p was the most abundant microRNA in CLL EVs. After 24h of incubation of CLL PBMC with CLL-EVs, 76% of monocytes were PKH67+ indicating they were the first cell type to integrate CLL-EVs while they only represent 3.5% of all PBMC ($p=0.0019$, $n=6$). Although, Mono + CLL-EVs display a fibroblast morphology similar to M2 macrophages. After 24h of incubation with CLL-EVs, miR-155-5p, miR-146a-5p, miR-132-3p were increased in monocytes (fold: +4.8, +4.5; +5.6, respectively; $p<0.05$, $n=9$) similarly to what happens in the differentiation of monocytes in NLC (fold: +5.6, +27.4, +12, respectively, $p<0.01$, $n=10$). Moreover, target of these microRNAs such as S1PR3 or KLF40 were decreased in Mono + CLL-EVs, in NLC and in Mono + Mimic ($p<0.05$, $n=11$). In addition, genes that were increased (MMP9, SPP1) or decreased (CCR2) after NLC differentiation display a similar trend in Mono + CLL-EVs ($n=10$, $p<0.05$). Multiplex immunoassay analysis ($n=3$) highlighted the increase of IL-10 (fold: +18.6), IL-8 (+6.1), IL-6 (+488.4), BAFF (+18.6), CCL2 (+4.9) and SDF-1α (+13.9) in Mono + CLL-EV produced in BCR stimulated conditions. These cytokines have already been described as increased in NLC or supporting CLL cell survival. Finally, CLL cells incubated with Mono + CLL-EVs showed a decreased apoptosis compared to co-culture with untreated monocytes (decrease of 18%±3.1, $p=0.0156$, $n=6$) highlighting the protective effect of these EV-transformed monocytes.

Conclusion: We showed that BCR stimulation modifies CLL EV microRNA content. The addition of EVs on monocytes lead to a shape change, an increase of several microRNAs, a decreased expression of some of their targets, an increase of several cytokines and an increased ability to rescue CLL cells from spontaneous apoptosis. Altogether, our data indicate that CLL-EVs induce the differentiation of monocytes into NLC supporting CLL cell survival.

Abstract ID: 1553156

Title: Treatment of symptomatic paraneoplastic fluidothorax in CLL with novel agents: a single-center case series.

Authors: Peter Turcsanyi, Eva Kriegova and Tomas Papajik

Introduction: Chronic lymphocytic leukemia (CLL) is the most common hematologic malignancy in western world, presenting with various clinical manifestations. CLL cells are mainly present in the peripheral blood, bone marrow and lymph nodes. As a rare compartment involvement could be a pleural space. We describe here a case series of four patients (P1–P4) with symptomatic CLL paraneoplastic fluidothorax, successfully treated by novel agents. Patients and cases description: P1. Woman, born in 1941, CIRS (Cumulative Illness Rating Scale): 8 (facial herpes zoster, residual paresis of ocular nerves, dyslipidemia, hypertension, osteoporosis). CLL was diagnosed in 2018 (in 77 years), stadium Binet B, Rai I., IGHV unmutated, del 6q. I.st line of treatment: 6 x RCD (rituximab, cyclophosphamide, dexamethasone) have been given from November 2019 to April 2020 due to symptomatic fluidothorax, evacuated several times with 60% CLL infiltration verificated by flow cytometry. Lymph nodes with a maximum to 1 cm was observed. Patient achieved partial remission (PR) and due to progression receiving 2nd line of therapy – reduced ibrutinib (140 mg/day) since July 2020. At this treatment, fluidothorax regressed completely. Last follow-up (FU) was May 2023 (progression free survival - PFS 34 months). P2. Man, born in 1948, CIRS: 9 (ischemic cardiac disease, atrial fibrillation, hypertension, hyperuricemia). CLL was diagnosed in 2012 (in 64 years), del 11 q, IGHV mutated. I.st line, 6 × FCR (fludarabine, cyclophosphamide, rituximab) was given from November 2013 to April 2013 with achieved complete remission (CR). Patient relapsed at September 2016 and from February to August 2017 patient received 5 × FCR, with CR 2. 3rd line of therapy R-idelalisib patient received since December 2018, with progression at November 2022 – massive fluidothorax with need of several evacuations. Fluid CLL infiltration and pleura infiltration (histology) was verified. Abdominal lymph nodes was up to 2 cm. Since December 2022, patient is receiving venetoclax and achieved CR of fluidothorax. Last FU April 2023 (PFS 5 months). P3. Man, born in 1951, CIRS: 8 (diabetes mellitus, diabetic foot disease, lower extremity ischemic disease). CLL was diagnosed in march 2020 (in 69 years), IGHV unmutated, 46 XY. 1st line treatment (1 × RCD, 3 × R- bendamustine) patient received from August 2021 to November 2021 due to generalized lymphadenomegalia (LAM) with maximum in retroperitoneal space up to 42 mm, fluidothorax and B symptoms), immunochemotherapy (ICT) had to be stopped due to infectious complications and patient achieved PR. From September 2022. patient started ibrutinib in the cause of progressive LAM and fluidothorax (70% CLL infiltration). In January 2022, there was no fluidothorax at skiagram and no palpable LAM. In February 2023 patient progressed in abdominal LAM (PFS 5 months), diagnosis of Richter transformation was established and after 3 cycles of ICT patient died in April 2023 due to progression (PD). P4. Man, born in 1969, CIRS: 2 (hypertension). CLL was diagnosed in March 2017 (in 48 years), IGHV unmutated, del 11 q, del 13 q. I.st line treatment was initiated at December 2017 due to cytopenia and LAM), after 3 cycles of RCD, it was continued with 2 cycles FCR to April 2018. Because of PD, treatment was switched from June 2018 to R-idelalisib. In February 2019, TP53 mutation was detected. Second line of therapy was successful until June 2022, when the patient progressed with massive lymphadenomegaly, bone lesions, cytopenia and symptomatic fluidothorax. After 1 cycle of RCD, with no effect. Then venetoclax was started at June 2022 and the patient achieved CR. Last FU April 2023 (PFS 10 months).
Results and conclusions: We present two patients where fluidothorax was observed at the time of diagnosis and two patients who developed fluidothorax after prior therapies. Fluidithoraxes were in two patients sensitive to ibrutinib and in two patients to venetoclax (refractory to idelalisib). Only one patient progressed during FU to Richter transformation. Two patients received ICT as a first line treatment and were refractory. In two patients, fluidithorax developed at idelalisib treatment. Although the number of patients presented is too small to conclude on the best treatment choice for CLL-related fluidothorax, it seems that BTK inhibitors and BCL2 inhibitors could be an effective choice. Grant support: IGA_LF_2023_010, IGA_LF_2023_005, MH_CZ-DRO(FNOL,00098892)

Abstract ID: 1553170

Title: The economic benefits of time off treatment: real-world HRU, costs, and subsequent treatment with fixed duration venetoclax among patients with chronic lymphocytic leukemia

Authors: Alan Skarbnik, Lori A Leslie, Nnadozie Emechebe, Dureshahwar Jawaid, Beenish S. Manzoor, Hasan Alhasani and Brian Hill

Background: Fixed-duration (FTD) venetoclax-based regimens are approved for the treatment of chronic lymphocytic leukemia/small lymphocytic leukemia (CLL/SLL) in first-line (1L) as well as relapsed/refractory (RR) settings. Prior studies have described FTD as related to clinical trials or total cost of care; however, there are limited data characterizing the real-world benefits of FTD with venetoclax regimens. Preliminary data suggest that the FTD of venetoclax regimens may provide off-therapy economic benefits. This study quantifies the healthcare resource utilization (HRU) and costs during and post-completion of venetoclax plus obinutuzumab (VO) or venetoclax plus rituximab (VR) therapy and evaluates subsequent treatment patterns in patients with CLL/SLL in 1L and RR settings over an extended period.
Methods: Patients aged ≥18 years diagnosed with CLL/SLL between 1/1/2010 and 6/30/2021 who initiated VO in 1L or VR in RR settings were identified in the Optum® Clinformatics® database (Eden Prairie, MN). This analysis is an update of a previous cohort with an extended identification period allowing for the identification of 115 additional patients (total Nf223). Patients were continuously enrolled in their health plan for 1 year pre- and post-initiation with VO or VR. The follow-up period was stratified into two phases: (1) on-treatment phase, defined as time in months from venetoclax initiation to end of treatment; and (2) off-treatment phase, defined as time in months from 1 day after the end of venetoclax treatment to end of continuous enrollment/1 day before next line of therapy, or death. Per-patient, per-month (PPPM) all-cause HRU and costs were summarized using mean, standard deviation, or median, and interquartile range (IQR) in both on- and off-treatment phases. The proportion of patients who received subsequent lines of therapy after initiation with VO or VR are reported.
Results: In 1L, 115 VO-treated patients with a median follow up of 23.3 months were identified, with a median age at venetoclax initiation of 70 years, and 71.3% were male. The median (IQR) Charlson Comorbidity Index (CCI) score without malignancies was 1.0 (0–2). The median (IQR) duration of the on- and off-treatment phases were 12.4 (11.3–13.5) and 10.2 (5.6–15.1) months, respectively. Mean PPPM all-cause costs were $17,186 and $4,927 in the on- and off-treatment phases, respectively, representing a 71% reduction in costs after treatment completion (Table 1). The on-treatment costs were driven mainly by medication costs ($14,230 PPPM) relative to medical costs ($2,956 PPPM), while medical costs ($4,106 PPPM) accounted for most of the off-treatment costs. The mean PPPM all-cause outpatient visits were higher in

Table 1. Mean (SD) all-cause costs ($) on and off treatment for patients in 1L and RR settings

Patient setting	All-cause costs	On-treatment	Off-treatment
1L (n=115)	Total costs	17,186 (4,978)	4,927 (11,076)
	Medication costs	14,230 (3,508)	821 (2,366)
	Medical costs	2,956 (3,045)	4,106 (10,863)
RR (n=108)	Total costs	16,478. (6,040)	2,801 (6,768)
	Medication costs	12,766 (4,355)	842 (2,845)
	Medical costs	3,713 (3,958)	1,959 (5,476)

1L, first-line treatment; RR, relapsed/refractory; SD, standard deviation.

the on- versus off-treatment phases (3.3 vs 1.8 visits). In patients treated with VO, only 9/115 (7.8%) patients moved on to a second line of therapy. In the RR setting, 108 patients with a median follow up of 24.0 months, median age at VR initiation of 73 years, and 58.3% male were identified. The median (IQR) CCI score without malignancies was 1.0 (0–3). The median (IQR) duration of the on- and off-treatment phases were 16.1 (11.0–23.6) and 0.2 (0.0–9.9) months. Mean PPPM all-cause costs were $16,478 and $2,801 in the on- and off-treatment phases, respectively, representing an 83% reduction in costs after treatment completion. Medication costs ($12,766) accounted for most of the total cost in the on-treatment phase, while medical costs ($1,959) were the primary drivers of the off-treatment costs. Furthermore, the mean PPPM all-cause outpatient visits were higher in the on-treatment phase (3.2 vs. 1.3). Less than one quarter (21/108 [19.4%]) of VR-treated patients received subsequent treatment during the follow-up period.

Conclusions: In this updated real-world cohort, patients treated with VO and VR had low rates of subsequent therapy during the available follow-up, consistent with previous findings, suggesting this is an effective therapy in these patients. There is also a reduction in healthcare cost when patients are off treatment. These findings illustrate the economic benefits of time off treatment as afforded by a FTD regimen. The full economic benefits of off-treatment in this analysis are limited by the duration of the follow-up, and future analyses with longer off-treatment period are warranted. Compared to indefinite therapy with Bruton's tyrosine kinase–inhibitor treatment, these results may carry implications not only for payers and access decisionmakers, but also considerations for shared decision making between physicians and patients.

Abstract ID: 1553178

Title: Activation of S100-A9/EMMPRIN axis triggers survival/proliferation pathways in leukemic cells. A novel target for chronic lymphocytic leukemia

Authors: Eugenia Payque, Gimena Dos Santos, Claudia Ortega, Angimar Uriepero, Agustin Correa, Rita Uría, Juliana Querol Rivas, Florencia Palacios, Cecilia Guillermo, Carolina Oliver, Victoria Irigoín, Ana Ines Landoni, Eva Sahakian, Javier Pinilla-Ibarz, Pablo Oppezzo and Maria Elena Marquez

Chronic lymphocytic leukemia (CLL) is a malignancy of CD5+ B-cells characterized by a defect in apoptosis in which leukemic cells are continuously supported by their microenvironment and frequently guided to proliferation. The tumor microenvironment (TME) of lymphoid tissues affects immune cell function playing an important role in the pathogenesis of hematological cancers by providing protective and supportive niches for malignant cells. CLL is an example of this TME dependence where progression occurs as the consequence of specific microenvironmental signals that support an imbalance between reduced cell turnover and excessive proliferation of leukemic cells. Antigen stimulation and inflammation are key events, commonly involved in the initiation and progression of CLL. Supporting this idea, our group proposed a direct link between inflammation and a progressive disease [1]. Our study described that pro-inflammatory S100-A9 protein is aberrantly expressed in CLL cells of progressive patients, exported to the serum in exosomes, and responsible of NF-kβ activation originating a positive activation loop during tumor progression. To gain deeper insights into the origins of the molecular mechanism underlying this observation and to better understand how inflammation may impact disease progression, we initiated this work by characterizing the expression levels of previously described receptors of S100-A9 (CD33, TLR4, receptor for advanced glycation end products –RAGE- and Extracellular Matrix Metalloprotease Inducer –EMMPRIN-) in CLL cells. Our results show that leukemic cells exhibit high expression of EMMPRIN and RAGE receptors, and low expression of TLR4 and CD33. Additionally, proteomic analysis of serum exosomes of progressive CLL identified the presence of S100-A9 protein but not S100A8, indicating that the active form in these patients is likely the homodimer of S100-A9 (main ligand of EMMPRIN receptor), and not the heterotetrametric form S100A8/S100-A9 (main ligand of RAGE receptor). Since EMMPRIN has been linked with metastasis and tumor progression and, in CLL associated with stroma interaction and NF-kβ activation, we focused on characterize its expression in CLL cells associating it with clinical evolution. Our results show that leukemic clone expresses EMMPRIN in an N-glycosylated form with significantly higher expression in unmutated patients compared with mutated CLLs and healthy donors ($n=36$; $n=28$ and $n=12$, respectively, p=***, Unpaired t test). Interestingly, this higher expression also correlates with earlier treatment requirement ($n=25$, $r=-0.61$; p=**, Spearman rank-test), suggesting a potential role for EMMPRIN receptor during disease evolution. Since we previously demonstrated that S100-A9/EMMPRIN axis activates NF-kβ pathway, we wonder if other survival/proliferative pathways also depend on this interaction. Thus, we analyze the phosphorylation of key residues involved in activation of Pi3K/AKT and MAPK/JNK pathways. Our findings demonstrate that stimulation with recombinant S100-A9 significantly increases the phosphorylation state of Ser176/180 in IKK, Ser473 and Thr308 in AKT, and Thr183/185 in JNK molecules, (p=****; p=****; p=*** and p=**, respectively, Unpaired t test), in CLL cells from 10 patients. Interestingly, these patients needed treatment earlier and depict high levels of

EMMPRIN expression. In contrast, not significant differences were found after S100-A9 incubation of CLL cells from indolent patients who depict lower EMMPRIN expression. These findings further support our previous data about that S100-A9/EMMPRIN axis have a major role during the disease progression status of progressive CLLs. To confirm these results we evaluated different downstream molecules involved in cell survival/proliferation known to be molecular targets of these pathways. After S100-A9 stimulation progressive patients depict significant changes confirming up-regulation of Mcl1, Bcl2, pRb-1 and Survivine proteins; up-regulation of CCL3 and CCL4 mRNAs, and down-modulation of p27 mRNA, a clear marker of quiescent cell status. Finally, we also confirm the specificity of our results using specific inhibitors either for S100-A9 (Tasquinimod and Paquinimod) or EMMPRIN (blocking antibody, -clon/UM-8D6-). Our findings show that S100-A9/EMMPRIN axis is engaged in NF-kβ and Pi3K/AKT activation, two key pathways strongly associated with tumor progression. CLL remains an incurable disease, underscoring the critical need for a deeper understanding of the mechanisms promoting tumor progression and/or refractoriness. This work describes for the first time a new survival/proliferation axis initiated by S100-A9/EMMPRIN interaction, which appears to be active in CLL patients during disease progression. Overall, our results raise new questions about the role of inflammation during CLL evolution and propose new targets to be explored within the heterogeneous biological and clinical scenario of CLL.

Abstract ID: 1553183

Title: Del8p and TNFRSF10B loss are associated with a poor prognosis and resistance to fludarabine in chronic lymphocytic leukemia

Authors: Ludovic Jondreville, Lea Dehgane, Cecile Doualle, Luce Smagghe, Beatrice Grange, Frederic Davi, Leticia Koch Lerner, Delphine Garnier, Clotilde Bravetti, Olivier Tournilhac, Damien Roos-Weil, Marouane Boubaya, Elise Chapiro, Santos A Susin and Florence Nguyen-Khac

Introduction: Chronic lymphocytic leukemia (CLL) is a heterogeneous disease, with a highly variable clinical course. Recurrent chromosomal abnormalities have a key role in CLL oncogenesis and drug resistance. We characterized a rare abnormality, the deletion of the short arm of chromosome 8 (del8p), associated with aggressive CLL. Additionally, we investigated the role of TNFRSF10 genes included in the minimal common deleted region.
Methods: We correlated patients' cytogenetic and clinical outcomes using standard statistical methods. We performed in vitro analyses in primary CLL cells and in TNFRSF10B CRISPR/Cas9 edited OSU-CLL cell lines using flow cytometry (annexin V and propidium iodide co-staining) for drug response assays, and ddPCR for gene expression assessment.
Results: Comparing the largest series to date of del8p CLL ($n=57$) to a non-del8p control cohort ($n=155$), del8p was significantly associated with poor prognostic factors: complex and highly complex karyotypes (33/46, 72% and 20/46, 44%, vs. 34/155 (22%) and 12/155 (8%) respectively, $p<0.001$), del11q (27/52, 52% vs. 27/155, 17%; $p<0.001$), del17p (20/55, 36% vs. 16/154, 10%; $p<0.001$) and unmutated IGHV (35/48, 73%, vs. 70/151, 46%; $p=0.002$). Del8p patients had a shorter time to first treatment (TTFT, median 0.25 vs 1.7y, $p=0.007$), worse overall survival (OS) (10year OS: 30 vs. 82%; $p<.0001$), and a higher risk of Richter transformation (RT) (10y: 22 vs. 5.5%, $p=.034$) (Figure 1). A multivariate analysis showed that large del8p and concomitant TP53 disruption had a negative impact on the OS. Interestingly, del8p patients treated with fludarabine-based regimens had a shorter time to next treatment (40 vs. 63 months; $p=.002$) and a shorter OS (10y OS: 46 vs. 82%; $p<.001$), including those with mutated IGHV (42 vs. 107 months; $p=.015$). We found that the TNFRSF10B gene in 8p21.3 (coding for a pro-apoptotic receptor activated by TRAIL) had been lost in 51/56 (91%) cases. TNFRSF10B

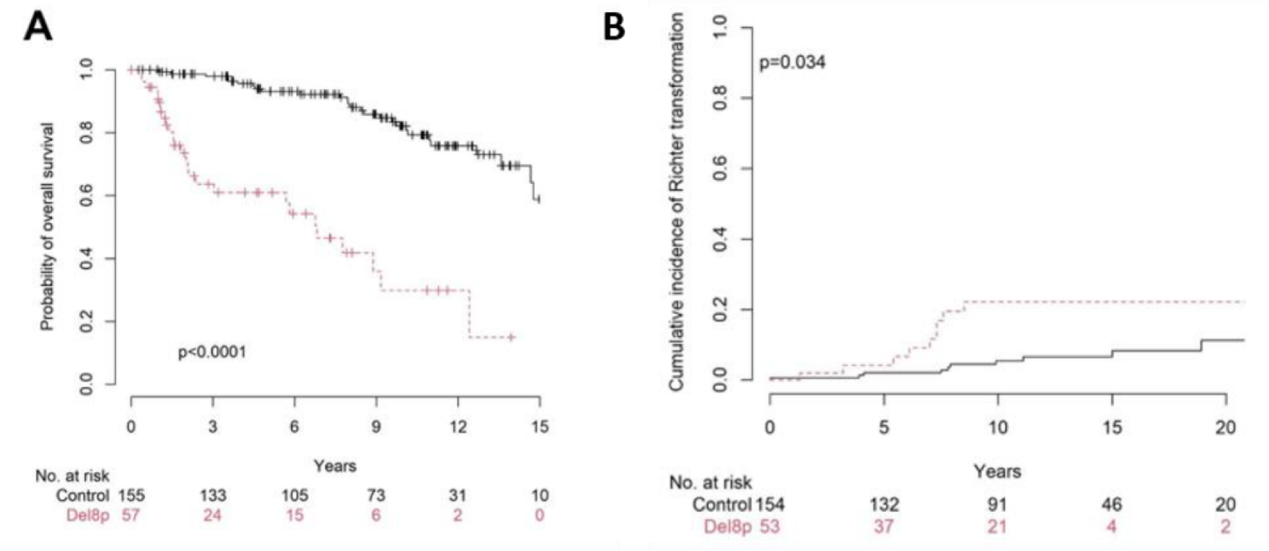

Figure 1. **Survival of del8p vs. non-del8p patients**. **A**. Overall survival; **B**. Cumulative incidence of Richter transformation

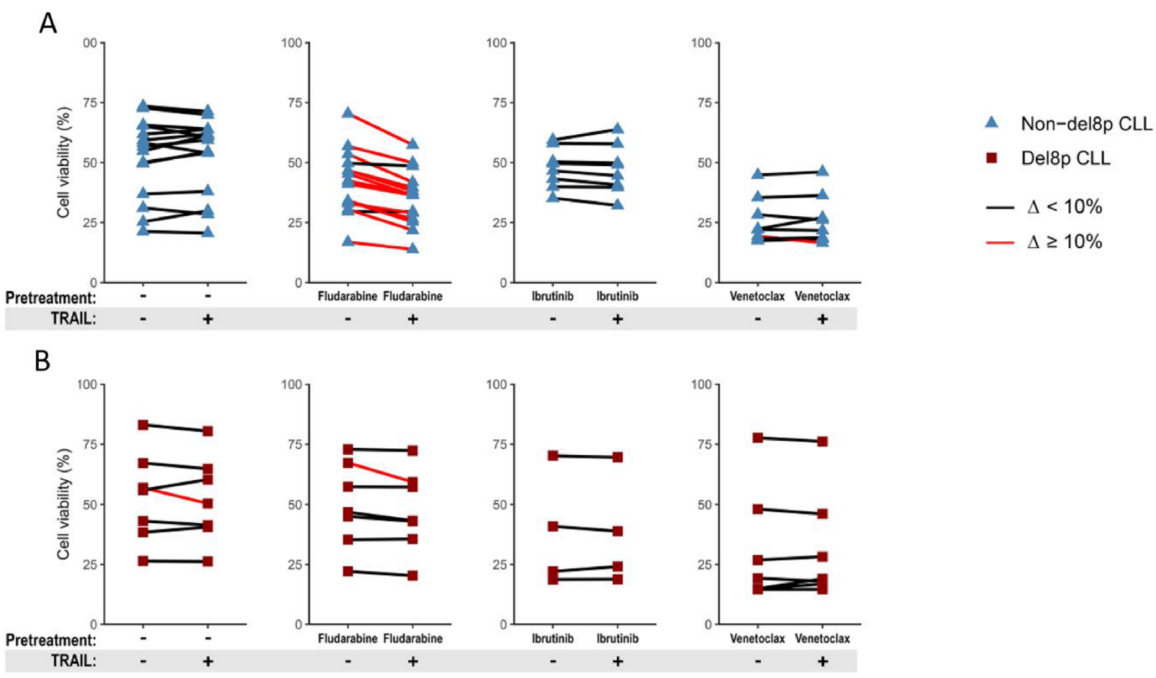

Figure 2. Fludarabine treatment specifically abrogates the decrease in cell viability induced by the fludarabine-TRAIL combination. Primary non-del8p (**A**) or del8p (**B**) CLL cells purified from various patients were treated (or not) with 10 µM fludarabine, 10 µM ibrutinib, or 1 nM venetoclax for 24 h and then cultured in the presence (200 ng/mL) or absence of TRAIL for 6h. The graphs show the cell viability (the percentage of viable cells, with co-negative annexin-V/PI staining) measured using flow cytometry. A cell viability decrease ≥ 10% in cells treated with TRAIL vs. cells not exposed to TRAIL was considered to be significant and is represented with a red line.

was haploinsufficient in del8p CLL: the TNFRSF10B expression was significantly lower in del8p CLL cells than in non-del8p CLL cells (2.4-fold; p<.001). We then demonstrated using CRISPR-edited cell lines that TNFRSF10B receptor was functional in inducing cell death in CLL cells. In primary CLL cells, TRAIL alone failed to induce significant cell death. We therefore hypothesized that exposure of cells to anti-CLL drugs might modulate TNFRSF10B expression, resulting in improved sensitivity to TRAIL. In non-del8p primary cells, TNFRSF10B expression was significantly greater after exposure to fludarabine (2.8-fold), but not after ibrutinib or venetoclax. This increase was not observed in del8p cells. We then performed a sequential approach to evaluate the cytotoxic effect of TRAIL with fludarabine. We observed that TRAIL had an additional cytotoxic effect in 13/15 (87%) of non-del8p samples. By contrast, TRAIL + fludarabine failed to elicit a synergistic cytotoxic effect in 6/7 del8p samples (Figure 2). We conclude that the lack of fludarabine-induced overexpression of TNFRSF10B abrogates the synergy between the purine analog and TRAIL. Finally, we hypothesized that p53 tumor suppressor protein was involved in fludarabine-induced TNFRSF10B expression. To check p53's activation after fludarabine treatment we measured the expression of three p53 target genes: MDM2, BAX and CDKN1A. In non-del8p samples, fludarabine induced a greater expression of all three genes: MDM2, 12.5-fold; BAX, 4.3-fold; CDKN1A, 8.7-fold. In contrast, the fludarabine-induced expression was substantially lower in del8p samples (2.2-fold, 1.0-fold and 3.4-fold, respectively), irrespectively of the presence or the absence of del17p. Thus, del8p in CLL appeared to interfere with the p53-dependent gene expression induced by fludarabine.

Conclusions: In this large cohort, we found that del8p is associated with poor cytogenetic and molecular prognostic factors, as well as with short TTFT and OS, and higher risk of RT. We also demonstrated that TNFRSF10B has an important role in fludarabine resistance in del8p CLL: we showed that del8p in CLL prevents the increase in expression of the TNRSF10B receptor and thus abrogates the apoptogenic synergy between fludarabine and TRAIL. These *in vitro* results are in line with our *in vivo* data showing that del8p CLL patients treated with fludarabine-based regimens have shorter OS. In patients who could benefit from the classical fludarabine-cyclophosphamide-rituximab treatment but who harbor del8p, other treatments (such as ibrutinib and venetoclax) might be more effective than fludarabine.

Abstract ID: 1553210

Title: The impact of BTK inhibitors on COVID-19 outcomes in patients with chronic lymphocytic leukemia: a real-world study in the Omicron wave

Authors: Shenmiao Yang and Xiaojun Huang

Objective: This study aims to examine the impact of Bruton tyrosine kinase inhibitors (BTKi) on the occurrence and severity of COVID-19 in patients with chronic lymphocytic leukemia (CLL) in the Omicron wave.
Methods: This was a single-center, retrospective study focusing on CLL patients. Data was collected through telephone

Table. Correlation analysis for risk factors associated with hypoxemia

Risk factors	Uni-variate analysis	P value	Multi-variate	P value
Age				
<65 years, n (%)	10 (25.6)	P=0.043		
≥65 years, n (%)	33 (45.2)			
COVID-19 vaccination				
No, n (%)	36 (43.9)	P=0.014		
Yes	5 (17.9)			
BTKi treatment				
No, n (%)	4 (16.0)	P=0.009	HR 4.014 (95% CI:	P=0.019
Yes, n (%)	39 (44.8)		1.253-12.883)	

Figure : Kaplan-Meier survival curve of CLL patients with COVID-19

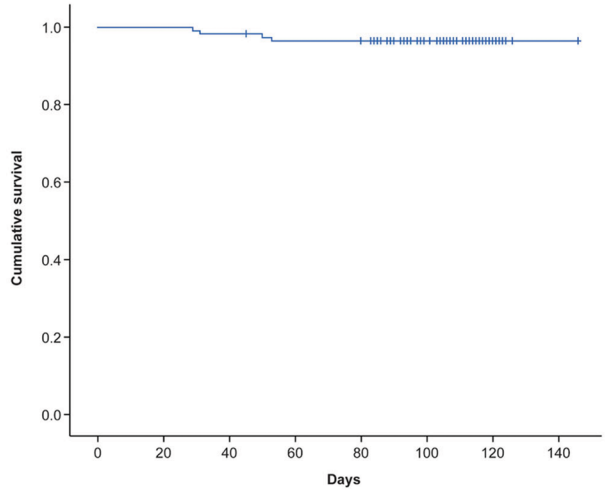

interviews, and a standardized questionnaire was used to gather information on demographics, COVID-19 outcomes, treatment history, and BTKi usage. Statistical analysis, including chi-square tests and logistic regression, was performed to assess the association between BTKi usage and COVID-19 outcomes. Kaplan–Meier survival curves were used to analyze the impact of BTKi on patient survival.

Results: In this study, 151 CLL patients were included, with 66.2% being male and the median age being 67 years. 117 (77.5%) patients took BTK inhibitor alone as the treatment. Most patients received ibrutinib ($n=68$; 58.1%) followed by zanubrutinib ($n=30$; 25.6%), acalabrutinib ($n=11$; 9.4%), and orelabrutinib ($n=8$; 6.8%). 34 patients did not receive any treatment. Most patients did not have progressive disease. 17 (50%) were vaccinated against COVID-19 in patients not receiving anti-leukemia treatment whereas only 17 (18%) of those were under BTKi treatment vaccinated ($p<0.001$). BTKi treatment was not associated with a higher risk of COVID-19 infection, but it was associated with a higher incidence of hypoxemia in patients with COVID-19. Among the CLL patients who received BTK inhibitors, 44.8% experienced hypoxemia. Univariate analysis identified age, lack of vaccination, and BTK inhibitor treatment as adverse risk factors for hypoxemia in CLL patients with COVID-19. Furthermore, multivariate analysis revealed that patients treated with BTK inhibitors had a four times higher incidence of exhibiting hypoxemia compared to CLL patients not receiving any treatment.

Conclusion: In conclusion, continuous BTKi was found to be a poor risk factor for severe COVID-19 outcomes in CLL patients.

Abstract ID: 1553263

Title: Occurrence and evolution of autoimmune cytopenias in chronic lymphocytic leukemia patients treated with venetoclax: a study of the French Innovative Leukemia Organization (FILO)

Authors: Aude Collignon, Morgane Nudel, Annie Brion, Kamel Laribi, Thomas Nivet, Fatiha Merabet, Loic Ysabaert, Olivier Tournilhac, Guillaume Le Guenno, Cecile Tomowiak, Emmanuelle Tchernonog, Jehan Dupuis, Habib Ghnaya, Nicolas Stocker, Alexandra Fayault, Marie-C Bene and Thérèse Aurran

Occurrence and Evolution of Autoimmune Cytopenias in Chronic Lymphocytic Leukemia Patients treated with Venetoclax: a study of the French Innovative Leukemia Organization (FILO).

Introduction: Autoimmune cytopenias (AICs) are a common complication in chronic lymphocytic leukemia (CLL) occurring in about 5–15% of cases, however their impact on survival is still controversial. Some drugs like fludarabine or ibrutinib are known to trigger AICs, but there is poor evidence regarding the role of venetoclax (VEN) in those events. Some authors have reported successful treatment of AIC with VEN, while some cases of emerging AICs were reported in VEN associated trials. Furthermore, its frequent use with anti-CD20 agents might represent a confounding factor to assess its impact on AIC. Here we present the results of a multicenter study of the FILO aiming to evaluate the outcome of AICs in CLL patients treated with VEN.

Methods: We retrospectively collected in all the FILO centers the cases of CLL patients who presented any kind of AICs [autoimmune hemolytic anemia (AIHA), autoimmune thrombocytopenia (AIT), autoimmune erythroblastopenia (AIEB), aplastic anemia (AA) or autoimmune neutropenia (AIN)] before or after treatment with VEN. Regarding CLL response by itself, iwCLL criteria were used except for bone marrow biopsy criteria, then we defined CR as clinical CR. Regarding AICs, response criteria were used as already published [1].

Results: Sixteen patients were included from 9 FILO centers in France. Twelve patients (75%) had background history of

Table 1 Characteristics of the patients.

	Number of patients (%)
Median age (years, range)	81 (65–90)
Hierarchical cytogenetics (FISH)	
Del(17p)	5 (31)
Del(11q)	3 (19)
Trisomy 12	0
Normal	5 (31)
Del(13q)	1 (6)
Other	2 (12)
Mutated *TP53*	
Yes	5 (31)
No	9 (56)
Unknown	2 (12)
IGHV gene mutation status	
Unmutated	8 (50)
Unknown	8(50)
Complex karyotype	
Yes	7 (44)
No	9 (56)
Number of previous lines	2(1–8)
Patients with previous event of AIC	12(75)
AIHA	7(44)
AIT	5(31)
AIEB	2(12)
EVANS syndrome	1(6)
Median number of AIC events	1,5 (1-10)

AICs before VEN initiation (see Table 1 for detailed characteristics). When starting VEN treatment, 13/16 (81%) had a progressive CLL (lymphocytosis or tumoral syndrome) and 12 out of 16 patients (75%) had an active AIC: 6 AIHA, 4 AIT, 1 Evans syndrome (ES) and 1 AIEB. Seven patients (58%) had rituximab in association to VEN. On VEN treatment, regarding AICs outcome, 8 patients achieved complete remission (CR) (67%, one patient had initial worsening of AIHA and then achieved CR), 2 partial response (17%) and 2 patients were in failure (17%). Regarding the CLL, 8 out of 12 achieved clinical CR (67%), 3 (25%) in PR and one (8%) in progression. There seemed to be a correlation between the response of the CLL and the AIC: all patients who achieve a CR of the CLL were also in CR regarding the AIC. In the same way, the 2 patients in failure regarding the AIC were in progression and PR of the CLL. Two patients in CR presented an occurrence of their AIC at 5months and 11 months after stopping VEN. The first one achieve CR once again at reintroduction of VEN. Within the four patients (25%) who did not have an active AIC at the time of VEN, all developed AICs on VEN: 2 AIHA, 1AIT and 1 AIEB, at 2.9 months in median (1.9–4.3) after initiation of the treatment. Fifty percent of the patients had rituximab in association to VEN. VEN was definitely stopped for all 4 patients at D0 of the AIC for 2 patients, D1 and D38 for the 2 others.

Conclusion: VEN can be both the cause or the treatment of AICs associated with CLL. When introduced while an AIC is active, it results in CR of the AIC in a majority of the cases and seems to be correlated with the response of the CLL. It is more difficult to conclude about the AIC triggered by VEN in this retrospective setting, because VEN was stopped quasi immediately after AIC and never reintroduced.

Abstract ID: 1553355

Title: Kinetics of lymphocytosis during Btk covalent inhibitors in treatment naïve chronic lymphocytic leukemia patients. An Italian multicenter experience of real life

Authors: Idanna Innocenti, Antonio Mosca, Annamaria Tomasso, Andrea Galitzia, Lydia Scarfò, Francesca Morelli, Eugenio Galli, Roberta Laureana, Giulia Benintende, Veronica Mattiello, Sabrina Chiriu, Maria Ilaria del Principe, Giulia Zamprogna, Massimo Gentile, Nicole Fabbri, Francesco Autore, Maria Chiara Montalbano, Giuliana Farina, Vanessa Innao, Caterina Patti, Paolo Sportoletti, Alberto Fresa, Gioacchino Catania, Marta Coscia, Alessandra Tedeschi, Alessandro Sanna, Andrea Visentin, Livio Trentin, Marzia Varettoni, Paolo Ghia, Roberta Murru and Luca Laurenti

Introduction: In chronic lymphocytic leukemia (CLL) patients (pts) the first phase of treatment with covalent Bruton's tyrosine kinase inhibitors (cBTKi), Ibrutinib or Acalabrutinib, is characterized by an increased absolute lymphocyte count (ALC), regardless of previous lines of treatment. Ibrutinib, as first-line therapy, induces lymphocytosis in about 57% of pts, and it is more frequent in IGHV mutated CLL patients. This phenomenon, due to the shift of neoplastic lymphocytes from the neoplastic nodal compartment into peripheral blood, is transient in most patients, resolving within 8 months, but can rarely persist over 12 months, without any impact on survival; the terms Partial response with lymphocytosis was coined due to this phenomenon. Despite lymphocytosis in Ibrutinib has been widely investigated, little is known about the effective presence, the kinetics and duration of lymphocytosis in patients treated with Acalabrutinib.

Aims: The main purpose of this study is to define, in a real-life setting, the kinetics of drug-induced lymphocytosis in CLL patients treated with Acalabrutinib or Ibrutinib, in order to underline any possible differences in terms of entity and duration of this phenomenon.

Methods: In our multicentric retrospective study we enrolled 204 pts (127 male and 77 female), treated in the first line with cBTKi (136 Ibrutinib and 68 Acalabrutinib) from 16 different Italian centers, between April 2016 and November 2022, with last follow up in April 2023. For each patient we collected data about the burden of disease at baseline (in terms of staging, lymph nodes involvement, presence of splenomegaly), and the biological features of the disease (cytogenetic aberrations and molecular mutations, IGHV status). Then we evaluated the ALC at the baseline and at well-defined time-points (after two weeks, 1, 2, 3, 6, 9, 12 months) over an observation period of 1 year. Patients' characteristics are reported in Table 1.

Results: The main differences between the two groups are observed in FISH and TP53 status, with more prevalent 17p- and mutated TP53 in Ibrutinib-treated patients ($p=0.04$ and $p=0.007$). We observed a median ALC increase after the beginning of therapy in both groups. Median lymphocytosis was higher than baseline during the first month of treatment in both cohorts. A progressive decline in median ALC occurred from the second month of treatment in both groups: at this time-point, median lymphocyte count was 62% of baseline in Acalabrutinib cohort versus 84% in Ibrutinib cohort ($p=0.025$). From the sixth month to the end of the study, we found a statistical difference in the ALC with higher counts in the Ibr group. Indeed, at this time point the median ALC was 6960/microL in Acalabrutinib compared to 11010/microL in Ibrutinib group (13 vs. 30% of baseline), at the ninth month it was 4550/microL vs. 8230/

Clinical and Biological characteristics and results 204 patients (April 2016 - November 2022)					
Follow up: 12 months		All patients n=204	Ibrutinib arm n=136	Acalabrutinib arm N=68	P-value
Age (163/204)	Median years	72	73	71	0.593
Gender (204/204)	M, n (%)	127 (62)	82 (60)	45 (66)	0.413
	F, n (%)	77 (38)	54 (40)	23 (34)	
Rai Stadium (204/204)	A, n (%)	23 (11)	20 (15)	3 (4)	
	B, n (%)	92 (45)	63 (46)	29 (43)	**0.040**
	C, n (%)	89 (44)	53 (39)	36 (53)	
Lymph nodes (203/204)	Absent	13	11	2	0.34
	< 5 cm	118	80	38	
	5-10 cm	46	27	19	
	> 10 cm	26	18	8	
Splenomegaly (204/204)	n	138	89	49	0.34
FISH, n	del 17p (198/204)	48	42	6	**0.0007**
	del 11q (199/204)	19	6	13	**0.0005**
	del 13q (198/204)	63	46	17	0.272
	trisomy 12 (198/204)	36	23	13	0.591
Molecular Biology, n	TP53 (193/204)	66	59	7	**< 0.001**
	NOTCH1 (127/204)	14	6	8	**0.028**
IgVH mutational status, n	mutated	65	44	21	
	unmutated (168/204)	93	64	29	0.464
Median ALC at different timepoints					
		All	Ibrutinib arm	Acalabrutinib arm	P-value
At baseline					
Absolute/microL (normal range 1000-3000)		66950	63270	82905	0.337
1 month					
Absolute/microL		68950	65170	78450	0.848
% of baseline		110	113	93	0.126
2 months					
Absolute/microL		36720	36280	37750	0.373
% of baseline		81	84	62	**0.025**
3 months					
Absolute/microL		25250	24240	26250	0.613
% of baseline		56	59	48	0.089
6 months					
Absolute/microL		10150	11010	6960	0.090
% of baseline		26	30	13	**0.024**
9 months					
Absolute/microL		6800	8230	4550	**0.012**
% of baseline		16	20	10	**0.013**
12 months					
Absolute/microL		4960	5520	2740	**0.003**
% of baseline		11	13	8	0.071

Table 1: Clinical and Biological characteristics and results

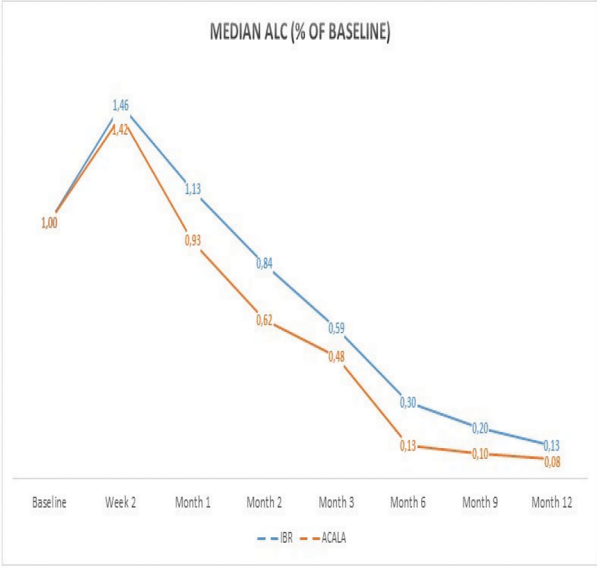

Figure 1. Median ALC trend in terms of percentage of baseline in the two groups of patients

microL (10 vs. 20% of baseline) and at one-year timepoint it was 2740/microL vs. 5520/microL (8 vs. 13% compared to baseline) in the Acalabrutinib versus Ibrutinib group, respectively. Results are reported in Table 1.

Conclusions: Acalabrutinib seems to determine, like Ibrutinib, an increase of ALC immediately after the starting of therapy. Therefore, lymphocytosis appears as a cBTKi-class effect. Despite this, the kinetics of lymphocytosis is not overlapping when comparing the two drugs. From the sixth month of treatment, ALC reached almost-normal values in the Acalabrutinib group, with significant statistical differences compared to Ibrutinib. These data suggest that lymphocytosis appears to be less long-lasting in patients treated with Acalabrutinib than in those ones treated with Ibrutinib, and the response criterion of partial response with lymphocytosis may also have a different duration during treatment with cBTKi.

Abstract ID: 1553461

Title: Anti-CD19 CAR T-cell therapy for patients with Richter syndrome: a LYSA Study from the DESCAR-T Registry

Authors: Hedi Bensaber, Emmanuel Bachy, Remy Dulery, David Beauvais, Thomas Gastinne, Bruno Villemagne, Louise Roulin, Sophie De Guibert, Pierre Feugier, Emmanuelle Ferrant, Cristina Castilla Llorente, Etienne Paubelle, Thomas Longval, Amandine Fayard, Jacques-Olivier Bay, Elodie Gat, Steven Le Gouill, Roch Houot and Romain Guieze

Background: Richter syndrome (RS) refers to the onset of aggressive lymphoma, mostly diffuse large B-cell lymphoma (DLBCL), in patients with chronic lymphocytic leukemia (CLL). The outcome of RS patients is usually very poor with short survival (typically <1 year) due to chemoresistance. Indeed, chemoimmunotherapy regimens used in de novo DLBCL failed to induce a significant complete remission rate (CRR) (R-CHOP, 7%; ofatumumab-CHOP, 27%) [1,2]. CD19-targeted chimeric antigenic receptor (CAR) T-cell therapy such as axicabtagene ciloleucel (axi-cel) and tisagenlecleucel (tisa-cel) have been transformative for patients with relapsed/refractory DLBCL. Here, we aimed to investigate the efficacy and safety profile of CD19-CAR T-cell therapy for patients with RS.

Methods: In this Lymphoma Study Association/ Lymphoma Academic Research Organization (LYSA/LYSARC) study, we conducted an analysis of the DESCAR-T registry which collects real-life data of patients treated with approved CD19-directed CAR T-cell therapies (axi-cel and tisa-cel) since 1 July 2018 in France. We selected patients with biopsy-proven RS of DLBCL histology, treated by tisa-cel or axi-cel in either the frontline or relapse setting. Data regarding prior CLL history were collected in addition to the DESCAR-T registry data. The data cut-off was 3 May 2023. The primary endpoint was best CRR according to Cheson IWG 2014 (Lugano Classification) after CAR-T cell infusion. Secondary endpoints were overall response rate (ORR), immune effector cell-associated neurotoxicity syndrome (ICANS), and cytokine release syndrome (CRS) incidence and grading (ASTCT Consensus) as well as hematological toxicity (NCI CTCAE v5.0).

Results: CD19-directed CAR T-cell therapy was planned for 17 patients from 12 November 2019 to 26 July 2022, 15 were infused and subsequently included in the present analysis (1 patient refused the infusion and 1 was not infused due to disease progression). Median age was 61 [42–76] years and sex ratio M/F was 1.5. CLL cytogenetic features at baseline were as follows: 2/10 (20%) patients had 17p deletion, 6/9 (60%) 11q deletion and 3/7 (43%) complex karyotype. TP53 mutations were seen in 5/8 (62%) patients and 5/7 (71%) patients harbored unmutated IGHV. Median number of prior therapeutic lines for CLL before RS was 2 [0–9]. Of the 15 patients who were infused, 3 (20%) did not receive any prior therapy for CLL. Nine (60%) patients received chemo-immunotherapy, 9 (60%) had been exposed to ibrutinib including 4 (26.7%) to both ibrutinib and venetoclax (data collection ongoing for one patient). Median time from CLL diagnosis to RS was 7 [0-22] years. Thirteen (87%) patients received ≥1 prior lines of therapy for RS and bridging therapy was administered to 13 (87%) patients. Evaluation for disease

status prior CAR T-cell infusion revealed progression for 8 (53.3%) patients, complete response in 1 (6.6%), partial response in 3 (20%) and stable disease in 2 (13.3%) (1 patient non-evaluated). After a median follow-up of 11.7 [0–24] months, best CRR was 40% and best ORR was 53.3%. One-year progressive free survival (PFS) rate was 40.7% and one-year overall survivor (OS) rate was 46.6%. Following CAR T-cell infusion with axi-cel (7 patients) or tisa-cel (8 patients), 8 (53.3%) patients were alive, 7 (46.6%) patients died (3 from acute toxicity with two CRS and one neurotoxicity, and 4 from disease progression). All but one (93.3%) patient presented with CRS, 5 (33.3%) with grade >2. Tocilizumab was administered to 13 (87%) patients. Six (40%) patients had ICANS, 5 (33.3%) with grade >3. Regarding hematotoxicity, 8 (53.3%) patients presented with grade >2 thrombocytopenia, 5 (33.3%) with grade >2 anemia, and 8 with (53.3%) grade >2 neutropenia. One case of macrophage activation syndrome was reported. Five (33.3%) patients were admitted to intensive care. A total of 8 (53.3%) patients had infections.

Conclusions: CD19-directed CAR T-cell therapy showed high response rates and an encouraging survival in our series of heavily pretreated RS patients. Frequency of CAR T-cell-specific adverse events was in the range of what is observed in de novo DLBCL while severity appeared higher [3,4].

Abstract ID: 1553534

Title: Incidence of arrhythmia in chronic lymphocytic leukemia (CLL) patients treated with ibrutinib: a real-world retrospective analysis from two Italian centers.

Authors: Roberta Murru, Idanna Innocenti, Andrea Galitzia, Annamaria Tomasso, Valeria Oggianu, Luca Laurenti and Giorgio La Nasa

Introduction: Ibrutinib, the first-in-class BTK inhibitor, has significantly improved the natural history of chronic lymphocytic leukemia (CLL) in both treatment-naïve (TN) and relapsed/refractory (R/R) patients but its beneficial effects on progression-free survival (PFS) and overall survival (OS) may be outweighed by off-target effects. Ibrutinib is currently in widespread clinical use, which has led to an increase in the frequency of both common and uncommon adverse events (AEs), less frequently observed in early clinical trials. Up to 29% of patients discontinue ibrutinib treatment because of side effects. In particular, atrial fibrillation (AF) is the most common reason, ranging from 5 to 20% in clinical trials and 8 to 25% in clinical practice. We currently know that predisposing risk factors and cardiac comorbidities seem to be the main elements that define an increased risk of AF.

Aims: To evaluate: the cumulative incidence (CI) of AF over time and its clinical impact on event-free survival (EFS), [event defined as AF, definitive treatment discontinuation (TD), disease progression, or death from any cause], PFS and OS; associations between clinical factors and higher incidence of AF; the incidence of cardiovascular events (CE) during treatment and long-term follow-up (FU); changes in cardiac medication during treatment; the length of drug exposure; causes of TD.

Methods: Unselected CLL patients treated with ibrutinib for at least 6 months between 01/2014 and 12/2022 were enrolled in a double-center retrospective cohort study. There were no exclusion criteria. Data were obtained from medical records. Demographic and treatment data, biological characteristics of disease, and concomitant cardiac comorbidities were collected. FU ended May 01, 2023. AF and all AEs were described according to CTCAE 5.0.

Results: We enrolled 179 patients (M/F: 112/67), characteristics are summarized in Table 1. The median age was 70 years (36–83). IGHV unmutated was detected in 85 (47%) patients and mutated in 51 (29%). TP53/del17p disruptions were detected in 63 patients (35%). Fifty-nine CLL patients received ibrutinib as TN and 120 as R/R, with a median number of lines of therapy of 1 (1–6). The median FU was 24.2 months (0.3–102.8). The median time to drug discontinuation was 41.4 months with a CI of TD of 32% at 24 months. There was no difference in TD between TN and R/R ($p = 0.232$). Specifically, the CI of TD was 29% in TN and 33% in R/R at 24 months. Now a day 103 (58%) CLL patients were on treatment, while 76 (42%) had discontinued ibrutinib therapy. TD was mainly due to progression and Richter's transformation (RT) (21%), followed by toxicity (18%). Among toxicities, CE led to TD in 6/33 patients (18%) [3 acute coronary syndrome (ACS), 3 AF]. The most common AEs were AF (11%), always defined ≤3 CTCAE; infections (12%); ACS (2%). Second malignancies were observed in 10% (*n* 18). No major bleeding was recorded. Nineteen of 20 AF patients started DOACs. The CI of AF was 4 and 9% at 12 and 24 months, respectively. We found a statistical difference ($p = 0.01$) between patients with or without anemia (7 vs. 4% at 12 months; 25 vs. 6% at 24 months). In addition, previous arrhythmias negatively impacted on CI of AF ($p = 0.02$). PFS was 77% at 24 months (median PFS: 53.4 months). EFS was 59% at 24 months (median EFS: 31.3 months). OS was 86% at 24 months, with median not reached at 5 years. AF had no significant impact on OS; however, TD for any cause negatively impacted on OS (75 vs. 96% in the no-discontinuation group at 24 months, $p<0.0001$). Finally, only discontinuation due to progression had a worse outcome, while discontinuation due to toxicity had a similar outcome to the continued-therapy group. Main causes of death were progression (n°10), RT (n°9), infection (n°9), and COVID-19 (n°6).

Conclusions: Our real-world data show that CLL patients treated with ibrutinib have outcomes similar to those seen in clinical

	Tot N=179	No AF N = 159	AF N = 20	p-Value
Gender				0.483
M	102 (56.98%)	89 (55.97%)	13 (65.0%)	
F	77 (43.02%)	70 (44.03%)	7 (35.0%)	
	N=179	N = 159	N = 20	
Age at start ibrutinib (years) (Mean ± SD)	68.98 ± 8.82	68.91 (± 9.05)	69.46 (± 6.93)	0.945
	Range (36.42; 83.47)	Range: (36.42; 83.47)	Range: (55.24; 80.92)	
	N=179	N = 159	N = 20	
N° Treat Before Ibru (Mean ± SD)	1.12 ± 1.12	1.11 (± 1.09)	1.25 (± 1.37)	0.906
	Range: (0.0; 6.0)	Range: (0.0; 6.0)	Range: (0.0; 5.0)	
	N=179	N = 159	N = 20	
IGHV				0.573
Mutated	51(37.5%)	44 (36.36%)	7 (46.67%)	
Unmutated	85 (62.5%)	77 (63.64%)	8 (53.33%)	
	N=136	N = 121	N = 15	
TP53 disruptions				0.628
Yes	63 (35.2%)	55 (34.59%)	8 (40.0%)	
No	116 (64.8%)	104 (65.41%)	12 (60.0%)	
	N=179	N = 159	N = 20	
RAI STAGE				0.111
0	23(13.86%)	23 (15.65%)	0 (0.0%)	
I	21 (12.65%)	18 (12.24%)	3 (15.79%)	
II	65 (39.16%)	58 (39.46%)	7 (36.84%)	
III	31 (18.67%)	24 (16.33%)	7 (36.84%)	
IV	26 (15.66%)	24 (16.33%)	2 (10.53%)	
	N=166	N = 147	N = 19	
BINET STAGE				0.493
A	45(27.11%)	42 (28.57%)	3 (15.79%)	
B	66 (39.76%)	57 (38.78%)	9 (47.37%)	
C	55(33.13%)	48 (32.65%)	7 (36.84%)	
	N=166	N = 147	N = 19	
ECOG				0.89
0	42 (55.26%)	30 (53.57%)	12 (60.0%)	
1	32 (42.11%)	24 (42.86%)	8 (40.0%)	
2	1 (1.32%)	1 (1.79%)	0 (0.0%)	
3	1 (1.32%)	1 (1.79%)	0 (0.0%)	
	N=76	N = 56	N = 20	
CIRS SCORE (global) (Mean ± SD)	4.35 ± 2.76	4.25 (± 2.93)	4.65 (± 2.25)	0.45
	Range: (0.0; 11.0)	Range: (0.0; 11.0)	Range: (0.0; 9.0)	
	N079	N = 59	N = 20	
PRIOR HYSTORY ARRYTHMIA				0.041
Yes	9 (11.39%)	4 (6.78%)	5 (25.0%)	
No	70 (88.61%)	55 (93.22%)	15 (75.0%)	
	N=79	N = 59	N = 20	
VALVULAR DISEASE				>0.999
Yes	12 (15.58%)	9 (15.79%)	3 (15.0%)	
No	65 (84.42%)	48 (84.21%)	17 (85.0%)	
	N=77	N = 57	N = 20	
HYPERTENSION				0.798
Yes	36 (46.75%)	26 (45.61%)	10 (50.0%)	
No	41 (53.25%)	31 (54.39%)	10 (50.0%)	
	N=77	N = 57	N = 20	
HEMORRHAGE				0.755
Yes	17 (21.52%)	12 (20.34%)	5 (25.0%)	
No	62 (78.48%)	47 (79.66%)	15 (75.0%)	
	N=79	N = 59	N = 20	
INFECTIONS				0.278
Yes	22 (12.29%)	18 (11.32%)	4 (20.0%)	
No	157 (87.71%)	141 (88.68%)	16 (80.0%)	
	N=179	N = 159	N = 20	
DEFINITIVE DISCONTINUATION IBRUT	76 (42.46%)	65 (40.88%)	11 (55.0%)	0.241
Yes	103 (57.54%)	94 (59.12%)	9 (45.0%)	
No	N=179	N = 159	N = 20	
SECONDARY MALIGNANCIES	18 (23.08%)	15 (25.86%)	3 (15.0%)	0.376
Yes	60 (76.92%)	43 (74.14%)	17 (85.0%)	
No	N=78	N = 58	N = 20	

Table 1. Patients' characteristics and groups comparison according to AF.

trials when consistently treated according to guidelines, resulting in fewer unnecessary treatment discontinuations with minimal impact on treatment armamentarium. The risk of AF, reaching its maximum effect during long-term FU, is likely a class effect of BTKi, but AF does not per se affect the outcome of patients treated with ibrutinib.

Abstract ID: 1553594

Title: Optical genome mapping and fluorescence in situ hybridization is the best combination to identify genomic complexity and TP53 deletions in CLL patients

Authors: Joanna Kamaso, Anna Puiggros, Rocío García-Serra, Marina Munné, María Rodríguez-Rivera, Carme Melero, Silvia Ramos-Campoy, Marta Salido, Eva Gimeno, Rack Katrina, Barbara Dewaele and Blanca Espinet

Introduction: Fluorescence in situ hybridization (FISH) is the gold-standard cytogenetic technique for the detection of the most frequent chromosomal alterations (CA) in chronic lymphocytic leukemia (CLL). In 2000, Döhner et al. established a hierarchical model for risk stratification including the following groups: isolated del13q, no abnormalities (normal), trisomy 12, del11q and del17p. Furthermore, complex karyotype (CK, ≥3 CA) identified by chromosome banding analysis (CBA) is also a poor prognostic and potentially predictive biomarker. Optical genome mapping (OGM) is a novel method that relies on the imaging of long DNA molecules (>250 Kb) labeled at specific sites. The unique pattern of labels throughout the genome allows their

	FISH		OGM		
Genomic alterations	Nº of patients (%) n=56	Median % of altered nuclei (range)	Nº of patients (%) n=56	Median % VAF (range)	Nº of FISH positive patients detected (%)
del(13)(q14)	35 (63%)	72 (6-98)	29 (52%)	45 (5-87)	29/35 (82.8%)
Trisomy 12	10 (18%)	58 (11-90)	9 (16%)	35 (28-42)	9/10 (90.0%)
del(11)(q22q23)	15 (27%)	64 (11-98)	14 (25%)	43 (3-53)	14/15 (93.3%)
del(17)(p13)	8 (14%)	38 (15-97)	4 (9%)	37 (15-46)	5/8 (62.5%)
Risk group according to Döhner hierarquical classification	**Nº of patients (%) n=56**		**Nº of patients (%) n=56**		
13q deletion as sole abnormality	13 (23%)		15 (27%)		
Trisomy 12	9 (16%)		7 (13%)		
del(11)(q22q23)	15 (27%)		14 (25%)		
del(17)(p13)	8 (14%)		5 (9%)		
Normal FISH	11 (20%)		15 (27%)		

CBA

46,XY,add(11)(q23),del(11)(q21q23)[9]/46,XY[11]

OGM

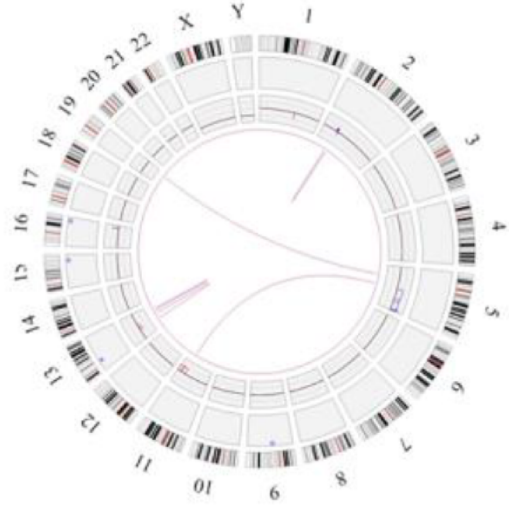

Gain	2p16.1p15 [2Mb]
Loss	2p14 [2Mb]
Translocation	fus(2;2)(p16.1;p14)
Gain	5q14.3q35.3 [88Mb]
Translocation	t(5;11)(q14.3;q22.1)
Loss	11q22.1q25 [34Mb]
Translocation	fus(13;13)(q14.11;q21.32)
Translocation	fus(13;13)(q31.1;q31.3)

genomic location to be precisely mapped permitting the detection of both balanced and unbalanced abnormalities with high resolution. OGM has shown promising results for CK assessment in CLL [1]. This study aims to determine the ability of OGM to detect poor prognostic biomarkers in CLL by evaluating the concordance with FISH and CBA results to investigate the potential of OGM as a routine diagnostic test.
Methods: Fifty-six CLL patients from two European centers with FISH (13q, CEP12, ATM and TP53) and CBA data available were included. FISH was performed on fixed peripheral blood (PB) cells ($n=39$) or after IL2+DSP30 cultures ($n=17$). CBA was performed on IL2+DSP30 PB cultures ($n=56$) and in parallel TPA cultures ($n=39$). For OGM analysis, DNA was extracted from whole PB ($n=22$) or PBMC ($n=34$). Clinically relevant CA (2p, 8q, 12 gains; 6q, 8p, 11q, 13q, 15q, 17p deletions; IGH, IGK, IGL, BCL2 rearrangements), other translocations and CA ≥5Mb detected with OGM were compared with those obtained by conventional techniques.
Results: Sixty-eight abnormalities were detected by FISH in the 56 patients. Of these, OGM detected 57 (84%). No additional variants were detected by OGM in the loci investigated by FISH. All FISH abnormalities present in >24% cells were identified by OGM. For the 11 abnormalities detected by FISH in ≤24% cells, OGM confirmed the aberration in four cases (4/11, range of FISH clonality percentage: 12–18%) but did not detect the abnormality in seven (7/11, range: 6–24%, median 16%). Importantly, this latter group included 27% (3/8) of cases with 17p deletions (range: 15–17%) (Table 1). If OGM was implemented as a stand-alone technique this would result in reclassification of 70% (7/10) of patients with discordant OGM/FISH results. More specifically, 4/7 patients would change from high-risk to low-risk (Table 1). Nevertheless, two of these discordant cases show high complexity by both CBA and OGM, which is a predictor of worse prognosis.Comparing CBA and OGM results, OGM detected a greater proportion of patients with CA (88 vs. 77%, $p=0.193$). The median number of aberrations was also higher with OGM (3 (1–65) vs. 2 (1–13), $p=0.469$). Among the 13 patients with a normal karyotype, 6/13 showed 1 to 4 aberrations and 1/13 showed high complexity (23 CA) by OGM. Regarding patients with abnormal karyotype, OGM detected abnormalities in 42/43 patients but failed to detect an isolated 6q deletion present in 14% nuclei in one case. OGM also identified chromothripsis and chromoplexy, in 3 cases each with a further case demonstrating both. Patients with CK ($n=12$; 8/12 with ≥5 CA) showed a significantly higher median number of aberrations by OGM compared with those with an abnormal non-CK ($n=31$) (10 (5–65) vs. 3 (0–13), $p<0.001$). Of note, 11 of the latter (35%) showed ≥5 aberrations by OGM (Figure 1), which was the minimum number of CA in the CK group. Remarkably, in cases with ≥5 CA by CBA (High-CK), the minimum number of aberrations by OGM was 6.
Conclusions: (1) OGM is a robust method to assess genome wide aberrations in CLL genome-wide; (2) Its independence of cell cultures and a higher genomic resolution increases the detection rate of genomic complexity. To define clear genomic complexity criteria by OGM, additional studies are needed and its clinical impact should be validated; (3) OGM sensitivity is limited and small cell clones (<15–25%) could be missed. Thus, FISH for del17p (TP53) detection should be maintained in the routine management of CLL patients.

Acknowledgements

2021SGR00025, PI21/00022, FEHH-AstraZeneca.

Abstract ID: 1553617

Title: Phase 1/2 Study of zilovertamab and ibrutinib: durable responses suggest a novel mechanism for synthetic lethality in TP53 aberrant disease

Authors: Michael Choi, Hun Ju Lee, Tanya Siddiqi, Joanna Rhodes, William Wierda, Jacqueline Barrientos, Iris Isufi, Joseph Tuscano, Nicole Lamanna, Suki Subbiah, Jean Koff, Lori A Leslie, Alec Goldenberg, Gina Chung, James Breitmeyer, Salim Yazji, Elisabeth Coates, Emanuela Ghia, Michael Wang, Catriona Jamieson and Thomas Kipps

Background: Zilovertamab (Zilo) is a humanized monoclonal antibody that inhibits the tumor-promoting activity of the cancer stem cell receptor, ROR1, which is highly expressed in many hematologic malignancies but not on normal adult tissues.
Methods: Patients (Pts) with relapsed or refractory (RR) MCL or MZL or treatment-naïve (TN) or RR CLL were enrolled in the overall trial. Part 1 (Dose Escalation in CLL & MCL) evaluated multiple doses up to Zilo 600 mg IV q4wks + Ibrutinib (Ibr) 420mg (CLL) or 560mg (MCL) daily, which was selected for Part 2 (Dose Expansion in CLL, MCL & MZL) and Part 3 (CLL only; pts randomized 2:1 to Zilo + Ibr vs. Ibr alone). Results from the CLL cohorts, including the subgroup with del(17p) or TP53 mutation (TP53 mut) are updated. Patient Characteristics: To date, 62 pts with CLL were treated. 34 patients (12 TN and 22 RR) in parts 1 & 2 were efficacy evaluable. In Part 3, 23 CLL pts on Zilo + Ibr (16) or Ibr (7) were evaluable. Across these parts, 10 pts (5 TN and 5 R/R) with CLL had TP53 mutation or del(17p). Safety: AEs are summarized for all pts in both the CLL and MCL cohorts. The most frequent (≥30%) treatment emergent adverse events (TEAEs) for all MCL & CLL pts on Zilo + Ibr ($n=85$) were diarrhea (45.9%), fatigue (45.9%), contusion (38.8%) and cough (30.6%). The most frequent (≥5%) grade ≥3 TEAEs were hypertension (10.6%), pneumonia (8.2%), atrial fibrillation (AF, 7.1%), neutropenia (7.1%), and fatigue (5.9%). Grade ≥3 hematologic lab abnormalities (not all treatment emergent) were decreases in neutrophils (11.8%), platelets (4.7%), and hemoglobin (3.5%). Efficacy in CLL: In parts 1–3, mPFS was not reached (NR) with median f/u of 40 mos for parts 1&2 and ~30 mos in part 3. Post-hoc analysis of the pts with del(17p) or TP53 mut showed a 100% landmark PFS and OS at 42 and 40 mos, respectively. To date, no patient with CLL with del(17p) or mutTP53 has had disease progression.
Correlative science: Preclinical studies have previously shown that cancer cells with TP53 mut are more dependent on NRF2 for stress and antioxidant response. Samples from patients treated with Zilo + Ibr (but not Ibr alone) showed suppression of NRF2 gene expression, supporting the hypothesis that CLL cells with TP53 mut or del(17p) are more sensitive to the effects of NRF2 inhibition.
Conclusions: Zilo + Ibr is well-tolerated with a safety profile that is comparable to Ibr alone. For pts with CLL, Zilo + Ibr is very active and results in durable remissions. The PFS and OS for the subgroup with TP53 mut/del(17p) are particularly encouraging in reference to other trials of BTK inhibitors, maintaining 100% PFS and OS at ~42 mos. Suppression of NRF2 via inhibition of ROR1 may represent a novel strategy for treatment of TP53 mut CLL.

Abstract ID: 1553702

Title: Switching from covalent BTKI to BCL2i is associated with improved clinical outcomes compared to switching to a different covalent BTKI in patients with CLL/SLL treated in the real-world setting

Authors: Toby A. Eyre, Catherine C. Coombs, Nicole Lamanna, Jennifer Brown, Beenish S. Manzoor, Nilanjan Ghosh, Hande H. Tuncer, Alan Skarbnik, Matthew Davids, Nnadozie Emechebe, Hasan Alhasani, Lori A Leslie, Lindsey Roeker, Chaitra Ujjani, Isabelle Fleury, Barbara Eichhorst, Brian Hill, Joanna Rhodes, Frederick Lansigan, Paul Barr, Laurie Pearson, Christopher P. Fox, Yun Choi, Christopher E. Jensen, Dureshahwar Jawaid, Kaitlin Kennard, Irina Pivneva, Talissa Watson, Annie Guerin and Mazyar Shadman

Introduction: Targeted agents, such as covalent BTKi- (cBTKi; i.e. acalabrutinib, ibrutinib, zanubrutinib) and BCL2i- based regimens (i.e. venetoclax), have demonstrated improved treatment efficacy and safety compared to CT/CIT for patients with CLL/SLL. However, some patients discontinue for reasons other than disease progression (PD) and switch to targeted agent with the same or different mechanism of action (MOA). This study assessed real-world treatment outcomes of patients with CLL/SLL who switched to a cBTKi- or BCL2i-based regimen following discontinuation of a cBTKi-based regimen.

Methods: Data from the CLL Collaborative Study of Real-World Evidence (CORE), an international, retrospective observational study involving 23 centers, were included in this study. Adult BCL2i-naïve patients diagnosed with CLL/SLL were included if they discontinued their cBTKi-based regimen for reasons other than PD or completion of therapy and switched to a cBTKi or BCL2i-based regimen. Based on switching patterns, patients were classified into 2 mutually exclusive cohorts: cBTKi (i.e. cBTKi-cBTKi) or BCL2i (i.e. cBTKi-BCL2i). Treatment outcomes of the studied therapy included overall response (OR), progression-free survival (PFS), and time to next treatment or death (TTNT-D). OR was defined as complete or partial response. PFS was defined as the time from cBTKi or BCL2i initiation to PD/death (event), censoring at last follow-up date. TTNT-D was defined as the time from cBTKi or BCL2i initiation to initiation of next treatment/death (event), censoring at last follow-up date. Regression models, controlling for age at cBTKi or BCL2i initiation, sex, time from CLL/SLL diagnosis to cBTKi or BCL2i initiation, duration of discontinued cBTKi therapy, ECOG, and lactate dehydrogenase (LDH), assessed the odds of achieving an OR via a logistic regression and the time to PD/death and time to next treatment/death via a Cox proportional hazards (PH) regression.

Results: A total of 121 BCL2i-naïve patients who discontinued their first cBTKi-based regimen in any line of therapy and switched to a subsequent treatment with a cBTKi- (cBTKi: 44 [36.4%]) or a BCL2i-based regimen (BCL2i: 77 [63.6%]) were included in the study. The most common subsequent regimen following cBTKi discontinuation was a second-generation cBTKi regimen (34/44 [77.3%]; acalabrutinib [30/34], zanubrutinib [4/34]) or BCL2i (venetoclax monotherapy: 43/77 [55.8%] and venetoclax + anti-CD20: 33/77 [42.9%]). Most common reason for prior cBTKi discontinuation was intolerance (cBTKi: 79.6%, BCL2i: 80.5%). The majority of patient characteristics were not significantly different between cohorts: median age at cBTKi or BCL2i initiation (cBTKi: 71.5 years, BCL2i: 69.0 years), gender (male: cBTKi: 63.6%, BCL2i: 68.8%), unmutated IGHV (cBTKi: 47.7%, BCL2i: 37.7%), and with del(17p)/TP53 mutation (cBTKi: 20.5%, BCL2i: 27.3%); however, there were some significant differences: median time from CLL/SLL diagnosis to cBTKi or BCL2i initiation (BTKi: 91.0 months, BCL2i: 62.6 months), median duration of discontinued-cBTKi (cBTKi: 19.6 months, BCL2i: 10.8 months), ECOG Performance Status 0 (cBTKi: 50.0%, BCL2i: 27.3%), and elevated LDH (cBTKi: 29.5%, BCL2i: 46.8%; Table 1). Median follow-up duration was 11.6 months for cBTKi and 16.4 months for BCL2i. Among 79 patients with recorded response, the OR was higher for BCL2i than cBTKi (cBTKi: 62.5%, BCL2i: 83.6%). The odds of achieving a response were significantly higher for BCL2i than cBTKi (unadjusted: 3.1 times [CI: 1.0; 9.1]; adjusted: 4.6 times [CI: 1.2; 18.0]). The PFS KM estimates were higher for BCL2i in relation to cBTKi at 12 months (cBTKi: 79.1%, BCL2i: 87.3%) and 24 months (cBTKi: 73.0%, BCL2i: 78.0%). Cox PH results revealed that treatment with BCL2i reduced the hazard of progression/death by 70% (unadjusted HR: 0.6 [CI: 0.3; 1.5]; adjusted HR: 0.3 [CI: 0.1; 0.8], $p = 0.023$) compared to cBTKi. The results were similar for TTNT-D (KM estimates at 12 months: cBTKi: 81.1%, BCL2i: 84.7%; at 24 months: cBTKi:

Table: Patient characteristics for cBTKi and BCL2i cohorts

Patient characteristics	BTKI cohort N = 44	BCL2i cohort N = 77	P-value
Age at cBTKi or BCL2i initiation (years), Mean± SD [Median]	70.2 ± 9.2 [71.5]	68.7 ± 9.6 [69.0]	0.41
Time from CLL/SLL diagnosis to cBTKi or BCL2i initiation (months), Mean± SD [Median]	98.4 ± 54.6 [91.0]	76.4 ± 66.7 [62.6	0.07
Number of prior lines, Mean± SD [Median]	1.7 ± 1.0 [1.0]	1.7 ± 0.8 [2.0]	0.98
Time to cBTKi discontinuation, (months), Mean± SD [Median]	22.8 ± 19.8 [19.6]	14.3 ± 17.1 [10.8]	0.01*
Male sex, N (%)	28 (63.6)	53 (68.8)	0.56
Race, N (%)			0.98
White	36 (81.8)	63 (81.8)	
Others	6 (13.6)	10 (13.0)	
Number of prior lines, N (%)			0.44
1	25 (56.8)	37 (48.1)	
2	11 (25.0)	28 (36.4)	
3+	8 (18.2)	12 (15.6)	
Rai staging, N (%)			0.98
Stage 0	5 (11.4)	9 (11.7)	
Stage I - IV	28 (63.6)	50 (64.9)	
ECOG, N (%)			0.03*
Grade 0	22 (50.0)	21 (27.3)	
Grade 1 - 3	14 (31.8)	42 (54.5)	
Elevated lactate dehydrogenase (LDH), N (%)	13 (29.5)	36 (46.8)	0.04*
Unmutated IGHV, N (%)	21 (47.7)	29 (37.7)	0.38
With del(17p)/TP53 mutation	9 (20.5)	21 (27.3)	0.59

*Significant at p<.05

69.6%, BCL2i: 71.1%; unadjusted HR: 0.8 [CI: 0.4; 1.9]; adjusted HR: 0.4 [CI: 0.1; 1.0], $p = 0.055$).

Conclusion: Patients who switched to a BCL2i-based regimen were more likely to respond to therapy and had lower hazard of progression/death; TTNT-D results also suggested a possible benefit of BCL2i over cBTKi. Switching to BCL2i-based regimens post-cBTKi demonstrates better treatment outcomes compared to cycling through consecutive cBTKis, further highlighting the effectiveness of BCL2i in real-world settings. Given the dynamic treatment landscape in CLL, the impact of switching to agent(s) with a different MOA or choosing to retreat with agent(s) in the same class are key considerations in optimizing clinical care.

Abstract ID: 1553733

Title: T cells from chronic lymphocytic leukemia patients are not exhausted but show signs of senescence, providing alternative clues for improvement

Authors: Fleur S. Peters, Chiara Montironi, Gaspard Cretenet, Ide Spaanderman, Eric Eldering and Arnon Kater

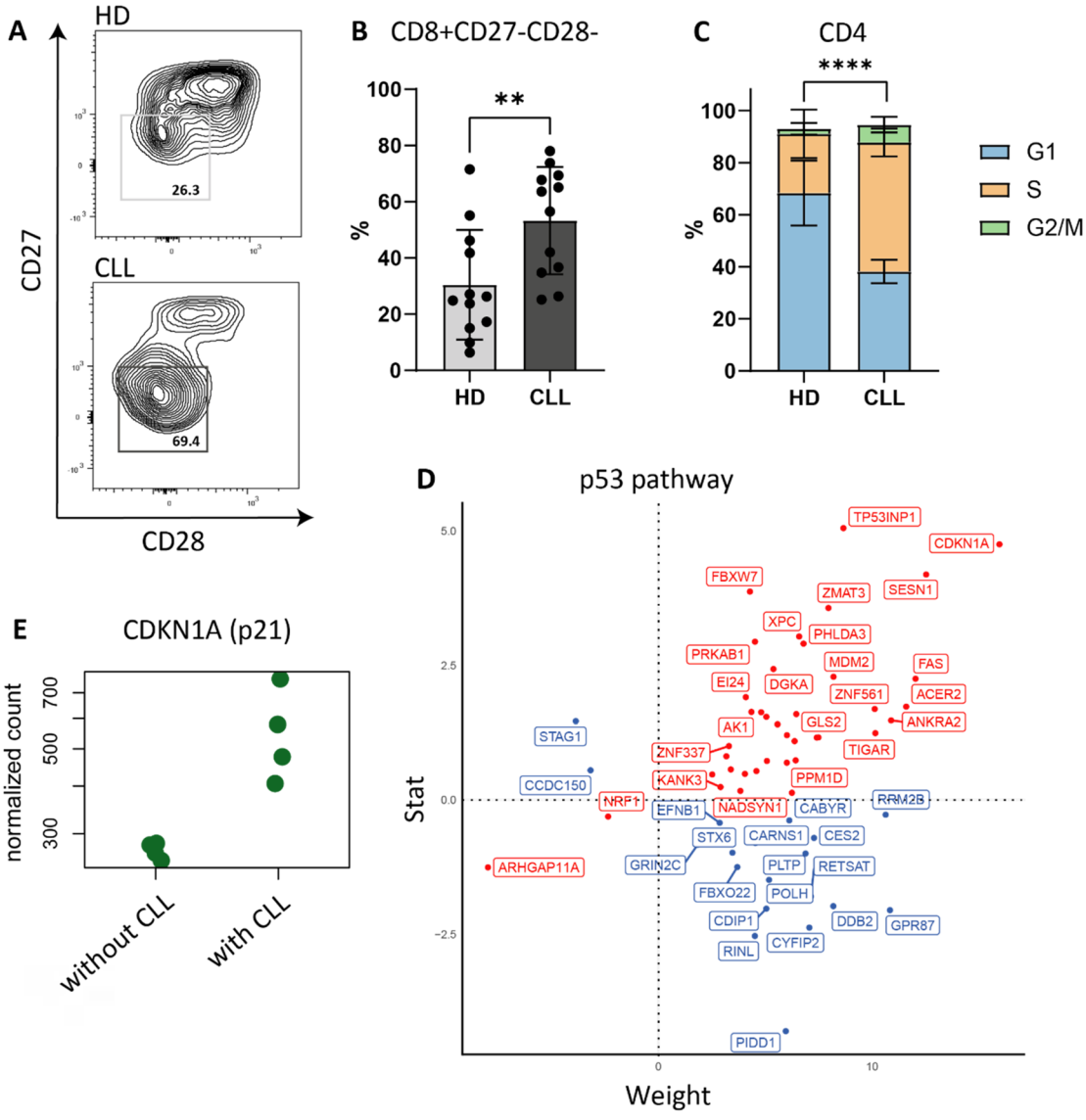

Figure 1. A Example FACS plots of CD27 and CD28 expression within CD8⁺ T cells of age-matched healthy donors (HD) and chronic lymphocytic leukemia (CLL) patients. **B** Percentage of CD27 and CD28 double-negative cells within CD8⁺. **C** Percentages of CD4⁺ cells in the different cell cycle phases measured using the FxCycle dye by flow cytometry in HD and CLL. **D** Gene expression of p53 pathway genes in CD4⁺ cells cultured in presence vs in absence of CLL cells, the y-axis indicates a measure for differential expression and the x-axis depicts the weight of each gene in the pathway as determined using the PROGENy pathway activity inference within the decoupleR package. **E** Normalized counts of the CDKN1A (encoding p21) gene in CD4⁺ cells cultured in absence or presence of CLL cells

Introduction: Chronic lymphocytic leukemia (CLL) is currently an incurable disease and there is an unmet need for novel therapeutic strategies. Utilization of T cells to target CLL is a promising strategy, but so far, has not been successful in the majority of CLL patients. Exhaustion of T cells has been proposed as contributing factor to the acquired T-cell dysfunction patients develop. However, we have demonstrated that reduced levels of activation and metabolic impairments of CLL T cells are rescued upon in vitro elimination of CLL cells [1], which indicates that the cells are not (terminally) exhausted. We hypothesize that instead of exhaustion, senescence is the dominant dysfunctional T-cell state in CLL patients. Senescent T cells share common features with senescent somatic cells such as cell-cycle arrest, decline in proliferation and activation, but are able to produce high amounts of pro-inflammatory cytokines, features that have been previously described for CLL T cells. Here we study phenotypical and molecular characteristics of senescence in CLL T cells.
Methods: We assessed expression of cell-surface proteins that characterize senescent T cells (e.g. absence of CD27/CD28 and presence of PD1/CD57/KLRG1) with flow cytometry. To measure cell-cycle progression, T cells were stimulated through CD3/CD28 for 5 days and, using a DNA dye, the different cell-cycle phases were measured with flow cytometry. To study the direct effect of CLL cells on autologous T cells, T cells were stimulated in the presence or absence of their CLL cells. On day 2 the CD4+ T cells were FACS-sorted and mRNA sequencing was performed to investigate the activity of molecular pathways. Results We found that CLL patients have increased proportions of CD27-CD28- T cells compared to age-matched healthy donors (HD) (Figure 1(A,B)). In accordance with previous findings [2], expression of KLRG1 was increased on CLL T cells and furthermore, a CD27-CD28–PD1+CD57+KLRG1¬+ subset was more abundant within the CLL T cells compared to HD. Senescent cells are typically cell-cycle arrested and when stimulating T cells *in vitro* through CD3/CD28, we observed a strikingly distinct cell-cycle pattern whereby a larger proportion of CLL T cells resided in S and G2/M phases (Figure 1(C)). RNA sequencing on CD4+ T cells stimulated with CD3/CD28 in the presence or absence of their autologous CLL cells revealed that CLL cells induced a clear inflammatory gene signature, indicated by upregulation of TNF and NFκB pathways. Pathways related to cell cycle such as E2F transcription factors and G2/M progression were repressed in presence of CLL. A potential cause for cell-cycle arrest and senescence is DNA damage. In our transcriptome data we observed activity of the p53 pathway when T cells were stimulated with CLL cells present as well as upregulated expression of ATM and CDKN1A (encoding p21) (Figure 1(D,E)); a possible indication of an activated DNA damage response. In addition, our group has also demonstrated that CLL T cells were specifically impaired in mitochondrial metabolism whilst glycolysis was largely intact, that CLL T cells have decreased TCA intermediates and increased reactive oxygen species (ROS) upon stimulation [3], which are all indicators of senescence. Potential intervention in MAPK or ATM signaling to alleviate senescence in the CLL T cells is to be investigated.
Conclusion: We conclude that the dominant T-cell dysfunctional state in CLL is more fitting with senescence rather than exhaustion. These two T-cell states arise by distinct mechanisms and also require different means of reinvigoration in the context of immunotherapy. MAPK/p38 signaling is specifically activated in senescent cells, which could also be activated by DNA damage. Further study is warranted on how these signals can be interrupted to restore function of T cells in for example chimeric antigen receptor (CAR) T-cell therapy.

Abstract ID: 1553741

Title: Real-world evidence on venetoclax in chronic lymphocytic leukemia: The KROHEM (Croatian cooperative group for hematological diseases) experience

Authors: Dino Dujmovic, Sandra Bašić-Kinda, Ida Ivek, Barbara Dreta, Marija Ivic, Ozren Jaksic, Antonia Mrdeža, Goran Rinčić, Karla Mišura, Slobodanka Kolonić Ostojić, Hrvoje Holik, Ivana Budisavljevic, Toni Valkovic, Ivan Zekanovic, Ivan Krecak, Nika Popović, Vlatko Pejša, Igor Aurer and Antonija Miljak

Real-world evidence on venetoclax in chronic lymphocytic leukemia: The KROHEM (Croatian cooperative group for hematological diseases) experience Chronic lymphocytic

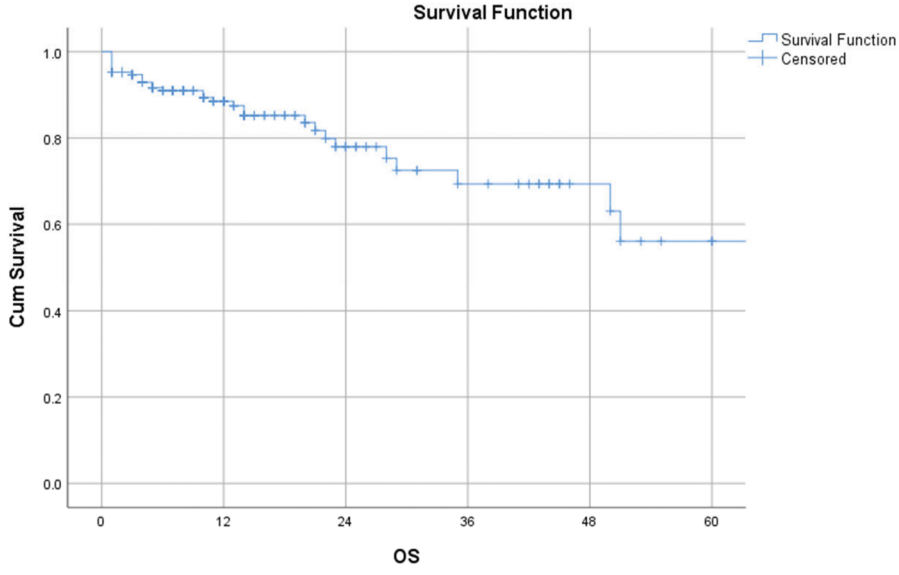

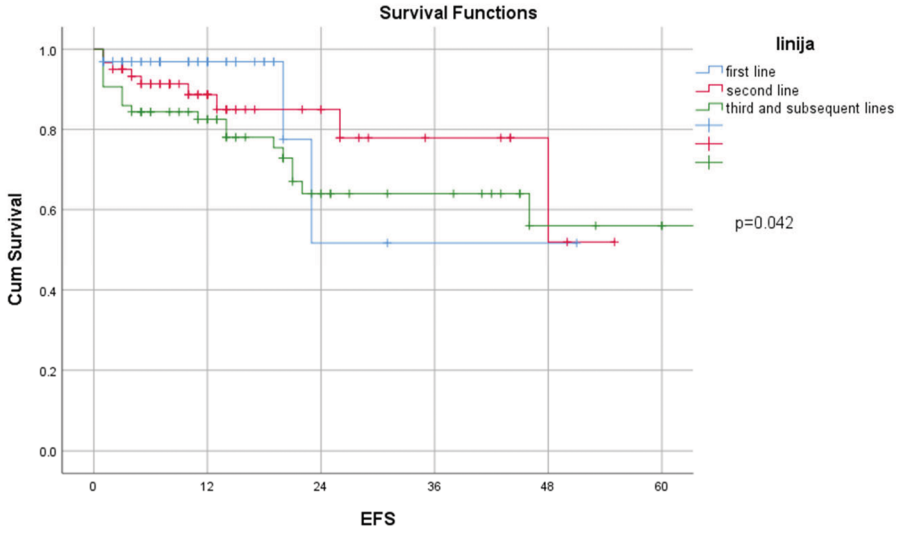

leukemia (CLL) is the most common form of leukemia in the western adult population. The B cell lymphoma-2 (BCL-2) family proteins play a key role in regulating intrinsic apoptosis and in many cancers have a major impact on tumor survival and therapy resistance. Hence, the role of BCL-2 inhibitors is very beneficial in the treatment of CLL. Venetoclax is the first selective, orally bioavailable BCL-2 inhibitor in use for both frontline and relapse/refractory CLL. In this trial we conducted a multicenter retrospective chart analysis of patients with chronic lymphocytic leukemia treated with venetoclax to describe outcomes and toxicities. From 2017 to 2023 a total of 188 patients were treated. Median age at venetoclax initiation was 66 years (range 33–90), median prior lines of therapies was 2 (1–6), 42 pts (22%) had del(17p). 64(34%) was treated frontline, 60(32%) received venetoclax as a second line and 64(34%) in later lines. Prior to venetoclax initiation, 33(17%) received a BTK inhibitor and 83(44%) received anti CD20 monoclonal antibody. 75 patients (40%) received venetoclax as a monotherapy while 113(60%) received venetoclax in combination either with rituximab or obinutuzumab. Overall response rate(ORR) was 85% in all analyzed cohorts with 94 (50%) patients achieved complete remission. 14 (7%) patients were not yet evaluated, 6 (3%) did not respond to treatment and died early in treatment and 6 (3%) patients progressed during treatment. Patients treated in first line had an overall response rate of 100% and in those patients that received venetoclax as a second line had an ORR of 96%. Almost all non responders that died early in treatment or those with early progression were patients treated in third or subsequent lines of therapy. After a median follow up of 12 months estimated median overall survival (OS) was not reached, 2-year OS for the whole cohort was 83.5%. Figure 1. Event free survival (EFS) was 83%. When we analyzed the patients by the treatment lines, in first line EFS was 93.8%, in second line 85% and third and subsequent lines it was 70.3% with a statistically significant difference ($p=0.042$). Figure 2. Adverse event of any grade occurred in 50% of the patients during venetoclax therapy. The most frequent adverse events where hematological and non hematological adverse events events include: infections including COVID 19 , tumor lysis syndrome, diarrhea, and elevated liver enzymes. Grade III/IV adverse events occurred in 86(45%) patients, mostly neutropenia (90%), but only 33(18%) needed hospitalization because of febrile neutropenia. 67(35%) had a temporary treatment discontinuation due to adverse events and 53(28%) patients had a dose reduction. In only 11(6%) patients venetoclax treatment was permanently discontinued due to toxicity. Richters transformation occurred in 18 (10%) patients. Of those patients 16 were in second or subsequent lines while patients had a concurrent Richters transformation at the beginning of treatment. Two patients developed secondary malignancy(breast cancer and skin cancer). Our real-life data tend to confirm that venetoclax used as monotherapy or in combination with rituximab or Obinutuzumab is effective treatment for both untreated and relapse/refractory CLL patients. Our data are very similar to the clinical trials data although our follow up is shorter. Adverse events were observed at a similar incidence as in the clinical trials, and the most of adverse events were easily manageable.

Abstract ID: 1553753

Title: Impaired long-term antibody persistence after primary immunization with pneumococcal vaccines in patients with chronic lymphocytic leukemia compared to immunocompetent controls

Authors: Magdalena Kättström, Camilla Virta, Merit Melin, Nina Ekström, P-O Andersson, Ylva Hammarlund, Sandra Lockmer, Ingmar Nilsson, Daniel Roth, Magnus Svensson, Tobias Tolf, Eva Kimby, Torbjörn Norén, Bertil Uggla and Simon Athlin

Background: Patients with chronic lymphocytic leukemia (CLL) have an increased risk of invasive pneumococcal disease (IPD). Impaired immune response to pneumococcal vaccination calls for improved vaccination strategies. In a previous randomized study of treatment-naïve CLL patients [1] we showed that a T-cell dependent conjugated pneumococcal vaccine (PCV13) induced a superior immune response compared to non-T cell dependent polysaccharide vaccine (PPSV23), estimated both by enzyme-linked immunosorbent assay for IgG titers and opsonophagocytic assay (OPA) for antibody functionality. Follow-up studies of long-term pneumococcal antibody persistence in CLL patients after PCV13 and PPSV23 are lacking, and there are no recommendations on revaccination strategies.

CLL patients						Healthy controls					
Group A			Group B			Group C			Group D		
PCV13-PCV13-PPSV23			PPSV23-PCV13-PCV13			PCV13-PCV13			PPSV23-PCV13		
N	N >0,35	% >0,35	N	N >0,35	% >0,35	N	N >0,35	% >0,35	N	N >0,35	% >0,35
36	16	44	38	13	34	9	8	89	22	18	82

Aim: To assess the long-term antibody persistence after primary immunization with PCV13 or PPSV23 in CLL patients and healthy controls, and the response to revaccination with PCV13 + PPSV23 or PCV13 + PCV13.
Method: Seventy-four CLL patients from our previous study were included 4–6 years after primary immunization with PCV13 (Group A, $n=36$) or PPSV23 (Group B, $n=38$). In addition, thirty-one immunocompetent controls were recruited, primary immunized with PCV13 (Group C, $n=9$) or PPSV23 (Group D, $n=22$) 3–7 years previously. The CLL patients and controls were assessed for antibody persistence and then revaccinated with PCV13. After 8 weeks, the CLL patients received a second revaccination with either PPSV23 (Group A) or PCV13 (Group B), but the controls received no further vaccine. Serum samples were collected before and 8 weeks after first revaccination, 8 weeks after second revaccination and after 12, 18, 24 and 30 months. A bead-based multiplex immunoassay was used for quantitation of IgG (µg/mL) against PCV13-related serotypes (1, 3, 4, 5, 6A, 6B, 7F, 9V, 14, 18C, 19A, 19F and 23F). Rates of serotype-specific IgG levels ≥0.35 µg/mL for >50% (7–13/13) of the serotypes were calculated in CLL patients and controls and used to evaluate persistent antibody levels.
Results: After a median time of 5 years after primary immunization, the rate of persistent antibody levels in CLL patients were lower compared to controls (29/74, 39% versus 26/31, 84%; $p<0.001$). No significant difference in rates of persistent antibody levels was seen after primary immunization with PCV13 or PPSV23 in CLL patients (44 vs. 34%, p=NS) or controls (89 vs. 82%, p=NS), see Table 1. Median time from primary immunization was similar between the four groups (Group A, 65; B, 65.5; C, 60.5; D, 60 months). Median time from CLL diagnosis to revaccination in group A and B were 91 and 85 months, respectively, and hypogammaglobulinemia was seen in 19/74 (26%) CLL patients. Fifty-eight patients (78%) were still treatment-naïve, 9 (12%) were off treatment in remission and 6 (8%) had ongoing treatment with BTK inhibitors or anti-CD20 antibodies.
Conclusion: CLL patients have impaired long-term antibody persistence 5 years after primary immunization with pneumococcal vaccines compared to immunocompetent controls. Whether CLL patients will benefit from pneumococcal revaccinations is currently being analyzed.

Abstract ID: 1553843

Title: Real-world dosing patterns and outcomes in patients with chronic lymphocytic leukemia patients with or without dose adjustment of first-line ibrutinib

Authors: Kerry Rogers, Xiaoxiao Lu, Bruno Edmond, Zhijie Ding, Patrick Lefebvre, Marie-Hélène Lafeuille, Heena Mavani, Zaina Qureshi and Nilanjan Ghosh

Introduction: Patients treated for chronic lymphocytic leukemia (CLL) with ibrutinib, a once-daily Bruton's tyrosine kinase inhibitor with dosing flexibility options, may adjust their daily dose to help prevent recurrence or worsening of adverse events, while preserving efficacy. This real-world study describes outcomes for patients with CLL treated with first-line (1L) ibrutinib who did or did not have a dose adjustment.
Methods: Electronic medical records from the Acentrus database (1/1/2016–4/30/2022) were used to identify patients with CLL initiated on 1L ibrutinib (index date). The first 6 months post-index were used to identify patients who remained on a starting dose of 420 mg/day or with dose adjustment (reducing to a dose lower than 420 mg/day; reasons for adjustment not available). Treatment adherence (measured using proportion of days covered [PDC] and medication possession ratio [MPR]) and time to next treatment (TTNT) were described for patients with and without dose adjustment. Descriptive analyses are reported for all patients and for the subgroup with high cardiovascular (CV) risk, defined as having a pre-existing CV comorbidity or a high CV risk score (CV subgroup).
Results: In total, 1,171 patients with CLL were initiated on 1L ibrutinib at the recommended dose of 420 mg/day (Table 1). Of those, 1,038 (88.6%) remained on 420 mg for ≥6 months (mean age =70.2 years, 33.6% female, median follow-up: 30.5 months); 229 (19.6%) had a dose adjustment at any time post-index (median time to adjustment: 5.5 months) and 126 had an adjustment during the first 6 months (mean age =72.2 years, 42.9% female, median follow-up: 35.1 months). Mean PDC and MPR were descriptively higher in patients with dose adjustment (overall: PDC =0.81, MPR =0.84; CV subgroup: PDC =0.78, MPR =0.81) relative to patients with no adjustment (overall: PDC =0.70, MPR =0.73; CV subgroup: PDC =0.69, MPR =0.72). Median TTNT was not reached, regardless of the dose adjustment status; 12-month Kaplan-Meier rates were similar for patients with (overall: 89.1%; CV subgroup: 92.7%) and without adjustment (overall: 92.5%; CV subgroup: 92.0%).
Conclusions: Among patients with CLL initiating with standard-of-care 1L ibrutinib, 19.6% had a dose adjustment. Those with adjustment had descriptively higher treatment

Table 1.

	Overall $N=1,171$	CV subgroup $N=724$
Dose adjustment at any time, *n* (%)	**229 (19.6%)**	**154 (21.3%)**
Time to first adjustment, months, mean ± standard deviation [median]	9.0 ± 9.2 [5.5]	8.5 ± 8.7 [5.4]
Staying on reduced dose for the remainder of 1L treatment, *n* (%)	138 (60.3%)	93 (60.4%)
Returning to 420 mg/day, *n* (%)	25 (10.9%)	14 (9.1%)
Further reduced dose following initial adjustment, *n* (%)	22 (9.6%)	17 (11.0%)
Other dosing patterns following adjustment, *n* (%)	44 (19.2%)	30 (19.5%)
Dose adjustment within first 6 months, *n* (%)	**126 (55.0%)**	**88 (57.1%)**
No dose adjustment during first 6 months, *n* (%)	**1,038 (88.6%)**	**634 (87.6%)**

adherence with no detriment to TTNT, relative to those who maintained 420 mg/day starting dose, regardless of baseline CV risk. These findings are consistent with other real-world studies and suggest that ibrutinib dose adjustment can be an effective treatment strategy that does not negatively affect efficacy while being well-tolerated outside of clinical trials.

Abstract ID: 1553850

Title: Loss of AID exacerbates the malignant progression of CLL

Authors: Chih-hang Tang, Avery Lee, Sai Ravi Pingali, Javier Pinilla-Ibarz, Carl De Trez and Chih-Chi Hu

Introduction: One of the major prognostic indicators for chronic lymphocytic leukemia (CLL) is the mutational status of the immunoglobulin heavy chain locus (IgHV). Patients with mutated IgHV have longer survival and a better response to chemotherapy than those with unmutated IgHV. This immunoglobulin mutation status is mediated by activation-induced cytidine deaminase (AID), an enzyme primarily expressed in B cells and during the germinal reaction when two gene-modifying processes critical for antibody function occur: class switch recombination and somatic hypermutation. In human patients, it has been shown that there is a correlation between higher levels of AID mRNA and a worse prognosis, although circulating CLL cells do not express AID protein. In contrast, the expression of AID has been shown to be targetable to kill CLL cells and may be important in the development of the relatively indolent mutated CLL. The function of AID in the progression of mutated versus unmutated CLL is not well understood, and the molecular mechanisms behind the development of CLL in an AID-deficient background have not been thoroughly studied.
Hypothesis, methods, and results: We generated an AID knockout CLL mouse model, AID-/-/Eμ-TCL1, and found that these mice die significantly earlier than their AID-proficient counterparts. As shown by immunoblots, AID-deficient Eμ-TCL1 CLL cells exhibited higher B cell receptor (BCR) signaling and a higher ER stress response compared to Eμ-TCL1 controls, particularly through activation of the IRE1/XBP1s pathway. Analysis of mRNA expression by qPCR in AID deficient B cells showed higher levels of spliced and unspliced XBP1 mRNA; knockout of secretory IgM from AID deficient B cells caused downregulation of XBP1s expression. Further, flow cytometry showed that AID-/-/Eμ-TCL1 CLL cells downregulate the tumor suppressive SMAD1/S1PR2 pathway and have altered migration. AID-/-/Eμ-TCL1 mice exhibited increased CLL cells in the livers, lungs, and peritoneal cavities by immunohistochemistry. Translationally, CLL cells from patients with IgHV-unmutated disease express higher levels of XBP1s mRNA compared to those from patients with IgHV-mutated CLL. Treatment of CLL cells from mice and human patients with combinations of the S1PR2 agonist CYM-5520 and the IRE1/XBP1s pathway inhibitor B-I09 delivered enhanced cytotoxicity.
Conclusions: We found that AID deficiency leads to upregulation of the IRE1/XBP1s pathway in both B cells and CLL cells. This upregulation of XBP1 is transcriptionally augmented by the increased secretory IgM found in AID-deficient B cells. The higher levels of XBP1s found in AID-/-/Eμ-TCL1 CLL cells support BCR signaling, contributing to CLL growth and survival. Conversely, downregulation of the SMAD1/S1PR2 pathway in AID-deficient CLL cells results in altered CLL migration, with leukemia cells homing to the non-lymphoid organs of the AID-/-/Eμ-TCL1 mice, potentially explaining their shorter survival. Finally, combined targeting of S1PR2 and XBP1s could be a useful strategy for CLL therapy. Our studies thus reveal novel mechanisms by which the loss of AID leads to worsened CLL and may explain why IgHV-unmutated CLL is more aggressive than IgHV-mutated CLL.

Abstract ID: 1553858

Title: Real-world treatment outcomes in patients with chronic lymphocytic leukemia or small lymphocytic lymphoma who were treated with first-line single-agent ibrutinib vs chemoimmunotherapy

Authors: Ruibin Wang, Zhijie Ding, Xiaoxiao Lu, Heena Mavani, Jinghua He, Zaina Qureshi and Javier Pinilla

Background: Real-world evidence on Bruton Tyrosine Kinase Inhibitor treatment vs chemoimmunotherapy (CIT) for patients with chronic lymphocytic leukemia or small lymphocytic lymphoma (CLL/SLL) has been limited to certain practice settings; research using a large and more comprehensive data source is warranted.
Methods: This retrospective cohort study evaluated treatment outcomes among patients with CLL/SLL treated with first-line (1L) ibrutinib (IBR) or CIT using the US claims data from the Komodo Health payer-complete dataset, derived from >150 private insurers and >140 million insured individuals from 2015 to 2022. This study included adult patients with CLL/SLL who initiated 1L single-agent IBR or CIT (defined as no prior CLL/SLL treatment for ≥12 months in the baseline period) on or after March 2016. Time to next treatment (TTNT) was defined as the time from initiation (index date) of 1L treatment to treatment add-on or switch to a next line of therapy ≥29 days post-index and was compared using Cox proportional hazards models. Cohorts were balanced on baseline characteristics using inverse probability of treatment weights.
Results: A total of 3570 1L IBR- and 2391 CIT-treated patients were included, with the mean age 68 vs. 64 years, 63 vs. 66% male, and mean Quan-Charlson Comorbidity Index score 2.87 vs 3.05, respectively. Median follow-up was 26 vs. 31 months, and 13% vs. 26% of patients recorded a next treatment during the study period for IBR and CIT, respectively. At 1-, 3-, and 5-year post-index, the probabilities (95% confidence interval [CI]) of not initiating a new treatment were 92% (91–93%), 83% (81–84%) and 76% (73–78%) vs. 88% (87–89%), 70% (68–73%) and 56% (53–60%) for the IBR and CIT cohorts, respectively. After controlling for baseline characteristics, 1L IBR patients were significantly less likely to initiate the next line of therapy during the study period (hazard ratio 0.61, 95% CI 0.54–0.69, $p<0.001$).
Conclusions: 1L single-agent IBR was associated with a significantly lower risk of advancing to next line of treatment compared to CIT in this large claims-based data set, reinforcing real-world effectiveness of 1L IBR for CLL in an insured US patient population.

Abstract ID: 1553860

Title: Real-world assessment of dosing patterns and treatment outcomes in patients with chronic lymphocytic leukemia who initiated first-line single-agent ibrutinib in an integrated claims-based database

Authors: Nilanjan Ghosh, Ruibin Wang, Zhijie Ding, Xiaoxiao Lu, Jinghua He, Heena Mavani, Zaina Qureshi and Kerry Rogers

Introduction: In patients with chronic lymphocytic leukemia or small lymphocytic lymphoma (CLL/SLL) who are receiving ibrutinib (IBR), a once-daily Bruton's tyrosine kinase inhibitor, dose modifications may be recommended for managing clinical events during treatment.

Methods: This retrospective cohort study aimed to describe real-world dosing patterns and treatment outcomes in CLL/SLL patients who did or did not have a dose adjustment (DA) after initiation of first-line (1L) single-agent IBR. The study was conducted using health insurance claims data from the Komodo Health payer complete dataset, derived from >150 private insurers in the U.S. and >140 million individuals from 2015 to 2022 with age and geographic representation of the insured U.S. population including patients from the community practice setting. Included CLL/SLL patients initiated on 1L single-agent IBR at the recommended dose of 420 mg/day on or after 4 March 2016. The IBR initiation date was defined as the index date and 1L single-agent IBR treatment was defined as having no other CLL/SLL treatment within 12 months before and 28 days after index. Dosing patterns between index and the end of patient follow-up (earliest of initiation of next line of therapy, end of enrollment, or end of data availability) were described. Further, patients with or without a DA to a dose lower than 420 mg/day during the first 6 months after index were classified into two separate cohorts. Adherence (measured by proportion of days covered [PDC] and medication possession ratio [MPR]) and time to next treatment (TTNT; a surrogate measure of treatment efficacy) after IBR initiation were assessed descriptively in these two cohorts. All analyses were repeated in the corresponding subgroups of patients with high cardiovascular (CV) risk (defined as pre-existing CV comorbidity or high-risk CHA2DS2-VASc score).

Results: 3174 patients initiated 1L IBR at 420 mg/day. Mean age at index was 67 years. Over a median follow-up period of 19.9 months, 18% ($n=562$) had a DA; of those, 50% ($n=280$) experienced DA within the first 6 months after IBR initiation, 85% ($n=478$) received 280 mg/day as the first

Figure. Kaplan-Meier survival curves of time to next treatment among patients treated with 1L single-agent ibrutinib with or without a dose adjustment within 6 months from index date

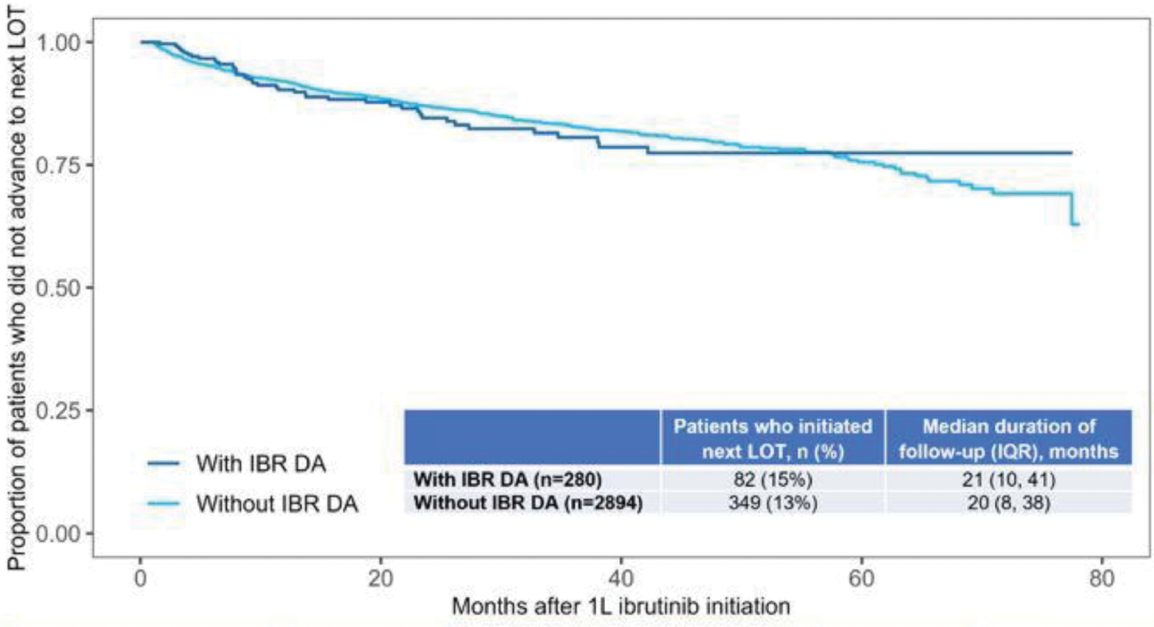

	Patients who initiated next LOT, n (%)	Median duration of follow-up (IQR), months
With IBR DA (n=280)	82 (15%)	21 (10, 41)
Without IBR DA (n=2894)	349 (13%)	20 (8, 38)

	6 months	12 months	24 months	48 months	72 months
With IBR DA (n=280)					
At risk, n	244	195	129	43	6
Probability of not initiating next LOT (95% CI)	97% (95%, 99%)	90% (87%, 94%)	85% (80%, 90%)	77% (71%, 84%)	77% (71%, 84%)
Without IBR DA (n=2894)					
At risk, n	2294	1904	1236	433	62
Probability of not initiating next LOT (95% CI)	95% (94%, 96%)	92% (91%, 93%)	87% (85%, 88%)	80% (77%, 82%)	69% (65%, 74%)

Abbreviations: 1L, first-line; DA, dose adjustment; IBR, ibrutinib; LOT, line of therapy

reduced dose, 70% ($n=396$) stayed on the first reduced dose for the remainder of 1L therapy, 12% ($n=68$) returned to 420 mg/day, and 13% ($n=74$) further reduced the dose. Similar dosing patterns were observed in the subgroup of high CV risk patients ($n=2334$). In the cohort of patients with a DA within the first 6 months after IBR initiation ($n=280$) and the cohort of patients who remained on 420 mg/day for ≥6 months ($n=2894$), 55 and 65% of patients were male, the mean baseline Quan Charlson Comorbidity Index score was 2.87 and 2.83, and 77% ($n=216$) and 73% ($n=2118$) had high CV risk, respectively. Mean PDC was 0.67 and 0.68, and mean MPR was 0.68 and 0.70 in patients with and without a DA, respectively. In the analysis of TTNT, the Kaplan–Meier estimates were similar between the two cohorts (Figure 1); the probability of not initiating the next line of therapy within 12 months was 90% (95% confidence interval [CI]: 87%, 94%) and 92% (95% CI: 91%, 93%) for the cohort with a DA and the cohort without a DA, respectively. Findings of adherence and TTNT were similar for the high CV risk subgroups.

Conclusions: In CLL/SLL patients who initiated 1L single-agent IBR at a dose of 420 mg/day, only 18% had a DA during a median follow-up of 20 months, suggesting that the recommended starting dose was generally well-tolerated. Measures of adherence and probabilities of not initiating the next line of therapy were numerically comparable in patients with or without a DA. These findings highlight that IBR dose modification may be an effective treatment strategy when dose modifications are warranted in the real-world.

Abstract ID: 1553863

Title: Genomic alterations and outcomes with fixed-duration ibrutinib + venetoclax: results from the phase 3 GLOW Study in patients with previously untreated CLL

Authors: Arnon Kater, Brendan Hodkinson, Carol Moreno, Talha Munir, Mark-David Levin, Carsten Niemann, Keqin Qi, Pierre Sinet, Kurt Baeten, Donne Bennett Caces and Srimathi Srinivasan

Introduction: IGHV mutation status and specific genomic aberrations are prognostic for chemoimmunotherapy in CLL. We explored the prognostic impact on fixed-duration ibrutinib + venetoclax (Ibr + Ven) in the phase 3 GLOW study.

Methods: The GLOW study aimed to evaluate the impact of baseline (BL) genomic alterations on undetectable minimal residual disease (uMRD) at 3 months after end of treatment (EOT +3) and progression-free survival (PFS) of Ibr + Ven and Clb + O in patients (pts) with previously untreated CLL. Pts aged ≥65 or 18–64 years with cumulative illness rating scale score >6 or creatinine clearance <70 mL/min were randomized 1:1 and stratified by del(11q) and IGHV status. Pts with del(17p) or known TP53 mutation were excluded. Del(11q),

Figure. PFS outcomes within Ibr+Ven arm according to chromosomal and genetic alterations.

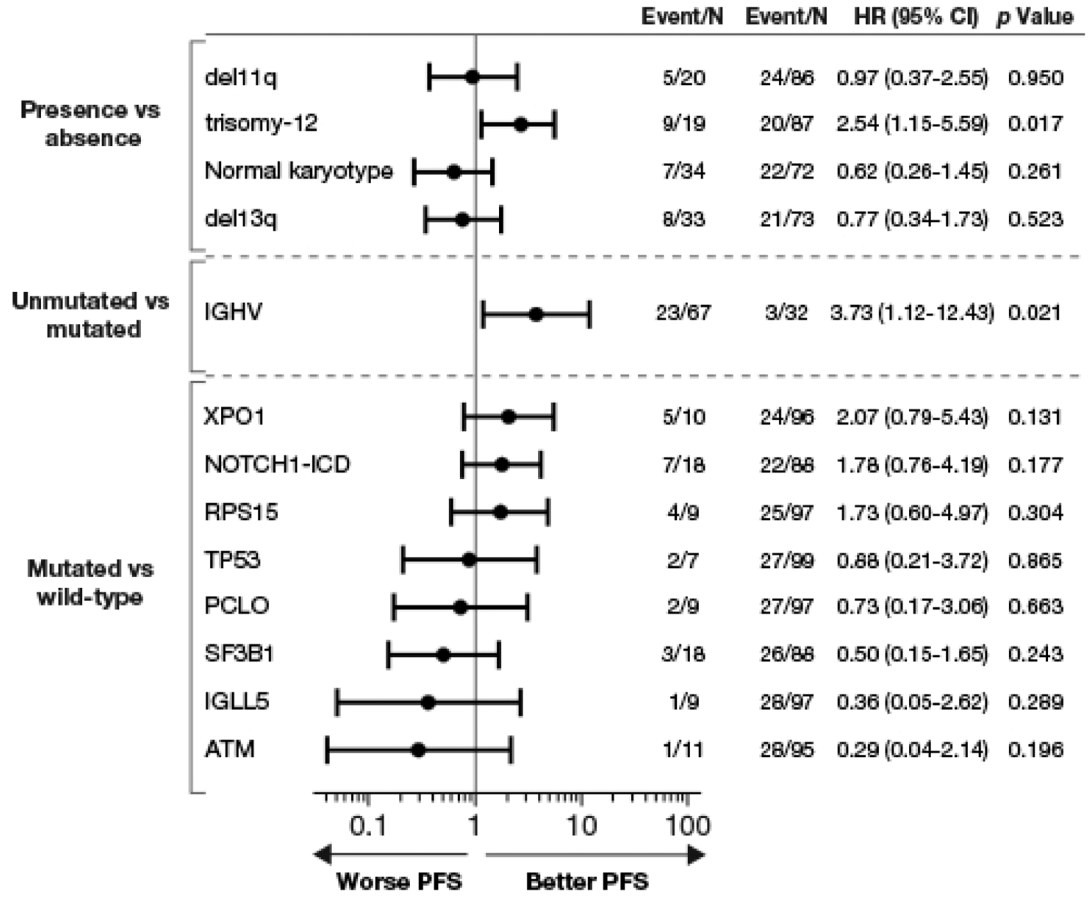

trisomy-12 (+12), and del(13q) were assessed by fluorescence in situ hybridization, IGHV mutation status by DNA-based next-generation sequencing (NGS) (98% cutoff), and exome-scale gene mutation analysis by NGS (Personalis ImmunoID NeXT), with genes ≥7% frequency, TP53, and MGA included. Cox proportional hazard models, Kaplan-Meier estimates, and log-rank tests were used to analyze time-to-event variables. Fisher's Exact test was used for association between binary variables. NGS was used to assess uMRD (< 10−4) in peripheral blood. Reported p-values are nominal.

Results: Incidences of BL genomic aberrations in both arms based on Dohner hierarchy: 18.5% del(11q), 19.4% +12, and 29.4% del(13q). IGHV was unmutated (uIGHV) in 58.8% and mutated (mIGHV) in 31.8%. Most frequent gene mutations: NOTCH1-ICD (17.5%), SF3B1 (17.5%), ATM (11.8%), XPO1 (7.1%) and RPS15 (7.1%), with TP53mut detected in 4.3%. Mutations in SF3B1, IGLL5* and del(13q) were more frequent in mIGHV, whereas NOTCH1-ICD*, ATM, XPO1*, RPS15*, TP53, MGA*, and del(11q) were more frequent in uIGHV (p<0.01 denoted by *). uMRD rates at EOT +3 were 54.7% for Ibr+Ven and 39.0% for Clb+O. For Ibr+Ven, uMRD rates trended higher in pts with del(13q) vs without (66.7 vs. 49.3%) and in uIGHV vs mIGHV (59.7 vs. 40.6%), and trended lower in pts with +12 (42.1 vs. 57.5%) or NOTCH1 (38.9 vs. 58.0%) vs without; differences were not significant (NS). For Clb+O, uMRD rates trended higher for pts with +12 (50.0 vs. 36.1%), and lower for pts with SF3B1 (26.3 vs. 41.9%) or ATM (28.6 vs. 40.7%); differences were NS. Except for +12 and IGLL5, Ibr+Ven achieved higher uMRD rates vs Clb+O across major mutations. With median follow up of 46 months, PFS was significantly improved for Ibr+Ven vs Clb+O (hazard ratio [HR], 0.214 [95% confidence interval [CI], 0.138–0.33], p<0.0001), as was overall survival (HR 0.487 [95% CI, 0.262–0.907]; nominal p=0.0205). For Ibr+Ven, +12 (HR 2.54 [CI, 1.15–5.59]) and uIGHV (HR 3.73 [CI, 1.12–12.43]) were associated with shorter PFS vs wild-type (wt) and mIGHV, respectively (Figure 1), noting both had an imbalance in non-progression-related on-treatment deaths (3/19 vs 4/87 [+12 vs wt]; 6/67 vs. 0/32 [uIGHV vs mIGHV]). PFS was significantly improved with Ibr+Ven vs Clb+O across all genomic subgroups, except +12 (HR 0.58), NOTCH1mut (HR 0.42) and IGLL5mut (HR 0.15), which favored Ibr+Ven but were NS.

Conclusion: With median follow-up of nearly 4 years in GLOW, uIGHV status and presence of +12 were associated with shorter PFS with fixed-duration Ibr+Ven in previously untreated CLL; however, imbalances in early non-progression events and small sample size may limit interpretation of findings. PFS in pts treated with Ibr+Ven was significantly improved vs Clb+O across most genomic subgroups, including mIGHV and uIGHV. Presence of +12 trended in favor of Ibr+Ven that was NS.

Abstract ID: 1553880

Title: Real-world effectiveness and safety of tixagevimab/cilgavimab lower dosage regimen in pre-exposure prophylaxis in patients undergoing treatment for chronic lymphocytic leukemia

Authors: Martin Šimkovič, Dominika Écsiová, Pavel Vodárek, Josef Malý, Lukáš Smolej and Petra Rozsívalová

Introduction: The global health crisis initiated by severe acute respiratory syndrome coronavirus 2 (SARS-CoV-2) since 2019 has predominantly affected vulnerable patient populations, including those with chronic lymphocytic leukemia (CLL) due to their advanced age, comorbidities and complex immune impairment. Low rates and duration of antibody responses to the SARS-CoV-2 vaccines have been observed mainly in older patients with hypogammaglobulinemia treated with anti-CD20 monoclonal antibodies and/or targeted oral inhibitors. Consequently, the introduction of a fixed combination of long-acting monoclonal antibodies, tixagevimab/cilgavimab (T/C) neutralising SARS-CoV-2 in pre-exposure prophylactic strategy demonstrated efficacy prior the emergence of the Omicron variant. Omicron variant pandemic surge has been associated with a milder course of COVID-19 disease and a decline in hospitalization and fatality rates in general population; however older immunocompromised patients with comorbidities still warrant prophylactic and early treatment approach. Objectives: This single-centre retrospective study aimed to examine the effectiveness and safety of T/C in prevention of SARS-CoV-2 infection mitigation of severe course of COVID-19. We included all patients with CLL fulfilling the IWCLL criteria who were undergoing CLL treatment and received T/C at approved dose 150/150 mg every 6 months at a tertiary hematology centre in the Czech Republic. Prophylactic administration was offered to all patients undergoing treatment for CLL. We performed statistical analyses with the SPSS software (version 25.0). Kaplan–Meier curves were used to evaluate time to COVID-19.

Results: A total of 81 consecutive patients on active treatment of CLL who received pre-exposure prophylaxis with T/C from April 8, 2022 to December 15, 2022 with prevailling Omicron variant were included in this study. Fourteen (17%) patients received a follow-up prophylactic dose of T/C 150/150 mg after six months from initial administration. The median age at T/C administration was 71 years (range 42–90), and 44 (54%) were men. Regarding prognostic characteristics, we observed an unmutated immunoglobulin heavy chain variable region gene (IGHV) in 57/78 (73%) patients. Del(17p) and/or TP53 mutation were detected in 20 (25 %). Full details of baseline demographic and clinical characteristics are presented in Table 1. At the median follow-up of 47 weeks,

Table 1. Patient demographics and baseline characteristics.

Total number of patients	81
Age at CLL diagnosis, median (range)	62 (37–79)
Age at tixagevimab/cilgavimab administration, median (range)	71 (42–90)
Males, *n* (%)	44 (54)
Prognostic markers	
Unmutated IGHV, *n* (%)*	57 (73)
Del(17p) and/or mutation *TP53*, *n* (%)	20 (25)
Del(11q), *n* (%)	32 (40)
Trisomy 12, *n* (%)	13 (16)
Del13q as a sole abnormality, *n* (%)	15 (19)
Complex karyotype, *n* (%)	11 (14)
Hypogammaglobulinemia, *n* (%)†	38 (52)
Obesity, *n* (%) ‡	28 (35)
CIRS score, median (range)	6 (2–14)
Major comorbidities, *n* (%)	49 (60)
SARS-CoV-2 vaccine in history, *n* (%)	73 (90)
Type of treatment for CLL at administration of tixagevimab/cilgavimab	
Idelalisib, *n* (%)	3 (4)
Chemoimmunotherapy, *n* (%)	6 (7)
Venetoclax, n (%)	32 (40)
Anti-CD20 monoclonal antibody, *n* (%)	35 (43)
BTK inhibitor, n (%)	41 (51)

*IGHV available in 78 pts; †data available in 73 pts; ‡defined as body mass index (BMI) ≥ 30. *Abbreviations*: n: number of patients; CLL: chronic lymphocytic leukemia; IGHV: immunoglobulin heavy chain variable region: TP53: tumour protein p53; BTK: Bruton tyrosine kinase

31 (38%) patients acquired SARS-CoV-2 infection despite T/C prophylactic administration. Figure 1 depicts the time to COVID-19 after the first dose of T/C. Notably, in our cohort no patients died as a result of SARS-CoV-2 infection nor were admitted to the intensive-care unit; 8 (10%) patients were hospitalized at a standard ward, and 5 (6%) patients required oxygen therapy. The majority of patients (90%) received at least one dose of anti-SARS-CoV-2 vaccine. T/C intramuscular administration was tolerated well. Only 1 (1%) patient on ibrutinib reported red skin nodules five days post T/C prophylaxis. This minor adverse event was successfully managed with topical treatment, and importantly, it did not reoccur in subsequent T/C administration.

Conclusion: Our data show that T/C 150/150 mg failed to prevent COVID-19 in about a third of patients during CLL treatment. However, most CLL patients who developed COVID-19 after prophylactic T/C had a mild infection with a low hospitalization rate. We will present updated results, including a comparison with CLL patients who did not receive prophylaxis with T/C. Additionally, we will evaluate the impact of different CLL treatment regimens on the T/C effectiveness.

Abstract ID: 1553895

Title: Significance of TP53 aberrations in context of other pathogenic sequence variants in patients with chronic lymphocytic leukemia in the era of targeted therapy

Authors: Zuzana Kubová*, Veronika Kašková*, Anna Petráčková, Peter Turcsanyi, Jiřina Maňáková, Petr Gajdoš, Vít Doleží, Tomas Papajik, Eva Kriegová and Jakub Savara

*Kubová and Kašková have contributed equally to this work.

Backround: Significant progress has been made in the treatment of chronic lymfocytic leukemia (CLL) over the past few decades. Targeted therapy replaced chemoimunotherapy in most patients. Improvement of progression-free survival (PFS) first-and other-line Bruton tyrosin kinase inhibitors (BTKi)-based therapy, even in patients with TP53 disrupted CLL, has been seen.

Aim: Analysis of the prognostic value of both isolated TP53 aberrations and in combination with other CLL associated pathogenic sequence variants (PSV) in the cohort of mostly pretreated CLL patients treated with BTKi.

Methods: We analyzed a cohort of 83 BTKi treated patients with CLL, who were treated between years 2014 and 2022 at University Hospital in Olomouc. Patients were mostly pretreated $N=77$ (93%), even 11 patients (13%) by four and more lines of therapy, 6 patients (7%) were treatment naive. Men slightly predominated, $N=49$ (59%), median of age was 67 years in range of 46–85 years. According to BTKi type, Ibrutinib was mostly used $N=73$ (88 %). We evaluated TP53 mutations by next-generation sequencing (NGS) and 17p deletions by fluorescence in situ hybridization (FISH), other PSV by both NGS and FISH according to type. As part of the analysis, we compared patients in individual subgroups, who were TP53wt (without mutation and/or 17p deletion) versus patients with TP53 aberration (with mutation and/or deletion of 17p), subsequently significance of individual type of TP53 aberrations and PFS effect of other CLL associated PSV alone and in combination with TP53 disruption.

Results: In the whole cohort of patients, 38 (46%) patients with TP53 aberration were identified. Improvement of survival has been seen in both wtTP53 and TP53 disrupted groups comparing to patients treated with chemoimmunotherapy, however longer PFS was demonstrated in patients with TP53wt ($p=0.017$). Median PFS was not reached in these patients compared to 40 months in patients with TP53 disruption. Significant effect of biallelic aberration compared to TP53wt patients was demonstrated ($p=0.012$), while in TP53 mutated patients this trend was only indicated ($p=0.086$). High proportion of other CLL PSV in TP53 disrupted subgroup were observed ($N=29$; 76 %). The most common aberrations were SF3B1 mutation and del(11q) in 32% respectively 48%. PFS impact of isolated other CLL PSV (most common NOTCH1 $p=0.870$, ATM $p=0.127$, SF3B1 $p=0.799$) was not confirmed in wtTP53 subgroup in comparison with noNOTCH resp. noATM resp. noSF3B1 together with noTP53. While PFS impact of combination of other variants (NOTCH1 $p=0.021$, ATM $p=0.002$, SF3B1 0.009) in presence of TP53 was confirmed compared to noPSV together with wtTP53. To support these results that TP53 disruption has impact only in combination of other pathogenetic sequence variants, we analyzed subgroup of patients with isolated TP53 disruption without any other most common changes compared to patient with no changes at all and we found that the difference of PFS between these two groups did not reached significance (p=0.312).

Conclusion: Despite improvement of survival in our BTKi treated cohort, negative prognostic value of TP53 aberration remained preserved. Importantly, negative effect of TP53 on PFS/OS only occurred in combination with other pathogenetic sequence variants in NOTCH1 or ATM or SF3B1 genes. Studies on larger cohorts are needed to confirm our observations.

Abstract ID: 1554121

Title: Outcomes of tixagevimab/cilgavimab pre-exposure prophylaxis in chronic lymphocytic leukemia patients- a single center experience

Authors: Pratik Shah, Iris Li, Kanti R. Rai, Jacqueline Barrientos and Joanna Rhodes

Introduction: Patients with CLL have an increased susceptibility to infections secondary to complex immune interactions, innate immunity dysfunction, and with treatment with immunosuppressants. This leads to infections accounting for the majority (60%) of deaths in CLL [1]. Recently, SARS-CoV-2, the virus, which causes COVID-19 infection has been an infectious etiology of concern. Development of tixagevimib/cilgavamib shows in vitro neutralizing capacity against the omicron variant in addition to earlier SARS-CoV-2 strains (alpha, beta, gamma, and delta) [2]. Tixagevimib/cilgavamib, a combination of two long-acting antibodies, was authorized for emergency use for pre-exposure prophylaxis of SARS-CoV-2 infection in moderate to severely immunocompromised patients by the FDA from December 2021 to January 2023 [3]. CLL patients were not studied specifically in the pivotal clinical trials, and tixagevimib/cilgavamib, so the CLL-specific outcomes are not well described.

Methods: We conducted a single institution, IRB approved, retrospective study evaluating tixagevimab/cilgavimab administration for use of pre-exposure prophylaxis in patients

with confirmed CLL treated at our institution prior to January 2023. We aimed to observe SARS-CoV-2 infection rates in primary series vaccinated (BNT162b2,mRNA1273, and AD26.COV2.S) CLL patients and infection rates in patients post tixagevimab/cilgavimab.

Results: We identified 90 CLL patients vaccinated with the primary SARS-CoV-2 series at our institution who were included in this retrospective review. 23/90 (25.6%) patients had one bout of SARS-CoV-2 infection with 21 patients having mild infections (treated in the ambulatory setting), 1 patient with moderate disease (requiring supplemental oxygen and hospitalization), and 1 patient with severe disease (requiring ICU stay). Of these patients 27/90 (30%) were administered Tixagevimab/cilgavimab prior to Jan 2023. Of the patients that were administered Tixagevimab/cilgavimab, 3/27 (11.1%) patients had one bout of SARS-CoV-2 infection post-administration, all of whom were classified as having mild disease. Of note, these patients that were infected post-administration did receive treatment with monoclonal antibodies. 4/27 of the patients administered Tixagevimab/cilgavimab had SARS-CoV-2 prior to and did not have any documented infections post administration. Of the 3 patients with documented post administration SARS-CoV-2 infections 2 patients also had a documented SARS-CoV-2 infection prior to administration.

Conclusions: Tixagevimab/cilgavimab has been part of the advances in SARS-CoV-2 pre-exposure prophylaxis for immunocompromised patients including CLL patients. As our data suggests we have observed a general trend towards decreased rates of infections in patients that were treated with tixagevimab/cilgavimab. In addition, it appeared that even for patients that were infected post administration of tixagevimab/cilgavimab, 2/3 of those patients had a documented SARS-CoV-2 infection prior to administration as well. As of January 2023 the FDA revised the recommendation regarding tixagevimab/cilgavimab use given that it appeared that the majority of current SARS-CoV-2 strains in the community are not susceptible to tixagevimab/cilgavimab. While tixagevimab/cilgavimab is not currently approved for use given its lack of efficacy to current strains, previous RCTs and the data that we have observed in our study does appear to indicate that a pre-exposure prophylaxis strategy may be beneficial in CLL patients, and warrants continue exploration in clinical studies [3].

Abstract ID: 1554137

Title: A retrospective study evaluating the sequence of BTKi and venetoclax, with a focus on toxicity

Authors: Zachary Arnold, Jordan Lundberg, Lindsay Rosen, Seema Bhat, Kerry Rogers, Michael Grever, Jennifer Woyach, Eric McLaughlin and Adam Kittai

Introduction: The Bruton's Tyrosine Kinase inhibitors (BTKi), ibrutinib, acalabrutinib, and zanubrutinib, and the BCL2 inhibitor (BCL2i), venetoclax (VEN), are FDA approved, and considered standard of care for the treatment of treatment-naïve (TN) and relapsed/refractory (R/R) chronic lymphocytic leukemia (CLL)/small lymphocytic lymphoma (SLL). Although the current treatment paradigm promotes the use of BTKi followed by BCL2i or vice versa, data behind the efficacy of this sequence is limited to real-world retrospective studies. As such, safety of second line BCL2i or BTKi after front-line BCL2i or BTKi has not been well-studied.

Methods: We performed a single-center, retrospective cohort study to evaluate therapy-related toxicities in patients who received venetoclax after BTKi for the treatment of CLL/SLL. We aimed to also evaluate and compare efficacy/safety of patients who received BTKi after venetoclax, but we had an insufficient number of patients. Clinical data was collected for adult patients who received treatment for CLL/SLL with a BTKi then venetoclax between 31 December 2009 and 20 October 2022. We assessed toxicities by assessing grade 3 or higher toxicities, dose reductions, and treatment discontinuations. Efficacy was assessed by determining progression-free survival (PFS), and overall survival (OS). Descriptive statistics were used to summarize safety data. Survival outcomes were estimated using Kaplan–Meier methods from the initiation date of venetoclax. Results We identified 215 patients treated with a BTKi and venetoclax in the electronic medical record. 60 patients were included in the final analysis, having received a BTKi then venetoclax in sequence. The study population was comprised of primarily white ($n=56$, 93.3%) males ($n=40$, 66.7%) with a median age of 58 years (range: 40–81) at diagnosis. 15 patients (25%) were treated with a BTKi then venetoclax for TN disease, and 45 patients (75%) were treated with this sequence for R/R disease. Median prior lines of therapy were 2 (range: 0–9) for the entire cohort, and 3 (range: 1–9) for patients who had R/R disease. 45 patients (75%) received venetoclax without concurrent anti-CD20 monoclonal antibody therapy. With a median exposure to therapy of 15 months (range: 1–48), patients experienced a grade 3 or higher toxicity rate of 76.7%. The most common grade 3 or higher toxicity was neutropenia, which occurred in 31 patients (54.4%), followed by thrombocytopenia in 19 patients (32.2%). Tumor lysis syndrome (TLS) occurred in 9 patients (15%), in which 4 patients (6.7%) experienced clinical TLS. The high rate of TLS may be related to high baseline TLS risk or dose escalation over a shorter timeframe than the licensed schedule in CLL, however, these variables were not collected. Venetoclax dose reduction occurred in 13 patients (22.8%) and seven patients (11.7%) discontinued venetoclax secondary to adverse drug events. After a median follow-up of 23 months (range: 1–91), utilizing the initiation date of venetoclax, median PFS was 31.9 months (95% CI, 20.2–40.3) and median OS was 44.8 months (95% CI, 31.9–Not reached (NR)). Patients that were TN prior to the BTKi/VEN sequence had a median PFS of 59.0 months (95% CI, 8.1–NR) and a median OS of NR (95% CI, 16.7–NR). Patients who were R/R prior to the BTKi/VEN sequence had a median PFS of 27.3 months (95% CI, 19.4–39.6) and a median OS of 36.9 months (95% CI, 31.8–NR) (Figure 1).

Conclusion: In this real-world retrospective cohort study of patients with R/R CLL/SLL who received treatment with a BTKi then venetoclax, the rate of grade 3 or higher toxicities during venetoclax therapy was similar to previously published clinical trials [1]. The current study adds real-world survival data with a median PFS that compares similarly with clinical trial data from the MURANO trial, which demonstrated a four-year PFS estimate of 57.3% [2] and a trial by Jones JA, et al., demonstrating a median PFS of 24.7 months [3] in a largely R/R population who received the BTKi/VEN sequence. Additionally, due to recent publications supporting the use of a BTKi plus venetoclax, future retrospective studies comparing the sequence of BTKi then venetoclax with BTKi plus venetoclax are warranted.

Figure 1. (A) Progression-free and overall survival for patients who were treatment naïve prior to BTKi/VEN. (B) Progression-free and overall survival for patients who were relapsed/refractory prior to BTKi/VEN

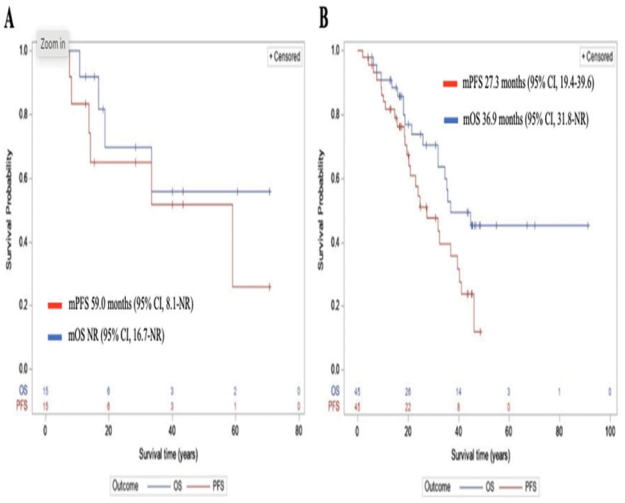

Abstract ID: 1554253

Title: LYN kinase programs stromal fibroblasts to facilitate leukemic survival via regulation of c-JUN and THBS1

Authors: Alexander vom Stein, Rocio Rebollido-Rios, Anton von Lom, Daniel Bachurski, France Rose, Katarzyna Bozek, Ali Abdallah, Viktoria Kohlhas, Björn Häupl, Thomas Oellerich, Phuong-Hien Nguyen and Michael Hallek

Non-hematopoietic stromal cells of the tumor microenvironment (TME) are increasingly recognized for facilitating disease progression and resistance to therapy in various lymphomas. In CLL, these stromal cells have an activated phenotype allowing for the diverse support of leukemic cells, e.g. via cytokines and direct cell contact. Here we demonstrate that an increased expression of LYN kinase in stromal cells of the CLL-TME stimulates their leukemia-promoting polarization and thus supports leukemic progression: We previously discovered that LYN kinase promotes the formation of a supportive leukemic niche. ImagingMassCytomety analysis of primary CLL lymph node samples revealed a significantly increased expression of LYN kinase especially within fibroblasts in the leukemic microenvironment. The absence of LYN in non-hematopoietic stromal cells consistently reduced leukemic expansion *in vivo*, and LYN-deficient fibroblasts showed reduced leukemic support in vitro. This indicated a CLL-supportive function for LYN kinase expression in stromal fibroblasts. A multi-omic characterization of the LYN-deficient fibroblasts revealed an extensive transcriptional reprogramming, affecting predominantly inflammation-, cytokine- and extracellular matrix-related cellular signatures. Combined, these changes indicated a reduced 'CAF-like' activation of fibroblasts upon LYN depletion, which could be validated on primary pancreatic cancer specimens. In particular, the perturbated extracellular matrix deposition was shown to decrease viability in CLL coculture experiments. Specifically, increased THBS1 expression impaired CLL cell viability via ligation to CD47. Mechanistically, epigenetic analyses identified a reduced c-Jun expression following LYN deficiency, leading to the transcriptional reprogramming with reduced inflammatory signaling and disinhibition of THBS1 expression. Lastly, we could demonstrate that the stromal reprogramming also affected interaction with other components of the TME: CD4+ and CD8+ T cells cultured in vitro with LYN-deficient fibroblasts showed a reduced activation and modulated exhaustion marker expression, indicating a change in stromal immunomodulatory capacity. All in all, this works highlights the role of stromal LYN kinase expression for induction of a 'CAF-like', leukemia supportive transcriptional reprogramming in stromal fibroblasts. By regulating transcription factors like c-Jun, LYN kinase governs inflammatory signatures and extracellular matrix deposition in fibroblasts. LYN deficiency reduces c-Jun levels and disinhibits THBS1 expression, inducing CLL cell apoptosis.

Abstract ID: 1554425

Title: Concomitant use of venetoclax 100 mg and ketoconazole to treat CLL in a public center in Brazil

Authors: Fernanda Marques, Verena Pfister, Pedro Fernandes, Vinicius Molla, Mihoko Yamamoto, Matheus Gonçalves and Celso Arrais-Rodrigues

Introduction: Venetoclax, a potent and selective B-cell lymphoma 2 (BCL-2) inhibitor, has demonstrated substantial efficacy as a monotherapy and in combination with other agents in the treatment of chronic lymphocytic leukemia (CLL). Its use has led to high response rates, durable remissions, and long survival, both in treatment-naive and relapsed/refractory CLL patients. However, the metabolism of venetoclax primarily relies on the cytochrome P450 enzyme CYP3A4, which can be influenced by concurrent administration of strong CYP3A4 inhibitors, including ketoconazole, itraconazole, clarithromycin, and ritonavir. These drugs have the potential to interact with venetoclax by inhibiting its metabolism resulting in elevated venetoclax plasma concentrations, increasing the risk of adverse events, particularly tumor lysis syndrome. Consequently, dose adjustments of venetoclax are necessary when coadministering with these inhibitors. Venetoclax availability in the public setting in Brazil is currently limited, with irregular donations being the only possible source. Therefore, we have made the decision to utilize the strong CYP3A4 inhibitor ketoconazole to save venetoclax tablets in an effort to maximize treatment opportunities for as many patients as possible. Objective: The objective of this analysis was to evaluate the efficacy and safety of the combination therapy of ketoconazole, low-dose venetoclax, and rituximab in the treatment of patients with chronic lymphocytic leukemia (CLL).
Methods: Patients received venetoclax starting on day 22 of cycle 1, with a 5-week dose ramp-up (20, 50, 100, and 200 mg). Subsequently, they received venetoclax 100 mg in combination with ketoconazole 200 mg daily until completion of cycle 12 (for patients in the first line of treatment) or cycle 24 (for patients in further treatment lines). Intravenous rituximab was also administered for six cycles, 375 mg/m^2 in cycle 1 and 500 mg/m^2 in cycles 2–6. All patients included in

the analysis had received a minimum of 6 months of treatment at the time of data collection.

Results: A total of 21 treatment regimens for 18 patients were included in this analysis. The median duration of venetoclax treatment was 12 months, ranging from 6 to 24 months. Six patients (29%) received the treatment as a first-line therapy, 5 (24%) as a second-line therapy, 8 (38%) as a third-line therapy, and the remaining patients received it in further lines of treatment. The overall response rate was 100%, with 14 treatments leading to a complete response and 7 treatments to a partial response. Among the partial responders, 4 patients are still receiving treatment, and 2 patients completed six months of treatment and were referred to an allogeneic stem cell transplantation. The most common grade 3 or 4 adverse event observed was neutropenia, which occurred in 12 treatments. Notably, no cases of grade 2 or higher hepatic toxicity related to ketoconazole were reported. Additionally, there were no treatment-related deaths observed in the study. At a median follow-up of 19 months (range: 6–33), the median progression-free survival (PFS) has not been reached, and the PFS at 24 months was 83%. Three cases of disease progression occurred after 26, 30, and 39 months of treatment. All three patients were successfully retreated with the same treatment combination and achieved at least a partial response again. The median overall survival (OS) has not been reached, and the OS at 24 months was 95%. Three deaths were recorded during the study period: one patient died from acute myelogenous leukemia, one patient from a myocardial infarction, and one patient due to an unrelated intestinal bleeding.

Conclusions: Our data indicate that the combination of ketoconazole, low-dose venetoclax, and rituximab showed favorable tolerability and promising effectiveness in patients with CLL. This treatment approach could serve as a valuable alternative for patients in regions with restricted availability of targeted therapies. Further studies and larger-scale investigations are warranted to confirm these observations and validate the potential benefits of this combination regimen in the management of CLL in similar settings.

Abstract ID: 1554470

Title: Unveiling the role of Siglec-6 in regulating b cell functions: implications for chronic lymphocytic leukemia therapeutics

Authors: Natarajan Muthusamy, Jessica Nunes, Rakeb Tafesse, Elizabeth Perry, Xioakui Mo, Meixiao Long and Christoph Rader

B cell Chronic lymphocytic leukemia (B-CLL) is a malignancy of CD5+CD23+CD19+ B lymphocytes. It is the most prevalent adult leukemia in the western world, accounting for more than 4000 deaths in the United States every year. It is characterized by activated B cell receptor (BCR) signaling that in turn promotes several downstream cell survival pathways and migration to pro-survival niches such as the bone marrow, lymph nodes and spleen tumor microenvironment (TME). The only curative therapy for CLL is allogeneic hematopoietic stem cell transplantation, which is associated with undesirable risks for the elderly patients. BCR signaling inhibitors are effective agents for CLL treatment, but therapeutic resistance and relapse remain problematic, necessitating the identification of new CLL targets that can bypass current disease resistance. Sialic-acid-binding immunoglobulin-like lectins (Siglecs) are a family of cell surface glycoproteins that were shown to play a role in tumor immunosurveillance and immunosuppression, thereby making them attractive anti-cancer targets. Our study focuses on evaluating a novel Siglec member, Siglec-6, which was recently found to be upregulated on B cells from CLL patients but not on healthy donor B cells. To study the biological role of Siglec-6, we generated a novel human (hu) Siglec-6 transgenic mouse model that expresses huSiglec-6 on B cells. We observed a selective decrease in antigen specific immunoglobulin responses in response to T independent and T dependent antigens in the huSiglec-6 mice. Interestingly, decreased proliferation of B cells in response to B cell activation was observed in huSiglec-6 mice, pointing to a role for Siglec-6 as a negative regulator of B cell immune response and proliferation. The molecular signals that direct B-CLL trafficking to the TME is an ongoing field of study, and interfering with B-CLL cell migration to or adhesion within these organs serves to target and eliminate survival of B-CLL cells. We show for the first time that CLL patient derived bone marrow stromal cells (BMSCs) express the ligand of Siglec-6, sialyl Tn (sTn). Mass spectrometry analysis revealed interaction of Siglec-6 with DOCK8, a guanine nucleotide exchange factor. We utilized the CRISPR-Cas9 system to generate novel MEC1-002 Siglec-6 and DOCK8 knock-out cell lines to explore the signaling pathways involved in Siglec-6 functions. Genetic ablation or antibody blocking revealed a novel role for Siglec-6 in migration and adhesion of B-CLL cells to CLL-BMSCs in vitro and compromised migration to bone marrow and spleen in vivo. Stimulation of MEC1-002 CLL cells with sTn resulted in Cdc42 activation, WASP protein recruitment and F-actin polymerization, which are all associated with cell migration. To evaluate the therapeutic potential of Siglec-6, we crossed our huSiglec-6 transgenic mouse model with the TCL1 CLL mouse model to obtain Siglec-6 x TCL1 mice which develop Siglec-6+ leukemia. An immunocompetent mouse model using humanized CD3 mice engrafted with Siglec-6+ leukemia showed improved overall survival when treated with a huSiglec-6/huCD3-bispecific T-cell-recruiting antibody (T-biAb). This T-biAb also induced rapid killing of CLL cells in a CLL patient-derived xenograft model. Taken together, our studies uncover a novel role for Siglec-6 in regulating the BCR signaling pathway, proliferation of B cells, and homing of B-CLL cells to pro-survival niches. As therapies that target Siglecs become more common for the treatment of various types of cancer, our need to understand the biological role of these Siglecs and our search for new drug targets intensify. Our ability to adapt current treatment regimens to newly discovered targets is paramount to effective treatment of CLL patients, and understanding how these new disease targets regulate CLL function is thus a driving factor in taking these therapies to clinical trials. Our findings thus suggest that Siglec-6 is an effective therapeutic target for the treatment of CLL patients and warrants further exploration into the exact mechanism by which Siglec-6+ CLL cells interact with the TME, and the biological role of Siglec-6 in other leukemias.

Abstract ID: 1554484

Title: Prognosis analysis and validation of fatty acid metabolism-related signature in chronic lymphocytic leukemia

Authors: Bihui Pan, Zhangdi Xu, Kaixin Du, Jiale Zhang, Li Wang, Jianyong Li, Jiazhu Wu and Wei Xu

Background: Chronic lymphocytic leukemia (CLL) is the most common leukemia in the western world. Although the treatment landscape for CLL is rapidly evolving, there are still part of patients develop disease refractory and relapse, which shows CLL's heterogeneity. Therefore, it is important to distinguish high-risk patients from CLL population during the early stage of the disease and apply a more suitable treatment strategy. Fatty acid (FA) metabolism contributes to tumorigenesis, progression, and therapy resistance through enhanced lipid synthesis, storage, and catabolism. In this study, we aimed to construct a prognostic model to improve the risk stratification of CLL and reveal the link between FA metabolism and CLL.

Methods: The differentially expressed fatty acid metabolism-related genes (FMGs) in CLL were filtered through univariate Cox regression analysis based on public databases. Patients in the cohort are divided into 2 clusters. Enrichment analysis of prognostic fatty acid (FA) metabolism-related genes was performed to explore functional enrichment. CIBERSORT and single-sample gene set enrichment analysis (ssGSEA) were performed to estimate the immune infiltration score and immune-related pathways. Besides, the least absolute shrinkage and selection operator (LASSO) Cox algorithms were carried out to establish a novel prognostic model.

Results: We obtained CLL RNA microarray profiles from public database and identified 15 prognostic-related FMGs. CLL patients were divided into two molecular clusters based on the expression of FMGs. The Kaplan–Meier analysis showed that patients in Cluster 1 had statistically significant worse TFS ($p<0.001$) and OS ($p<0.001$). KEGG functional analysis showed that several pathways, including the chemokine signaling pathway, IL-17 signaling pathway, NF-κB signaling pathway, PD-L1expression and PD-1 checkpoint pathway in cancer, and T cell receptor signaling pathway were enriched. Then, we conducted LASSO Cox regression analysis to establish the FA metabolism-related prognostic index (FAPI), exhibiting similar prognostic significance. Finally, a novel nomogram prognostic model including CLL-IPI was constructed, exhibiting reliable effectiveness and accuracy.

Conclusion: In conclusion, we established a reliable predictive signature based on FA metabolism-related genes and constructed a novel nomogram prognostic model, supporting the potential preclinical implications of FA metabolism in CLL research.

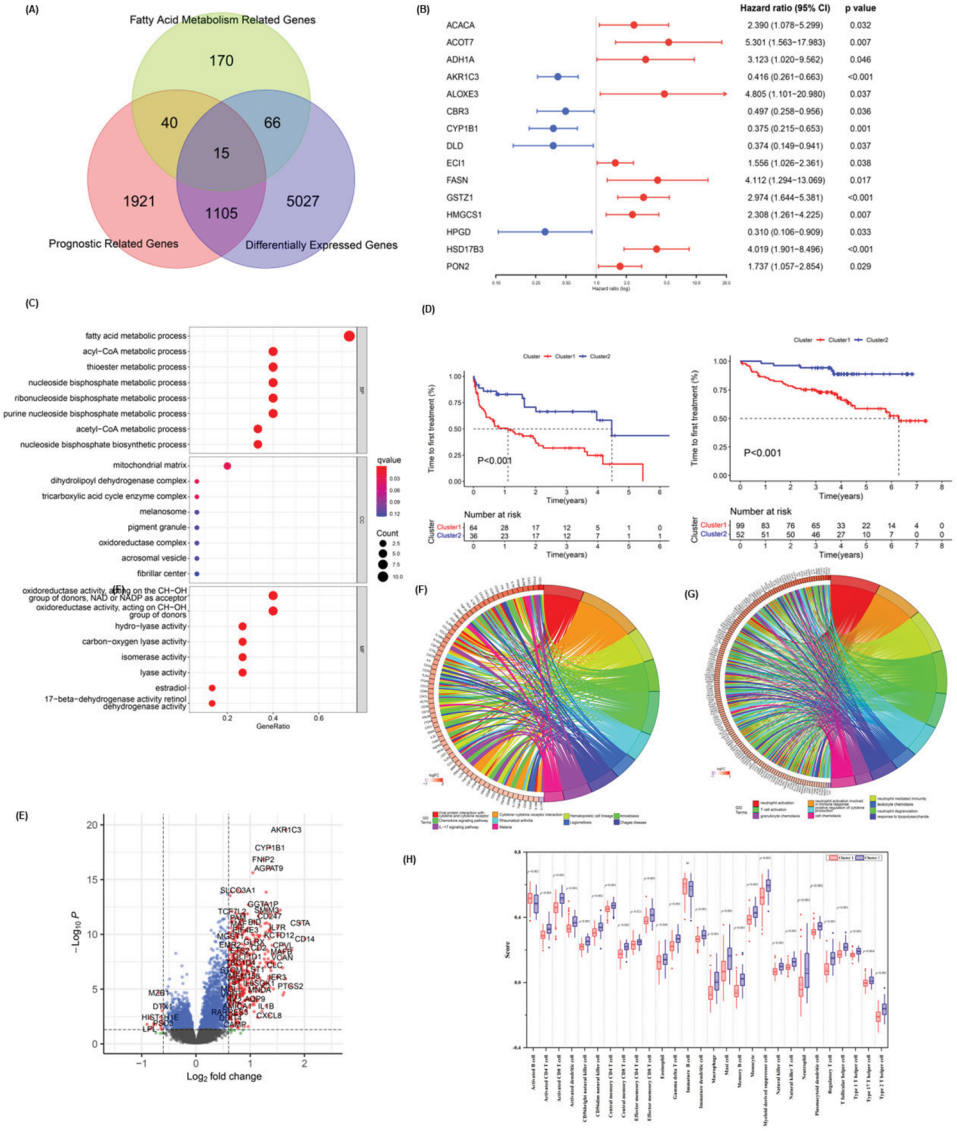

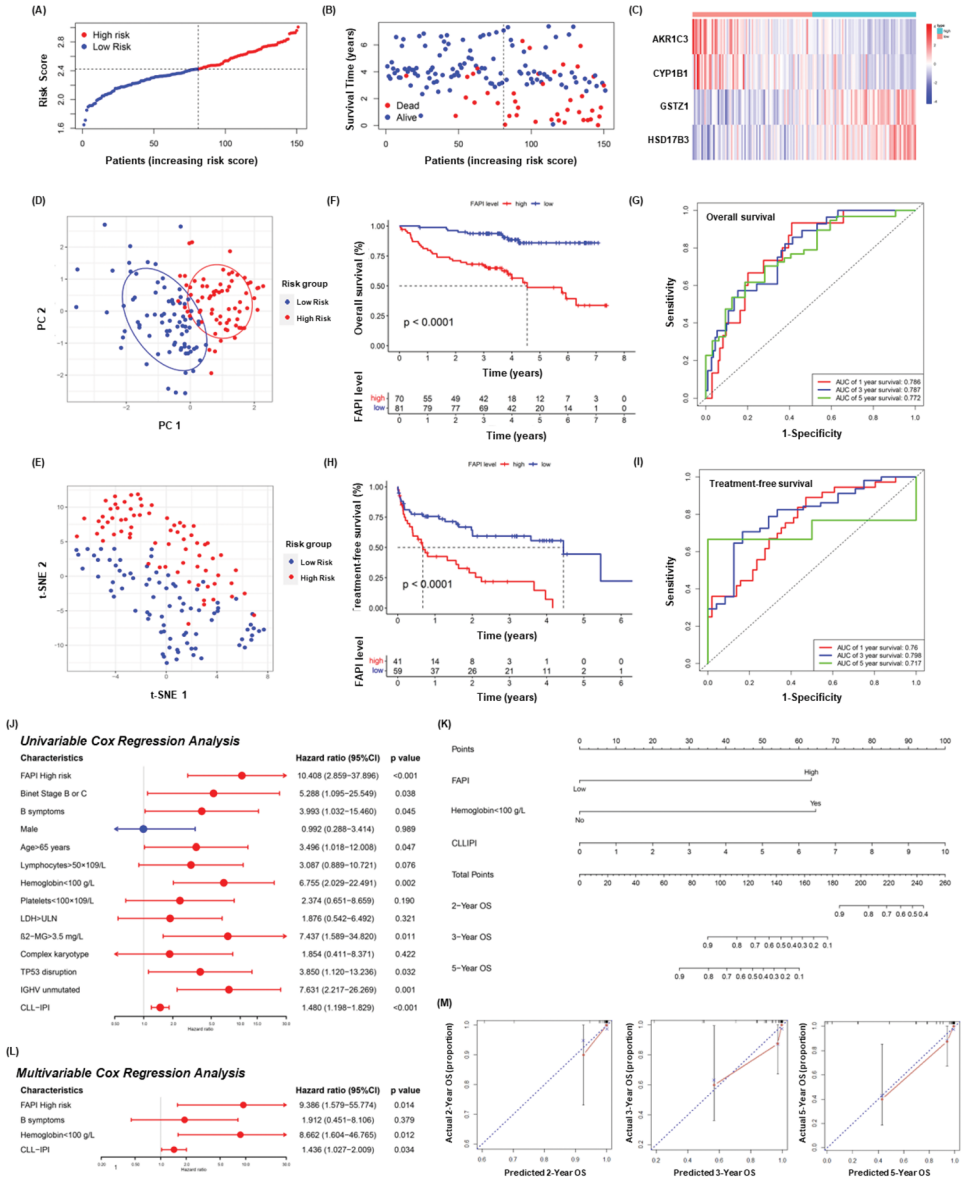

Abstract ID: 1554496

Title: SH2-Flow: a multiplex single cell phosphotyrosine profiling tool for B-cell malignancies

Authors: Kazuya Machida, Evan Jellison, Bruce Mayer and Ji Yu

Introduction: Aberrant activation of tyrosine kinases leads to oncogenic cell signaling, causing cancer cell proliferation, invasion, and metastasis; targeted tyrosine kinase inhibitors of the B cell receptor (BCR) pathway, particularly BTK inhibitors, have shown promising clinical results in chronic lymphocytic leukemia (CLL) and non-Hodgkin's lymphoma. However, resistance to BTK inhibitors, possibly due to de novo mutations in BCR signaling molecules, and relapse after long-term therapy are problems in clinical practice. Therefore, it is important to monitor changes in pathogenic signaling pathways before, during, and after chemotherapy throughout disease progression. There are many prognostic and therapeutic markers based on gene mutations and protein expression, some of which have been successfully incorporated into clinical practice. However, BCR signaling markers that directly reflect the activation status of signaling pathways have not yet been established. We previously developed SH2 profiling to detect changes in the global tyrosine phosphorylation state of cancer cells using the SH2 domain, a major pTyr-binding module, as a probe. We hypothesized that the phosphotyrosine phosphorylation profile measured by SH2 profiling is a promising tool for monitoring the BCR pathway in B-cell malignancies. The primary goal of current study is to develop a clinically adoptable single-cell phosphotyrosine-SH2 profiling assay platform integrating advanced flow cytometry technologies. The new assays (termed SH2-Flow) is multiplexed, largely automated, and optimized for detecting SH2–pTyr interactions in B-cell malignancy cells at the single cell level.

Results: First, we established a flow cytometry-compatible 'BCR-SH2 panel' containing 36 SH2 domains involved in BCR signal regulation (Table 1). The probe protein consists of an N-terminal GST and a C-terminal Halo-His tag, which can be conjugated with a fluorescent dye. Global measurements of protein expression and solubility showed that the majority of

#	SH2	Gene symbol	Gene ID	Protein function
1	GST-Halo	n/a	n/a	Control
2	Arg	ABL2	27	Tyrosine kinase
3	Blk	BLK	640	Tyrosine kinase
4	Blnk	BLNK	29760	Adaptor
5	BRDG1	STAP1	26228	Adaptor
6	Btk	BTK	695	Tyrosine kinase
7	CblA	CBL	867	Ubiquitin ligases
8	Crk	CRK	1398	Adaptor
9	CrkL	CRKL	1399	Adaptor
10	Csk	CSK	1445	Tyrosine kinase
11	Eat2	SH2D1B	117157	Adaptor
12	FynA	FYN	2534	Tyrosine kinase
13	Grb2	GRB2	2885	Adaptor
14	Grb7	GRB7	2886	Adaptor
15	Hck	HCK	3055	Tyrosine kinase
16	Lck	LCK	3932	Tyrosine kinase
17	Lyn	LYN	4067	Tyrosine kinase
18	Nck1	NCK1	4690	Adaptor
19	Nck2	NCK2	8440	Adaptor
20	p85a	PIK3R1	5295	Phosphoinositide kinase
21	PLCg1	PLCG1	5335	Phospholipase
22	PLCg2	PLCG2	5336	Phospholipase
23	RasGAP	RASA1	5921	GTPase activating protein
24	SH3BP2	SH3BP2	6452	Adaptor
25	ShcA	SHC1	6464	Adaptor
26	SHIP1	INPP5D	3635	Inositol phosphatase
27	SHIP2	INPPL	3636	Inositol phosphatase
28	SHP-1	PTPN6	5777	Tyrosine phosphatase
29	SHP-2	PTPN11	5781	Tyrosine phosphatase
30	Stat1	STAT1	6772	Transcription factor
31	STAT5B	STAT5B	6777	Transcription factor
32	Syk	SYK	6850	Tyrosine kinase
33	Tec	TEC	7006	Tyrosine kinase
34	Vav1	VAV1	7409	Guanine nucleotide exchange factor
35	Vav2	VAV2	7410	Guanine nucleotide exchange factor
36	Vav3	VAV3	10451	Guanine nucleotide exchange factor
37	Zap70	ZAP70	7535	Tyrosine kinase

	Marker		CD45 Barcode				SH2			
Dye	APC	PerCP Cy5.5	BV510	PECy7	APC H7	BV605	AF488	R6G	AF700	AF405
Group	CD19	CD20	CD45	CD45	CD45	CD45	SH2-1	SH2-2	SH2-3	SH2-4
A	X	X	X				3BP2	Arg	BLNK	Blk
B	X	X	X	X			BTK	CrkL	CSK	EAT2
C	X	X	X	X	X		Grb7	GH	Grb2	Fyn
D	X	X	X	X	X	X	Lck	Lyn	Nck2	p85a
E	X	X	X		X		PLCg1	GAP	SHIP2	SHP-2
F	X	X	X			X	ZAP70	Syk	Vav2	STAT5B

proteins are expressed in soluble form. PTyr-binding activity was confirmed by an established quantitative dot-blot assay using stimulated and unstimulated cancer cells. Purified domains were conjugated to fluorescent dyes with various emission spectra by on-column labeling or direct lysate labeling. Labeling efficiency and binding activity of the labeled SH2 domains were assessed by cell staining using SDS gels and fluorescent imagers. Two assay formats were developed to perform a multiplex SH2 flow cytometry assay that can easily detect SH2 binding to cell lines and peripheral blood mononuclear cells (PBMCs) with low background. The 4-plex assay was used for analysis of three time points of CLL PBMC samples (pretreatment, short-term treatment and long-term treatment) showing both probe-specific and sample-specific binding patterns; the 24-plex assay employs a barcoding strategy with CD47 antibodies (Figure 1). Using this method, we analyzed four PBMC samples from four CLL patients with various clinical characteristics which indicates the presence of different SH2 domain binding sites in the CLL cells.

Conclusions: We have established a dye-labeled BCR-SH2 panel that can be used for flow cytometry as well as imaging and other SH2 profiling assays. The 4-plex and 24-plex assay formats have been developed, allowing the versatile application of SH2 profiling in research and diagnosis. Preliminary analyses using CLL PBMC have shown that SH2-Flow has the sensitivity and specificity to select patient subgroups that reflect differences in treatment status and clinical course. Efforts are currently underway to further evaluate the value of SH2-Flow in profiling a CLL cohort, which may lead to the discovery of new biomarkers based on signaling status.

Abstract ID: 1554519

Title: Impact of T-cell co-stimulatory molecule CLECL1 expressing CLL cells on CLL disease progression and transformation to Richter's syndrome

Authors: Shih-Shih Chen, Xiao Jie Yan, Martina Cardillo, Anita Ng, Gonzalo Blanco Ares, Morgan King-Richards, YuJu Chen, Yasmine Kieso and Nicholas Chiorazzi

Disease progression of chronic lymphocytic leukemia (CLL) is highly dependent on elements in secondary lymphoid tissues. In these niches, stromal cells produce chemokines to recruit T cells and CLL cells, and their crosstalk produces factors such as IL-4 that promote tumor survival and growth. CLECL1 (C-type lectin-like protein 1) is a T-cell costimulatory molecule that instructs T cells to produce IL-4. We found CLECL1 expression on the surface of CLL cells. Importantly, CLECL1+ but not CLECL1− cells express AID, an enzyme that drives aberrant somatic hypermutation associated with Richter's transformation. While the level of CLECL1 is associated with first time to treatment in CLL, patients with Richter's and accelerated CLL have significantly higher levels of membrane CLECL1. Thus, here we investigated the role of CLECL1 in CLL and Richter's transformation. Bulk RNAseq analyses of CLL cells suggest that the expression of CLECL1 correlates with IL-4-related gene expression and associates with genes expressed in G2/M. Indeed, flow cytometry analyses confirm that CLECL1+ cells are mainly in the G2/M phase of the cell cycle, whereas CLECL1− cells are chiefly in G1/S or undergoing apoptosis. CLECL1+ CLL cells are more activated, expressing higher levels of cell interaction molecules and activation markers, consistent with CLECL1+ CLL cells being generated from CLECL1− cells. Indeed, in vitro stimulation of CLECL1− cells with anti-IgM+IL-4 converts CLECL1− to CLECL1+ cells. Similar results were also seen when CLECL1− cells are stimulated with soluble anti-CD3 antibody activated autologous T cells; however, T-cell induced CLECL1 expression is only seen in U-CLL but not in M-CLL patients, emphasizing a role of CLECL1 in more aggressive CLL. Immunohistochemistry staining of patient lymph nodes shows co-localization of CLECL1+ B cells, Ki67-expressing cells, and T cells. Thus, we investigated the function of CLECL1 in T-cell growth and cytokine production. We first identified direct binding of recombinant CLECL1 (rCLECL1) protein to both naïve (Tn) and memory (Tmem) T cells in CLL patients. When Tn and Tmem cells were incubated with rCLECL1, both subsets responded with enhanced proliferation and IL-4 production. Similar results were seen when we cocultured CLECL1+ but not CLECL1− CLL B cells with unseparated T cells or each subset of T cells. When the same experiment was carried out with samples taken from two CLL patients before and after transformation into Richter's syndrome, we found significant better ability of CLECL1+ Richter's patient cells to induce IL-4 production but not the proliferation of T cells, compared to their counterparts at the CLL stage. To mimic tissue niches, this experiment was repeated in the presence of lymph node stromal cells obtained from normal donors. Interestingly, both CLL and Richter's cells attached to stromal cells and reduced CXCR4 expression, potentially in response to CXCL12 chemokines produced by lymphatic stromal cells. Importantly, we also observed enhanced CLECL1 expression in malignant B cells co-cultured with stromal cells; these B cells were also better at inducing IL-4 producing T cells. Finally, to see the key function of CLECL1 in CLL B cells, we sorted CLECL1+ and CLECL1− populations from MEC-1, OSU and RAJI cells line, and cultured these cells separately for 3 days. We found significantly better growth of the CLECL1+ than CLECL1- fractions in all three cell lines, supporting the findings that CLECL1 levels is associated with the activation and survival of B cells. To further understand whether separating out CLECL1 expressing cells can achieve better clinical outcome in vivo, we used patient derived xenografts. Injection of NSG mice with autologous CD3+ T cells plus CLECL1− PF cells led to significantly reduced numbers of CLL B and T cells in the spleens of recipient mice. In this model, Th2 cells outgrew Th1 T cells, and removing CLECL1−expressing cells significantly reduced the number of Th2 T cells in the spleens. We are currently repeating this experiment in Richter's patients. Overall, this study suggests that CLECL1−expressing CLL cells are a key subset that drives CLL survival and proliferation and shapes a Th2-biased tumor microenvironment, although whether the CLECL1+ fraction is the source of Richter's transformation remains elucidated. Overall, these results strongly suggest that CLECL1+ cells in the PF of CLL clones are potentially key targets for therapy.

Abstract ID: 1550344

Title: NX-2127 and NX-5948, two clinical stage cereblon-recruiting BTK degraders, facilitate T-cell functionality in CLL

Authors: Tiana Huynh, Sonia Rodriguez-Rodriguez, Carly Roleder, Janine Powers and Alexey Danilov

Introduction: Inhibitors targeting Bruton's tyrosine kinase (BTK) altered the treatment paradigm in chronic lymphocytic leukemia (CLL). In addition to direct anti-neoplastic effects, BTK inhibitors ibrutinib and acalabrutinib were found to favorably modulate T-cell function in pre-clinical and clinical studies of CLL. Specifically, treatment with ibrutinib down modulated expression of T-cell exhaustion markers, shifted T-cell polarization towards a pro-inflammatory TH1 phenotype, and improved overall T-cell number and repertoire diversity. However, resistance to BTK inhibitors eventually occurs due to the development of mutations in BTK. As a result, Targeted Protein Degradation has emerged as a strategy to circumvent acquired resistance to BTK inhibition. The compounds NX-2127 and NX-5948 were designed to induce BTK degradation by recruiting the E3 ubiquitin ligase, cereblon (CRBN), which was originally recognized for its modulation of the immune system. However, only NX-2127, and not NX-5948, was designed to

maintain CRBN immunomodulatory function. The effects of BTK degraders on T-cell functionality are not known. Furthermore, it is unclear to what extent CRBN modulation contributes to pre-clinical (and ultimately clinical) activity of BTK degraders. Here, we began to address these questions using the bifunctional NX-2127 and immunomodulatory neutral NX-5948 compounds.

Methods: Peripheral blood mononuclear cells were isolated from CLL patients. CLL cells were treated with drugs for 24 hours and BTK, Aiolos, and Ikaros levels were assessed by immunoblotting. CD3+ T-cells were purified using Dynabeads. For apoptosis and activation assays, CD3+ T-cells were stimulated with αCD3/CD28 and concurrently treated with drugs. T-cells were then analyzed through flow cytometry for apoptosis (Annexin V) and activation (CD69, CD25, HLA-DR, PD-1, and CD38) after 24, 48, and 72 hours. For polarization assays, naïve CD4+ T-cells were stimulated with αCD3/CD28 and treated with drugs for 7 or 14 days under TH1/Treg/TH2-differentiation conditions. Flow cytometry was used to detect IFN-γ and IL-2 (TH1); CD25 + FoxP3+ T-cells (Tregs); and IL-4 (TH2). For immunological synapse assays, αCD3/CD28-stimulated CD3+ T-cells and CLL cells were treated with drugs for 24 hours. T-cells and CLL cells were then combined at a ratio of 1:1, stained with CellTracker, F-actin, and granzyme B, and imaged using immunofluorescent confocal microscopy. NX-2127 and NX-5948 were provided by Nurix Therapeutics, Inc. BTK inhibitor ibrutinib and CRBN modulator lenalidomide were used as controls at 1 μM concentrations.

Results: Treatment of CLL cells with 0.1-1 μM NX-2127 and NX-5948 resulted in degradation of BTK. Furthermore, NX-2127, but not NX-5948, induced dose-dependent degradation of Aiolos and Ikaros (known CRBN substrates), thereby confirming that only NX-2127 possessed CRBN immunomodulatory activity. Exposure of CD3+ T-cells to 0.1–1 μM NX-2127 or NX-5948 was not accompanied by either apoptosis or reduced cell proliferation for up to 72 hours. Neither early (CD69) nor late (CD25, HLA-DR, and PD-1) activation of CD4+ and CD8+ T-cells was disrupted in the presence of either compound. Interestingly, we observed an increase in the activation marker CD38 within CD4+ and CD8+ T-cells treated with NX-2127, but not with NX-5948. A similar effect was observed with both ibrutinib and lenalidomide. *In vitro* polarization assays indicated that treatment with 1 μM NX-2127, but not NX-5948, resulted in a dramatic and significant upregulation of both IFN-γ and IL-2 under TH1-polarizing conditions, to a degree which significantly exceeded the effect of either ibrutinib or lenalidomide. At the same time, BTK degraders did not alter T-cell differentiation under TH2-polarizing conditions as indicated by unchanged IL-4 expression. Additionally, NX-2127 and lenalidomide significantly reduced differentiation of Tregs when used in higher concentrations (1 μM). This effect was not observed with either immunomodulatory-neutral NX-5948 or ibrutinib. Immunofluorescent confocal microscopy revealed that NX-2127 enhanced immunological synapse formation to levels comparable to those of lenalidomide. Synapses were not induced by ibrutinib.

Conclusions: CRBN-recruiting BTK degraders NX-2127 andNX-5948 induce degradation of BTK in primary CLL cells and do not interfere with T-cell activation and survival in vitro. More importantly, CRBN-immunomodulatory activity was required to upregulate CD38 (an IFN response gene), promote T-cell differentiation towards a TH1 phenotype, downregulate Treg differentiation, and facilitate immunological synapse formation, suggesting NX-2127 has the potential to reverse the immunosuppressive environment of CLL. Overall, our findings provide a strong rationale for continued investigation of these BTK degraders in CLL and lymphoid malignancies.

Abstract ID: 1551267

Title: Increased susceptibility to *Streptococcus pneumoniae* pulmonary infection in the Eμ-TCL1 adoptive transfer mouse model of CLL

Authors: Ana Colado, Juliana Bernatowiez, Chiara Cassarino, Valeria Sarapura Martinez, Martín Bertini, Fernando R. Bezares, Mónica Vermeulen, Romina Gamberale, Mirta Giordano and Mercedes Borge

Infectious complications continue to be a major cause of morbidity and mortality in patients with CLL. The reason of this increased risk is multifactorial and is associated with immunosuppression generated by treatment, but also by the disease itself. In fact, treatment-naïve patients are at higher risk of infections than healthy population, and infections during the treatment-naïve period are associated with worse treatment-free survival and overall survival [1]. Bacterial pneumonia, involving *Streptococcus pneumoniae* (Spn), is a frequent serious infection among untreated patients [2]. Early immune response to Spn is critical to control bacterial burden and disease outcome. Although innate immune alterations were described in CLL, if these mechanisms are defective in the Spn *in vivo* response is unknown. By using a murine adoptive transfer model of CLL, we aimed to study the susceptibility to Spn pulmonary infection in the context of untreated CLL and to characterize innate immune parameters involved in the early response to the bacteria. Female C57BL/6 mice (8–10 weeks old) were intraperitoneally injected with 20×106 leukemic cells obtained from spleens of full leukemic Eμ-TCL1 mice (C57BL/6 background). CLL burden was determined in the adoptively transferred (AT)-TCL1 mice with the percentage of leukemic cells (CD5+ CD19+) in the peripheral blood (PB) assessed by flow cytometry (FC). Leukemic mice (>60% of CD5+ CD19+ cells in PB) and control mice (age-matched C57BL/6) were intranasally (i.n.) infected with a total of 2×106 CFU of Spn serotype 3 (clinical isolate provided by the Antimicrobial Service from 'Dr. Carlos G. Malbrán' Institute, Argentina) (Figure 1(A)). For survival experiments, mice were daily controlled for 11 days. In other set of experiments, bronchoalveolar lavage fluid (BALF) analysis from infected mice was performed. To this aim mice were euthanized 24 hs after infection and the BALF was obtained to determine: bacterial load by serial dilution in Columbia blood agar plates, cell number and phenotype by FC, IL-1β and TNF-α by ELISA and total protein, Lactate Dehydrogenase (LDH) and myeloperoxidase (MPO) by colorimetric assays. Statistical analysis was performed with Prism v7 (GraphPad). Values of $p<0.05$ was considered significant. Spn-infected AT-TCL1 mice showed an increased mortality rate compared to Spn-infected control mice and non-infected AT-TCL1 mice (Figure 1(B)). At 24hs after infection, AT-TCL1 mice showed a higher bacterial burden than control mice in the BALF, suggesting impairment in bacterial growth control-mechanisms (Figure 1(C)). We also observed higher levels of inflammatory parameters in BALF from leukemic mice such as total protein, TNF-α and IL-1β levels (Figure 1(D–F)). Interestingly we found no difference in LDH values

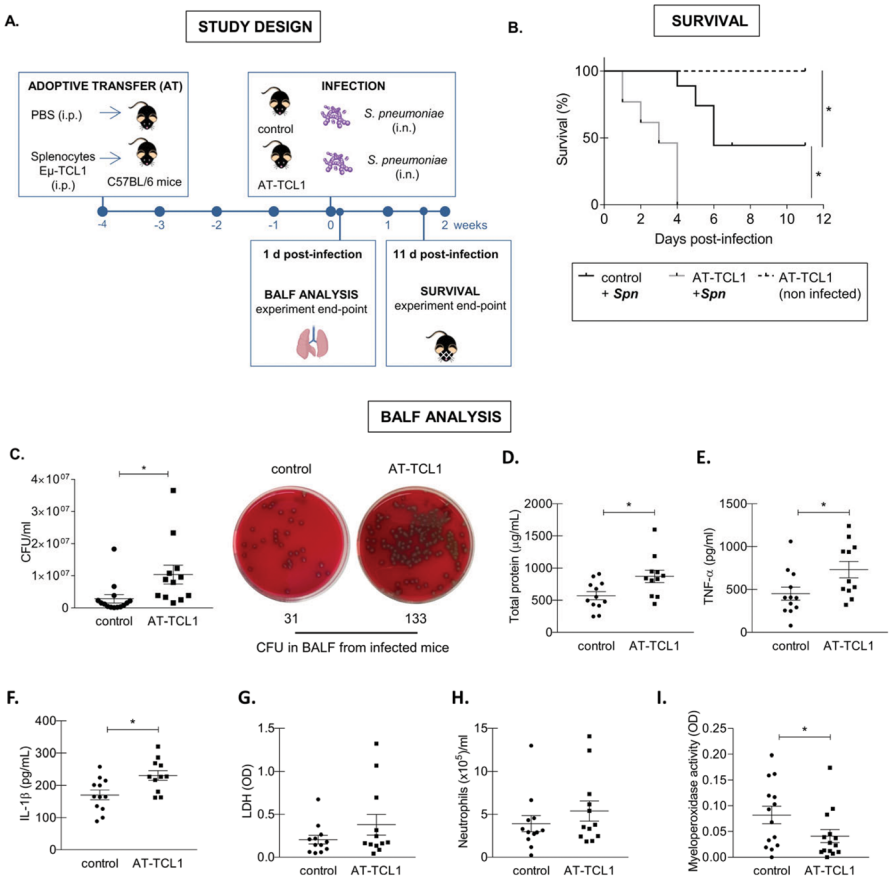

Figure 1. A. Female C57BL/6 mice (8-10 weeks old) were intraperitoneally (i.p.) injected with 20 x 10^6 leukemic cells (AT-TCL1) obtained from spleens of full leukemic Eμ-TCL1 mice. Control mice were injected with PBS. After 4 weeks, leukemization was confirmed by flow cytometry (>60% of $CD5^+$ $CD19^+$ cells in peripheral blood) and mice were infected intranasally (i.n.) with a total of 2 x 10^6 Colony forming units (CFU) of *Streptococcus pneumoniae (Spn)* serotype 3. BALF analysis and survival experiments were performed. **B.** Survival of control + *Spn* (infected), AT-TCL1+ *Spn* (infected) and AT-TCL1 (non-infected) mice (n= 4 per group). Results from 3 independent experiments are shown. Log-rank (Mantel-Cox) test, *statistically significant, p values were corrected by the Bonferroni method for multiple comparisons **C-I.** Control and AT-TCL1 mice (>60% $CD19^+CD5^+$ cells in peripheral blood) were i.n. infected as describe in methods. Mice were euthanized 24 hs after infection and the BALF was obtained for further determinations. **(C)** CFU obtained from the BALF. CFU were counted by plating serial dilutions in Columbia blood agar plates. Results from 4 independent experiments are shown. Representative plates are shown in the right. Mean ± SEM, *p<0.05, Mann Whitney test. **(D)** Total protein was evaluated with the BCA Protein Assay Kit. TNF-α **(E)** and IL-1β **(F)** were measured by ELISA. **(G)** Lactate Dehydrogenase (LDH) was determinate with a colorimetric commercial kit. **(H)** Neutrophils per 1 ml of BALF were determined. Cell number/ml was determined by microscopy and neutrophils were calculated with the % obtained by flow cytometry analysis of Ly6G + cells. **(I)** Myeloperoxidase (MPO) was determinate with a colorimetric commercial kit. Mean ± SEM, *p<0.05, Mann Whitney test.

between control and leukemic mice (Figure 1(G)), suggesting similar levels of lung damage in both cases. Moreover, we found similar numbers of neutrophils in the BALF of AT-TCL1 and control mice after 24hs of infection (Figure 1(H)). This is different from what was previously reported in a urinary tract infection model in AT-TCL1 where a defect in neutrophil recruitment to the infection site was found [3] Remarkably, despite a similar neutrophil-recruitment to the lung, AT-TCL1 mice showed lower levels of MPO in the BALF than control mice (Figure 1(I)). Our results show that CLL predisposes to an impaired control of bacterial growth and to a higher mortality rate in a model of Spn pulmonary infection. The increased bacterial count in the BALF of AT-TCL1 mice was accompanied with a rise in inflammatory parameters, suggesting that at least some early innate-immune mechanisms, such as pro-inflammatory cytokines release and neutrophil recruitment, are preserved. On the other hand, and given the central role of MPO in bacterial clearance by neutrophils, the lower levels of MPO found in the BALF of AT-TCL1 infected mice, suggests that the increased susceptibility to Spn lung infection could be partially related to a deficiency in killing mechanism by neutrophils.

Abstract ID: 1551356

Title: Clinical outcomes in patients with chronic lymphocytic leukemia (CLL) treated with veneto-clax-based regimens

Authors: Paul Hampel, Kari Rabe, Yucai Wang, Saad Kenderian, Wei Ding, Eli Muchtar, Jose Leis, Amber Koehler, Mazie Tsang, Ricardo Parrondo, Rachel Bubik, Susan Schwager, Curtis Hanson, Esteban Braggio, Susan Slager, Min Shi, Daniel Van Dyke, Timothy Call, Neil Kay and Sameer Parikh

TABLE 1: Baseline characteristics at the time of venetoclax start

Parameter		Number (%) or Median [range]			
		All patients	Firstline	Relapsed/ BTKi-naïve	Relapsed/BTKi-exposed
N		**155**	**55**	**17**	**83**
Age, years		66 [41-93]	65 [41-84]	67 [51-83]	68 [43-93]
Males		108 (70)	36 (66)	12 (71)	60 (72)
Prior lines of therapy		1 [0-11]	0	1 [1-6]	3 [1-11]
Combination with anti-CD20mAb	Rituximab	45 (29)	0 (0)	8 (47)	37 (45)
	Obinutuzumab	80 (52)	55 (100)	9 (53)	16 (19)
	Monotherapy	30 (19)	0 (0)	0 (0)	30 (36)
Rai stage, n=148	0	20 (14)	2 (4)	2 (13)	16 (20)
	I-II	62 (42)	30 (58)	5 (31)	27 (34)
	III-IV	66 (45)	20 (39)	9 (56)	37 (46)
Absolute Lymphocyte Count (x 10^9/L)*, n=150		22.4 [0-539]	80.7 [0-539]	16.2 [4-108]	13.0 [0.3-533]
IGHV mutation status*, n=129	Unmutated	93 (72)	20 (39)	8 (57)	8 (13)
FISH*, n=134	None detected	20 (15)	11 (21)	4 (27)	5 (8)
	Other	5 (4)	0 (0)	0 (0)	5 (8)
	13q-	34 (25)	16 (30)	4 (27)	14 (21)
	Trisomy 12	23 (17)	11 (21)	2 (13)	10 (15)
	11q-	28 (21)	13 (25)	4 (27)	11 (17)
	17p-	24 (18)	2 (4)	1 (7)	21 (32)
Complex karyotype*, n=69	Complex (≥3 abnormalities)	27 (39)	3 (12)	3 (38)	21 (58)
TP53 Disruption (either del17p or *TP53* mutation)*, n=136	Present (Abnormal)	32 (24)	2 (4)	2 (13)	28 (41)

*not available for all patient

Introduction: We aim to identify factors that impact outcomes of venetoclax for patients with CLL treated in routine practice at a tertiary center. We report on the use of venetoclax in the most frequently encountered disease scenarios: first-line, relapsed/Bruton tyrosine kinase inhibitor (BTKi)-naïve, and relapsed/BTKi-exposed.

Methods: After IRB approval, we identified patients who received venetoclax therapy for CLL (between 4/2012 and 4/2023) from the Mayo Clinic CLL Database. Undetectable measurable residual disease (uMRD) was defined as <1 CLL cell per 10,000 leukocytes using 8-color flow cytometry on peripheral blood (PB) or bone marrow (BM). Overall survival (OS) was defined as the time from venetoclax start until date of death or last known to be alive. Treatment-free survival (TFS) after venetoclax was defined as the time from venetoclax start until the earliest of date of next treatment, or death. Kaplan–Meier was used to display OS and TFS. Multivariable Cox proportional hazards regression models were used to estimate associations of factors with time-to-event outcomes.

Results: A total of 155 patients received venetoclax: firstline therapy (in combination with obinutuzumab, $n=55$) and relapsed CLL ($n=100$; 17 had relapsed/BTKi-naïve CLL, and 83 had previously received BTKi [55 with progression after BTKi], relapsed/BTKi-exposed). The median follow-up for the

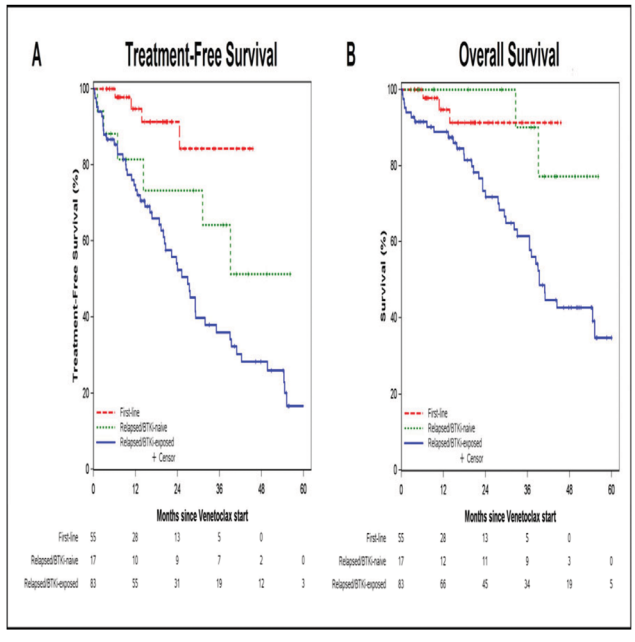

cohorts of first-line therapy, relapsed/BTKi-naïve, and relapsed/BTKi-exposed was 12.9, 37.0, and 27.6 months, respectively. Baseline characteristics at the time of venetoclax initiation for all patients are shown in Table 1. The median TFS for the overall cohort was 39.0 months. The median OS was 54.6 months. Among patients treated with venetoclax as first-line therapy ($n=55$), the 2-year TFS (Figure 1(A)) and 2-year OS rates were both 91% (Figure 1(B)). MRD testing was performed in 28 patients and was uMRD in 23 (82%) patients (only PB assessed, $n=7$; only BM assessed, $n=2$; PB and BM assessed, $n=14$). Detectable MRD was identified in 3 patients, and 2 patients had discordant results (PB uMRD and BM detectable disease). Among patients treated venetoclax in the relapsed/BTKi-naïve setting ($n=17$), the 2-year TFS rate was 73% (Figure 1(A)) and the 2-year OS rate was 100% (Figure 1(B)). MRD testing was performed in 7 patients and was uMRD in 7 (100%) patients (only PB assessed, $n=3$; only BM assessed, $n=2$; PB and BM assessed, $n=2$). The median time to first uMRD result was 14.1 months. Among relapsed/BTKi-exposed venetoclax-treated patients ($n=83$), the median TFS was 26.9 months (Figure 1(A)), and the median OS was 39.4 months (Figure 1(B)). In this subgroup, the median TFS for patients with ($n=55$) and without ($n=28$) prior disease progression on prior BTKi were 22.3 and 42.3 months, respectively. Median TFS with venetoclax monotherapy ($n=30$) was 24.0 months, venetoclax in combination with rituximab ($n=37$) was 26.9 months, and venetoclax in combination with obinutuzumab ($n=16$) was 39.0 months. BTKi-exposed patients that were chemotherapy-naïve ($n=27$) and chemotherapy-exposed ($n=56$) had median TFS of 29.1 and 24.0 months, respectively. MRD testing was performed in 28 patients and was uMRD in 16 (57%) patients (only PB assessed, $n=9$; only BM assessed, $n=2$; PB and BM assessed, $n=5$). Detectable MRD was identified in 11 patients, and 1 had discordant results (PB uMRD and BM detectable disease). The median time to first uMRD result was 11.5 months. TP53 disruption, unmutated IGHV genes, older age, complex karyotype (CK; defined as more than 3 chromosomal aberrations on CpG stimulated karyotype), and disease progression on prior BTKi were associated with shorter TFS in the overall cohort on univariate analysis. TP53 disruption, older age, CK, and disease progression on prior BTKi were associated with shorter OS in the overall cohort on univariate analysis. Multivariable analysis was performed by including only those patients where all variables significant in univariable analysis were available (OS model $n=65$, TFS model $n=53$). In these models, only CK was significantly associated with shorter TFS (HR 8.5; 95%CI 2.5–29.1; $p<0.001$) and shorter OS (HR 4.1; 95%CI 1.2–14; $p=0.03$).

Conclusions: Patients with BTKi-exposed CLL, particularly those with prior disease progression on BTKi, had worse outcomes. Our study identified CK as one of the most important baseline predictors of adverse TFS and OS in the overall cohort of patients, supporting karyotype assessment for prognostication prior to venetoclax treatment.

Abstract ID: 1551507

Title: Single center report on cohort of patients relapsed on Bruton Tyrosine Kinase inhibitors (BTKi)

Authors: Huayuan Zhu, Luomengjia Dai, Yeqin Sha, Ziyuan Zhou, Siqi Qian, Xiao Lu, Tonglu Qiu, Yi Miao, Shuchao Qin, Yi Xia, Lei Fan, Wei Xu and Jianyong Li

Introduction: Acquired BTK/PLCG2 mutations remain to be the driver of Bruton Tyrosine Kinase inhibitor (BTKi) resistance. But the underlying mechanisms need to be further explored. In this study, we retrospectively analyzed the clinical and biological characteristics of fifty-nine BTKi-resistant CLL patients in our center and made comparison with responsive cohort. Method We retrospectively collected and analyzed clinical and biological characteristics of 229 patients treated with Bruton Tyrosine Kinase inhibitors in our center (between 2014 and 2023), including 59 patients relapsed on BTKi and 170 patients in durable remission. Next-generation sequencing results acquired at the time of disease progression and treatment initiation were used to describe mutational landscape. High sensitivity droplet digital PCR (ddPCR) result was used to validate or detect additional drug resistant hotspot mutation.

Results: The median age was 65(range 33–88) and 55 (range 30–75) years in the durable remission cohort ($n=170$) and the relapsed cohort ($n=59$), respectively. Clinical and biological characteristics of above two cohorts at initiation of BTKi treatment were described and compared in Table1. IGHV unmutated status was enriched for the BTKi relapsed cohort. Besides, higher proportion of high-risk biological factors such as del(17p), del(11q) , TP53 aberrations were shown in the BTKi relapsed cohort. BTKi relapsed cohort was also enriched in bulky disease (40.8%) and the medium LDH was 289.3 IU/L (range 125–1191), which was significantly higher than the responsive cohort. Therefore, the relapsed cohort was enriched for patients with high-risk features, which may explain the inferior treatment response. Consistently, in the relapsed cohort, higher proportion of patients were stratified to high-risk (3–4 point) according to the four-factor prognostic score system developed for predicting the risk of BTKi resistance (50 vs 13.7%, $p<0.0001$). Resistance to BTKi occurred at a median exposure of 29.4 months. Among patients experienced disease progression, 13 were Richter transformation (12 with diffuse large B-cell lymphoma [DLBCL], 1 with Hodgkin lymphoma [HL]) while 46 were CLL progression (medium exposure were 9.5 months and 32.6 months, respectively, $p<0.001$). The most commonly used fragments in the relapsed cohort were 1–69 ($n=11$), 4–39 ($n=10$), 3–48 ($n=7$), and 3–9 ($n=6$), which is totally different from the responsive cohort. Mutational landscape was mapped using NGS results and showed that BTK/PLCG2 mutations were the most common mutation at the timepoint of disease progression. No significant difference was identified except for higher proportion of TP53 mutation (45 vs. 24%, $p=0.0056$) and EGR2 mutation (23 vs. 8%, $p=0.0105$) at the timepoint of disease progression. By integrating NGS and ddPCR results, 54.5% (30/55) patients relapsed on BTKi acquired BTK/PLCG2 mutation. BTK/PLCG2 mutation was detected in 34.3% (12/35), 83.3% (10/12), 70% (7/10) , 50%(1/2)patients relapsed on Ibrutinib, Zanubrutinib, Orelabrutinib and Acalabrutinib, respectively. BTK hotspot mutation analysis was carried and identified that BTKC481 mutation was the most common mutation and was detected in patients treated with all kinds of BTKis. Other mutations at the C481 site include C481R, C481Y, C481F. However, BTKT474 mutation was only detected in patients treated with Orelabrutinib (Figure 1). Four patients had PLCG2 mutations, including one concurrent with BTK mutation. Six patients had more than one mutation. Though higher proportion of TP53 mutation was identified at disease progression on BTKi, most patients had a stable mutation burden ($n=20$) or even a reduction of mutation burden

($n=8$) during the treatment of BTKi according to the matched NGS results of individual patient (Figure 4). Five patients gained TP53 mutation, all of whom exposed to cytotoxic drugs before BTKi treatment, including 4 exposed to FC-based regimen and 1 exposed to Chlorambucil.

Conclusion: Patients relapsed on BTKi have different clinical and biological characteristics from responsive ones. IGHV unmutated status was dominant in BTKi resistant cohort and the most frequently used fragments were different from that of the responsive cohort. Acquired BTK/PLCG2 mutations remained to be key drivers of BTKis resistance but other high-risk factors may affect the outcome of BTKi treatment and the underlying mechanisms should be explored in order to overcome BTKi resistance.

Table 1. Characteristics of patients at BTKi treatment initiation.

Characteristics at BTKis initiation		Percentage (%) or Median (range)		P value
		Relapsed cohort	Responsive cohort	
Age		55 (30-75)	65(33-88)	
Male : Female		35 : 24	118 : 52	
Number of prior therapies		1 (0-4)	0(0-6)	
BTKis	Ibrutinib	35/59 (59.3)	101/170 (59.4)	
	Zanubrutinib	12/59 (20.3)	33/170 (19.4)	
	Orelabrutinib	10/59 (16.9)	31/170 (18.2)	
	Acalabrutinib	2/59 (3.3)	4/170 (2.3)	
	Lox-305	0/59 (0)	1/170 (1.0)	
TTFT		10.96m (2.86-47.86m)	28.2m (1.00-138.23m)	0.0002
IGHV mutation status	Unmutated	47/55 (85.5)	78/158(49.4)	<0.0001
	Cannot be defined	1	1	
	Missing	3	12	
Rai stage	I-II	15/49 (30.6)	45/143 (31.5)	
	III-IV	34/49 (69.4)	94/143 (65.7)	
	Not applicable	10	27	
Binet stage	B	17/49 (34.7)	46/143 (32.2)	
	C	32/49 (64.6)	86/143 (60.1)	
	Not applicable	10	27	
LDH (IU/L)		289.3 (125-1191)	221 (92-1032)	0.0117
β2-MG (mg/L)		4.49 (2.52-7.18)	4.10(1.4-17.3)	0.2451
Bulky disease(≥5cm)	≥5cm	20/49 (40.8)	19/141(13.5)	<0.0001
	≥10cm	5/49 (10.2)	10/141(7.1)	0.5404
	Missing	10	29	
Four-factor prognostic score	Low risk(0-1)	10/32(31.3)	58/95(61.1)	<0.0001
	Interim risk(2)	6/32(18.8)	24/95(25.3)	
	High risk(3-4)	16/32(50.0)	13/95(13.7)	
	Missing	27	75	
FISH	17p-	21/50 (42.0)	15/107 (14.2)	0.0001
	11q-	18/41 (43.9)	21/93 (22.6)	0.0123
	13q14-	16/41(39.0)	46/86 (53.5)	0.1273
	+12	6/41(14.6)	20/83 (24.1)	0.2233
TP53 mutation	Yes	14/43 (32.6)	22/109 (20.2)	0.1060
	Missing	16	61	
TP53 Disruption	Yes	25/46 (54.3)	19/84 (22.6)	0.0003
	Missing	13		
Complex karyotype	≥3	13/34(38.2)	31/128 (24.2)	0.1024
	Missing	25	42	

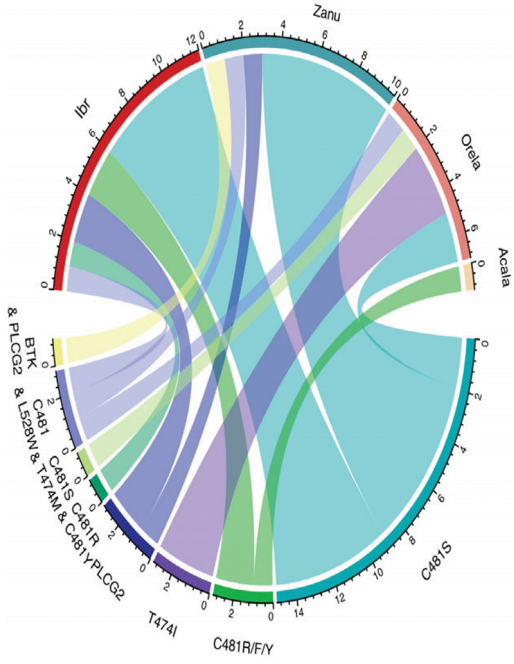

Abstract ID: 1551550

Title: PI3K inhibitor-resistant B-cell lymphomas show distinct functional phenotypes characterized by sensitivity to Bcl-2- or proteasome-inhibition

Authors: Johanne Hermansen, Paschalis Athanasiadis, Yanping Yin, Alberto J. Arribas, Lene Skou Nilsen, Anthony Mato, Fransesco Bertoni, Geir Tjønnfjord, Tero Aittokallio and Sigrid Skånland

Background: While patients with B-cell malignancies often have an initial response to targeted therapies, development of treatment intolerance or resistance is common. It is therefore important to identify clinically actionable biomarkers to guide selection of optimal treatment for the individual patient.

Aim: To identify biomarkers of treatment resistance and sensitivity in B-cell malignancies.

Methods: We studied lymphoma cell lines (KARPAS1718 and VL51) with induced resistance to the PI3K inhibitor idelalisib. RNA-sequencing, drug sensitivity screens ($n=97$ drugs), and (phospho) protein ($n=31$) profiling were performed on both the parental and resistant versions of the cell lines. To study clinical relevance, functional assays were performed on chronic lymphocytic leukemia (CLL) cells from treatment naïve ($n=8$) and idelalisib-intolerant/refractory patients ($n=13$).

Results: Compared to their isogenic parental counterparts, the idelalisib-resistant KARPAS1718 and VL51 cell lines presented with distinct functional phenotypes. The resistant KARPAS1718 strain remained sensitive to the Bcl-2 antagonist venetoclax while venetoclax sensitivity was reduced in the resistant VL51 strain. We found that Bcl-2 and Bim phosphorylation/expression correlated with venetoclax sensitivity in both parental and resistant cell lines. To test this *in vitro* observation in primary cells, we performed ex vivo drug sensitivity and (phospho)protein profiling on CLL cells from treatment naïve ($n=8$) and idelalisib-intolerant/refractory patients ($n=13$). In agreement with the cell line data, we found that Bcl-2/Bim phosphorylation/expression and venetoclax sensitivity was reduced in CLL cells from the idelalisib-intolerant/refractory patients compared to the treatment naïve patients. To identify effective drugs in idelalisib-resistant cells that were less responsive to venetoclax, we performed a target addiction scoring based on drug sensitivity screening of 97 drugs. Bcl-2 and histone deacetylase (HDAC) were identified as the top two target addictions across the four cell lines. We therefore tested combination treatment with a Bcl-2 antagonist (venetoclax) and an HDAC inhibitor (panobinostat). However, this combination was less effective in the idelalisib-resistant VL51 cell line than in the parental cell line. By performing RNA sequencing on the four cell lines, we found that BCL2 transcripts were reduced in the resistant VL51 cell line, in agreement with the observed reduction in Bcl-2 protein level. We further observed that RNA transcripts for the proteasome remained unchanged for both KARPAS1718 and VL51 cell lines. When these cell lines were treated with proteasome inhibitors (bortezomib or ixazomib), cell viability was effectively reduced in both the parental and resistant cell lines. Similarly, proteasome inhibitors were equally effective in CLL cells from treatment naïve and idelalisib-intolerant/refractory patients.

Conclusion/summary: Our findings suggest that idelalisib resistance associates with cell line-specific functional phenotypes, emphasizing the need for tailored treatment

selection. Proteasome inhibition may provide a broadly applicable salvage strategy for multi-refractory CLL. We are currently in the process of enrolling CLL patients who are relapsed/refractory to targeted therapies to the clinical trial IMPRESS-Norway (NCT04817956). These patients will be treated with the proteasome inhibitor bortezomib following a positive drug sensitivity test as a companion functional biomarker.

Abstract ID: 1551624

Title: Explainable machine learning to identify chronic lymphocytic leukemia based on gut microbiome data

Authors: Tereza Faitova, Ramtin Marandi and Carsten Niemann

Background: Recent studies have shown extensive crosstalk between our immune system and gut microbiome (GM). The host immune system plays a vital role in the maintenance of GM homeostasis by establishing a balance between eliminating invading pathogens and promoting the growth of beneficial microbes, whereas GM can modulate the immune system by cytokine production. As chronic lymphocytic leukemia (CLL) is, among others, characterized by high rate of infectious complications and an altered immune system, it is warranted to uncover the pattern of microbiome composition distinguishing CLL from other hematological malignancies and healthy cohorts. Thus, we aimed to investigate whether machine learning model would be able to classify patients with CLL based on microbiome and demographic data.

Methods: A Danish cohort including a total of 438 feces samples collected from different patient groups and healthy donors were analyzed. 87 samples were collected from patients with CLL, 161 from patients with hematological malignancies such as acute myeloid leukemia (AML), myelodysplastic syndrome (MDS), or severe aplastic anemia, 121 from patients undergoing major thoracic surgery, 58 from healthy individuals, and 11 from kidney donors. Feces samples of healthy individuals were chosen to match the CLL population with respect to age, demographic data, sample collection method, and sequencing platform. Taxonomical profiling was done using an in-house bioinformatics pipeline and the resulting dataset was randomly split into a training set with 80% used as an input for machine learning algorithms and 20% of individuals stratified by CLL in the blinded test set for which results are reported.

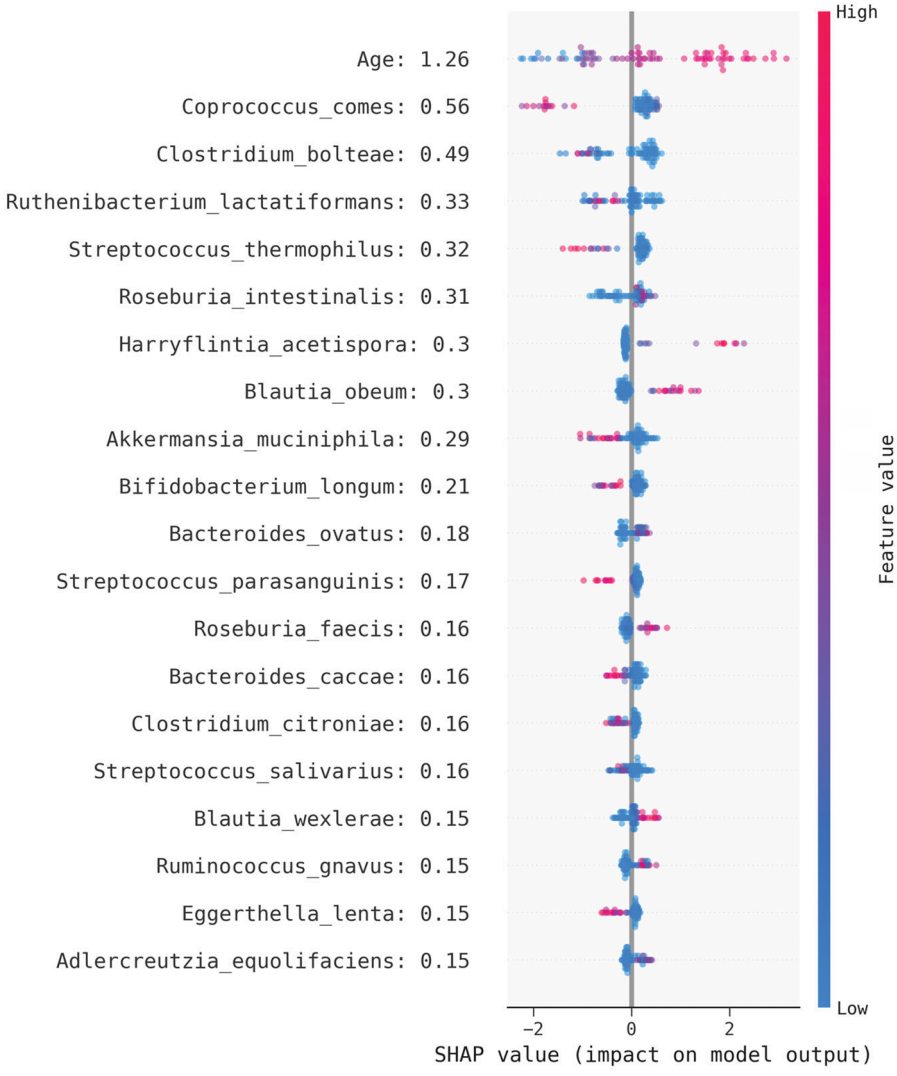

Results: Preliminary results suggested that age, Coprococcus comes and Costridium boltae were the 3 most informative features to identify CLL (Figure 1). Age had the highest contribution to the identification of CLL and was positively correlated with its SHAP values, which translates to increased chance of identifying CLL as age increases. Coprococcus comes was the second most contributing feature with its values being negatively correlated with SHAP values. In other words, the chance of identifying CLL decreases as the relative abundance of Coprococcus comes increases. Costridium boltae as the third most contributing feature followed a similar pattern seen in Coprococcus comes, only with less difference in relative abundances. The predictions were retrieved from the best performing model (LightGBM) achieving the area under the receiver operating characteristics curve, AUC =0.71 with specificity =0.92, sensitivity =0.44, positive predictive value =0.62, and negative predictive value =0.86 on the test set.
Conclusion: The presented results are preliminary data and thus we plan to further investigate the interaction between age and bacterial abundances in the included cohorts to avoid spurious correlations and predictions – updated analyses will be presented. Nonetheless, the results suggest that there exists a strong potential in using microbiome data for identifying disease states such as CLL. Incorporating cohorts with diverse hematological disease severities (AML, MDS, and aplastic anemia) alongside a healthy cohort, we aimed to elucidate the genuine microbiome pattern associated with CLL. By also encompassing other pathologies and considering the microbiome's potential reflection of health status, we believe we have accounted for a comprehensive representation. We observed several bacterial species being both negatively and positively correlated with identification of CLL, which offers a highly encouraging opportunity for exploring and implementing interventions aimed at modulating the microbiome through introduction of beneficial bacteria and/or elimination of pathogens. This knowledge could potentially lead to targeted interventions aimed at modulating the composition and function of the microbiota to improve disease outcomes for CLL patients.

Abstract ID: 1551688

Title: Expression of SIGLEC-10 ligands CD24 and CD52 limit T cell and CAR-T cell function in CLL

Authors: Jaco A. C. Van Bruggen, Fleur S. Peters, Gaspard Cretenet, Perry D. Moerland, Aldo Jongejan, J. Joseph Melenhorst, Gerritje J. W. van der Windt, Eric Eldering and Arnon Kater

Introduction: Disappointing success rates of autologous T cell-based therapies such as CAR T cell therapy in chronic lymphocytic leukemia (CLL) correlate with impaired activation and proliferation of T cells. These T cell defects are reversible upon removal of CLL cells, suggesting that unknown CLL-derived factor(s) are responsible for acquired T-cell dysfunction. The aim of this study is to investigate mechanisms by which CLL cells suppress T-cell activation.
Methods: We attempted to identify the mechanism of action in which CLL cells induce T cell dysfunction and whether these suppressive effects are mediated through a soluble factor secreted by CLL cells, or by contact-dependent mechanisms. CD40 activation of CLL cells results in increased expression of key surface-expressed adhesion and costimulatory molecules, but also in alterations of immune-modulatory cytokines secretion. This model has shown that the negative impact on T cell activation can be overcome by CD40-ligation of the CLL cells, at least partly because of improved antigen-presenting capacity [1].
Results: Prior works suggest that T cells in CLL cannot reach the same levels of activation as HD derived T cells, similar to exhausted T cells. However, such studies lack analysis of T cell activation over time. Our current observations revealed that the peak percentage of activated T cells occurred on day 4 in HD and day 5 in CLL indicating T cell activation in CLL occurs in a delayed fashion. When T cells are challenged with multiple rounds of stimulations in presence of autologous CLL cells, impaired cytokine production and a diminished proliferative capacity start to arise as early as after the first round of restimulation, compared to HD. Similarly, CLL-derived CAR-T cells don't proliferate when challenged with primary CLL cells multiple times in sequence but do so when the Jeko-1 cell line is presented as a target to kill. This indicates that CLL cells impose an immune restrictive environment on T cells including CAR-T cells. In order to study what CLL-mediated factor(s) underlies the acquired delay and dysfunction upon T cell activation, we made use of the well-established CD40 model. Impaired T-cell activation was alleviated by CD40-activated CLL cells, and occurred in a cell contact-dependent manner. However, CD40-stimulated CLL cells treated with the SRK-kinase inhibitor dasatinib were unable to restore T-cell function when co-cultured again with T cells, despite high expression of co-stimulatory receptors on CLL cells. Sialic acid-binding Ig-like lectin 10 (Siglec-10) ligands CD24 and CD52 were pinpointed as potential genes responsible for inhibiting T-cell function by CLL after transcriptome profiling of CD40-stimulated CLL cells treated with or without dasatinib. This was confirmed at the protein level. We also found elevated expression of their cognate receptor, Siglec-10, in CLL-derived T cells. Upon ligation of Siglec-10 and CD24 or CD52, Siglec-10 recruits phosphatases to dampen phosphorylation of key proteins downstream of the TCR such as ZAP70. To demonstrate a potential therapeutic opportunity, we included CD24 and CD52 blocking antibodies during T cell stimulation. Analysis of T cell activation over time revealed that the delay in CLL T cell activation was restored when blocking CD24 and CD52. Moreover, blocking CD24 and CD52 reduced expression of PD-1 on T cells despite presence of CLL cells. We also observed improved specific lysis of CLL cells co-cultured with HD or CLL-derived CAR-T cells. Blocking CD24 and CD52 also increased phosphorylation of CD3ζ and ZAP70 in CLL-derived T cells.
Conclusion: These results demonstrate that CLL-derived T cells are not terminally dysfunctional, but that TCR-mediated activation is suppressed by CLL cells in a contact-dependent manner. By blocking CD24 and CD52, (CAR-)T cell function could be efficiently restored even without transforming CLL cells into efficient APC through CD40 stimulation. Manipulating interactions of CD24 and CD52 with Siglec-10 may represent a therapeutic window of opportunity to enhance autologous based therapies in CLL such as CAR-T cell therapy.

Abstract ID: 1552104

Title: The RNA-binding protein Musashi2 is regulated by NOTCH1/KLF4 pathway and support tumor survival keeping CLL cells in proliferative niches during disease progression

Authors: Juliana Querol Rivas, Magalí Torres, Gabriel Fernandez, Eugenia Payque, Rita Uría, Maria Elena Marquez, Shih-Shih Chen, Ana Ines Landoni, Cecilia Guillermo, Nicholas Chiorazzi, Pablo Oppezzo and Florencia Palacios

Post-transcriptional regulation is an essential mechanism for the cells to control gene regulation where the RNA-binding proteins (RBPs) orchestrate the fate of the RNA molecules. Because of its critical role, a dysregulation of the RBPs can lead to cancer. Specifically, in chronic lymphocytic leukemia (CLL) high levels of the RBP Musashi2 (MSI2) has been related with tumor cell survival and poor prognosis underlining a key role for MSI2 during disease evolution [1]. The increase in CLL-cells in patients stems from a small fraction of dividing CD5+ B cells. The growth of this proliferative fraction (PF) correlates directly with poor outcome, making the PF an important target for therapy. Interestingly, we observed higher MSI2 levels in CLL than healthy donors (HD) B cells, even higher in the PF. Downregulating MSI2 expression or blocking its function eliminates CLL-cells. These results allow us to propose that MSI2 itself, molecules that induce MSI2 expression or the downstream molecules that MSI2 regulates, could be responsible for the clinical course of CLL patients. Therefore, we studied the molecular mechanisms that induce MSI2 overexpression in CLL-B cells. Interestingly, in CLL-cells NOTCH1 suppresses the expression of the transcription factor Kruppel-like factor 4 (KLF4), a known negative regulator of MSI2 in adenocarcinoma. NOTCH1 is a transmembrane receptor that is cleaved upon engaging ligand with an intracellular domain migrating to the nucleolus and activating genes related to cell survival, as c-myc. As we observed for MSI2, higher NOTCH1 active forms were found in lymph nodes (LN) than peripheral blood (PB) of CLL-B cells. Because low levels of KLF4 were reported for CLL-B cells, we wondered whether MSI2 overexpression in CLL was due to alterations in the NOTCH1/KLF4 pathway. To answer this, we first determined at mRNA levels by quantitative PCR KLF4/MSI2 expression in CLL-cells and HD. Results showed that there was a negative correlation between KLF4/MSI2 ($r=0.68$; $p=0.009$). To further study the role of NOTCH1/KLF4/MSI2, poor outcome CLL patients (previously selected for activated NOTCH1), were treated with NOTCH1 inhibitor (gamma-secretase) and NOTCH1/KLF4/MSI2 levels were determined. NOTCH1 inhibition increased KLF4 levels ($p=0.01$) and downregulates MSI2 and c-myc expression ($p<0.05$). To confirm that the decrease expression of MSI2 it is because of the negative action of KLF4 on MSI2 promoter, chromatin immunoprecipitation using anti-KLF4 and PCR MSI2 promotor amplification was performed. Remarkably, treated CLL-cells exposed to NOTCH1 inhibitor immunoprecipitated a fragment corresponding to the MSI2-promoter, indicating that KLF4 effectively binds and negatively regulates MSI2 expression in CLL-cells. Results suggested that MSI2 overexpression in LN and in activating/dividing cells is due to the absence of KLF4 regulated by NOTCH1. Which are the molecules that MSI2 regulates in the active microenvironment it is now a relevant question to answer. Because MSI2 regulates different targets in a cell type-specific manner, we studied MSI2´s role in activated/dividing CLL-cells. To do this, we analyzed the proteomes of MSI2 knock-down in activated (CpG-ODN + IL15) CLL-B cells ($n=12$) and compare with the control. Results showed that MSI2 knock-down significantly increased the levels of 12 proteins ($p \leq 0.01$) consistent with MSI2 functioning as a mRNA inhibitor of a set of molecules involved in cell migration. To confirm these results, we selected and verified protein levels expression by flow cytometry of Fer (non-tyrosine-protein kinase receptor), VAV1 (guanine nucleotide exchange factors) and its active form (phosphorY174). Since Fer/VAV1 plays a role in the cytoskeleton regulation, we also knocked-down MSI2 in CLL-B cells from the same cohort and evaluated by microscopy cytoskeleton rearrangement of cells bound to fibronectin-coated slides, showing that MSi2 downregulation in activated cells present more elongated cells implying an active cytoskeleton. Because: 1-high MSI2 levels are associated to poor outcome, 2-there is more MSI2 in LN > PB, even more in dividing-cells and 3-in activated cells MSI2 inhibit cell migration, we hypothesize that MSI2 may be playing a role on keeping the cells in solid-tissues receiving surviving signals, favoring disease progression. Altogether, our results provide novel findings about the molecular mechanisms that regulates MSI2 expression, highlighting the role of NOTCH1/KLF4 pathway in this protein and the potential function of MSI2 inhibiting CLL-cell migration in an active microenvironment supporting CLL progression, which postulate new tools to modulate/prevent disease progression, potentially rendering CLL more manageable for patients.

Abstract ID: 1552701

Title: A study of frontline therapy in adults aged 80+ years with chronic lymphocytic leukemia (CLL)

Authors: Mazie Tsang, Paul Hampel, Kari Rabe, Wei Ding, Jose Leis, Saad Kenderian, Yucai Wang, Eli Muchtar, Amber Koehler, Curtis Hanson, Min Shi, Susan Slager, Neil Kay and Sameer Parikh

Background: Although CLL primarily affects older adults (median age 71 years), limited data exists about the outcomes of adults who are 80+ years old because they are under-enrolled on clinical trials.
Methods: The Mayo Clinic CLL Database was used to conduct a retrospective cohort study of adults 80+ years at the time of frontline CLL treatment. Kaplan–Meier analysis was used to plot OS, and cumulative incidence was used to plot TTNT, accounting for competing risk of death. The Mayo Clinic IRB approved the study.
Results: Our study included 216 patients who were age 80+ at the time of frontline CLL therapy between 1/1995 and 11/2022 (Table 1). The median time from CLL diagnosis to initiation of frontline therapy was 3.1 years. The median OS after start of frontline therapy was 3.9 years. The median OS was 3.3 years (95% CI 2.6–4.2) for patients who received alkylating agents (e.g. chlorambucil, $n=96$), 3.8 years (95% CI 2.8–not reached [NR]) for purine analogues (e.g. fludarabine, $n=11$), 3.9 years (95% CI 3.2–4.9) for anti-CD20 monoclonal antibody monotherapy (e.g. obinutuzumab, $n=64$), and not reached (95% CI 3.3–NR) for novel agents ($n=43$) ($p=0.02$). The types of novel agents included ibrutinib ($n=19$), acalabrutinib ($n=16$), venetoclax ($n=7$), and orelabrutinib ($n=1$). There was no difference in OS between 36 patients who received a BTKi compared to the 7 patients who received venetoclax based therapy. At a median follow-up time of 6.7 years from the first visit, 143 patients died from the following: progressive CLL ($n=63$), infections ($n=12$), other cancer ($n=11$), non-CLL reasons ($n=21$). Cause of death was unavailable for 36 patients. On multivariable

analyses, older age (i.e. any 5-year increase in age) was associated with a 50% increased risk of death (HR 1.5, 95% CI 1.2–1.9, $p=0.001$), and treatment with non-novel agents was associated with 3.2 times increased risk of death (HR 3.2, 95% CI 1.2–8.9, $p=0.02$). Of the 216 patients, 76 patients required second-line therapy; the median TTNT was 4.2 years (95% CI 2.9–NE). The most used second-line agents were monoclonal antibodies alone (20/76, 26%) and single-agent alkylators (18/76, 24%).

Conclusion: When compared to all other CLL treatments, novel agents such as BTKi and venetoclax-based treatments are associated with significantly improved OS in CLL patients 80+ years when used in the frontline setting. Further research is warranted to evaluate the patient-reported outcomes and needs of older adults with CLL in the era of novel agents.

Table 1 Baseline patient characteristics ($N=216$)

Pre-treatment	*N* (%) or Median (range)
Age	83 (80–95)
Sex	
Female	70 (32)
Male	146 (68)
Labs	
Absolute lymphocyte count ($\times10^9$/L)	33.8 (0.4–360.5)
White blood cell count ($\times10^9$/L)	42.8 (2.2–610)
Hemoglobin (g/dL)	11.4 (6.3–16.3)
Platelet count ($\times10^9$/L)	144 (3–748)
FISH, pretreated	
Missing	90
Normal	28 (22.2)
13q-	38 (30.2)
Trisomy 12	29 (23.0)
11q-	20 (15.9)
17p-	11 (8.7)
IGHV mutation status	
Missing	115
Unmutated	59 (58.4)
CLL-IPI risk group	
Missing	142
Low	1 (1.4)
Intermediate	10 (13.5)
High	54 (73.0)
Very high	9 (12.2)

Abstract ID: 1552892

Title: Single-cell transcriptomic analysis of CLL cells at ibrutinib plus venetoclax relapse and targeting using BCL-2/BCL-xL PROTACs PZ18753b and WH25244

Authors: Daisy Diaz Rohena, Arnau Peris Cuesta, Bailey Slawin, Janani Ravikrishnan, Chaomei Liu, Charmelle Williams, Wanyi Hu, Peiyi Zhang, Phillip Thompson, William Wierda, Nitin Jain, Sachet Ashok Shukla, Guangrong Zheng, Daohong Zhou, Jennifer Woyach and Deepa Sampath

Management of CLL in the clinic has been dramatically improved with the use of targeted therapeutics. Venetoclax treatment causes apoptosis of CLL cells via inhibition of the anti-apoptotic protein Bcl-2. Ibrutinib treatment inhibits the Bruton's Tyrosine Kinase (BTK) and interrupts the B cell receptor signaling which is critical for CLL survival. While these therapies can induce deep responses when used as monotherapies or in combination, outcomes on subsequent treatments are suboptimal for patients who relapse. We aimed to evaluate drivers of relapse in CLL patients treated with venetoclax and ibrutinib, via single cell RNA sequencing (sc-RNA-seq), to propose novel strategies for therapeutic targeting. Peripheral blood mononuclear cells were isolated from CLL samples ($n=3$) collected upon relapse to, both, venetoclax and ibrutinib treatment, which were administered in combination or sequentially. From sc-RNA-seq data, 12 clusters were identified in the integrated relapsed samples. 4 CLL clusters were distinguished and had a distinct transcriptome profile from naïve B cells, NK cells and T cells. The main enriched pathway within the relapsed CLL clusters was BCR signaling. Interleukin-mediated (IL-2, IL-3 and IL-5), ErbB and Fc epsilon receptor I signaling pathways were also enriched. Notably, 3 out of 4 CLL clusters had high expression of BCL-2, and most cells expressing MCL-1 or BCL-xL also

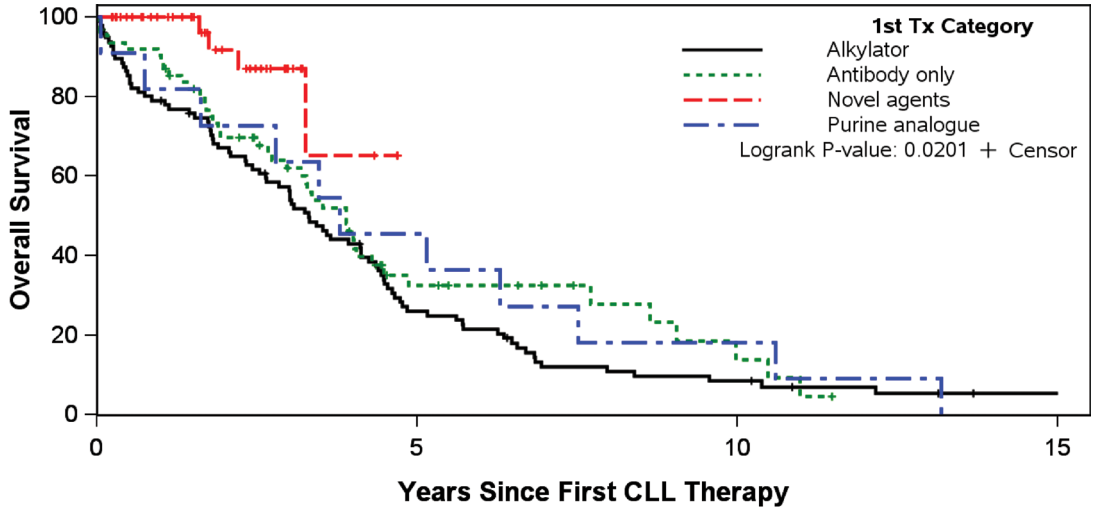

co-expressed BCL-2. We analyzed paired samples from a CLL patient (CLL-3) collected at baseline and at relapse, which occurred after cessation of fixed-duration treatment with venetoclax and ibrutinib. While the CLL clusters were shared at baseline and relapse, the proportion of cells in each cluster was vastly altered at relapse. Particularly, CLL cells from cluster 3 represented 4% of CLL cells at baseline versus 36% at relapse, suggesting their role in driving relapse. An analysis of the marker genes led to identify a high B-cell receptor (BCR) score in CLL cluster 3, including high expression of MAP3K8, FOSB8, JUND and NFKB1 genes. Moreover, the relapsed sample had an increased number of CLL cells expressing transcripts from the BCL-2 family of anti-apoptotic proteins, including BCL-2, BFL-1 (encoded by BCL2A1), MCL-1 and BCL-xL (encoded by BCL2L1). The observation that BCL-2 and BCL-xL remain relevant in relapsed CLL led us to propose a targeted therapeutic strategy. Knowing that BCL-xL inhibition in the clinic has been limited by platelet toxicity, PROTACs PZ18753b and WH25244 were synthesized from navitoclax (BCL-2/BCL-xL dual inhibitor) linked to a VHL E3 ligase ligand to target Bcl-2 and Bcl-xL for degradation, with improved specificity to cancer cells while sparing platelets. CLL cells from treatment naïve patients (n = 5) or OSU-CLL cells expressing wildtype (WT) or mutant Bcl-2 (G101V, F104L, R107-110dup or A113G) were treated with venetoclax, navitoclax, PROTACs PZ18753b or WH25244, or negative controls (NC) lacking VHL recruitment PZ18753b-NC or WH25244-NC. Viability was evaluated by Cell Titer Glo assay, and apoptosis by flow cytometric detection of active BAX and BAK, mitochondrial cytochrome C, and AnnexinV binding. Protein degradation and inhibition was evaluated by Western Blot and NanoBRET assay, respectively. PZ18753b and WH25244 exposure led to key events of the mitochondrial apoptosis pathway in treatment naïve primary CLL cells: BAK and BAX transformation, cytochrome C release and phosphatidyl serine exposure. The potency of these PROTACs was improved 1.6- and 6.5-fold for PZ8753b and WH25244, respectively, when compared to their precursor, navitoclax. Importantly, CLL cells were sensitive to these PROTACs at concentrations known to be non-toxic to human platelets. Sensitivity to venetoclax was similar to WH25244, with 50% death occurring between 0.5 and 4 nM. Apoptosis was associated with degradation of Bcl-xL in a VHL-dependent manner. Moreover, OSU-CLL cells incorporating BCL-2 mutations were up to 4.3-fold more sensitive to WH25244 than venetoclax. Cell death of OSU-CLL cells upon treatment with WH25244 was preceded by degradation of Bcl-xL and wildtype or mutant Bcl-2. We anticipate that venetoclax-relapsed primary CLL cells showing high Bcl-xL dependency by single cell sequencing will retain sensitivity to PZ18753b and WH25244. PZ18753b and WH25244 have preclinical efficacy in baseline CLL and can degrade, both, Bcl-xL and mutant Bcl-2 proteins, which are known to confer venetoclax resistance. This translational study supports the development of novel therapeutics for the treatment of CLL subgroups with adverse clinical prognosis and will open new frontiers as we better understand the biology of this disease.

Abstract ID: 1553021

Title: *ZMYM3* mutations dysregulate histone acetylation and impact the outcome of chronic lymphocytic leukemia patients

Authors: Alberto Rodríguez Sánchez, Miguel Quijada Álamo, Claudia Pérez Carretero, Luis A. Corchete Sánchez, Cristina Miguel García, Sandra Santos Mínguez, Eva Lumbreras González, Julio Dávila Valls, Alfonso García De Coca, María Jesús Vidal Manceñido, Rocío Benito Sánchez, Ana E. Rodríguez Vicente and Jesús María Hernández Rivas

Recent next-generation sequencing (NGS) studies have identified mutations in more than 200 candidate driver genes in chronic lymphocytic leukemia (CLL), most of which occur in frequencies of less than 5% of CLL patients. One of these genes is *ZMYM3*, which is mutated in 2–4% of CLL cases, that has been suggested to play a role in chromatin remodeling. Nevertheless, the clinical and biological impact of *ZMYM3* mutations in CLL has not been explored. To assess the clinical implications of these mutations, 487 CLL patients were analyzed by targeted NGS to evaluate the mutational status of 54 CLL-related genes. We detected that *ZMYM3* was mutated in 6.2% ($n = 30/487$) of CLL patients. Variants identified were predominantly loss-of-function, mainly frameshift mutations (~70%), which were distributed throughout *ZMYM3* coding sequence, with a particular exception of a recurrent mutation observed in 6 patients (p.P48fs). Regarding to their mutational profile, 70% of *ZMYM3* patients ($n = 21$) harbored mutations in *NOTCH1* and in negative regulators of the NOTCH signaling pathway such as *FBXW7*, *SPEN* or *MED12*, which suggests a cooperation between both events in CLL pathobiology. Among the 409 cases with clinical data, *ZMYM3* mutations associated with a shorter time to first treatment (median: 35 vs. 52 months; $p = 0.010$). Moreover, *ZMYM3* mutations stratified the clinical outcome of early stage CLL subgroups such as Binet stage A (48 vs. 108 months, $p = 0.002$) or Rai 0/1 (48 vs. 91 months, $p = 0.016$). To determine the biological implications of *ZMYM3* mutations, we used the CRISPR/Cas9 system to design an *in vitro* CLL model based on the CLL-derived HG3 cell line, mimicking the most frequent truncating mutation in *ZMYM3* (*ZMYM3*) identified in our cohort (p.P48fs) ($n = 3$). These mutations were introduced in HG3 wild-type (WT) cells ($n = 3$) and *NOTCH1* mutated cells (*NOTCH1*) ($n = 3$), which harbor the most frequent *NOTCH1* mutation reported in CLL (p.P2514fs), to simultaneously combine both mutations and generate *ZMYM3 NOTCH1* cells ($n = 3$). We first evaluated the impact of *ZMYM3* mutations in CLL transcriptome by RNA sequencing (RNA-seq). Compared to WT cells, *ZMYM3* cells showed 155 differentially expressed genes (DEGs: fold change [FC] > 2; false discovery rate [FDR] < 0.05), while *NOTCH1* cells exhibited 86 DEGs. Notably, *ZMYM3 NOTCH1* cells showed a profound transcriptional dysregulation with a total of 690 DEGs, most of which were downregulated (458 vs 232). Gene set enrichment analysis (GSEA) revealed that DEGs were enriched for apoptosis, signaling by interleukins, inflammatory response or DNA damage repair in *ZMYM3* cells. Interestingly, GSEA analysis revealed an upregulation of genes involved in histone deacetylation. Given the proposed role of *ZMYM3* as a component of a histone deacetylase complex, we evaluated the impact of these mutations on global histone acetylation. We identified a reduction of histone H4 acetylated levels in *ZMYM3* compared with WT cells ($p < 0.05$), while we did not observe significant differences in histone H3 acetylation. Altogether, these results suggest that *ZMYM3* mutations may alter gene expression through reduction of histone acetylation. At the functional level and consistent with the transcriptional

changes, *ZMYM3* cells had a reduced ability to arrest cell cycle in G2/M phase after DNA damage ($p<0.05$) and showed an abnormal DNA damage repair by persistence of γH2AX foci ($p<0.05$); and fewer RAD51 and BRCA1 foci than WT cells ($p<0.001$) in DNA lesions. In line with these results, *ZMYM3* CLL patients showed a higher average number of mutated CLL drivers than *ZMYM3* patients ($p<0.0001$), which collectively suggests a role of *ZMYM3* mutations in genome instability. In addition, we evaluated the impact of *ZMYM3* in the apoptotic pathway. First, *ZMYM3* cells showed increased levels of the anti-apoptotic proteins BCL2 and, to a lesser extent, MCL1 and BCL-XL. Second, expression of initiator or executor caspase-8, -3 and -7, was reduced in *ZMYM3* cells. This altered protein expression correlated with a higher apoptosis evasion of *ZMYM3* cells, as shown by annexin V/PI staining, which was potentiated in *ZMYM3 NOTCH1* cells ($p<0.001$), and leaded to an improved growth capacity ($p<0.05$). In conclusion, our work shows that *ZMYM3* mutations highly associate with *NOTCH1* mutations and have an impact in the outcome of CLL patients, especially in early-stage cases. Moreover, we demonstrate that *ZMYM3* mutations reduce histone H4 acetylation levels and alter gene expression of CLL cells, resulting in impaired DNA damage repair and promoting apoptosis evasion.

Abstract ID: 1553093

Title: Time-limited venetoclax-rituximab is effective for patients with Bruton tyrosine kinase exposed chronic lymphocytic leukaemia, but durable treatment-free remissions are uncommon

Authors: Thomas Lew, Rory Bennett, Victor Lin, Ashley Whitechurch, Sasanka Handunnetti, Paula Marlton, Yandong Shen, Stephen Mulligan, Joshua Casan, Piers Blombery, Constantine S. Tam, Andrew Roberts, John Seymour, Phillip Thompson and Mary Ann Anderson

Although time-limited anti-CD20 antibody and venetoclax therapy is highly effective for patients (pts) with chronic lymphocytic leukaemia (CLL), there are minimal data regarding its effectiveness among patients previously exposed to Bruton tyrosine kinase inhibitors (BTKi). In the phase III MURANO study, which established venetoclax-rituximab as a standard of care in relapsed/refractory CLL, pts with BTKi-exposed disease were poorly represented ($n=5$) [1]. Although continuous venetoclax monotherapy has been shown to be effective in BTKi exposed patients [2], venetoclax-rituximab and the potential for time-limited remissions in this context, is poorly described to date.

Aim: To describe the clinico-pathologic characteristics and outcomes of a cohort of pts treated with venetoclax-based therapy for CLL after prior BTKi-exposure. Method: We retrospectively reviewed 49 pts consecutively treated with venetoclax-based therapy for CLL after prior BTKi-exposure at the Royal Melbourne Hospital and Peter MacCallum Cancer Centre, the Princess Alexandra Hospital and Royal North Shore Hospital between June 2011 and Feb 2023. Baseline clinico-pathologic variables, treatment, response and outcome data were collected. The Kaplan-Meier method was used to estimate progression-free survival (PFS) and overall survival (OS).

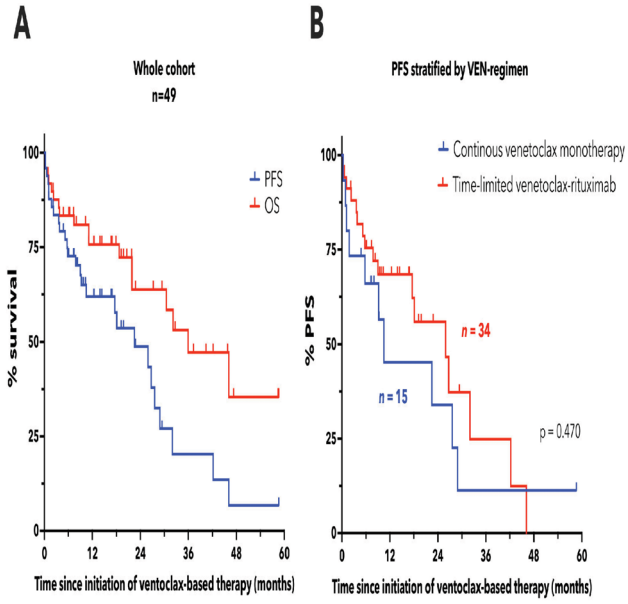

Results: The median age was 70 (range, 47–86) years and the median number of prior therapies, including BTKi-containing regimen, was 2 (range 1–7). 86% of pts were chemoimmunotherapy-exposed. Median time to disease progression after initial BTKi-containing therapy was 32 (range 1–91) months. At the time of venetoclax-based therapy, most pts had high-risk disease genetics: IGHV unmutated (20/23; 87%), complex karyotype (16/22; 73%), del(17p) and/or TP53-mutated (27/40; 68%). Thirty-four (69%) pts received venetoclax-rituximab intended as time-limited therapy; 15 (31%) received continuous venetoclax monotherapy. Among 37 pts evaluated for response, the objective response rate was 76% (complete response rate: 54%). The median PFS after venetoclax initiation was 22.5 (95%CI 9.2–28.9) months and the median OS was 35.9 (95%CI 21.9–NE) months (Figure 1(A)). The median PFS for pts receiving continuous venetoclax-monotherapy was 10.5 (95%CI 1.1–28.9) months and 25.9 (95%CI 9–42.2) for those receiving venetoclax-rituximab ($p=0.470$) (Figure 1(B)). However, patients who received venetoclax-monotherapy were more heavily pre-treated (median 3 prior lines, range 1–7) compared to patients receiving venetoclax-rituximab (median 2 prior lines, range 1–5) ($p=0.179$).

Conclusion: In this heavily pre-treated cohort of mostly chemoimmunotherapy-exposed pts, enriched for high-risk genetics, venetoclax-based therapy was effective against BTKi-exposed CLL. With a median PFS after venetoclax initiation of ~26 months, venetoclax-rituximab appears to be comparable to other therapies for pts with BTKi-exposed CLL, such as pirtobrutinib [3] However, progressive disease during or shortly after fixed-duration therapy is common and durable time-limited remissions in this context are infrequently observed. The implications of these data for pts who progress after first-line BTKi are unclear.

Abstract ID: 1553624

Title: LYN kinase and its regulator CSK as key players in CLL-supporting macrophages

Authors: Viktoria Kohlhas, Maximilian Koch, Julia Saggau, Hendrik Jestrabek, Luca

Schreurs, Rebekka Zölzer, Rocio Rebollido-Rios, Alexander vom Stein, Daniel Bachurski, France Rose, Katarzyna Bozek, Simon Tröder, Branko Zevnik, Björn Häupl, Thomas Oellerich, Michael Hallek and Phuong-Hien Nguyen

The expression of several B-cell receptor-associated kinases such as LYN, BTK, PI3Kδ and PKC-β in bystander cells of the CLL tumor microenvironment (TME) were shown to contribute actively to the leukemia-promoting niche [1–3]. LYN kinase was an essential factor for disease progression, although activation of this kinase in B cells seemed to play only a minor role in CLL development *in vivo* [4,5]. In contrast, LYN expression in the microenvironment was essential for CLL growth, which could be attributed to the failure of both LYN-knockout macrophages and stromal fibroblasts to fully support CLL cell survival [6]. Using CRISPR/Cas9 editing in murine zygotes, we generated a mouse model harboring a point mutation (K275R) in the kinase domain of LYN, leading to an inactivation of its kinase function. LYN-K275R mice exhibit a massive reduction in tyrosine phosphorylation with an alleviated phenotype compared to LYN-knockout mice. In adoptive transfer experiments, CLL progression was significantly delayed in LYN-K275R recipients. The viability of primary CLL cells cultured with LYN-K275R bone marrow-derived macrophages was significantly reduced, indicating that the kinase function of LYN in macrophages is the important mediator of CLL support. Alongside the *in vivo* findings, we established a library of tyrosine kinase knockout macrophage cell lines to investigate the potential roles of tyrosine kinases in the CLL-TME dialog. For this purpose, we successfully conducted a functional arrayed CRISPR/Cas9 knockout screen of all known tyrosine kinases in the THP-1 cell line. THP-1 monocytes stably expressing the Cas9 nuclease were transduced with lentiviral particles containing sgRNAs targeting all human tyrosine kinases. Single gene knockout THP-1 monocytes were differentiated into macrophages and cocultured with primary CLL cells. CLL cell survival was measured as a read-out for the supportive capacity of the THP-1 feeder cells. We discovered a dozen single-gene knockouts with consistently reduced CLL cell survival support, with LYN being identified among the top targets, adding further weight to our *in vivo* findings. Importantly, we detected a significantly enhanced expression of LYN in macrophages of the CLL lymph node compared to those of healthy individuals, implying the clinical relevance of LYN. Interestingly, the deletion of CSK, the major negative regulator of SRC family kinases (SFK) including LYN, also led to a robust decrease in CLL-feeding capacity of macrophages. LYN and CSK knockout THP-1 macrophages did not show detectable differences in viability and phagocytosis. Although CSK knockout resulted in the increased activation of other SFK, LYN expression was starkly diminished in CSK-knockout macrophages, which was solely dependent on the kinase activity of CSK. These results indicate that the signaling axis governed by LYN and its negative regulator CSK in macrophages are crucial for CLL cell survival. Further validation of these findings with LYN and CSK knockouts in additional macrophage cell lines and in primary macrophages is ongoing. Our current studies are focusing on deciphering the molecular mechanisms, by which LYN and its regulator CSK in macrophages influence CLL cell survival using transcriptome, proteome, and secretome analyses. Our acquired results will not only unravel the signaling pathways involving tyrosine kinases that are critical for the CLL-TME dialog but also open new venues for novel combinatory treatment regiments, in which available kinase inhibitors can be redesigned for remodeling of the CLL TME.

Abstract ID: 1553769

Title: Sensitive monitoring of sequential targeted therapy resistance in relapsed/therapy refractory chronic lymphocytic leukemia

Authors: Lili Kotmayer, Tamas Laszlo, Donat Alpar and Csaba Bödör

Targeted therapies, including the BTK inhibitor ibrutinib and the Bcl-2 inhibitor venetoclax, have transformed the therapeutic landscape of relapsed/therapy refractory chronic lymphocytic leukemia (R/R CLL) demonstrating previously unmet efficacy and high response rates across heavily pre-treated patient populations. Despite the prolonged progression-free survivals, secondary or acquired resistance and subsequent progressive CLL occur in some patients and are the leading cause of treatment failure. Since eventual loss of efficacy and sequential resistance to both ibrutinib and venetoclax confer dismal outcomes, early detection of secondary resistance could potentially allow for the introduction of alternative treatment strategies with ideal timing over the disease course and the identification of patients who may benefit from change of therapy. With a series of studies, our specific aims were to develop a droplet digital polymerase chain reaction (ddPCR)-based method for the detection of the most frequent resistance mutations conferring secondary resistance to ibrutinib or venetoclax therapy. We further aimed to dissect the temporal heterogeneity observed in R/R CLL in the context of targeted therapy by the molecular monitoring of the BTK p.Cys481Ser and BCL-2 hotspot mutations relevant in acquired ibrutinib and venetoclax resistance, respectively. Our ultimate goal was to aid the standard-of-care monitoring of the efficacy of ibrutinib and venetoclax therapies in CLL. Serial peripheral blood (PB) samples were collected from 83 R/R CLL patients treated with ibrutinib. This cohort comprised a subset of 126 patients investigated within the framework of the nationwide Hungarian Ibrutinib Resistance Analysis Initiative. Further PB samples were collected from 67 patients with R/R CLL treated with venetoclax monotherapy or venetoclax in combination with rituximab. Progressive disease and relapse were defined as the emergence of at least one novel symptom based on the iwCLL criteria for active disease and change of therapy was issued at the physician's discretion in both cohorts. Screening and quantitative assessment of the BTK p.Cys481Ser and selected BCL2 resistance mutations (p.Gly101Val and p.Asp103Tyr) were performed by ddPCR using assays designed for the discriminative analysis of mutant and wild-type alleles. Reactions were carried out on the QX200 Droplet Digital PCR platform (Bio-Rad Laboratories, California, USA) according to the manufacturer's instructions. In the ibrutinib- and venetoclax-treated patient groups, median follow up time was 40 and 23 months, respectively, with both cohorts representing the largest real-world patient populations in which resistance mutations have been longitudinally monitored at the date of publishing. In 83 ibrutinib-treated R/R CLL patients, BTK p.Cys481Ser was detected in nearly half of the cases with 80% of the mutation-bearing patients showing signs of disease progression. In the venetoclax-treated patient population, BCL2 p.Gly101Val and p.Asp103Tyr were detected in 10.4 and 11.9% of the cases, respectively, with 4 patients harbouring both alterations. Ten out of eleven (90.9%) patients

carrying p.Gly101Val and/or p.Asp103Tyr experienced relapse or disease progression, representing 43.5% (10/23) of all cases developing secondary venetoclax resistance during the follow-up period. Intriguingly, 21 patients receiving ibrutinib have experienced relapse or disease progression during the follow up and were administered subsequent venetoclax therapy. Of this patient subpopulation, 18 cases were found to harbour the BTK p.Cys481Ser resistance mutation with the emergence of the variant predating the first clinical observation of resistance with a median of 11 months. Sequential resistance to ibrutinib and venetoclax occurred in 11 cases, with 3 patients carrying both BTK p.Cys481Ser and either of the two BCL2 hotspot mutations. In summary, with the ultra-sensitive ddPCR-based analyses of one mutation hotspot associated with ibrutinib resistance and two hotspots linked to venetoclax failure, we successfully identified the underlying molecular mechanisms in two-thirds (32/44 and 10/23 of all ibrutinib- and venetoclax-resistant cases, respectively) of the patients undergoing relapse or disease progression during targeted treatments. Molecular monitoring of sequential resistance to ibrutinib and venetoclax by ddPCR is a feasible method able to capture the temporal heterogeneity observed in R/R CLL. Our results imply the selected gene mutations as promising potential molecular biomarkers for use in the standard-of-care diagnostic work-up of targeted therapy resistance in CLL.

Abstract ID: 1553902

Title: Mutations and translocations associated with venetoclax resistance in chronic lymphocytic leukemia (CLL)

Authors: Kiyomi Mashima, Yanan Kuang, Stacey Fernandes, Samantha Shupe, Rayan Fardoun, Mariia Mikhaleva, Aishath Naeem, Benjamin Hanna, Cloud P. Paweletz, Matthew Davids and Jennifer Brown

Introduction: The B-cell lymphoma-2 (BCL-2) protein inhibitor venetoclax (VEN) is a key drug for treatment of chronic lymphocytic leukemia (CLL). We aim to evaluate the gene mutations detected during VEN treatment in CLL including BCL2 G101V mutation.

Methods: We retrospectively reviewed 126 patients (pts) who received VEN at Dana-Farber Cancer Institute between 2010 and 2022. Thirty-nine pts who had at least one clinical sequencing test during VEN treatment were available, with 138 next generation sequencing (NGS).

Results: As the clinical NGS does not include BCL-2, we performed a droplet digital PCR (ddPCR) assay to detect BCL2 G101V mutations in 72 DNA samples obtained from peripheral blood or bone marrow mononuclear cells on the same day or within three months of clinical sequencing. NGS was performed at disease progression in 20 pts (Group PD) and on treatment without progression in 19 pts (Group NP). Nine-teen pts in the PD group and 15 pts in the NP group had DNA samples for ddPCR. The median observation period (days from VEN initiation to evaluation with NGS) was 347.5 [7 – 2599] and 553 [16 –1480] days in the NP and PD groups, respectively. Pts with complex karyotype (NP vs PD, 23.5 % vs 65.0%, P = 0.02) and del(13q) (NP vs. PD, 15.8 vs 50.0%, $p = 0.02$) were significantly enriched in the PD group. In addition, pts in the PD group showed a trend toward having more prior treatment regimens (NP vs PD, treatment before VEN, 0/1/2+: 15.8%/31.6%/52.6% vs 0.0%/20.0%/80.0%, $p = 0.096$). Nineteen PD pts and 15 NP pts had DNA for ddPCR to evaluate BCL2 G101V mutation. BCL2 G101V mutation was detected more frequently in PD pts compared to NP pts with higher median variant allele frequency (mVAF), but these differences were not significant (PD vs. NP, 36.8 vs. 20.0 %, $p = 0.28$, VAF: 4.68 vs. 0.17%, $p = 0.21$). Our clinical sequencing data showed that SF3B1 mutations significantly co-occurred with BCL2 G101V mutations (57.1% in BCL2 G101V vs. 8.33% in those without, $p = 0.035$, mVAF 27.8 vs 0.3%). These data also showed that ASXL1 (31.6%) and NOTCH1 (31.6%) (both $p = 0.016$) mutations were detected only in the PD group (mVAF: ASXL1 19.3%; NOTCH1 52.9%) (Figure 1). TP53, SF3B1, BRAF, CUT1, PPMD1, SH2B3, and XPO1 tended to be higher in the PD group but not significantly. (mVAF PD vs. NP, p value: TP53, 11.1 vs. 5.35%, 0.064; SF3B1, 22.8 vs. 15.65%, 0.14, respectively). ATM mutations tended to be lower in the PD group (PD vs. NP, 15.7 vs 40.0% p value $p = 0.11$), as we also saw in our BTK inhibitor PD cohort (BTK-i abstract for iwCLL 2023). We recently demonstrated that copy number loss of 8p from whole exome sequencing data was associated with VEN resistance [1]. In this analysis, the most common chromosomal change detected by karyotype was loss of chr 8 (PD vs NP 25 vs. 0%, $p = 0.0228$). Moreover, unbalanced translocations caused loss of chr 8p in 4 of 5 cases during VEN (one of 5 was monosomy 8) (Table 1). These findings confirm our

Table 1. Translocations detected in G-banding test during venetoclax treatment

Groups	Balanced translocations	Unbalanced translocations
PD	translocation 1q21; 14q32	derivative 5p15
	translocation 4q12; 9p22	derivative 6q21
		derivative 8q10; 17q10
		derivative 8q10; 21q10
		derivative 8q11.1
		derivative 8p23
		derivative 10q12
		derivative 14q32
		derivative 15p11.1
		derivative 16q11.2
		derivative 17p11.2
		derivative 17q22
NP	translocation 6p23; 13q13	derivative 4q31
		derivative 15q10; 17q10
		derivative 20p13

Figure 1. Mutations detected in all pts according to venetoclax response

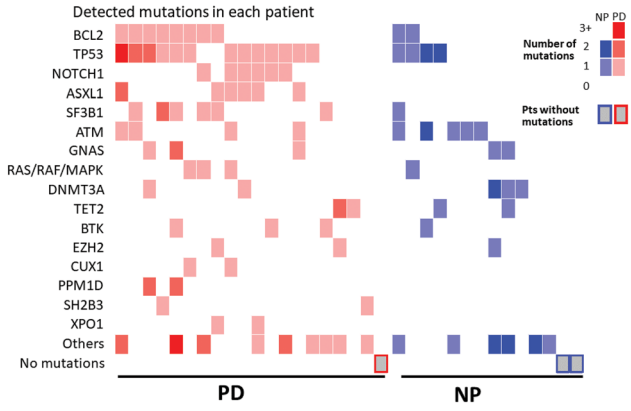

recent report (total of 6 pts with loss of 8p, 4 acquired during VEN vs 2 preexisting) in a largely independent cohort (total of 7 pts with loss of 8p, 5 acquired during VEN vs. 2 preexisting). Four patients were overlapping including the 2 with pre-existing 8p loss, one with acquired loss of 8p during VEN and the other without loss of 8p. All of these pts with loss of 8p detected during VEN in our cohort had complex karyotype with 5 or more abnormalities. The next most frequent translocated locus was chr 17 (PD vs NP 25 vs. 5.6%, $p=0.101$).

Conclusions: We retrospectively analyzed gene mutations among venetoclax treated pts and showed that ASXL1 and NOTCH1 were frequently mutated in the resistant cohort. We also evaluated BCL2 G101V mutations using ddPCR and demonstrated that SF3B1 gene mutations were highly co-mutated with BCL-2. Notably, copy number loss of 8p is related to venetoclax resistance and the majority of these events are caused by unbalanced translocations in the context of highly complex karyotype.

Abstract ID: 1554007

Title: Generation and preclinical evaluation of a novel ROR1-specific CAR T-cells against chronic lymphocytic leukemia

Authors: Md Kamrul Hasan, Christopher Oh, Christina Girgis, George Widhopf, Charles Prussak and Thomas Kipps

Receptor tyrosine kinase-like orphan receptor 1 (ROR1) is an oncoembryonic surface antigen expressed on chronic lymphocytic leukemia (CLL) B cells, but not on normal B cells or virtually all normal postpartum tissues. We generated chimeric antigen receptor (CAR) constructs using intracellular co-stimulatory domains of CD137 and CD3zeta with a CD28 transmembrane domain and IgG4 spacer region presenting an anti-ROR1-scFv (single-chain fragment variable). We utilized the humanized scFv binding domain of zilovertamab (formerly UC-961 and then cirmtuzumab), which showed high affinity and specificity for human ROR1 and a highly favorable safety profile in Phase-1 clinical evaluation [1]. Moreover, we generated constructs with extracellular stalks of varying lengths by using IgG4-derived heavy-chain constant (CH) regions or Hinge region, namely Hinge domain alone, Hinge-CH2, and Hinge-CH2-CH3, allowing us to evaluate whether the stalk length factored in the efficacy of this anti-ROR1 CAR. The chimeric genes encoding these constructs each were inserted into lentivirus vectors for transduction of human primary T cells. Transduction of primary T cells from healthy donors with each construct generated cells with high proportions of anti-ROR1 CAR-expressing T cells that specifically could bind a fluorochrome-labeled recombinant protein with the ROR1 extracellular domains, as assessed via flow cytometry. When T cell populations with comparable proportions of anti-ROR1 CAR T cells were compared for their cytotoxic activity against radioactive chromium (Cr51)-labeled ROR1-target cells for Cr51 release assays at various effector cell (E): target cell (T) ratios, we observed comparable specific killing by T cells expressing either of these different constructs, thus distinguishing these anti-ROR1 CAR constructs from other anti-ROR1 CAR constructs reported by other investigators. We selected for subsequent study the anti-ROR1 CAR construct with the shortest stalk, namely the one with only the Hinge region. We used this anti-ROR1 CAR construct to generate anti-ROR1 CAR T-cells from healthy donors or patients with CLL. We performed Cr51-assays with varying E:T ratios to interrogate the cytotoxic activity of ROR1-CAR T-cells for primary CLL cells and the CLL-derived cell line MEC1, or MEC1 cells transfected to express ROR1 (named MEC1-ROR1). We found that anti-ROR1-CAR T-cells derived from T cells of healthy donors or from patients with CLL were highly cytotoxic for allogeneic or autologous primary CLL cells, CLL cells with high-risk adverse genetic features (e.g. mutant TP53/del(17p), complex cytogenetics), or MEC1-ROR1 cells, but not MEC1 cells lacking expression of ROR1. Pretreatment of CLL cells with the anti-ROR1 mAb zilovertamab inhibited the capacity of anti-ROR1-CAR T-cells to kill CLL, demonstrating that the cytotoxic activity of anti-ROR1-CAR T-cells for CLL cells is specific for ROR1. Moreover, we found that anti-ROR1 CAR T cells lacked cytotoxic activity for normal B cells, which lack ROR1, even when placed in co-culture with ROR1-expressing CLL cells. Furthermore, anti-ROR1 CAR T cells, but not activated T cells, were highly effective in clearing luciferase-labeled MEC1-ROR1 cells engrafted in immune-deficient mice. We conclude that lentivirus encoding this anti-ROR1 CAR construct can generate anti-ROR1 CAR T cells using T cells of healthy donors or patients with CLL that are highly effective in killing ROR1-expressing leukemia cells in vitro or in vivo. Moreover, the anti-ROR1 CAR T cells generated using this construct may provide for selective killing of CLL cells without affecting normal CD19/CD20-expressing B cells of patients with CLL, thereby mitigating the risk for further enhancing immune deficiency, such as observed in patients treated with anti-CD19 CAR T cell therapy.

Abstract ID: 1554112

Title: Combining CD19 CAR T cells with T cell-engaging bispecific antibody treatment enhances efficacy in murine models of CLL and ex vivo patient cultures

Authors: Alessia Floerchinger, Berit J. Brinkmann, Tobias Roider, Peter-Martin Bruch, Antonia Angeli, Sibylle Ohl, Norman Mack, Mariana Coelho, Philipp M. Roessner, Sascha Dietrich and Martina Seiffert

Failure of adaptive immunity and immunotherapy such as immune checkpoint blockade (ICB) and chimeric antigen receptor (CAR) T cell therapy has been linked to dysfunctional effector T cells in chronic lymphocytic leukemia (CLL) patients. Chronic exposure to tumor (neo)antigens in an immunosuppressive microenvironment results in T cell exhaustion with limited reactivation upon immunotherapy. Despite an increasing number of effective tumor-targeting treatment options for CLL, patients are frequently suffering from refractory disease when malignant cells resistant to standard therapy emerge. CLL is still considered incurable with an urgent clinical need for additional treatment modalities for therapy-resistant cases. We therefore aimed to exploit CAR T cell therapy in combination with additional immunostimulation to overcome the lack of response in CLL as opposed to other B cell malignancies, such as acute lymphoblastic leukemia (ALL), where CD19-CAR T cells are an effective and safe treatment strategy. Clinically relevant drugs were screened for candidates improving CAR T cell therapy in an in vitro system based on several B cell non-Hodgkin lymphoma (B-NHL) cell lines cocultured with healthy donor-derived CD19-CAR T cells or non-transduced (NT) control T cells for four days. Bispecific antibody (BsAb) treatment targeting CD20 as tumor antigen and CD3 on T cells was included in the screening, aiming to maximize tumor cell killing via combined forces of CD19-CAR T cells and bystander endogenous T cells engaged to kill CD20-positive cells. In this model system, the addition of BsAb had only minor effects on CAR T cell expansion and tumor cell killing, but was highly beneficial for NT T cell proliferation and cytotoxicity. We hypothesized that BsAb-mediated activation of non-transduced endogenous T cells in the physiological context may complement CAR T cell therapy and improve overall anti-tumor response. The fully immunocompetent Eμ-TCL1 mouse model of CLL was used to evaluate the potential of this combination approach in vivo. Monotherapies with either murine CD20-BsAb or CD19-CAR T cells were established in this model, both demonstrating dose-dependent efficacy in terms of CLL cell killing. Following lymphodepletion via low dose irradiation, the CAR T cell treatment was titrated to define an injected cell number with suboptimal treatment efficacy leading to relapse of animals after initial response to mimic key challenges in the clinical reality. Combination of CAR T therapy with subsequent injections of BsAb resulted in reduced tumor load and prolonged survival compared to both monotherapies. Intriguingly, preliminary data indicate that this higher efficacy is accompanied by improved CAR T cell expansion under BsAb therapy. In the long term, not only bystander T cells, but also CAR T cells may hence benefit from repeated BsAb stimulation. To validate these findings in a relevant *ex vivo* setting mimicking the cellular composition of CLL patient lymph nodes, the combination treatment was tested in primary lymph node-derived samples of CLL ($n=4$) and other B-NHL ($n=20$) patients containing both malignant B cells and tumor-experienced T cells. Addition of CD20-BsAb enhanced overall tumor cell killing in cocultures with CAR T cells and improved activation and proliferation of autologous T cells marked by increased percentages of CD25+, Granzyme B+and Ki67+ cells. Therefore, CAR T cell-mediated cytotoxicity can be complemented by BsAb-induced tumor cell killing mediated by autologous T cells in the *ex vivo* setting of primary lymph node cultures. In conclusion, our data suggest that combination of CAR T cell and BsAb therapies can enhance therapeutic efficacy in CLL and other B-NHL. Both bystander T cell activation and improved long term expansion or persistence of CAR T cells with repeated BsAb restimulation seem to contribute to this improved tumor control.

Abstract ID: 1554414

Title: T-cell transcriptional and mitochondrial fitness reprogramming in CLL Using PI3Kδ inhibitors

Authors: Wael Gamal, Melanie Mediavilla-Varela, Kamira Maharaj, Angimar Uriepero, Vishaal Kunta, Eva Sahakian and Javier Pinilla-Ibarz

T-cell dysfunction associated with chronic lymphocytic leukemia (CLL) presents a major barrier for successful adoptive cell therapy in patients. This problem is attributed to the phenotypic skewness of CLL T cells towards terminal differentiation phenotypes that, in most cases, cannot tolerate the ex vivo stimulation and expansion protocols. Importantly, a handful of recent reports have demonstrated metabolic defects in T cells from CLL patients, which represent a new facet for the T-cell dysfunction problem in this disease. Nevertheless, the field is still lacking sufficient studies to validate these metabolic abnormalities, in order to correlate with the differentiation and transcriptional changes of T cells in the preclinical Eμ-TCL1 murine model. PI3K signaling pathway is a main regulator of T-cell differentiation and metabolic programming following antigen recognition. Previous evidence has shown that T cells can maintain proliferative capacity following PI3K/AKT inhibition resulting in durable T cell phenotypes with enhanced functional capacity. Despite these observations, specific application of this knowledge in CLL is still required to improve adoptive cell therapies. In this study, (1) we utilized the Eμ-TCL1 preclinical model for uncovering the potential correlation between the mitochondrial/metabolic defects and the exhausted-like features of T cells in CLL and (2) we investigated the potential benefits of ex vivo priming of Eμ-TCL1 T cells. By using a PI3Kδ inhibitor, Idelalisib, we asked to improve the metabolic fitness and T-cell transcriptional reprogramming (more naïve/less-differentiated T-cell phenotypes with high persistence and effective cytotoxicity). In this study, CLL was induced in mice via adoptive transfer (AT) of leukemic splenocytes from transgenic Eμ-TCL1 mice into wild type (WT) recipients. Multiparameter flow cytometry and transmission electron microscopy (TEM) analyses revealed the accumulation of small-sized depolarized mitochondria with significant changes in reactive oxygen species (ROS) levels in AT Eμ-TCL1 CD8+ T cells. These abnormalities were associated with the expansion of specific Eμ-TCL1 CD8+ T-cell populations with high EOMES and low TCF-1 expression, and a significant increase in effector phenotypes highly expressing immune suppressive markers such as PD-1 and Tim-3. Upon ex vivo activation of AT Eμ-TCL1 CD8+ T cells for 5–6 days using CD3/CD28 dynabeads and 60IU/ml hIL-2, we found significant loss in mitochondrial spare respiratory capacity (SRC), using mitochondrial stress test, compared to activated WT controls. Nanostring gene expression analysis comparing metabolic gene expression profiles of AT Eμ-TCL1 versus WT CD8+ T cells revealed upregulation of glycolysis, mitochondrial respiration, T-cell receptor and costimulatory pathways. On the other hand, there was a downregulation in autophagy, AMPK and amino acid transporter pathways. For *ex vivo* reprogramming experiments, AT Eμ-TCL1 CD8+ T cells were primed with 5μM dose of idelalisib (CAL-101) and activated using CD3/CD28 dynabeads and 60IU/ml hIL-2 for 5–7 days. Idelalisib-treated Eμ-TCL1 T-cell cultures showed comparable expansion to vehicle-treated cells. Flow cytometric analysis showed

significant increase in central memory CD8+ T-cell populations with marked CD62L expression intensity in idelalisib-treated cultures compared to more effector and terminally differentiated phenotypes in vehicle-treated counterparts. Interestingly, the idelalisib-induced effect was associated with a shift in the transcriptional signature of Eμ-TCL1 CD8+ T cells into significantly less EOMES and TOX expression and a significant upregulation of TCF-1. This indeed was accompanied by downregulation of immune checkpoint markers such as Tim-3 and KLRG-1. From a metabolic perspective, idelalisib treatment maintained high expression of PGC-1α in Eμ-TCL1 CD8+ T cells and resulted in an increase in oxygen consumption rate and mitochondrial SRC compared to the more terminally differentiated vehicle-treated cells. This increase in mitochondrial capacity was also demonstrated by the increase in mitochondrial membrane potential and ROS production. Finally, to demonstrate the functional advantage of *ex vivo* CLL T-cell reprogramming, we performed a cytotoxicity study of idelalisib-treated cells against autologous Eμ-TCL1 CLL cells. Compared to vehicle controls, PI3K inhibition in Eμ-TCL1 T cells resulted in a significantly higher killing capacity at various effector: target ratios. In conclusion, we characterized for the first time the mitochondrial defects of CD8+ T cells from the Eμ-TCL1 murine model and outlined the correlation of these defects with the T-cell transcriptional changes in this disease. Additionally, we demonstrated successful application of *ex vivo* PI3K inhibition on Eμ-TCL1 T cells for improving adoptive cell therapy product quality and effectiveness, which can be translated into CLL patient studies.